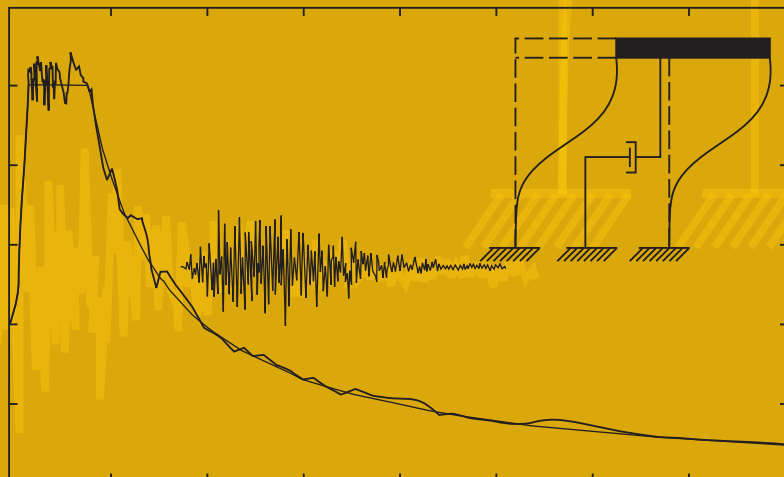


Earthquake Resistant Design of Structures



Pankaj Agarwal
Manish Shrikhande



EARTHQUAKE RESISTANT DESIGN OF STRUCTURES

PANKAJ AGARWAL

Assistant Professor

*Department of Earthquake Engineering
Indian Institute of Technology Roorkee*

and

MANISH SHRIKHANDE

Assistant Professor

*Department of Earthquake Engineering
Indian Institute of Technology Roorkee*

PHI Learning Private Limited

New Delhi-110001
2011

EARTHQUAKE RESISTANT DESIGN OF STRUCTURES
Pankaj Agarwal and Manish Shrikhande

© 2006 by PHI Learning Private Limited, Delhi. All rights reserved. No part of this book may be reproduced in any form, by mimeograph or any other means, without permission in writing from the publisher.

ISBN-978-81-203-2892-1

The export rights of this book are vested solely with the publisher.

Thirteenth Printing

...

...

July, 2014

Published by Asoke K. Ghosh, PHI Learning Private Limited, Rimjhim House, 111, Patparganj Industrial Estate, Delhi-110092 and Printed by Rajkamal Electric Press, Plot No. 2, Phase IV, HSIDC, Kundli-131028, Sonepat, Haryana.

To
Our Parents

Contents

<i>Preface</i>	<i>xxi</i>
<i>Contributors</i>	<i>xxv</i>

Part I EARTHQUAKE GROUND MOTION

1. Engineering Seismology	3-44
1.1 Introduction	3
1.2 Reid's Elastic Rebound Theory	3
1.3 Theory of Plate Tectonics	4
1.3.1 Lithospheric Plates	6
1.3.2 Plate Margins and Earthquake Occurrences	7
1.3.3 The Movement of Indian Plate	9
1.4 Seismic Waves	10
1.4.1 Body Waves	10
1.4.2 Surface Waves	11
1.5 Earthquake Size	13
1.5.1 Intensity	13
1.5.2 Isoseismal Map	18
1.5.3 Earthquake Magnitude	18
1.5.4 Energy Released in an Earthquake	23
1.5.5 Earthquake Frequency	23
1.6 Local Site Effects	24
1.6.1 Basin/Soil Effects	24
1.6.2 Lateral Discontinuity Effects	27
1.6.3 Effect of the Surface Topography	28

1.7	Internal Structure of the Earth	30
1.7.1	Crust	30
1.7.2	Upper Mantle	31
1.7.3	Lower Mantle	31
1.7.4	Core	32
1.8	Seismotectonics of India	32
1.9	Seismicity of India	34
1.10	Classification of Earthquakes	35
1.11	Tsunami	36
1.11.1	Tsunami Velocity	37
1.11.2	Run-up and Inundation	37
	<i>Summary</i>	38
	<i>Glossary of Earthquake/Seismology</i>	38
	<i>References</i>	41
2.	Seismic Zoning Map of India	45–58
2.1	Introduction	45
2.2	Seismic Hazard Map	45
2.3	Seismic Zone Map of 1962	48
2.4	Seismic Zone Map of 1966	50
2.4.1	Grade Enhancement	51
2.4.2	Review of Tectonic	51
2.5	Seismic Zone Map of 1970	52
2.6	Seismic Zone Map of 2002	56
2.7	Epilogue	56
	<i>Summary</i>	58
	<i>References</i>	58
3.	Strong Motion Studies in India	59–69
3.1	Introduction	59
3.2	Understanding the Nature of Ground Motions	60
3.2.1	Source Effect	60
3.2.2	Path Effect	62
3.2.3	Site Effect	63
3.3	Estimation of Ground Motion Parameters	64
3.4	The Indian Perspective	65
3.5	Utilization of Strong Motion Data	65
	<i>Summary</i>	66
	<i>References</i>	66
4.	Strong Motion Characteristics	70–87
4.1	Introduction	70

4.2	Terminology of Strong Motion Seismology	73
4.2.1	Amplitude Parameters	73
4.2.2	Duration of Strong Motion	74
4.2.3	Fourier Spectrum	74
4.2.4	Power Spectrum	75
4.2.5	Response Spectrum	76
4.2.6	Seismic Demand Diagrams	79
4.2.7	Spatial Variation of Earthquake Ground Motion	80
4.2.8	Damage Potential of Earthquakes	81
<i>Summary</i>	86
<i>References</i>	86
5.	Evaluation of Seismic Design Parameters	88-107
5.1	Introduction	88
5.2	Types of Earthquakes	88
5.2.1	Intensity	89
5.2.2	Magnitude	89
5.3	Fault Rupture Parameters	90
5.4	Earthquake Ground Motion Characteristics	91
5.4.1	Amplitude Properties	91
5.4.2	Duration	93
5.4.3	Effect of Distance	93
5.4.4	Ground Motion Level	96
5.4.5	Geographical, Geophysics and Geotechnical Data	96
5.5	Deterministic Approach	97
5.6	Probabilistic Approach	98
5.6.1	Example	100
5.7	Response Spectra	101
5.8	Design Spectrum	101
<i>Summary</i>	105
<i>References</i>	106

Part II STRUCTURAL DYNAMICS

6.	Initiation into Structural Dynamics	111-114
6.1	Introduction	111
6.2	Mathematical Modelling	112
<i>Summary</i>	114
<i>References</i>	114

7. Dynamics of Single Degree of Freedom Systems.....	115-128
7.1 Introduction	115
7.2 Free Vibration of Viscous-Damped SDOF Systems	116
7.2.1 Underdamped Case ($\zeta < 1$)	118
7.2.2 Critically-damped Case ($\zeta = 1$).....	118
7.2.3 Overdamped Case ($\zeta > 1$).....	118
7.3 Forced Vibrations of SDOF Systems	120
7.3.1 Response of SDOF Systems to Harmonic Excitations	120
7.3.2 Excitation by Base Motion	122
7.3.3 Response of SDOF Systems to a Finite Duration Excitation	122
7.3.4 Response of SDOF Systems to a Short Duration Impulse	124
7.3.5 Response of SDOF Systems to General Dynamic Excitation	125
7.4 Vibration Isolation	126
<i>Summary</i>	128
<i>References</i>	128
8. Theory of Seismic Pickups.....	129-136
8.1 Introduction	129
8.2 The Physics of Operation.....	129
8.3 Which Parameter to Measure?	131
8.4 Seismometers	132
8.4.1 Displacement Pickups	132
8.4.2 Velocity Pickups	132
8.5 Accelerometers	133
8.5.1 Servo-accelerometers	135
8.5.2 Calibration of Accelerometers	136
<i>Summary</i>	136
<i>References</i>	136
9. Numerical Evaluation of Dynamic Response	137-143
9.1 Numerical Solution Based on Interpolation of Excitation	137
9.2 Numerical Solution Based on Approximation of Derivatives	139
9.3 Stability and Accuracy Considerations	141
<i>Summary</i>	143
<i>References</i>	143
10. Response Spectra.....	144-156
10.1 Introduction	144
10.2 Fourier Spectra	144

10.3	Response Spectra	146
10.3.1	Formulation	147
10.3.2	Solution: Initially at Rest	148
10.3.3	Solution: General Conditions	151
10.3.4	Smooth Spectrum	154
10.3.5	Seismic Demand Diagrams	154
<i>Summary</i>	155
<i>References</i>	155

11. Dynamics of Multi-Degree-of-Freedom Systems 157–188

11.1	Introduction	157
11.2	System Property Matrices	158
11.3	Dynamics of Two Degree of Freedom Systems.....	159
11.4	Free Vibration Analysis of MDOF Systems	162
11.4.1	Orthogonality Conditions	163
11.5	Determination of Fundamental Frequency	165
11.5.1	Rayleigh Quotient	165
11.5.2	Stodola Method	165
11.5.3	Converging to Higher Modes	166
11.6	Forced Vibration Analysis	169
11.6.1	Mode-superposition Method	170
11.6.2	Excitation by Support Motion	171
11.6.3	Mode Truncation	175
11.6.4	Static Correction for Higher Mode Response	176
11.7	Model Order Reduction in Structural Dynamics	177
11.8	Analysis for Multi-Support Excitation	178
11.9	Soil–Structure Interaction Effects	181
11.9.1	Dynamic Analysis including SSI Effects	182
<i>Summary</i>	187
<i>References</i>	187

Part III CONCEPTS OF EARTHQUAKE RESISTANT DESIGN OF REINFORCED CONCRETE BUILDING

12.	Earthquake and Vibration Effect on Structures: Basic Elements of Earthquake Resistant Design	191–206
12.1	Introduction	191
12.2	Static and Dynamic Equilibrium	192
12.3	Structural Modelling	194
12.3.1	Structural Models for Frame Building	194

12.4 Seismic Methods of Analysis	196
12.4.1 Code-based Procedure for Seismic Analysis	197
12.5 Seismic Design Methods	198
12.5.1 Code-based Methods for Seismic Design.....	198
12.6 Response Control Concepts	199
12.6.1 Earthquake Protective Systems	200
12.7 Seismic Evaluation and Retrofitting	201
12.7.1 Methods for Seismic Evaluation	202
12.7.2 Methods for Seismic Retrofitting	203
12.8 Seismic Test Methods	204
12.8.1 Methods for Seismic Testing	204
<i>Summary</i>	205
<i>References</i>	205
13. Identification of Seismic Damages in RC Buildings during Bhuj Earthquake.....	207-225
13.1 Introduction	207
13.2 Reinforced Concrete Building Construction Practices	208
13.3 Identification of Damage in RC Buildings	210
13.3.1 Soft Storey Failure	211
13.3.2 Floating Columns	212
13.3.3 Plan and Mass Irregularity	213
13.3.4 Poor Quality of Construction Material and Corrosion of Reinforcement ..	214
13.3.5 Pounding of Buildings	215
13.3.6 Inconsistent Seismic Performance of Buildings	216
13.4 Damage to Structural Elements	217
13.5 Damage to Non-Structural Panel Elements	219
13.5.1 Damage to Infill Walls	219
13.5.2 Damage to Exterior Walls	220
13.6 Damage to Water Tank and Parapets	220
13.7 Damage to Vertical Circulation Systems	221
13.7.1 Damage to Staircase	221
13.7.2 Damage to Elevator	222
13.8 Effect of Earthquake on Code Designed Structures	222
13.9 Lessons Learnt from Damages of RC Buildings	223
<i>Summary</i>	224
<i>References</i>	224
14. Effect of Structural Irregularities on the Performance of RC Buildings during Earthquakes	226-238
14.1 Introduction	226

14.2	Vertical Irregularities	227
14.2.1	Vertical Discontinuities in Load Path	227
14.2.2	Irregularity in Strength and Stiffness	230
14.2.3	Mass Irregularities	232
14.2.4	Vertical Geometric Irregularity	233
14.2.5	Proximity of Adjacent Buildings.....	233
14.3	Plan Configuration Problems	234
14.3.1	Torsion Irregularities	234
14.3.2	Re-entrant Corners	236
14.3.3	Non-parallel Systems	236
14.3.4	Diaphragm Discontinuity	237
14.4	Recommendations	237
	<i>Summary</i>	238
	<i>References</i>	238

15. Seismoresistant Building Architecture 239-248

15.1	Introduction	239
15.2	Lateral Load Resisting Systems	239
15.2.1	Moment Resisting Frame	240
15.2.2	Building with Shear Wall or Bearing Wall System	240
15.2.3	Building with Dual System	240
15.3	Building Configuration	241
15.3.1	Problems and Solutions	241
15.4	Building Characteristics	243
15.4.1	Mode Shapes and Fundamental Period	243
15.4.2	Building Frequency and Ground Period	244
15.4.3	Damping	244
15.4.4	Ductility	244
15.4.5	Seismic Weight	245
15.4.6	Hyperstaticity/Redundancy	245
15.4.7	Non-structural Elements	245
15.4.8	Foundation Soil/Liquefaction	246
15.4.9	Foundations	246
15.5	Quality of Construction and Materials	246
15.5.1	Quality of Concrete	247
15.5.2	Construction Joints	247
15.5.3	General Detailing Requirements	247
	<i>Summary</i>	248
	<i>References</i>	248

Part IV
SEISMIC ANALYSIS AND MODELLING OF
REINFORCED CONCRETE BUILDING

16. Code Based Procedure for Determination of Design Lateral Loads	251-281
16.1 Introduction	251
16.2 Seismic Design Philosophy	251
16.3 Determination of Design Lateral Forces	252
16.3.1 Equivalent Lateral Force Procedure	253
16.3.2 Dynamic Analysis Procedure	259
<i>Summary</i>	280
<i>References</i>	280
17. Consideration of Infill Wall in Seismic Analysis of RC Buildings	282-291
17.1 Introduction	282
17.2 Structural and Constructional Aspects of Infills	282
17.3 Failure Mechanism of Infilled Frame	283
17.4 Analysis of Infilled Frames	284
17.4.1 Equivalent Diagonal Strut	285
<i>Summary</i>	290
<i>References</i>	290
18. Step-by-Step Procedure for Seismic Analysis of a Four-storeyed RC Building as per IS 1893 (Part 1): 2002	292-326
18.1 Introduction	292
18.2 Equivalent Static Lateral Force Method	293
18.2.1 Step 1: Calculation of Lumped Masses to Various Floor Levels	293
18.2.2 Step 2: Determination of Fundamental Natural Period	294
18.2.3 Step 3: Determination of Design Base Shear	294
18.2.4 Step 4: Vertical Distribution of Base Shear	295
18.3 Response Spectrum Method	296
A: Frame without Considering the Stiffness of Infills	296
18.3.1 Step 1: Determination of Eigenvalues and Eigenvectors	296
18.3.2 Step 2: Determination of Modal Participation Factors	299
18.3.3 Step 3: Determination of Modal Mass	299
18.3.4 Step 4: Determination of Lateral Force at Each Floor in Each Mode	300
18.3.5 Step 5: Determination of Storey Shear Forces in Each Mode	301
18.3.6 Step 6: Determination of Storey Shear Force due to All Modes	302
18.3.7 Step 7: Determination of Lateral Forces at Each Storey	304
B: Frame Considering the Stiffness of Infills	305

18.4	Time History Method	311
18.4.1	Step 1: Calculation of Modal Matrix	312
18.4.2	Step 2: Calculation of Effective Force Vector	314
18.4.3	Step 3: Calculation of Displacement Response in Normal Coordinate	314
18.4.4	Step 4: Displacement Response in Physical Coordinates	316
18.4.5	Step 5: Calculation of Effective Earthquake Response Forces at Each Storey	319
18.4.6	Step 6: Calculation of Storey Shear	321
18.4.7	Step 7: Calculation of Maximum Response	324
	<i>Summary</i>	324
	<i>References</i>	325
	<i>Appendix 1: Linear Interpolation of Excitation</i>	325
19.	Mathematical Modelling of Multi-storeyed RC Buildings	327–337
19.1	Introduction	327
19.2	Planar Models	327
19.2.1	Shear Beam Model	328
19.2.2	Flexure Beam Model	328
19.2.3	Idealized Plane Frame Model	329
19.2.4	Equivalent Shear Wall Frame Model	330
19.2.5	Plane Frame Model of Coupled Shear Walls	330
19.3	3D Space Frame Model	331
19.4	Reduced 3D Model	331
19.5	Some Important Issues in Modelling	331
19.5.1	Modelling of Floor Diaphragms	331
19.5.2	Modelling of Soil-Foundation	334
19.5.3	Foundation Models	334
19.5.4	Soil Models	335
19.5.5	Modelling of Staircases	336
19.5.6	Modelling of Infills	336
	<i>Summary</i>	336
	<i>References</i>	337

Part V

EARTHQUAKE RESISTANT DESIGN (ERD) OF REINFORCED CONCRETE BUILDINGS

20.	Ductility Considerations in Earthquake Resistant Design of RC Buildings	341–370
20.1	Introduction	341
20.2	Impact of Ductility	342
20.3	Requirements for Ductility	342

20.4	Assessment of Ductility	342
20.4.1	Member/Element Ductility	343
20.4.2	Structural Ductility	345
20.5	Factors Affecting Ductility	346
20.6	Ductility Factors	347
20.7	Ductile Detailing Considerations as per IS 13920: 1993	348
<i>Summary</i>	370
<i>References</i>	370
21.	Earthquake Resistant Design of a Four-storey RC Building Based on IS 13920: 1993	371–391
21.1	Introduction	371
21.2	Preliminary Data for Example Frame	371
21.3	Loading Data	373
21.4	Analysis of Sub-frame 4-4	373
21.4.1	Dead Load Analysis	373
21.4.2	Live (Imposed) Load Analysis	375
21.4.3	Earthquake Load Analysis	376
21.5	Load Combinations	377
21.6	Design of Sub-Frame 4-4	382
21.6.1	Design of a Flexure Member	382
21.6.2	Design of Exterior Columns	385
21.6.3	Design of Interior Columns	387
21.6.4	Detailing of Reinforcements	389
<i>Summary</i>	390
<i>References</i>	391
22.	Earthquake Resistant Design of Shear Wall as per IS 13920: 1993	392–403
22.1	Introduction	392
22.2	Description of Building	392
22.3	Determination of Design Lateral Forces	393
22.4	Design of Shear Wall	397
22.5	Detailing of Reinforcements	402
<i>Summary</i>	403
<i>References</i>	403
23.	Capacity Based Design—An Approach for Earthquake Resistant Design of Soft Storey RC Buildings.....	404–424
23.1	Introduction	404
23.2	Preliminary Data for (G+3) Plane Frame	405
23.2.1	Determination of Loads	406

23.3 Step-by-Step Procedure for Capacity Based Design	409
23.3.1 Step 1: Seismic Analysis of Frame (G+3)	409
23.3.2 Step 2: Determination of Flexural Capacity of Beams	412
23.3.3 Step 3: Establishing a Strong Column–Weak Beam Mechanism	414
23.3.4 Step 4: Determination of Moment Magnification Factors for Columns	415
23.3.5 Step 5: Capacity Design for Shear in Beams	417
23.3.6 Step 6: Capacity Design for Shear in Columns	418
23.3.7 Step 7: Detailing of Reinforcements	419
<i>Summary</i>	421
<i>References</i>	421
<i>Appendix 1: Beam Flexural Capacity Calculation as per Design Aid IS456: 1978.....</i>	422
<i>Appendix 2: Determination of Moment Magnification Factor at Every Joint</i>	423

Part VI

EARTHQUAKE RESISTANT DESIGN (ERD) OF MASONRY BUILDINGS

24. Identification of Damages and Non-Damages in Masonry Buildings from Past Indian Earthquakes..... 427–448

24.1 Introduction	427
24.2 Past Indian Earthquakes	427
24.3 Features of Damages and Non-damages	429
24.3.1 Bhuj Earthquake, January 26, 2001	429
24.3.2 Chamoli Earthquake, March 29, 1999	431
24.3.3 Jabalpur Earthquake, May 22, 1997	433
24.3.4 Killari Earthquake, September 30, 1993	436
24.3.5 Uttarkashi Earthquake, October 20, 1991	438
24.3.6 Bihar-Nepal Earthquake, August 21, 1988	441
24.4 Lessons Learnt	444
24.5 Recommendations	445
<i>Summary</i>	445
<i>References</i>	446
<i>Appendix 1: Muzaffarabad Earthquake of October 8, 2005</i>	446

25. Elastic Properties of Structural Masonry..... 449–462

25.1 Introduction	449
25.2 Materials for Masonry Construction	449
25.2.1 Unit	449
25.2.2 Mortar	450
25.2.3 Grout	451
25.2.4 Reinforcement	451

25.3	Elastic Properties of Masonry Assemblage	452
25.3.1	Compressive Strength	452
25.3.2	Flexural Tensile Strength	455
25.3.3	Shear Strength	456
<i>Summary</i>	460
<i>References</i>	460
26.	Lateral Load Analysis of Masonry Buildings	463–485
26.1	Introduction	463
26.2	Procedure for Lateral Load Analysis of Masonry Buildings	464
26.2.1	Step 1: Determination of Lateral Loads	465
26.2.2	Step 2: Distribution of Lateral Forces	468
26.2.3	Step 3: Determination of Rigidity of Shear Wall	470
26.2.4	Step 4: Determination of Direct Shear Forces and Torsional Shear Forces	474
26.2.5	Step 5: Determination of Increase in Axial Load Due to Overturning	479
26.2.6	Step 6: Walls Subjected to Out-of-plane Bending	483
<i>Summary</i>	484
<i>References</i>	485
27.	Seismic Analysis and Design of Two-storeyed Masonry Buildings	486–502
27.1	Introduction	486
27.2	Building Data	486
27.3	Step 1: Determination of Design Lateral Load	488
27.4	Step 2: Determination of Wall Rigidities	489
27.5	Step 3: Determination of Torsional Forces	492
27.6	Step 4: Determination Increase in Axial Load due to Overturning	495
27.7	Step 5: Determination of Pier Loads, Moments and Shear	498
27.8	Step 6: Design of Shear Walls for Axial Load and Moments	500
27.9	Step 7: Design of Shear Walls for Shear	500
27.10	Step 8: Structural Details	501
<i>Summary</i>	501
<i>References</i>	502
Part VII		
SEISMIC EVALUATION AND RETROFITTING OF REINFORCED CONCRETE AND MASONRY BUILDINGS		
28.	Seismic Evaluation of Reinforced Concrete Buildings: A Practical Approach	505–523
28.1	Introduction	505

28.2 Components of Seismic Evaluation Methodology.....	506
28.2.1 Condition Assessment for Evaluation	506
28.2.2 Field Evaluation/Visual Inspection Method	509
28.2.3 Concrete Distress and Deterioration Other than Earthquake	519
28.2.4 Non-destructive Testing (NDT).....	519
<i>Summary</i>	522
<i>References</i>	522
29. Seismic Retrofitting Strategies of Reinforced Concrete Buildings	524–555
29.1 Introduction	524
29.2 Consideration in Retrofitting of Structures	528
29.3 Source of Weakness in RC Frame Building	528
29.3.1 Structural Damage due to Discontinuous Load Path	529
29.3.2 Structural Damage due to Lack of Deformation	529
29.3.3 Quality of Workmanship and Materials	533
29.4 Classification of Retrofitting Techniques	533
29.5 Retrofitting Strategies for RC Buildings	535
29.5.1 Structural Level (or Global) Retrofit Methods	535
29.5.2 Member Level (or Local) Retrofit Methods	541
29.6 Comparative Analysis of Methods of Retrofitting	550
<i>Summary</i>	553
<i>References</i>	553
30. Seismic Retrofitting of Reinforced Concrete Buildings—Case Studies	556–575
30.1 Introduction	556
30.2 Methodology for Seismic Retrofitting of RC Buildings	557
30.3 Case Study 1: Seismic Retrofitting of RC Building with Jacketing and Shear Walls	558
30.4 Case Study 2: Seismic Retrofitting of RC Building with Bracing and Shear Wall	560
30.5 Case Study 3: Seismic Retrofitting of RC Building with Steel Bracing	562
30.6 Case Study 4: Seismic Retrofitting of RC Building by Jacketing of Frames	564
30.7 Case Study 5: Seismic Retrofitting of RC Building with Shear Walls and Jacketing	565
30.8 Case Study 6: Seismic Retrofitting of RC Building by Adding Frames	567
30.9 Case Study 7: Seismic Retrofitting of RC Building by Steel Bracing and Infill Walls	568
30.10 Case Study 8: Seismic Retrofitting of RC Building with Shear Walls	570
30.11 Case Study 9: Seismic Retrofitting of RC Building by Seismic Base Isolation ..	571
30.12 Case Study 10: Seismic Retrofitting of RC Building by Viscous Damper	573
<i>Summary</i>	574
<i>References</i>	575

31. Seismic Provisions for Improving the Performance of Non-engineered Masonry Construction with Experimental Verifications	576–590
31.1 Introduction	576
31.2 Criteria for Earthquake Resistant Provisions	577
31.3 Salient Features of Earthquake Resistant Provisions	577
31.4 Seismic Strengthening Features	577
31.5 Experimental Verification of Codal Provisions	582
31.5.1 Features of Model	583
31.5.2 Seismic Strengthening Arrangements	584
31.6 Shock Table Test on Structural Models	585
31.6.1 Behaviour of Models in Shock Tests	586
31.6.2 Recommendations	589
<i>Summary</i>	590
<i>References</i>	590
32. Retrofitting of Masonry Buildings	591–624
32.1 Introduction	591
32.2 Failure Mode of Masonry Buildings	592
32.2.1 Out-of-plane Failure	592
32.2.2 In-plane Failure	593
32.2.3 Diaphragm Failure	593
32.2.4 Failure of Connection	593
32.2.5 Non-structural Components	594
32.2.6 Pounding	595
32.3 Methods for Retrofitting of Masonry Buildings	595
32.3.1 Repair	596
32.3.2 Local/Member Retrofitting	596
32.3.3 Structural/Global Retrofitting	596
32.4 Repairing Techniques of Masonry	596
32.4.1 Masonry Cracking	596
32.4.2 Masonry Deterioration	601
32.5 Member Retrofitting	602
32.5.1 Retrofitting Techniques	602
32.6 Structural Level Retrofitting Methods	605
32.6.1 Retrofitting Techniques	606
32.7 Seismic Evaluation of Retrofitting Measures in Stone Masonry Models	618
32.7.1 Behaviour of Retrofitted Models	620
32.7.2 Findings	621
<i>Summary</i>	621
<i>References</i>	622
Index	625–634

Preface

The vast devastation of engineered systems and facilities during the past few earthquakes has exposed serious deficiencies in the prevalent design and construction practices. These disasters have created a new awareness about the disaster preparedness and mitigation. With increased awareness came the demand of learning resource material which directly address the requirements of professionals without any circumlocution. While the recommended codes of practice for earthquake resistant design do exist but those only specify a set of criteria for compliance. These design codes throw little light on the basic issue of *how to design*. The problem becomes more acute as students graduate with degrees in civil/structural engineering without any exposure to earthquake engineering in most of the universities/institutes. The short-term refresher courses routinely offered by various institutes and universities for professionals achieve little more than mere familiarization with the subject matter. Any *short-term* approach to the learning process, which requires the relevant ideas and concepts to be assimilated, is doomed to fail. Realizing the practical difficulties of professionals in attending any long-term direct contact academic programme on earthquake engineering, a six-month modular course in distance education mode was offered by IIT Roorkee in 2004. The course was well-received and culminated in a two-day workshop at Roorkee which was attended by a large number of participants, providing valuable feedback. This book derives its origin from the set of lecture notes prepared for the participants with later additions to incorporate some of the suggestions made in the feedback workshop.

The guiding principle in developing the content of this book has been to provide enough material—at one place—to develop the basic understanding of the issues as required for correctly interpreting and using the standard codes of practices for earthquake resistant design. The objective is to present the essentials in a clear and concise manner with adequate illustrations, while intentionally steering clear of some of the advanced topics which require more rigorous mathematical treatment.

This book is divided into seven parts, each dealing with a specific aspect of earthquake engineering. We start with the discussion of the physics of the earthquake generation, the evolution of the seismic zoning map of India, characteristics of the earthquake strong ground motions, and determination of seismic design parameters in the first part on *Earthquake Ground Motions*. The second part on *Structural Dynamics* is concerned with the study of

analytical treatment of vibration problems. Starting with an introductory chapter on Mathematical Modelling for Structural Dynamics Problems, the theory of structural dynamics is developed gradually to the level of dynamics of complex structural systems including multi-support excitation and dynamic soil-structure interaction analysis. The treatment is intentionally focused on deterministic problems in time domain as most of the professional engineers do not feel comfortable with the probabilistic framework and frequency domain methods. The basic philosophy of the earthquake resistant design is discussed along with the deficiencies in the prevalent design and construction practices with the help of several case studies in the third part on *Concepts of Earthquake Resistant Design of Reinforced Concrete Buildings*. Simple architectural considerations that go a long way in improving the seismic performance of reinforced concrete (RC) buildings are also discussed. The modelling issues, including the modelling of infill panels, and seismic analysis of RC framed buildings are elaborated through several worked-out examples in the fourth part on *Seismic Analysis and Modelling of Reinforced Concrete Buildings*. The actual design calculations as per relevant IS codes are presented for the seismic design of four-storey RC framed buildings and RC shear walls are described in the fifth part on *Earthquake Resistant Design of Reinforced Concrete Buildings*. A detailed example on the capacity design method to handle the soft-storey problem in RC framed buildings has also been presented. The modelling, analysis and design of masonry buildings to resist earthquake load forms the thrust of part six entitled *Earthquake Resistant Design of Masonry Buildings*. Finally, the seventh part on *Seismic Evaluation and Retrofitting of Reinforced Concrete and Masonry Buildings* elaborates upon the very challenging problem of seismic evaluation and retrofitting/strengthening of existing buildings. A state-of-the-art compilation of methods and materials has been presented along with experimental verification in some case studies. Thus a gamut of earthquake engineering starting from seismology and seismic hazard analysis to analytical study of dynamic behaviour to design and retrofit of RC and masonry buildings has been presented in a single volume.

This book is the result of team work. We have received tremendous support and cooperation from our colleagues and students in bringing it to this form and are greatly indebted to them, in particular, to Prof. Susanta Basu and Prof. S.K. Thakkar who read early drafts and offered useful suggestions for improvement in addition to contributing some chapters for the book. Dr. J.P. Narayan pitched in with his expertise in the engineering seismology to contribute a chapter introducing the basic seismological concepts. Mr. V.V.S. Dadi helped with the calculations and Mr. J.P. Singh and Mr. Hemant Venayak helped with the figures. We greatly appreciate the kind support extended to us by the staff of Prentice-Hall of India, New Delhi. We particularly admire the seemingly infinite patience of Ms. Seema Zahir, who readily accepted numerous revisions/corrections till the last moment. Finally, we are grateful to our wives, Mahima and Ashwini, for their support during the period when time was at a premium.

Although this book is primarily designed to serve as a textbook for undergraduate and postgraduate students of civil engineering, it can also be used as a reference book for regular academic courses on design of reinforced concrete and masonry buildings. The book will also serve the needs of structural designers as a ready reckoner for most of the commonly

encountered problems in earthquake resistant design and construction. Only the problems related to earthquake resistant design of buildings have been addressed in this book to restrict it to a reasonable size. It is planned to address the problems concerning earthquake resistant design of other structural types in another volume. It is but natural that some errors might have crept into the text of such volume. We will appreciate if such errors are brought to our notice. Suggestions for improvement of the book are also welcome.

**PANKAJ AGARWAL
MANISH SHRIKHANDE**

Contributors

Jay Prakash Narayan

Assistant Professor, Department of Earthquake Engineering
Indian Institute of Technology Roorkee

Shashikant Thakkar

Railway Bridge Professor
Department of Civil Engineering
Indian Institute of Technology Roorkee

Susanta Basu

Professor, Department of Earthquake Engineering
Indian Institute of Technology Roorkee

PART I

Earthquake Ground Motion

Chapter 1

Engineering Seismology

1.1 INTRODUCTION

Seismology is the study of the generation, propagation and recording of elastic waves in the earth, and the sources that produce them (Table 1.1). An earthquake is a sudden tremor or movement of the earth's crust, which originates naturally at or below the surface. The word natural is important here, since it excludes shock waves caused by nuclear tests, man-made explosions, etc. About 90% of all earthquakes result from tectonic events, primarily movements on the faults. The remaining is related to volcanism, collapse of subterranean cavities or man-made effects. Tectonic earthquakes are triggered when the accumulated strain exceeds the shearing strength of rocks. Elastic rebound theory gives the physics behind earthquake genesis. This chapter includes elastic rebound theory, plate tectonics, earthquake size, earthquake frequency and energy, seismic waves, local site effects on the ground motion characteristics, interior of the earth and seismicity of India.

TABLE 1.1 A list of natural and man-made earthquake sources

Seismic Sources	
Natural Source	Man-made Source
• <i>Tectonic Earthquakes</i>	• Controlled Sources (Explosives)
• <i>Volcanic Earthquakes</i>	• Reservoir Induces Earthquakes
• <i>Rock Falls/Collapse of Cavity</i>	• Mining Induces Earthquakes
• <i>Microseism</i>	• Cultural Noise (Industry, Traffic, etc.)

1.2 REID'S ELASTIC REBOUND THEORY

After the devastating 1906 San Francisco, California earthquake, a fault trace was discovered that could be followed along the ground in a more or less straight line for 270 miles. It was found that the earth on one side of the fault had slipped compared to the earth on the other side of the fault up to 21 feet. This fault trace drew the curiosity of a number of scientists, but

nobody had yet been able to explain what was happening within the earth to cause earthquakes. From an examination of the displacement of the ground surface which accompanied the 1906 earthquake, H.F. Reid, Professor of Geology at Johns Hopkins University, concluded that the earthquakes must have involved an “elastic rebound” of previously stored elastic stress (Reid, 1911). The gradual accumulation and release of stress and strain is now referred to as the “elastic rebound theory” of earthquakes.

Suppose continuously increasing shear forces are acting on two blocks of an unstrained existing fault (Figure 1.1a). Further, assume that these stresses are trying to move the western block northward and the eastern block southward. Because of friction, there is no movement initially, but the blocks are distorted so that lines originally straight across the fault have become oblique (Figure 1.1b).

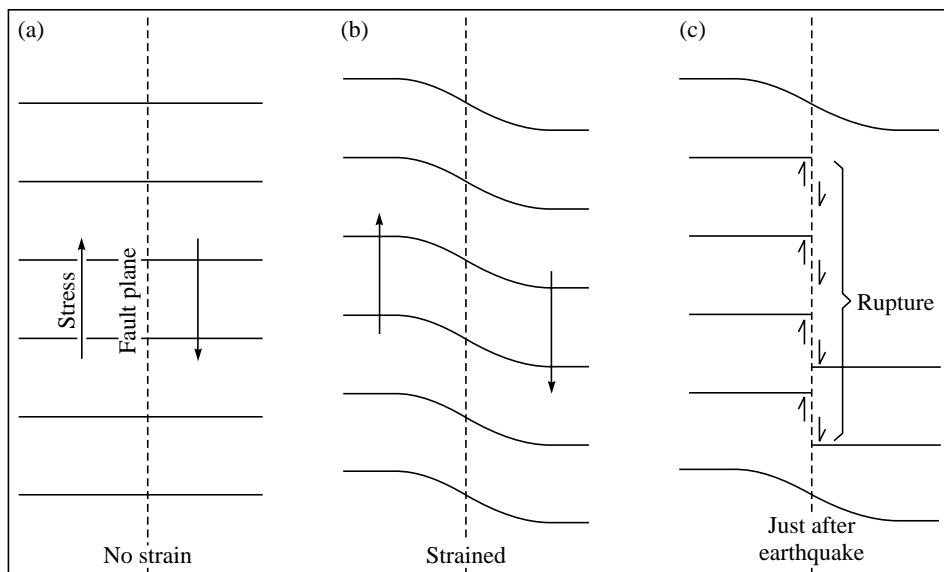


FIGURE 1.1 Schematic representation of elastic rebound theory (after Mussett and Khan, 2000).

The weakest part of the fault slips suddenly when the strain becomes more than what the fault can support. The rupture from the weakest part extends rapidly along the fault plane, allowing the blocks on either side of it to ‘jerk’ into a less strained condition. The half arrows beside the fault in Figure 1.1c show the extent of this sudden displacement, called the elastic rebound. The accumulated energy in the strained volume of rock is suddenly released in the form of seismic waves and a part is converted into heat or other forms.

1.3 THEORY OF PLATE TECTONICS

The epicentres of earthquakes are not randomly distributed over the earth’s surface. They tend to be concentrated in narrow zones. Why is it so? And why are volcanoes and mountain

ranges also found in these zones, too? An explanation to these questions can be found in plate tectonics, a concept which has revolutionized thinking in the Earth Sciences in the last few decades. The epicentres of 99% earthquakes are distributed along narrow zones of *interplate* seismic activity. The remainder of the earth is considered to be *aseismic*. However, no region of the earth can be regarded as completely earthquake-free. About 1% of the global seismicity is due to *intraplate* earthquakes, which occur away from the major seismic zones. The seismicity map is one of the important evidences in support of the plate tectonic theory, and delineates the presently active plate margins (Figure 1.2).

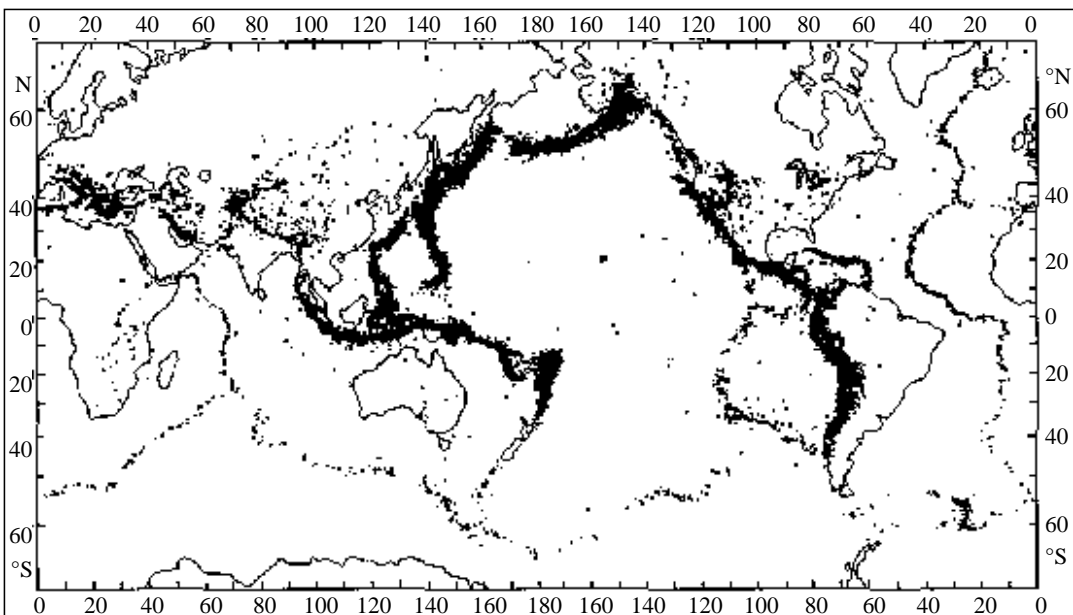


FIGURE 1.2 Geographical distribution of epicentres of 30,000 earthquakes occurred during 1961-1967 illustrates the tectonically active regions of the earth (after Barazangi and Dorman, 1969).

The pioneering work was done by Alfred Wegener, a German meteorologist and geophysicist, towards the development of the theory of plate tectonics. He presented his continental drift theory in his 1915 book '*On the Origin of Continents and Oceans*'. He proposed that at one time all the continents were joined into one huge super continent, which he named **Pangaea** and that at a later date the continents split apart, moving slowly to their present positions on the globe. Wegener's theory was not accepted since he could not satisfactorily answer the most fundamental question raised by his critics, i.e. what kind of forces could be strong enough to move such large masses of solid rock over such great distances? Further, Harold Jeffreys, a noted English geophysicist, argued correctly that it was physically impossible for a large mass of solid rock to plough through the ocean floor without breaking up, as proposed by Wegener. But, Wegener persisted in his study of the idea, finding more and more supporting evidences like fossils and rocks of vastly different climates in the past that could only be explained by a relocation of the particular continent to different latitudes.

Wegener died in 1930 and his **continental drift theory** was not accepted by most of the scientific community in spite of numerous supporting evidences. Continental drift theory was hotly debated off and on for decades even after his death and was largely dismissed as being eccentric, preposterous, and improbable. However, in the beginning of 1950s, wealth of new evidences emerged to revive the debate about Wegener's provocative ideas and their implications. In particular, four major scientific developments spurred the formulation of theory of the plate tectonics.

- (i) Demonstration of the ruggedness in the form of oceanic ridges, island arcs, trenches and youthness of the ocean floor.
- (ii) Confirmation of repeated reversals of the earth magnetic field in the past and development of paleomagnetism.
- (iii) Emergence of the seafloor-spreading hypothesis and associated recycling of oceanic crust. Hess (1962) first recognized the sea floor spreading at the oceanic ridges.
- (iv) Precise documentation that the world's earthquake and volcanic activity is concentrated along oceanic trenches and submarine mountain ranges.

After fifty years of publication of Wegener's continental drift theory (1915), finally the science of plate tectonics, although in a modified form, came to the rescue of his intellectual honour and his life's work was vindicated.

According to the theory of plate tectonics, the outermost layer of the earth, known as lithosphere, is broken into numerous segments or plates. The plates comprising crust and upper mantle are floating on the asthenosphere, which is viscous in nature. A plate may be purely continental, oceanic or both continental and oceanic.

1.3.1 Lithospheric Plates

The crust and uppermost mantle down to a depth of about 70-100 km under deep ocean basins and 100-150 km under continents is rigid, forming a hard outer shell called the *lithosphere*. Beneath the lithosphere lies the *asthenosphere*, a layer in which seismic velocities often decrease, suggesting lower rigidity. It is about 150 km thick, although its upper and lower boundaries are not sharply defined. This weaker layer is thought to be partially molten; it may be able to flow over long periods of time like a viscous liquid or plastic solid, in a way that depends on temperature and composition. The asthenosphere plays an important role in plate tectonics, because it makes possible the relative motion of the overlying lithospheric plates.

Earthquake epicentres are not evenly distributed over the surface of the globe, but occur predominantly in well-defined narrow seismic zones that are often associated with volcanic activity. These narrow zones are: (a) the circum-Pacific 'ring of fire'; (b) the Alpine-Himalayan belt and (c) the world-circling oceanic ridges. These seismic zones subdivide the lithosphere laterally into tectonic plates (Figure 1.3). There are twelve major plates (Antarctica, Africa, Eurasia, India, Australia, Arabia, Philippines, North America, South America, Pacific, Nazca, and Cocos) and several minor plates (e.g., Scotia, Caribbean, Juan de Fuca, etc.).

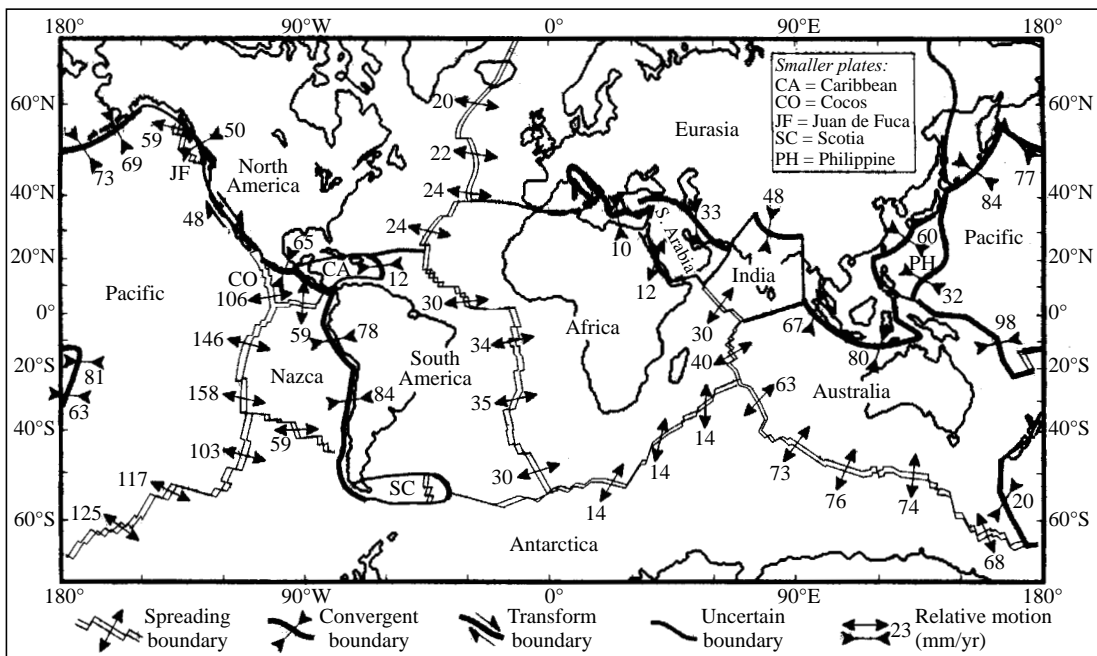


FIGURE 1.3 The major and minor lithospheric plates. The arrows indicate relative velocities in mm/year at different types of active plate margins (After: DeMets et al., 1990).

1.3.2 Plate Margins and Earthquake Occurrences

Barazangi and Dorman (1969) published the locations of all earthquakes occurred in period 1961–1967, to relate the earthquake occurrences with plate tectonics (Figure 1.2). The epicentres of most of the earthquakes are confined to narrow belts, which define the boundaries of the plates. The interiors of the plates are largely free of large earthquakes, but they are not aseismic. The different lithospheric plates comprising both crust and upper mantle move relative to each other across the surface of the globe (Figure 1.3). There are three types of plate margins:

- Constructive plate margin/Divergent boundaries*—where new crust is generated as the plates pull away from each other.
- Destructive plate margin/Convergent boundaries*—where crust is destroyed as one plate drives under another.
- Conservative plate margin/Transform boundaries*—where crust is neither produced nor destroyed as the plates slide horizontally past each other.

Divergent boundaries

Divergent boundaries occur along spreading centres where plates are moving apart and new crust is created by upward movement of molten magma (Figure 1.3). Figure 1.4 depicts a schematic representation for divergence boundary. The well-known divergent boundary is the Mid-Atlantic Ridge. The rate of spreading along the Mid-Atlantic Ridge averages about 2.5 cm/yr. Divergence

boundaries in continental regions are known as rift zones. The distribution of earthquakes defines a narrow band of seismic activity close to the crest of an oceanic ridge and rift zone. The earthquakes occur at shallow depths (2-8 km) and are mostly small. The occurrence of earthquake with magnitude greater than six is rare.

The point is that the lithosphere is very thin and weak at divergence boundaries, so the strain build up is not enough to cause large earthquakes.

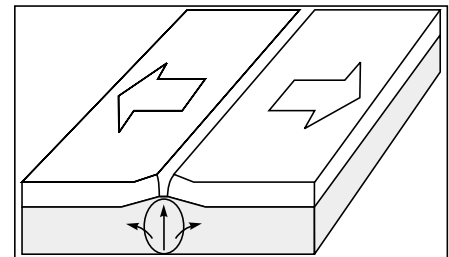


FIGURE 1.4 Schematic representation of divergence boundary.

Convergent boundaries

The earth's unchanging size implies that the crust must be destroyed at about the same rate as it is being created at divergence boundaries, as surmised in sea floor spreading hypothesis. Such destruction of crust takes place along convergent boundaries where plates are moving toward each other, and one plate sinks under another. The location where sinking of a plate occurs is called *subduction zone*. Convergence can occur between an oceanic and a continental plate, or between two oceanic plates, or between two continental plates. The ten largest earthquakes since 1900 on the globe have occurred along the subduction zones, including the 26th December 2004 earthquake in Indonesia which had triggered a massive tsunami.

Oceanic-continental convergence

If by magic we could pull a plug and drain the Pacific Ocean, we would see the most amazing sight, a number of long narrow, curving trenches thousands of kilometres long and 8 to 10 km deep cutting into the ocean floor. Trenches are the deepest parts of the ocean floor and are created by subduction. At the oceanic-continent boundaries, oceanic plate subducts due to higher density (Figure 1.5). Strong, destructive earthquakes and the rapid uplift of mountain ranges towards the side of overriding plate are common at the convergence boundaries. Oceanic-continental convergence also sustains many of the earth's active volcanoes on the side of overriding plate.

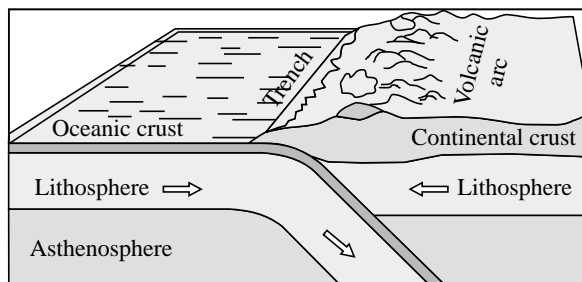


FIGURE 1.5 Schematic representation of oceanic-continental convergence.

Oceanic-oceanic convergence

When two oceanic plates converge, older one is usually subducted under the other, and in the process a trench is formed. The Mariana's Trench (paralleling the Mariana Islands), for example,

marks the location where the fast-moving Pacific Plate converges against the slow moving Philippine Plate. Subduction processes in oceanic-oceanic plate convergence also result in the formation of volcanoes. Such volcanoes are typically strung out in chains called *island arcs*.

Continental-continental convergence

The Himalayan mountain range dramatically demonstrates one of the most visible and spectacular consequences of plate tectonics. When two continents meet head-on, neither is subducted because the continental rocks are relatively light and, like two colliding icebergs, resist downward motion. Instead, the crust tends to buckle and be pushed upward or sideways (Figure 1.6).

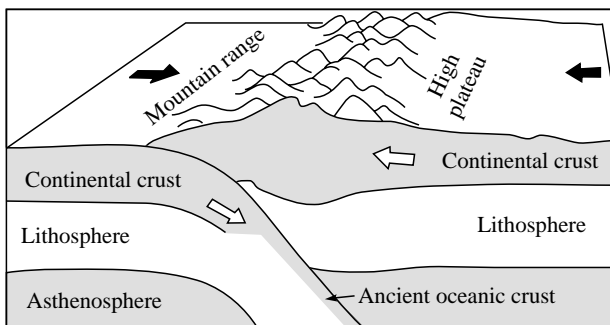


FIGURE 1.6 Schematic representation of continental-continental convergence.

About 40 to 50 million years ago the boundary between Indian plate and the Eurasian plate was oceanic-continental in nature and later on it became continental-continental convergence after consumption of the Tethys Sea.

Transform boundaries

The zone between two plates sliding horizontally past one another is called a *transform-fault boundary*, or simply a *transform boundary* (Figure 1.7). The concept of transform fault originated with Canadian geophysicist J. Tuzo Wilson, who proposed that these large faults or *fracture zones* connect two spreading centres (divergent plate boundaries) or, less commonly, trenches (convergent plate boundaries). Most transform faults are found on the ocean floor. However, a few occur on land, for example, the San Andreas Fault zone in California. Along the transform boundaries, the earthquakes occur at shallow depth, unaccompanied by volcanic activity. The friction between the plates can be so great that very large strains can build up before they are periodically relieved by large earthquakes.

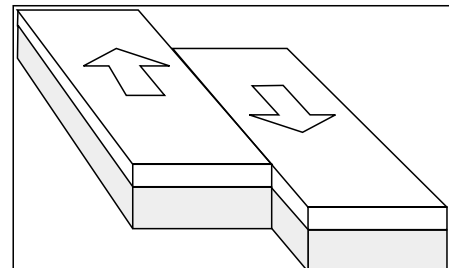


FIGURE 1.7 Schematic representation of transform boundary.

1.3.3 The Movement of Indian Plate

Among the most dramatic and visible creations of plate-tectonic forces are the lofty Himalayas, which stretches 2,900 km along the border between India and Tibet. After splitting of Pangaea,

about 200 million years ago, India began to forge northward. About 225 million years ago, India was a large island still situated off the Australian coast, and Tethys Sea separated India from the Eurasian continent. About 80 million years ago, India was located roughly 6,400 km south of the Eurasian continent, moving northward at a rate of about 9 m a century. By studying the history and ultimately the closing of the Tethys Sea, scientists have reconstructed India's northward journey (Figure 1.8). Immense Himalayan mountain range began to form between 40 and 50 million years ago, when two large landmasses, India and Eurasia, driven by plate movement, collided. Both these continental landmasses have same rock density, so one plate could not be subducted under the other. Further, the rate of northward movement of India reduced to about 4.5 m a century after collision. The collision and associated decrease in the rate of plate movement are interpreted to mark the beginning of the rapid uplift of the Himalayas.

1.4 SEISMIC WAVES

Seismic waves are classified into two groups: **body waves**, which travel through the earth in all directions and to all depths, and **surface waves**, whose propagation is limited to a volume of rock within a few seismic wavelengths of the earth's surface. The uses and analysis methods for the two types of waves are substantially different. Body waves are used for resource exploration purposes and for the study of earthquakes. Surface waves are used to delineate the layered-earth structure.

1.4.1 Body Waves

Two types of body waves exist: **compressional waves (P)** and **shear waves (S)**. P-waves are similar to sound waves. They obey all the physical laws of the science of acoustics. The mass particle motion of a P-wave is in the direction of the propagation of the wave. In addition, P-waves cause a momentary volume change in the material through which they pass, but no concomitant momentary shape change occurs in the material.

S-waves, or **shear waves**, as they are commonly called, move in a direction perpendicular to the direction of particle motion. Vertically and horizontally polarised S-waves are known as

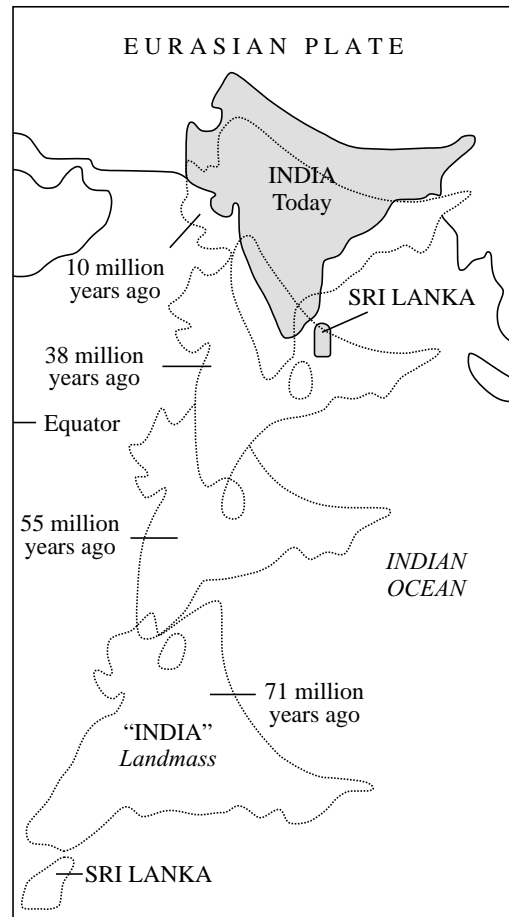


FIGURE 1.8 Schematic representation of movement of Indian plate.

SV-wave and SH-wave, respectively. They are sometimes called secondary waves because they travel more slowly than P-waves in the same material. S-waves do not change the instantaneous volume of the materials through which they pass, but as they pass through materials, they distort the instantaneous shape of those materials. The velocity of S-wave is directly related to the shear strength of materials. S-waves do not propagate through fluids as those do not have any shear strength.

1.4.2 Surface Waves

A disturbance at the free surface of a medium propagates away from its source partly as seismic surface waves. Surface waves, sometimes known as L-waves, are subdivided into Rayleigh (L_R) and Love waves (L_Q). These surface waves are distinguished from each other by the type of motion of particles on their wavefronts.

Rayleigh waves

Lord Rayleigh (1885) described the propagation of Rayleigh wave along the free surface of semi-infinite elastic half-space. In the homogeneous half-space, vertical and horizontal components of particle motion are 90° out of phase in such a way that as the wave propagates, the particle motion describes a retrograde ellipse in the vertical plane, with its major axis vertical and minor axis in the direction of wave propagation. The resulting particle motion can be regarded as a combination of P- and SV-vibrations (Figure 1.9). In the case of a layered and

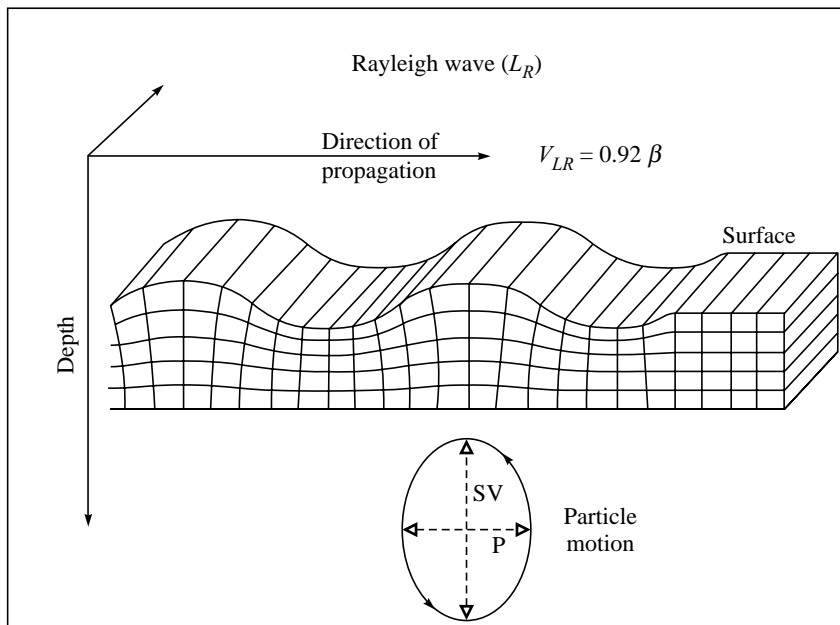


FIGURE 1.9 Schematic representation of movement of particle during Rayleigh wave propagation (after Lowrie, 1997).

dissipative medium, the path is always elliptical but not necessarily retrograde. Further, the axis of the ellipse may not be vertical and horizontal since the phase difference between vertical and horizontal displacement can be different from 90° . The velocity of Rayleigh wave is very much dependent on the Poisson's ratio and it is equal to 0.9194 times to that of S-wave in the Poisson's solid (Poisson's ratio = 0.25). The particle displacement is not confined entirely to the surface of the medium but the passes of the Rayleigh waves also displace the particle below the free surface up to a depth equal to the wavelength. In a uniform half space, the amplitude of particle displacement decreases exponentially with depth.

Love waves

A.E.H. Love (1911) explained the mechanism of generation of Love waves in horizontal soil layer overlying the half-space (Figure 1.10). When the angle of reflection at the base of soil layer is more than the critical angle, SH-waves are trapped in the soil layer. The constructive interference of reflected SH-waves from the top and bottom of the soil layer generate horizontally travelling Love waves. The particle motion is in horizontal plane and transverse to the direction of wave propagation. The velocity of Love wave lies between the velocity of S-wave in the soil layer and in the half-space. The velocity of Love wave with short wavelength is close to the velocity S-wave in soil layer and velocity of longer wavelength Love wave is close to the S-wave velocity in half-space. This dependence of velocity on wavelength is termed dispersion. Love waves are always dispersive, because they can only propagate in a velocity-layered medium.

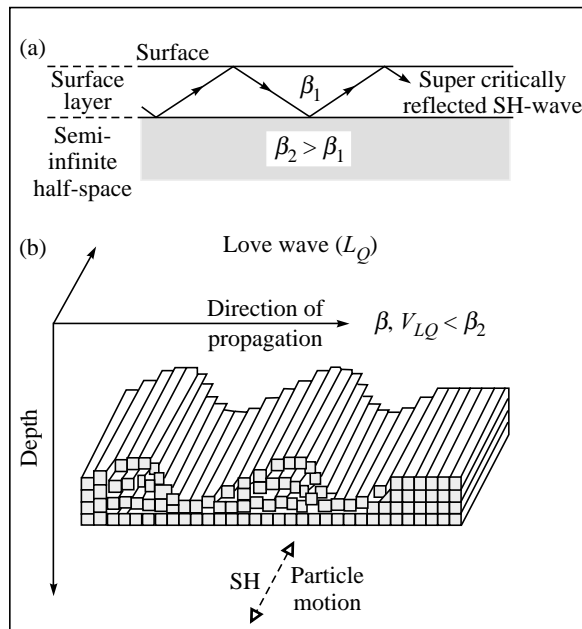


FIGURE 1.10 Schematic representation of movement of particle during Love wave propagation (after Lowrie, 1997).

1.5 EARTHQUAKE SIZE

1.5.1 Intensity

Seismic intensity scale is a way of measuring or rating the effects of an earthquake at different sites. The assignment of intensity of an earthquake does not require any instrumental records. It depends very much on the acuity of the observer, and is in principle subjective. Intensity to different places of an affected area can be assigned based on visual observations and interviews of residents or based on evaluation of questionnaires completed by residents of that area. Intensity data are very much useful for the development of seismic risk map of a region or country. Seismic risk maps are useful in planning safe sites for important structures like nuclear power plants or large dams. Risk maps are also valuable to insurance companies. Intensity data is also important in determination of historic seismicity of a region.

The Rossi-Forel intensity scale, developed in the late 19th century, have ten stages to describe the earthquake effects in increasing order. Mercalli (1902) proposed an intensity scale in which earthquake severity was classified in twelve stages. The Mercalli intensity scale was modified in 1931 to suit the building conditions in the United States. The modified version is widely known as Modified Mercalli Intensity (MMI) scale. The Medvedev-Spoonheuer-Karnik (MSK) intensity scale introduced in 1964 also has twelve stages and differs from the MMI scale mainly in details. The MSK (Table 1.5) and MMI (Table 1.6) intensity scales are commonly used to seek information on the severity of effects of an earthquake. Intensity ratings are expressed as Roman numerals. The intensity scale differs from the magnitude scale in that the effects of any one earthquake vary greatly from place to place, so there may be many intensity values for one earthquake. On the other hand, there is only one magnitude value for an earthquake.

MSK intensity scale

In assigning the MSK intensity at a site due attention is paid to the type of structures (Table 1.2), percentage of damage to each type of structure (Table 1.3) and grade of damage to different type of structures (Table 1.4) and details of intensity scale (Table 1.5). The main features of MSK intensity scale are as follows:

TABLE 1.2 Type of structures (buildings)

Type of structures	Definitions
A	Buildings in fieldstone, rural structures, unburnt-brick houses, clay houses.
B	Ordinary brick buildings, buildings of the large-block and prefabricated type, half-timbered structures, buildings in natural hewn stone.
C	Reinforced buildings, well-built wooden structures.

TABLE 1.3 Definition of quantity

Quantity	Percentage
Single, few	About 5
Many	About 50
Most	About 75

TABLE 1.4 Classification of damage to buildings

<i>Grade</i>	<i>Definitions</i>	<i>Descriptions</i>
G1	Slight damage	Fine cracks in the plaster; fall of small pieces of plaster.
G2	Moderate damage	Small cracks in walls; fall of fairly damaged large pieces of plaster, pantiles slip off; cracks in chimneys; parts of chimney brakes.
G3	Heavy damage	Large and deep cracks in walls; fall of chimneys.
G4	Destruction	Gaps in walls; parts of buildings may collapse; separate parts of the building lose their cohesion; and inner walls collapse.
G5	Total damage	Total collapse of buildings.

TABLE 1.5 Details of MSK intensity scale

<i>Intensity</i>		<i>Descriptions</i>
I	Not noticeable	The intensity of the vibration is below the limit of sensibility; the tremor is detected and recorded by seismographs only.
II	Scarcely noticeable (very slight)	Vibration is felt only by individual people at rest in houses, especially on upper floors of the buildings.
III	Weak, partially observed only	The earthquake is felt indoors by a few people, outdoors only in favourable circumstances. The vibration is like that due to the passing of a light truck. Attentive observers notice a slight swinging of hanging objects, somewhat more heavily on upper floors.
IV	Largely observed	The earthquake is felt indoors by many people, outdoors by few. Here and there people awake, but no one is frightened. The vibration is like that due to the passing of a heavily loaded truck. Windows, doors and dishes rattle. Floors and walls crack. Furniture begins to shake. Hanging objects swing slightly. Liquids in open vessels are slightly disturbed. In standing motorcars the shock is noticeable.
V	Awakening	(a) The earthquake is felt indoors by all, outdoors by many. Many sleeping people awake. A few run outdoors. Animals become uneasy. Buildings tremble throughout. Hanging objects swing considerably. Pictures knock against walls or swing out of place. Occasionally pendulum clocks stop, Unstable objects may be overturned or shifted. Open doors and windows are thrust open and slam-back again.

Contd.

TABLE 1.5 Contd.

<i>Intensity</i>	<i>Descriptions</i>
	Liquids spill in small amounts from well-filled open containers. The sensation of vibration is like that due to heavy object falling inside the buildings. (b) Slight damages in buildings of Type A are possible. (c) Sometimes changes in flow of springs.
VI Frightening	(a) Felt by most indoor and outdoor people. Many people in buildings are frightened and run outdoors. A few persons lose their balance. Domestic animals run out of their stalls. In few instances dishes and glassware may break, books fall down. Heavy furniture may possibly move and small steeple bells may ring. (b) Damage of Grade I is sustained in single buildings of Type B and in many of Type A. Damage in a few buildings of Type A is of Grade 2. (c) In few cases cracks up to widths of 1 cm is possible in wet ground; in mountains occasional landslips; change in flow of springs and in level of well water are observed.
VII Damage of buildings	(a) Most people are frightened and run outdoors. Many find it difficult to stand. The vibration is noticed by persons driving motorcars. Large bells ring. (b) In many buildings of Type C damage of Grade I is caused; in many buildings of Type B damage is of Grade 2. Most buildings of Type A suffer damage of Grade 3, a few of Grade 4. (c) In single instances landslips of roadway on steep slopes; cracks in roads; seams of pipelines damaged; cracks in stone walls.
VIII Destruction of buildings	(a) Fright and panic; also persons driving motorcars are disturbed. Here and there branches of trees break off. Even heavy furniture moves and partly overturns. Hanging lamps are damaged in part. (b) Most buildings of Type C suffer damage of Grade 2, and a few of Grade 3. Most buildings of Type B suffer damage of Grade 3, and most buildings of Type A suffer damage of Grade 4. Many buildings of Type C suffer damage of Grade 4. Occasional breaking of pipe seams. Memorials and monuments move and twist. Tombstones overturn. Stone-walls collapse. (c) Small landslips in hollows and on banked roads on steep slopes; cracks in ground up to widths of several

Contd.

TABLE 1.5 Contd.

<i>Intensity</i>	<i>Descriptions</i>
	cm. Water in lakes becomes turbid. New reservoirs come into existence. Dry wells refill and existing wells become dry. In many cases change in flow and level of water is observed.
IX General damage to buildings	<p>(a) General panic; considerable damage to furniture. Animals run to and fro in confusion and cry.</p> <p>(b) Many buildings of Type C suffer damage of Grade 3, and a few of Grade 4. Many buildings of Type B show damage of Grade 4, and a few of Grade 5. Many buildings of Type A suffer damage of Grade 5. Monuments and columns fall. Considerable damage to reservoirs; underground pipes partly broken. In individual cases railway lines are bent and roadway damaged.</p> <p>(c) On flat land overflow of water, sand and mud is often observed. Ground cracks to widths of up to 10 cm, on slopes and river banks more than 10 cm; furthermore a large number of slight cracks in ground; falls of rock, many landslides and earth flows; large waves in water. Dry wells renew their flow and existing wells dry up.</p>
X General destruction of buildings	<p>(a) Many buildings of Type C suffer damage of Grade 4, and a few of Grade 5. Many buildings of Type B show damage of Grade 5; most of Type A have destruction of Grade 5; critical damage to dams and dykes and severe damage to bridges. Railway lines are bent slightly. Underground pipes are broken or bent. Road paving and asphalt show waves.</p> <p>(b) In ground, cracks up to widths of several cm, sometimes up to 1 m. Parallel to water course occur broad fissures. Loose ground slides from steep slopes. From river-bank and steep coasts, considerable landslides are possible. In coastal areas, displacement of sand and mud; change of water level in wells; water from canals, lakes, rivers, etc., thrown on land. New lakes occur.</p>
XI Destruction	<p>(a) Severe damage even to well built buildings, bridges, water dams and railway lines; highways become useless; underground pipes destroyed.</p> <p>(b) Ground considerably distorted by broad cracks and fissures, as well as by movement in horizontal and vertical directions; numerous landslips and falls of rock. The intensity of the earthquake requires to be</p>

Contd.

TABLE 1.5 Contd.

<i>Intensity</i>	<i>Descriptions</i>
XII	Landscape changes (a) Practically all structures above and below the ground are greatly damaged or destroyed. (b) The surface of the ground is radically changed. Considerable ground cracks with extensive vertical and horizontal movements are observed. Falls of rock and slumping of river-banks over wide areas, lakes are dammed; waterfalls appear, and rivers are deflected. The intensity of the earthquake requires to be investigated specially.

The details of Modified Mercalli Intensity (MMI) scale is given in Table 1.6 and is also used to seek information on the effects of an earthquake like MSK intensity scale.

TABLE 1.6 Details of MMI intensity scale

<i>Intensity</i>	<i>Descriptions</i>
I	Vibrations are recorded by instruments. People do not feel any earth movement.
II	People at rest upstairs notice shaking. A few people might notice movement if they are at rest and/or on the upper floors of tall buildings.
III	Shaking felt indoors; hanging objects swing. Many people indoors feel movement. Hanging objects swing back and forth. People outdoors might not realize that an earthquake is occurring.
IV	Dishes rattle; standing cars rock; trees shake. Most people indoors feel movement. Hanging objects swing. Dishes, windows, and doors rattle. The earthquake feels like a heavy truck hitting the walls. A few people outdoors may feel movement. Parked cars rock.
V	Doors swing; liquid spills from glasses; sleepers awake. Almost everyone feels movement. Sleeping people are awakened. Doors swing open or close. Dishes are broken. Pictures on the wall move. Small objects move or are turned over. Trees might shake. Liquids might spill out of open containers.
VI	People walk unsteadily; windows break; pictures fall off walls. Everyone feels movement. People have trouble walking. Objects fall from shelves. Pictures fall off walls. Furniture moves. Plaster in walls might crack. Trees and bushes shake. Damage is slight in poorly built buildings. No structural damage.
VII	Difficult to stand; plaster, bricks, and tiles fall; large bells ring. People have difficulties in standing. Drivers feel their cars shaking. Some furnitures break. Loose bricks fall from buildings. Damage is slight-to-moderate in well-built buildings; considerable in poorly built buildings.
VIII	Car steering affected; chimneys fall; branches break; cracks in wet ground. Drivers

Contd.

TABLE 1.6 Details of MMI intensity scale

<i>Intensity</i>	<i>Descriptions</i>
	have trouble steering. Houses that are not bolted down might shift on their foundations. Tall structures such as towers and chimneys might twist and fall.
	Well-built buildings suffer slight damage. Poorly built structures suffer severe damage. Tree branches break. Hillsides might crack if the ground is wet. Water levels in wells might change.
IX	General panic; damage to foundations; sand and mud bubble from ground. Well-built buildings suffer considerable damage. Houses that are not bolted down move off their foundations. Some underground pipes are broken. The ground cracks. Reservoirs suffer serious damage.
X	Most buildings destroyed; large landslides; water thrown out of rivers. Most buildings and their foundations are destroyed. Some bridges are destroyed. Dams are seriously damaged. Large landslides occur. Water is thrown on the banks of canals, rivers, lakes. The ground cracks in large areas. Railroad tracks are bent slightly.
XI	Railway tracks bend; roads break up; large cracks appear in ground; rocks fall. Most buildings collapse. Some bridges are destroyed. Large cracks appear in the ground. Underground pipelines are destroyed. Railroad tracks are badly bent.
XII	Total destruction; “waves” seen on ground surface; river courses altered; vision distorted. Almost everything is destroyed. Objects are thrown into the air. The ground moves in waves or ripples. Large amounts of rock may move.

1.5.2 Isoseismal Map

A contour on a map bounding areas of equal intensity is an isoseismal and a map having different isoseismals for a particular earthquake is an isoseismal map. The intensity is usually strongest near the earthquake epicentre and decreases with distance and at large distance the earthquake is no longer felt by anyone. Other factors such as the local geology beneath a particular site, the regional geology and the orientation of the earthquake fault can affect intensity. The numbers on the map represent relative shaking strength and can be qualitatively interpreted. Earthquake isoseismal maps provide valuable documents of macro-seismic effects of large earthquakes. Isoseismal maps of past earthquakes help us to understand the nature of the earthquakes in a particular region. Scientifically, it is still a far cry to predict an earthquake, and to be able to take effective steps for minimizing the damage due to the same. So, in the absence of earthquake prediction, the use of isoseismal map for long term planning and development of seismic zoning maps or seismic hazard maps is the best approach.

1.5.3 Earthquake Magnitude

Earthquake magnitude is a measure of the amount of energy released during an earthquake. Depending on the size, nature, and location of an earthquake, seismologists use different methods to estimate magnitude. Since magnitude is the representative of the earthquake itself, there is thus only one magnitude per earthquake. But magnitude values given by different

seismological observatories for an event may vary. The uncertainty in an estimate of the magnitude is about ± 0.3 unit. Seismologists often revise magnitude estimates as they obtain and analyze additional data.

Richter magnitude (M_L)

One of Dr. Charles F. Richter's most valuable contributions was to recognize that the seismic waves radiated by earthquakes could provide good estimates of their magnitudes. Richter (1935) collected the recordings of seismic waves from a large number of earthquakes and constructed a diagram of peak ground motion versus distance (Figure 1.11). The logarithm of recorded amplitude was used due to enormous variability in amplitude. Richter inferred that the larger the intrinsic energy of the earthquake, the larger the amplitude of ground motion at a given distance.

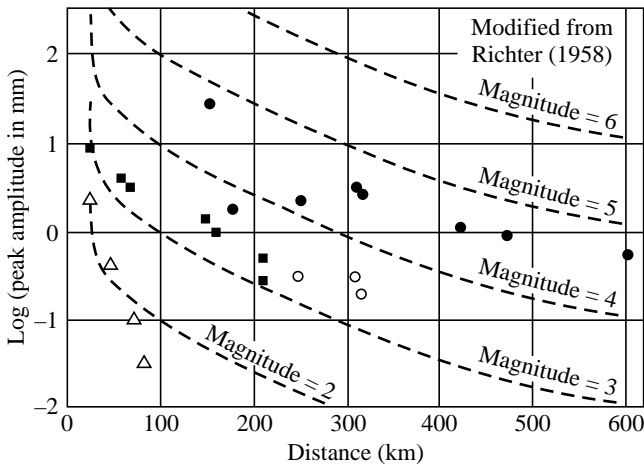


FIGURE 1.11 A plot of log of peak amplitude in mm versus epicentral distance of earthquakes recorded in Southern California (different symbols represent different earthquakes).

The idea of a logarithmic earthquake magnitude scale struck into the mind of Richter after analysing the roughly parallel curves generated by different size earthquakes on the plot of log of the recorded amplitude at various epicentral distances. The parallel nature of curves for different earthquakes suggested that a single number could quantify the relative size of different earthquakes. He proposed zero magnitude for an earthquake that would produce a record with amplitude of $1.0 \mu\text{m}$ at a distance of 100 km from the epicentre on Wood-Anderson (WA) seismograph with 1.25 Hz natural frequency and 2800 magnification factor. The logarithmic form of Richter magnitude scale (M_L) is given as:

$$M_L = \log_{10} A - \log_{10} A_0 \quad (1.1)$$

where A_0 is the amplitude for zero magnitude earthquakes at different epicentral distances and A is the recorded amplitude in μm . The zero magnitude amplitude can be computed for different epicentral distances taking into account the effects of geometrical spreading and absorption of considered wave.

The Richter scale used in Southern California for different epicentral distances and 18 km fixed focal depth is as follows.

$$M_L = \log_{10} A \text{ (mm)} + \text{Distance correction factor } \sigma \quad (1.2)$$

Distance correction factor ‘ σ ’ is log of inverse of zero magnitude amplitude measured in mm at an epicentral distance ‘ Δ ’ in km. The distance correction factors for different epicentral distances are given in Table 1.7. The distance correction factors given in Table 1.7 cannot be used in other regions of the world since considered focal depth was constant. So, to compute M_L in any other region like Himalayas, first zero magnitude amplitude at different epicentral distances should be determined according to the original definition of M_L at 100 km and different focal depths taking into account the geometrical spreading and appropriate measure of absorption. Since, sufficient time resolution of high frequency records is no longer a problem, therefore, frequency dependent distance correction factors, matched with Richter scale at 100 km distance, have been developed based on epicentral as well as hypo-central distances (Hutton and Boore, 1987; Kim, 1998; Langston et al., 1998).

TABLE 1.7 Distance correction factors (σ) for M_L (Elementary Seismology, Richter, 1958)

Δ (km)	$\sigma(\Delta)$						
0	1.4	90	3.0	260	3.8	440	4.6
10	1.5	100	3.0	280	3.9	460	4.6
20	1.7	120	3.1	300	4.0	480	4.7
30	2.1	140	3.2	320	4.1	500	4.7
40	2.4	160	3.3	340	4.2	520	4.8
50	2.6	180	3.4	360	4.3	540	4.8
60	2.8	200	3.5	380	4.4	560	4.9
70	2.8	220	3.65	400	4.5	580	4.9
80	2.9	240	3.7	420	4.5	600	4.9

Although, Richter magnitude was originally developed using earthquake records of WA-seismometer in Southern California but the records of any short period seismometers can be used. Now, procedures are available to synthesise precisely the response characteristics of WA-seismograph from digital broadband recordings (Plesinger et al., 1996).

Magnitude is a measure of seismic energy released which, in turn, is proportional to $(A/T)^2$, where A is the ground motion trace amplitude, and T as the period of the considered wave. So, the general form of Richter magnitude scale based on measurements of ground displacement amplitudes A of considered wave with periods T is,

$$M = \log_{10} (A/T)_{\max} + \sigma(\Delta, h) + C_r + C_s \quad (1.3)$$

where $\sigma(\Delta, h)$, distance correction factor at an epicentral distance ‘ Δ ’ and focal depth ‘ h ’. C_r is the regional source correction term to account for azimuth dependent source directivity and C_s is the station correction factor dependent on local site effects. (A/T) for different periods are computed and maximum of them is used in the magnitude computation.

Surface wave magnitude

As more seismograph stations were installed around the world, it became apparent that the method developed by Richter was strictly valid only for certain frequency and distance ranges. Further, at large epicentral distances, body waves are usually attenuated and scattered so that the resulting motion is dominated by surface waves. On the other hand, the amplitude of surface waves, in case of deep focus earthquakes is too small. So, in order to take advantage of the growing number of globally distributed seismograph stations, new magnitude scales that are an extension of Richter's original idea were developed. These include *body-wave magnitude* (m_B) and *surface-wave magnitude* (M_S). Each is valid for a particular period range and type of seismic wave.

A commonly used equation for computing M_S of a shallow focus (< 50 km) earthquake from seismograph records between epicentral distances $20^\circ < \Delta < 160^\circ$ is the following one proposed by Bath (1966).

$$M_S = \log_{10} (A_s/T)_{\max} + 1.66 \log_{10} \Delta + 3.3 \quad (1.4)$$

Where A_S is the amplitude of the horizontal ground motion in 'μm' deduced from the surface wave with period T (around 20 ± 2 seconds) and epicentral distance Δ is in degree.

Body wave magnitude (m_B)

Gutenberg (1945) developed body wave magnitude m_B for teleseismic body-waves such as P, PP and S in the period range 0.5 s to 12 s. It is based on theoretical amplitude calculations corrected for geometric spreading and attenuation and then adjusted to empirical observations from shallow and deep-focus earthquakes.

$$m_B = \log_{10}(A/T)_{\max} + \sigma(\Delta, h) \quad (1.5)$$

Gutenberg and Richter (1956) published a table with distance correction factors $\sigma(\Delta, h)$ for body waves, which enable magnitude determinations. These distance correction factors are used when ground motion trace amplitudes are measured in 'μm'.

Duration magnitude (M_D)

Analogue paper and tape recordings have a very limited dynamic range of only about 40 dB and 60 dB, respectively. M_L cannot be determined since these records are often clipped in case of strong and near earthquakes. Therefore, alternative duration magnitude scale M_D has been developed. Duration from the P-wave onset to the end of the coda (back-scattered waves from numerous heterogeneities) is used in computations. Aki and Chouet (1975) reported that for a given local earthquake at epicentral distances lesser than 100 km the total duration of a signal is almost independent of distance, azimuth and property of materials along the path. This allows development of duration magnitude scales without a distance term.

$$M_D = a_0 + a_1 \log D \quad (1.6)$$

a_0 and a_1 are constant and D is the duration in seconds. The values of these constants vary region to region according to crustal structure, scattering and attenuation conditions. They have to be determined locally for a region with the help of available M_L .

Moment magnitude

In case of large earthquakes, the various magnitude scales (M_L , m_B or M_S) based on maximum amplitude and period of body waves or surface waves under estimate the energy released due to saturation. Recently, seismologists have developed a standard magnitude scale, known as moment magnitude. Moment magnitude is calculated using moment released during an earthquake rupture. The moment released depends on the physical dimension of the rupture (A), shear strength of the rock (μ) and the average displacement on the fault plane (d).

Figure 1.12 shows a schematic diagram of the strained fault just before the rupture. In this figure, a couple of the shear forces acting on the either side of the fault are considered, ‘ $2b$ ’ distance apart. The moment of the couple (M_0) is simply ‘ $F \cdot 2b$ ’. Now, if ‘ d ’ is the displacement, the strain (γ) developed by the couple is ‘ $d/2b$ ’. The value of considered force can be obtained in terms of shear strength rock and area of rupture, using stress–strain relationship.

$$\sigma = F/A = \mu \cdot \gamma = \mu \cdot d/2b \quad \text{or} \quad F = \mu \cdot A \cdot d/2b$$

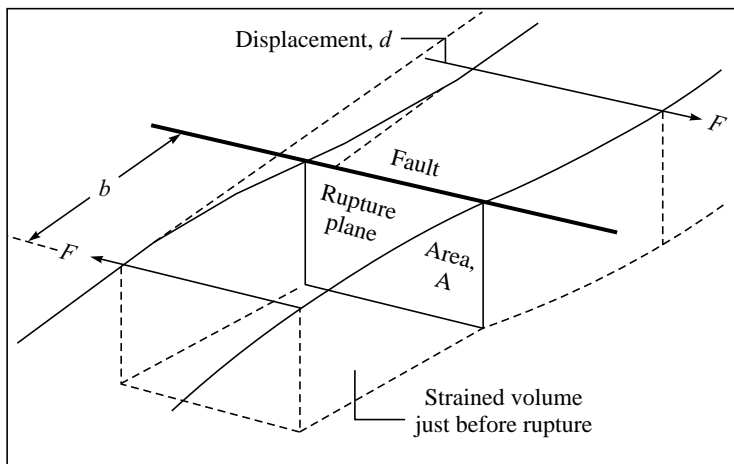


FIGURE 1.12 Schematic diagram for seismic moment determination (after Mussett and Khan, 2000).

Finally, moment can be computed as

$$M_0 = \mu A d \quad (1.7)$$

The moment magnitude M_w can be obtained using following relation (Kanamori, 1977; Hanks and Kanamori, 1979).

$$M_w = \frac{2}{3} [\log_{10} M_0(\text{dyne-cm}) - 16.0] \quad (1.8)$$

The rigidity ‘ μ ’ is measured using samples of rock or is estimated from knowledge of the rocks in the area. Aftershocks are believed to reveal the rupture area because most of them lie on a plane. The simplest way to measure the length ‘ L ’ and average displacement ‘ d ’ of a fault is to look at the newly faulted surface, or fault break. The seismic moment can also be estimated from the long period components of seismograms (Bullen and Bolt, 1985).

1.5.4 Energy Released in an Earthquake

The earthquake magnitude is defined in terms of logarithm of the amplitude of recorded seismic wave, and energy of a wave is proportional to the square of its amplitude. So, there should be no surprise that the magnitude is also related to the logarithm of the energy. Several equations have been proposed for this relationship in the past. An empirical formula worked out by Gutenberg and Richter (Gutenberg, 1956), relates the energy release E to the surface-wave magnitude M_S

$$\log_{10} E = 4.4 + 1.5 M_S \quad (1.9)$$

where E is in Joules. An alternative version of the energy—magnitude relation, suggested by Bath (1966) for magnitudes $M_S > 5$, is,

$$\log_{10} E = 5.24 + 1.44 M_S \quad (1.10)$$

The logarithmic nature of each formula means that the energy release increases very rapidly with magnitude. For example, when the magnitudes of two earthquakes differ by 1, their corresponding energies differ by a factor 28 ($=10^{1.44}$) according to Bath's equation, or 32 ($10^{1.5}$) according to the Gutenberg-Richter formula.

More recently, Kanamori came up with a relationship between seismic moment and seismic wave energy. It gives:

$$\text{Energy} = (\text{Moment})/20,000 \quad (1.11)$$

For this relation moment is in units of dyne-cm, and energy is in units of erg.

1.5.5 Earthquake Frequency

On this globe, the annual frequency of small earthquakes is very large and that of large earthquakes is very small (Table 1.8). According to a compilation published by Gutenberg and Richter in 1954, the mean annual number of earthquakes in the years 1918–1945 with magnitudes 4–4.9 was around 6000, while there were only on an average about 100 earthquakes per year with magnitudes 6–6.9. The relationship between annual frequency (N) and magnitude

TABLE 1.8 Earthquake frequencies since 1900 (based on data from the USGS/ NEIC) and the estimated mean annual energy release based on Bath (1966)

Earthquake magnitude	Number per year	Annual energy (10^{15} Joule yr^{-1})
≥ 8.0	0–1	0–600
7–7.9	18	200
6–6.9	120	43
5–5.9	800	12
4–4.9	6,200	3
3–3.9	49,000	1
2–2.9	$\approx 350,000$	0.2
1–1.9	$\approx 3,000,000$	0.1

(M_S) is logarithmic and is given by an equation of the form

$$\log N = a - bM_S \quad (1.12)$$

The value of ‘ a ’ varies between about 8 and 9 from one region to another, while ‘ b ’ is approximately unity for regional and global seismicity. Most of the time ‘ b ’ is assumed to be equal to 1; ‘ b >1 in an area generally means that small earthquakes occur frequently; ‘ b <1 indicates an area that is more prone for a larger earthquake. In volcanic areas where there is lots of earthquake swarms ‘ b ’ >1. Along subduction zones and continental rifts the value of ‘ b <1. The mean annual numbers of earthquakes in different magnitude ranges are listed in Table 1.8.

1.6 LOCAL SITE EFFECTS

Significant differences in structural damage in basin as compared with the surrounding exposed rocks, or even in the basin itself from place to place, have been observed during earthquakes. The amplitude of shaking in basin can be more than 10 times stronger than the surrounding rocks. Other geological conditions, which affect amplitude and signal duration, are topography (ridge, valley and slope variation) and the lateral discontinuities. The historical references regarding earthquake damage due to local site condition extend back to nearly 200 years (Wood, 1908; Reid, 1910).

Mac Murdo (1924) noted that the buildings situated on the rock were not much affected as those situated on the soil cover during Kutch earthquake (1819). Recent examples regarding the intense effects of local site conditions include Michoacan earthquake (1985) which caused only moderate damage in the vicinity of its epicenter but caused heavy damage some 400 km away in the Mexico city (Dobry and Vacetic, 1987), damage caused by the Loma Prieta, California earthquake (1989) in the city of San Francisco and Oakland (USGS, 1990) and damage pattern observed during Bhuj earthquake of January 26, 2001 (Narayan et al., 2002).

1.6.1 Basin/Soil Effects

Study of different aspects of basin effects on the ground motion characteristics needs special attention since most of urbanized areas are generally settled along river valleys over young, soft, surficial soil deposits.

Impedance contrast

Seismic waves travel faster in hard rocks than in softer rocks and sediments. As the seismic waves pass from hard medium to soft medium, their celerity decrease, so they must get bigger in amplitude to carry the same amount of energy. If the effects of scattering and material

TABLE 1.9 Classification of local geology in different category

LOCAL SITE EFFECTS	
A. Basin/soil	B. Topography
a. Impedance contrast	a. Ridge
b. Resonance	b. Valley
c. Trapping	c. Slope/slope variation
d. Focusing	
e. Basin-edge	C. Strong Lateral
f. Damping	discontinuities

damping are neglected, the conservation of elastic wave energy requires that the flow of energy (energy flux, $\rho V_S v^2$) from depth to the ground surface be constant. Therefore, with decrease in density (ρ) and S-wave velocity (V_S) of the medium, as waves approach the ground surface, the particle velocity (v), must increase. Thus, shaking tends to be stronger at sites with softer soil layers.

Resonance

Tremendous increase in ground motion amplification occurs when there is resonance of signal frequency with the fundamental frequency or higher harmonics of the soil layer. Various spectral peaks characterize resonance patterns. For one-layer 1D structures, this relation is very simple:

$$f_0 = V_{S1}/4h \text{ (fundamental mode) and } f_n = (2n + 1)f_0 \text{ (harmonics)}$$

where V_{S1} is the S-wave velocity in the surficial soil layer, and h is the thickness. The amplitudes of these spectral peaks are related mainly to the impedance contrast and sediment damping.

Damping in soil

Absorption of energy occurs due to imperfect elastic properties of medium in which the collision between neighbouring particles of the medium is not perfectly elastic and a part of the energy in the wave is lost instead of being transferred through the medium. This type of attenuation of the seismic waves is referred to as anelastic damping. The damping of seismic waves is described by a parameter called as **quality factor** (Q). It is defined as the fractional loss of energy per cycle, $2\pi/Q = -\Delta E/E$, where ΔE is the energy lost in one cycle and E is the total elastic energy stored in the wave. If we consider the damping of a seismic wave as a function of the distance and the amplitude of seismic wave, we have

$$A = A_0 \exp\left(-\frac{\pi r}{Q\lambda}\right) = A_0 \exp(-\alpha r) \quad (1.13)$$

where $\alpha = \omega/2QV$ is absorption coefficient. This relation implies that higher frequencies will be absorbed at a faster rate.

Basin edge

Intense concentrations of damage parallel to the basin-edge had been observed due to strong generation of surface waves near the edge, during recent earthquakes (Northridge earthquake, 1994; Kobe earthquake, 1995 and Dinar earthquake, 1995). The conclusion that basin-edge induces strong surface waves had been drawn in many studies by examining the phase and group velocities, polarity and arrival azimuth (Bard and Bouchan, 1980 a, b 1985; Hatayama et al., 1995; Kawase, 1996; Pitarka et al., 1998; Narayan, 2003a, 2004, 2005). Surface waves start generating near the edge of the basin when frequency content in the body wave exceeds the fundamental frequency of the soil and their amplitudes decrease with increase of edge-slope (Narayan, 2004, 2005).

Figure 1.13a shows the vertically exaggerated basin-edge models having different thickness of single soil layer over the bed-rock. Figure 1.13b depicts the vertical component of ground motion, computed for thickness of soil layer as 195 m using a double-couple source (dip = 45°,

rake = 60° and strike = 90°) just below the edge at a depth of 13.7 km with a dominant frequency 1.0 Hz. The P- and S-waves velocities and densities were taken as 1396.5 m/s, 400.0 m/s and 1.9 g/cm^3 for soil and 3464.1 m/s , 2000.0 m/s and 2.5 g/cm^3 for half space (hard rock). The ground response was computed at 26 equidistant (105 m apart) receiver points. Figure 1.13b reveals four well-separated wavelets at receiver points some distance away from the edge. The differential ground motion in north-south direction clearly depicts horizontally travelling surface waves since vertically travelling body waves are more or less removed (Figure 1.13c).

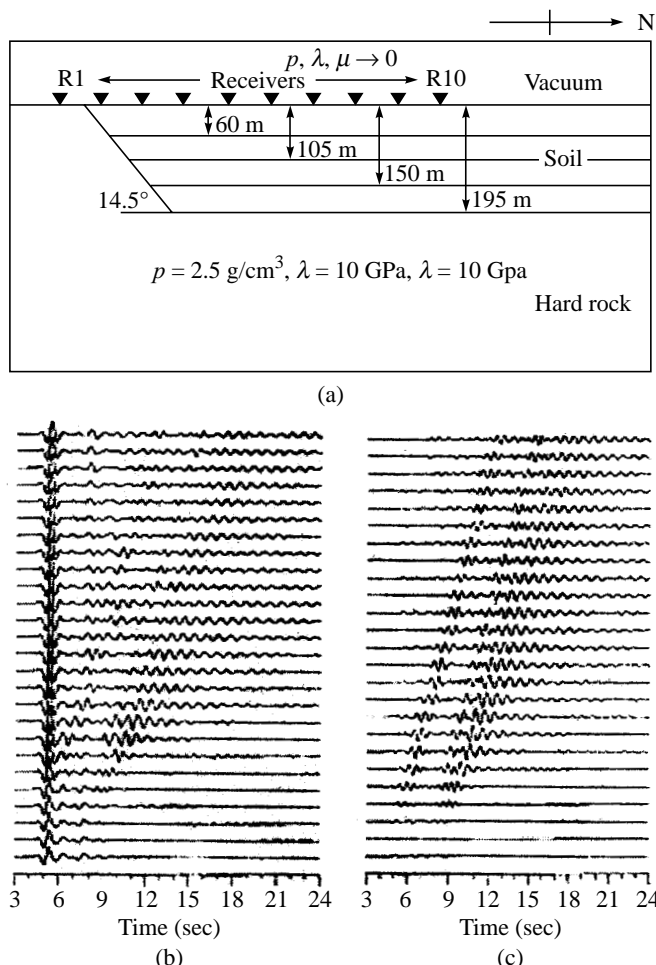


FIGURE 1.13 (a) Vertically exaggerated basin-edge model, (b) vertical component of ground displacement, and (c) the differential ground displacement corresponding to the vertical component of ground motion at 26 receiver points (after Narayan, 2005).

The generation of surface waves near the edge was confirmed on the basis of the large coherence in recording stations, increase of travel time of later phases as we move away from the edge, estimated group velocity of later phases and the analysis of differential ground motion (Narayan, 2005). Both P-wave and S-wave have caused generation of Rayleigh waves.

The major conclusions drawn in papers of Bard and Bouchan (1980 a, b), Hatayama et al. (1995), Kawase (1996) Pitarka, et al. (1998) and Narayan (2003a, 2004, 2005) are listed below.

- Basin-edge induces strong surface waves near the edge.
- Edge-induced surface waves propagate normal to edge and towards the basin.
- Surface waves start generating near the edge of the basin when frequency content in the body wave exceeds the fundamental frequency of the soil deposit.
- Surface wave amplitude decreases with increase of edge-slope.
- Damage caused by edge-induced surface waves is confined in a narrow zone (width 2.5–3.5 km) parallel to the edge, and at some distance (0.5–1.0 km).
- Surface wave amplitude increases with the decrease of propagation velocity in soil. Further, their characteristics are highly variable with change in propagation velocity and thickness of soil deposit.
- The characteristics of edge-induced surface waves are also very much dependent on the angle of incidence of body waves.
- Edge-induced surface waves develop significant differential ground, the main cause of damage during earthquakes, in addition to amplification and prolongation of the signal.

Basement topography

The focusing and defocusing effects caused by basement topography are strongly dependent on the azimuth and angle of incidence of waves. Seismic waves traveling upward from depth may be redirected by subtle irregularities at geological interfaces, particularly the basement topography. The effects of focusing and defocusing are maximum for normal incidence of waves and it decreases with increase of angle of incidence. Similarly, azimuth also affects the focusing and defocusing effects. This effect reveals the importance of considering not only the surficial soil layer but also the basement topography for seismic microzonation.

Trapping of waves

The fundamental phenomenon responsible for the increase of duration of motion over soft sediments is the trapping and multiple reflections of seismic waves due to the large impedance contrast between soft sediments and underlying bedrock. Sometimes, when a wave enters a basin through its edge, it can become trapped within the basin if post-critical incidence angles develop, causing total internal reflection at the base of the layer. Waves that become trapped in deep sedimentary basins can therefore be potentially very damaging.

1.6.2 Lateral Discontinuity Effects

There are numerous consistent macroseismic observations showing a significant increase in intensity of damage in narrow zones located along lateral discontinuities, i.e. areas where a softer material lies besides a more rigid one. An amplitude amplification and local surface wave generation in the softer medium and large differential motion caused by shorter wavelength of the surface wave can explain the observed damage. In past, a number of field observations

(Narayan and Rai, 2001) and theoretical studies have reported significant increase of damage in the narrow zone located along strong lateral discontinuities (Moczo and Bard, 1993).

1.6.3 Effect of the Surface Topography

It has often been reported after destructive earthquakes in hilly areas that buildings located at hill tops suffer much more damage than those located at the base: examples of such observations may be found in Levret et al., 1986 (Lambesc, France, 1909 earthquake), Siro, 1982 (Irpinia, Italy, 1980 earthquake), Celebi, 1987 (Chile, 1985 earthquake) and Narayan and Rai, 2001 (Chamoli, 1999 earthquake).

There are also very strong instrumental evidences that surface topography considerably affects the amplitude and frequency contents of ground motion (Pedersen et al., 1994). A review of such instrumental studies and results may be found in Geli et al. (1988), Aki (1988) and more recently in Faccioli (1991). The theoretical and numerical models have also predicted a systematic amplification of ground motion at ridge crest (convex part) and deamplification in valley (concave parts) of the surface topography (Kawase and Aki, 1990; Sanchez-Sesma, 1990; Faccioli, 1991; Narayan and Rao, 2003; Narayan, 2003b).

Narayan and Rao (2003) reported surface wave generation near the top of the ridge and their propagation towards the base of the ridge, in addition to amplification of ground motion with elevation and slope of the ridge using 2.5 D model (Narayan, 2001). Narayan (2003b) reported strong generation of surface waves for weathering thickness more than one-eighth of wavelength. He reported on the basis of the simulated results that damage to the built environment may be maximum on the top of the ridge, if it is not weathered. But, if the velocity of the weathered material is very less as compared to the underlying rock formation, maximum damage may be more near the base of the ridge, due to large amplitude and duration of the generated surface waves. Some of the findings of the above-mentioned studies are listed below.

- Ground motion amplification increases with ridge-slope.
- Maximum amplification ($2\pi/\phi$ times, where ϕ is the crest angle) occurs at the crest of the triangular wedge type topography relative to the base for wavelength comparable to width of the base (Figure 1.14).

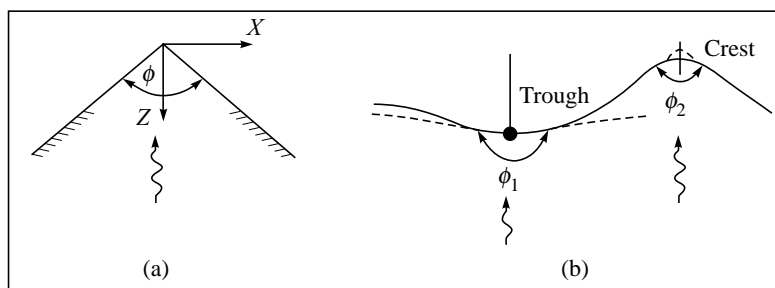


FIGURE 1.14 Characterization of simple topographic irregularities; (a) notation for a triangular wedge; (b) approximation of actual ground surface (solid line) at trough and crest by wedges, (after Faccioli, 1991).

- De-amplification ($2\pi/\phi$ times) occurs in valley relative to the top of the valley.
- Topographic amplification decreases with increase of angle of incidence of body waves.
- Ridge amplification increases with elevation (Figure 1.15).

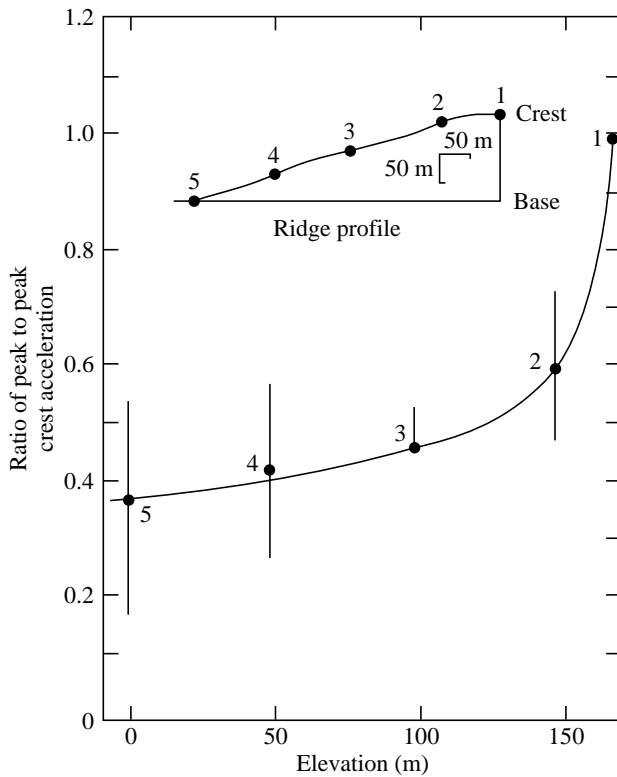


FIGURE 1.15 Variation of average amplification factor with elevation (after Jibson, 1987).

- Surface waves are generated near the top of the topography.
- The presence of neighbouring ridges accentuates the topographic effects.
- Interference between the incident waves and outgoing diffracted waves produces rapidly varying amplitude and phase, thereby causing differential ground motion along the slope of the topography.
- The amplitude of ridge-weathering-induced surface wave increases towards its base, if thickness of weathering is more than one-eighth of the wavelength.
- Decrease of weathering velocity increases the amplitude of ridge-induced surface waves.
- Complicated damage pattern occurs on hills with variable slopes. Generally, houses situated on or near the slope-change suffer more damage.
- In general, theoretical studies predict lower amplification than those obtained by analysis of recorded motion.

1.7 INTERNAL STRUCTURE OF THE EARTH

The delineation of internal structure of the Earth, different discontinuities and nature of material between two major discontinuities is mainly based on the analysis of the recorded reflected and refracted seismic waves. In broad sense, the internal structure of the earth is divided into three concentric cells, namely crust, mantle and core according to the chemical property of the materials (Figure 1.16). Further, crust is divided as upper and lower crust, mantle as upper and lower mantle and core as inner core and outer core. The crust and mantle together are also classified as lithosphere, asthenosphere and mesosphere, on the basis of physical property of the materials. Following subheadings describe crust, mantle and core in brief along with the discovery of major discontinuities.

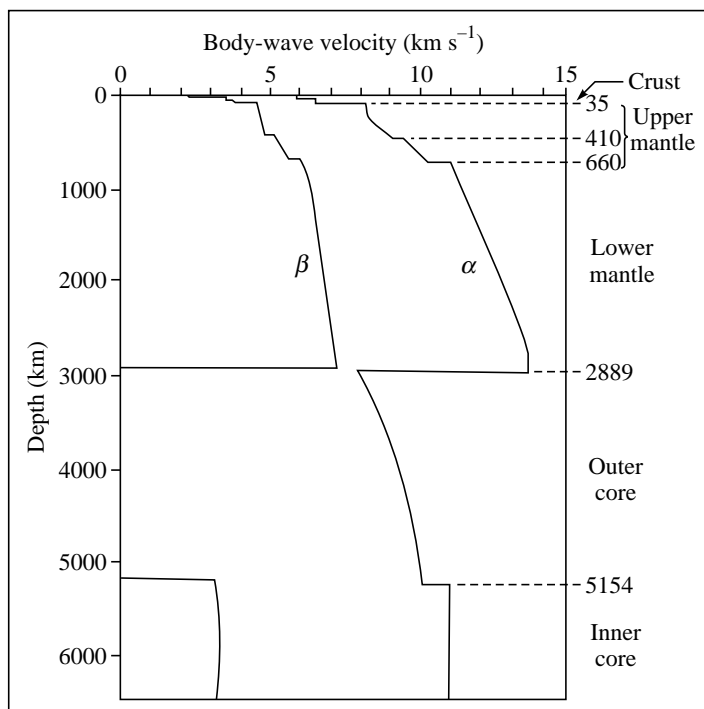


FIGURE 1.16 Internal structure of the earth based on P- and S-waves velocity variations (after Kennett and Engdahl, 1991).

1.7.1 Crust

Andrija Mohorovicic (1909) found only direct P-wave (Pg) arrivals near the epicentre during the analysis of an earthquake in Croatia. But beyond 100 km two P-wave arrivals were recorded and direct P-wave was overtaken by the second P-wave (Pn). He concluded that it is only possible when Pn has travelled at greater speed. Mohorovicic identified Pn as a refracted wave from the upper mantle. According to his calculations, the velocity of direct P-wave and refracted P-wave was 5.6 km/s and 7.9 km/s, respectively; and the estimated depth, at which sudden

increase of velocity occurred was 54 km. Now, this seismic discontinuity between crust and mantle, where there is sudden increase of seismic wave velocity, is called as *Mohorovicic discontinuity*, or simply *Moho*.

V. Conrad (1925) found faster P-wave (P^*) and S-wave (S^*) as compared to Pg and Sg waves during the analysis of Tauern earthquake of 1923 (Eastern Alps) in upper crustal layer. The estimated velocities of P^* and S^* waves (6.29 km/s and 3.57 km/s, respectively) were lesser than the velocities of Pn and Sn waves refracted from the Moho. Conrad inferred the existence of a lower crustal layer with higher velocity as compared to the upper crustal layer. The interface separating the crustal mass into upper and lower crust is called as *Conrad discontinuity*, in honour of V. Conrad.

Worldwide analysis of recorded reflected and refracted seismic waves reveals that the structures of the crust and upper mantle are very complex. The thickness of crust is highly laterally variable. It is 5–10 km in oceanic region, below the mean water-depth of about 4.5 km. The vertical structure of continental crust is more complicated than that of oceanic crust. The thickness of continental crust varies from 35 to 40 km under stable continental areas and 50 to 60 km under young mountain ranges.

1.7.2 Upper Mantle

The Mohorovicic discontinuity defines the top of the mantle. The average depth of Moho is 35 km, although it is highly variable laterally. Several discontinuities of seismic wave velocity and velocity gradients exist in the upper mantle. The uppermost mantle, 80–120 km thick, is rigid in nature in which velocity of seismic wave increases with depth. This rigid part of uppermost mantle together with crust forms the *lithosphere*. The lithosphere play an important role in plate tectonics.

There is an abrupt increase of seismic wave velocity (3 – 4%) at depth of around 220 ± 30 km. This interface is called as the *Lehmann discontinuity*. Between the base of lithosphere and the Lehmann discontinuity, there is low velocity layer (LVL) with negative velocity gradients. The average thickness of LVL is around 150 km. This LVL is known as *asthenosphere*, which also plays an important role in plate tectonics. Asthenosphere behaves as viscous fluid in long term and thus decouples the lithosphere from the deeper mantle.

The travel-time versus epicentral-distance curves of body wave show a distinct change in slope at epicentral distance of about 20° . This is attributed to a discontinuity in mantle velocities at a depth of around 400 km. This is interpreted as due to a petrological change from an olivine-type lattice to a more closely packed spinel-type lattice. A further seismic discontinuity occurs at a depth of 650–670 km. This is a major feature of mantle structure that has been observed world-wide. In the transition zone between the 400 km and 670 km discontinuities there is a further change in structure from β -spinel to γ -spinel, but this is not accompanied by appreciable changes in physical properties.

1.7.3 Lower Mantle

The lower mantle lies just below the important seismic discontinuity at 670 km. Its composition is rather poorly known, but it is thought to be consisting of oxides of iron and magnesium as

well as iron-magnesium silicates with a perovskite structure. The uppermost part of the lower mantle between 670 and 770 km depth has a high positive velocity gradient. Beneath it, there is great thickness of normal mantle, characterized by smooth velocity gradients and the absence of seismic discontinuities. Just above the core-mantle boundary an anomalous layer, approximately 150–200 km thick, has been identified in which body-wave velocity gradients are very small and may even be negative.

1.7.4 Core

R.D. Oldham first detected the fluid nature of the outer core seismologically in 1906. He observed that, if the travel-times of P-waves observed at epicentral distances of less than 100° were extrapolated to greater distances, the expected travel-times were less than those observed. This meant that the P-waves recorded at large epicentral distances were delayed in their path. Oldham inferred from this the existence of a central core in which the P-wave velocity was reduced. Gutenberg (1914) verified the existence of a shadow zone for P-waves in the epicentral range between 105° and 143° . Gutenberg also located the depth of top of outer core at about 2900 km. A modern estimate for this depth is 2889 km. It is characterized by very large seismic velocity change and is the most sharply defined seismic discontinuity. In honour of Gutenberg, the core-mantle boundary is known as the *Gutenberg seismic discontinuity*.

Inga Lehmann (1936), a Danish seismologist, reported weak P-wave arrivals within the shadow zone. She interpreted this in terms of a rigid inner core with higher seismic velocity at depth of around 5154 km. Thus core has a radius of 3480 km and consists of a solid inner core surrounded by a liquid outer core.

1.8 SEISMOTECTONICS OF INDIA

Himalaya is one of the tectonically most active belts of the world and one of the rare sites of active continent-continent collision. A major portion of the strain due to collision is taken up in the thrusting phenomenon along the Himalayas while the remaining strain is distributed north of it in a wide area from Tibetan Plateau to Pamirs. The push from the Asian side has given rise to compression from north producing gigantic thrusts progressing from north to south.

The northward movement of the Indian plate and the continued convergence process along the Himalayas has transmitted large northerly compression in the Indian Peninsula, causing NE oriented faults (Figure 1.17). The other tectonic features like ENE trending Narmada Son graben and NW trending Godavari and Mahanadi grabens are older. Sometimes the NW faults have been displaced by the younger NE faults. Present-day tectonics as indicated by seismicity study shows strike-slip fault either along NE or NW trending faults by reactivation. Normal faults along Narmada, Godavari and Koyna rifts are also reactivated occasionally. However, the faults in Peninsular India are small and so only moderate earthquakes have occurred except in Kutch region. The source of stress responsible for tectonic activity in the Kutch region is not well defined.

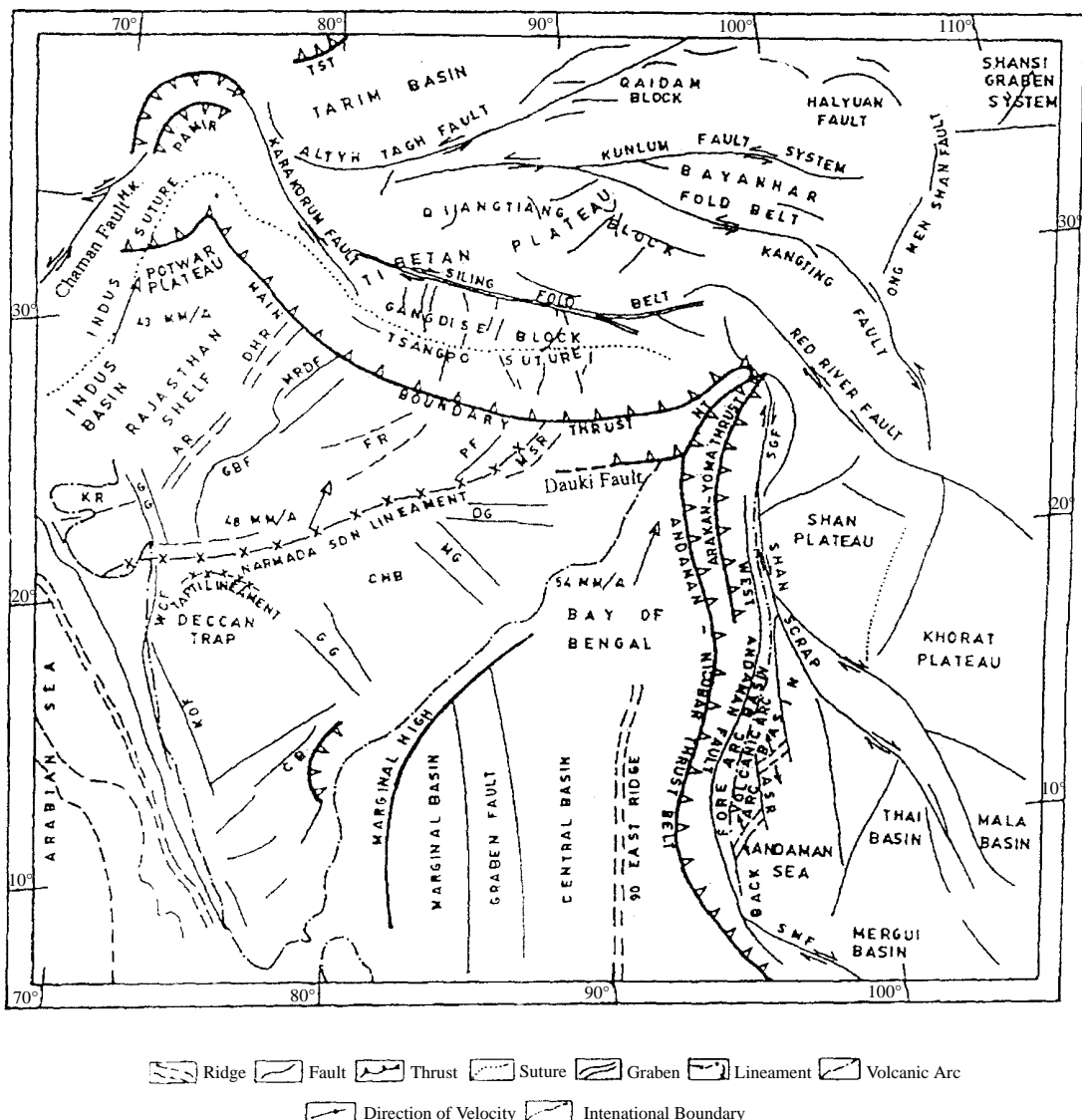


FIGURE 1.17 Tectonic map showing the major geomorphologic features in India and adjoining regions. AR—Aravalli Ridge; ASR—Andaman Spreading Ridge; CB—Cuddapah Basin; CG—Cambay Graben; CHB—Chhattisgarh Basin; DG—Damodar Graben; DHR—Delhi-Hardwar Ridge; FR—Faizabad Ridge; GBF—Great Boundary Fault; GG—Godavari Graben; HK—Hindukush; KOF—Koyna Fault; KR—Kutch Ridge; MG—Mahanadi Graben; MRDF—Moradabad Fault; MSR—Monghyr Saharsa Ridge; NT—Naga Thrust; SGF—Sagaing Fault; SHF—Sumatra Fault; TST—Tien Shan Thrust; WCF—West Coast Fault (after Khan, 2004).

1.9 SEISMICITY OF INDIA

Earthquakes have been occurring in the Indian subcontinent from the times immemorial but reliable historical records are available for the last 200 years (Oldham, 1883). From the beginning of 20th century, more than 700 earthquakes of magnitude 5 or more have been recorded and felt in India, as given in the catalogues prepared by US National Oceanographic and Atmospheric Administration, India Meteorological Department, National Geophysical Research Institute (Figure 1.18). The seismicity of India can be divided in four groups, namely, Himalayas region, Andaman Nicobar, Kutch region and Peninsular India. Some of the damaging earthquakes which have occurred in these four regions are listed in Table 1.10.

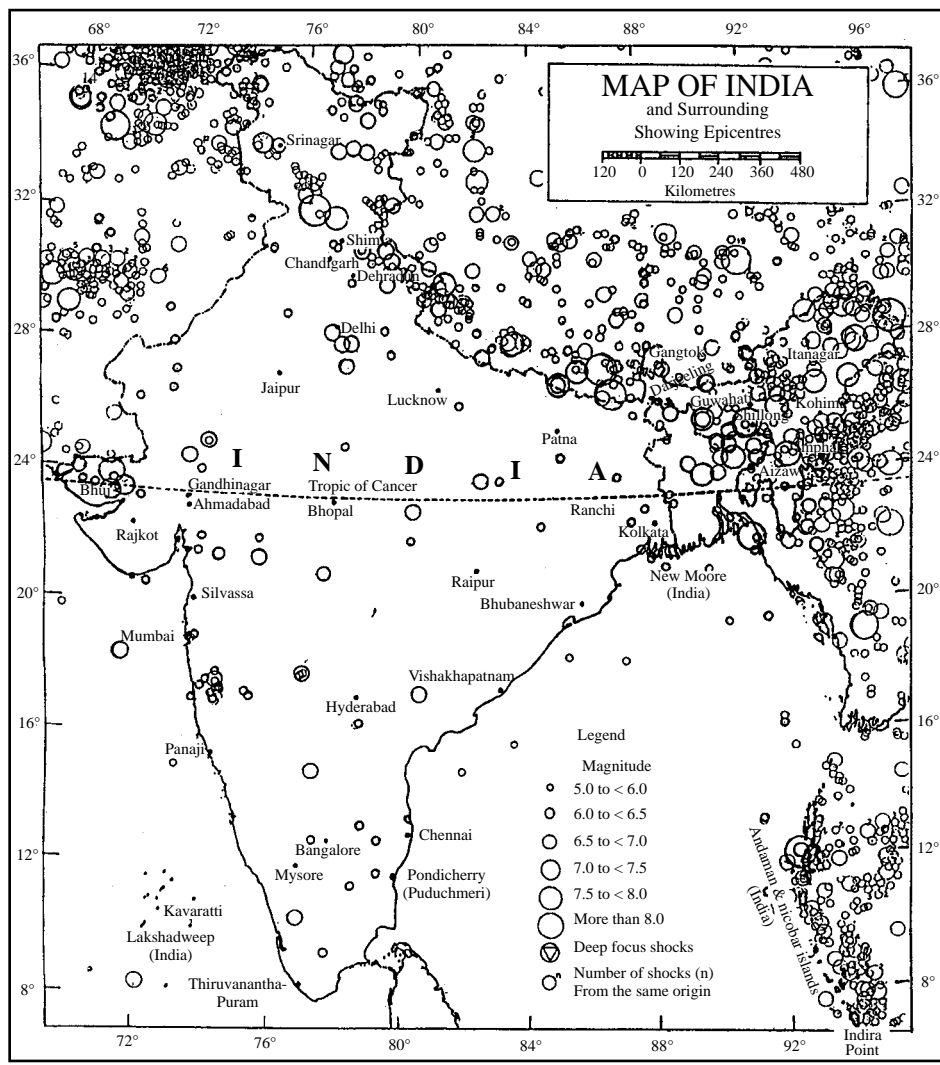


FIGURE 1.18 Seismicity map of India (after, IS:1893 (Pt. 1): 2002).

TABLE 1.10 List of damaging earthquakes in India

		<i>Himalayan Region</i>	<i>Year</i>	<i>Magnitude/ Intensity</i>	<i>Death</i>
<i>S. No.</i>	<i>Name</i>	<i>Location</i>			
1.	Kashmir Earthquake	Srinagar, J. & K.	1885	—	3,000
2.	Shillong Earthquake	Shillong, Plateau	1897	8.7	1,600
3.	Kangra Earthquake	Kangra, H.P.	1905	8.5	20,000
4.	Bihar-Nepal Earthquake	Bihar-Nepal border region	1934	8.3	10,000
5.	Assam Earthquake	Assam	1950	8.5	1,526
6.	Bihar-Nepal Earthquake	Bihar-Nepal border region	1988	6.5	1,000
7.	Indo-Burma Earthquake	India-Burma Border	1988	7.3	—
8.	Uttarkashi Earthquake	Uttarkashi, Uttaranchal	1991	7.0	768
9.	Chamoli Earthquake	Chamoli, Uttaranchal	1999	6.8	103
<i>Andaman Nicobar</i>					
1.	Andaman-Nicobar Earthquake	Andaman-Nicobar Trench	1941	8.1	—
<i>Kutch Region</i>					
1.	Samaji Earthquake	Samaji, Delta of Indus	1668	X	—
2.	Kutch Earthquake	Kutch, Gujarat	1819	8.0	2,000
3.	Anjar Earthquake	Anjar, Gujarat	1956	6.1	115
4.	Bhuj Earthquake	Bachau, Gujarat	2001	6.9	20,000
<i>Peninsular India</i>					
1.	Bombay-Surat Earthquake	Bombay-Surat	1856	VII	—
2.	Son Valley Earthquake	Son Valley	1927	6.5	—
3.	Satpura Earthquake	Satpura	1938	6.3	—
4.	Balaghat Earthquake	Balaghat, M.P.	1957	5.5	—
5.	Koyna Earthquake	Koyna	1967	6.0	177
6.	Ongole Earthquake	Ongole, Bhadrachalam	1967	5.4	—
7.	Broach Earthquake	Broach	1970	5.4	26
8.	Latur Earthquake	Latur, Maharashtra	1993	6.2	10,000
9.	Jabalpur Earthquake	Jabalpur, M.P.	1997	6.0	54

1.10 CLASSIFICATION OF EARTHQUAKES

1. Based on location
 - (a) Interplate
 - (b) Intraplate
2. Based on epicentral distances
 - (a) Local earthquake $< 1^\circ$
 - (b) Regional earthquake $1 - 10^\circ$
 - (c) Teleseismic earthquake $> 10^\circ$
3. Based on focal depth

(a) Shallow depth	0–71 km	(a) Mircoearthquake < 3.0
(b) Intermediate depth	71–300 km	(b) Intermediate earthquake 3–4
4. Based on magnitude
 - (a) Mircoearthquake < 3.0
 - (b) Intermediate earthquake 3–4

- | | | |
|---------------------|----------|--|
| (c) Deep earthquake | > 300 km | (c) Moderate earthquake 5–5.9
(d) Strong earthquake 6–6.9
(e) Major earthquake 7–7.9
(f) Great earthquake > 8.0 |
|---------------------|----------|--|

1.11 TSUNAMI

Tsunami is a series of large waves of extremely long period caused by a violent, impulsive undersea disturbance or activity near the coast or in the ocean. The waves become extremely dangerous and damaging when they reach the shore. The word tsunami is composed of the Japanese words “tsu” (which means harbour) and “nami” (which means “wave”). They are sometimes called seismic sea waves or, erroneously, tidal waves. In case of tsunami waves, energy extends to the ocean bottom and water flows straight. Near the shore, tsunami energy is concentrated in the vertical direction by the reduction in water depth, and in the horizontal direction by shortening of the wavelength due to reduction in velocity. There are various aspects of tsunami waves which are studied by researchers namely plate tectonics responsible for generation, propagation and observation, inundation, run-up build-up near the coast due to geometry of coast, resonance in bays, etc.

The destructive tsunamis are generated from large (dislocation of several metres), shallow earthquakes with epicentre or fault line near or on the ocean floor. Tsunamis generally occur in the oceanic subduction zones of lithospheric plates. The sudden vertical displacements over large areas, disturb the ocean's surface, displace water, and generate destructive tsunami waves. A ‘**tsunami earthquake**’ is defined as an earthquake that excites much larger tsunami than expected from its seismic waves (Kanamori, 1972; Abe, 1973). Usually, earthquakes with Richter magnitude larger than 7.5 produce destructive tsunami waves. Table 1.11 shows a list of ten deadliest tsunamis in Indian Ocean. The wavelength of the tsunami waves and their period depend on the generating mechanism and the dimensions of the source event. The period of the

TABLE 1.11 List of ten deadliest tsunamis in Indian Ocean

Year	Deaths	Location*
Dec. 26, 2004	220000+	Sumatra
Aug. 27, 1883	36500	Java/Sumatra
Jan. 26, 1941	5000	Andaman Sea
Sept. 3, 1861	1700	Sumatra
Jun. 16, 1819	1543+	Arabian Sea
Nov. 28, 1945	1000+	Arabian Sea
Feb. 16, 1861	905	Sumatra
April 2, 1762	500	Bay of Bengal
Aug. 19, 1977	500	Sunda Islands
Jan. 4, 1907	400	Sumatra

* Includes deaths from the tsunami and the earthquake.

tsunami waves may range from 5 to 90 minutes. On the open ocean, the wavelength of a tsunami may be as much as 200 km (Figure 1.19). In the deep ocean, the height of the tsunami from trough to crest may range from only a few centimetres to a metre or more. In shallow waters near the shoreline, however, the tsunami height may build up to several metres.

1.11.1 Tsunami Velocity

The velocity of a tsunami wave (V_{Tsu}) whose wavelength is sufficiently large compared to the water depth (25 or more times the depth) is given by the following expression (Satake, 2002):

$$V_{\text{Tsu}} = \sqrt{gh} \quad (1.14)$$

where ‘g’ is the acceleration due to earth’s gravity field and ‘h’ is the depth of water. The tsunami velocity may vary from 35 km/hr to 950 km/hr for the range of water depth 10 m to 7.0 km (Figure 1.19).

1.11.2 Run-up and Inundation

Although infrequent, tsunamis are among the most terrifying and complex physical phenomena and have been responsible for great loss of life and extensive destruction to property. Damage due to tsunami is caused by large run-up (elevation reached by seawater measured relative to some stated datum), inundation (distance between the inundation line and the shore), wave impact on structures and erosion.

As the tsunami wave approaches the coast, the wavelength is shortened and the wave energy is directed upward, thus increasing their heights considerably, as shown in Figure 1.19. The amplitude of tsunami waves may grow up to 30–35 m near the shore. Depending upon the

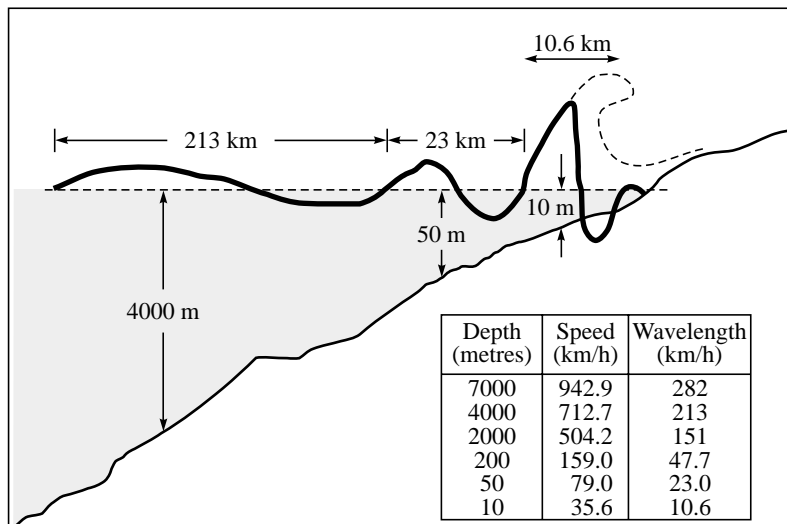


FIGURE 1.19 Velocity and wavelength variation with water depth of a tsunami with period about 18 minutes, and an illustration for amplitude amplification near the shore.

water depth and the coastal configuration, the waves may undergo extensive refraction, another process that may converge their energy to particular areas on the shore and thus increase the heights and inundation even more. Field surveys are carried out after every large tsunami for assessment of run-ups and inundation limits and to collect associated data from eyewitnesses such as the number of waves, arrival time of waves and the largest wave.

SUMMARY

Seismology is the study of generation, propagation and recording of elastic waves in the earth and of sources that produce them. An earthquake is a sudden tremor or movement of earth's crust, which originates naturally at or below the surface. About 90% of all earthquakes result from tectonic events, primarily movements of the faults. The remaining proportion is related to volcanism, collapse of sub-terranean cavities, or man-made effects. The epicenters of earthquakes are not randomly distributed over the earth's surface. They tend to be concentrated in narrow zones. This chapter describes in detail the elastic rebound theory, seismic waves, local site effects on ground motion characteristics, interior of the earth and movement of Indian plate along with its seismotectonic features.

GLOSSARY OF EARTHQUAKE/SEISMOLOGY

- **Active fault.** A fault that is likely to have another earthquake some time in the future. Faults are commonly considered to be active if they have moved one or more times in the past.
- **Aftershocks.** Earthquakes that follow the largest shock of an earthquake sequence. They are smaller than the mainshock and continue over a period of weeks, months, or years. In general, the larger the mainshock, the larger and more numerous the aftershocks, and the longer they will continue.
- **Alluvium.** Loose gravel, sand, silt, or clay deposited by streams.
- **Aseismic.** This term describes a fault on which no earthquakes have been observed.
- **Attenuation.** When you throw a pebble in a pond, it makes waves on the surface that move out from the place where the pebble entered the water. The waves are largest where they are formed and gradually get smaller as they move away. This decrease in size, or amplitude, of the waves is called attenuation.
- **Basement.** Harder and usually older igneous and metamorphic rocks that underlie the main sedimentary rock sequences (softer and usually younger) of a region and extend downward to the base of the crust.
- **Bedrock.** Relatively hard, solid rock that commonly underlies softer rock, sediment, or soil; a subset of the basement.
- **Benioff zone.** A dipping planar (flat) zone of earthquakes that is produced by the interaction of a downgoing oceanic crustal plate with a continental plate. These earthquakes can be produced by slip along the subduction thrust fault or by slip on faults within the downgoing plate as a result of bending and extension as the plate is pulled into the mantle. Also known as the Wadati-Benioff zone.

- **Body wave.** A seismic wave that moves through the interior of the earth, as opposed to the surface waves that travel near the earth's surface. P- and S-waves are body waves.
- **Crust.** The outermost major layer of the earth, ranging from about 10 to 65 km in thickness worldwide. The uppermost 15 to 35 km of crust is brittle enough to produce earthquakes.
- **Core.** The innermost part of the earth. The outer core extends from 2500 to 3500 miles below the earth's surface and is liquid metal. The inner core is the central 500 miles and is solid metal.
- **Earthquake.** This term is used to describe both sudden slip on a fault, and the resulting ground shaking and radiated seismic energy caused by the slip, or by volcanic or magmatic activity, or other sudden stress changes in the earth.
- **Earthquake hazard.** Anything associated with an earthquake that may affect the normal activities of people. This includes surface faulting, ground shaking, landslides, liquefaction, tectonic deformation, tsunamis, and seiches.
- **Earthquake risk.** The probable building damage, and number of people that are expected to be hurt or killed if a likely earthquake on a particular fault occurs. Earthquake risk and earthquake hazard are occasionally used interchangeably.
- **Epicentre.** The point on the earth's surface vertically above the point in the crust where seismic rupture begins
- **Fault.** A fracture along which the blocks of crust on either side have moved relative to one another parallel to the fracture. **Strike-slip faults** are vertical (or nearly vertical) fractures where the blocks have mostly moved horizontally. If the block opposite to an observer looking across the fault moves to the right, the slip style is termed right lateral; if the block moves to the left, the motion is termed left lateral. **Dip-slip faults** are inclined fractures where the blocks have mostly shifted vertically. If the rock mass above an inclined fault moves down, the fault is termed **normal**, whereas if the rock above the fault moves up, the fault is termed **reverse (or thrust)**. Oblique-slip faults have significant components of both slip styles.
- **Foreshocks.** Foreshocks are relatively smaller earthquakes that precede the largest earthquake in a series, which is termed the mainshock. Not all mainshocks have foreshocks.
- **Hypocentre.** The point within the earth where an earthquake rupture starts. Also commonly termed the focus.
- **Intensity.** A number (written as a Roman numeral) describing the severity of an earthquake in terms of its effects on the earth's surface and on humans and their structures. There are many intensity values for an earthquake, depending on where you are, unlike the magnitude, which is one number for each earthquake.
- **Intraplate and interplate.** **Intraplate** pertains to process within the earth's crustal plates. **Interplate** pertains to process between the plates.
- **Isoseismal.** A contour or line on a map bounding points of equal intensity for a particular earthquake.
- **Left-lateral.** If you were to stand on the fault and look along its length, this is a type of strike-slip fault where the left block moves toward you and the right block moves away.

- **Lithosphere.** The outer solid part of the earth, including the crust and uppermost mantle. The lithosphere is about 100 km thick, although its thickness is age dependent (older lithosphere is thicker). The lithosphere below the crust is brittle enough at some locations to produce earthquakes by faulting, such as within a subducted oceanic plate.
- **Love wave.** A type of seismic surface wave having a horizontal motion that is transverse (or perpendicular) to the direction the wave is travelling.
- **Magnitude.** A number that characterizes the relative size of an earthquake. Magnitude is based on measurement of the maximum motion recorded by a seismograph. Several scales have been defined, but the most commonly used are (1) local magnitude (M_L), commonly referred to as "Richter magnitude," (2) surface-wave magnitude (M_S), (3) body-wave magnitude (m_B), and (4) moment magnitude (M_W).
- **Mainshock.** The largest earthquake in a sequence, sometimes preceded by one or more foreshocks, and almost always followed by many aftershocks.
- **Mantle.** The part of the earth's interior between the metallic outer core and the crust.
- **Moho.** The boundary between the crust and the mantle in the earth. The boundary is between 25 and 60 km deep beneath the continents and between 5 and 10 km deep beneath the ocean floor.
- **Oceanic spreading ridge.** A fracture zone along the ocean bottom where molten mantle material comes to the surface, thus creating new crust. This fracture can be seen beneath the ocean as a line of ridges that form as molten rock reaches the ocean bottom and solidifies.
- **Oceanic trench.** A linear depression of the sea floor caused by the subduction of one plate under another.
- **P-wave.** A seismic body wave that shakes the ground back and forth in the same direction and the opposite direction as the wave is moving.
- **Plate tectonics.** A theory supported by a wide range of evidence that considers the earth's crust and upper mantle to be composed of several large, thin, relatively rigid plates that move relative to one another. Slip on faults that define the plate boundaries commonly results in earthquakes. Several styles of faults bound the plates, including thrust faults along which plate material is subducted or consumed in the mantle, oceanic spreading ridges along which new crustal material is produced, and transform faults that accommodate horizontal slip (strike slip) between adjoining plates.
- **Rayleigh wave.** A seismic surface wave causing the ground to shake in an elliptical motion, with no transverse, or perpendicular, motion.
- **Recurrence interval.** The average time span between large earthquakes at a particular site. Also termed return period.
- **Reflection.** The energy or wave from an earthquake that has been returned (reflected) from a boundary between two different materials within the earth, just as a mirror reflects light.
- **Refraction.** The deflection, or bending, of the ray path of a seismic wave caused by its passage from one material to another having different elastic properties. Bending of a tsunami wave front owing to variations in the water depth along a coastline.
- **Right-lateral.** If you were to stand on the fault and look along its length, this is a type of strike-slip fault where the right block moves toward you and the left block moves away.

- **Ring of Fire.** The zone of earthquakes surrounding the Pacific Ocean which is called the Circum-Pacific belt about 90% of the world's earthquakes occur there. The next most seismic region (5–6% of earthquakes) is the Alpide belt (extends from Mediterranean region, eastward through Turkey, Iran, and northern India).
- **S-wave.** A seismic body wave that shakes the ground back and forth perpendicular to the direction the wave is moving, also called a shear wave.
- **Sand boil.** Sand and water that come out onto the ground surface during an earthquake as a result of liquefaction at shallow depth.
- **Seismic gap.** A section of a fault that has produced earthquakes in the past but is now quiet. For some seismic gaps, no earthquakes have been observed historically, but it is believed that the fault segment is capable of producing earthquakes on some other basis, such as plate-motion information or strain measurements.
- **Seismicity.** The geographic and historical distribution of earthquakes.
- **Seismic moment.** A measure of the size of an earthquake based on the area of fault rupture, the average amount of slip, and the force that was required to overcome the friction sticking the rocks together that were offset by faulting. Seismic moment can also be calculated from the amplitude spectra of seismic waves.
- **Seismic zone.** An area of seismicity probably sharing a common cause. Example: “The Himalayan Zone.”
- **Seismogenic.** Capable of generating earthquakes.
- **Seismogram.** A record written by a seismograph in response to ground motions produced by an earthquake, explosion, or other ground-motion sources.
- **Seismology.** The study of earthquakes and the structure of the earth, by both naturally and artificially generated seismic waves.

REFERENCES

- [1] Abe, K., “Tsunami and Mechanism of Great Earthquakes”, *Physics of the Earth Planet Interiors*, 7: 143–153, 1973.
- [2] Aki, K. and Chouet, B., “Origin of Coda Waves: Source, Attenuation and Scattering Effects”, *Journal of Geophysical Research*, 80: 3322, 1975.
- [3] Aki, K., “Local Site Effects on Strong Ground Motion”, In *Earthquake Engineering and Soil Dynamics II—Recent Advances in Ground Motion Evaluation*, J.L. Von Thun (Ed.), Geotechnical Special Publication No. 20, 103–155, American Society of Civil Engineering, New York, 1988.
- [4] Barazangi, M. and Dorman, J., “World Seismicity Map Compiled from ESSA, Coat and Geodetic Survey, Epicenter Data, 1961–1967”, *Bulletin of the Seismological Society of America*, 59: 369–380, 1969.
- [5] Bath, M., “Earthquake Energy and Magnitude”, *Physics and Chemistry of the Earth*, Ahren, L.H. Press, 115–165, 1966.
- [6] Bard, P.Y. and Bouchon, M., “The Seismic Response of Sediment-filled Valleys—Part 1: The Case of Incident SH Waves”, *Bulletin of the Seismological Society of America*, 70: 1263–1286, 1980a.

- [7] Bard, P.Y. and Bouchon, M., "The Seismic Response of Sediment-filled Valleys—Part 2: The Case of Incident P and SV Waves", *Bulletin of the Seismological Society of America*, 70: 1921–1941, 1980b.
- [8] Bard, P.Y. and Bouchon, M., "The Two-dimensional Resonance of Sediment-filled Valleys", *Bulletin of the Seismological Society of America*, 75: 519–541, 1985.
- [9] Bullen, K.E. and Bolt, B.A., *An Introduction to the Theory of Seismology*, Cambridge University Press, Cambridge, 1985.
- [10] Celebi, M., "Topographical and Geological Amplifications Determined from Strong-motion and Aftershock Records of the 3 March 1985 Chile Earthquake", *Bulletin of the Seismological Society of America*, 77: 1147–1167, 1987.
- [11] Conrad, V., "Laufzeitkurven Des Tauernbebens", vom 28: 59: 1–23, Mitt.Erdb.-Komm. Wien, 1925.
- [12] DeMets, et al., *Current Plate Motions*, 101: 425–478, 1990.
- [13] Faccioli, E., "Seismic Amplification in the Presence of Geological and Topographic Irregularities", *Proceedings of 2nd International Conference on Recent Advances in Geotechnical Earthquake Engineering and Soil Dynamics*, St. Louis, Missouri, 2: 1779–1797, 1991.
- [14] Geli, L., Bard, P.Y. and Jullien, B., "The Effect of Topography on Earthquake Ground Motion: A Review and New Results", *Bulletin of the Seismological Society of America*, 78: 42–63, 1988.
- [15] Gutenberg, B., *The Energy of Earthquakes*, 112: 1–14, 1945.
- [16] Gutenberg, B. and Richter, C.F., *Seismicity of Earth and Related Phenomenon*, Princeton University Press, Princeton, New Jersey, 1945.
- [17] Gutenberg, B., "Magnitude Determination for Deep Focus Earthquakes", *Bulletin of the Seismological Society of America*, 35: 117–130, 1956.
- [18] Hatayama, K., Matsunami, K., Iwata, T. and Irikura, K., "Basin-induced Love Wave in the Eastern Part of the Osaka Basin", *Journal of Physics of the Earth*, 43: 131–155, 1995.
- [19] Hutton, L.K. and Boore, D.M., "The M_L Scale in Southern California", *Bulletin of the Seismological Society of America*, 77: 6: 2074–2094, 1987.
- [20] Jibson, R., "Summary on Research on the Effects of Topographic Amplification of Earthquake Shaking on Slope Stability", *Open-File-Report-87-268*, USGS, California, 1987.
- [21] Kanamori, H., "Mechanism of Tsunami Earthquake", *Physics of the Earth Planet, Interiors*, 6: 246–259, 1972.
- [22] Kanamori, H., "The Energy Release in Great Earthquakes", *Tectonophysics*, 93: 185–199, 1977.
- [23] Hank, T.C. and Kanamori, H., "A Moment Magnitude Scale", *JGR*, 84: 2348–2350, 1979.
- [24] IS: 1893, *Indian Standard Criteria for Earthquake Resistant Design of Structures*, Part 1, BIS, New Delhi, 2002.
- [25] Kawase, H., "The Cause of Damage Belt in Kobe: 'The Basin-edge Effect', Constructive Interference of the Direct S-Waves with the Basin Induced Diffracted/Rayleigh Waves", *Seismological Research Letters*, 67: 25–34, 1996.

- [26] Kawase, H. and Aki, K., “Topography Effect at the Critical SV Wave Incidence: Possible Explanation of Damage Pattern by the Whitter Narrow”, *Earthquake of 1 October 1987, Bulletin of the Seismological Society of America*, 80: 1–22, California, 1990.
- [27] Kennett, B.L.N. and Engdahl, E.R., “Travel Times for Global Earthquake Location and Phase Identification”, *International Journal of Geophysics*, 105: 429–465, 1991.
- [28] Khan, P.K., “Recent Seismicity Trend in India and Adjoining Regions”, *ISET, New Lett.*, October 2003–July 2004, 10–14, 2004.
- [29] Kim, W.Y., “The M_L Scale in Eastern North America”, *Bulletin of the Seismological Society of America*, 88(4): 935–951, 1998.
- [30] Langston, C.A., Brazier, R., Nyblade, A.A., and Owens, T.J., “Local Magnitude Scale and Seismicity Rate for Tanzania, East Africa,” *Bulletin of the Seismological Society of America*, 88(3): 712–721, 1998.
- [31] Levret, A., Loup, C., and Goula, X., “The Provence Earthquake of June 11, 1909 (France): New Assessment of Near Field Effects”, *Proceedings of the 8th European Conference of Earthquake Engineering*, Lisbon, 2, p. 4.2.79, 1986.
- [32] Love, A.E.H., *Some Problems of Geodynamics*, Cambridge University Press, 1911.
- [33] Lowrie, W. *Fundamentals of Geophysics*, Cambridge University Press, 1997.
- [34] MacMurdo, J., “Papers Relating to the Earthquake which Occurred in India in 1819”, *Philosophical Magazine*, 63: 105–177, 1824.
- [35] Moczo, P. and Bard, P.Y., “Wave Diffraction, Amplification and Differential Motion Near Strong Lateral Discontinuities”, *Bulletin of the Seismological Society of America*, 83: 85–106, 1993.
- [36] Mohorovicic, A., “Das Beben Vom 8×1909 ”, *Jb. Met. Obs. Zagreb*, 9, 1–63, 1909.
- [37] Mussett, A.E. and Khan, M.A., *Looking into the Earth: An Introduction to Geological Geophysics*, Cambridge University Press, 2000.
- [38] Narayan, J.P., “Site Specific Strong Ground Motion Prediction Using 2.5-D Modelling”, *Geophysical Journal International*, 146: 269–281, 2001.
- [39] Narayan, J.P. and Rai, D.C., “An Observational Study of Local Site Effects in the Chamoli Earthquake”, *Proceedings of Workshop on Recent Earthquakes of Chamoli and Bhuj*, 273–279, 2001.
- [40] Narayan, J.P., Sharma, M.L. and Ashwani Kumar, ‘A Seismological Report on the January 26, 2001 Bhuj, India Earthquake’, *Seismological Research Letters*, 73: 343–355, 2002.
- [41] Narayan, J.P. and Prasad Rao, P.V., “Two and Half Dimensional Simulation of Ridge Effects on the Ground Motion Characteristics”, *Pure and Applied Geophysics*, 160: 1557–1571, 2003.
- [42] Narayan, J.P., “2.5D Simulation of Basin-edge Effects on the Ground Motion Characteristics”, *Proceedings of Indian Academy of Sciences (Science of the Earth Planet)*, 112: 463–469, 2003a.
- [43] Narayan, J.P., “Simulation of Ridge Weathering Effects on the Ground Motion Characteristics”, *Journal of Earthquake Engineering*, 7: 447–461, 2003b.
- [44] Narayan, J.P., “3D Simulation of Basin-edge Effects on the Ground Motion Characteristics”, *13WCEE*, August 1–6, Paper No. 3333, Vancouver, Canada, 2004.

- [45] Narayan, J.P., "Study of Basin-edge Effects on the Ground Motion Characteristics Using 2.5-D Modelling", *Pure and Applied Geophysics*, 162: 273–289, 2005.
- [46] Oldham, R.D., "A Catalog of Indian Earthquakes from the Earliest Times to the End of A.D., 1869", *Memoir X*, Geological Survey of India, 1883.
- [47] Oldham, R.D., "The Constitution of the Interior of the Earth, as Revealed by Earthquakes", *Quarterly Journal of Geological Society of London*, 62: 456–75, 1906.
- [48] Pedersen, H., Hatzfeld, D., Campillo, M., and Bard, P.Y., "Ground Motion Amplitude Across Ridges", *Bulletin of the Seismological Society of America*, 84: 1786–1800, 1994.
- [49] Pitarka, A., Irikura, K., Iwata, T., and Sekiguchi, H., "Three-dimensional Simulation of the Near Fault Ground Motion for 1995", Hyogo-ken Nanbu (Kobe), Japan earthquake, *Bulletin of the Seismological Society of America*, 88: 428–440, 1998.
- [50] Plesinger A., Zmeskal, M., and Zednik, J., *Automated Pre-processing of Digital Seismograms: Principles and Software*. Version 2.2, E. Bergman (Ed.), Prague and Golden, 1996.
- [51] Rayleigh, Lord, "On-wave Propagated Along the Plane Surface of an Elastic Solid", *Proceedings of the London Mathematical Society*, 17: 4–11, 1885.
- [52] Reid, H.F., *The California Earthquake of April 18, 1906*, Publication 87, 21, Carnegie Institute of Washington, Washington, D.C., 1910.
- [53] Reid, H.F., "The Elastic Rebound Theory of Earthquakes", *Bulletin of Department of Geology*, 6: 413–444, University of Berkeley, 1911.
- [54] Richter, C.F., "An Instrumental Earthquake Magnitude Scale", *Bulletin of the Seismological Society of America*, 25: 1–32, 1935.
- [55] Richter, C.F., *Elementary Seismology*, W.H. Freeman, San Francisco, 1958.
- [56] Sánchez-Sesma, F.J., "Elementary Solutions for the Response of a Wedge-shaped Medium to Incident SH and SV Waves", *Bulletin of the Seismological Society of America*, 80: 737–742, 1990.
- [57] Satake, K., *Tsunamis, International Handbook of Earthquake and Engineering Seismology—Part B*, Lee et al. (Eds.), 437–451, 2002.
- [58] Siro, L. "Southern Italy November 23, 1980 Earthquake", *Proceedings of 7th European Conference on Earthquake Engineering*, Athens, Greece, 1982.
- [59] Wood, H.O., "Distribution of Apparent Intensity in San-Francisco, in the California Earthquake of April 18, 1906", *Report of the State Earthquake Investigation Commission*, 1: 220–245, Carnegie Institute of Washington, Washington, D.C., 1908.

Chapter 2

Seismic Zoning Map of India

2.1 INTRODUCTION

The goal of seismic zoning is to delineate regions of similar probable intensity of ground motion in a country, for providing a guideline for provision of an adequate earthquake resistance in constructed facilities, as a step to disaster mitigation. Various social, economic, and political considerations govern the prescription of a minimum standard of safeguard against earthquake in the design of a structure. These are (i) economic concept of ‘acceptable risk’, and (ii) answer to social question ‘How safe is safe enough’. The strongest intensity of likely ground motion is based on the answers to the above two posers. In terms of pure economic theory, earthquake causes two types of losses known as primary and secondary losses. A *primary loss* is irrecoverable loss, which results in the loss of human life in earthquake. All other losses incurred due to earthquake that can be recouped are termed as *secondary losses*. Thus minimum standard in a code to withstand earthquake is prescribed such that complete collapse of structure is prevented which ensures that no human life is lost. This requires a forecast of the strongest intensity of likely ground motion at a particular site during the service life of structure. Thus estimate of acceleration, velocity, displacement, frequency content and duration of expected maximum strong motion is required for a site. Seismic zoning map of a country segregates country in various areas of similar probable maximum intensity of ground motion. The maximum intensity is fixed in such a way that the lifeline/critical structures will remain functional and there is low possibility of collapse for structures designed with the provision provided in the code even for the occurrence of earthquake with higher intensity. Thus a structure designed with the provision of code can suffer damage of both structural and non-structural type. The damage is repairable but its economic viability is not warranted.

2.2 SEISMIC HAZARD MAP

Geological Survey of India (GSI) prepared a seismic hazard map in 1935 (Auden, 1959) of three zones (Figure 2.1) depicting likely damage scenario namely, *severe*, *moderate* and *slight*. This map also showed areas, which experienced damaging Modified Mercalli (MM) intensity VIII (Rossi-Forel intensity ‘higher than VII’) in the past earthquakes.

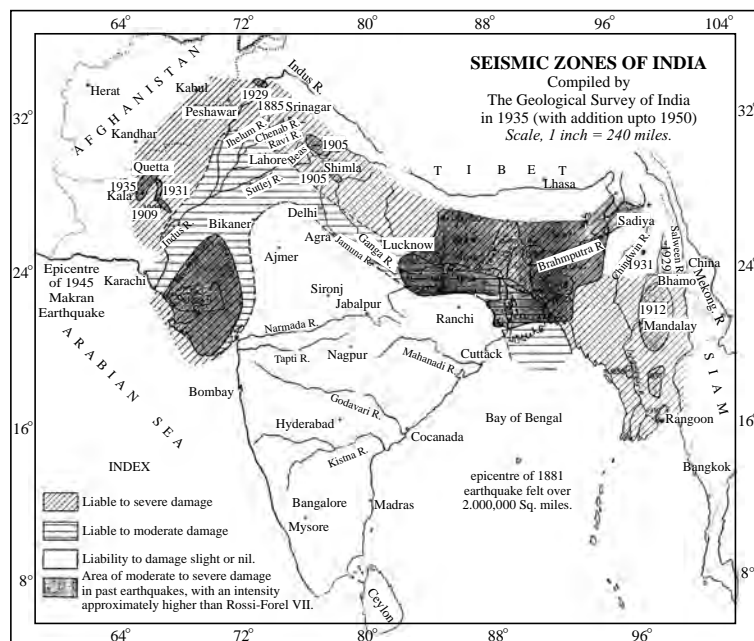


FIGURE 2.1 Seismic zones of Indian subcontinent compiled by the Geological Survey of India in 1935 (with additions up to 1950).

West (1937) presented a seismic hazard zone map (Figure 2.2) showing three zones. These zones were

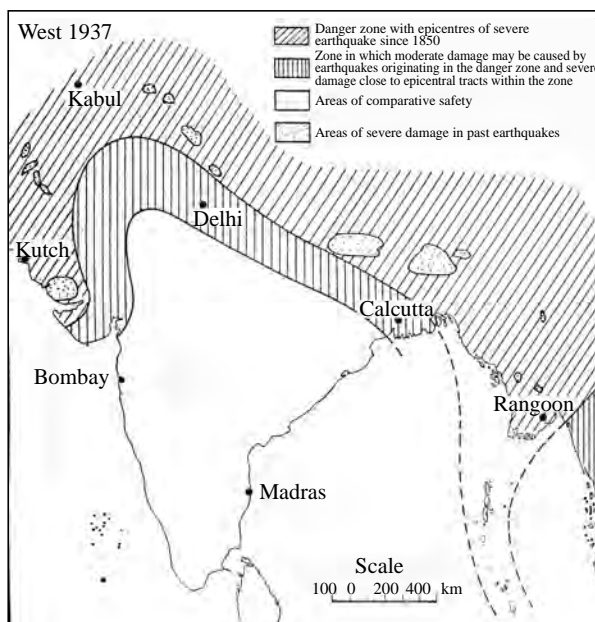


FIGURE 2.2 Earthquake Damage Zone of India by West (1937).

- (i) danger zone that encompasses epicentres of all past earthquakes causing severe damage (MM intensity 'X and above') since 1850,
- (ii) a zone of moderate damage, which might be caused by earthquakes originating in the danger zone and severe damage close to the epicentre region might be caused by the earthquake originating within this zone, and
- (iii) areas of comparative safe zone of slight or no damage.

These two maps relied on the epicentre data of past earthquakes without any reference to the tectonic setting of Indian subcontinent.

By evaluating peak horizontal ground acceleration based on earthquake occurrence data from 1904 to 1950 Jai Krishna (1958 and 1959) developed four-zone seismic map (Figure 2.3). These zones are

- (i) very heavy damage zone corresponding to magnitude 8 anywhere in this zone,
- (ii) heavy damage zone with probable maximum accelerations of 0.3 g due to an epicentre of magnitude 8 earthquake along southern margins of very heavy damage zone,
- (iii) moderate damage zone of ground accelerations between 0.1–0.3 g, and
- (iv) light damage zone corresponding to ground accelerations less than 0.1 g. This map also advocates no seismic consideration in Indian peninsular regions as it was considered to be stable plateau.

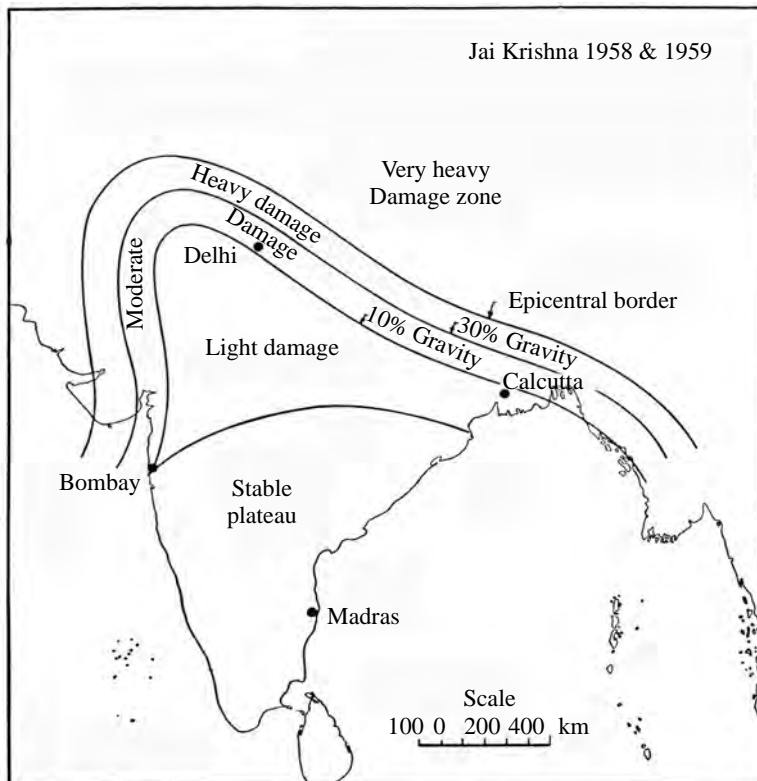


FIGURE 2.3 Seismic Zoning Map of India by Jai Krishna (1958 and 1959).

Mithal and Srivastava (1959) classified occurrence of earthquakes in India on thickness of continental shelf using geophysical data and based on Assam (1897 and 1950), Kangra (1905) and Bihar-Nepal (1934) earthquakes. Three seismic zones (Figure 2.4) named as belt of frequent, occasional and rare earthquakes are of continental shelf thickness of more than 1500 m, less than 1500 m and shield blocks of marginal overburden, respectively.

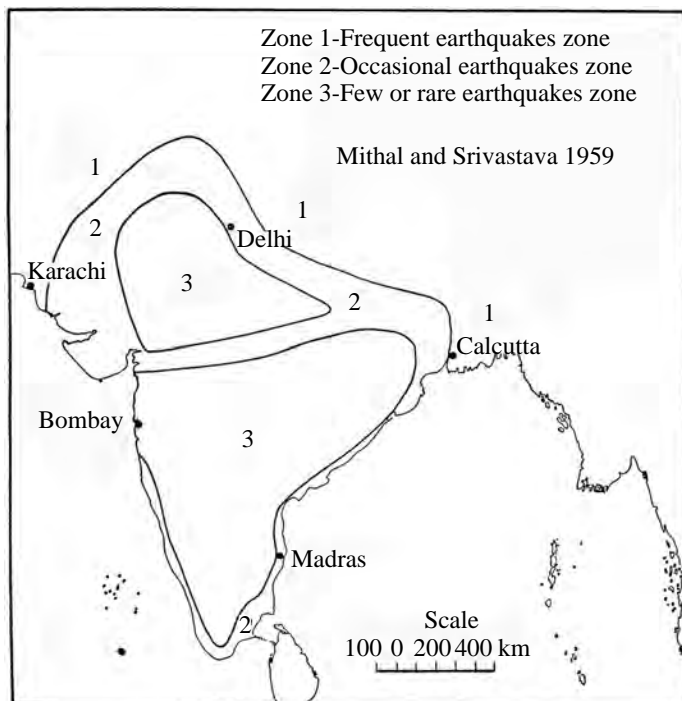


FIGURE 2.4 Seismic Belts of India by Mithal and Srivastava (1959).

2.3 SEISMIC ZONE MAP OF 1962

The Bureau of Indian Standards (BIS) constituted a multi-disciplinary committee of Engineers, Geologist and Seismologist in 1960 to prepare a code of practice for earthquake resistant design of structures. The first comprehensive seismic zoning map was developed by the consensus view of the above committee drawn from various organizations that deal with physics of earthquake and mitigation efforts associated with the earthquake hazard. In view of scanty data of past earthquakes in the country, the committee agreed that evolution of zoning map based only on statistical approach is not likely to provide a representative seismic hazard appraisal. Broad seismotectonics framework of the country was considered to be the basis of the seismic zoning. This was augmented by preliminary tectonic map prepared by GSI and map of epicentres of past earthquakes prepared by the India Meteorological Department (IMD). These maps were included in the Indian Standard Recommendation for Earthquake Resistant Design of Structure IS: 1893–1962. The committee utilized the average intensity attenuation (intensity-magnitude-distance) relationship to draw idealized isoseismal of twenty-three major earthquakes that

produced intensities ‘less than V’, V, VI, VII, VIII, IX and ‘X and above’ in twelve point MM scale. Envelopes for various MM intensities stated as above were drawn. These envelopes were modified to take into account of past seismic activity of smaller magnitude earthquakes, the trend of principal tectonic features and local ground condition (lithological groups).

The isoseismal around Delhi were modified in conformity to the trend of Aravalli Hills. Bellary isoseismal was also modified in the activity trend of minor shocks that occurred in the region extending from Chennai in Tamil Nadu to Thiruvananthapuram in Kerala. A seismic zoning map having seven zones (Figure 2.5), was adopted in IS: 1893–1962. In this recommendation

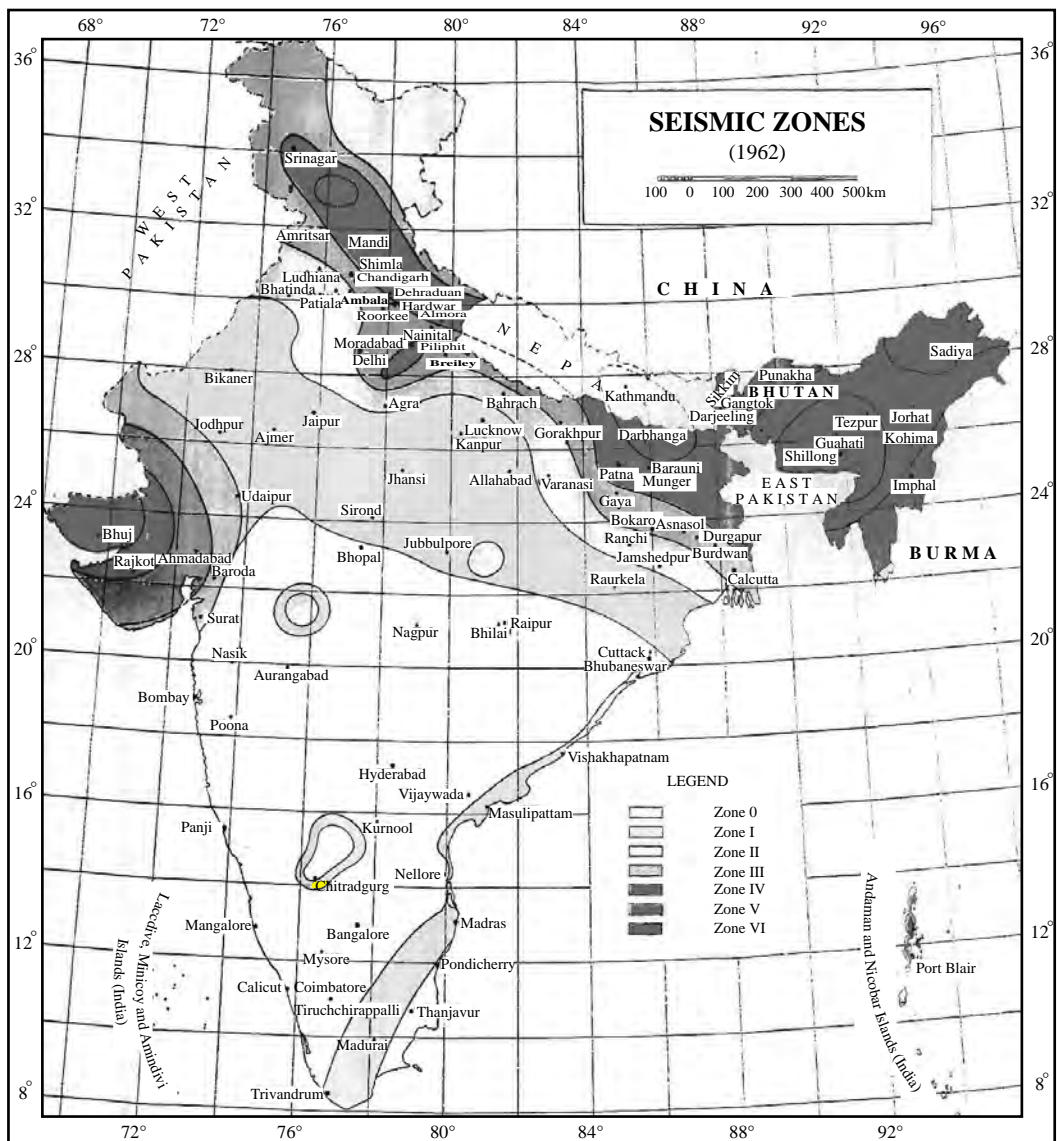


FIGURE 2.5 Seismic Zoning Map of IS: 1893–1962.

the zone corresponding to MM intensity of less than five is termed as zone 0 (zero), to suggest that lateral loading on the structure was envisaged to be small so that the design of structure to carry vertical loads with proper factor of safety was considered to be adequate.

Guha (1962) prepared a seismic regionlisation map (Figure 2.6) with the premise that past earthquake data (epicentres) contains all the information pertaining to seismo-tectonic setup of the country. Isoseismals were drawn and five seismic regions corresponding to MM intensity below V, VI, VII–VIII, IX–X and XI were termed as no damage, moderate damage, heavy damage and very heavy damage. The presumption of availability of historic seismicity data is implicit in the assumption made to prepare the seismic regionalization map.

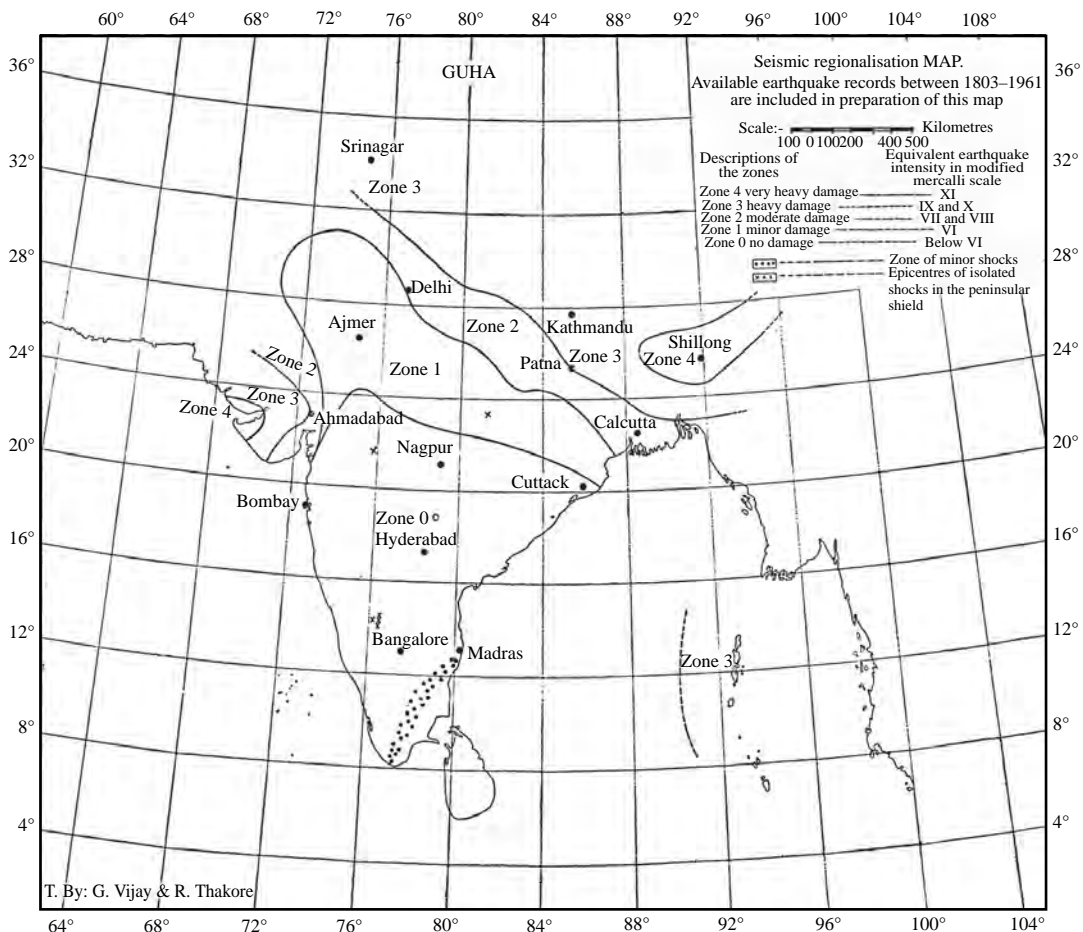


FIGURE 2.6 Seismic Regionalisation Map by Guha (1962).

2.4 SEISMIC ZONE MAP OF 1966

The presence of narrow zones of MM intensity V–VII (Seismic zones I–III) around the Gujarat region contained in seismic zoning map in IS: 1893–1962 was noted as deficiency. The

map included in the published volume was so small that the regions between MM intensity V–VI (seismic zone I-II) boundaries were not visible at the southern part from the east of Vadodara in Gujarat. Moreover, IMD had assigned magnitudes to many historical earthquakes using correlation between magnitude and felt area. Tectonic Map was published by GSI in 1964 at the time of International Geological Congress. The BIS committee revised the seismic zoning map to account for new available information of the historic data and to provide additional emphasis on geology and tectonics in demarcating zones. The committee also decided that the number of zones and methodology need no changes. The major modifications can be grouped as:

2.4.1 Grade Enhancement

Magnitude 8.3 Kutch earthquake of June 16, 1819 had similar grade of damage as of June 12, 1897 Shillong earthquake of magnitude 8.7, January 15, 1934 Bihar-Nepal earthquake of magnitude 8.3 and August 15, 1950 Rima (Assam) earthquake of magnitude 8.6. Based on higher felt area data it was inferred that source of Satpura and Rewa earthquake was of higher potential and consequently the grade of isoseismal of these earthquakes were increased. Consequently isoseismal of Satpura and Rewa earthquakes were elongated taking into account, alignment of Naramda rift as the causative tectonic feature. In this revision isoseismal of Coimbatore earthquake of February 8, 1900 were drawn, the location of Kangra earthquake of 1905 was corrected and the area of MM intensity ‘X and above’ were drawn, based on the observed data. The area of ‘X and above’ intensity at Kangra was graded as zone VI. A region of Zone V based on intensity-magnitude-distance relationship was also introduced around this zone. Bellary earthquake was associated to Dharwarian strike resulting in re-orientation of isoseismal to Northwest-Southeast direction corresponding to Dharwarian trend. Isoseismal V was redrawn taking into account of Oldham’s hypothesis of faulted coastal line (Krishnaswamy, 1977). Based on tectonic setup and occurrence of earthquake in the region it was extended to cover only the ‘marginal depression’ that forms a mobile belt in Maharashtra that underlie the Deccan traps, corresponding to the GSI’s tectonic map.

2.4.2 Review of Tectonic

The activity of past earthquakes were associated to deep-seated trends of Moradabad and Sohna faults in the basement rock of the Gangetic plains from the studies of IMD, which resulted in changing the shape of MM intensity VIII isoseismal. Intensities of Manipur, Tripura and Andaman were enhanced based on available seismic data and tectonic setup. The origin of earthquakes in the Kashmir region was associated to the Himalayan thrust, resulting in the change of shape and grade. The shapes of isoseismals of the entire Northern region (Himachal Pradesh, Haryana and Uttar Pradesh) were modified in the direction parallel to the Himalayan trend. The same philosophy was followed in the north-eastern region also. Isoseismal around Nagaland was modified to conform to tectonics of the region. Corresponding to the trend of Western Ghat, isoseismal in the Kerala region was also redrawn.

The incorporation of changes as above is recommended in IS: 1893–1966 (Figure 2.7) resulted in reduction of the embayment of Zones III and IV in the northern region and the extent of Zone 0 in the southern part of Indian Peninsula in comparison with that of IS: 1893–1962.

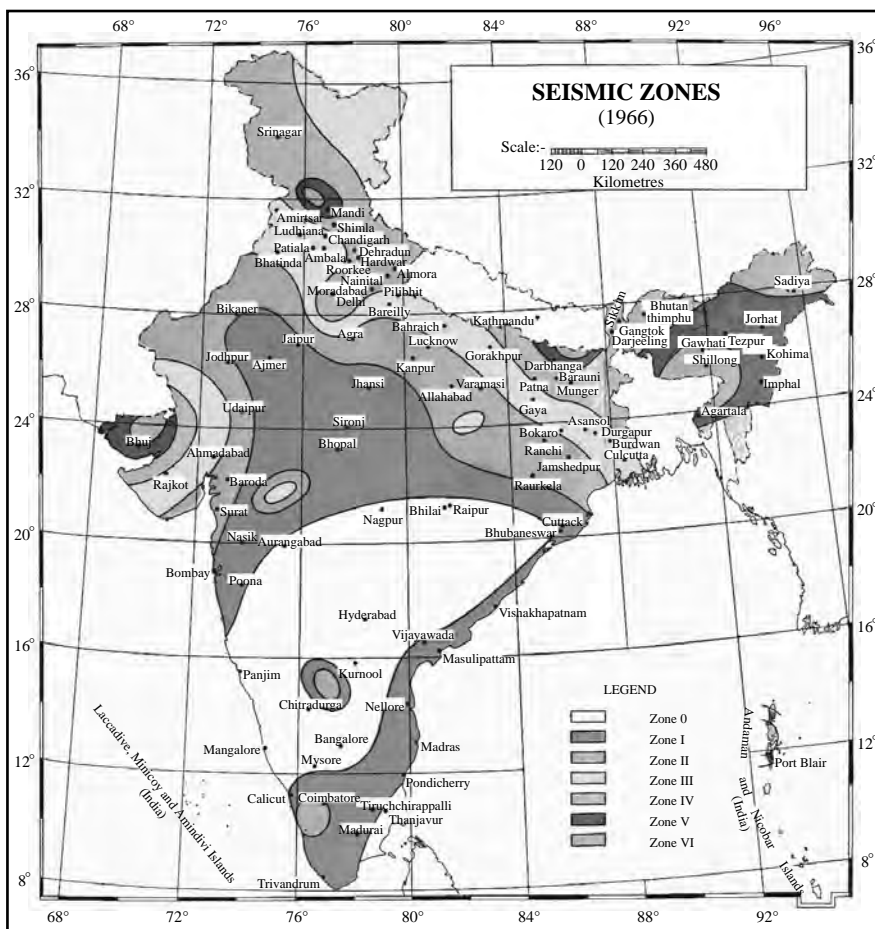


FIGURE 2.7 Seismic Zoning Map of IS: 1893–1966.

2.5 SEISMIC ZONE MAP OF 1970

Just after the publication of the first revision of IS: 1893–1966, magnitude 6.5 Koyna earthquake of December 11, 1967 occurred in Peninsular Shield of India. The second revision of IS: 1893 was taken up in 1968 to review the given low seismic status of the Indian peninsular region and the revised version appeared in 1970 as IS: 1893–1970. The committee by a process of compromise and consensus view of the different disciplines agreed to use seismo-tectonic approach by recognizing geological history and tectonic character of different areas of the country. It was decided that the number of seismic zones would be reduced to five in the revised version instead of seven. The insignificant variation of design provision between the zones corresponding to MM intensity ‘below V’ and V leading to the decision that a single zone of MM intensity below VI would be kept in the revised version. The availability of strong motion data indicated that zones corresponding to MM intensities IX and ‘X and above’ were capable of producing comparable ground acceleration. Thus, these two zones were decided to be merged

to one and termed as MM intensity 'IX and above' zone. Epicentre location, steep geothermal gradient, movement of crust, geomorphic evidence of offset of small landforms, stratigraphic evidence, gravity anomalies were utilised in demarcating seismo-tectonic setup of India. Krishnaswamy (in Srivastava, 1969) proposed five principal seismo-tectonic units (Figure 2.8 and Table 2.1) based on these. The proposed seismo-tectonic units are as follows:

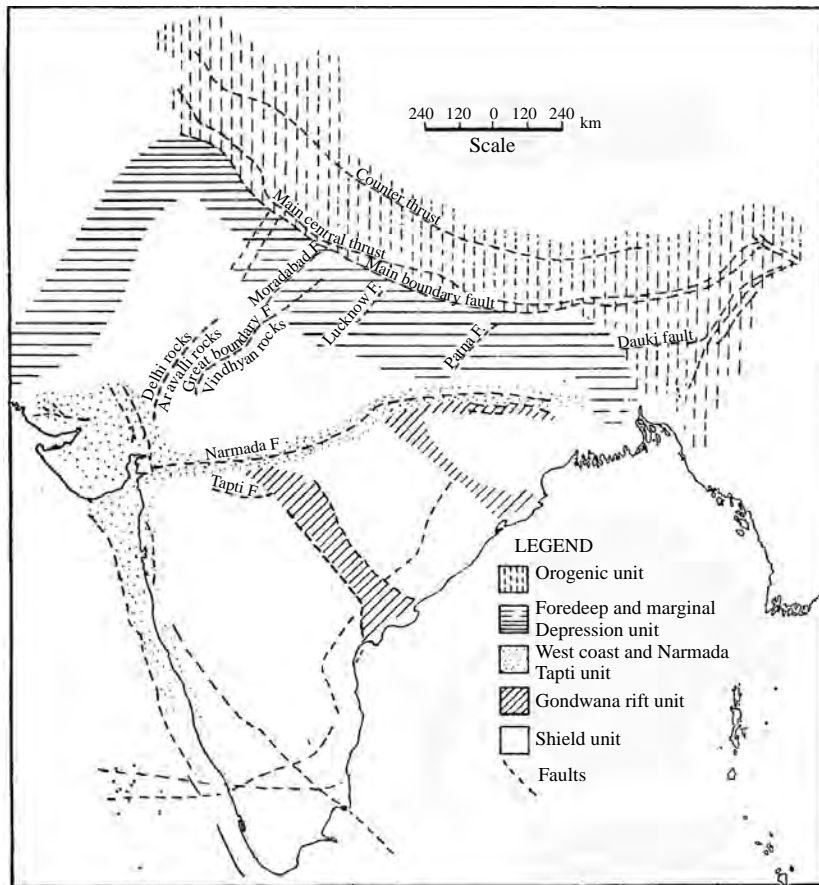


FIGURE 2.8 Generalised tectonic unit of Indian subcontinent (Krishnaswamy (in Srivastava, 1969)).

1. Shield unit of peninsular India with ancient faults and localized seismic activity encompassed by MM intensity 'less than VI' and VI.
2. Gondwana rift unit of peninsular India with Mesozoic fault movements and the later adjustments that includes the Gondwana graben and adjacent platform cover of peninsular shield with Mesozoic Tertiary sediments were in general of MM intensity VII.
3. West Coast and Narmada-Tapti unit of peninsular shield that is segmented by Tertiary-Quaternary fault movements including the West Coast, Narmada-Son and Tapti rift zone and their extension corresponding to MM intensity VII with islands of MM intensity VIII.

TABLE 2.1 Generalised tectonic units of India with decreasing magnitude and frequency of earthquake occurrence (after Krishnaswamy (in Srivastava, 1969)).

Tectonic unit	Name	Description	Earthquake occurrence		Seismic zones
			Earthquake occurrence	Seismic zones	
1. Orogenic	Orogenic unit of Cenozoic folding and faulting. The Shillong Massif, which has been greatly affected by this faulting, has been included in this zone.	Common shocks of magnitude 5–6.5 with a number of shocks of magnitude 6.5–7.5, a few shocks of magnitude 7.5–8 and occasional shocks greater than 8 originating on some of the major Himalayan thrust and faults (Satlita thrust, Pinjor thrust, Central Himalayan thrust, Dauki faults, etc.)	Common shocks of magnitude 5–6 with a few shocks of magnitude 6–7 and occasional shocks of magnitude 7.5–8 originating along active faults in the basement (Patna fault? or other basement faults, Kutch faults).	III and IV with islets of V	IV and V
2. Foredeep and marginal depression	Unit of Himalayan foredeep and marginal depression (where the boundary is not positively established, some of the marginal parts of the shield may really be included in this zone. The Tectonic Map provisionally defines the boundary at 200–1000 m contour of the basement at margin of the shield).	Unit of Shield with Tertiary–Quaternary fault movement including the West coast seismogenic zone, the Narmada–Son rift zone, the Tapti rift zone and their postulated extensions.	Common shocks of magnitude 5–6 with a few shocks of magnitude 6–7 in Narmada and Tapti rifts. Past epicentres can be related to extensions of partly mapped faults. Maximum recorded magnitude on West coast Zone 6.6–7, on Narmada rift 6.5, Tapti rift 6.25.	III with islets of IV	III
3. West coast and Narmada-Tapti			Occasional shocks of magnitude 5–6 with few centres, which may have magnitude 6–6.5 and may be related to the boundary faults of the Gondwana basin and faults of limited extent in the Mesozoic–Cenozoic cover on the platform.		
4. Gondwana rifts	Unit of shield with Mesozoic fault movements and later adjustments, include Gondwana rift zone and adjacent parts of the shield, marginal parts of the peninsular shield to the east and north with platform cover of Mesozoic–Cenozoic sediments.	Generally aseismogenic and partitioned areas of the peninsular shield with ancient faults and with localized seismogenic features.	Occasional shocks of magnitude 5–6 with exceptional activity along local faults in the Archaeans with magnitude 6–6.5.	I and II with islets of III	I and II with islets of III
5. Shield					

4. Himalayan foreland basins (foredeep) and marginal depression units generally contains areas of MM intensities VII and VIII with islets of MM intensity 'IX and above'.
5. Mountain belts (Orogenic area) that formed by folding and faulting of earth's crust in the era beginning from Tertiary period to the present time (Cenozoic) encompassing zones of MM intensity 'VIII and above' in general.

The seismic zones I-V in this IS: 1893–1970 (Figure 2.9) broadly follows the trends of above stated five seismo-tectonic units in general. The demarcated seismo-tectonic provinces had earthquakes of different focal depths. Earthquake magnitude and frequency show an overall increase in general as the zone increase from zone I to zone V with some exception. The following modifications were also made besides the defined seismic zones on the basis of the five seismo-tectonic provinces as above.

Four new separate islets were demarcated as zone V (MM intensity 'IX and above') to take into account the postulated higher seismic status in view of tectonic/past earthquake. These were islets:



FIGURE 2.9 Seismic Zoning Map of IS: 1893–1970.

- (i) around Srinagar relating to down-dip extension of Pinjal thrust,
- (ii) epicentral tract of 1905 Kangra earthquake was related to the extension of Sattilata thrust and an island around Dharmshala in Himachal Pradesh was introduced,
- (iii) around western Nepal and Pithoragarh of Uttarakhand was associated with extension of Himalayan thrust and
- (iv) epicentral tract of 1934 Bihar-Nepal earthquake in seismic zone IV.

An islet of zone IV encompassing epicentral region of 1967 Koyna earthquake was also introduced in the new Western coast seismic zone III. Seismic status of entire Assam, Mizo hills, Tripura and northeast part of Kashmir were enhanced by one based on tectonics and seismicity. In recognition of total tectonic framework entire Andaman island was demarcated as zone V. Two new seismic zones of level III were introduced along Western coast and along marginal depression in Rajasthan. Seismic status of parts of Indo-Gangetic trough was raised due to re-demarcation in accordance to tectonic features. Narmada-Son-Tapti zone was merged with Damodar graben in the east. The isoseismals for Bellary and Coimbatore earthquakes were redrawn due to revised estimates of magnitudes. The islet around Coimbatore was nonexistent due to introduction of costal belt of seismic zone III in the Western coast. The entire Lakshadweep group of islands was in seismic zone III in conformity to Western coast belt. The seismic zone I was limited on the basis of extent of platform cover and past earthquake data resulting in curtailment of extent of zone I.

Srivastava (1974) indicated that the correlation of likely maximum Richter magnitude with the seismic zones I-V was ‘less than 5’, 5-6, 6-6.5, 6.5-7 and ‘greater than 7’. The maximum magnitude as indicated might be ‘maximum considered magnitude’.

2.6 SEISMIC ZONE MAP OF 2002

BIS constituted a committee to review seismic status of Indian peninsular shield due to magnitude 6.2 Killari (Latur) earthquake of September 30, 1993. The committee decided to enhance seismic zone I to seismic zone II. It was also decided that an interim revision to review seismic status of peninsular India be made as a revised map based on probabilistic hazard analysis would be made in future. The committee decided to do a pattern analysis of earthquake hazard using a combination of seismo-tectonics and probabilistic method for Peninsular India below latitude N 22°. The recently available instrumental seismic data were used in this study. The result of the study had enhanced extent of seismic zone III to include area beyond Chennai in the south and removal of islets of zone III surrounding epicentral tract of Bellary earthquake. Thus a four-zone seismic zoning map was adopted in IS: 1893–2002 (Figure 2.10). It is to be noted that probabilistic assessment portrays the total hazard from all sources around a site whereas the deterministic assessment is in general based on a single source.

2.7 EPILOGUE

The proposed hazard maps prior to IS: 1893–1962 presumed that earthquake processes in the recent past in all likelihood would be the same as those in the near future. These maps were primarily based on the effects of four Himalayan earthquakes and Kutch earthquake. Mital and

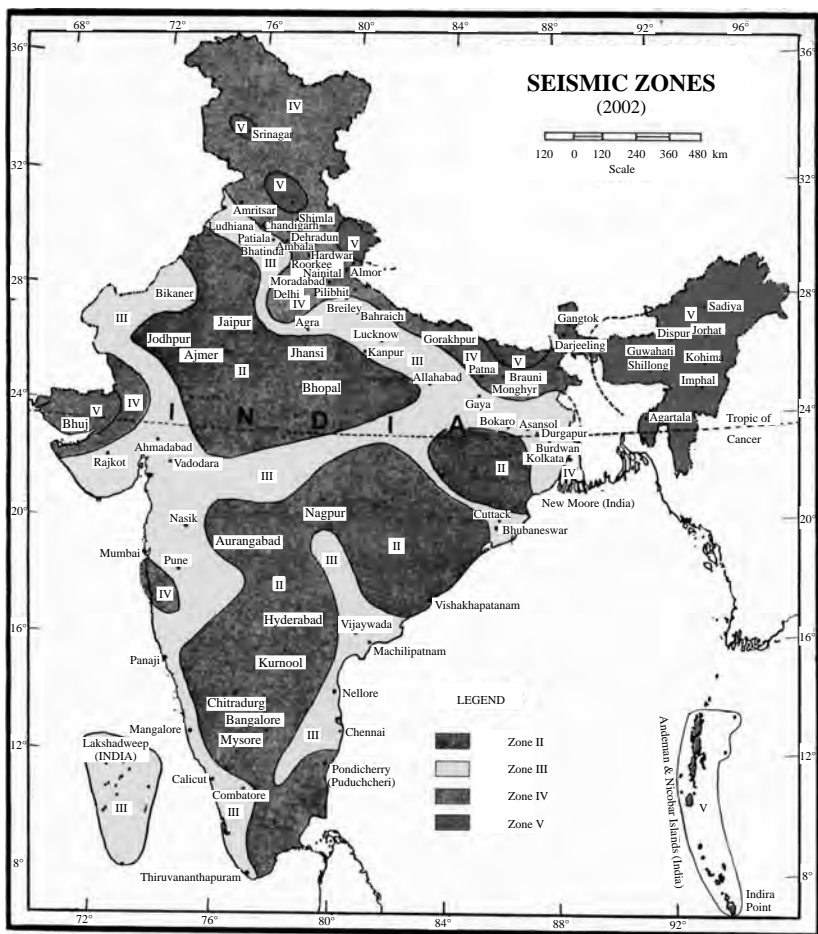


FIGURE 2.10 Seismic Zoning Map of IS: 1893–2002.

Srivastava (1959) did not consider 1819 Kutch earthquake for establishing the seismic belt. More importance was given to geologic and tectonic setup in demarcating the seismic zoning map from the revision of 1966 onwards. The seismic zone V in the BIS code in the Bhuj region in Gujarat can only be justified by the deterministic zoning method. The occurrence of earthquake in this region is very infrequent that result in long return period. The hazard determined in this region using probabilistic theory will be lower than that determined using deterministic theory. Similarly islets of seismic zone V in the seismic zone IV in the northern region is due to the observed estimated intensities of past earthquakes. These islets in the zoning map are due to the use of deterministic theory.

The decision of the BIS is to have a new revised zoning map using probabilistic framework. This needs to have an answer to ‘acceptable risk’ and answer to the ‘safety level’. The present committee of BIS must be extended to include member of planning commission and finance/commerce ministry to establish the minimum requirement of safety and acceptable risk. Moreover, prior to embarking on probabilistic zoning basis map for the country, boundaries of

different seismo-tectonic block of the entire country should be made.

SUMMARY

The description of perceived threat from earthquakes in different parts of the country in the form of a map began in 1935. The most recent revision of this map was taken up in 2002. This evolution of seismic zoning map of Indian subcontinent is described in this chapter. The basis and data used in the preparation of these zoning maps are discussed. The future trends in the preparation of seismic zoning map on the basis of the probabilistic hazard analysis is also discussed.

REFERENCES

- [1] Auden, J.B., "Earthquake in Relation to Damodar Valley Project", *Earthquake Engineering Seminar*, H.L. Sally (Ed.), University of Roorkee, India, pp. 212–216, 1959.
- [2] West, W.D., "Earthquake in India (Presidential Address)", *24 Indian Science Congress*, pp. 189–227, 1937.
- [3] Krishna, J., "Earthquake Engineering Problems in India", *Journal of Institution of Engineers*, India, 1958.
- [4] Krishna, J., "Seismic Zoning of India", *Earthquake Engineering Seminar*, H.L. Sally, (Ed.), University of Roorkee, India, pp. 24–31, 1959.
- [5] Mithal, R.S. and Srivastava, L.S., "Geotectonic Position and Earthquakes of Ganga-Brahmaputra Region", in H.L. Sally, (Ed.), *Earthquake Engineering Seminar*, University of Roorkee, India, pp. 217–233, 1959.
- [6] IS: 1893–1962, *Indian Standard Recommendations for Earthquake Resistance of Structures*, Indian Standards Institute, New Delhi, 1962.
- [7] Guha, S.K. "Seismic Regionalisation of India", *Second Symposium on Earthquake Engineering*, University of Roorkee, India, 1962.
- [8] IS: 1893–1966, *Indian Standard Recommendations for Earthquake Resistance of Structures* (First Revision), Indian Standards Institute, New Delhi 1967.
- [9] Krishnaswamy V.K., "The Evolution of Seismic Zoning Map of India", *Souvenir Volume*, H.M. Choudhury, (Ed.), *Sixth World Conference of Earthquake Engineering*, Prabhat Press, Uttar Pradesh, pp. 77–89, 1977.
- [10] IS: 1893–1970, *Indian Standard Criteria for Earthquake Resistance of Structures* (Second Revision), Indian Standards Institute, New Delhi, 1971.
- [11] Srivastava L.S., "A Note on the Seismic Zoning Map of India", *Bulletin of the Indian Society of Earthquake Technology*, 6(4): pp. 185–194, 1969.
- [12] Srivastava, L.S., "Seismic Zoning Map of India", *Earthquake Engineering—Jai Krishna Sixtieth Birth Anniversary Commemoration Volume*, Sarita Prakashan, Meerut, India, pp. 49–65, 1974.
- [13] IS: 1893, *Indian Standard Criteria for Earthquake Resistance of Structures—Part 1: General Provisions and Buildings* (Fifth Revision), Bureau of Indian Standards, New Delhi, 2002.

Chapter 3

Strong Motion Studies in India

3.1 INTRODUCTION

The UNESCO had declared the nineties as the *International Decade for Natural Disaster Reduction (IDNDR)*. Ironically, this decade also witnessed four earthquakes of magnitude 6.0 and above occurring in the Himalayas, central India, and the peninsular region resulting into approximately 10000 casualties and many more injuries. These figures would have been much higher, if these earthquakes had occurred in the neighbourhood of large urban centres, as was seen in the case of the Bhuj earthquake of January 2001. This earthquake alone accounted for more than 15000 lives in addition to having a crippling effect on the economy of the region. These disastrous consequences could have been avoided had the systems been designed to withstand earthquake ground motions. Quoting from the declaration of the United Nations International Decade for Natural Disaster Reduction (UNIDNDR) Yokohama Convention 1994:

The impact of natural disasters in terms of human and economic losses has risen in recent years, and society in general has become more vulnerable to natural disasters. Those usually most affected by natural and other disasters are the poor and socially disadvantaged groups in developing countries as they are least equipped to cope with them.

Disaster prevention, mitigation, preparedness and relief are four elements which contribute to and gain from the implementation of sustainable development policies. These elements, along with environmental protection and sustainable development, are closely interrelated. Therefore, nations should incorporate them in their development plans and ensure efficient follow-up measures at the community, sub-regional, regional, national and international levels.

Disaster response alone is not sufficient, as it yields only temporary results at a very high cost. We have followed this limited approach for too long. This has been further demonstrated by the recent focus on response to complex emergencies which, although compelling should not divert from pursuing a comprehensive approach.

The facts are clear—we cannot prevent big, destructive earthquakes from occurring. These pose a continuing threat to lives and property in more than 55% of the area of this country. However, it is possible to avoid the disastrous consequences of an earthquake and that precisely

is the objective of every seismic design code of practice. The seismic design codes are framed primarily with the objective of prevention of loss of life. In order to meet this objective it is essential that the structures/constructed facilities respond to the expected earthquake ground motions at the site in a designated manner, which in turn depends on the nature of ground motion exciting the structure. Thus the reliability of achieving the life safety performance objective of any constructed facility is governed by the most uncertain element in the chain—*expected ground motion*. The strong motion studies are aimed at reducing the uncertainties in the specification of expected earthquake ground motions for designing any structure.

3.2 UNDERSTANDING THE NATURE OF GROUND MOTIONS

The complexity of earthquake ground motion is primarily due to three factors: (i) the seismic waves generated at the time of earthquake fault movement are not of a uniform character (source effect), (ii) as these waves pass through the earth on their way from the fault to the project site, they are modified by the soil and rock media through which they pass (path effect), and (iii) once the seismic waves reach the project site, they undergo further modifications, which are dependent upon the characteristics of the ground and soil at the site (local site effects). Each of these factors will be discussed with reference to the possible implications for design recommendations.

3.2.1 Source Effect

Earthquake is a manifestation of rapid release of stress waves during a brittle rupture of rock mass along a geologic fault zone. The size and type of rupture has a significant influence on the nature of ground motion. The size of the earthquake is proportional to the size of fault rupture area which, in turn, is proportional to the total energy released—a measure of the *magnitude* of the earthquake. The potential of a geologic fault to generate large earthquakes is estimated from the past seismicity data. In general, a large magnitude earthquake (with large fault rupture area) will result in a longer duration of shaking and vice versa.

These inferences about the characteristics of earthquake ground motions have been drawn from the study of strong motion data recorded over the years. Nevertheless, the nature of the ground motion in the neighbourhood of fault rupture (near-field say, within a radius of 20-60 km) is further influenced by the movements along the fault, which are not accounted for in these inferences. Though existence of some of these effects had been postulated as early as 1985 [29], those could not be verified for the lack of recorded strong motion data in the near-field. With the deployment of dense arrays of strong motion recording instruments, the database of quality strong motion records is building up (see, e.g., <http://db.cosmos-eq.org>) which also includes the near-field strong motion data from several recent earthquakes. Analyses of the near-field strong motion data points to three distinct effects described as follows:

(i) Rupture directivity effect

The rupture directivity effect is essentially a manifestation of Doppler's effect in seismic wave propagation and affects the ground motion in fault parallel direction. This occurs when the

velocity of rupture is close to the velocity of shear waves in the rock mass near the source. The seismic waves observed at a site in the direction of fault rupture will have higher frequency in comparison to the waves observed at an equally spaced site in the direction away from the direction of fault rupture. This phenomenon is illustrated schematically in Figure 3.1. In particular, the rupture directivity effect results in a large amplitude, short duration pulse at the site in the direction of rupture and a small amplitude, long duration pulse at the site in the direction opposite to the direction of fault rupture.

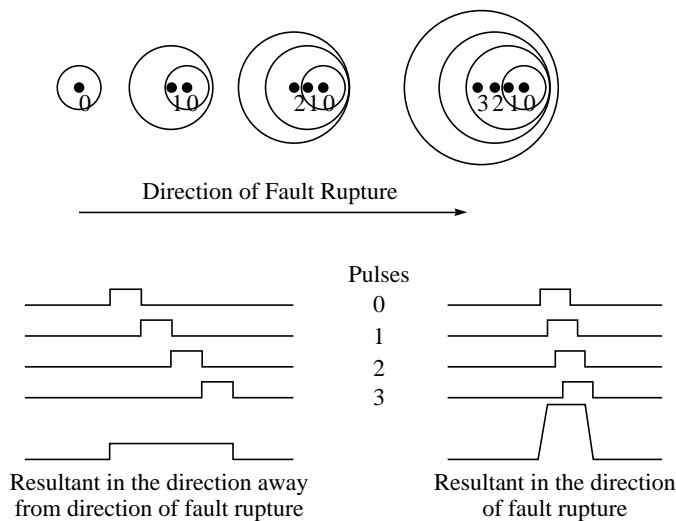


FIGURE 3.1 Illustration of directivity effect on ground motion at sites toward and away from direction of fault rupture (after [29]).

(ii) Fling effect

Some near-field strong motion data recorded on modern digital equipment during the 1999 Turkey and Taiwan earthquakes show some permanent ground displacement that occurs across a ruptured fault. This static displacement, termed *fling step*, occurs over a finite time interval of several seconds as the fault slip is developed. The fling step involves a large, unidirectional velocity pulse to accommodate this displacement in the slip-parallel direction and is not strongly coupled with the rupture directivity pulse. In strike-slip faulting, the directivity pulse occurs on the strike-normal component while the fling step occurs on the strike-parallel component. In dip-slip faulting both the fling step and the directivity pulse occur on the strike-normal component. A schematic illustration of the orientations of fling step and rupture directivity pulse are shown in Figure 3.2.

The feature of rupture directivity effect, that is most damaging to structures is the large velocity pulse, which can lead to one yield reversal with a large ductility demand. On the other hand, fling step affects the peak velocity and displacement of ground motions. These near fault source effects, which comprise of brief and impulsive ground motions, can not be adequately described in frequency domain which characterizes a uniform distribution of energy throughout the duration of motion. Thus the conventional characterization of design ground motion in the

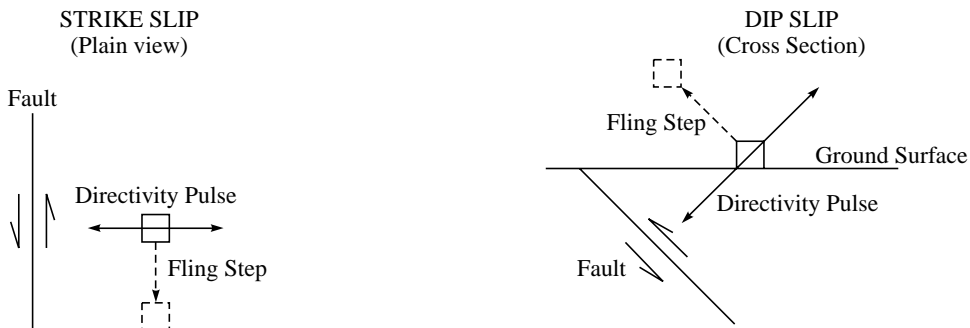


FIGURE 3.2 Schematic illustration of the orientations of fling step and directivity pulse in strike-slip and dip-slip faults (after [32]).

form of response spectra needs to be augmented with a simplified description of the near-source pulses in time domain. A simple characterization is indeed possible with the use of Peak Horizontal Velocity (PHV), approximate period of the dominant pulse (T_v), and the number of significant half-cycles of motion in the larger, fault-normal direction [16].

(iii) Hanging wall effect

The hanging wall effect is primarily due to the proximity of much of the fault to the sites on hanging wall side. It has been observed to have the most pronounced effect for periods shorter than about 1 s, and at locations away from the top-edge of the fault on the hanging wall side. The rupture directivity effect, on the other hand, is due to rupture propagation and radiation pattern effects. It is more pronounced for periods longer than 1 s, and is concentrated over the top edge of the fault. The relationship between the rupture directivity effect and the hanging wall effect is thus complementary both in the region of influence and the affected period range, thereby increasing the degree of spatial variation of strong ground motion around dipping faults [2].

Sites on the hanging wall of a dipping fault have closer proximity to the fault as a whole than do the sites at the same closest distance on the foot wall side, causing larger short period motions on the hanging wall than on the foot wall. The hanging wall effect is observed to be the greatest in the closest distance range of 8 to 18 km for periods of 0 to 0.6 s, and decreases to unity at 5 s [1].

3.2.2 Path Effect

Although the total energy released during an earthquake is a constant parameter for a particular seismic event the specific energy, which is defined as the seismic energy per unit volume, decreases due to advancing wavefront. This decrease is purely geometrical in nature as the volume of the medium over which the total seismic energy is distributed increases as the wavefront advances. When the earthquake energy is released from a fault below the ground surface, body waves travel away from the source in all directions. If we assume the rupture zone to be a point source, the wavefronts will be spherical and it can be proved that the geometric

attenuation will cause the amplitude of the body waves to decrease at a rate of $1/r$, where r represents the radius of the wavefront. It has also been shown that the geometric attenuation of surface waves occurs at a rate of $1/\sqrt{r}$ [7]. Thus the surface waves attenuate much more slowly than the body waves, which also explains the fact that the ground motion at large epicentral distances predominantly comprises surface wave. In addition to these geometric attenuation effects, the seismic waves also experience an attenuation of amplitudes on account of the dissipation of seismic energy due to material damping in the soil. A combination of both these effects represents the influence of path effects on the nature of ground motion at a site.

3.2.3 Site Effect

Incorporation of the site effects in ground motion estimation procedures is aimed at reducing the uncertainty in the ground motion estimates as measured by the standard error of the regression analysis and also to remove the potential bias in median estimates. The site effects represent the local influences on the nature of ground motion and include the local ground response, basin effects, and the surface topography. The *local ground response* refers to the response of shallow geological deposits to the vertically propagating body waves. The modelling should ideally involve the full soil profile up to the bed rock level at the site but for deep alluvial deposits, reasonable estimates can usually be obtained by considering the soil profile only up to a depth of 100–120 m. The *basin effects* correspond to the influence of two or three-dimensional extent of the sedimentary basin structures on ground motions, including critical body wave reflections and surface wave generation at basin edges. The dividing line between the local ground response effects and the basin effects is rather arbitrary and usually the local ground response effects refer to the one-dimensional response of soil column and basin effects are considered account for the observed ground motion characteristics that deviate from the predictions of one-dimensional analysis. The presence of ridges and valleys at the site can also have some influence on the nature of ground motion. An approximate estimate of these effects for certain cases of ridge-valley terrain is possible by using analytical solutions for some idealized geometries [24].

The effect of soil layer on the nature of surface ground motion can be divided into two principal components: (i) the predominant period of surface ground motion, and (ii) spectral amplification with respect to the bed rock motion. These effects may be studied by analyzing the recorded strong motion data after eliminating the source and path effects from the strong motion recordings. Two different approaches have been adopted to achieve this end: (i) by comparing the strong motion recorded on soil site with motions from a reference site (usually rock) [5, 31], and (ii) without using any reference site recordings [11, 19].

(i) Reference Site Approach

If a reference site can be found in the close vicinity of the soil site then the motions at both sites are expected to have similar source and path effects. Thus a comparison of the two motions provides an estimate of the local site effect. In practice ratios of either response spectra, or (smoothed) Fourier spectra of the motions recorded at soil site and the reference site is taken to be a representative of the *transfer function* of the soil column at the site. The predominant period

and amplification factor can be estimated from the location and amplitude of peaks of derived transfer functions.

(ii) Non-reference Site Approach

Since the availability of a rocky outcrop in the close vicinity of the site can not always be guaranteed, a few approaches have been proposed for estimation of site effects, which do not require availability of reference site data. A very popular approach is to take the ratio of the spectrum of horizontal component of motion with respect to the spectrum of the vertical component of the motion (termed as H/V ratio) at the same site. This spectral ratio is considered as the transfer function of the site. The ease of applicability of this approach has lured many to adopt this approach in site characterization studies. However, it has been shown that the estimates (predominant period and amplification factors) predicted by H/V ratios are not stable for the same site using different records [25]. Yet another non-reference site approach involves normalization of the spectra of recorded motions by a reference spectrum for rocky site obtained from some attenuation relationships [30].

Since the data from large, strong earthquakes in near-field region of intense motions is quite sparse, the use of microtremor data and/or records from small, frequent earthquakes has been proposed to study the site effects [14, 17]. Unfortunately, the behaviour of soil column during strong motions generated by large, strong earthquakes differs substantially from that during small earthquakes (weak motions). In particular, the large strain levels associated with the strong motions during large earthquakes force the soil to respond non-linearly as against an essentially linear response during small strain weak motions. It has been shown in several studies in different regions of the world that site effects estimated by using weak motion records, or the microtremor data do not correlate well with the observed behaviour of the soil during strong earthquakes [3, 6, 18, 25, 38, 40, 41, 42, 44].

3.3 ESTIMATION OF GROUND MOTION PARAMETERS

In such a scenario, the estimates of site effects using the transfer function theory of linear systems do not seem to be of much use in estimating the expected motions due to strong, damaging earthquakes. It is, therefore, more rational to relate the ground motion parameter of interest directly in terms of earthquake size, type of fault rupture, source to site distance, surface geology at the site, depth to bedrock level at the site, etc. to represent the mechanics of ground motion process as closely as possible. The co-efficients of these predictive relationships are obtained by regression analyses of recorded strong motion data. With the inclusion of more data with time, the uncertainties in the estimated design ground motions should decrease. A generic expression for this purpose generally takes the form [15]:

$$\ln Y = c_1 + c_2 M + c_3 M c_4 + c_5 \ln [R + c_6 \exp(c_7 M)] + c_8 R + f_1(\text{source}) + f_2(\text{site})$$

where Y represents the desired ground motion parameter (assumed to be distributed log-normally), M is a measure of the size of the earthquake, R is a measure of source-to-site distance, f_1 and f_2 are some suitable functions of source parameters (e.g., type of faulting, etc.) and local site conditions (soil/rock), respectively. Usually, such relations provide the median estimate of

the ground motion parameter in question. The uncertainties associated with this estimate are reflected in the error term $\sigma_{\ln Y}$ of the regression. Such predictive relations have indeed been developed for the Fourier and pseudo-spectral velocity spectra [36, 37, 39], peak ground acceleration [8, 10, 12, 13] and strong motion duration [21, 22, 43], etc.

3.4 THE INDIAN PERSPECTIVE

The strong motion studies were taken up in India in 1976 on the recommendations of the planning commission. Two types of strong motion recording instruments namely, **Roorkee Earthquake School Accelerograph (RESA)** and the **Structural Response Recorders (SRR)** were designed and fabricated at the Department of Earthquake Engineering, Indian Institute of Technology, Roorkee (then, University of Roorkee). Today, the department maintains a network of over 200 accelerographs and 350 SRRs in the Himalayan and sub-Himalayan belt as shown in Figure 3.3. Seventeen earthquakes have been recorded by the instruments of this network till date with the most recent one being the Kutch earthquake of January 26, 2001 [9]. The data recorded by this network of strong motion instruments has been of immense help in development of the standard spectral shape in the recent revision of the seismic design code IS-1893 (Part 1): 2002 [23]. Currently work is in progress for the installation of 3-dimensional array of strong motion accelerographs in Tehri to study the effects of soil column response at various elevations. The analysis of data recorded by this network will aid in the development of a more rational basis for design of underground facilities. The strong motion data recorded by this network, will also allow studies on the effect of topography, and basin structure. In addition to the free-field earthquake recording instruments, the department also maintains networks of accelerometers in several high-rise buildings in different parts of the country.

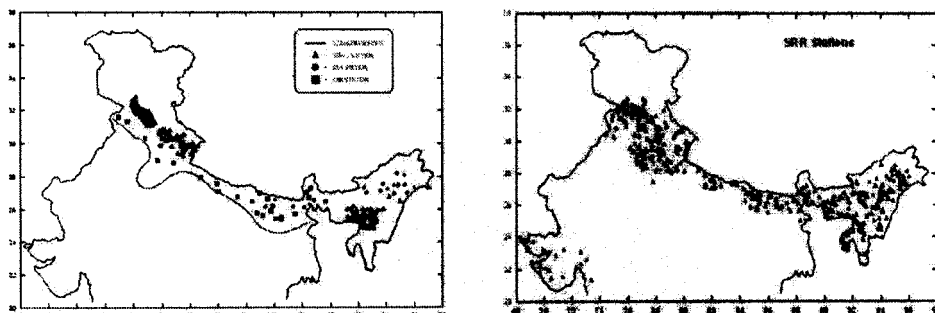


FIGURE 3.3 Installations of free-field Strong Motion Accelerographs (SMA) and Structural Response Recorders (SRR) by Department of Earthquake Engineering, Indian Institute of Technology, Roorkee.

3.5 UTILIZATION OF STRONG MOTION DATA

There can be no short-cuts for developing specifications for design earthquake ground motions, which have to be derived on the basis of analyses of recorded strong motion data. The commonly

recommended approach of using easily available weak motion data instead of data from less frequent strong earthquakes may lead to gross errors in land-use planning in addition to leading to unsafe designs [25]. Strong motion data helps in developing a better understanding of (i) ground response near fault ruptures of large earthquakes, (ii) effects of severe shaking on different sub-surface structures and geologic materials, and (iii) ground response in areas that are prone to liquefaction. Analysis of strong motion records also leads to the development of improved methods for generating artificial earthquake motions for regions where the data from real earthquakes are not available [27, 28]. The data recorded by the network of instruments in high-rise buildings can be used for deriving information for remote monitoring of the health of the building, the locations and extent of repair works required, and to verify adequacy of the analytical modeling and design guidelines.

The strong motion data as recorded by the strong motion instruments, however, are not directly useful for strong motion studies. The raw data has to be first processed and corrected for various possible sources of errors which might have crept in during the process of recording. A detailed discussion of the various issues of strong motion data processing may be found in other publications [4, 20, 26, 33, 34, 35].

SUMMARY

This chapter contains discussion of the various issues involved in strong motion studies—primarily a discussion of what, why, and how. The emphasis is on developing an understanding of the problem of characterizing design earthquake ground motions. This will help readers to interpret correctly the relevant clauses in design codes and also in making a judicious decision in special cases requiring special attention beyond the scope of the standard codes of practice.

REFERENCES

- [1] Abrahamson, N.A. and Silva, W.J., "Empirical Response Spectral Attenuation Relations for Shallow Crustal Earthquakes". *Seismological Research Letters*, 68: 94–127, 1997.
- [2] Abrahamson, N.A. and Somerville, P.G., "Effects of the Hanging Wall and Foot Wall on Ground Motions Recorded during the Northridge Earthquake", *Bulletin of the Seismological Society of America*, 86: S93–S99, 1996.
- [3] Aki, K., Chin, B.-H., and Kato, K., "Seismological and Geotechnical Studies of Local Site Effects on Strong and Weak Motions", In *Proceedings of the International Symposium on the Effects of Surface Geology on Seismic Motion, ESG1992, Odawara, Japan*, Pages I: 97–110, IASPEI/IAEE Joint Working Group on ESG, Association for Earthquake Disaster Prevention, Tokyo, Japan, 1992.
- [4] Boore, D.M., Stephens, C.D., and Joyner, W.B., "Comments on Baseline Correction of Digital Strong Motion Data: Examples from the 1999 Hector Mine, California Earthquake", *Bulletin of the Seismological Society of America*, 92(4): 1543–1560, 2002.

- [5] Borcherdt, R.D., "Effects of Local Geology on Ground Motion Near San Francisco Bay". *Bulletin of the Seismological Society of America*, 60: 29–61, 1970.
- [6] Bresnev, I.A. and Wen, K.-L., "Nonlinear Soil Response—A Reality?", *Bulletin of the Seismological Society of America*, 86: 1964–1978, 1996.
- [7] Bullen, K.E., *An Introduction to the Theory of Seismology*, Cambridge University Press, London, 1953.
- [8] Campbell, K.W., "Near Source Attenuation of Peak Horizontal Acceleration", *Bulletin of the Seismological Society of America*, 71: 2039–2070, 1981.
- [9] Chandra, B., Thakkar S.K., Basu S., Kumar A., Shrikhande M., Das J., Agarwal P., and Bansal M.K., "Strong Motion Records", *Earthquake Spectra*, Supplement A to Volume 18: 53–66, 2002.
- [10] Crouse, C.B., "Ground-motion Attenuation Equations for Earthquakes on the Cascadia Subduction Zone". *Earthquake Spectra*, 7(2): 201–236, 1991.
- [11] Field, E.H. and Jacob, K.H., "A Comparison and Test of Various Site Response Estimation Techniques, Including Three that are Non Reference-site Dependent". *Bulletin of the Seismological Society of America*, 85: 1127–1143, 1995.
- [12] Joyner, W.B. and Boore, D.M., "Method for Regression Analysis of Strong Motion Data", *Bulletin of the Seismological Society of America*, 83: 469–487, 1993 (Errata in 1994).
- [13] Joyner, W.B. and Boore, D.M., "Errata: Method for Regression Analysis of Strong Motion Data". *Bulletin of the Seismological Society of America*, 84: 955–956, 1994.
- [14] Konno, K. and Ohmachi, T., "Ground-motion Characteristics Estimated from Spectral Ratio between Horizontal and Vertical Components of Microtremor". *Bulletin of the Seismological Society of America*, 88(1): 228–241, 1998.
- [15] Kramer, S.L., *Geotechnical Earthquake Engineering*, Pearson Education, Singapore, 1996 (Indian reprint 2003).
- [16] Krawinkler, H. and Alavi, B., "Development of Improved Design Procedures for Near Fault Ground Motions", In *SMIP98, Seminar on Utilization of Strong Motion Data*, Oakland, California, 1998.
- [17] Lermo, J. and Chavez-Garcia, F.J., "Are Micro-tremors Useful in Site Response Evaluation?", *Bulletin of the Seismological Society of America*, 84: 1350–1364, 1994.
- [18] Mohammadioun, B., "Nonlinear Response of Soils to Horizontal and Vertical Bedrock Earthquake Motion", *Journal of Earthquake Engineering*, 1(1): 93–119, 1997.
- [19] Nakamura, Y., "Clear Identification of Fundamental Idea of Nakamura's Technique and its Applications". In *Proceedings of the 12th World Conference on Earthquake Engineering*, Vol. 5, Paper # 2656, Auckland, New Zealand, 2000.
- [20] Novikova, E.I. and Trifunac, M.D., "Digital Instrument Response Correction for the Force Balance Accelerometer". *Earthquake Spectra*, 8(3): 429–442, 1992.
- [21] Novikova, E.I. and Trifunac, M.D., "Modified Mercalli Intensity Scaling of the Frequency Dependent Duration of Strong Ground Motion", *Soil Dynamics and Earthquake Engineering*, 12: 309–322, 1993.
- [22] Novikova, E.I. and Trifunac, M.D., "Duration of Strong Ground Motion in Terms of Earthquake Magnitude, Epicentral Distance, Site Conditions, and Site Geometry", *Earthquake Engineering and Structural Dynamics*, 23: 1023–1043, (1994).

- [23] IS-1893, *Indian Standard Criteria for Earthquake Resistant Design of Structures—Part I: General Provisions and Buildings*. Bureau of Indian Standards, New Delhi, 2002.
- [24] Sanchez-Sesma, F., “Elementary Solutions for Response of a Wedge-shaped Medium to Incident SH- and SV-Waves”, *Bulletin of the Seismological Society of America*, 80: 737–742, 1990.
- [25] Shrikhande, M. and Basu, S., “Strong Motion versus Weak Motion: Implications for Microzonation Studies”, *Journal of Earthquake Engineering*, 8(1): 159–173, 2004.
- [26] Shrikhande, M., Basu, S., and Kumar, A., “Earthquake Strong Motion Data Processing”, In *Atlas of Indian Strong Motion Records*, M. Shrikhande (Ed.), Department of Earthquake Engineering, Indian Institute of Technology Roorkee, 2001.
- [27] Shrikhande, M. and Gupta, V.K., “Synthesizing Ensembles of Spatially Correlated Accelerograms”, *Journal of Engineering Mechanics, ASCE*, 124(11): 1185–1192, 1998.
- [28] Shrikhande, M. and Gupta, V.K., “On the Characterization of the Phase Spectrum for Strong Motion Synthesis”, *Journal of Earthquake Engineering*, 5(4): 465–482, 2001.
- [29] Singh, J.P., “Earthquake Ground Motions: Implications for Designing Structures and Reconciling Structural Damage”. *Earthquake Spectra*, 1(2): 239–270, 1985.
- [30] Sokolov, V.Y., Loh, C.H., and Wen, K.L., “Empirical Study of Sediment-filled Basin Response: The case of Taipei city”. *Earthquake Spectra*, 16(3): 681–707, 2000.
- [31] Steidl, H.J., Tumarkin, A.G., and Archuleta, R.J., “What is a reference site?”, *Bulletin of the Seismological Society of America*, 86: 1733–1748, 1996.
- [32] Stewart, J.P., Chiou S.-J., Bray J.D., Graves R.W., Somerville P.G., and Abrahamson N.A., “Ground Motion Evaluation Procedures for Performance Based Design”. *PEER Report 2001/09*, Pacific Earthquake Engineering Research Centre, Berkeley, 2001.
- [33] Sunder, S. and Connor, J., “A New Procedure for Processing Strong-motion Earthquake Signals”. *Bulletin of the Seismological Society of America*, 72(2): 643–661, 1982.
- [34] Sunder, S. and Schumacker, B., “Earthquake Motions Using a New Data Processing Scheme”, *Journal of Engineering Mechanics, ASCE*, 108(EM6): 1313–1329, 1982.
- [35] Trifunac, M.D., “A Note on Correction of Strong-motion Accelerograms for Instrument Response”, *Bulletin of the Seismological Society of America*, 62(1): 401–409, (1972).
- [36] Trifunac, M.D., “Influence of Local Soil and Geologic Site Conditions on Fourier Spectrum Amplitudes of Recorded Strong Motion Accelerations”, *Technical Report 87-04*, Department of Civil Engineering, University of Southern California, Los Angeles, 1987.
- [37] Trifunac, M.D., “Fourier Amplitude Spectra of Strong Motion Acceleration: Extension to High and Low Frequencies”, *Earthquake Engineering and Structural Dynamics*, 23: 389–411, 1994.
- [38] Trifunac, M.D., Hao, T.Y., and Todorovska, M.I., “On the Recurrence of Site Specific Response”. *Soil Dynamics and Earthquake Engineering*, 18: 569–592, 1999.
- [39] Trifunac, M.D. and Lee, V.W., “Preliminary Empirical Model for Scaling Fourier Amplitude Spectra of Strong Ground Acceleration in Terms of Earthquake Magnitude, Source to Station Distance, Site Intensity and Recording Site Conditions”, *Technical Report 85-03*, Department of Civil Engineering, University of Southern California, Los Angeles, 1985.

- [40] Trifunac, M.D. and Todorovska, M.I., “Nonlinear Soil Response as a Natural Passive Isolation Mechanism—the 1994 Northridge, California, Earthquake”, *Soil Dynamics and Earthquake Engineering*, 17: 41–51, 1998.
- [41] Trifunac, M.D. and Todorovska, M.I., “Can Aftershock Studies Predict Site Amplification Factors: Northridge, CA, Earthquake of 17 January 1994”, *Soil Dynamics and Earthquake Engineering*, 19: 233–251, 2000.
- [42] Trifunac, M.D. and Todorovska, M.I., “Long Period Microtremors, Microseisms and Earthquake Damage: Northridge, CA, Earthquake of 17 January 1994”, *Soil Dynamics and Earthquake Engineering*, 19: 253–267, 2000.
- [43] Trifunac, M.D. and Westermo, B.D., “A Note on the Correlation of Frequency-Dependent Duration of Strong Earthquake Ground Motion with the MMI and Geologic Condition at the Recording Stations”, *Bulletin of the Seismological Society of America*, 67(3): 917–927, 1977.
- [44] Udwadia, F.E. and Trifunac, M.D., “Comparison of Earthquake and Micro-tremor Ground Motions in El Centro, California”, *Bulletin of the Seismological Society of America*, 63: 1227–1253, 1973.

Chapter 4

Strong Motion Characteristics

4.1 INTRODUCTION

The characteristics of strong motion in the vicinity of causative fault (near field) is strongly dependent on the nature of faulting. The motion depends on source parameters such as fault shape, its area, maximum fault dislocation, complexity of slipping process, stress drop and the distance of fault plane from the ground surface. The elastic properties of the material through which the generated seismic waves travel also influence the strong motion characteristics. A component trace of acceleration is known as **accelerogram**. Figure 4.1 shows a record of analog accelerograph, obtained during Uttarkashi earthquake of October 20, 1991 in epicentral area, in fact, at Uttarkashi itself. It shows traces of three components (accelerograms), two fixed traces and two traces of relative time marks—two pulses per second. Conventionally trace two is termed as longitudinal (N15°W), trace four is termed as vertical and trace six is termed as transverse (N75°E). By visual inspection following approximate estimate can be made of the parameters of the shock:

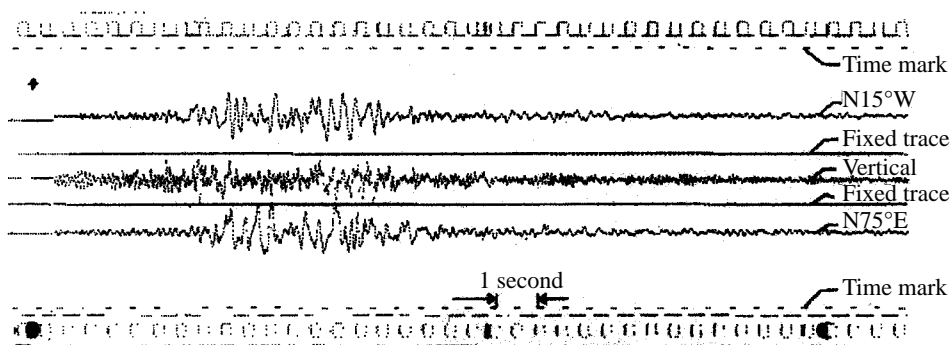


FIGURE 4.1 Traces of analog records of Uttarkashi earthquake.

- (i) peak acceleration by using acceleration trace and its calibration data,
- (ii) duration of strong shaking,
- (iii) frequency of predominant wave and rough idea of frequency range,
- (iv) amplitude and frequency relation between horizontal and vertical accelerogram, and
- (v) approximate distance of hypocentre from the recording station.

An accelerogram is a time history of acceleration composed of non-periodic sequences of acceleration pulses. The earthquake ground acceleration is a random function of time and thus its instantaneous value can not be predicted in deterministic sense. However, the unpredictable fluctuations show some degree of statistical regularity. This makes it possible to describe instantaneous value within a specified range. The area under the acceleration pulse is a measure of vibrations transmitted to the structure with foundation on the ground. The amplitude of the pulse is often taken as a measure of severity of ground shaking which could be termed as satisfactory if the duration of all pulses are similar. However, an accelerogram is generally composed of pulses of various durations. Thus not only peak of amplitude but also frequency content of the record is necessary in characterization of accelerogram. The temporal evolution of an accelerogram is composed of three parts (Figure 4.2), viz. rise, strong motion and decay. The effect of ground shaking is mostly dependent on duration of strong motion part. The accelerogram is rich in high frequencies near the causative faults. The high frequency components attenuate faster than the low frequency components, therefore the contribution of high frequency components is reduced in the accelerograms recorded at large distances from the fault. Further, the amplitude of ground acceleration decreases with increasing distance from the causative faults. Moreover, the vertical component of the ground acceleration is richer in high frequencies than the two horizontal components at a recording station. Figures 4.3 and 4.4 show the three orthogonal components of the motion recorded at Uttarkashi and Karnaprayag during the Uttarkashi earthquake. The epicentral distance of Karnaprayag is greater than that of Uttarkashi and this difference shows up in the ground motion characteristics at the two locations.

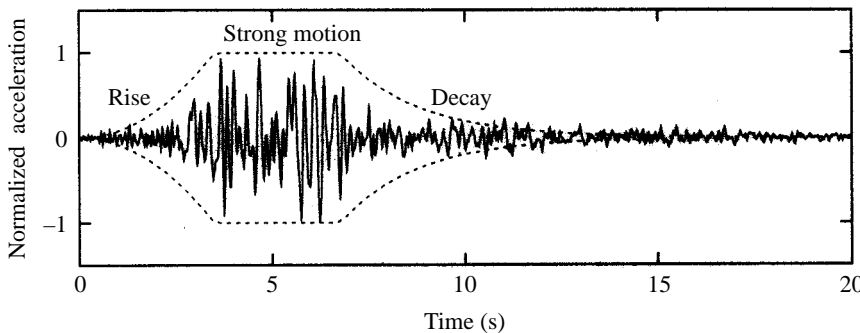


FIGURE 4.2 Temporal evolution of an accelerogram.

The ground velocity and displacement can be obtained by direct integration of an accelerogram. For an analog accelerogram, integrated record to obtain velocity and displacement is an approximate one, as the initial conditions at trigger of accelerograph are not known. For engineering purposes, the ground acceleration is the most significant parameter of strong motion, being directly proportional to the inertia force imposed on the structures. The ground

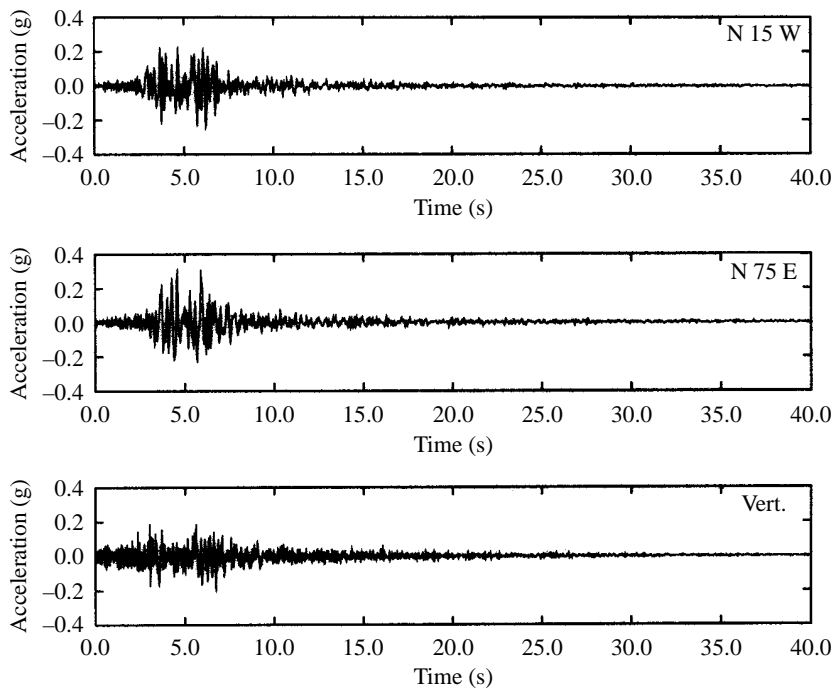


FIGURE 4.3 Three components of the motion recorded at Uttarkashi.

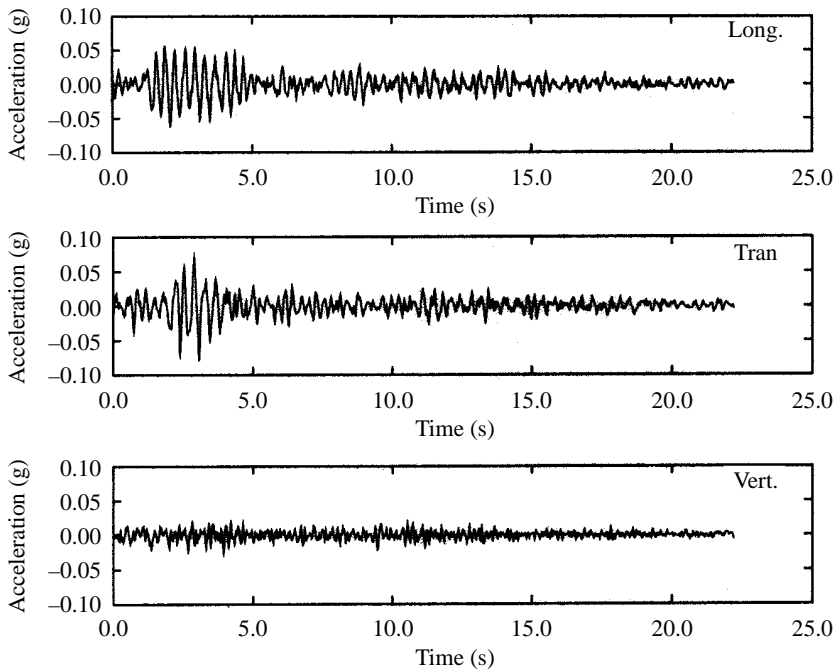


FIGURE 4.4 Three components of the motion recorded at Karnaprayag.

velocity is better correlated with the intensity of damage and it is also directly related with the energy transmitted to the structures. The ground displacement, however, is important for design of underground pipelines and is also an indicator of the amount of strain the foundation of a large structure will be subjected to.

4.2 TERMINOLOGY OF STRONG MOTION SEISMOLOGY

Due to the random nature of ground motion during a strong earthquake, it is not possible to characterize it for design purposes by means of the time histories of a recorded ground motion. Some of the physical quantities and derived parameters which are used to describe various aspects of the ground motion are described as follows:

4.2.1 Amplitude Parameters

The amplitude parameters of the ground motion were the earliest of the strong motion parameters to be proposed. Typically, the peak values of the ground acceleration, velocity and displacement give an idea of the severity of shaking at a site, predominant period of vibration, etc.

Peak Acceleration

The Peak Horizontal Acceleration (PHA) is the most commonly used measure of the intensity of shaking at a site and is taken to be the largest absolute value of the horizontal acceleration recorded at a site. It is also possible to extract the maximum of the vector sum of two orthogonal components of the horizontal ground acceleration recorded at a site. Ground motions with high peak accelerations are usually, but not always, more damaging than those with lower peak acceleration. However, a short duration stray pulse with large amplitude may not cause any significant damage as there is very little time available for the system to respond to such excitation. Therefore, the duration of the excitation is also an important consideration in estimating the damage potential of a ground motion.

v/a ratio

As the *peak accelerations (a)* and *peak velocities (v)* are usually associated with the motion of different frequencies, the ratio v/a can be related to the frequency content of the motion. For earthquake motions that include several frequencies, the parameter $2\pi v/a$ can be interpreted as the period of vibration of an equivalent harmonic wave, thereby providing an indication of the predominant period of the ground motion. It has been observed that v/a ratio for rocky sites are substantially lower than those for alluvium.

ad/v^2 ratio

The ratio of the peak acceleration-displacement product to the square of the peak velocity can be related to the sharpness or flatness of the response spectrum. For harmonic motions, this ratio

is unity and for steady-state square acceleration wave it is 1/2, whereas for most earthquake motions this ratio ranges between 5–15.

4.2.2 Duration of Strong Motion

Several definitions have been proposed for the strong motion duration of an accelerogram. However, one of the most widely used definitions refers to the duration of the strong motion as the time interval in which 90% of the total contribution to the energy of the accelerogram ($\int [\ddot{x}(t)]^2 dt$) takes place [22]. Usually the time interval between 5% and 95% contributions is taken as the strong motion duration.

4.2.3 Fourier Spectrum

The frequency content (distribution of energy with respect to frequencies) of an accelerogram is represented by Fourier Spectrum. The Fourier transform of an accelerogram $\ddot{x}(t)$ is given by,

$$X(\omega) = \int_{-\infty}^{\infty} \ddot{x}(t) e^{-i\omega t} dt \quad (4.1)$$

Assuming ground acceleration as non-zero in $t \in (0, T]$ the Equation (4.1) can be written as,

$$X(\omega) = \int_0^T \ddot{x}(t) \cos(\omega t) dt - i \int_0^T \ddot{x}(t) \sin(\omega t) dt \quad (4.2)$$

Fourier amplitude and phase spectra of earthquake ground motion are defined using Equation (4.2) as,

$$|X(\omega)| = \sqrt{\left[\int_0^T \ddot{x}(t) \cos(\omega t) dt \right]^2 + \left[\int_0^T \ddot{x}(t) \sin(\omega t) dt \right]^2} \quad (4.3)$$

$$\phi(\omega) = -\tan^{-1} \left\{ \frac{\int_0^T \ddot{x}(t) \sin(\omega t) dt}{\int_0^T \ddot{x}(t) \cos(\omega t) dt} \right\} \quad (4.4)$$

Although phase spectrum is considered to be relatively of lesser importance than amplitude spectrum, both amplitude and phase spectra are required for unique definition of ground acceleration. It has long been established that the non-stationary characteristics of an accelerogram are described by its phase spectrum [15, 16, 20, 21]. Fourier amplitude spectra of velocity and displacement can be obtained by dividing acceleration and Fourier amplitude spectrum ordinate by frequency and square of frequency value respectively. Figure 4.5 shows normalized Fourier amplitude spectra for displacement, velocity and acceleration of N15°W component of Uttarkashi earthquake, recorded at Uttarkashi. It is to be noted that the bandwidth of predominant frequency for displacement is narrowest and that of acceleration is the broadest. It also demonstrates that acceleration, velocity and displacement are controlled by different frequency bands.

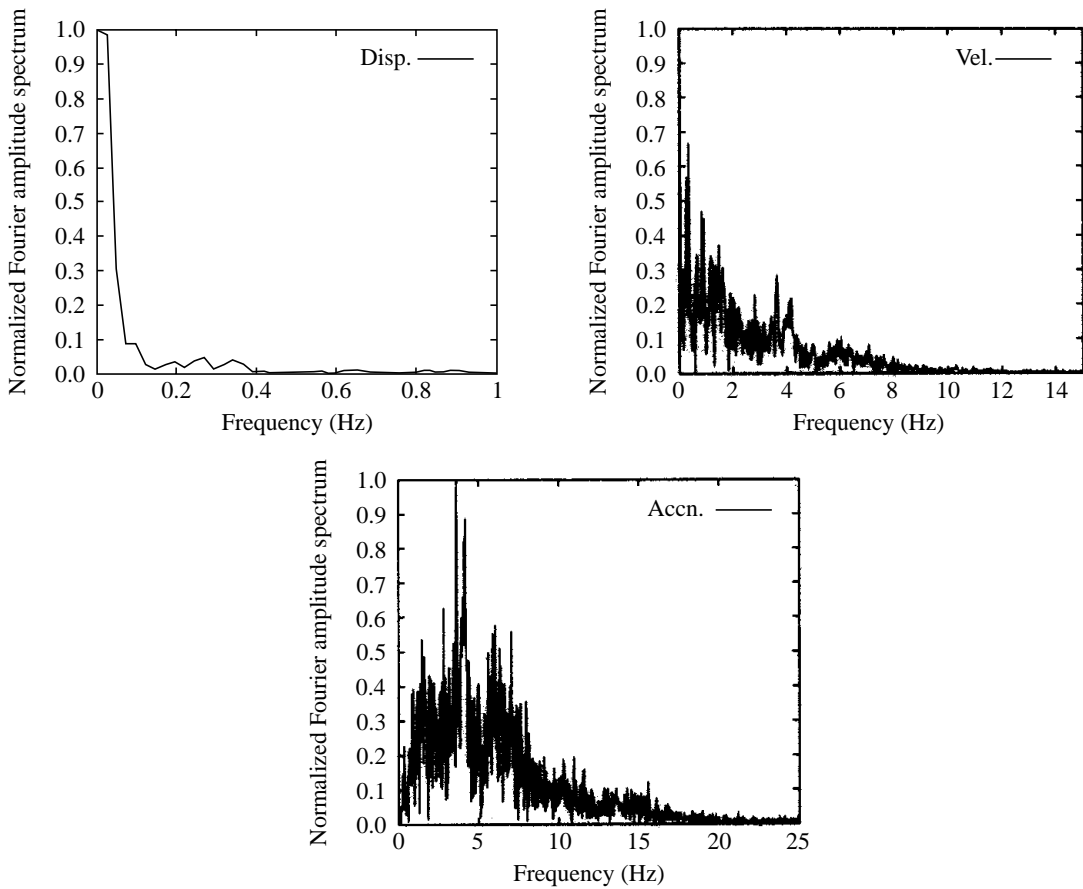


FIGURE 4.5 Normalized Fourier amplitude spectrum of displacement, velocity and acceleration at Uttarkashi (Component: N15°W).

4.2.4 Power Spectrum

The power spectrum is an alternate representation of the frequency content of a time history. It is closely related to the Fourier amplitude spectrum of the records as,

$$S(\omega) = \frac{1}{2\pi T} \mathcal{E}[|X(\omega)|^2] \quad (4.5)$$

where $S(\omega)$ = power spectrum,

$|X(\omega)|$ = Fourier amplitude spectrum,

$\mathcal{E}[\cdot]$ = mathematical expectation operator, and

T = duration of the record.

In routine accelerogram processing, the expectation operator is generally replaced by a moving window averaging operator.

4.2.5 Response Spectrum

Ever since Housner [6] presented the use of *response spectrum* in seismic analysis, it has been adopted as a standard way of representation of effect of ground acceleration on structures. It reflects frequency content, amplitude of ground motion and effect of subsequent filtering by the structure. The response of an oscillator, initially at rest, is given by,

$$x(t) = -\frac{1}{\omega_d} \int_0^t \ddot{x}_g(\tau) e^{-\zeta\omega_n(t-\tau)} \sin \omega_d(t-\tau) d\tau \quad (4.6)$$

where $\omega_d = \omega_n \sqrt{1 - \zeta^2}$ is the damped natural frequency. The plot of maximum relative response $x(t)$ of linear elastic SDOF system, initially at rest with prescribed damping ratio ζ subjected to a ground acceleration versus natural period, or frequency of vibration is defined as relative displacement response spectrum and is denoted as,

$$\begin{aligned} S_d(\zeta, \omega_n) &\equiv S_d(\zeta, T_n) = |x(t)|_{\max} \\ &= \frac{1}{\omega_d} \left[\left\{ \int_0^t \ddot{x}_g(\tau) e^{-\zeta\omega_n(t-\tau)} \sin \omega_d(t-\tau) d\tau \right\}_{\max} \right]_{\max} \end{aligned} \quad (4.7)$$

where natural period of vibration $T_n = 2\pi/\omega_n$. For a specified ground motion the Equation (4.6) is numerically integrated and the resulting maximum relative displacement value gives one value of S_d for a given set of ω_n and ζ . Typically this integration is carried out at uniform frequency interval in a prescribed range of frequency for different ratios of ζ . The quantity within the curly brackets of Equation (4.7) has the unit of velocity. The absolute maximum of this quantity is termed as pseudo relative velocity response spectrum (psv) $S_{pv}(\zeta, \omega_n)$ and is given as,

$$S_{pv}(\zeta, \omega_n) \equiv S_{pv}(\zeta, T_n) = \left[\left\{ \int_0^t \ddot{x}_g(\tau) e^{-\zeta\omega_n(t-\tau)} \sin \omega_d(t-\tau) d\tau \right\}_{\max} \right]_{\max} \quad (4.8)$$

Thus for lightly damped system (i.e., $\omega_d \approx \omega_n$)

$$S_d(\zeta, \omega_n) \equiv \frac{1}{\omega_d} S_{pv}(\zeta, \omega_n) \approx \frac{1}{\omega_n} S_{pv}(\zeta, \omega_n) \quad (4.9)$$

The relative displacement response spectra asymptotically approaches maximum ground displacement for highly flexible structure. Formally the limiting value of $S_d(\zeta, \omega_n)$ is,

$$\lim_{\omega_n \rightarrow 0} S_d(\zeta, \omega_n) = |x_g(t)|_{\max} \quad (4.10)$$

This implies that the mass remains stationary for all practical purposes and only the ground moves, as the linear elastic SDOF system is composed of spring with negligible stiffness.

Differentiation of Equation (4.6) with respect to time t gives,

$$\begin{aligned} \dot{x}(t) &= -\int_0^t \ddot{x}_g(\tau) e^{-\zeta\omega_n(t-\tau)} \cos \omega_d(t-\tau) d\tau \\ &+ \frac{\zeta}{\sqrt{1 - \zeta^2}} \int_0^t \ddot{x}_g(\tau) e^{-\zeta\omega_n(t-\tau)} \sin \omega_d(t-\tau) d\tau \end{aligned} \quad (4.11)$$

The relative velocity spectrum is similarly defined as,

$$S_v(\zeta, \omega_n) \equiv S_v(\zeta, T_n) = [\dot{x}(t)]_{\max} \quad (4.12)$$

For lightly damped structure $\zeta \approx 0$, the second term of Equation (4.11) can be neglected and thus the expression for relative velocity spectrum reduces to

$$S_v(0, \omega_n) = \left[\int_0^t \ddot{x}_g(\tau) \cos \omega_n(t - \tau) d\tau \right]_{\max} \quad (4.13)$$

From Equation (4.8) the undamped relative pseudo-velocity response spectra can be obtained as,

$$S_{pv}(0, \omega_n) = \left| \int_0^t \ddot{x}_g(\tau) \sin \omega_n(t - \tau) d\tau \right|_{\max} \quad (4.14)$$

It is easy to see from the Equation (4.13) that as $\omega_n \rightarrow 0$, the relative velocity spectrum $S_v \rightarrow |\dot{x}_g(t)|_{\max}$ and from the Equation (4.14) the relative pseudo-response $S_{pv} \rightarrow 0$ as the mass remains stationary. Hudson [10, 11] has shown that numerically $S_v(0, \omega_n)$ and $S_{pv}(0, \omega_n)$ are almost equal except for very long period structure. However, variation is considerable in case of highly damped structure. Figure 4.6 shows relative velocity spectra S_v and pseudo-relative velocity spectra S_{pv} for damping ratios $\zeta = 0.02$ and 0.20 of longitudinal (N15°W) component of Uttarkashi record. The absolute acceleration response of the oscillator can be written as,

$$\begin{aligned} \ddot{x}_m(t) &= \ddot{x}(t) + \ddot{x}_g(t) \\ &= -\omega_n^2 x(t) - 2\zeta\omega_n \dot{x}(t) \end{aligned} \quad (4.15)$$

The absolute acceleration spectra is similarly defined as,

$$S_a(\zeta, \omega_n) = S_a(\zeta, T_n) = [\ddot{x}_m(t)]_{\max} \quad (4.16)$$

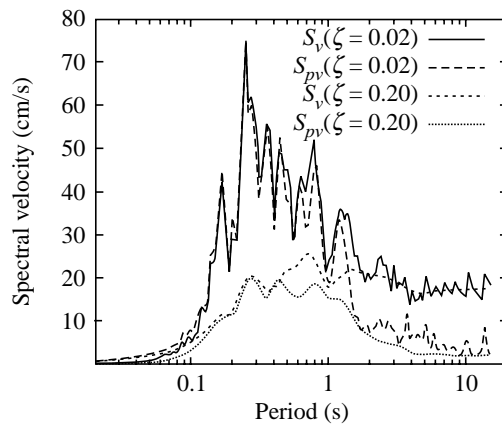


FIGURE 4.6 Comparison of spectral and pseudo-spectral velocity of longitudinal component recorded at Uttarkashi for different damping ratios.

It may be seen that for damping ratio $\zeta \in (0.0, 0.20)$

$$S_a(\zeta, \omega_n) \approx \omega_n S_{pv}(\zeta, \omega_n) = S_{pa}(\zeta, \omega_n) \quad (4.17)$$

where $S_{pa}(\zeta, \omega_n)$ is called **absolute pseudo-acceleration spectral response** and the Equation (4.17) becomes equality for $\zeta = 0$. Absolute pseudo-acceleration spectra $S_{pa}(\zeta, \omega_n) \leq S_a(\zeta, \omega_n)$. This difference might be important for rigid systems. Figure 4.7(a) shows absolute acceleration response spectra $S_a(0.05, \omega_n)$ and absolute pseudo acceleration response spectra $S_{pa}(0.05, \omega_n)$ of longitudinal (N15°W) component of motion at Uttarkashi. Figure 4.7(b) shows the enlarged view of the plot in the period range 5–15 s to illustrate the difference in S_a and S_{pa} ordinates at long periods. The limiting value of absolute acceleration spectra is achieved for infinitely stiff structure, as there is no relative motion between ground and mass, hence

$$\lim_{\omega_n \rightarrow \infty} S_a(\zeta, \omega_n) = |\ddot{x}_g(t)|_{\max} \quad (4.18)$$

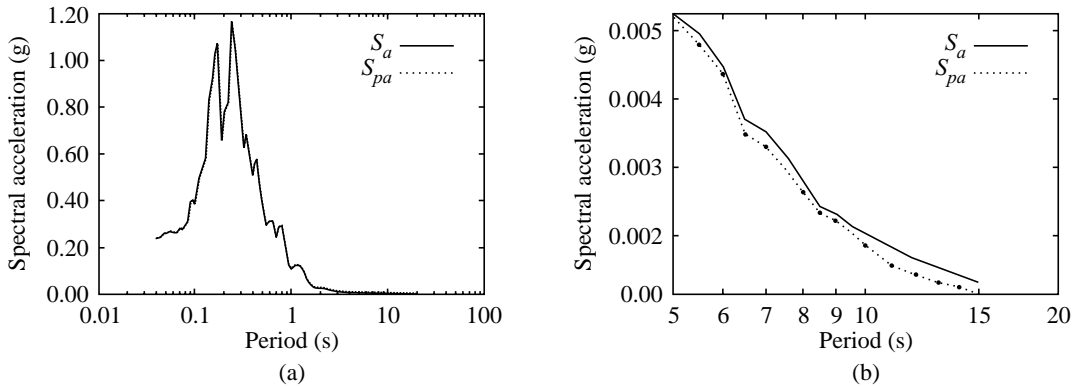


FIGURE 4.7 Comparison of spectral and pseudo-spectral acceleration of longitudinal component recorded at Uttarkashi for 5% damping.

The maximum spring force developed in the oscillator is $kS_d(\zeta, \omega_n) = mS_{pa}(\zeta, \omega_n)$, whereas $mS_a(\zeta, \omega_n)$ is the maximum of total elastic and damping forces. The maximum strain energy input is,

$$E_I = \frac{k}{2} [S_d(\zeta, \omega_n)]^2 \quad (4.19)$$

and the maximum stain energy per unit mass is,

$$E_s = \frac{k}{2m} [S_d(\zeta, \omega_n)]^2 = \frac{1}{2} [\omega_n S_d(\zeta, \omega_n)]^2 = \frac{1}{2} [S_{pv}(\zeta, \omega_n)]^2 \quad (4.20)$$

The total energy of the system is,

$$E_T(t) = \frac{m}{2} [\dot{x}(t)]^2 + \frac{k}{2} [x(t)]^2 \quad (4.21)$$

For an undamped linear elastic SDOF system, substitution of $x(t)$ by the Equation (4.6) and $\dot{x}(t)$ by the Equation (4.11), the Equation (4.21) reduces to,

$$\sqrt{\frac{2E_T(t)}{m}} = \sqrt{\left[\int_0^t \ddot{x}_g(\tau) \cos(\omega_n \tau) d\tau \right]^2 + \left[\int_0^t \ddot{x}_g(\tau) \sin(\omega_n \tau) d\tau \right]^2} \quad (4.22)$$

which at the end of accelerogram $t = T$ is identical to Fourier amplitude spectrum $|X(\omega)|$ of the ground acceleration evaluated at frequency ω_n . The maximum of the Equation (4.22) is pseudo-relative velocity spectrum $S_{pv}(0, \omega_n)$. If the relative response reaches maximum at the end of accelerogram duration, then $|X(\omega)| = S_{pv}(0, \omega_n)$. In general, $|X(\omega)| \leq S_{pv}(0, \omega_n)$. Figure 4.8 shows relative velocity response spectrum S_{pv} for undamped system and Fourier spectrum $|X(\omega)|$ of longitudinal component recorded at Uttarkashi.

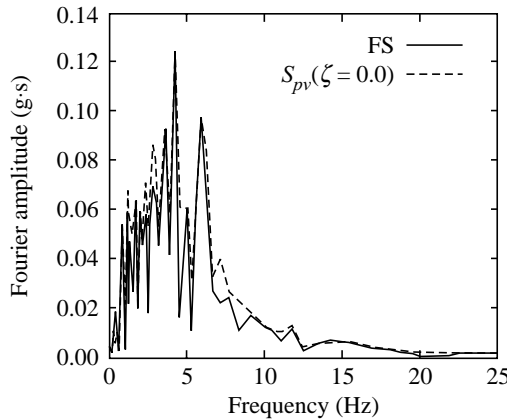


FIGURE 4.8 Comparison of pseudo-spectral velocity spectrum for 0% damping and the Fourier spectrum of longitudinal component recorded at Uttarkashi.

4.2.6 Seismic Demand Diagrams

The recent thrust in the development of performance-based engineering concepts has necessitated representation of the ground motion spectral characteristics in a new format, viz., Acceleration-Displacement Response Spectrum (ADRS) format. The spectral accelerations are plotted against spectral displacements, with the periods (T_n) being represented by radial lines. An estimate of inelastic demands imposed on a structure by an earthquake is obtained from the linear elastic response spectra computed for equivalent damping ratios related to a specified level of ductility. The capacity diagram of a building is obtained from the relationship between the base shear and roof displacement (push-over curve). The roof displacement and the base shear are converted to the spectral displacement and spectral acceleration by the use of mode participation factor and effective modal mass for the fundamental mode. The performance of a building in any earthquake can be assessed by superimposing the capacity diagram on the seismic demand diagram. The intersection of the capacity curve and the seismic demand curve provides an estimate of the yield strength and the displacement demand. The elastic demand diagrams for

the motions recorded at Ahmedabad during the Kutch Earthquake of January 26, 2001 are shown in Figure 4.9.

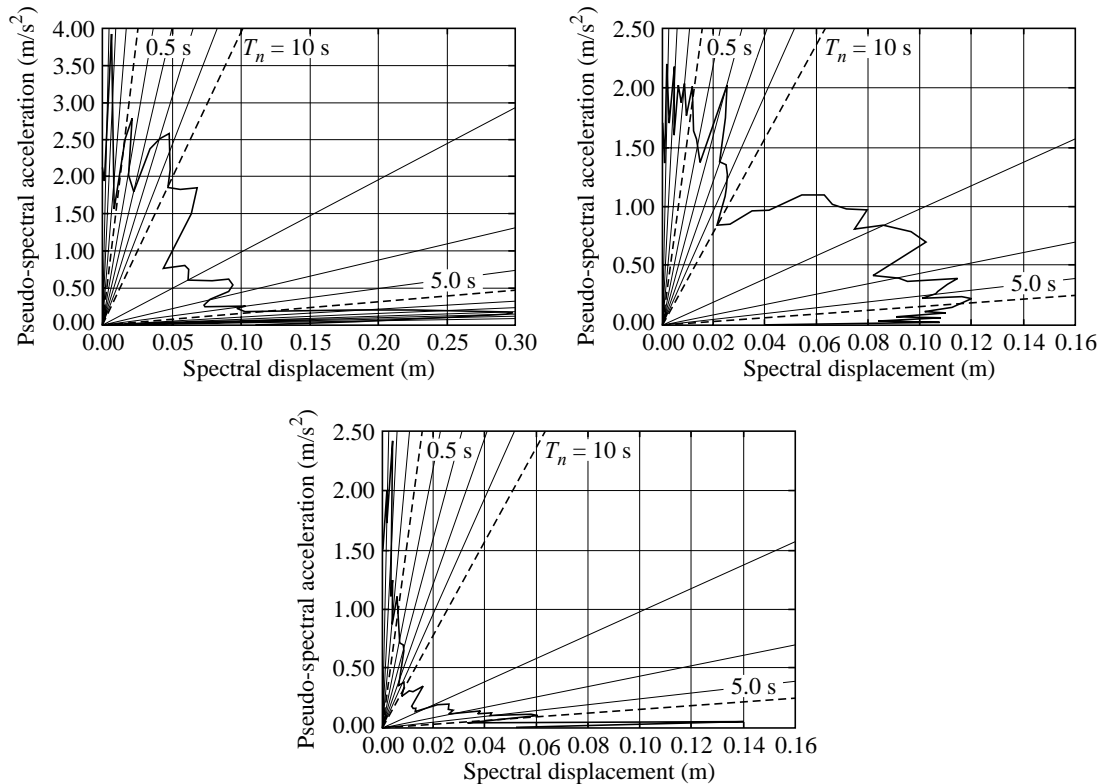


FIGURE 4.9 Demand Diagram for N78°E, N12°W and Vertical Component of January 26, 2001 Kutch earthquake recorded at Ahmedabad (Damping 5%).

4.2.7 Spatial Variation of Earthquake Ground Motion

In several situations, the seismic input is required to be applied at different points in space, e.g., in the case of long-span bridges, or pipelines. For seismic analysis of such spatially extended structures, it is important to account for possible variations in the earthquake ground motion at different points in space. Even in the case of simple building systems with raft foundations, it has been reported that the spatial variation of ground motion results in increase in rocking and torsional components of excitation due to averaging of ground motion by the rigid basemat [14].

The spatial variation of seismic ground motions is generally modeled as the product of two functions representing two distinct phenomena, viz., (i) the incoherence effect—caused by changes in waveform due to multiple reflections, diffractions, etc. owing to heterogeneities and asperities along the travel path between two stations and, (ii) the wave propagation effect—accounting for the finite delay in wave arrivals at a distant station due to finite propagation

velocities, and is given as

$$\gamma_{jk}(i\omega) = \frac{S_{jk}(i\omega)}{\sqrt{S_{jj}(\omega)S_{kk}(\omega)}} \approx |\gamma_{jk}(i\omega)| \exp\left(i\omega \frac{r_{jk}}{v_{\text{app}}}\right) \quad (4.23)$$

where $\gamma_{jk}(i\omega)$ is known as the **coherency function** and is a measure of correlation between the given pair of time-histories, $S_{jk}(i\omega)$ is the **cross-power spectral density function** for the pair of motions recorded at stations j and k , $S_{jj}(\omega)$ and $S_{kk}(\omega)$ are the respective auto-power spectral density functions of the motions at stations j and k , r_{ij} represents the projected horizontal separation between stations j and k , and v_{app} denotes the **surface apparent velocity** of propagation of the wave at frequency ω .

Although seismic waves of different frequencies, in general, travel with different speeds it is common to prescribe a constant value for v_{app} for all frequencies because of inherent difficulties in the estimation of this parameter. The first factor, on the right hand of Equation (4.23), represents the effect of incoherence and can be either derived from entirely theoretical considerations [12, 25], or is empirically obtained from the analysis of strong motion array data [4, 5], and the second factor represents the effect of propagation delay due to finite velocities.

4.2.8 Damage Potential of Earthquakes

The potential of an earthquake to inflict damage on engineered facilities has always been a matter of great concern to all engineers. Very often a situation is encountered wherein one is forced to choose between several alternative ground motion time histories to verify the adequacy of a particular design to resist the design level earthquake motion. Since the design earthquake loads are usually specified in the form of design spectra, artificial/synthetic accelerograms are generated so as to be compatible with the design specifications. However, the solution to the problem of synthesizing a spectrum compatible accelerogram is not unique and it is possible to have several different synthetic accelerograms which are compatible with the specified design spectrum. Thus it is desirable to use that time history which has the maximum potential for damage. It is therefore necessary to derive a set of parameters derived from earthquake records that may be considered as measures of the severity of ground shaking at the site. Further, the correlation between three orthogonal components of the ground acceleration vector at a location is assumed to be negligible in seismic analysis. However, the recorded components are generally correlated which may introduce some bias in the analysis results. To eliminate these correlation effects, the resolution of the ground motion components along the principal direction has been suggested in the past [13, 17]. The principal directions and resolution of the ground motion components along these principal directions have been discussed below. Further, several strong motion parameters which are used to measure the severity of the ground motions have been explained.

Earthquake motions along principal axes

The seismic design loads on structures are usually specified in terms of a set of normalized design (response) spectra for horizontal and vertical motions expected at a site. These spectral shapes are generally derived from the statistical analysis of the spectral ordinates of previously

recorded earthquake motions in the region. In deriving the spectral shape for horizontal motions, it is common to consider the stronger of the two horizontal components of ground motion in these analyses. Since the directivity of a future earthquake is random, the same spectral shape is used for the two orthogonal horizontal directions for a conservative estimate of the expected seismic loading. Further, the two orthogonal horizontal components of design earthquake are generally assumed to be uncorrelated. However, if these spectral shapes were derived from the recorded components of the ground motions, the estimates of the expected spectral ordinates are likely to be biased and also unconservative. The bias in these estimates results from the finite correlation between the recorded components of the motions. In order to eliminate this bias, it is desirable to consider the uncorrelated components of the ground motion in statistical analysis.

Let the three translational components of ground acceleration recorded along the three orthogonal transducer axes of the accelerograph denoted by $a_i(t)$; ($i = x, y, z$) be defined as,

$$\begin{aligned} a_x(t) &= e(t)b_x(t) \\ a_y(t) &= e(t)b_y(t) \\ a_z(t) &= e(t)b_z(t) \end{aligned} \quad (4.24)$$

where $b_i(t)$; ($i = x, y, z$) are stationary random processes and $e(t)$ is a deterministic modulating function. Assuming the ground acceleration process to be Gaussian with zero mean, the three dimensional ground acceleration process can be completely characterized in a probabilistic sense through the covariance matrix

$$[\mu(t, \tau)] = \begin{bmatrix} \mu_{xx} & \mu_{xy} & \mu_{xz} \\ \mu_{yx} & \mu_{yy} & \mu_{yz} \\ \mu_{zx} & \mu_{zy} & \mu_{zz} \end{bmatrix} \quad (4.25)$$

where, μ_{ij} (= $\mu_{ij}(t, \tau) = E[a_i(t)a_j(t + \tau)]$) represents the covariance between two orthogonal components $a_i(t)$ and $a_j(t)$ and $E[\cdot]$ represents the mathematical expectation (ensemble average) operator. As a first approximation, real earthquake accelerograms can be represented by shot or white noise processes [7]. In such a situation, the random variables $a_i(t)$ and $a_j(t + \tau)$ would be statistically uncorrelated for non-zero values of time difference τ . Hence, the elements of the covariance matrix of the ground acceleration process may approximated by $\mu_{ij} = E[a_i(t)a_j(t)]$. Substituting from Equation (4.24) into Equation (4.25), the covariance matrix can be written as,

$$[\mu(t)] = e^2(t)[\beta] \quad (4.26)$$

where, $\mu_{ij}(t) = E[a_i(t)a_j(t)]$ and β_{ij} (= $E[b_i(t)b_j(t)]$) is the time invariant covariance of stationary processes $b_i(t)$ and $b_j(t)$, for $i, j = x, y, z$. Further, the components of motion along an arbitrary set of orthogonal axes x' , y' , z' can be transformed to components along orthogonal axes x , y , z by a simple transformation as,

$$\begin{pmatrix} a_x(t) \\ a_y(t) \\ a_z(t) \end{pmatrix} = [A] \begin{pmatrix} a_{x'}(t) \\ a_{y'}(t) \\ a_{z'}(t) \end{pmatrix} \quad (4.27)$$

where $[A]$ is the orthogonal transformation matrix satisfying the relation $[A]^T[A] = [I]$. Thus the covariance matrix for the axis x' , y' , z' is obtained as

$$\begin{aligned} [\mu'(t)] &= [A]^{-1}[\mu(t)][A]^{-1}^T \\ &= [A]^T[\mu(t)][A] \\ &= e^2(t)[A]^T[\beta][A] \end{aligned} \quad (4.28)$$

This transformation of three-dimensional ground motion is identical to the transformation of three-dimensional state of stress. Therefore it can be proved that there exists a set of principal axes along which the components of motion have maximum, minimum and intermediate values of variance and zero covariance. The directions of the principal axis are given by the eigenvectors of the covariance matrix of the recorded motions whereas the corresponding eigenvalues are the principal variances [13, 17]. Since the off-diagonal terms in a covariance matrix indicate quantitatively the correlation between the corresponding components, the components along the principal axes are fully uncorrelated with respect to each other. Moreover, the three components of motion along the principal axes are statistically independent of each other, provided that the ground motions are assumed to be adequately represented by *Gaussian random processes*. For a small class of stationary random processes, *viz.*, ergodic processes, the ensemble statistics are same as the temporal statistics and thus time averages taken over a single sample of the random process provide complete statistical information about the process. For all other types of random processes such a duality between ensemble and temporal statistics does not exist. In a practical application, however, the desired statistical properties of random processes are often estimated by examining individual members from the ensembles of processes [3]. Thus the covariances in Equation (4.26) can be obtained by considering the temporal averaging over any single member of the process, i.e.,

$$\beta_{ij} = \langle b_i^r(t)b_j^r(t) \rangle$$

where, the superscript r denotes the r th sample from the ensemble of the process and angular brackets represent time averaging over the duration of motion.

It has been reported [17] that there exists a strong correlation between the direction of one of the principal axis (most often the major principal axis) and the general direction to the fault-slip zone. However, analysis of data from San Fernando earthquake of February 9, 1971 indicates that this correlation is not very strong. Further, it was observed that one of the principal directions is usually aligned with the vertical direction [13]. For the Indian earthquakes also, no correlation could be established between the directions of principal components of the recorded motions and the direction of the rupture of fault plane [18, 19].

Measures of severity

Various parameters have been defined to characterize severity of strong shaking. The Peak Ground Acceleration (PGA) is the most widely used parameter to measure severity of earthquake. However, the PGA is a rather poor parameter for measuring severity of strong motion due to various reasons such as, its possible association with a pulse of very high frequency, amplification due to irregular local topography, interaction of large structure at the site of recording, etc. The popularity of PGA as a measure of severity of ground motion is partly because of it being the

only parameter that can be directly measured by an instrument—all other strong motion parameters are derived from the processing of strong motion data. Further, the PGA measure is intuitively appealing to the engineers as it is proportional to the maximum inertia force imposed on a structure during an earthquake. Several parameters that have been proposed as replacements for PGA as a measure of severity of ground shaking are discussed below.

Arias defined *earthquake intensity* as sum of the total energy per unit weight, stored in undamped oscillators uniformly distributed with respect to their frequencies at the end of the earthquake [2]:

$$I_A = \frac{\pi}{2g} \int_0^{T_D} [\ddot{x}(t)]^2 dt \quad (4.29)$$

where, $\ddot{x}(t)$ refers to the ground acceleration, g is acceleration due to gravity and T_D represents the earthquake duration. Thus duration and amplitude is implicitly considered in the definition of I_A . Since $\ddot{x}(t) = 0$ for $t > T_D$, the Equation (4.29) can also be written as,

$$I_A = \frac{\pi}{2g} \int_0^{\infty} [\ddot{x}(t)]^2 dt = \frac{1}{2g} \int_0^{\infty} |X(\omega)|^2 d\omega \quad (4.30)$$

where, $|X(\omega)|$ is the Fourier amplitude spectrum of $\ddot{x}(t)$. Thus I_A will be large for strong motion with significant amount of high frequency components, high amplitude and long duration.

Housner used the mean square acceleration during the rise time of strong motion to define earthquake average power [9]. Let

$$I = \int_0^{T_D} [\ddot{x}(t)]^2 dt \quad (4.31)$$

be the total energy in a strong motion. The earthquake average power is defined as,

$$P_a = \frac{1}{T_S} \int_{t_{0.05}}^{t_{0.95}} [\ddot{x}(t)]^2 dt \quad (4.32)$$

where, $t_{0.05}$ and $t_{0.95}$ are the time t at which I has 5% and 95% value respectively and the rise time is defined as ($T_S = t_{0.95} - t_{0.05}$) the duration of strong motion part of an accelerogram [22]. The root mean square of P_a is the measure of average rate of input energy to an elastic system and is denoted as $rms_a = \sqrt{P_a}$. The larger value of P_a is obtained for an accelerogram which is of short duration and impulsive in nature. The value of earthquake power and Arias intensity is comparable. Both I_A and P_a are fairly good indicator of damage potential for brittle structure.

The elastic response spectra indicate directly how a linear elastic single degree of freedom (SDOF) system responds to strong ground motion. It also indicates maximum elastic deformation produced in structures having periods in the range of computation. However, it cannot be a good predictor of damage potential as the damage is primarily an inelastic phenomenon. For ductile structure the damage depends on duration of strong motion, number of stress reversals and amplitude of vibration excursions. Number of stress reversal and inelastic deformation are largely dependent on strong motion duration. To measure intensity of ground shaking from the elastic response of structure Housner [8] proposed an average response in a range of periods.

This measure is defined as spectral intensity and is given by

$$SI(\zeta) = \int_{0.1}^{2.5} S_v(\zeta, T) dT \quad (4.33)$$

where, T is the period of SDOF, and $S_v(\zeta, T)$ represents the relative velocity spectrum. Although originally it was proposed for damping ratio of $\zeta = 0.02$, but presently it is customary to calculate $SI(0.05)$. In the range of period $T \in [0.1, 2.5]$ and for lightly damped structure $S_v(\zeta, \omega_0) \approx S_{pv}(\zeta, \omega_0)$ and the Equation (4.33) reduces to

$$SI(\zeta) \approx \int_{0.1}^{2.5} S_{pv}(\zeta, T) dT = \frac{1}{2\pi} \int_{0.1}^{2.5} S_{pa}(\zeta, T) T dT \quad (4.34)$$

Here, S_{pv} and S_{pa} respectively refer to the pseudo-velocity and pseudo-acceleration spectra. The Equation (4.34) implies that spectral intensity is higher for strong motion with richer content of long period waveforms. The limitation of SI as a measure of damage potential parameter of earthquake is inherited from the definition of response spectra. The effect of duration of strong motion is not accounted for in response spectra. Thus spectral intensity SI value of strong motion records of approximately similar duration should be compared for any meaningful conclusion.

Since a high value of PGA in a record could be due to large amplitude stray pulse, it is not a reliable parameter to measure the severity of ground motion. An alternative parameter Effective Peak Acceleration (EPA) has been defined by Watabe and Tohdo [23]. The EPA is defined as the peak value of amplitude truncated ground acceleration time history for which the spectrum intensity is 90% of that for the original time history. This way the effect of any spurious peak in the recorded time history is eliminated.

Araya and Saragoni simultaneously accounted for the effect of maximum amplitude, duration and frequency content of strong motion in prescribing earthquake destructiveness potential factor as [1]:

$$P_D = \frac{I_A}{\mu_0^2} \quad (4.35)$$

where I_A is Arias intensity and μ_0 is the intensity of zero crossing defined as N_0/T_D . N_0 is the total number of zero crossing in an accelerogram in total duration T_D with positive and negative slope. Among all the proposed damage potential parameters the Equation (4.35) is most rational for linear elastic structure. However, it does not consider effect of inelastic deformations which is primarily responsible for damage.

A criterion of equivalent number of yield cycles (N)—based on inelastic deformations of SDOF systems for a specified ductility ratio was proposed by Zahrah and Hall [24]. This parameter is defined as the ratio of the total energy dissipated by yielding (E_H) in a structure when subjected to ground motion to the area under the resistance-displacement curve for the structure when it is loaded monotonically until it reaches the same maximum displacement it experiences during the excitation, i.e.,

$$N = \frac{E_H}{\omega_0^2 U_Y^2 (\mu - 1)} \quad (4.36)$$

where, ω_n denotes the natural frequency of the SDOF structure, U_Y represents the yield deformation, and μ is the specified ductility. The smallest value N can have is 1; in this case, the structure yields only in one direction and reaches its maximum displacement.

SUMMARY

A discussion of various issues involved in the engineering interpretation of strong motion data is presented. Starting with the explanation of basic terminology used in strong motion seismology the reader is guided through the different forms of characterization of ground motions. The chapter concludes with a discussion of the various parameters used to quantify the damage potential of the earthquake ground motion recorded at a site. This will help in developing an understanding about the ground motion characterization and the parameters used to indicate the severity of the motion at a site.

REFERENCES

- [1] Araya, R. and Saragoni, G.R., "Earthquake Accelerogram Destructiveness Potential Factor", In *Proceedings of the Eighth World Conference on Earthquake Engineering, San Francisco, California, U.S.A.*, pp. II: 835–842, Prentice Hall Inc., New Jersey, 1984.
- [2] Arias, A., "A Measure of Earthquake Intensity". In *Seismic Design for Nuclear Power Plants*, R.J. Hansen, (Ed.), pp. 438–469. MIT Press, Cambridge, Massachusetts, 1970.
- [3] Bendat J.S. and Piersol A.G., *Random Data*, 2nd ed., John Wiley and Sons, 1986.
- [4] Hao, H., Oliviera, C.S., and Penzien, J., "Multiple-Station Ground Motion Processing and Simulation Based on SMART-1 Array Data", *Nuclear Engineering and Design*, 111: 293–310, 1989.
- [5] Harichandran, R.S. and Vanmarcke, E.H., "Stochastic Variation of Earthquake Ground Motion in Space and Time", *Journal of Engineering Mechanics, ASCE*, 112: 154–174, 1986.
- [6] Housner, G.W., "Calculating the Response of an Oscillator to Arbitrary Ground Motion", *Bulletin of the Seismological Society of America*, 31: 143–149, 1941.
- [7] Housner, G.W., "Characteristics of Strong Motion Earthquakes", *Bulletin of the Seismological Society of America*, 37(1): 19–31, 1947.
- [8] Housner, G.W., "Spectrum Intensities of Strong Motion Earthquakes", In *Proceedings of the Symposium of Earthquake and Blast Effects on Structures*, Earthquake Engineering Research Institute, Los Angeles, California, pp. 21–36, 1952.
- [9] Housner, G.W., "Measures of Severity of Earthquake Ground Shaking". In *Proceedings of the US National Conference on Earthquake Engineering*, Earthquake Engineering Research Institute, Ann Arbor, Michigan, pp. 25–33, 1975.
- [10] Hudson, D.E., "Response Spectrum Techniques in Engineering Seismology", In *Proceedings of the First World Conference on Earthquake Engineering*, Earthquake Engineering Research Institute, Los Angeles, California, Vol. 4, pp. 1–12, 1956.

- [11] Hudson, D.E., "Some Problems in the Application of Spectrum Technique to Strong Motion Earthquake Analysis", *Bulletin of the Seismological Society of America*, 52(2): 417–430, (1962).
- [12] Kiureghian, A. Der, "A Coherency Model for Spatially Varying Ground Motions". *Earthquake Engineering and Structural Dynamics*, 25: 99–111, 1996.
- [13] Kubo, T. and Penzien, J., "Analysis of Three-dimensional Strong Ground Motions Along Principal Axes, San Fernando Earthquake", *Earthquake Engineering and Structural Dynamics*, 7: 265–278, 1979.
- [14] Luco, J.E. and Wong, H.L., "Response of a Rigid Foundation to a Spatially Random Ground Motion", *Earthquake Engineering and Structural Dynamics*, 14(6): 891–908, 1986.
- [15] Nigam, N.C., "Phase Properties of a Class of Random Processes", *Earthquake Engineering and Structural Dynamics*, 10: 711–717, 1982.
- [16] Ohsaki, Y., "On the Significance of Phase Content in Earthquake Ground Motions", *Earthquake Engineering and Structural Dynamics*, 7: 427–439, 1979.
- [17] Penzien, J. and Watabe, M., "Characteristics of 3-dimensional Earthquake Ground Motions", *Earthquake Engineering and Structural Dynamics*, 3: 365–373, 1975.
- [18] Shrikhande, M., Das, J.D., Bansal, M.K., Kumar, A., Basu, S., and Chandra, B., "Analysis of Strong Motion Records from Dharmshala Earthquake of April 26, 1986", In *Proceedings of the Eleventh Symposium on Earthquake Engineering*, Department of Earthquake Engineering, University of Roorkee, India, Dec. 17–19, pp. 281–285, 1998.
- [19] Shrikhande, M., Das, J.D., Bansal, M.K., Kumar, A., Basu, S., and Chandra, B., "Strong Motion Characteristics of Uttarkashi Earthquake of October 20, 1991 and its Engineering Significance", In *Research Highlights in Earth System Science; Volume 2: Seismicity*, O.P. Varma, (Ed.), Indian Geological Congress, Roorkee, India, pp. 337–342, 2001.
- [20] Shrikhande, M. and Gupta, V.K., "Synthesizing Ensembles of Spatially Correlated Accelerograms", *Journal of Engineering Mechanics, ASCE*, 124(11): 1185–1192, 1998.
- [21] Shrikhande, M. and Gupta, V.K., "On the Characterization of the Phase Spectrum for Strong Motion Synthesis", *Journal of Earthquake Engineering*, 5(4): 465–482, 2001.
- [22] Trifunac, M.D. and Brady, A.G., "A Study on the Duration of Strong Earthquake Ground Motion", *Bulletin of the Seismological Society of America*, 65: 581–626, 1975.
- [23] Watabe, M. and Tohdo, M., "Analyses on Various Parameters for the Simulation of Three-dimensional Earthquake Ground Motions", In *Transaction of the 5th International Conference on Structural Mechanics in Reactor Technology, 13–17 August 1979*, Number K1/1 in K(a), pp. 1–11, Berlin, Germany, 1979.
- [24] Zahrah, T.F. and Hall, W.J., "Earthquake Energy Absorption in SDOF Structures", *Journal of Structural Engineering, ASCE*, 110(8): 1757–1772, 1984.
- [25] Zerva, A. and Shinouzuka, M., "Stochastic Differential Ground Motion", *Structural Safety*, 10: 129–143, 1991.

Chapter 5

Evaluation of Seismic Design Parameters

5.1 INTRODUCTION

Most of the earthquake occurrences are concentrated in narrow belts along plate boundaries. These earthquakes are known as **interplate earthquakes**. The earthquakes occurring within a plate are known as **intraplate earthquakes**. The origins of intraplate earthquakes are still poorly understood. Tectonic earthquakes are generated by the process of faulting. Sudden deformation of rock causes earthquake. Earthquake originates at depth (*focus*) and thus theory of earthquake occurrence has inherent uncertainties because of its development from the inference on the rocks at the surface. A fault is a fracture or a zone of fractures along which rocks on opposite side have been displaced relative to each other. The manifestation of fault is the differential movement parallel to the surface of fracture. The plate boundaries are the main faults (*sources*). There also exist some intraplate faults in Indian region. These faults are in a state of stress due to natural forces acting on them. The very rapid release of this state of stress generates earthquake motion. This release produces seismic waves that cause shaking of the ground. The structures supported on the ground are subjected to this shaking and as a result, experience deformations (stresses), that must be accounted for in earthquake resistant design. Thus understanding of earthquake process and its effect on ground motion is needed for evaluation of seismic design parameters.

5.2 TYPES OF EARTHQUAKES

The earthquakes can be classified into three categories according to its depth of focus. These are:

- (i) *Shallow focus earthquakes* are earthquakes with depth of focus < 70 km. Nearly 80% of total earthquakes are shallow focus earthquakes. These types of earthquakes are of greater concern for earthquake resistant design.
- (ii) *Intermediate focus earthquakes* are earthquakes with depth $\in [70, 30]$ km.
- (iii) *Deep focus earthquakes* are earthquakes having focal depth > 300 km.

5.2.1 Intensity

Intensity is a qualitative measure of the strength of an earthquake. It gives a gradation of strength of earthquake using observed damage to structures and/or ground and reaction of humans to the earthquake shaking. An earthquake has many intensities, the highest near the maximum fault displacement and progressively to lower grade at further away. Since the measure is not instrumental, intensity can be assigned to historical earthquakes also. The popular intensity scale is the Modified Mercalli (*MMI*) scale with twelve gradation denoted by Roman numerals from I to XII. Another intensity scale developed for central and eastern European states is known as Medvedev-Sponheuer-Karnik (*MSK*) intensity scale. The twelve gradation *MSK* scale differs with *MMI* in details only. Like many other countries, IS 1893 (Part 1), the Indian Standard: 2002, also refers to the *MSK* scale [14]. An isoseismal map shows intensities of a past earthquake in a contoured form of line of equal intensities. Note that the defined scale is subjective in nature and depend on social and prevailing construction practices. Revision of intensity scale from time to time is made so that gradations of intensity as per current construction practices are made.

5.2.2 Magnitude

The magnitude is a quantitative or absolute measure of the size of an earthquake. It can be correlated to the amount of wave energy released at the source of an earthquake. The elastic wave energy is that portion of total strain energy stored in lithospheric rock that is not consumed as mechanical work (e.g. through faulting) during an earthquake. There are various magnitude scales in use. These scales differ from each other because those are derived from measuring different wave components of an earthquake. Richter [25] defined magnitude of local earthquake in southern California for shallow earthquake having epicentral distance $\Delta < 600$ km. Local (Richter) magnitude (M_L) is logarithm to the base 10 of the maximum seismic wave (velocity) amplitude in microns (10^{-3} mm) recorded on Wood-Anderson seismograph (having period 0.8 s, nearly critical damping and magnification 2800) at a distance (Δ) 100 km from the epicentre of earthquake. Richter magnitude can be scaled for any seismograph of about 1 s period using instrumental amplification corrected amplitude of ground motion. Later other scales were defined for larger and/or distant earthquakes ($\Delta > 600$ km). Surface wave (S-wave) magnitude (M_S) is defined on the basis of the amplitude of surface (Rayleigh) wave of period about 20 s and 80 km wavelength. M_S is valid for an aperture $\Delta > 15^\circ$ (approximately 1,650 km distance). The amplitude of compressional and dilatational wave (P-wave) through the earth is not dependent on focal depth. The body wave magnitude (m_b) is defined as the maximum amplitude of P-wavengroup on vertical component seismograph of period about 1 s and less than 10 km wavelength. This scale is routinely used to describe size of an earthquake at present. Both M_S and m_b are determined using maximum trace amplitude and epicentral distances. The size of smaller earthquake (micro-earthquake) and near earthquake (distance $\Delta < 200$ km) is often reported as duration magnitude (M_D). This scale is based on signal duration (length of seismograph trace). However, the definition of signal duration is not unique and subjective in nature. Maruyama [16] and Burridge and Knopoff [6] among others established the point force equivalence of fault slip (dislocation) as a double couple. The total moment of this slip is a function of time and is given by $M_0 = GAs$, where G is the modulus of rigidity (taken as

3×10^4 MPa for crust and 7×10^4 MPa for mantle in most of the seismic moment calculation), A is the surface area in m^2 of ruptured fault and s is the average slip in m across fault. The value of this moment as time $t \rightarrow \infty$ is known as the *seismic moment*. However, only geodetic data can provide M_0 as $t \rightarrow \infty$. Further, estimate of M_0 is also made from low frequency end of the seismic spectrum (period much larger than 20 s). This far-field seismic parameter is a direct measure of the extent of faulting and is used for comparison with near-field geodetic and geological measurements. It may also be noted that surface wave, magnitude M_S is an energy measure and is determined by seismic wave amplitude at a period approximately in the range of 18 s to 22 s. The moment magnitude M_W as defined by Hanks and Kanamori [11] is given by,

$$M_W = 2/3 \log M_0 - 6.7 \quad (5.1)$$

M_W is intrinsically related to seismic moment M_0 (Nm). For values at about 6.5 the m_b and M_S scales coincide. The small earthquakes (< 6.5) are better represented by m_b scale and M_S scale underestimates the same. The magnitude scales (M_L , m_b and M_S) saturate at some upper bound. M_L and m_b saturate at about 6.5 and 7 respectively. Upper bound of M_S is about 8.5. Since, M_L , m_b and M_S are determined from seismic wave of particular period and wavelength that is much shorter than the earthquake source size of great earthquakes (magnitude eight or larger). The M_W scale adequately measures the size of the source since the scale is independent of particular wave type.

5.3 FAULT RUPTURE PARAMETERS

Tocher [29], Slemmons [28] and Wells and Coppersmith [32] among others studied the correlations of fault rupture parameters (*e.g.* length and displacement) to assess the future earthquake potential in a region. Based on 216 worldwide past earthquake Wells and Coppersmith gave relationship between moment magnitude M_W and fault rupture parameters. For all styles of faulting, some of the relations are

$$\begin{aligned} M_W &= 1.16 \log(L) + 5.08 \pm 0.28; & \log(L) &= 0.69 M_W - 3.22 \pm 0.22 \\ M_W &= 2.25 \log(W) + 4.06 \pm 0.41; & \log(W) &= 0.32 M_W - 1.01 \pm 0.15 \\ M_W &= 0.98 \log(A) + 4.07 \pm 0.24; & \log(A) &= 0.91 M_W - 3.49 \pm 0.24 \end{aligned} \quad (5.2)$$

where, L , W and A are surface rupture length (km), down-dip rupture width (km) and rupture area (km^2) respectively. Similar relationships between moment magnitude M_W and displacement are also reported. These are,

$$\begin{aligned} M_W &= 0.74 \log(D_m) + 6.69 \pm 0.40; & \log(D_m) &= 0.82 M_W - 5.46 \pm 0.42 \\ M_W &= 0.82 \log(D_a) + 6.93 \pm 0.39; & \log(D_a) &= 0.69 M_W - 4.80 \pm 0.36 \end{aligned} \quad (5.3)$$

where, D_m is maximum surface displacement (m) and D_a is average surface displacement (m). The maximum surface displacement provides the largest slip at a point along a rupture and average surface displacement gives the mean displacement along the length of rupture. They also presented relations for different styles of faulting but concluded that difference is insignificant.

Further conclusions are,

- (i) L is equal to 75% of the subsurface rupture length,
- (ii) the average surface displacement per event is about 50% of the maximum surface displacement per event, and
- (iii) the average subsurface displacement on the fault plane is bounded by the average surface displacement and the maximum surface displacement.

5.4 EARTHQUAKE GROUND MOTION CHARACTERISTICS

The earthquake ground motion of sufficient strength that affect human and their environment (*strong ground motion*) are of interest for earthquake resistant design. The strong motions are measured by *accelerographs* and its record is time history of acceleration (*accelerogram*). The temporal evolution of an accelerogram is composed of three parts *viz.* rise, strong motion and decay. It is composed of non-periodic sequences of acceleration pulses of various durations. Thus not only peak of amplitude but also frequency content of record is necessary to characterize accelerogram. The characteristic of strong motion in the vicinity of causative fault (*near field*) is strongly dependent on the nature of faulting. The motion depends on source parameters such as fault shape, its area, maximum fault dislocation, and complexity of slipping process, stress drop, and the distance of fault plane from ground surface. The elastic properties of the material through which the generated seismic waves travel also influence the strong motion. The effect of ground shaking is mostly dependent on duration of strong motion part. The earthquake ground acceleration is generally broadband in frequency composition. It is rich in high frequencies in the near fields. The high frequency components attenuate faster than the low frequency components, therefore the contribution of high frequency components is reduced in the accelerograms recorded at large distances from the fault. Further, the amplitude of ground acceleration decreases with increasing distance from the causative faults in general. Moreover, in general the vertical component of the ground acceleration is richer in high frequencies than the two horizontal components.

5.4.1 Amplitude Properties

Horizontal component of acceleration is primarily used to report ground motion as structures are designed for vertical loads and margin of safety in the vertical direction are usually adequate for earthquake induced vertical load. The common amplitude measure of a ground motion is the largest horizontal acceleration and known as horizontal peak ground acceleration (*PGA*). The largest dynamic forces induced in very stiff structures are closely related *PGA*. Historic earthquakes can have only intensity information. Various authors have attempted to propose relation between *MMI* and *PGA*. Ambraseys [2] proposed such a relation using southern European earthquakes as $\log a = 0.36 I_{MM} - 0.16$. Later, using 187 records of 57 western USA earthquake with *MMI* between III and X, Trifunac and Brady [30] gave a relation as $\log a = 0.30 I_{MM} + 0.014$. Murphy and O'Brien [20], using worldwide data of 1465 records having more

than 900 records with peak horizontal ground acceleration greater than 10 cm/s^2 and *MMI* in the range I to X, also proposed correlation between *MMI* and *PGA* as $\log a = 0.25 I_{MM} + 0.25$. These relationships are shown in Figure 5.1. Horizontal ground velocity is derived from accelerogram and have less contribution from high frequency component than acceleration record. Most buildings are in the range of the frequency content of ground velocity. Thus peak ground velocity (*PGV*) v is a better indicator of damage potential. Trifunac and Brady [30] also proposed a correlation between *MMI* and *PGV*. The ratio of *PGV* and *PGA* is a representation of the frequency content of the motion. This ratio can be interpreted as the period of vibration of an equivalent harmonic wave and thus provides an indication of the significant periods of the ground motion [26]. The peak ground displacement *PGD* d is the most inaccurate ground motion information because of long period noise in the record and errors in filtering and integration of accelerograms. The displacement record is associated with lower frequency component of ground motion. Statistical analysis (Mohraz [19], Newmark and Hall [23]) on ground motion was carried to estimate ground motion properties. These studies suggest use of both v/a and ad/v^2 to estimate ground motion parameters. According to Newmark and Rosenbleuth [24] for earthquake of engineering interest the ratio ad/v^2 ranges between 5 and 15. This ratio can be considered as a measure for the sharpness of response spectrum in the velocity region. Small ratio indicates a sharp response spectrum while a large value corresponds to a flat spectrum in the velocity region. Note that all the amplitude parameters discussed are peak in a single cycle of ground motion. The damage in structure is essentially cumulative damage and it requires repeated cycle of high amplitudes. The use peak amplitudes for design purpose are generally questioned on this ground. This leads to the concept of effective peak acceleration (*EPA*) and effective velocity related acceleration A_v . The pseudo velocity corresponding to A_v is termed as effective peak velocity (*EPV*). Let S_a be the mean pseudo-acceleration value in the period $T \in [0.1, 0.5] \text{ s}$ and S_v be the pseudo-velocity value at about 1 s. For 5% critical damping NEHRP, 1997 [21] specifies the *EPA* is defined as $A_a = S_a/2.5$ and the *EPV* is similarly defined as $V_v = S_v/2.5$.

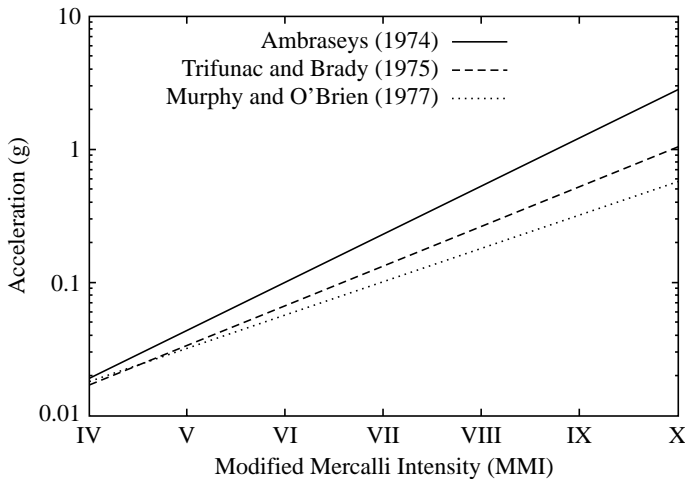


FIGURE 5.1 PGA-MMN relations.

5.4.2 Duration

Strong motion duration is related to the time required to release of the accumulated strain energy in the causative fault. Thus, duration of strong motion increases with increasing earthquake magnitude. As stated earlier it has a strong influence on damage. Housner [13] uses the mean square acceleration during the rise time of strong motion to define earthquake average power. Let

$$I = \int_0^{t_d} a^2(t) dt \quad (5.4)$$

be the total energy in a strong motion. The earthquake average power is defined as

$$P_a = \frac{1}{t_s} \int_{t_{0.05}}^{t_{0.95}} a^2(t) dt \quad (5.5)$$

where, $t_{0.05}$ and $t_{0.95}$ are the time t at which I has 5% and 95% value respectively. The former is known as the rise time and the later is known as the decay time respectively. Trifunac and Brady [31] defined t_s as the duration of strong motion part of an accelerogram and is defined as $t_s = t_{0.95} - t_{0.05}$.

5.4.3 Effect of Distance

Attenuation law gives the effect of distant earthquake to the site and is expressed as peak ground motion. The attenuation relationships in the literature can be broadly classified into three different types. The first one corresponds to those proposed by Bolt and Abrahamson [4]. These relations are in the form of Pearson family of probability curves as functions of source to site distance in various ranges of moment magnitude. They concluded that the data does not indicate increase of PGA systematically with the increase of magnitude in the near-source region. The second group of attenuation relation is of the form presented by Campbell [7]. These relations indicate that influence on PGA of site to source distance and magnitude is non-separable. The last group of attenuation relationships are popularly known as Joyner and Boore [15] type. Basic feature of this relationship is separability of influence of magnitude and site to source distance on PGA . Using western USA earthquake data, relations for larger PGA , which are valid for similar range of closest distance to surface rupture from site $d \leq 370$ km, were given by Bolt and Abrahamson [4]. These relations are specified for different ranges of moment magnitude M_W and are given by

$$A = \begin{cases} 1.20 [R^2 + 1]^{0.033} \exp(-0.066 R) & \text{for } M_W \in [5.0, 6.0], R = d + 23 \text{ and } \sigma_A = 0.06 \text{ g} \\ 1.20 [R^2 + 1]^{0.042} \exp(-0.044 R) & \text{for } M_W \in [6.0, 7.0], R = d + 25 \text{ and } \sigma_A = 0.10 \text{ g} \\ 0.24 [R^2 + 1]^{0.10} \exp(-0.022 R) & \text{for } M_W \in [7.0, 7.7], R = d + 15 \text{ and } \sigma_A = 0.05 \text{ g} \end{cases} \quad (5.6)$$

where, σ_A is the standard error of one observation (*i.e.* standard deviation of the prediction error). These relations show similar trend in attenuation as predicted by the equation (5.6) in $M_W \in [5.0, 7.0]$, but exhibit an entirely different trend in the range of $M_W \in [7.0, 7.7]$. This

deviation in trend is mainly due to the use of nonlinear regression in this study. This study also attempts to define a significant (effective) peak acceleration. On the basis of worldwide earthquake data Campbell [7] proposed attenuation relationships for peak value of both horizontal and vertical components of ground acceleration. These relationships are defined for moment magnitude M_W and the shortest distance R from site to the zone of seismogenic rupture on the fault. For peak horizontal ground acceleration (PGA), defined as the geometric mean of the PGA of two horizontal components, in units of g ($= 981 \text{ cm/s}^2$), the relation is given by,

$$\begin{aligned} \ln A = & 3.512 + 0.904M_W - 1.328 \ln \sqrt{R^2 + [0.149 \exp(0.647 M_W)]^2} \\ & + [1.125 - 0.112 \ln R - 0.0957M_W] f + [0.440 - 0.171 \ln R] s_s \\ & + [0.405 - 0.222 \ln R] s_h + \epsilon \end{aligned} \quad (5.7)$$

where, the following are recommended:

$f = 0$ for strike-slip faulting; $f = 0.5$ for normal faulting; $f = 1$ for reverse, thrust, reverse-oblique and thrust-oblique faulting; $s_s = s_h = 0$ for alluvium or firm soil (Quaternary deposit with depth $> 10 \text{ m}$); $s_s = 1$, $s_h = 0$ for soft rock (Tertiary sedimentary deposits and soft volcanic deposits); $s_s = 0$, $s_h = 1$ for hard rock (Cretaceous and older sedimentary deposits, metamorphic rock, crystalline rock, and hard volcanic deposits like basalt); and ϵ is error of the regression relation having mean zero and standard deviation σ . In this study magnitude data was postulated as $M_W = M_S$ for $M_S \geq 6.0$ and $M_W = M_L$ for $M_L < 6.0$. The standard deviation σ is correlated with $\ln A$ as,

$$\sigma = \begin{cases} 0.55 & \text{if } A < 0.068 \text{ g} \\ 0.173 - 0.140 \ln A & \text{if } 0.068 \text{ g} \leq A \leq 0.21 \text{ g} \\ 0.39 & \text{otherwise} \end{cases} \quad (5.8)$$

However, a correlation between σ and M_W is also reported in this study as,

$$\sigma = \begin{cases} 0.889 - 0.691 M_W & \text{if } M_W < 7.4 \\ 0.38 & \text{otherwise} \end{cases} \quad (5.9)$$

The equation (5.8) is found to be more robust than equation (5.9) by *r-squared* value. Further, the shortest distance from site to rupture zone depends on the average depth h to the top of the seismogenic rupture zone of a presumed earthquake. In absence of any information it is recommended as

$$h = \begin{cases} 0.5 [h_t + h_b - W \sin \alpha + \dots] & \text{if } h \geq h_t \\ h_t & \text{otherwise} \end{cases} \quad (5.10)$$

where, h_t and h_b respectively are the depth to the top and bottom of the seismogenic crust in km, α is the angle of dip of the fault plane, and W is the down-dip rupture width in km. Down-dip rupture width W can be estimated using following empirical relation obtained by Wells and Coppersmith [32]

$$\log W = -1.01 + 0.32 M_W \pm 0.15 \quad (5.11)$$

The source to site distance R is defined as

$$R = \sqrt{h^2 + d^2} \quad (5.12)$$

where, d is the closet distance from site to surface projection of the rupture zone in km. Campbell [7] recommends this attenuation relationship for $M_W \geq 5$ and source to site distance $R \leq 60$ km. This study also reports fitted equations for peak vertical acceleration, peak ground velocity and pseudo-absolute acceleration response spectra. An equation of Joyner and Boore [15] type for PGA in units of g was proposed by Boore *et al.* [5] using moment magnitude M_W , distance d in km from site to the surface projection of fault rupture and average shear-wave velocity V_s in units of m/s. This relation is given by,

$$\ln A = b_1 + b_2 (M_W - 6) + b_3 (M_W - 6)^2 + b_5 \ln R + b_V (\ln V_s - \ln V_A) \quad (5.13)$$

where, b_1, b_2, b_3, b_5, b_V are empirical constants, h denotes a fictitious depth parameter, V_A is a fictitious normalising shear-wave velocity determined by regression analysis, and $R = \sqrt{d^2 + h^2}$ represents the source to site distance. The geometric mean of two horizontal component of ground acceleration is used as peak acceleration in this study. The standard deviation of the regression is given by

$$\sigma_r = \sqrt{\sigma_1^2 + \sigma_c^2} \quad (5.14)$$

$$\sigma_{\ln A} = \sqrt{\sigma_e^2 + \sigma_r^2} \quad (5.15)$$

where, σ_e and σ_r are the standard deviation of earthquake to earthquake variability, determined in the second stage of regression, and all other components of variability respectively. In equation (5.14), σ_1 is the standard deviation of first stage of regression, and σ_c is the needed correction in standard deviation for randomly oriented horizontal component of ground acceleration. The shear-wave velocity, V_s is used in the proposed relation to define site conditions. A time weighted average shear-wave velocity value is used in the analysis and is recommended as 30 m divided by shear-wave, travel time from surface to 30 m below. The authors recommend b_1 value according to the type of fault mechanism as

$$b_1 = \begin{cases} -0.313 & \text{for strike-slip mechanism} \\ -0.117 & \text{for reverse-slip mechanism} \\ -0.242 & \text{for unspecified mechanism} \end{cases} \quad (5.16)$$

Other recommended smooth parameters are $b_2 = 0.527$, $b_3 = 0$, $b_5 = -0.778$, $b_V = -0.371$, $V_A = 1396$ m/s, $h = 5.57$ km, $\sigma_1 = 0.431$, $\sigma_c = 0.226$, $\sigma_r = 0.486$, $\sigma_e = 0.184$ and $\sigma_{\ln A} = 0.520$. The authors recommend this attenuation relation for moment magnitude $M_W \in [5.5, 7.5]$ and $d \leq 80$ km. This study also provides empirical relations for pseudo-acceleration response spectra in units of g at 5% damping for randomly oriented horizontal component of ground acceleration.

5.4.4 Ground Motion Level

The important consideration in evaluation of design forces is the consequences of damage of a particular type of structure from shaking, from ground failure, etc. Well-designed and constructed structure will be less susceptible to damage than old, poorly constructed structure. Very important structures, such as dams and nuclear power plants, whose failure would lead to disaster from secondary phenomena, should be provided with least susceptibility to damage than ordinary masonry buildings, which may be permitted to undergo repairable non-structural damage but prevented from structural failure and collapse. Thus the design criteria for very important structures will be different from that of ordinary and/or conventional buildings. The engineering project site with such structure, therefore, requires special consideration in defining appropriate levels of severity of ground motion at a given site to permit analysis of the behaviour of the structure to remain functional during and after the earthquake. One of these levels can be considered to be the maximum ground motion that reasonably can be expected to occur at the site once during lifetime of the structure. The earthquake corresponding to this level of ground motion is often called as Design Basis Earthquake (*DBE*). The other level may correspond directly to ultimate safety requirements. This level of ground motion has a very low probability of being exceeded and represents the maximum level of ground motion on the basis of estimates of upper threshold magnitude of seismic sources. The earthquake corresponding to the ultimate safety requirements is often called as Maximum Credible Earthquake (*MCE*). The *DBE* is derived on the basis of historical earthquakes that have affected the site, expressed as ground motion having a defined probability of not being exceeded during the service life of the facility and may be derived using probabilistic approach or the approach may include seismotectonic consideration (combined probabilistic and seismotectonic approach). An alternative to rigorous probabilistic analysis for evaluation of *DBE*, when data on earthquake is meagre or not available, *DBE* is taken as a fraction (e.g. 0.4 for the bridge site) of *MCE*, where *MCE* is determined by rigorous application of seismotectonic method. The *MCE* is derived on the basis of maximum earthquake potential inside the seismotectonic province of the site or adjoining seismotectonic provinces associated with or not associated with specific tectonic structures, and combined probabilistic and seismotectonic approach may also be used based on available data on earthquake occurrence. However, design earthquake has to be prescribed so that duration and frequency content of ground motion is included for ground motion specification. There can be more than one design earthquake for a particular site.

5.4.5 Geological, Geophysical and Geotechnical Data

The identification of seismic sources is of prime importance for evaluation of ground motion level. Various geological and geophysical parameters are studied to identify seismic sources. These studies include earthquake history, geological record of past seismic activity, tectonic maps, recent tectonic movement, surface landforms indicators, lineaments map from remote sensing, etc. It also includes other parameters such as abrupt change in ground water level, steep gravity gradient, magnetic gradient, difference in seismic wave velocities in the region, etc. Moreover, local topography, properties of soil and its strength, area of subsidence and/or settlement, etc., shall be used. It is necessary to ascertain faults by ground verification of remotely sensed lineaments map. The tectonic (structural geology) map of an area gives

information about the type of rocks to be found and indicates faults in a geographic region. It is necessary to determine evidence of any motion in recent times. Locations of epicentres of all available seismic data (instrumental and historical) in the region are to be plotted to determine possible trend to indicate active faulting. A fault that does not extend to earth surface and normally terminates upward at the axial region of convex upward fold (*Anticline*) is known as blind fault. This fault cannot be examined and is thus associated with very high uncertainties. But this type of fault has a very great effect on level of ground motion estimation and is often very difficult to incorporate in the evaluation. Different faults have different degree of activity. Specific definition of fault activity is given for regulatory purpose. For quantitative assessment of activity, some time a capable fault is defined as a fault that had surface displacement within past 10,000 years (*Holocene* active). Generally faults originate as small fracture, successive earthquakes propagate (lengthen) it. If a site does not belong to a very active complex tectonic zone, chances of new fault breaking are almost none for the service life of a structure.

5.5 DETERMINISTIC APPROACH

When the causative fault cannot be identified, it is very difficult to avoid arbitrariness in specifying *MCE*. The standard practice is to determine the intensity of the site (from the available isoseismal map of the region) from the strongest earthquake that has ever occurred around the site. Lacking strong motion accelerogram record, it is customary to increase the scale factor by one for the specification of *MCE*. Many earthquake intensity-acceleration relationships are available in the literature. These data suggest that the median value of the maximum ground velocity is approximately 20 cm/s for *MMI* intensity VIII and changes by a factor of 2 for each unit of change of intensity. The peak acceleration of 0.167 g thus correspond to *MMI* intensity VIII, since a velocity of 122 cm/s corresponds to a peak acceleration of g. The correlation between *MMI* and peak ground velocity is almost independent of the property of local soil. The relationship between peak velocity and peak ground acceleration is dependent slightly on local soil condition. But the *MMI* is strongly correlated with damage and the damage is dependent on local soil condition. Hence, local soil condition is implicitly taken into account in arriving at peak ground velocity. When faults exist around the site, the earthquake of maximum considered magnitude associated with each fault is determined from past seismic data. However, care should be taken to ascertain the type of magnitude (*e.g.* body wave magnitude, surface wave magnitude, local or Richter magnitude, moment magnitude, *etc.*) in the reported data. From the known length of faults from tectonic map, it is ascertained that the identified faults, associated with highest magnitude, are capable to release that amount of energy. It is customary to increase these magnitudes by 1/2 for *MCE*. The epicentres of these earthquakes are assumed to be the closest point on the faults from the site. The depth of focus of an earthquake gives the depth at which the strains build up in the earth's crust and/or Upper Mantle resulting in fracture generating seismic waves. The rocks in the immediate vicinity of a site are often not strong enough to store the energy for earthquake of magnitude of engineering significance (magnitude greater or equal to five) in a few km of the upper depth due to weathering and other natural processes. This depth plus half of the idealized down-dip rupture width, *W*, is taken for the depth of focus of each earthquake in a causative fault if no specific information of fault dip is

available. The effect of these distant earthquakes on the faults to the site, expressed as peak ground motion (e.g. acceleration, velocity and displacement), is obtained via attenuation law. Various attenuation laws are available in the literature (e.g. [2], [9] etc.). One of them is due to Esteva and Villaverde [10] and is given by

$$a = 5600 \exp(0.8M_L)/(R + 40)^2 \quad (5.17)$$

$$v = 32 \exp(M_L)/(R + 25)^2 \quad (5.18)$$

$$d = (1 + 200R^{-0.6}) v^2/a \quad (5.19)$$

where, a is PGA in gal, v is PGV (cm/s), d is PGD (cm) and R is focal (hypocentral) distance (km). M_L is the Richter magnitude and 40 km and 25 km are empirical constants to account for the volume of lithospheric rock that participates in releasing the stored energy. The above laws indicate more rapid reduction in value of high frequency component of ground motion.

5.6 PROBABILISTIC APPROACH

Various workers (Cornell [8], Esteva [9], Algermissen and Perkins [1], McGuire [17] and Basu [3], etc.) developed methodology and techniques for the probabilistic estimations of ground motion. The combined statistical and seismotectonic approach for the evaluation of ground motion parameter (acceleration, velocity and displacement) at a site involves identification of seismotectonic province of the site and seismic sources in which future significant earthquake can originate, determine the rate at which earthquake can occur in different sources, obtain the frequency distribution of depth of focus and magnitude in various sources, and establish a ground motion attenuation to account for the effect of focal distance of earthquake on the site. The analysis is carried out with the assumption that the available data is not exhaustive and contain error in locations (say 0.1 degree), depth estimates, magnitude etc. The statistical tool available for analysis is Bayesian analysis, and can be carried out on the lines of Basu [3] for evaluation of ground acceleration in following steps:

- (i) The data are sorted out for different seismic sources.
- (ii) A modular source of arc length 150 km at the surface of the earthquake with the project site as its center and of 150 km depth is taken and seismically active faults lying within modular source are considered as area sources.

Locations of floating earthquakes (not associated with faults) in the modular source are considered temporarily stationary and spatially homogeneous; and occurrence of earthquake is equally likely in the latitude and longitude direction. The focal depth data with assigned value of 33 km (average depth of Moho) are assumed to be distributed uniformly within 16 to 51 km for estimation of focal depth distribution. A mixed truncated lognormal distribution is fitted in the modular source and area sources. The probability density function of focal depth for $h \in (0, h_0]$ is,

$$f_H(h) = \sum_{i=1}^2 \frac{P_i}{\sqrt{2\pi}\sigma_i h \Phi[(\ln h_0 - v)/\sigma_i]} \exp[-(\ln h - v)^2/(2\sigma_i^2)] \quad (5.20)$$

where, $0 < P_1 < 1$, $P_2 = 1 - P_1$ and $\Phi(\cdot)$ is the probability distribution function of $N(0, 1)$. The estimation of parameters (P_1 , σ_1 , σ_2 , v) are formulated as minimum Chi-square problem. The magnitude, M_L , of earthquake is independent of rate of occurrences of earthquake. The magnitude distribution is estimated in two ways in accordance with available data. The probability density function corresponding to the bilinear frequency-magnitude relation with an upper and lower threshold is given by

$$f_{M_L}(m) = K_1 \beta \exp[(m_0 - m)\beta + (m_1 - m)\lambda U(m - m_1)], \quad m \in (m_0, m_2] \quad (5.21)$$

where, $1/K_1 = [\lambda + \beta - \lambda \exp\{(m_0 - m)\beta\} - \beta \exp\{(m_0 - m_2)\beta + (m_1 - m_2)\lambda\}] / (\lambda + \beta)$, and $m_0 < m_1 < m_2$. The $U(\cdot)$ is Heaviside function. It is assumed that $m_0 = 5$ is the lower threshold magnitude. The estimation of parameters (λ , β , m_1 , m_2) are obtained using minimum Chi-square estimation method. Physical interpretation of equation (5.21) is that there exist two different processes, one leading to release of energy below magnitude m_1 , and other above that. A linear relation can also be used with upper threshold magnitude m_2 that takes care of the ultimate strength against rupture of underlain strata. The parameter, m_2 is inferred from historical and/or geological data. Normalisation of linear frequency-magnitude relation with upper and lower threshold leads to the probability density function as

$$f_{M_L}(m) = K_2 \beta \exp[(m_0 - m)\beta], \quad m \in (m_0, m_2] \quad (5.22)$$

where, $1/K_2 = 1 - \exp[(m_0 - m_2)\beta]$. The attenuation law correlating peak ground acceleration with earthquake parameters for a source including the effect of scatter in the past data is assumed to be

$$y = a \exp[bm - c \ln(r + d) + \theta] \quad (5.23)$$

where, m is the magnitude, r is the focal distance (km), y is the peak ground acceleration (gal) and θ is a normal random variable. Esteva and Villaverde [10] have suggested values of a , b , c and d as 5600, 0.8, 2.0 and 40 km, respectively and normal random variable θ is of mean 0.04 and variance 0.4096. The occurrence of an earthquake is assumed to be in accordance with Poisson process with intensity, μ_i , for magnitude greater than five. The posterior intensity of earthquake arrival is estimated through Bayesian statistics and by using past regional (Newmark and Rosenblueth [24]) seismic data. Under the assumption of mutual statistical independence of various sources at project site, it can be shown that, the probability distribution function of maximum acceleration, Y_{\max} , can formally be

$$F_{r_{\max}}(y) = \exp \left\{ \sum_{i=1}^{n+1} t\mu_i P[Y_i > y] \right\} \quad (5.24)$$

in which μ_i is the intensity of earthquake arrival in its source, n is the number of faults in the modular source at site, and $P[Y_i > y]$ is the probability of exceeding peak acceleration, y , at the site due to the i^{th} source. From equation (5.24) t -year return period of PGA , y , is obtained as,

$$t = 1 / \left\{ \sum_{i=1}^{n+1} P[Y_i > y] \right\} \quad (5.25)$$

Substituting t , numerically the t -year acceleration is obtained at the site solving equation (5.25) numerically for y . In general peak acceleration (velocity, displacement) for 100 years service life of the structure for various exceedence probability are evaluated from equation (5.24). The level of probability is chosen with the consideration of the consequence of failure. A low exceedence probability is taken for atomic power plant structures (say 0.05). For dams less conservative exceedence probability (say 0.25) may be taken. The choice of the ground motion parameter with prescribed exceedence probability is made on an engineering judgment based on permissible damage to the structures and prescribing the levels of design ground motion.

5.6.1 Example

Himalayan belt, including parts of Indo-Gangetic planes, can be divided into three seismic provinces. Major earthquakes up to magnitude 6.5 have occurred in western Himalayas. The limited data on depth of focus of earthquakes, for which fault plane solutions are available, do not show clear-cut relationship with probable extension of the known thrusts and faults. Both the longitudinal and transverse features are capable of future seismic activity in the region. In the absence of instrumental evidence and precise depth evaluation of the seismological lineaments in relation to the project site for evaluation of design earthquake parameters can be selected on the following criteria:

1. As fault plane solution indicates probabilities of seismic slip both along the longitudinal as well as transverse tectonic lineaments in Himalayas, deep seated extensions of the tectonic planes related with the major thrusts and faults can act as capable faults.
2. The idealized width of slipped fault is about 30 km for magnitude 6.5. The focal depth is estimated to be 20 km based on the assumption that the rock in first 5 km depth in the immediate vicinity of site may not be strong enough to store the strain energy. Though the depth of focus of damaging earthquakes in the region are noted to vary from about 25 km to about 100 km, a conservative estimate of depth of focus of 20 km could be adopted for the *MCE*. Based on the seismotectonic setup of the region, the following set of earthquake parameters reported in Table 5.1 are considered for evaluation of *PGA* due to the *MCE* along the major faults around site based on the attenuation law proposed by McGuire [18]

$$y = b_1 \frac{10^{b_2 m}}{(r + 25)^{b_3}} \quad (5.26)$$

TABLE 5.1 Earthquake parameters at site

<i>Seismic source</i>	<i>Magnitude</i>	<i>Focal depth (km)</i>	<i>Hypocentral distance (km)</i>	<i>Peak horizontal acceleration (g)</i>
Srinagar Thrust	6.5	20	26	0.16
MCT	7.0	20	37	0.20
MBF (NB)	7.0	20	27	0.25
MBF (SB)	7.2	20	48	0.19

where, r is the hypocentral distance (km) and m is the magnitude. All empirical coefficients, reported by McGuire [18] for projections of horizontal PGA , PGV and PGD also, are reproduced in Table 5.2. The probabilistic approach for the same site gives PGA of 0.23 g with exceedence probability of 0.25 for 100-year service life of the structure. The PGA of 0.25 g corresponding to MCE can be recommended for the site by combining both deterministic and probabilistic approach for evaluation of acceleration response spectra.

TABLE 5.2 Parameters for attenuation laws

<i>Observation</i>		<i>Coefficients</i>	
y	b_1	b_2	b_3
Acceleration (g)	0.482	0.278	1.301
Velocity (m/s)	0.0564	0.401	1.202
Displacement (mm)	3.93	0.434	0.885

5.7 RESPONSE SPECTRA

Earthquake engineers prefer to report interaction between ground acceleration and structural systems through response spectrum as popularised by Housner [12]. It reflects frequency content, amplitude of ground motion and effect of subsequent filtering by the structure. Acceleration spectrum is a plot of natural period of vibration of a single degree of freedom (SDOF) oscillator with a specific value of damping versus peak absolute acceleration of oscillator mass when subjected to a base acceleration equal to the earthquake accelerogram (*i.e.*, ground acceleration). The value of the spectral acceleration at zero periods, known as zero period acceleration (ZPA), is the PGA because oscillator is composed of infinitely stiff linear spring. The relative displacement response spectrum asymptotically approaches maximum ground displacement for highly flexible structure. This implies that the mass remains stationary for all practical purposes and only the ground moves as the linear elastic *SDOF* system is composed of spring with negligible stiffness. In-between the two extremes period, the value of spectral acceleration at a particular period is a constant multiplier, known as amplification factor, of peak ground acceleration. The amplification factor at short-period increases with increase of period and reaches a maximum at the sub-soil period and then it decreases with increase of period in general. The amplification factor for rocky site condition is higher than that of alluvium site condition at short periods and vice versa at long-periods. The amplification factor reduces with increase of hypocentral distance from the site and peak amplification occurs at longer period.

5.8 DESIGN SPECTRUM

The design response spectrum is a smooth response spectrum specifying level of seismic resistance required for design. Thus the design spectrum is a specification of the required strength of structure. The strength is frequency dependent and also dependent on maximum velocity, maximum displacement and maximum acceleration in various ranges of frequencies.

Three straight lines bound the general shape of the smooth spectra on a logarithmic tripartite graph as shown in Figure 5.2. At low frequency range the spectral displacement S_d = maximum ground displacement d ; and in the high frequency range, the spectral acceleration S_a = maximum ground acceleration a . As we proceed from low to high frequency, there exist five different regions. These are:

- (i) a transition from maximum ground displacement to amplified spectral displacement,
- (ii) amplified displacement,
- (iii) amplified velocity,
- (iv) amplified acceleration and
- (v) a transition from amplified spectral acceleration to ground acceleration.

The design spectrum can be obtained from maximum ground velocity, displacement and acceleration if the amplifications are known. Table 5.4 gives the amplification factors for larger

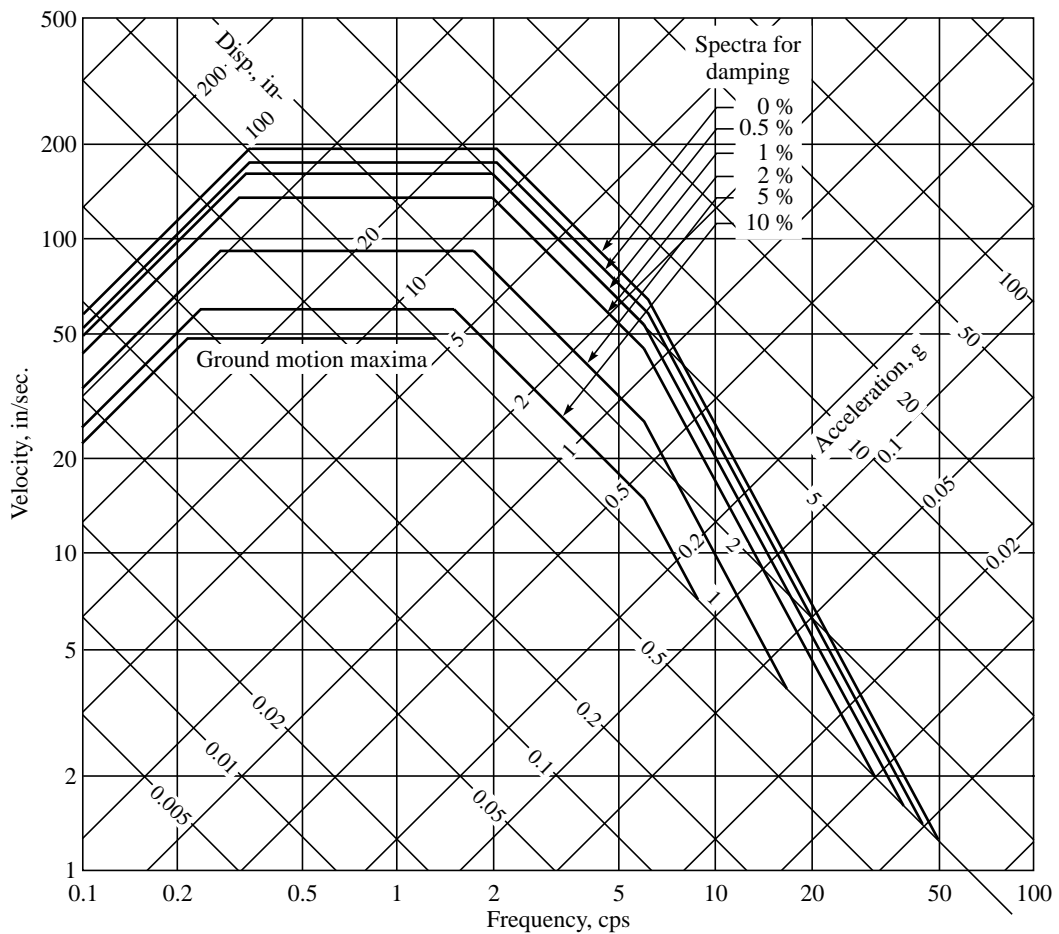


FIGURE 5.2 Design spectra recommended by Newmark et al. [22] for 1 g PGA at 84.1 percentile.

horizontal and vertical component of earthquake. Newmark et al. [22] proposed transition from amplified ground acceleration to ground acceleration begin at 6 Hz. for all damping values and end at 40, 30, 17.0 and 9.0 Hz, for critical damping ratio 0.5, 2.0, 5.0 and 10.0 per cent, respectively. Corresponding to 1 g ZPA, the peak ground velocity is 122 cm/s and displacement is 91 cm for alluvial soil, and 58 cm/s and 30 cm for the rock. The measure of width of the spectrum is $ad/v^2 = 6$ for both type of spectra. Figure 5.2 shows the spectrum for alluvial soil recommended by Newmark et al., for 1 g ZPA. Figure 5.3 shows the 84.1 percentile (*i.e.* mean + one standard deviation), 5% critical damping spectra for the horizontal component of earthquake motion by Seed et al. [27]. Mohraz [19] studied three components of ground motion. The mean value of the ratio of smaller and larger horizontal component (RS) is 0.83 and that of vertical and larger horizontal component (RV) is 0.48. The 84.1 percentile values are RS = 0.98 and RV = 0.65 which indicates that both horizontal components are almost equal and the vertical component is approximately 2/3 of the larger horizontal component. Figure 5.4 shows average spectra normalized to 1 g ZPA for 2% critical damping. Tables 5.3–5.5 give the ground motion parameter, amplification factor for alluvium and proposed site design spectra coefficients. Given the PGA is a , using Tables 5.3–5.5, 50 or 84.1 percentile horizontal design response spectrum can be obtained. The spectral values are $S_d = \text{factor} \times d$, $S_v = \text{factor} \times v$ and $S_a = \text{factor} \times a$ where d , v and a are PGD, PGV and PGA respectively from Table 5.3. From Table 5.4, design spec-

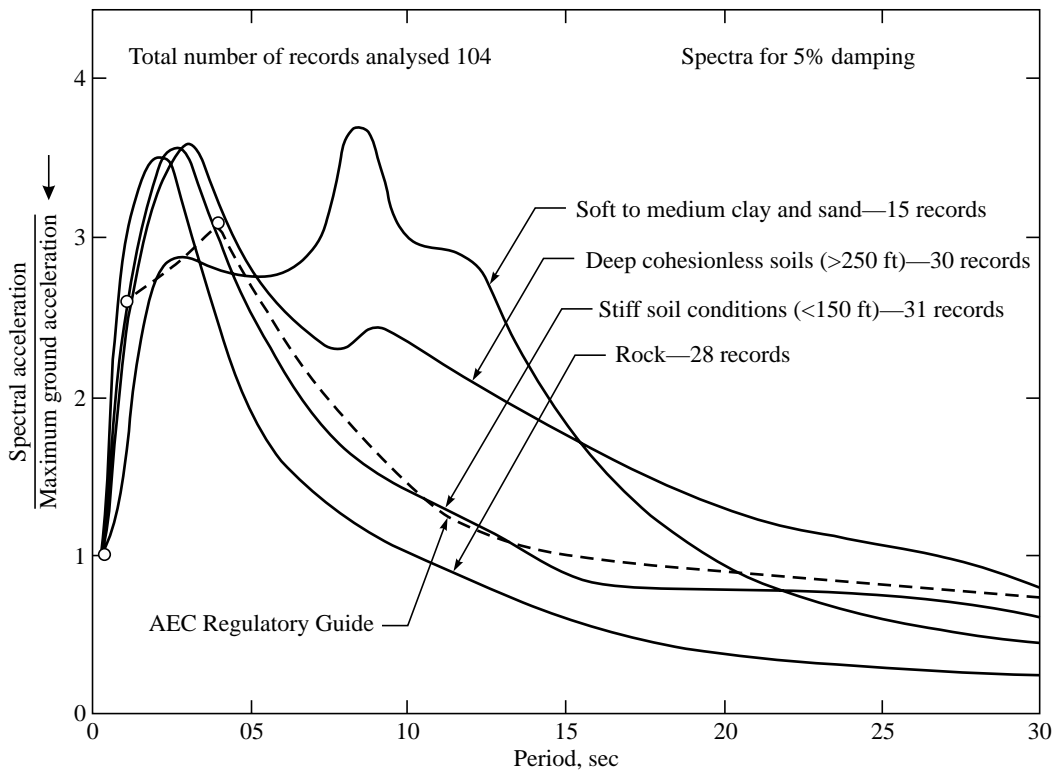


FIGURE 5.3 Design spectra recommended by Seed [27] for 5% damping at 84.1 percentile.

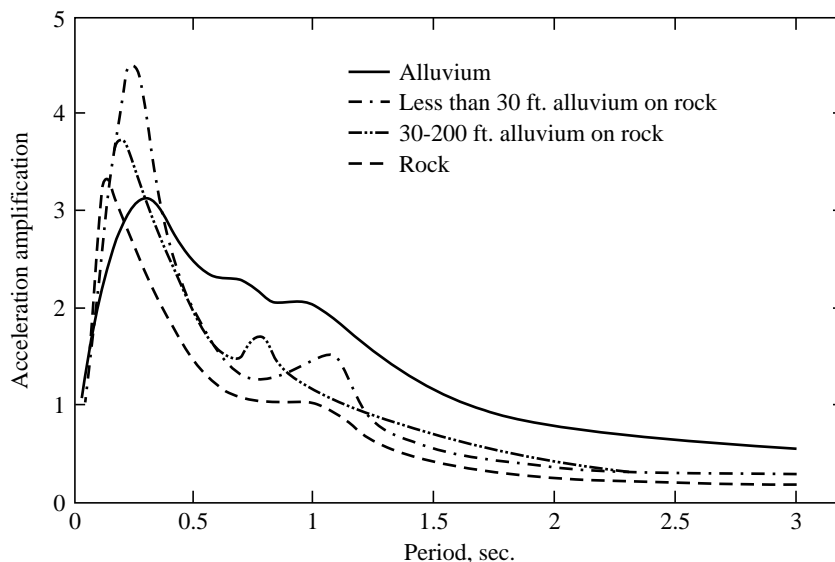


FIGURE 5.4 Average design spectra recommended by Mohraz for 2% damping.

TABLE 5.3 Ground motion parameters (after Mohraz (1976))

Site condition	Larger horizontal				Vertical			
	v/a (m/s)/g	ad/v^2	v m/s	d mm	v/a (m/s)/g	ad/v^2	v m/s	d mm
Rock	0.686	6.9	0.686	330.0	0.787	7.6	0.787	480.0
Alluvium underlain by rock < 9 m deep	0.940	5.2	0.940	467.0	0.940	8.5	0.940	765.0
Alluvium underlain by rock between 9-61 m deep	0.838	5.6	0.838	401.0	0.838	9.1	0.838	650.0
Alluvium	1.295	4.3	1.295	734.0	1.295	5.0	1.295	856.0

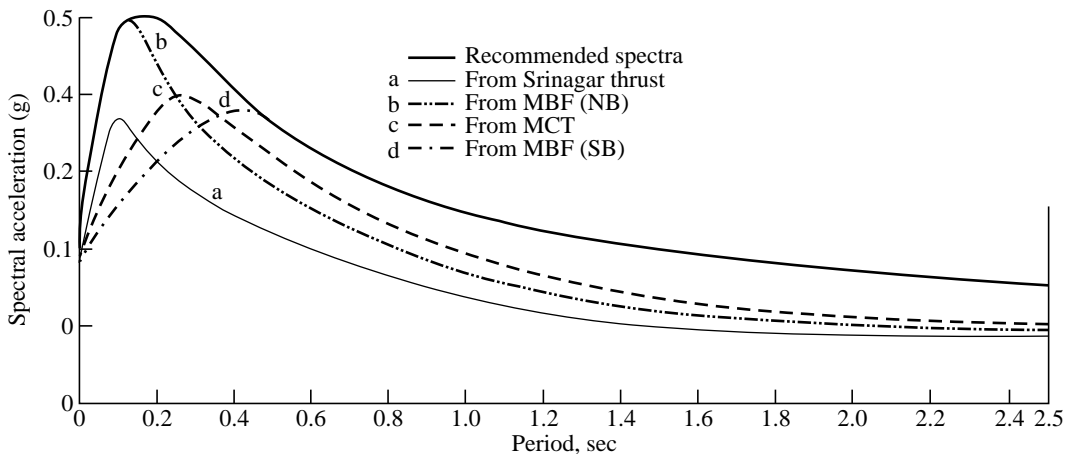
TABLE 5.4 Amplification factors (5% damping) for larger horizontal component (after Mohraz (1976))

Site condition	Percentile					
	50		84.1		50	
	Displacement		Velocity		Acceleration	
Rock	1.83	2.71	1.28	1.90	1.98	2.82
Alluvium underlain by rock < 9 m deep	2.53	3.30	1.33	2.09	2.60	3.38
Alluvium underlain by rock between 9-61 m deep	1.85	2.73	1.47	2.19	2.29	2.94
Alluvium	2.07	2.78	1.44	2.08	2.01	2.58

TABLE 5.5 Site design coefficient (after Mohraz (1976))

Site category	Coefficients		
	Displacement	Velocity	Acceleration
Rock	0.50	0.50	1.05
Alluvium underlain by rock	0.75	0.75	1.20

trum value can be obtained as site coefficients \times design spectrum value for alluvium site. According to the geological condition of site, taking averaged spectral acceleration as a guide, the spectral acceleration of each faults are drawn. An envelope, of all these spectral acceleration of various causative faults for a particular site, is called acceleration spectrum of *MCE*. The acceleration spectrum corresponding to *DBE* is obtained by multiplying a fraction less than equal to half to the spectral acceleration of *MCE*. Figure 5.5 corresponds to the spectral acceleration for *MCE* of rocky site with earthquake parameters given in Table 5.1. The spectral acceleration for *DBE* is used for working stress design and that of *MCE* is used for ultimate design.

**FIGURE 5.5 Acceleration spectrum for MCE for 10% damping.**

SUMMARY

The seismic design parameters and ground motion characteristics are discussed in this chapter. Both deterministic and probabilistic approaches to determine ground motion level are presented. Various factors influencing the design ground motion parameters are discussed. Finally, the construction of design spectrum needed for earthquake resistant design calculations is elaborated at the end.

REFERENCES

- [1] Algemisen, S.T. and Perkins D.M., "A Technique for Seismic Zoning—General Consideration and Parameter", In *Proceedings of the International Conference of Microzonation for Safer-Construction, Research and Application*, Vol. II, pp. 865–878, Seattle, Washington, 1972.
- [2] Ambraseys, N.N., "The Correlation of Intensity with Ground Motions", In *Advances in Engineering Seismology in Europe*, Trieste, 1974.
- [3] Basu, S., "Statistical Analysis of Seismic Data and Seismic Risk Analysis of Indian Peninsula", *Ph.D thesis*, Department of Civil Engineering, IIT Kanpur, India, 1977.
- [4] Bolt, B.A. and Abrahamson, N.A., "New Attenuation Relations for Peak and Expected Accelerations of Ground Motion", *Bulletin of the Seismological Society of America*, 72(6): 2307–2321, 1982.
- [5] Boore, D.M., Joyner, W.B., and Fumal, T.E., "Equations for Estimating Horizontal Response Spectra and Peak Acceleration for Western North American Earthquakes: A Summary of Recent Work", *Seismological Research Letters*, 68(1): 128–140, 1997.
- [6] Burridge, R. and Knopoff, L., "Body Force Equivalents for Seismic Dislocation", *Bulletin of the Seismological Society of America*, 54: 1875–1888, 1964.
- [7] Campbell, K.W., "Empirical Near-source Attenuation Relationships for Horizontal and Vertical Components of Peak Ground Acceleration, Peak Ground Velocity, and Pseudo-absolute Acceleration Response Spectra", *Seismological Research Letters*, 68(1): 154–179, 1997.
- [8] Cornell, C.A., "Engineering Seismic Risk Analysis", *Bulletin of the Seismological Society of America*, 58(5): 1583–1606, 1968.
- [9] Esteva, L., "Bases Para la Formulacion de Decisiones de Diseño Sísmico", *Technical Report*, Institute de Ingenieria, UNAM, Mexico, 1968.
- [10] Esteva, L. and Villaverde, R., "Seismic Risk Design Spectra and Structural Reliability", In *Proceedings of Fifth World Conference on Earthquake Engineering*, Rome, pp. 2586–2596, 1974.
- [11] Hanks, T.C. and Kanamori, H., "A Moment Magnitude Scale", *Journal of Geophysical Research*, 84(B5): 2348–2350, 1979.
- [12] Housner, G.W., "Calculating the Response of an Oscillator to Arbitrary Ground Motion", *Bulletin of the Seismological Society of America*, 31:143–149, 1941.
- [13] Housner, G.W., "Measures of Severity of Earthquake Ground Shaking", In *Proceedings of the US National Conference on Earthquake Engineering*, Earthquake Engineering Research Institute, Ann Arbor, Michigan, pp. 25–33, 1975.
- [14] IS-1893, *Indian Standard Criteria for Earthquake Resistant Design of Structures—Part 1: General Provisions and Buildings*, Bureau of Indian Standards, 2002.
- [15] Joyner, W.B. and Boore, D.M., "Peak Horizontal Acceleration and Velocity from Strong-motion Records Including Records from the 1979 Imperial Valley, California Earthquake", *Bulletin of the Seismological Society of America*, 71: 2011–2038, 1981.
- [16] Maruyama, T., "On the Force Equivalents of Dynamic Elastic Dislocations with Reference to the Earthquake Mechanism", *Bulletin of Earthquake Research Institute*, Tokyo University, 41: 467–486, 1963.

- [17] McGuire, R.K., "Seismic Structural Response Risk Analysis, Incorporating Peak Response Regressions on Earthquake Magnitude and Distance", *Technical Report* 75-51, Department of Civil Engineering, MIT Press, Cambridge, Massachusetts, 1975.
- [18] McGuire, R.K., "Seismic Design Spectra and Mapping Procedures Using Hazard Analysis Based Directly on Oscillator Response", *Earthquake Engineering and Structural Dynamics*, 5: 211-234, 1977.
- [19] Mohraz, B., "A Study of Earthquake Response Spectra for Different Geologic Condition", *Bulletin of the Seismological Society of America*, 66: 915-932, 1976.
- [20] Murphy, J.R. and O'Brien, L.J., "The Correlation of Peak Ground Acceleration Amplitude with Seismic Intensity and Other Physical Parameters", *Bulletin of the Seismological Society of America*, 67(3): 877-915, 1977.
- [21] NEHRP, "Recommended Provisions for Seismic Regulation for New Buildings and Other Structures", *Technical Report*, Building Safety Council for Federal Emergency Management, Washington D.C., 1997.
- [22] Newmark, N.M., Blume, J.A., and Kapur, K.K., "Seismic Design Spectra for Nuclear Power Plants", *Journal of Power Division, ASCE*, 99(02): 873-889, 1973.
- [23] Newmark, N.M. and Hall, W.J., "Earthquake Spectra and Design", *Technical Report*, Earthquake Engineering Research Institute, Berkeley, California, 1982.
- [24] Newmark, N.M. and Rosenblueth, E., "Fundamentals of Earthquake Engineering", Prentice Hall, Inc., New Jersey, 1971.
- [25] Richter, C.F., *Elementary Seismology*, W.H. Freeman and Co., San Francisco, California, 1958.
- [26] Seed, H.B. and Idriss, I.M., "Ground Motions and Soil Liquefaction during Earthquakes", *Technical Report*, Earthquake Engineering Research Institute, Berkeley, California, 1982.
- [27] Seed, H.B., Ugas, C., and Lysmer, J., "Site Dependent Spectra for Earthquake-resistant Design", *Bulletin of the Seismological Society of America*, 66: 221-243, 1976.
- [28] Slemmons, D.B., "Determination of Design Earthquake Magnitudes for Microzonation", in *Proceedings of 3rd International Earthquake Microzonation Conference*, pp. 119-130, 1982.
- [29] Tocher, D., "Earthquake Energy and Ground Breakage", *Bulletin of the Seismological Society of America*, 48(2): 147-153, 1958.
- [30] Trifunac, M.D. and Brady, A.G., "On the Correlation of Seismic Intensity with Peaks of Recorded Strong Motion", *Bulletin of the Seismological Society of America*, 65: 139-162, 1975.
- [31] Trifunac, M.D. and Brady, A.G., "A Study on the Duration of Strong Earthquake Ground Motion", *Bulletin of the Seismological Society of America*, 65: 581-626, 1975.
- [32] Wells, D.L. and Coppersmith, K.J., "New Empirical Relationships among Magnitude, Rupture Length, Rupture Width, Rupture Area and Surface Displacement", *Bulletin of the Seismological Society of America*, 84(4): 974-1002, 1994.

PART II

Structural Dynamics

Chapter 6

Initiation into Structural Dynamics

6.1 INTRODUCTION

Any study of vibrations and related topics requires an understanding of the basic question—what is vibration? Basically, vibration is an oscillatory motion of a particle or a body about a reference position. Such motion may be simple harmonic (sinusoidal) or complex (non-sinusoidal). The most striking feature of any vibrating body is the effect of inertia which comes into play by virtue of Newton's second law of motion, which states that the rate of change of momentum of any body in motion is equal to the external forces acting on it, that is,

$$F(t) = \frac{d}{dt}(mv) \quad (6.1)$$

where, $F(t)$ is the external (time varying) force applied on the body, m denotes the mass (a measure of inertia) of the body, and v represents the instantaneous velocity of the body. Equation (6.1) describes the instantaneous equilibrium that exists between various forces acting on the system, if we assume the time rate of change of momentum—which has the units of force—to be a fictitious inertia force. Energy considerations often play an important role in vibration problems. From the consideration of the principle of conservation of energy, any vibrating system will, in general, have three constituents: (i) a mechanism to store the kinetic energy; (ii) a mechanism for energy dissipation/loss; and (iii) a mechanism to store the potential energy, responsible for the elastic restoring force in the vibrating system. An example of the most elementary form of a dynamical system, which every student of science is familiar with, is a *simple pendulum*, shown in Figure 6.1. This simple system is a classic demonstration of the energy conversions that take place in any dynamical system, once it is set into motion. Let us recapitulate some of the basic aspects of the dynamics of this simple system. The pendulum is set into motion by taking the bob to the extreme position

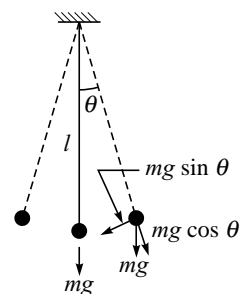


FIGURE 6.1 A simple pendulum.

and then releasing it. When the bob is at the extreme position the potential energy of the system is at its maximum while the kinetic energy is minimum. As the bob approaches the mean position during its downward swing, the potential energy is gradually converted into the kinetic energy of the bob so much so that at the mean position the kinetic energy is at its maximum with potential energy being zero. This energy conversion goes on in every half cycle as long as these oscillations persist. The oscillations eventually subside due to frictional losses caused by the resistance offered by the air to the motion of bob.

Having observed the physical phenomenon, it is then natural to enquire—is it possible to develop a mathematical model for describing it? The answer is a resounding *yes*. In fact, mathematical modelling is an integral part of the study of structural dynamics. The solution of the differential equation governing the mathematical model correspond to the observed physical phenomenon. The governing differential equation, also known as the equation of motion, is a second order differential equation in time. The most important (and many a time quite difficult one) aspect of structural dynamics is the formulation of equation of motion. In general, the governing equation of a vibrating system can be developed by adopting any of the following five approaches:

1. Newton's second law of motion,
2. Application of d'Alembert's principle,
3. Principle of virtual work,
4. Hamilton's principle, and
5. Lagrange's equation

Of these, the first two approaches are based on the principles of *vector mechanics*, whereas the latter two approaches are based on *variational principles*. The approaches based on vector mechanics are physically intuitive but invariably become intractable in case of complex configurations. On the other hand, the variational approaches depend on scalar work-like quantities and can accommodate very complex systems without any difficulty. However, the variational approaches are more abstract and lack the physical intuitive appeal afforded by the vector mechanics approaches. The principle of virtual work is an extension of the equilibrium methods in the sense that it is a statement of no work being done by a system of forces, in equilibrium, in moving through a set of virtual displacements consistent with the geometric constraints. For the purpose of introductory exposition to structural dynamics the methods based on vector mechanics will suffice for establishing the equation(s) of motion.

6.2 MATHEMATICAL MODELLING

The study of structural dynamics involves developing an insight into the dynamic behaviour of the structural systems by investigating the behaviour of their models under the influence of dynamic loads, such as blast, winds, earthquakes, heavy rotating machinery, etc. The models used in these investigations can be either small-scale laboratory models for experimental studies, or can be mathematical models for analytical studies. The development of an appropriate mathematical model for a specific study requires an understanding of the basic phenomenon and a clear idea of the basic mechanics.

For example, let us consider the development of a mathematical model for the lateral load analysis of a simple portal frame shown in Figure 6.2. Since the mass of columns is very small in comparison with that of the slab, it is reasonable to assume that the entire mass of the portal is concentrated at the slab level.¹ Further, we note that the axial rigidity of the beam and slab is very large in comparison with the stiffness of columns in the lateral deformations. Thus it is a good approximation to assume that the beam/slab is infinitely rigid and entire lateral deformation is due to the flexural deformations in columns. Since, the change in length of the columns due to lateral deformations (assumed to be small) is not very significant, it is a good first order approximation to assume that the axial stretch in the columns is negligible. Moreover, as the beams are usually cast monolithically with the columns, the joint can be assumed to be rigid as the relative rotation between beam and column at the joint will be negligible. With these simplifying kinematic constraints, the lateral displacement of the rigid beam/slab is the only possible mode of deformation in the system. Since the entire mass is concentrated at the slab level, the inertial effects in the model can be completely determined from the knowledge of the motion of the slab. The model resulting from all the above mentioned simplifying assumptions is known as the *shear building* model. The origin of this nomenclature is that the shear force is constant across the height of the column. It cannot be overemphasized here that the mode of deformation in columns is purely *flexural*. This also brings us to the concept of *dynamic degrees of freedom*, which is defined as the total number of displacements (and rotations) required to completely determine the inertial effects in a dynamical system. Accordingly, the lateral deformation of the portal frame of Figure 6.2 under the influence of a lateral load $F(t)$ can be represented as the response of a single-degree-of-freedom system shown in Figure 6.3. This is a typical discrete spring-mass-dashpot mechanical analog for the response of portal frame to lateral loads. The parameters of discrete model are related to the physical system (portal frame) as:

- mass m is the total mass of the beam and slab of the frame and serves as the storage for kinetic energy,
- spring of stiffness k represents the combined stiffness of two columns for lateral deformations and stores the internal strain energy due to column deformations, and

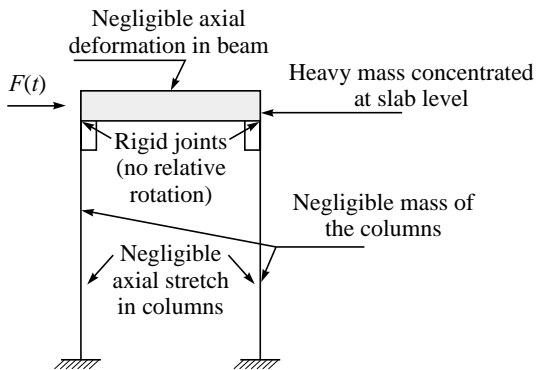


FIGURE 6.2 A simple portal frame.

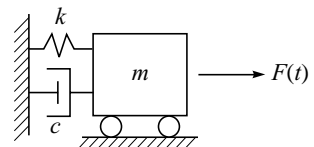


FIGURE 6.3 Equivalent single degree of freedom system.

¹Actually, it is also possible to account for the mass/inertia properties of the columns by adding one-third of the total mass of the columns and in-fill panels to the mass of the beam/slab. This “one-third” rule which is widely adopted in all codes of practice for earthquake resistant design has its basis in the total kinetic energy equivalence criterion.

- dashpot with damping coefficient c represents the energy dissipation due to various sources,
- the excitation $F(t)$ is the lateral force $F(t)$ applied on the portal frame.

Since the essential properties of the dynamical system have been segregated into independent, discrete elements, such a model is also known as a *lumped parameter model* as against a *distributed parameter model* or continuous system wherein all the properties are distributed continuously throughout. Though all physical systems are essentially distributed parameter system, it is nevertheless possible to get a fairly good estimate of the response of a continuous system by investigating the behaviour of a suitable lumped parameter model. We shall see, in the next chapter, how the dynamic behaviour of such a system can be described by means of a second order linear differential equation with constant coefficients.

SUMMARY

This chapter provides a general introduction to the study of vibration problems. The process of transforming a physical phenomenon into a mathematical model suited for numerical experimentation is described. This should enable a reader to put in proper perspective, the detailed mathematical formulation of vibration problems in the following chapters.

REFERENCES

- [1] Clough, R.W. and Penzien, J., *Dynamics of Structures*, 2nd ed., McGraw-Hill, New York, 1993.
- [2] Craig, R.R., Jr., *Structural Dynamics*, John Wiley & Sons, New York, 1981.
- [3] Humar, J.L., *Dynamics of Structures*, Prentice Hall, Inc., 1990.
- [4] Hurty, W.C. and Rubinstein, M.F., *Dynamics of Structures*, Prentice-Hall of India, New Delhi, 1967.
- [5] Warburton, G.B., *The Dynamical Behaviour of Structures*, 2nd ed., Pergamon Press, 1976.

Chapter 7

Dynamics of Single Degree of Freedom Systems

7.1 INTRODUCTION

In the preceding chapter we have noted that from the considerations of conservation of energy any vibrating system will, in general, have three constituents: (i) a mechanism to store the kinetic energy, which is also responsible for the generation of inertia force; (ii) a mechanism for energy dissipation/loss; and (iii) a mechanism to store the potential energy, responsible for the elastic restoring force in the vibrating system. In the simplest possible idealisation of a vibrating system, these three mechanisms may be considered to be lumped into discrete elements as shown in Figure 6.3. The mass/inertia element(m) stores the kinetic energy, the spring element (k) stores the potential energy, the dashpot (c) represents the viscous damper for dissipation/loss of energy, and $F(t)$ is an external time varying force. The system shown in Figure 7.1 is a Single Degree of Freedom (SDOF) system because it is only required to monitor a single quantity, *viz.*, the movement of the mass (m), to completely describe the vibration of the system. In general the number of independent displacements required to define the displaced positions of all the masses relative to their original position is called the number of degrees of freedom for vibration analysis. A single degree of freedom (SDOF) system is the simplest possible mathematical model in structural dynamics.

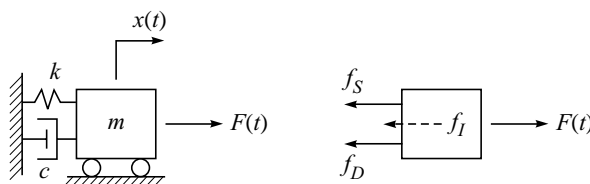


FIGURE 7.1 Single degree of freedom system (SDOF).

The motion of the mass m is governed by Newton's second law of motion. In order to derive the governing equation of motion, let us consider the various forces acting on the mass m as shown in the accompanying Free Body Diagram (FBD). The forces f_S and f_D represent the

elastic restoring force and the force developed in the damper, respectively. These forces, along with the external force $F(t)$ act on the mass (m), which then cause the change in momentum of the mass in accordance with Newton's second law as,

$$\frac{d}{dt}(m\dot{x}) = F(t) - f_S - f_D \quad (7.1)$$

where, $x(t)$ denotes the displacement of mass m from its original position of rest. For the special case of civil engineering structures, the mass of the system does not change with time, and therefore, the rate of change of momentum can be considered to have the same effect as that of applying a *fictitious* inertia force f_I directed opposite to the direction of motion for considering the instantaneous equilibrium of forces acting on the mass. This simplified interpretation of Newton's second law of motion (valid only when the mass of the system is time invariant) is popularly known as the **d'Alembert's principle**.

$$f_I = F(t) - f_S - f_D \quad (7.2)$$

Thus the inertia force $f_I = m\ddot{x}$ (mass \times acceleration), spring force $f_S = kx$ (spring constant \times spring deformation) and damping force $f_D = c\dot{x}$ (coefficient of viscous damping \times relative velocity between the two ends of the dashpot).¹ By substituting these relations in Equation (7.2), we get,

$$m\ddot{x} + c\dot{x} + kx = F(t) \quad (7.3)$$

Equation (7.3) is a linear second order differential equation with constant parameters. The general solution for this equation is given by,

$$x(t) = x_h(t) + x_p(t) \quad (7.4)$$

where, $x_h(t)$ is the solution of the corresponding homogeneous equation obtained by making the right hand side zero; and $x_p(t)$ is the particular solution which depends on the specific form of applied force $F(t)$. The homogeneous solution of this second order differential equation contains two arbitrary constants which can be evaluated by using the initial conditions $x(0)$ and $\dot{x}(0)$, i.e., the displacement and velocity of the mass at the onset of vibration.

7.2 FREE VIBRATION OF VISCOUS-DAMPED SDOF SYSTEMS

For a particular case when there is no external force acting on the system, it is still possible to make the mass vibrate by giving some arbitrary initial conditions. The ensuing motion of

¹This is only a convenient mathematical model for the energy dissipation mechanism in a vibrating system and is actually an expression of the viscous drag in a laminar flow. In real structural systems, energy dissipation actually takes place in different ways and the most important of them is the energy loss due to inter-granular friction between the particles of a vibrating system. However, incorporating a dry friction damping behaviour would result in a nonlinear equation of motion. Since the magnitude of damping force is generally very small in comparison to the other forces acting on the system, a viscous damping model (leading to a linear equation!) serves well to get a rational estimate of system response for engineering design.

the mass is then termed as the *free vibration* and is given by the solution of differential equation

$$m\ddot{x} + c\dot{x} + kx = 0$$

or,

$$\ddot{x} + 2\zeta\omega_n\dot{x} + \omega_n^2x = 0 \quad (7.5)$$

where, ω_n is defined by $\omega_n^2 = k/m$ and ζ is defined by $\zeta = c/c_{cr}$ with $c_{cr} = 2m\omega_n = 2k/m = 2\sqrt{km}$. The constant ω_n is called the *undamped circular natural frequency*, measured in rad/s; ζ is a dimensionless quantity called the *viscous damping factor*; and c_{cr} is called the critical damping coefficient. The parameters ω_n and ζ play important roles in determining the response of SDOF systems.

In order to determine the solution of Equation (7.5), let us assume a solution in the form $x(t) = Xe^{\lambda t}$. Substituting this assumed solution in the governing equation yields a characteristic equation

$$\lambda^2 + 2\zeta\omega_n\lambda + \omega_n^2 = 0 \quad (7.6)$$

which has the roots at

$$\lambda_{1,2} = -\zeta\omega_n \pm \omega_n\sqrt{\zeta^2 - 1} \quad (7.7)$$

The magnitude of the damping factor (ζ) can be used to distinguish three cases: *underdamped* ($0 < \zeta < 1$), *critically damped* ($\zeta = 1$), and *overdamped* ($\zeta > 1$). Figure 7.2 illustrates the response for these three cases. For the underdamped case the motion is oscillatory in nature with a decaying amplitude. For the overdamped case there is no oscillation, and amplitude decays slowly. For the critically damped system there is no oscillation, and the amplitude decays more rapidly than in either the underdamped or overdamped cases.

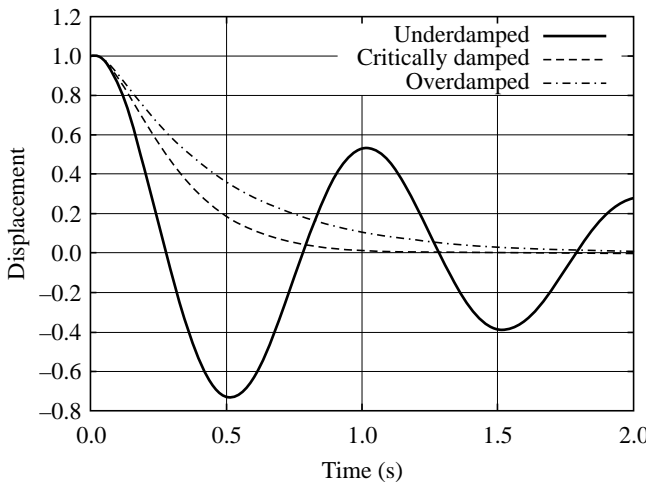


FIGURE 7.2 Response of single degree of freedom systems.

7.2.1 Underdamped Case ($\zeta < 1$)

For $\zeta < 1$, it is convenient to write Equation (7.7) in the form

$$\begin{aligned}\lambda_{1,2} &= -\zeta\omega_n \pm i\omega_n\sqrt{1^2 - \zeta^2} \\ &= -\zeta\omega_n \pm i\omega_d\end{aligned}\quad (7.8)$$

where ω_d is known as the *damped circular natural frequency*. Using Euler's formula, the general solution, $x(t)$, can be written in the form,

$$x(t) = e^{-\zeta\omega_n t} (A_1 \cos \omega_d t + A_2 \sin \omega_d t) \quad (7.9)$$

The coefficients A_1 and A_2 are determined from the initial conditions $x(t = 0) = x_0$ and $\dot{x}(t = 0) = \dot{x}_0$ and the solution is then given by

$$x(t) = e^{-\zeta\omega_n t} \left[x_0 \cos \omega_d t + \left(\frac{\dot{x}_0 + \zeta\omega_n x_0}{\omega_d} \right) \sin \omega_d t \right] \quad (7.10)$$

Although the value of ζ has an effect on the frequency ω_d , the most pronounced effect of damping is on the rate at which the motion dies out, that is, on the $e^{-\zeta\omega_n t}$ term.

7.2.2 Critically-damped Case ($\zeta = 1$)

When $\zeta = 1$, the Equation (7.7) gives only one solution as $\lambda = -\omega_n$. The response for the case of repeated roots is then given by

$$x(t) = e^{-\omega_n t} (A_1 + A_2 t) \quad (7.11)$$

where, A_1 and A_2 are determined from the initial conditions x_0 and \dot{x}_0 . The solution in terms of the initial conditions can be derived as,

$$x(t) = e^{-\omega_n t} [x_0(1 + \omega_n t) + \dot{x}_0 t] \quad (7.12)$$

The free-vibration response of a critically damped system does not involve oscillations about the zero-displacement position, instead the system returns to zero-displacement position asymptotically by virtue of the decayed exponential term of Equation (7.12). However, there will be precisely one crossing of the zero-displacement position if the initial displacement and initial velocity were of opposite signs.

7.2.3 Overdamped Case ($\zeta > 1$)

For $\zeta > 1$, the Equation (7.7) gives two distinct, negative real roots. The solution is then given by,

$$\begin{aligned}x(t) &= e^{-\zeta\omega_n t} (A_1 \cosh \omega^* t + A_2 \sinh \omega^* t) \\ &= e^{-\zeta\omega_n t} \left(x_0 \cosh \omega^* t + \frac{\dot{x}_0 + \zeta\omega_n x_0}{\omega^*} \sinh \omega^* t \right)\end{aligned}\quad (7.13)$$

where, $\omega^* = \omega_n \sqrt{\zeta^2 - 1}$ and the coefficients A_1 and A_2 are determined from the initial conditions x_0 and \dot{x}_0 . The trend is similar to that for the critically damped systems except that the system returns to the zero-position more slowly.

Practical utility of free vibration analysis

Although the preceding discussion has been fairly mathematical in nature, the basic concepts presented there in have immense practical utility. A point in the case is the experimental determination of dynamic characteristics (*i.e.*, natural frequency and damping) of real structures. The dynamic parameters, so estimated, can serve as a valuable check for validating the mathematical model of the structure and verify some of the modelling assumptions. Figure 7.3 shows a comparison between the free vibration response recorded during an actual test and that for a mathematical model using viscous damping model for the same set of parameters. Note the similarity in the general trend of response even though the two curves differ in detail. The response from the viscously damped model is a simplified representation of actual behaviour which is a combined effect of several different energy loss mechanisms simultaneously at work.

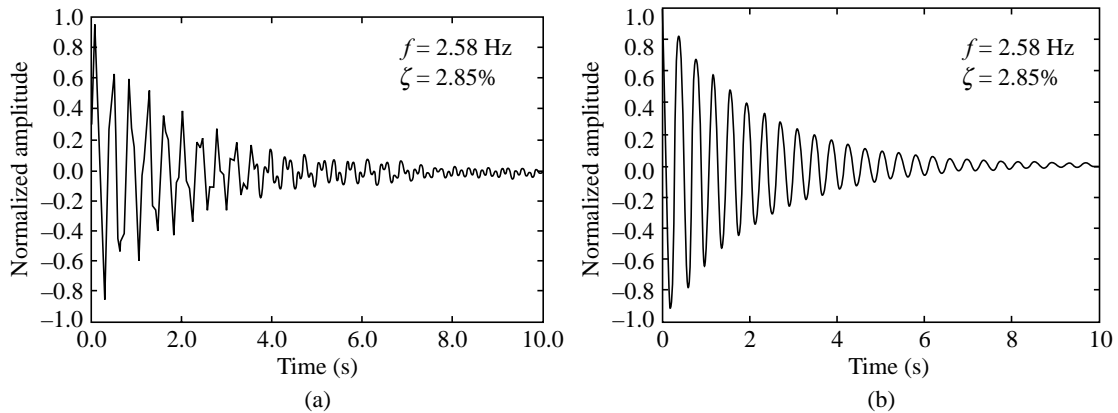


FIGURE 7.3 Free vibration response (a) from field test data, and (b) theoretical curve for viscously damped system.

The determination of (damped) natural frequency follows from its definition and is estimated by determining the number of cycles completed in the vibration record per unit time. The determination of damping from free vibration records, unfortunately, is not so straightforward. However, the procedure does simplify a lot, if we decide to ascribe energy loss to only one damping mechanism. For example, assuming viscous damping behaviour the equivalent viscous damping parameter may be estimated by using the method of *logarithmic decrement*. Let

us consider any two positive peaks x_n and x_{n+1} which occur at times $n\left(\frac{2\pi}{\omega_d}\right)$ and $(n + 1)\frac{2\pi}{\omega_d}$, respectively. The ratio of these two amplitudes is given by using Equation (7.10)

$$\frac{x_n}{x_{n+1}} = \exp\left(-\frac{2\pi\zeta\omega_n}{\omega_d}\right) \quad (7.14)$$

By taking the natural logarithm of both sides and substituting for ω_d , we get,

$$\delta = \ln \frac{x_n}{x_{n+1}} = \frac{2\pi\zeta}{\sqrt{1-\zeta^2}} \quad (7.15)$$

where, δ is known as the *logarithmic decrement*. In practice it is more convenient to measure the peak-to-trough amplitudes instead of peaks or troughs due to the absence of zero baseline in the experimental records. It can be shown that the same result for logarithmic decrement (as in Equation (7.15)) also holds for peak-to-trough amplitudes. Further, in the case of lightly damped systems, it might be more convenient to measure amplitudes which spaced a few cycles (say, m) apart. It can be shown that in this case the equation for logarithmic decrement changes to

$$\delta = \frac{x_n}{x_{n+m}} = \frac{2m\pi\zeta}{\sqrt{1-\zeta^2}}$$

which is commonly used in practice.

7.3 FORCED VIBRATIONS OF SDOF SYSTEMS

The dynamical systems may be set into motion by several types of excitations. These forcing functions may either be harmonic or non-harmonic, periodic or aperiodic, etc. Further, the response may also differ on account of the duration of exposure to the applied excitation. The nature of the response of a SDOF system to harmonic excitation is significantly different from that for a finite duration excitation. We shall begin with the response of SDOF systems excited by harmonic excitations, which has great practical significance since any periodic function can be decomposed into a sum of harmonic functions by using Fourier series². The results of this section have an important bearing on the design of vibration recording instruments, industrial vibration isolators, and shock absorbers.

7.3.1 Response of SDOF Systems to Harmonic Excitations

The governing differential equation for a SDOF system as shown in Figure 2.1 with $F(t) = F_0 \sin \omega t$ is given by,

$$m\ddot{x} + c\dot{x} + kx = F_0 \sin \omega t \quad (7.16)$$

Let us assume the initial conditions given as x_0 and \dot{x}_0 . Moreover, the particular solution of this

²Under a fairly general set of conditions, any periodic function $f(t)$ can be expressed as:

$$f(t) = a_0 + \sum_{j=1}^{\infty} \left(a_j \cos j \frac{2\pi t}{T} + b_j \sin j \frac{2\pi t}{T} \right)$$

where T is the period of $f(t)$. For more details consult any text on Applied Mathematics, such as, E. Kreyszig, *Advanced Engineering Mathematics*, Wiley Interscience.

equation will be harmonic of the same frequency as that of the excitation albeit with a phase lag. Thus the particular solution (or, steady-state response) is given by,

$$x_p(t) = X \sin(\omega t - \phi) \quad (7.17)$$

where, X is the *steady-state amplitude* and ϕ is the *phase angle* of the steady-state response relative to the excitation. The determination of these two parameters of the steady-state response is facilitated by the use of rotating vectors as shown in Figure 7.4. It can be readily established from the Figure 7.4 that

$$F_0^2 = (kX - \omega^2 mX)^2 + (\omega c X)^2, \quad \text{and} \quad (7.18)$$

$$\tan \phi = \frac{\omega c}{k - \omega^2 m} \quad (7.19)$$

This can be rewritten as,

$$D_s = \frac{X}{X_{st}} = \frac{1}{[(1 - \eta^2)^2 + (2\zeta\eta)^2]^{1/2}}, \quad \text{and} \quad (7.20)$$

$$\tan \phi = \frac{2\zeta\eta}{1 - \eta^2} \quad (7.21)$$

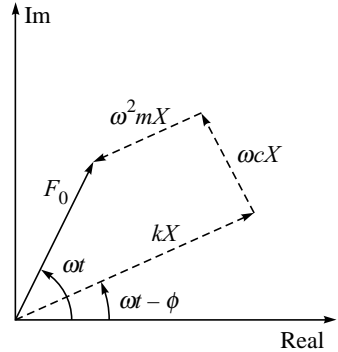


FIGURE 7.4 Force polygon.

where, $X_{st} = F_0/k$ is the static deflection if the force F_0 was applied statically, $\eta = \omega/\omega_n$ is known as the tuning ratio and ζ is the damping ratio defined earlier. The steady-state magnification factor D_s and the phase angle ϕ are plotted in Figure 7.5. From Equations (7.17) to (7.21) and Figure 7.5 the following significant features of steady-state response can be observed:

- (i) the motion described by Equation (7.17) is harmonic and is of the same frequency as the excitation.

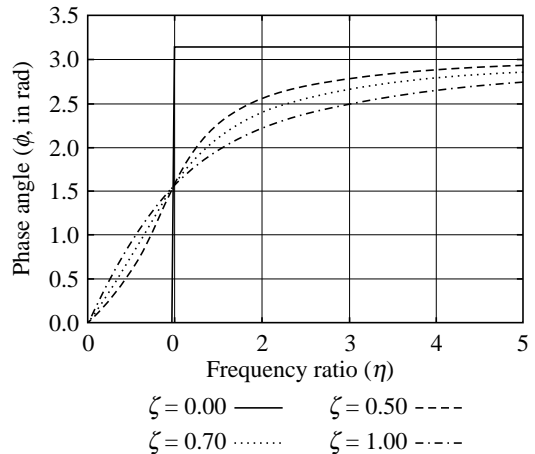
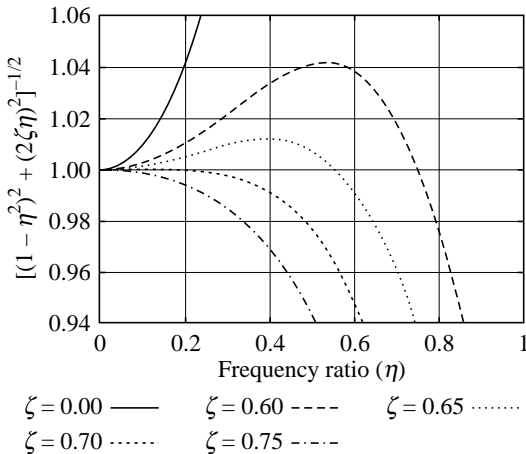


FIGURE 7.5 Magnification and phase of response of SDOF system to different excitation frequencies.

- (ii) The amplitude of the steady-state response is a function of the amplitude and frequency of the excitation as well as that of the natural frequency and damping factor of the system. The steady-state magnification factor can be considerably greater than unity or less than unity.
- (iii) The steady-state response $x_p(t) = X \sin(\omega t - \phi)$ and the excitation $F(t) = F_0 \sin \omega t$, are not in phase, that is, they do not attain their maximum values at the same instant. The response lags the excitation by a phase angle ϕ . This corresponds to a time lag of ϕ/ω .
- (iv) At resonance, $\eta = 1$, the amplitude is limited only by the damping force, and $(D_s)_{\eta=1} = 1/2\zeta$. Also, at resonance the response lags excitation by 90° .

The total response of the SDOF system can be given by superimposing the homogeneous solution on the particular solution ($x(t) = x_h(t) + x_p(t)$). The homogeneous solution is the free-vibration solution as derived earlier. The unknown parameters in the homogeneous solution can be determined by imposing the initial conditions on the total response solution of the SDOF system. Since the homogeneous part of the solution gradually decays with time—in a damped system—it is referred to as *starting transient*.

7.3.2 Excitation by Base Motion

Let us now consider the situation when the external force acting on the mass is $F(t) = 0$. Instead the support point is moving as $x_g(t) = X_g \sin \omega t$. Let $x_m(t)$ denote the absolute displacement of the mass relative to its original position of rest and $x(t)$ be the motion of the mass relative to the moving base, i.e., $x_m(t) = x(t) + x_g(t)$. The equation of motion for this system can now be written as,

$$m\ddot{x} + c(\dot{x}_m - \dot{x}_g) + k(x_m - x_g) = 0 \quad (7.22)$$

This equation can be rewritten as,

$$m\ddot{x} + c\dot{x} + kx = -m\ddot{x}_g \quad (7.23)$$

This equation is now completely analogous to the standard equation of the motion of a SDOF system and can be solved for the relative displacement response by the standard procedures.

7.3.3 Response of SDOF Systems to a Finite Duration Excitation

Let us now consider the response of a SDOF system subjected to a rectangular pulse of finite duration, T , as shown in Figure 7.6. The governing equation of motion for this system is given by

$$m\ddot{x} + c\dot{x} + kx = \begin{cases} F_0; & 0 \leq t \leq T \\ 0; & t > T \end{cases} \quad (7.24)$$

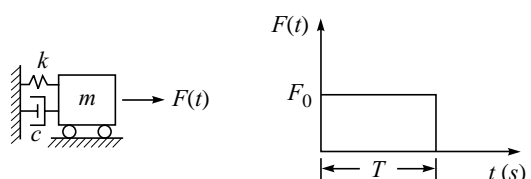


FIGURE 7.6 SDOF system excited by a finite duration rectangular pulse.

The above equation resembles the equation of motion for forced vibration for $0 \leq t \leq T$ and describes the free vibrations of SDOF oscillator for $t > T$. Accordingly, the response of the SDOF system can be considered in two phases:

(i) response during $0 \leq t \leq T$, the forced-vibration era, which comprises a homogeneous solution and a particular solution:

$$\begin{aligned}x(t) &= x_h(t) + x_p(t); 0 \leq t \leq T \\&= e^{-\zeta\omega_n t} [A_1 \cos \omega_d t + A_2 \sin \omega_d t] + \frac{F_0}{k} \\&= e^{-\zeta\omega_n t} \left[\left(x_0 - \frac{F_0}{k} \right) \cos \omega_d t + \frac{\dot{x}_0 + \zeta\omega_n(x_0 - F_0/k)}{\omega_d} \sin \omega_d t \right] + \frac{F_0}{k}\end{aligned}$$

where x_0 and \dot{x}_0 are the initial displacement and initial velocity of the oscillator mass at $t = 0$, and

(ii) free vibration response subsequent to the removal of the applied external force:

$$\begin{aligned}x(t-T) &= e^{-\zeta\omega_n(t-T)} [A_1 \cos \omega_d(t-T) + A_2 \sin \omega_d(t-T)]; t > T \\&= e^{-\zeta\omega_n(t-T)} \left[x_T \cos \omega_d(t-T) + \frac{\dot{x}_T + \zeta\omega_n x_T}{\omega_d} \sin \omega_d(t-T) \right]\end{aligned}$$

where, x_T and \dot{x}_T denote the displacement and velocity at the end of forced vibration era, at $t = T$.

The effect of the duration of application of excitation pulse on the response of a SDOF oscillator is shown in Figure 7.7, wherein the dynamic response has been normalized by the static response F_0/k . Four pulses of duration $T = [0.25T_n, 0.5T_n, 2T_n, 4T_n]$ (where T_n = natural period of the oscillator—assumed to be 0.1 s for numerical study) have been considered. It is worthwhile studying these plots in some detail. The following points emerge (with respect to the finite duration rectangular pulse):

- (i) The response of oscillator to a pulse of very short duration (with respect to the natural period) closely resembles the free vibration response of oscillator due to non-zero initial velocity.
- (ii) The time of occurrence of the maximum oscillator response—for the pulse width $T \leq 0.5T_n$, the maximum response occurs in the free-vibration phase *after* the excitation has ceased to act on the oscillator. It is, therefore, prudent while studying the dynamic response of a structural system to finite duration excitations to compute the response beyond the duration of excitation for a few cycles. This is particularly important for lightly damped systems.
- (iii) When the pulse duration is relatively large ($T > 0.5T_n$), the response during the forced-vibration era oscillates about the static response (unit normalized response), and the free vibration response oscillates about the zero-level. This shift of mean position occurs instantaneously after the excitation ceases to exist.

These observations can be used to derive analytical procedures for computing dynamic response of oscillators for arbitrary loadings as discussed in the following.

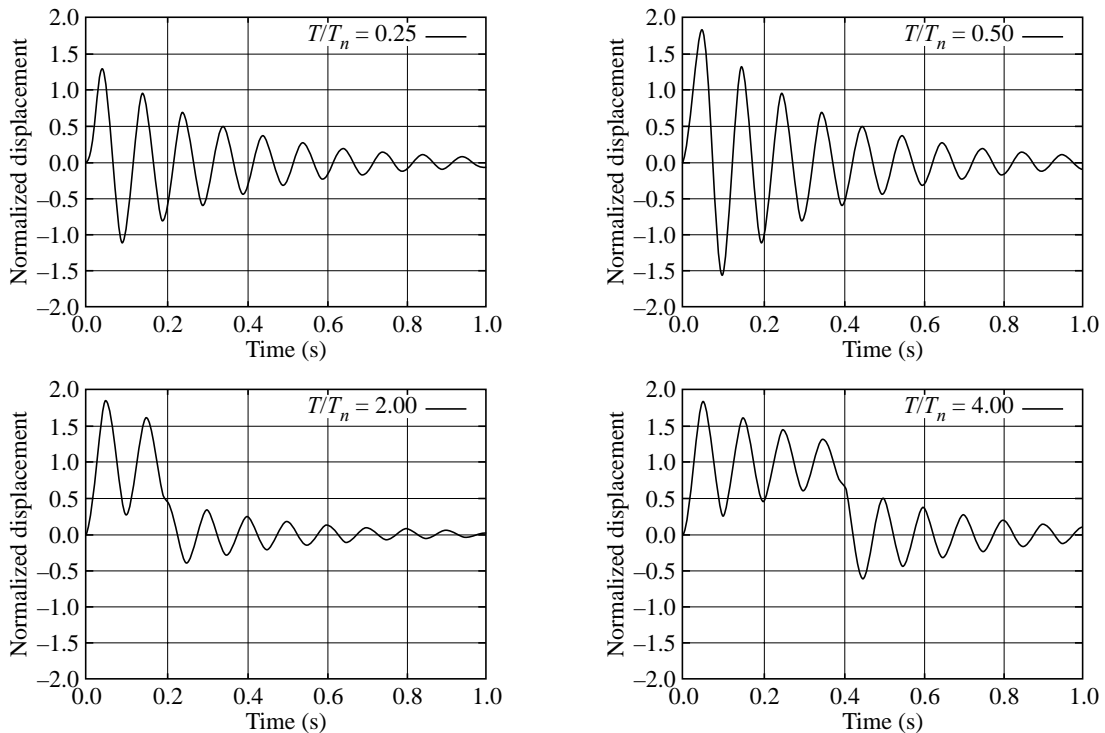


FIGURE 7.7 Effect of finite duration of excitation on response of SDOF system ($T_n = 0.1$ s, and $\zeta = 0.05$).

7.3.4 Response of SDOF Systems to a Short Duration Impulse

Let us consider a SDOF system, initially at rest, that is excited by an impulse of magnitude I . Since the impulse acts on the system for a very small time, it can only effect an instantaneous change in the momentum of the mass without altering its position. Therefore the mass, initially at rest, experiences a change in velocity but the instantaneous displacement remains zero. The velocity imparted to the mass by the impulse I is given by $\dot{x}_0 = I/m$ from the conservation of momentum principle. Thus the mass will start free-vibration after the removal of impulse with initial velocity as $\dot{x}_0 = I/m$ and initial displacement $x_0 = 0$. When the applied impulse is of unit magnitude, the resulting free vibration solution is known as the *unit impulse response function* and is given by,

$$h(t) = \frac{1}{m\omega_d} e^{-\zeta\omega_d t} \sin \omega_d t \quad (7.25)$$

The response due to an impulse is closely approximated by response to short duration pulse as seen in the first plot of Figure 7.7 for $T = 0.25T_n$. This useful approximation can be clubbed with the principle of superposition to develop a versatile analytical procedure.

7.3.5 Response of SDOF Systems to General Dynamic Excitation

A general method for evaluating the response of SDOF systems to an arbitrary form of the excitation can be derived on the basis of unit impulse response function developed earlier. The method is based on the principle of superposition and hence is strictly valid for linear systems only. Let us consider a SDOF system subjected to some arbitrary forcing function $F(t)$. This arbitrary excitation can be considered to be a sequence of pulses of infinitesimal duration $d\tau$ and magnitude equal to the amplitude of the forcing function $F(t = \tau)$ as shown in Figure 7.8. The response of the system to an impulse $dI = F(\tau)d\tau$ is denoted by $dx(t)$ and is given by,

$$dx(t) = \left(\frac{dI}{m\omega_d} \right) e^{-\zeta\omega_n(t-\tau)} \sin \omega_d(t - \tau) \quad (7.26)$$

The total response at time t will be the sum of the response due to all incremental impulses occurring prior to time t . Therefore,

$$x(t) = \frac{1}{m\omega_d} \int_0^t F(\tau) e^{-\zeta\omega_n(t-\tau)} \sin \omega_d(t - \tau) d\tau \quad (7.27)$$

This integral is known as *Duhamel integral* and can be used to compute the response of SDOF system to any arbitrary excitation. This equation can also be written as

$$x(t) = \int_0^t F(\tau) h(t - \tau) d\tau \quad (7.28)$$

and in this form it is commonly referred to as the *convolution integral*. It may be noted that the effect of non-zero initial conditions has not been considered in the response. The free-vibration response due to non-zero initial conditions should be superposed with the forced vibration response computed by using Duhamel integral to get the complete response. Since the forcing functions are usually available as tabulated values for different time instants, the Equation (7.27) needs to be evaluated numerically by replacing the continuous integral by a finite summation with a uniform pulse width (step size) Δt approximating the infinitesimal $d\tau$. As the above formulation is based on the superposition of impulse response functions, it is necessary to ensure that the pulse duration Δt used in actual evaluation of the response is indeed small enough to closely resemble this assumed behaviour. Moreover, Δt should also be small enough to assume the force amplitude to be constant within the interval. The effect of magnitude of Δt on the computed response is shown in Figure 7.9. These plots represent the response of a SDOF oscillator excited by a rectangular pulse of width $T = 4T_n$ computed analytically, and numerically by using Duhamel integral (convolution integral) for different values of Δt . It can be seen that for a large Δt the numerically computed response is a poor approximation for the analytical solution, especially in the free vibration era. Further, for any finite choice of Δt , the numerically evaluated response always lags behind the *true* (analytical) response and the amount

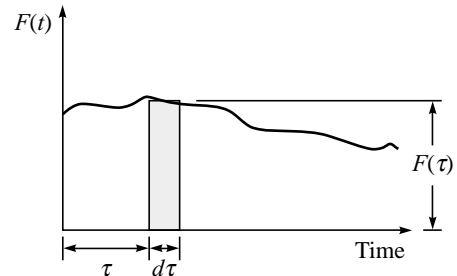


FIGURE 7.8 Arbitrary forcing function as a series of impulses.

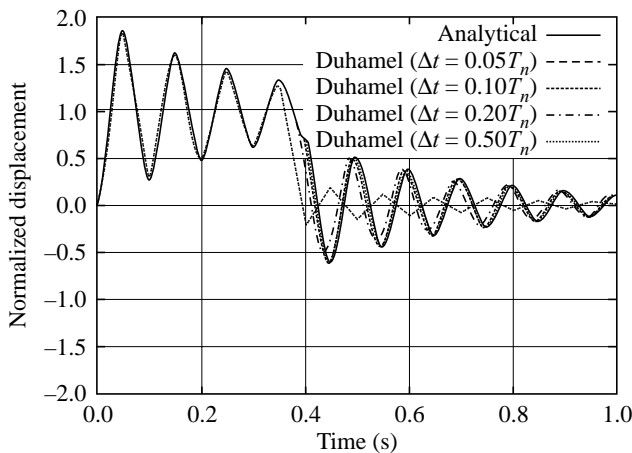


FIGURE 7.9 Effect of step size on numerical evaluation of Duhamel integral.

of lag is proportional to the choice of Δt . It can, therefore, be concluded that $\Delta t \leq 0.1T_n$ for reasonable accuracy in the computed response.

The formulation for numerical evaluation of Duhamel integral is discussed in a later chapter on the numerical evaluation of dynamic response.

7.4 VIBRATION ISOLATION

Several industrial units have machines with reciprocating parts installed at various places in the structure. These machine installations should be carefully planned and proper mountings should be designed lest these machine vibrations should transfer to other parts of the structure and interfere with the daily operations. Let us consider the schematic representation of a SDOF system shown in Figure 7.10, where the mass now represents the vibrating machine, the force $F(t) = F_0 \sin \omega t$ represents the harmonic force generated during its operation, and spring and dashpot denote the properties of the mounting system to be designed such that the force transmitted to the base (reaction) is kept under some specified limit.

The concepts developed in the study of response of SDOF system to harmonic excitations are used for designing the vibration isolators. Since the machines typically operate for long durations at a certain frequency, the starting transients can be neglected. The displacement, $x(t)$, of machine can be given by Equations 7.17 to 7.21. The total force transmitted to the support is given by (assuming that the supporting system is rigid enough not to deform significantly due to these transmitted forces):

$$\begin{aligned} R(t) &= kx(t) + c\dot{x}(t) \\ &= kX \sin(\omega t - \phi) + c\omega X \cos(\omega t - \phi) \end{aligned} \quad (7.29)$$

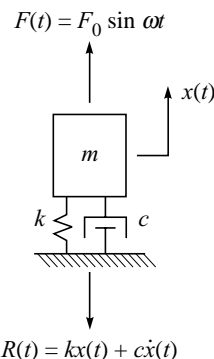


FIGURE 7.10 Transmission of vibrations from reciprocating machines.

where the two terms respectively represent the force developed in spring and dashpot. It can be seen from Figure 7.4 that these two forces are out of phase by 90° . Thus the amplitude of the total harmonic force transmitted to the support is,

$$\begin{aligned} R_{\max} &= X(k^2 + \omega^2 c^2)^{1/2} \\ &= F_0 \frac{[1 + (2\zeta\eta)^2]^{1/2}}{[(1 - \eta^2)^2 + (2\zeta\eta)^2]^{1/2}} \end{aligned} \quad (7.30)$$

where η and ζ respectively denote the tuning ratio and the damping ratio of the mounting system.

Let us define transmissibility ratio (TR) as the ratio of the amplitude of the force transmitted to the support to the amplitude of the applied harmonic force,

$$\begin{aligned} \text{TR} &= \frac{R_{\max}}{F_0} \\ &= \frac{[1 + (2\zeta\eta)^2]^{1/2}}{[(1 - \eta^2)^2 + (2\zeta\eta)^2]^{1/2}} \end{aligned} \quad (7.31)$$

which is shown in Figure 7.11 for a range of damping and tuning parameters. It may be noted from this figure that the TR curves for all damping ratios intersect at $\eta = \sqrt{2}$ for $\text{TR} = 1.0$. Further, following inferences can be drawn from these plots:

- (i) For $\eta < \sqrt{2}$, the amplitude of the transmitted force is always greater than the amplitude of imposed harmonic force and adding more damping to the mounting system contributes to the reduction in amplitude of the transmitted force.
- (ii) For $\eta > \sqrt{2}$, the amplitude of the transmitted force is always smaller than the amplitude of imposed harmonic force. Further, adding more damping to the isolator system is not beneficial for vibration isolation.

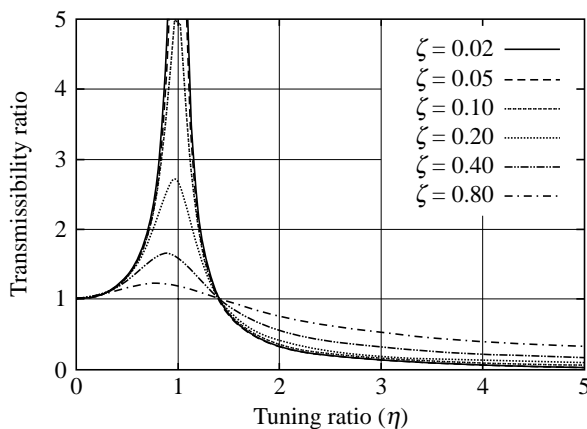


FIGURE 7.11 Vibration transmissibility ratio.

It might appear that one should always aim for a flexible isolator/mounting pads ($\eta > \sqrt{2}$) with very small damping so that the amplitude of the force transmitted to the support can have minimum isolation problem. However, such an isolator would lead to excessive displacement of the machine frame itself. Therefore, it is often preferred to have stiff isolators/mounting pads ($\eta < \sqrt{2}$) so that the machine frame itself does not vibrate so as to hinder its operation. For designing isolator to operate in this range, adding more damping to the system improves the performance of vibration isolators.

SUMMARY

The behaviour of the most elementary form of a dynamical system is described. The basic concepts of vibration analysis are presented with reference to this elementary system. Different aspects of the vibration problem are introduced such as, free vibration, forced vibration, harmonic and transient excitation, vibration isolation, etc. This background paves the way for assimilation of concepts from dynamics of more complex systems.

REFERENCES

- [1] Clough, R.W. and Penzien, J., *Dynamics of Structures*, 2nd ed., McGraw-Hill, New York, 1993.
- [2] Craig, R.R., Jr., *Structural Dynamics*, John Wiley & Sons, New York, 1981.
- [3] Humar, J.L., *Dynamics of Structures*, Prentice Hall, Inc., 1990.
- [4] Thomson, W.T., *Theory of Vibration*, 3rd ed., CBS Publishers, New Delhi, 1988.

Chapter 8

Theory of Seismic Pickups

8.1 INTRODUCTION

Often, small insignificant vibrations can excite the resonant frequencies of some structural parts and be amplified into major vibration/noise sources. Vibrations may also have adverse effects on human beings. The primary effects are task-performance interference, motion sickness, breathing and speech disturbance, and a hand-tool disease known as *white-finger*, in which nerves in the fingers are permanently damaged, resulting in the loss of touch sensitivity. It is always desirable to minimise the harmful effects of vibration through a suitable engineering design of products and systems. A fundamental requirement in all such vibration related problems is the availability of the characteristics of the expected vibrations. These vibration characteristics are derived from the analysis of the records obtained from various vibration measuring devices, known as *seismic pickups* or *transducers*.

8.2 THE PHYSICS OF OPERATION

A typical vibration measuring unit comprises of a mass supported by a spring and dashpot as shown in Figure 8.1. The inertia of the seismic mass causes it to lag behind the motion of the casing when the casing is subjected to some vibration, causing a deformation of the spring. By proper selection of mass, spring and dashpot, the relative motion measurement between mass and housing can be made proportional to either displacement, velocity or, the acceleration of the base with the help of an appropriate transducer. The equation of motion of such a system

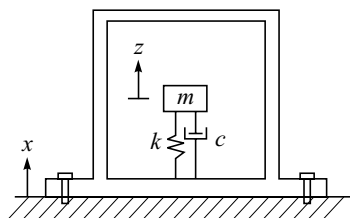


FIGURE 8.1 Schematic diagram of a seismic pickup.

is given as,

$$m\ddot{z} + c(\dot{z} - \dot{x}) + k(z - x) = 0 \quad (8.1)$$

where, z is the absolute displacement of mass m , x is the displacement of housing, c is the damping coefficient of dashpot, k is the stiffness of the spring and a ('') represents differentiation with respect to time. Defining the displacement of seismic mass relative to the base as $y(t) = z(t) - x(t)$, and rearranging the terms in the above equation,

$$\ddot{y} + 2\zeta\omega_n\dot{y} + \omega_n^2y = -\ddot{x} \quad (8.2)$$

where, ζ and ω_n represent the critical damping ratio and natural frequency of the oscillator. Transforming the time domain equation of motion as given by Equation (8.2) to the frequency domain,

$$Y(\omega) = X(\omega) \frac{\omega^2/\omega_n^2}{\left(1 - \frac{\omega^2}{\omega_n^2}\right) + i2\zeta\frac{\omega}{\omega_n}} \quad (8.3)$$

where, $Y(\omega)$ denotes the Fourier transform of the relative displacement $y(t)$ of the mass and $X(\omega)$ represents the Fourier transform of the base displacement $x(t)$. The amplitude and phase transfer function of the oscillator relating the relative displacement to the base displacement are given as,

$$\left| \frac{Y(\omega)}{X(\omega)} \right| = \frac{\frac{\omega^2}{\omega_n^2}}{\left[\left(1 - \frac{\omega^2}{\omega_n^2}\right)^2 + \left(2\zeta\frac{\omega}{\omega_n}\right)^2 \right]^{1/2}}; \quad (8.4)$$

and

$$\phi(\omega) = \tan^{-1} \left(\frac{2\zeta\frac{\omega}{\omega_n}}{1 - \frac{\omega^2}{\omega_n^2}} \right) \quad (8.5)$$

The variation of these functions with respect to the ratio of the frequency of the base motion to the natural frequency of the oscillator, also known as the tuning ratio $\eta \left(= \frac{\omega}{\omega_n}\right)$, for various values of the oscillator damping as shown in Figure 8.2. The parameters of the oscillator are selected depending on the quantity to be recorded and the usable range of frequencies.

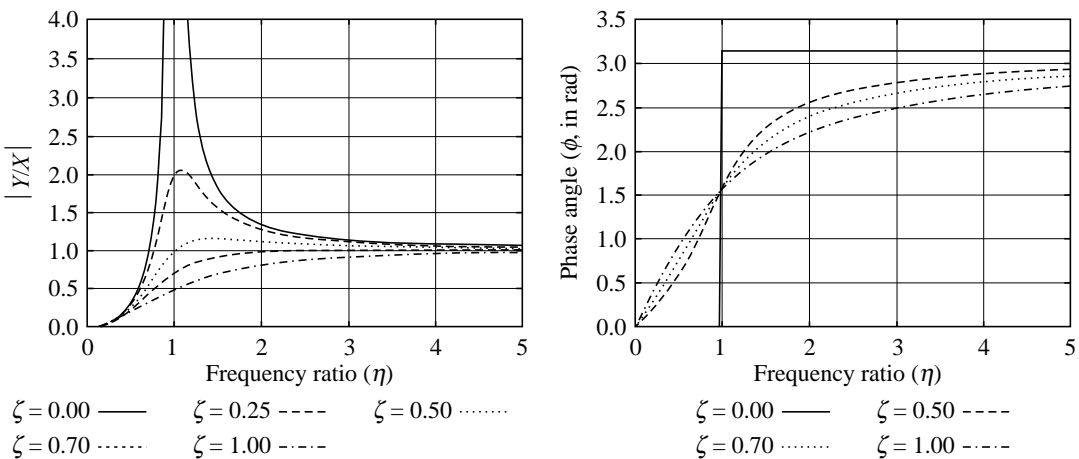


FIGURE 8.2 Amplitude and phase of the transfer function of transducer.

8.3 WHICH PARAMETER TO MEASURE?

If the amplitudes of displacement, velocity and acceleration of a certain vibration records are measured for the base motion of various frequencies, the resulting graphs of amplitudes v/s frequency are known as the *vibration spectra* and the shapes of these curves are referred to as *spectral shapes* (see Figure 8.3). It is possible to make a good judgement about which parameter to measure on the basis of these graphs. In particular, it is advantageous to select that parameter (displacement, velocity or acceleration) for the measurement which has the flattest vibration

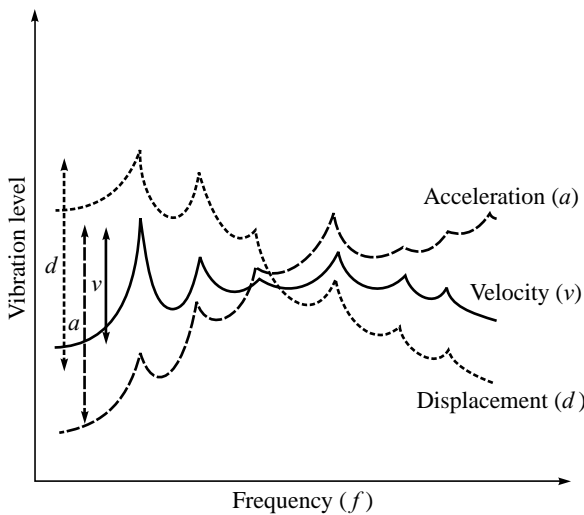


FIGURE 8.3 Typical vibration spectra.

spectrum, in the frequency-range of interest, in order to best utilise the dynamic range (the difference between the smallest and the largest values that can be measured) by the instrumentation.

Depending on the operating range of frequencies, the seismic-mass transducers may be classified as (i) seismometers and (ii) accelerometers. The difference in operation of these two basic types of seismic pickups is described in detail.

8.4 SEISMOMETERS

Seismometers are the instruments with very low natural frequency in comparison to the frequency of the vibrations to be measured so that the ratio ω/ω_n becomes very large. It may be noted from Figure 7.5, that as the frequency of the oscillator decreases, the relative displacement $Y(\omega)$ of the oscillator mass approaches the base displacement $X(\omega)$ irrespective of the value of damping. Thus the oscillator mass remains stationary while the casing of the instrument moves with the vibrating body. Due to the requirement of very low natural frequency, the seismometers are often of a very large size. Moreover, the dimensions of a seismometer unit are also governed by the peak to peak maximum displacement of the vibrating body which will be same as the maximum displacement of the vibrating base. Seismometers with an arrangement to store the vibrations measured by the seismometer on some kind of a storage device are known as seismographs. The seismometers can be designed to work as either displacement pickups, or velocity pickups.

8.4.1 Displacement Pickups

These are used to pickup the vibration of a body when there is no fixed reference point available, e.g. in determining the movement of the chassis of a vehicle. It is, therefore, required that the seismic mass should behave (as far as possible) as though it was fixed in space. This can be achieved by having a very heavy seismic mass attached to an extremely flexible spring which results in a system with a very low natural frequency ω_n . For frequencies of vibration well above the natural frequency of the pickup the displacement of the seismic mass relative to the casing is practically same as the the displacement of the casing but with the phase difference of 180° as shown in Figure 7.5. This means that as the casing moves in one direction, the seismic mass moves in the opposite direction. The relative motion of the seismic-mass may either be amplified optically to record the displacement trace on a photographic film/smoke paper, or be converted to a proportional voltage signal by using a potentiometer.

8.4.2 Velocity Pickups

A velocity pickup is designed like a displacement pickup, to have a low value of ω_n and to operate at angular frequencies well above ω_n so that the motion of the seismic mass is virtually the same as that of the casing but opposite in phase. The transducer is generally a coil of wire carried by the seismic mass which is suspended in a radial magnetic field so that a voltage proportional to velocity is generated in the coil when it is vibrated along the sensor axis. Since

the induced electro-motive force e.m.f. is proportional to the rate of intersection of the magnetic field, the generated voltage is proportional to the velocity of the vibrating body. Figure 8.4 shows the construction of a typical velocity pickup. The seismic mass consists mainly of a central rod with its associated nuts, washers and coil former. The rod connects two flexible diaphragms together, whose stiffness forms the *spring*. The coil former suspends the coil in a narrow annular slot in a cylindrical magnet—the magnetic field acting radially across the slot. The coil former may be made up of metal, so that eddy currents are generated in it to provide eddy current damping.

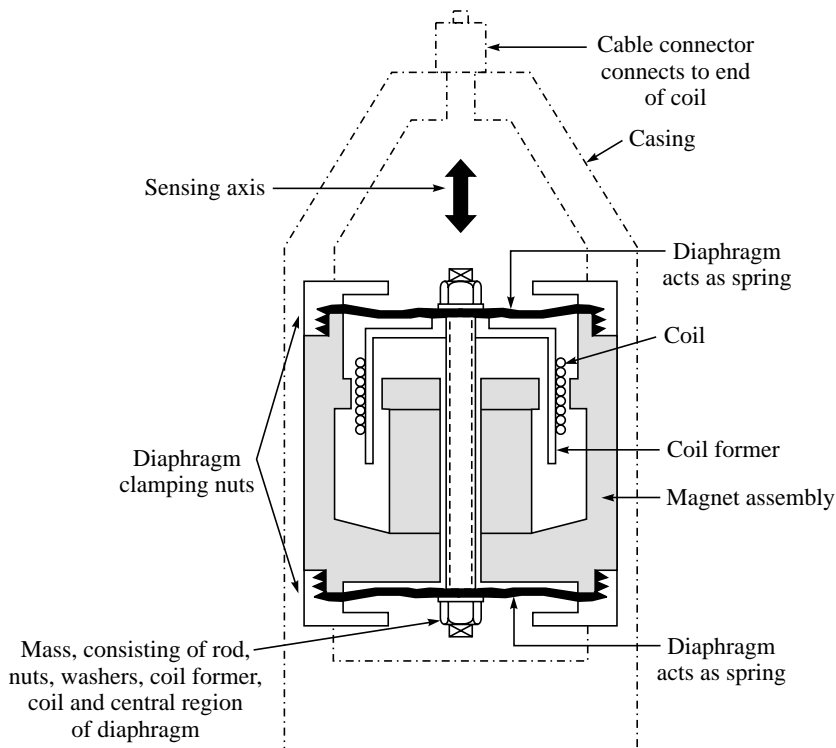


FIGURE 8.4 Schematic diagram of a velocity pickup.

Generally, seismometers are highly sensitive instruments and can pickup very small vibrations. Ironically, however, high sensitivity of these instruments make them unsuitable for recording the ground vibrations during a strong earthquake shaking. Most of these instruments cannot accommodate the large ground displacements occurring during such events.

8.5 ACCELEROMETERS

We have seen that by designing the pickup to have a very low value of ω_n it can be used as either a displacement or a velocity pickup. To measure accelerations, we must go to the other extreme, *i.e.*, make the natural frequency $\omega_n \gg \omega$ (*i.e.*, $\eta \approx 0$). As shown in Figure 7.5, for frequencies

well below the natural frequency of the pickup, the displacement of the seismic mass relative to the casing tends to be zero. Therefore, at these low frequencies the seismic mass must be experiencing the same acceleration as the casing. Considering Equation 8.4, the denominator approaches unity as $\eta \rightarrow 0$, so that

$$Y(\omega) = \frac{1}{\omega_n^2} \omega^2 X(\omega) \quad (8.6)$$

Thus the relative displacement, $Y(\omega)$, becomes proportional to the acceleration to be measured with a proportionality factor of $1/\omega_n^2$. A practical range of tuning ratio (η) can be determined for different damping ratios by studying the variation of the denominator of Equation 8.4. As shown in Figure 8.5, the denominator of Equation 8.4 remains unity for all practical purposes up to $\eta \leq 0.3$ for the damping of 70 per cent of the critical damping. This represents the maximum usable frequency range of the accelerometer. It may be noted that all other values of damping ratio result in a smaller usable frequency range for the accelerometer.

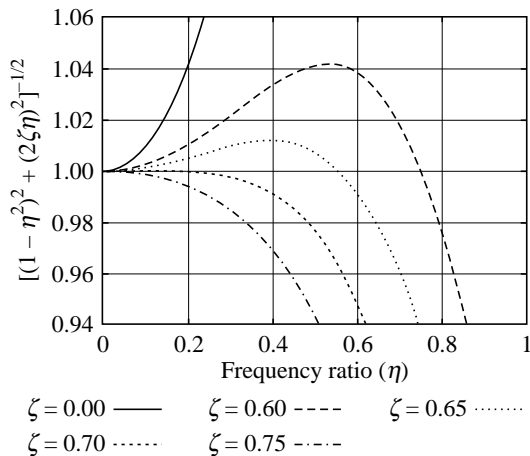


FIGURE 8.5 Amplitude spectrum of the transfer function of an accelerometer.

Thus the natural frequency of an accelerometer should be at least 3–4 times the highest frequency of the vibration to be recorded and all the smaller frequencies will be accurately measured by the accelerometer. Further, there may be phase shift between the ground motion and the relative displacements measured by the transducer. If the phase shift is same for waves of all frequencies, then the resulting signal would simply be shifted a little in time, which would be of no consequence for structural response calculations. If the phase shift is different for different frequencies, however, component waves will add up to give a distorted signal which will be quite different from the input signal. However, if the phase shift can be made a linear function of the frequency, then the resulting output signal will have the same shape as the input signal, with a small, constant shift of phase. Fortunately, it so happens that a transducer element having a damping of about 70% of critical possesses a phase-shift-frequency curve that is a good approximation to a straight line. Thus the same value of damping that gives an optimum amplitude response curve is also the best value from the stand point of phase shift.

8.5.1 Servo-accelerometers

The modern digital accelerographs make use of anti-aliasing filters and Analog to Digital Converter (ADC) to store data digitally through microprocessor. Moreover, instead of a mechanical sensor, a servo-accelerometer or Force Balance Accelerometer (FBA) is used to pickup the ground vibration. A schematic diagram of an FBA is shown in Figure 8.6. The acceleration to be measured is applied along the axial direction of the transducer. Relative displacement of the transducer mass M caused by the applied acceleration is sensed by a variable capacitance with sensitivity D (volts/m) and converted into a voltage output. This voltage is sent to an amplifier of gain k and a velocity-sensing pick-up, or to a phase-advancing network with transfer function $(1 + qd/dt)$. The output current is fed into a force generator with the amplitude modified by the generator constant G (N/Amp). The force produced completes the feed-back loop balancing the inertia force of the transducer mass caused by the acceleration, so that the mass M remains stationary relative to the instrument body. The FBAs have several advantages over mechanical accelerometers, such as:

- (i) broadening the frequency range of the measurement,
- (ii) the possibility to alter the natural frequency and damping of the transducer by changing the electrical constants, and
- (iii) significant reduction of cross-axis sensitivity due to practically zero relative movement of the mass.

The measurements of digital accelerometers are more accurate and reliable in comparison with those of analog instruments. The availability of the pre-event data, *i.e.* the data prior to the triggering of the instrument, substantially reduces the uncertainties associated with the initial velocity and initial displacement of the ground motion for computing the ground velocity and displacement time histories by integrating the recorded acceleration time history.

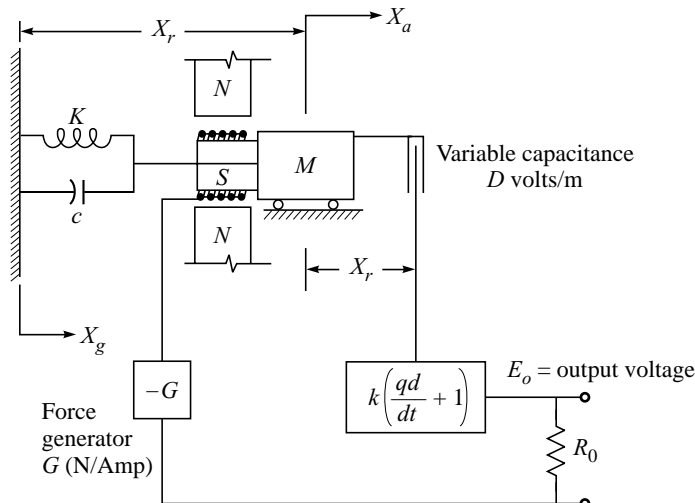


FIGURE 8.6 Force Balance Accelerometer block diagram. X_g is the absolute ground displacement, X_a denotes absolute displacement of the mass M and X_r represents the relative displacement of the mass.

8.5.2 Calibration of Accelerometers

The accelerometers capable of recording a constant acceleration (0 Hz/DC) signal can be calibrated using the earth's gravitational field. The accelerometer is mounted on a tilting table from which the angle θ between the sensing axis and the vertical can be measured. At $\theta = 0$, the force of gravity on the seismic mass is same as the force of inertia due to an acceleration of 9.81 m/s^2 . At any other angle θ the corresponding acceleration is $9.81 \cos \theta \text{ m/s}^2$. A simple 90° turn produces a traceable 1 g change in acceleration and a 180° rotation produces a 2 g change. By recording the output of the accelerometer for these acceleration levels a simple scale factor to convert the accelerometer output to acceleration units can be established. This is a simple and easy technique for testing the accelerometer before sending it out in the field.

SUMMARY

The aims and objectives of vibration recording and monitoring are discussed. This is followed by a detailed description of the principle of operation of vibration pickups. The important criteria for choosing an appropriate type of vibration pickup depending on the application are discussed.

REFERENCES

- [1] Crede, C.M. and Piersol, A.G., *Harris' Shock and Vibration Handbook*, 5th ed., McGraw-Hill Professional, 2001.
- [2] De Silva, C.W., *Vibration: Fundamentals and Practice*, CRC Press, 1999.
- [3] Rao, S.S., *Mechanical Vibrations*, 4th ed., Prentice Hall, Inc., 2003.
- [4] Thomson, W.T., *Theory of Vibration with Applications*, 3rd ed., CBS Publishers, New Delhi, 1988.

Chapter 9

Numerical Evaluation of Dynamic Response

Two distinct approaches exist to evaluate the dynamic response of SDOF systems—(i) by interpolation of the excitation, or (ii) by approximation of the derivatives in the differential equations of motion. The first approach is based on Duhamel integral and involves interpolation of the integrand of the Duhamel integral, and therefore, is strictly applicable only for linear systems. The second approach is applicable for both linear and nonlinear systems.

9.1 NUMERICAL SOLUTION BASED ON INTERPOLATION OF EXCITATION

If the excitation function $f(t)$ is specified as a set of discrete values $f_i = f(t_i)$ for $i = 0$ to N spaced at uniform interval of Δt . Assuming a linear variation of the excitation function within an interval, the variation of $f(\tau)$ within an interval may be given as,

$$f(\tau) = f(t_i) + \frac{\Delta f_i}{\Delta t} \tau \quad ; \quad 0 \leq \tau \leq \Delta t$$

where, $\Delta f_i = f(t_{i+1}) - f(t_i)$. The general solution for the dynamic response of an underdamped SDOF system within the time interval t_i and t_{i+1} is given by,

$$\begin{aligned} v_{i+1} &= e^{-\zeta\omega_n t} \left[v_i \cos \omega_d t + \frac{\dot{v}_i + \zeta\omega_n v_i}{\omega_d} \sin \omega_d t \right] \\ &\quad + \frac{1}{m\omega_d} \int_{t_i}^{t_{i+1}} f(\tau) e^{\zeta\omega_n(t-\tau)} \sin \omega_d(t-\tau) d\tau \end{aligned}$$

and $\dot{v}_{i+1} = \frac{dv_{i+1}}{dt}$

Substituting for $f(\tau)$ and evaluating the integral, the recurrence relations for displacement and

velocity may be obtained as,

$$v_{i+1} = Af_i + Bf_{i+1} + Cv_i + D\dot{v}_i$$

and

$$\dot{v}_{i+1} = A'\dot{f}_i + B'\dot{f}_{i+1} + C'v_i + D'\dot{v}_i$$

Alternatively, the recurrence relations may be arranged in a matrix form as,

$$\begin{pmatrix} v_{i+1} \\ \dot{v}_{i+1} \end{pmatrix} = \begin{bmatrix} A & B \\ A' & B' \end{bmatrix} \begin{pmatrix} f_i \\ f_{i+1} \end{pmatrix} + \begin{bmatrix} C & D \\ C' & D' \end{bmatrix} \begin{pmatrix} v_i \\ \dot{v}_i \end{pmatrix}$$

where, A, B, \dots, C', D' are the coefficients of the recurrence relation and are given in Table 9.1.

TABLE 9.1 Coefficients of recurrence relation for Duhamel integral

$A = \frac{1}{k\omega_d\Delta t} \left\{ e^{-\beta\Delta t} \left[\left(\frac{\omega_d^2 - \beta^2}{\omega_n^2} - \beta\Delta t \right) \sin \omega_d\Delta t - \left(\frac{2\omega_d\beta}{\omega_n^2} + \omega_d\Delta t \right) \cos \omega_d\Delta t \right] + \frac{2\beta\omega_d}{\omega_n^2} \right\}$
$B = \frac{1}{k\omega_d\Delta t} \left\{ e^{-\beta\Delta t} \left[\left(-\frac{\omega_d^2 - \beta^2}{\omega_n^2} \right) \sin \omega_d\Delta t + \left(\frac{2\omega_d\beta\Delta t}{\omega_n^2} \right) \cos \omega_d\Delta t \right] + \omega_d\Delta t - \frac{2\beta\omega_d}{\omega_n^2} \right\}$
$C = e^{-\beta\Delta t} \left[\cos \omega_d\Delta t + \left(\frac{\beta}{\omega_d} \right) \sin \omega_d\Delta t \right]$
$D = \frac{1}{\omega_d} e^{-\beta\Delta t} \sin \omega_d\Delta t$
$A' = \frac{1}{k\omega_d\Delta t} \left\{ e^{-\beta\Delta t} [(\beta + \omega_n^2\Delta t) \sin \omega_d\Delta t + \omega_d \cos \omega_d\Delta t] - \omega_d \right\}$
$B' = \frac{1}{k\omega_d\Delta t} [-e^{-\beta\Delta t} (\beta \sin \omega_d\Delta t + \omega_d \cos \omega_d\Delta t) + \omega_d]$
$C' = -\frac{\omega_n^2}{\omega_d} e^{-\beta\Delta t} \sin \omega_d\Delta t$
$D' = e^{-\beta\Delta t} \left[\cos \omega_d\Delta t - \left(\frac{\beta}{\omega_d} \right) \sin \omega_d\Delta t \right]$

where, $\beta = \zeta\omega_n$ and $\omega_d = \omega_n\sqrt{1-\zeta^2}$.

For reasonable accuracy in the computed response, it is necessary that the sampling interval $\Delta t \leq 0.1T_n$, T_n being the natural period of the SDOF oscillator. Use of too large sampling interval leads to the loss in temporal resolution and then it is possible that the correct maximum response might not be captured. Further, due to the finite size of pulse duration—used for summation approximation of the convolution integral—the numerically computed response is only an approximation to the exact (analytically derived) response. In particular, the amplitude of the computed response may differ from that derived analytically. Also the finite size of the pulse has the effect of introducing a phase shift in the computed response. The extent

of these deviations in amplitude and phase properties of the computed response from those of the exact solution depends on the ratio $\Delta t/T_n$. Generally, the choice of $\Delta t \leq 0.1T_n$ has been found to give satisfactory results for all practical purposes.

9.2 NUMERICAL SOLUTION BASED ON APPROXIMATION OF DERIVATIVES

If the variation of acceleration response within a time step is assumed to be approximated by a simple functional form, then it is possible to derive the corresponding variations in the velocity and displacement response which is consistent with the assumed variation of the acceleration response. For example, if the acceleration within a time step can be assumed to be constant given by the average value of acceleration at the beginning and end of the time step. Thus the acceleration during the interval t_i to t_{i+1} is given by,

$$\ddot{v}(\tau) = \frac{\ddot{v}_i + \ddot{v}_{i+1}}{2}$$

where, $\tau = (t - t_i)/\Delta t$ is the dimensionless time and varies from 0 to 1 during the interval t_i to t_{i+1} . The associated velocity and displacement during this interval are given by,

$$\begin{aligned}\dot{v}(\tau) &= \dot{v}_i + \int_0^\tau \ddot{v}(\theta) d\theta \\ &= \dot{v}_i + \tau \frac{\ddot{v}_i + \ddot{v}_{i+1}}{2} \\ v(\tau) &= v_i + \int_0^\tau \dot{v}(\theta) d\theta \\ &= v_i + \tau \dot{v}_i + \frac{\tau^2}{2} \cdot \frac{\ddot{v}_i + \ddot{v}_{i+1}}{2}\end{aligned}$$

Considering the dynamic equilibrium at the end of the interval, i.e., at t_{i+1} th instant,

$$m\ddot{v}_{i+1} + c\dot{v}_{i+1} + kv_{i+1} = f(t_{i+1})$$

Substituting from the approximated response derivatives we get,

$$\left(m + \frac{\Delta t}{2}c + \frac{\Delta t^2}{4}k \right) \ddot{v}_{i+1} = f(t_{i+1}) - (c + \Delta tk)\dot{v}_i - kv_i - \left(\frac{\Delta t}{2}c + \frac{\Delta t^2}{4}k \right) \ddot{v}_i$$

or,
$$\ddot{v}_{i+1} = \tilde{m}^{-1} \left\{ f(t_{i+1}) - (c + \Delta tk)\dot{v}_i - kv_i - \left(\frac{\Delta t}{2}c + \frac{\Delta t^2}{4}k \right) \ddot{v}_i \right\}$$

where, $\tilde{m} = m + \frac{\Delta t}{2}c + \frac{\Delta t^2}{4}k$ has been substituted for the sake of brevity. This equation can be

solved for the acceleration at the end of the interval, and which, in turn can be used to compute the velocity and displacement at the end of the time step as:

$$v_{i+1} = \frac{\Delta t^2}{4} \tilde{m}^{-1} f_i + \frac{\Delta t^2}{4} \tilde{m}^{-1} f_{i+1} + \left(1 - \frac{\Delta t^2}{2} \tilde{m}^{-1} k\right) v_i + \Delta t \left[1 - \frac{\Delta t}{4} \tilde{m}^{-1} (2c + \Delta t k)\right] \dot{v}_i$$

$$\dot{v}_{i+1} = \frac{\Delta t}{2} \tilde{m}^{-1} f_i + \frac{\Delta t}{2} \tilde{m}^{-1} f_{i+1} - \Delta t \tilde{m}^{-1} k v_i + \left[1 - \frac{\Delta t}{2} \tilde{m}^{-1} (2c + \Delta t k)\right] \dot{v}_i$$

In these relations the acceleration $\ddot{v}_i = m^{-1}(f_i - c\dot{v}_i - kv_i)$ has been eliminated by making use of the dynamic equilibrium equation at the instant t_i . Thus the solution marches in time from one instant to the next. Again these recurrence relations can be arranged in matrix form as,

$$\begin{pmatrix} v_{i+1} \\ \dot{v}_{i+1} \end{pmatrix} = \begin{bmatrix} A & B \\ A' & B' \end{bmatrix} \begin{pmatrix} f_i \\ f_{i+1} \end{pmatrix} + \begin{bmatrix} C & D \\ C' & D' \end{bmatrix} \begin{pmatrix} v_i \\ \dot{v}_i \end{pmatrix}$$

where A, B, \dots, C', D' are the coefficients of the recurrence relation and are given in Table 9.2.

TABLE 9.2 Coefficients of recurrence relation for constant average acceleration

$A = \frac{\Delta t^2}{4} \tilde{m}^{-1}$
$B = \frac{\Delta t^2}{4} \tilde{m}^{-1}$
$C = \left(1 - \frac{\Delta t^2}{2} \tilde{m}^{-1} k\right)$
$D = \Delta t \left[1 - \frac{\Delta t}{4} \tilde{m}^{-1} (2c + \Delta t k)\right]$
$A' = \frac{\Delta t}{2} \tilde{m}^{-1}$
$B' = \frac{\Delta t}{2} \tilde{m}^{-1}$
$C' = -\Delta t \tilde{m}^{-1} k$
$D' = \left[1 - \frac{\Delta t}{2} \tilde{m}^{-1} (2c + \Delta t k)\right]$

where, $\tilde{m} = m + \frac{\Delta t}{2} c + \frac{\Delta t^2}{4} k$.

Similar recurrence relations can be derived in the case of other forms of assumed variation of acceleration within a time-step leading to various time-marching schemes for numerical integration of equation of motion. Schematically, the recurrence relation for any time-marching

scheme may be written as,

$$\begin{Bmatrix} v \\ \dot{v} \end{Bmatrix}_{i+1} = \mathbf{A} \begin{Bmatrix} v \\ \dot{v} \end{Bmatrix}_i + \mathbf{L} \begin{Bmatrix} f_i \\ f_{i+1} \end{Bmatrix}$$

where \mathbf{A} is known as the amplification matrix, and \mathbf{L} is known as the load operator matrix.

9.3 STABILITY AND ACCURACY CONSIDERATIONS

As with any numerical procedure, the time marching schemes for numerical integration of equation of motion provide an approximation to the actual solution of the equations. The quality of the computed solution depends on the choice of time-marching algorithm and also on the time step for numerical integration. Two issues are of primary concern in the case of time marching algorithms. They are:

- (i) *Stability*: For what range of parameters, does the computed response for bounded input remains within bounds?
- (ii) *Accuracy*: What is the usable range of parameters to restrict the deviation of computed response from the exact solution within acceptable limits?

To investigate the stability of the algorithm, we consider the case of free vibration, *i.e.* $f(t) = 0$. Under these conditions, the quality of predicted response at n^{th} time step due to non-zero initial conditions depends only on the powers of amplification matrix \mathbf{A} as given below,

$$\begin{Bmatrix} v \\ \dot{v} \end{Bmatrix}_n = \mathbf{A}^n \begin{Bmatrix} v \\ \dot{v} \end{Bmatrix}_0 \quad (9.1)$$

For a single degree of freedom system, the matrix \mathbf{A} is of size 2×2 and hence will have 2 eigenvalues and corresponding eigenvectors. Let us assume that these eigenpairs are given as λ_{A1} , $\{\phi^{(1)}\}$ and λ_{A2} , $\{\phi^{(2)}\}$. Thus, invoking the linear independence property of eigenvectors, the initial state vector can be written as,

$$\begin{Bmatrix} v \\ \dot{v} \end{Bmatrix}_0 = \mathbf{\Phi} \mathbf{c} \quad (9.2)$$

Combining this with the recurrence equation (9.1) we get,

$$\begin{aligned} \begin{Bmatrix} v \\ \dot{v} \end{Bmatrix}_n &= \mathbf{A}^n \mathbf{\Phi} \mathbf{c} \\ &= \mathbf{\Phi} \mathbf{\Lambda}_A^n \mathbf{c} \end{aligned} \quad (9.3)$$

where, $\mathbf{\Lambda}_A$ is a diagonal matrix of eigenvalues λ_{Aj} of matrix \mathbf{A} . It is, therefore, clear that the contributions of original coefficients \mathbf{c} are reinforced by the powers of the eigenvalues, $\mathbf{\Lambda}_A^n$. In such a situation, bounded response can only be expected if and only if the modulus of the maximum eigenvalue does not exceed 1. Mathematically, it translates into stating that for

stability the spectral radius (ρ_A) of A should not exceed 1:

$$\rho_A = \max_j |\lambda_{Aj}| \leq 1 \quad (9.4)$$

In general, A can have real or complex eigenvalues and mere fulfilment of condition in Equation (9.4) does not ensure a satisfactory performance of the time marching scheme. It is, then, worthwhile to investigate the effects of eigenvalues of A on the performance of time marching scheme. Let us consider an arbitrary complex eigenvalue λ_{Aj} of A :

$$\begin{aligned} \lambda_{Aj} &= a_j + ib_j \\ &= \sqrt{a_j^2 + b_j^2} e^{i\theta_j}; \quad \theta_j = \tan^{-1} \frac{b_j}{a_j} \\ &= \rho_j e^{i\theta_j} \end{aligned} \quad (9.5)$$

Raising of this eigenvalue to n^{th} power yields

$$\begin{aligned} \lambda_{Aj}^n &= \rho_j^n e^{in\theta_j} \\ &= \rho_j^n (\cos n\theta_j + i \sin n\theta_j) \end{aligned} \quad (9.6)$$

The following inferences may be drawn:

- positive real eigenvalues do not lead to a change in sign,
- negative real eigenvalues lead to a change in sign at each step,
- complex eigenvalues *may* lead to changes in sign, this depending on each individual step,
- if the modulus of the eigenvalue is smaller than 1, the involution converges toward zero.

An algorithm for solving structural dynamics problem should be capable of reproducing a free, undamped oscillation. The reversal of direction of this oscillatory motion should not be dependent on the step-size of the integration and thus, a few complex eigenvalues must exist. If the modulus of all eigenvalues is indeed smaller than 1, stability is ensured, but the algorithm would simulate a damped motion, a phenomenon often referred to as *algorithmic damping*. Thus, to achieve a satisfactory performance, we must demand the presence of complex eigenvalues with a modulus of 1.

The above-mentioned issues have to be considered in the design of an algorithm for numerical integration of equation of motion. More often, an engineer is just interested in computing dynamic response by using whichever method is available (in the form of a coded programme). To ascertain the reliability and accuracy of the computer implementation of a numerical integration algorithm, it is essential to test the performance of the code for a few simple bench-mark problems. A simple test which can be quickly performed is to determine the free-vibration response of an undamped single degree of freedom system (with natural frequency ω_n rad/s) for these initial conditions:

- (i) A unit initial displacement with zero initial velocity, *i.e.*, $v_0 = 1.0$, $\dot{v}_0 = 0.0$
- (ii) Zero initial displacement with unit initial velocity, *i.e.*, $v_0 = 0.0$, $\dot{v}_0 = 1.0$.

The exact response for the first case is $v(t) = \cos \omega_n t$, whereas for the second case the solution is $v(t) = \sin \omega_n t$. The numerically evaluated response is then compared with the known solution to evaluate the performance of the algorithm. In addition, it may also be worthwhile to compare the numerically evaluated response to harmonic excitation with the closed-form solution of the problem discussed in the earlier chapter. In general, an error in numerically evaluated response shows up in either or both of the following forms:

Period elongation: It is the apparent change in the natural period of vibration caused due to finite approximation of the integration operator. A direct consequence of this error is the distortion in the computed response waveforms in comparison with the exact response due to incremental change in phase at each time step.

Artificial damping: Also known as *algorithmic damping*—this is caused by the deviation from unity of the modulus of the complex eigenvalues of the integration operator as discussed above. This leads to either artificial decay, or build-up of response amplitudes depending on whether the eigenvalue modulus is less than unity, or greater than unity, respectively.

The constant average acceleration algorithm is free from the artificial damping error but does lead to period elongation in the computed response. Due to good stability characteristics, the constant average acceleration algorithm is widely used in the numerical evaluation of response of linear/nonlinear systems.

SUMMARY

The analysis of vibration problems is too tedious and cumbersome for manual calculations. One has to resort to numerical methods for solution of vibration problems on a digital computer. The assumptions, formulation and limitations of the numerical algorithms used for the solution of vibration problems are discussed and some safeguards for the correct use of these numerical methods are described.

REFERENCES

- [1] Argyris, J.H. and Mlejnek, H.P., *Dynamics of Structures*, North-Holland, 1991.
- [2] Bathe, K.J., *Finite Element Procedures*, Prentice Hall, Inc., 1995.
- [3] Nickell, R.E., “On the Stability of Approximation Operators in Problems of Structural Dynamics”, *International Journal of Solids and Structures*, 7: 301–319, 1971.
- [4] Pego, P., “Alternative Characterization of Time Integration Schemes”, *Computer Methods in Applied Mechanics and Engineering*, 190: 2702–2727, 2001.

Chapter 10

Response Spectra

10.1 INTRODUCTION

Earthquake causes ground to vibrate and structures supported on ground are subjected to this motion. Thus the dynamic loading on the structure during an earthquake is not external loading but due to motion of supports. In general, the ground motions have three translational and three rotational components. Not much information is available regarding the properties of rotational components of ground motion due to difficulties in recording those. On the other hand, the characteristics of translational components are relatively better known as they are routinely recorded and processed during strong earthquakes by an instrument known as **accelerograph**. Moreover, it can be deduced from the analysis of vibration records obtained from different elevations in a structure during an earthquake that the rotational components are quite small in magnitude in comparison with translational components. Therefore, the effects of rotational components of ground motion are usually neglected in seismic analysis of structures. Further, the response of a structure is often obtained by subjecting structure to one component of ground translation (acceleration). The total response of structural system is obtained by combining response due to individual component, as method of superposition is valid for linear elastic systems. Since the natural frequencies of the structure are not known *a priori*, complications arise in the design of structure necessitating several iterations. In such a situation, a design engineer requires a prescription of seismic loading that reflects frequency content, amplitude of ground motion and effect of subsequent filtering by the structure. This information is provided by Response Spectra.

In this chapter frequency content of ground motion is discussed first by means of Fourier Spectrum and later the concept of response spectrum is introduced as a tool for quick dynamic analysis.

10.2 FOURIER SPECTRA

Frequency content of an accelerogram can be conveniently depicted by Fourier Spectra. Fourier transform of an accelerogram $\ddot{x}(t)$ is given by

$$X(\omega) = \int_{-\infty}^{\infty} \ddot{x}(t) e^{-i\omega t} dt \quad (10.1)$$

Assuming ground acceleration as non-zero in $t \in (0, t_d]$, the Equation (10.1) can be written as,

$$X(\omega) = \int_0^{t_d} \ddot{x}(t) \cos(\omega t) dt - i \int_0^{t_d} \ddot{x}(t) \sin(\omega t) dt \quad (10.2)$$

Fourier amplitude and phase spectra of strong motion are defined using Equation (10.2) as

$$|X(\omega)| = \sqrt{\left[\int_0^{t_d} \ddot{x}(t) \cos(\omega t) dt \right]^2 + \left[\int_0^{t_d} \ddot{x}(t) \sin(\omega t) dt \right]^2} \quad (10.3)$$

$$\phi(\omega) = -\tan^{-1} \left\{ \frac{\int_0^{t_d} \ddot{x}(t) \cos(\omega t) dt}{\int_0^{t_d} \ddot{x}(t) \sin(\omega t) dt} \right\} \quad (10.4)$$

Although phase spectrum (Equation (10.4)) is considered to be relatively of less importance than amplitude spectrum (Equation (10.3)), both amplitude and phase spectra are required for unique definition of ground acceleration. Fourier amplitude spectra of velocity and displacement can be obtained by dividing acceleration Fourier amplitude spectrum ordinate by frequency and square of frequency value respectively.

Figures 10.1–10.3 show normalized Fourier amplitude spectra for acceleration, velocity and displacement of N15°W component of accelerogram recorded at Uttarkashi during Uttarkashi earthquake of October 20, 1991. It is to be noted that the bandwidth of predominant frequency for displacement is narrowest and that of acceleration is the broadest. It also demonstrates that acceleration, velocity and displacement are controlled by different frequency bands.

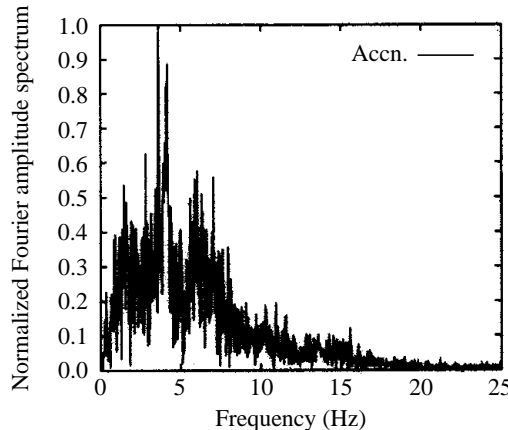


FIGURE 10.1 Normalized Fourier amplitude acceleration spectrum of N15°W component at Uttarkashi during Uttarkashi earthquake of October 20, 1991.

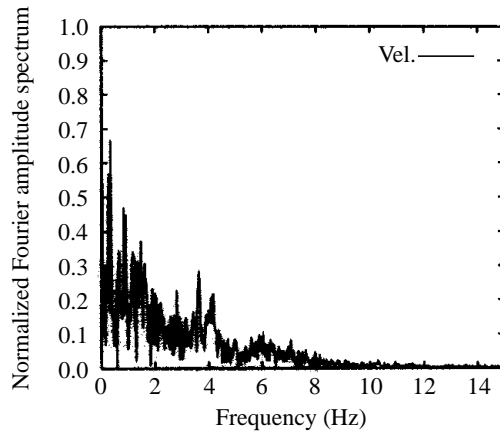


FIGURE 10.2 Normalized Fourier amplitude velocity spectrum of N15°W component at Uttarkashi.

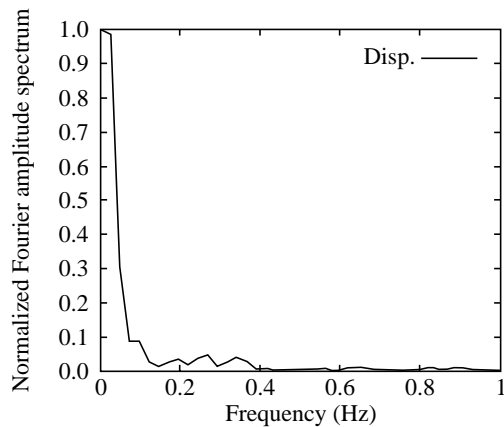


FIGURE 10.3 Normalized Fourier amplitude displacement spectrum of N15°W component at Uttarkashi.

10.3 RESPONSE SPECTRA

Earthquake engineers prefer to report interaction between ground acceleration and structural systems through response spectrum first proposed by Biot [1, 2,] and later popularised by Housner [3]. Response spectrum is a set of ordinates that describes maximum response of a set of Single Degree Freedom Systems (SDOF) subjected to a prescribed ground motion. Often a response spectrum is presented as a plot of maximum response of a set of SDOF systems subjected to a support (ground) motion as ordinate and corresponding natural frequencies (or, periods) of the SDOF system as abscissa.

10.3.1 Formulation

The equation of motion of a SDOF system subjected to support (ground) motion, as shown in Figure 10.4, may be written as

$$m\ddot{z} + c(\dot{z} - \dot{x}) + k(z - x) = 0 \quad (10.5)$$

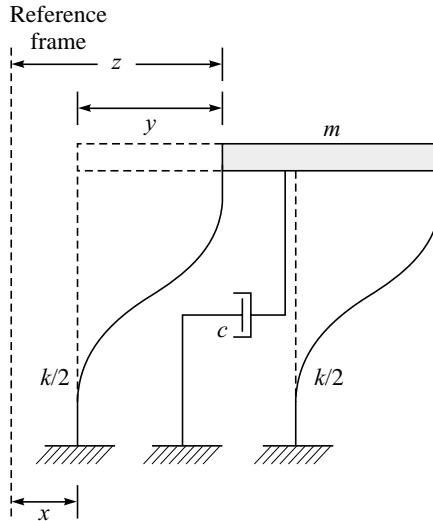


FIGURE 10.4 Single degree of freedom system excited by support motion

where, z is the absolute displacement of mass m , x is the displacement of ground, c is the damping coefficient of dash-pot and k is the stiffness of the spring. Dividing by m in equation (10.5) and replacing absolute displacement z by relative displacement $y = z - x$ gives,

$$\ddot{y} + 2\zeta\omega_n\dot{y} + \omega_n^2 y = -\ddot{x} \quad (10.6)$$

where ω_n is undamped natural frequency of the system and ζ is the damping ratio. The Equations (10.5) and (10.6) are ordinary second order differential equations with constant coefficients. Either of these can be used to find response of the SDOF system. The Equation (10.5) needs ground displacement $x(t)$ and velocity $\dot{x}(t)$ as input support motion. While the required support excitation is ground acceleration $\ddot{x}(t)$ for the Equation (10.6). The solution of these Equations (10.5) and (10.6) requires initial condition of the response and ground motion at the start of ground vibration. Thus the computation of response spectrum is an initial-value problem. The systems represented by Equations (10.5 and 10.6) are *incrementally linear systems*. These systems violate zero-in/zero-out property of linear system [15] if the systems are not initially at rest. The complexity of this solution was realised by Pecknold and Riddell [16], Malhotra [7] and Mylonakis and Syngros [9] among others. This initial-value problem is not well posed because support motion and/or initial condition are not properly defined. The ill posed problem creates complications in the solution if:

- (i) the system and ground motion are not initially at rest, and

- (ii) the prescribed ground motions (acceleration, velocity and displacement) are not compatible.

The accelerograph generally starts recording motion after a fixed threshold of acceleration level set up in the instrument is exceeded by the base motion. Thus, at the start of recording, ground displacement and velocity are not zero. Moreover, reported processed histories of ground acceleration, velocity and displacement are often incompatible (*i.e.* reported histories of velocity and displacement can not be obtained by integrating reported acceleration) due to the use of extra correction procedure employed for velocity and displacement correction than that of acceleration history correction of standard ground motion processing. Note that solution for well posed problem will give same solution using either of the Equation (10.5) or (10.6). These complications are ignored by engineers by assuming that the ground and structure are initially at rest and using only ground acceleration as input.

10.3.2 Solution: Initially at Rest

The Equation (10.6) is the standard equation of motion for a linear elastic SDOF system undergoing forced vibration due to support excitation. The solution of initially at rest system is given by Duhamel's integral as

$$y(t) = -\frac{1}{\omega_d} \int_0^t \ddot{x}(\tau) e^{-\zeta\omega_n(t-\tau)} \sin \omega_d(t-\tau) d\tau \quad (10.7)$$

where, $\omega_d = \omega_n \sqrt{1 - \zeta^2}$ is the damped natural frequency of SDOF system. The maximum relative response $y(t)$ of linear elastic SDOF system, initially at rest with prescribed damping ratio ζ subjected to a ground acceleration versus natural period or frequency of vibration is defined as relative displacement response spectrum and is denoted as

$$\begin{aligned} S_d(\zeta, \omega_n) &= S_d(\zeta, T_n) = |y(t)|_{\max} \\ &= \frac{1}{\omega_d} \left| \left\{ \int_0^t \ddot{x}(\tau) e^{-\zeta\omega_n(t-\tau)} \sin \omega_d(t-\tau) d\tau \right\} \right|_{\max} \end{aligned} \quad (10.8)$$

where, natural period of vibration $T_n = 2\pi/\omega_n$. For a prescribed accelerogram the Equation (10.7) is numerically integrated and the resulting maximum relative displacement value gives one value of S_d for a specified set of ω_n , and ζ . The numerical scheme for evaluating Duhamel's integral, originally proposed by Nigam and Jennings [13], has been discussed in the previous chapter. Typically, this integration is carried out at uniform frequency interval in a prescribed range of frequencies for different values of ζ . It is worth noting that the quantity within the curly brackets of Equation (10.8) has the unit of velocity. The absolute maximum of this quantity is termed as pseudo relative velocity response spectrum (*psv*) $S_{pv}(\zeta, \omega_n)$ and is formally given as,

$$S_{pv}(\zeta, \omega_n) \equiv S_{pv}(\zeta, T_n) = \left| \int_0^t \ddot{x}(\tau) e^{-\zeta\omega_n(t-\tau)} \sin \omega_d(t-\tau) d\tau \right|_{\max} \quad (10.9)$$

Thus for lightly damped system (*i.e.* $\omega_d \approx \omega_n$)

$$S_d(\zeta, \omega_n) \equiv \frac{1}{\omega_d} S_{pv}(\zeta, \omega_n) \approx \frac{1}{\omega_n} S_{pv}(\zeta, \omega_n) \quad (10.10)$$

The relative displacement response spectra asymptotically approaches maximum ground displacement for highly flexible structure. Formally, the limiting value of $S_d(\zeta, \omega_n)$ is,

$$\lim_{\omega_n \rightarrow 0} S_d(\zeta, \omega_n) = |x(t)|_{\max} \quad (10.11)$$

This implies that the mass remains stationary for all practical purposes and only the ground moves as the linear elastic SDOF system is composed of spring with negligible stiffness. Differentiation of Equation (10.7) with respect to time t gives,

$$\begin{aligned} \dot{y}(t) &= - \int_0^t \ddot{x}(\tau) e^{-\zeta\omega_n(t-\tau)} \cos \omega_d(t-\tau) d\tau \\ &\quad + \frac{\zeta}{\sqrt{1-\zeta^2}} \int_0^t \ddot{x}(\tau) e^{-\zeta\omega_n(t-\tau)} \sin \omega_d(t-\tau) d\tau \\ &= - \int_0^t \ddot{x}(\tau) e^{-\zeta\omega_n(t-\tau)} \cos \omega_d(t-\tau) d\tau - \zeta\omega_n y(t) \end{aligned} \quad (10.12)$$

The relative velocity spectrum is similarly defined as,

$$S_v(\zeta, \omega_n) \equiv S_v(\zeta, T_n) = |\dot{y}(t)|_{\max} \quad (10.13)$$

For lightly damped structure $\zeta \approx 0$, the second term of Equation (10.12) can be neglected and thus the relative velocity spectrum reduces to,

$$S_v(0, \omega_n) = \left| \int_0^t \ddot{x}(\tau) \cos \omega_n(t-\tau) d\tau \right|_{\max} \quad (10.14)$$

From the Equation (10.9) the undamped relative pseudo velocity response spectrum can be obtained as,

$$S_{pv}(0, \omega_n) = \left| \int_0^t \ddot{x}(\tau) \sin \omega_n(t-\tau) d\tau \right|_{\max} \quad (10.15)$$

It is easy to see from the Equation (10.14) that as $\omega_n \rightarrow 0$ the relative velocity spectrum $S_v \rightarrow |\dot{x}(t)|_{\max}$ and from the Equation (10.15) the relative psuedo response $S_{pv} \rightarrow 0$ because the mass does not move. Hudson [4, 5] has shown that numerically $S_v(0, \omega_n)$ and $S_{pv}(0, \omega_n)$ are almost equal except for very long period structure. However, variation is considerable in case of highly damped structure. Figure 10.5 shows relative velocity spectra S_v and pseudo relative velocity spectra S_{pv} for damping ratios $\zeta = 0.02$ and 0.20 of N15°W component of Uttarkashi record. By rearranging the terms in Equation (10.6), the absolute acceleration response of the linear elastic SDOF system can be obtained as,

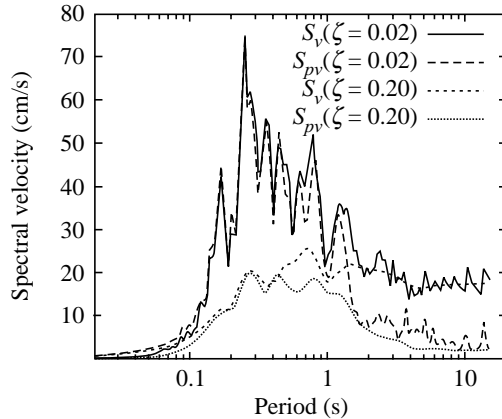


FIGURE 10.5 Comparison of spectral and pseudo-spectral velocity of N15°W component recorded at Uttarkashi for different damping ratios.

$$\begin{aligned}\ddot{z}(t) &= \ddot{x}(t) + \ddot{y}(t) \\ &= -\omega_n^2 y(t) - 2\zeta\omega_n \dot{y}(t)\end{aligned}\quad (1.16)$$

The absolute acceleration spectra is similarly defined as,

$$S_a(\zeta, \omega_n) \equiv S_a(\zeta, T_n) = |\ddot{z}(t)|_{\max} \quad (10.17)$$

It may be seen that for damping ratio $\zeta \in (0.0, 0.20)$

$$S_a(\zeta, \omega_n) \approx \omega_n S_{pv}(\zeta, \omega_n) \equiv S_{pa}(\zeta, \omega_n) \quad (10.18)$$

where, $S_{pa}(\zeta, \omega_n)$ is called *absolute pseudo acceleration spectral response* and the relation (10.18) reduces to equality for $\zeta = 0$. Absolute pseudo acceleration spectra $S_{pa}(\zeta, \omega_n) \leq S_a(\zeta, \omega_n)$. This difference might be important for rigid systems. Figure 10.6 shows absolute

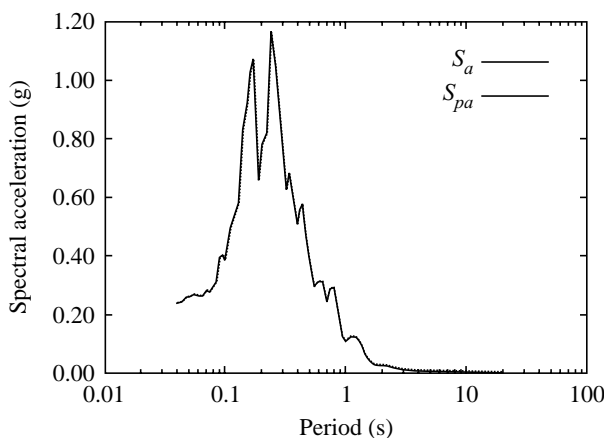


FIGURE 10.6 Comparison of spectral and pseudo-spectral acceleration of N15°W component recorded at Uttarkashi for 5% damping.

acceleration response spectra $S_a(0.05, \omega_n)$ and absolute pseudo acceleration response spectra $S_{pa}(0.05, \omega_n)$ of N15°W component of motion at Uttarkashi. The limiting value of absolute acceleration spectrum is achieved for infinitely stiff structure as there is no relative motion between ground and mass, hence

$$\lim_{\omega_n \rightarrow \infty} S_a(\zeta, \omega_n) = |\ddot{x}(t)|_{\max} \quad (10.19)$$

The maximum spring force developed in the oscillator is $kS_d(\zeta, \omega_n) = mS_{pa}(\zeta, \omega_n)$, while $mS_d(\zeta, \omega_n)$ is the maximum of total elastic and damping forces. The maximum strain energy input is,

$$E_I = \frac{k}{2} [S_d(\zeta, \omega_n)]^2 \quad (10.20)$$

and the maximum strain energy per unit mass is,

$$E_s = \frac{k}{2m} [S_d(\zeta, \omega_n)]^2 = \frac{1}{2} [\omega_n S_d(\zeta, \omega_n)]^2 = \frac{1}{2} [S_{pv}(\zeta, \omega_n)]^2 \quad (10.21)$$

The total energy of the system is,

$$E_T(t) = \frac{m}{2} [\dot{y}(t)]^2 + \frac{k}{2} [y(t)]^2 \quad (10.22)$$

For an undamped linear elastic SDOF system, substitution of $y(t)$ by the Equation (10.7) and $\dot{y}(t)$ by the Equation (10.12), the Equation (10.22) reduces to,

$$\sqrt{\frac{2E_T(t)}{m}} = \sqrt{\left[\int_0^t \ddot{x}(\tau) \cos(\omega_n \tau) d\tau \right]^2 + \left[\int_0^t \ddot{x}(\tau) \sin(\omega_n \tau) d\tau \right]^2} \quad (10.23)$$

which at the end of accelerogram $t = t_d$ is identical to Fourier amplitude spectrum $|X(\omega)|$ of the ground acceleration evaluated at frequency ω_n . The maximum of the Equation (10.23) is pseudo relative velocity spectrum $S_{pv}(0, \omega_n)$. If the relative response reaches maximum at the end of accelerogram duration, then $|X(\omega_n)| = S_{pv}(0, \omega_n)$. In general, $|X(\omega_n)| \leq S_{pv}(0, \omega_n)$. Figure 10.7 shows relative velocity response spectrum S_{pv} for an undamped system and Fourier spectrum $|X(\omega)|$ of N15°W component recorded at Uttarkashi.

10.3.3 Solution: General Conditions

The concepts of stiff and flexible system are necessary to obtain response spectrum when the ground motion are incompatible or when the

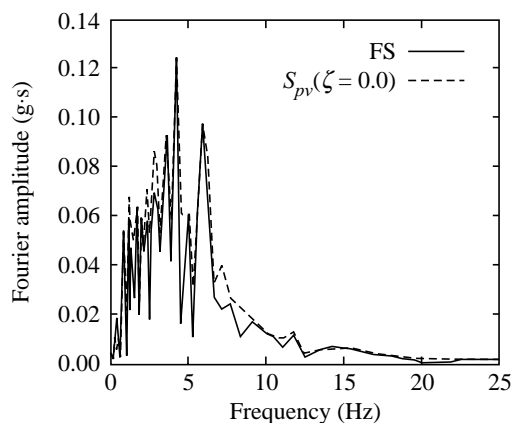


FIGURE 10.7 Comparison of pseudo-spectral velocity spectrum for 0% damping and the Fourier spectrum of N15°W component recorded at Uttarkashi.

system/ground is not initially at rest. A SDOF system excited by support excitation is considered to be stiff (flexible) if the natural frequency is larger (smaller) than the support excitation frequency. Response spectrum by definition encompasses response of both stiff and flexible SDOF systems as it prescribes maximum response for a set of SDOF systems. Moreover, absolute displacement response for a very flexible structure is zero and relative displacement response of a very stiff structure is zero. Thus, for a specified non-zero initial support motion both absolute and relative displacement cannot be simultaneously zero. This requires a reformulation of the problem. Let ω_c be a predominant (representative central) frequency of the excitation and $f(\omega_n, \omega_c)$ be a function such that $f(\omega_n, \omega_c)$ approaches unity as $\omega_n \rightarrow 0$ and vanishes as $\omega_n \rightarrow \infty$. One such generalised function is,

$$f(\omega_n, \omega_c) = \frac{1.0}{1.0 + \left(\frac{\omega_n}{\omega_c}\right)^\alpha} \quad (10.24)$$

where, $\alpha > 0$ and the function satisfies the specified limit conditions for both flexible and stiff SDOF systems. Define a displacement u by mixing absolute and relative displacement as,

$$u = y + z \left(\frac{\omega_c}{\omega_n}\right)^\alpha \quad (10.25)$$

Addition of Equation (10.6) and Equation (10.5) multiplied by $(\omega_c/\omega_n)^\alpha/m$ results in,

$$\ddot{u} + 2\zeta\omega_n\dot{u} + \omega_n^2 u = -\ddot{x} + \left(\frac{\omega_c}{\omega_n}\right)^\alpha [2\zeta\omega_n\dot{x} + \omega_n^2 x] \quad (10.26)$$

The Equation (10.26) is solved with the generalised initial condition $u(0) = \dot{u}(0) = 0$. Note that the solution requires acceleration, velocity and displacement of ground motion as excitation. Replacing absolute displacement z by $y + x$ from Equation (10.25) the relative displacement is obtained as,

$$y = \frac{u\omega_n^\alpha - x\omega_c^\alpha}{\omega_n^\alpha + \omega_c^\alpha} \quad (10.27)$$

The Equation (10.27) satisfies initial physical condition for both stiff and flexible SDOF systems. Using Equation (10.27) the relative displacement y is obtained from the values of the mixed displacement u . The required spectral displacement is the maximum of y at any time. In most of the cases, a simpler approximate method of solution than that of the general method presented above can be used satisfying limiting behaviour of SDOF system. In this method a frequency dependent initial condition is obtained from Equation (10.27) by using generalised initial condition $u(0) = \dot{u}(0) = 0$ as,

$$y(0) = \frac{-x(0)}{1.0 + \left(\frac{\omega_n}{\omega_c}\right)^\alpha},$$

and

$$\dot{y}(0) = \frac{-\dot{x}(a)}{1.0 + \left(\frac{\omega_n}{\omega_c}\right)^\alpha} \quad (10.28)$$

The Equation (10.6) is solved with the derived frequency dependent initial condition given by Equation (10.28). However, specification of parameter α and representative ground frequency ω_c need to be defined. Using simulation technique, the parameter $\alpha = 2$ is found to be satisfactory for response spectrum computation. There are several definition of predominant frequency ω_c of ground motion records in the literature [6, 8, 17]. The predominant ground frequency may be defined as the frequency at which relative velocity response of 5% damped SDOF system is maximum in the entire range of frequencies of ground motion. This frequency is insensitive to the initial condition of ground motion. Representative ground frequency can also be defined as,

$$\omega_c = \sqrt{\frac{PGA}{PGD}} \quad (10.29)$$

where, PGA is Peak Ground Acceleration and PGD is the Peak Ground Displacement. Use of Equation (10.29) is criticised on the ground that PGA and PGD occur at different frequencies of ground motion and thus it does not represent a single frequency. Use of former definition of predominant ground frequency needs additional computation of 5% damped relative velocity spectrum of ground motion with initially at rest condition.

The S-E component of 1940 El Centro accelerogram [14] is used to compute 2% damped response spectrum for initially at rest and at non zero condition. The accelerogram has peak ground values as $PGA = 0.3484$ g, $PGV = 0.334$ m/s and $PGD = 108.7$ mm. The predominant ground period from 5% relative damped velocity spectrum is 0.85 s. The Equation (10.29) gives period as 1.1 s. These two values are considered to be comparable for all practical purposes. The initial ground velocity and displacement are -0.04664 m/s and 21.59 mm. Use of two definition of predominant ground period gives almost identical result. Figure 10.8 shows 2% damped displacement spectrum. The solution using non-zero initial conditions satisfies physical

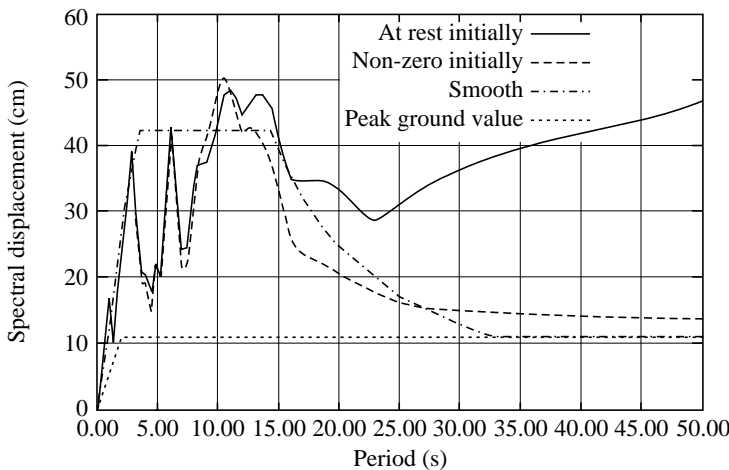


FIGURE 10.8 Displacement spectrum (damping 2%).

constraint for both stiff and flexible systems. The initially at rest solution satisfies physical condition of stiff systems.

10.3.4 Smooth Spectrum

The seismic design specification needs prescription of required strength of structure. In dynamic condition maximum allowable displacement, velocity and acceleration are needed. The design spectrum describes relative strength required at different periods for design purpose. Actual strength specification requires allowable stress values and damping. The design spectrum is derived from smooth spectrum of an ensemble of earthquake records. The smooth spectrum of S-E component of 1940 El Centro accelerogram is derived from the 2% damped spectrum using method proposed by NEHRP [11] and Nau and Hall [10]. Figure 10.9 shows derived smooth pseudo velocity spectrum. The corresponding displacement spectrum has been shown in Figure 10.8.

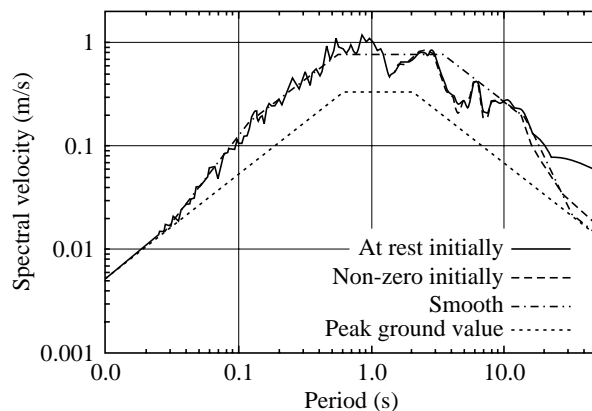


FIGURE 10.9 Pseudo velocity spectrum (damping 2%).

10.3.5 Seismic Demand Diagrams

The recent thrust in the development of performance-based engineering concepts has necessitated representation of the ground motion spectral characteristics in a new format, *viz.*, Acceleration-Displacement Response Spectrum (ADRS) format. The spectral accelerations are plotted against spectral displacements, with the periods (T_n) being represented by radial lines. An estimate of inelastic demands imposed on a structure by an earthquake is obtained from the linear elastic response spectra computed for equivalent damping ratios related to a specified level of ductility. The capacity diagram of a building is obtained from the relationship between the base shear and roof displacement (push-over curve). The roof displacement and the base shear are converted to the spectral displacement and spectral acceleration by the use of mode participation factor and effective modal mass for the fundamental mode. The performance of a building to any earthquake can be assessed by superimposing the capacity diagram on the seismic demand diagram. The intersection of the capacity curve and the seismic demand curve provides an estimate of the yield strength and the displacement demand. The elastic demand diagrams for

the accelerogram of January 26, 2001 Kutch earthquake recorded at Ahmedabad are shown in Figures 10.10 and 10.11.

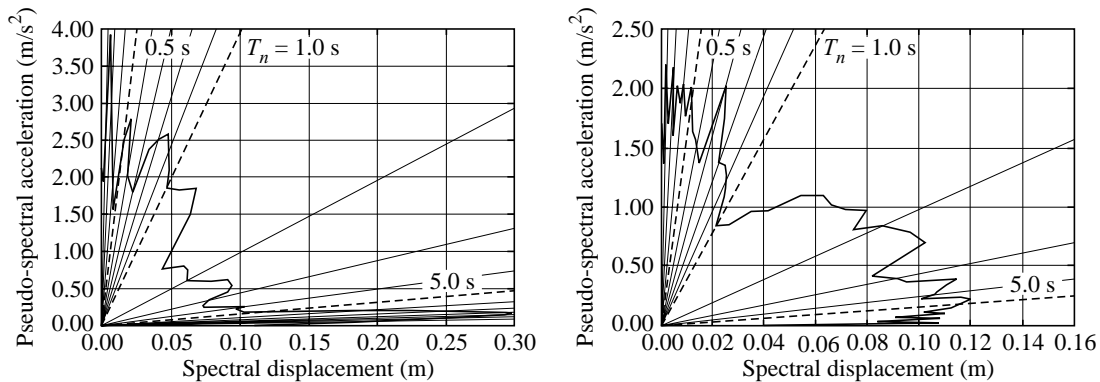


FIGURE 10.10 Demand diagram for N78°E and N12°W components (damping 5%).

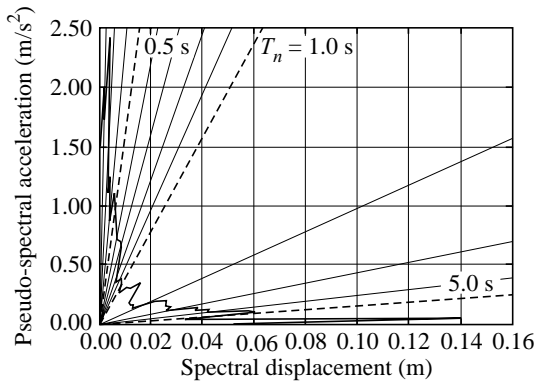


FIGURE 10.11 Demand diagram for vertical component (damping 5%).

SUMMARY

The concept of response spectrum (plural-spectra) is introduced. The importance of this elementary concept in seismic analysis and design is described. Alternate formulations for the response spectrum calculation and representation are described and their use in earthquake resistant design is discussed.

REFERENCES

- [1] Biot, M.A., "Theory of Elastic Systems Vibrating under Transient Impulse with Application to Earthquake-proof Buildings", *Proceedings of the National Academy of Sciences*, 19: 262–268, 1933.

- [2] Biot, M.A., "A Mechanical Analyser for the Prediction of Earthquake Stresses", *Bulletin of the Seismological Society of America*, 31: 151–171, 1941.
- [3] Housner, G.W., "Calculating the Response of an Oscillator to Arbitrary Ground Motion". *Bulletin of the Seismological Society of America*, 31: 143–149, 1941.
- [4] Hudson, D.E., "Response Spectrum Techniques in Engineering Seismology", In *Proceedings of the First World Conference on Earthquake Engineering*, 4: 1–12. Earthquake Engineering Research Institute, Los Angeles, California, 1956.
- [5] Hudson, D.E., "Some Problems in the Application of Spectrum Technique to Strong Motion Earthquake Analysis", *Bulletin of the Seismological Society of America*, 52(2): 417–430, 1962.
- [6] Kramar, S.L., *Geotechnical Earthquake Engineering*, Prentice Hall, Inc., New Jersey, 1996.
- [7] Malhotra, P.K., "Response Spectrum of Incompatible Acceleration, Velocity and Displacement Histories", *Earthquake Engineering and Structural Dynamics*, 30: 279–286, 2001.
- [8] Miranda, E. and Bertero, V.V., "Evaluation of Strength Reduction Factors for Earthquake-resistant Design", *Earthquake Spectra*, 10(2): 357–379, 1994.
- [9] Mylonakis, G. and Syngros, C., "Discussion of Response Spectrum of Incompatible Acceleration, Velocity and Displacement Histories", *Earthquake Engineering and Structural Dynamics*, 31: 1025–1031, 2002.
- [10] Nau, J.M. and Hall, W.J., "Scaling Methods for Earthquake Response Spectra", *Journal of Structural Engineering Division, ASCE*, 110(7): 1533–1548, 1984.
- [11] NEHRP, "Recommended Provisions for Seismic Regulation for New Buildings and Other Structures", *Technical Report*, Building Safety Council for Federal Emergency Management Agency, Washington D.C., 1997.
- [12] Newmark, N.M., "A Method of Computation for Structural Dynamics", *Journal of Engineering Mechanics Division, ASCE*, 85: 67–94, 1959.
- [13] Nigam, N.C. and Jennings, P.C., "Calculation of Response Spectra From Strong Motion Earthquake Records", *Bulletin of the Seismological Society of America*, 59(2): 909–922, 1969.
- [14] NOAA, *Earthquake Strong Motion: CDROM*, National Geophysical Data Center, Boulder Colorado, March 1996.
- [15] Oppenheim, A.V., Willsky, A.S., and Young, I.T., *Signals and Systems*, Prentice Hall, Inc., New Jersey, 1983.
- [16] Pecknold, D.A. and Riddell, R., "Effect of Initial Base Motion on Response Spectra". *Journal of Engineering Mechanics Division, ASCE*, 104(2): 485–491, 1978.
- [17] Rathje, E., Abrahamson, N., and Bray, J., "Simplified Frequency Content Estimates of Earthquake Ground Motions", *Journal of Geotechnical and Geoenvironmental Engineering, ASCE*, 124(2): 150–159, 1998.

Chapter 11

Dynamics of Multi-Degree-of-Freedom Systems

11.1 INTRODUCTION

A Multi-Degree-of-Freedom (MDOF) system, as the name suggests, is one that requires two or more independent coordinates to describe its motion. The coordinates normally used to describe the motion of a structural system, may be related to each other via some constraints, which could either be simple kinematic relations between various coordinates, or they could arise from the consideration of equilibrium of forces. The number of generalised (independent) coordinates is given by the difference between the total coordinates describing the motion of a system and the number of constraint relations. For example, consider the case of a double pendulum, which is constrained to move in XY plane as shown in Figure 11.1. In Cartesian coordinate system the positions of two masses m_1 and m_2 are described by two pairs of Cartesian coordinates (x_1, y_1) and (x_2, y_2) respectively. These four coordinates *viz.* x_1, y_1, x_2, y_2 , however, are related to each other through two constraint relations:

$$x_1^2 + y_1^2 = l_1^2, \quad (11.1)$$

and
$$(x_2 - x_1)^2 + (y_2 - y_1)^2 = l_2^2 \quad (11.2)$$

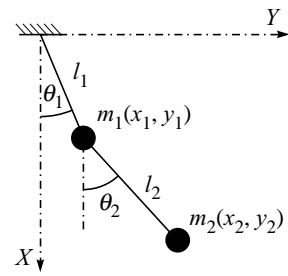


FIGURE 11.1 A double pendulum.

Thus the number of degrees of freedom (or, generalised coordinates) of the structural system is $4 - 2 = 2$. The angles θ_1 and θ_2 can be taken as the two independent generalised coordinates to describe the motion of the masses. In certain systems it is possible to eliminate dependent variables by using constraint relations and derive a set of generalised coordinates, are said to possess *holonomic* constraints. On the other hand, there may exist some constraints, called *nonholonomic* for which it is not possible to derive a set of independent coordinates. Nonholonomic constraints are rarely encountered in practice, so it will be assumed in the following that the equations of the dynamic equilibrium of the system are specified in the unconstrained coordinate system.

11.2 SYSTEM PROPERTY MATRICES

As mentioned earlier, every dynamical system comprises

- (i) a mechanism for storing strain energy due to deformations,
- (ii) some means of storing kinetic energy of the system in motion, and
- (iii) an energy dissipation mechanism.

In MDOF system, described by a set of N generalised coordinates (say, v_1, v_2, \dots, v_N), these energy functionals depend on the motion of the system described by the generalised coordinates.

$$\text{Potential energy} = U(v_1, v_2, \dots, v_N, t) = \frac{1}{2} \sum_{i,j=1}^N \frac{\partial^2 U}{\partial v_i \partial v_j} v_i v_j$$

$$\text{Kinetic energy} = T(\dot{v}_1, \dot{v}_2, \dots, \dot{v}_N, t) = \frac{1}{2} \sum_{i,j=1}^N \frac{\partial^2 T}{\partial \dot{v}_i \partial \dot{v}_j} \dot{v}_i \dot{v}_j$$

$$\text{Rayleigh dissipation function} = R(\dot{v}_1, \dot{v}_2, \dots, \dot{v}_N, t) = \frac{1}{2} \sum_{i,j=1}^N \frac{\partial^2 R}{\partial \dot{v}_i \partial \dot{v}_j} \dot{v}_i \dot{v}_j$$

where Rayleigh dissipation function represents the energy loss through velocity proportional viscous damping force.

The element c_{ij} of damping matrix (**C**) is given by the coefficient $\frac{\partial^2 R}{\partial \dot{v}_i \partial \dot{v}_j}$ and represents the damping force at i^{th} DOF corresponding to the unit velocity at j^{th} DOF with the velocities at all other DOFs remaining zero. The coefficient $\frac{\partial^2 U}{\partial v_i \partial v_j}$ is the element k_{ij} of stiffness matrix (**K**) and represents restoring force at the i^{th} DOF corresponding to the unit displacement at j^{th} DOF with displacements at all other DOFs being constrained to zero. Similarly, the coefficient $\frac{\partial^2 T}{\partial \dot{v}_i \partial \dot{v}_j}$ is the element m_{ij} of inertia matrix (**M**) and represents the inertia force at the i^{th} DOF corresponding to the unit acceleration at the j^{th} DOF with accelerations at all other DOFs being constrained to zero. The governing differential equation of motion for an MDOF system can be derived from the same principles as used in the case of SDOF systems. As an illustration, let us consider the 2-DOF system as shown in Figure 11.2. By invoking the d'Alembert's principle, the equations of motion for free vibration of this system can be written as,

$$m\ddot{v}_1 + 2c\dot{v}_1 - c\dot{v}_2 + 3kv_1 - kv_2 = 0$$

$$m\ddot{v}_2 - c\dot{v}_1 + 2c\dot{v}_2 - kv_1 + 3kv_2 = 0$$

which can be arranged in the matrix form as,

$$\begin{bmatrix} m & 0 \\ 0 & m \end{bmatrix} \begin{pmatrix} \ddot{v}_1 \\ \ddot{v}_2 \end{pmatrix} + \begin{bmatrix} 2c & -c \\ -c & 2c \end{bmatrix} \begin{pmatrix} \dot{v}_1 \\ \dot{v}_2 \end{pmatrix} + \begin{bmatrix} 3k & -k \\ -k & 3k \end{bmatrix} \begin{pmatrix} v_1 \\ v_2 \end{pmatrix} = \begin{pmatrix} 0 \\ 0 \end{pmatrix}, \quad \text{or} \quad \mathbf{M}\ddot{\mathbf{v}} + \mathbf{C}\dot{\mathbf{v}} + \mathbf{K}\mathbf{v} = \mathbf{0} \quad (11.3)$$

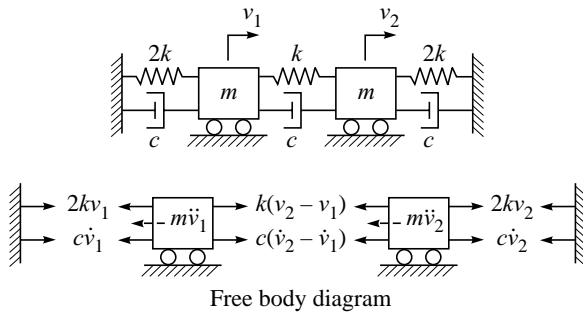


FIGURE 11.2 A 2-DOF system.

The nature of damping forces is assumed to be of the viscous type primarily as an approximate representation of the combined action of all energy dissipation mechanisms present in a vibrating system. Since the extent of damping in structural systems is usually very small, precise nature of the damping force is not very important for dynamic response computations.

11.3 DYNAMICS OF TWO DEGREE OF FREEDOM SYSTEMS

Let us consider the response of a harmonically excited 2-DOF (undamped) system as shown in Figure 11.3. The governing equation of motion for this system can be given as:

$$\begin{bmatrix} m_1 & 0 \\ 0 & m_2 \end{bmatrix} \begin{pmatrix} \ddot{v}_1 \\ \ddot{v}_2 \end{pmatrix} + \begin{bmatrix} k_1 + k_2 & -k_2 \\ -k_2 & k_2 \end{bmatrix} \begin{pmatrix} v_1 \\ v_2 \end{pmatrix} = \begin{pmatrix} F_0 \sin \omega t \\ 0 \end{pmatrix} \quad (11.4)$$

This system is the characteristic of an industrial building with a reciprocating machine installed at one of the floors. Since such machines typically operate at a fixed speed, the force exerted by these machines on the building floor will be harmonic and the steady-state response of the system to this harmonic excitation will also be harmonic of the same frequency.

Thus assuming the harmonic response as $\mathbf{v} = [v_1, v_2]^T = \sin \omega t [V_1, V_2]^T$, Equation (11.4) can be solved for the response amplitudes V_1 and V_2 of the two masses as:

$$\begin{bmatrix} k_1 + k_2 - \omega^2 m_1 & -k_2 \\ -k_2 & k_2 - \omega^2 m_2 \end{bmatrix} \begin{pmatrix} V_1 \\ V_2 \end{pmatrix} \sin \omega t = \begin{pmatrix} F_0 \sin \omega t \\ 0 \end{pmatrix}$$

or,

$$\begin{pmatrix} V_1 \\ V_2 \end{pmatrix} = \frac{1}{\Delta} \begin{bmatrix} k_2 - \omega^2 m_2 & k_2 \\ k_2 & k_2 + k_2 - \omega^2 m_1 \end{bmatrix} \begin{pmatrix} F_0 \\ 0 \end{pmatrix} \quad (11.5)$$

where $\Delta = \mu m_1^2 [\omega^4 - \omega^2 \{\omega_1^* + \omega_2^*(1 + \mu)\} + (\omega_1^* \omega_2^*)^2]$, $\omega_1^* = \sqrt{k_1/m_1}$, $\omega_2^* = \sqrt{k_2/m_2}$, and

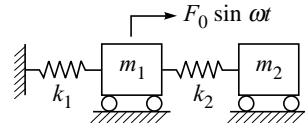


FIGURE 11.3 Harmonic excitation of a 2-DOF system.

$\mu = m_2/m_1$. Thus the system response can be given by,

$$\begin{aligned} v_1(t) &= \frac{F_0(k_2 - \omega^2 \mu m_1)}{\mu m_1^2 [\omega^4 - \omega^2 \{\omega_1^* + \omega_2^*(1 + \mu)\} + (\omega_1^* \omega_2^*)^2]} \sin \omega t \\ v_2(t) &= \frac{F_0 k_2}{\mu m_1^2 [\omega^4 - \omega^2 \{\omega_1^* + \omega_2^*(1 + \mu)\} + (\omega_1^* \omega_2^*)^2]} \sin \omega t \end{aligned} \quad (11.6)$$

It may be noted from Equations 11.6 that it is possible to force the amplitude of response of the first mass (m_1) to vanish by a suitable choice of parameters (also referred to as tuning) k_2 and m_2 (or, μ). This concept can be exploited in designing vibration absorbers for industrial structures and can be achieved by attaching an auxiliary/secondary mass to the primary structure which is subjected to a harmonic excitation. This can be quite effective, when the operating frequency of the reciprocating machine and a natural frequency of the supporting structure are nearly equal, causing large amplitude vibrations of the supporting structure due to resonance.

Let us assume for simplicity, that the second mass m_2 in Figure 11.3 is an auxiliary mass attached to the primary structure, which is excited by a reciprocating machine installed on the floor. The amplitude of displacement response (normalized with respect to the static deflection F_0/k_1) of the primary mass is shown in Figure 11.4(a) for a range of operating frequencies. The unbounded amplitude for $\omega/\omega_1^* = 1.0$, corresponds to the condition of resonance and it should be avoided ($\omega_1^* = \sqrt{k_1/m_1}$ represents the natural frequency of primary structure alone). Let us now consider the use of a tuned mass damper (or, vibration absorber) in altering the dynamic response of primary structure. Figures 11.4(b-f) show the response characteristics of primary structure with an auxiliary/secondary structure for different parametric variations. The objective is to find a suitable set of parameters for secondary structure, so as to limit the normalized response of primary structure to be less than unity in the neighbourhood of $\omega/\omega_1^* = 1$. The effect of adding a secondary structure is to split one resonant peak into two resonant peaks, corresponding to two natural frequencies of the combined 2-DOF system. A light ($\mu < 1$) secondary system attached to the primary structure by means of a relatively flexible attachment, does take away a significant part of the vibration energy from the primary structure at $\omega/\omega_1^* = 1$, as can be seen in Figure 11.4(b). However, such an arrangement is only effective (in reducing the vibration amplitude of primary mass) for a very small range of operating frequencies, by means of increasing the deformations in the secondary structure. Attaching a heavy secondary mass with a flexible spring is not at all effective, as can be inferred from Figure 11.4(c). Figure 11.4(d) shows that the use of a light mass and relatively stiff attachment does not lead to any significant change in the resonant frequency of the original structure and hence is not an effective solution for the vibration problem. Figures 11.4(e) and (f) show the performance for secondary structures comprising heavy mass with stiff attachments. By comparing these two figures, it may be noted that the two resonant peaks are well separated and are sufficiently away from the original location of resonant peak (for the primary structure alone) at $\omega/\omega_1^* = 1$. Further, the amplitude of displacement of primary structure vanishes at $\omega/\omega_1^* = 1$ and is less than the static deformation (F_0/k_1) for a wide range of operating frequencies. This effective range of operating frequencies increases with increase in the mass ratio ($\mu = m_2/m_1$).

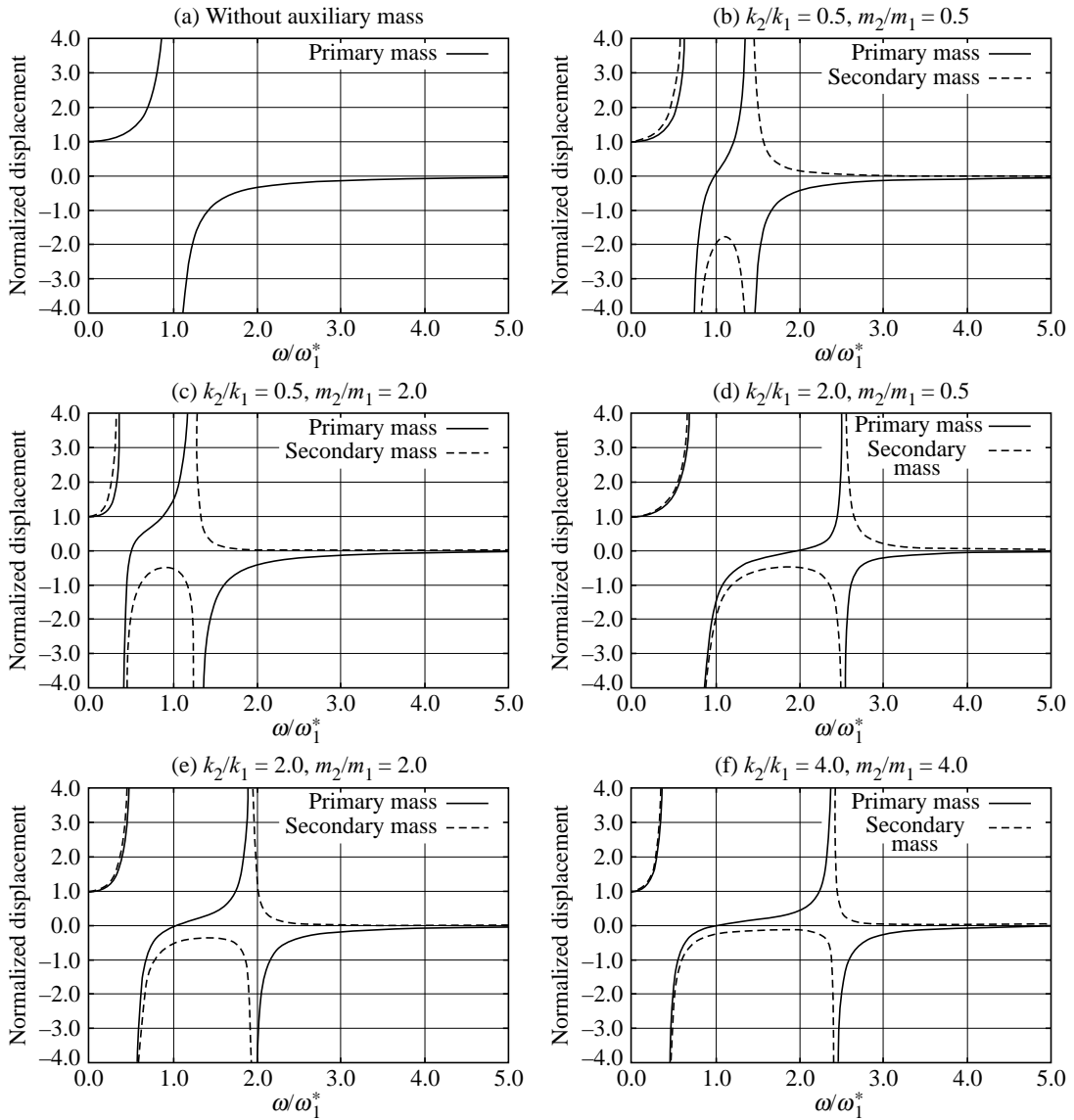


FIGURE 11.4 Performance of vibration absorber/tuned mass damper.

Thus a secondary structure with heavy absorber mass can be very effective in controlling machine induced vibrations in a building/structure. However, the large size associated with a heavy mass can sometimes impose a practical limitation on the usable range of operating frequencies. The required stiffness (k_2) of the secondary attachment can be calculated from the maximum allowable displacement of the secondary system (at $\omega = \omega_2^*$) $V_{2,\max} = F_0/k_2$.

11.4 FREE VIBRATION ANALYSIS OF MDOF SYSTEMS

By considering the fact that the damping levels are usually very small in structural systems, let us consider the response of an undamped MDOF system. The effect of damping will be dealt with at a later stage. The equation of free vibration then reduces to,

$$\mathbf{M}\ddot{\mathbf{v}} + \mathbf{K}\mathbf{v} = \mathbf{0} \quad (11.7)$$

We look for a solution in the form $v_i = q(t)\phi_i$, $i = 1, 2, \dots, N$, where the dependence on time and that on space variables can be separated. This implies that the ratio of amplitudes of any two coordinates is independent of time. Physically, it implies that all degrees of freedom perform synchronous motion and the system configuration does not change its shape during motion but only its amplitude changes.

Substituting for \mathbf{v} , the equation of motion may be written as,

$$\mathbf{M}\{\phi\}\ddot{q}(t) + \mathbf{K}\{\phi\}q(t) = \mathbf{0} \quad (11.8)$$

which is a set of N simultaneous equations of the type

$$\sum_{j=1}^N m_{ij}\phi_j\ddot{q}(t) + \sum_{j=1}^N k_{ij}\phi_jq(t) = 0; i = 1, 2, \dots, N \quad (11.9)$$

where the separation of variables leads to

$$\frac{-\ddot{q}(t)}{q(t)} = \frac{\sum_{j=1}^N k_{ij}\phi_j}{\sum_{j=1}^N m_{ij}\phi_j}; \quad i = 1, 2, \dots, N \quad (11.10)$$

Since the terms on either side of the equality sign are independent of each other, this equality can hold only when each of these terms are equal to a positive constant (say, ω^2).¹ Thus we have,

$$\ddot{q}(t) + \omega^2q(t) = 0 \quad (11.11)$$

$$\sum_{j=1}^N (k_{ij} - \omega^2m_{ij})\phi_j = 0; \quad i = 1, 2, \dots, N. \quad (11.12)$$

The solution of Equation (11.11) is $q(t) = \sin(\omega t - \alpha)$, a harmonic of frequency ω . Thus we may conclude that the motion of all coordinates is harmonic with same frequency ω and same phase difference α . However, it still needs to be established if such a synchronous, harmonic motion is possible for all frequencies. To investigate this issue let us consider the Equation

¹The choice of the sign is dictated by physical considerations. For a conservative system the displacements must remain finite at all instances. If we had chosen a negative constant then the solution would involve exponential functions which would grow without bounds with time t . The choice of positive constant, on the other hand, provides a harmonic solution which has finite energy at all times.

(11.12), which is a set of N simultaneous linear homogeneous equations in unknowns ϕ_j . The problem of determining constant (ω^2) for which the Equation (11.12) has a non-trivial solution is known as the *characteristic value* or *eigenvalue* problem. The eigenvalue problem may be rewritten, in matrix notation as,

$$(\mathbf{K} - \omega^2 \mathbf{M})\{\phi\} = \mathbf{0} \quad (11.13)$$

A non-trivial solution for Equation (11.13) is feasible only when the determinant of the coefficient matrix vanishes, *i.e.*,

$$|\mathbf{K} - \omega^2 \mathbf{M}| = 0 \quad (11.14)$$

The expansion of the determinant in Equation (11.14) yields an algebraic equation of N^{th} order in ω^2 , which is known as the characteristic equation. The roots of characteristic equation are known as the eigenvalues and the positive square root of these eigenvalues are known as the natural frequencies (ω_i) of the MDOF system. It is only at these N frequencies that the system admits synchronous motion at all coordinates. For stable structural systems with symmetric and positive definite stiffness and mass matrices the eigenvalues will always be real and positive. For each eigenvalue the resulting synchronous motion has a distinct shape and is known as *natural/normal mode shape* or *eigenvector*. The normal modes are as much a characteristic of the system as the eigenvalues are. They depend on the inertia and stiffness, as reflected by the coefficients m_{ij} and k_{ij} . These shapes correspond to those structural configurations, in which the inertia forces imposed on the structure due to synchronous harmonic vibrations are exactly balanced by the elastic restoring forces within the structural system. These eigenvectors are determined as the non-trivial solution of Equation (11.13). Since the determinant of the coefficient matrix evaluated at one of the natural frequencies is singular, a unique solution for eigenvectors can not be found. It is, however, possible to compute the amplitudes of the synchronous motion at $N - 1$ coordinates relative to the amplitude of motion at the remaining coordinate, which may be selected arbitrarily. Thus an additional constraint—known as *normalisation condition*—must be supplied in addition to Equation (11.13) to completely determine an eigenvector. Two of the most commonly used normalisation procedures are:

- (i) assume the amplitude of synchronous motion at the first degree of freedom as unity,
- (ii) constrain a *length* measure of the eigenvector to be unity. For example, for any eigenvector $\{\phi^{(i)}\}$ it is possible to determine elements of $\{\phi^{(i)}\}$ such that $\{\phi^{(i)}\}^T \mathbf{M} \{\phi^{(i)}\} = 1$. Such a normalisation, using mass/inertia matrix (\mathbf{M}) is known as *mass renormalisation* and the resulting mode shape is known as *mass orthonormal mode shape*.

It can be shown that the N eigenvectors of an N -DOF system completely span the N -dimensional vector space, and therefore, can be used as basis vectors for representing any N^{th} order vector. Since the condition of orthogonality is a necessary condition for any set of base vectors, it will now be shown that the eigenvectors also satisfy this condition.

11.4.1 Orthogonality Conditions

An important property of the mode shapes or eigenvectors is that they are mutually orthogonal with respect to the mass and stiffness matrices. More precisely, the product involving

multiplication of mode shapes corresponding to two different modes vanishes.

$$\{\phi^{(j)}\}^T [\mathbf{M}]\{\phi^{(i)}\} = M_i \delta_{ij} \quad \text{and} \quad \{\phi^{(j)}\}^T [\mathbf{K}]\{\phi^{(i)}\} = K_i \delta_{ij} \quad (11.15)$$

where M_i and K_i are called the *generalised mass* and *stiffness* respectively for the i^{th} mode and δ_{ij} is the *Kronecker delta*. For the case when mode shapes have been orthonormalized with respect to the mass, $M_i = 1$ and $K_i = \omega_i^2$.

In order to prove this proposition, let us assume that ω_i^2 and $\{\phi^{(i)}\}$ denote the eigenvalue and corresponding eigenvector for i^{th} mode and ω_j^2 and $\{\phi^{(j)}\}$ correspond to the $j(\neq i)^{\text{th}}$ mode. It follows that both of these eigenpairs satisfy Equation (11.13). Thus,

$$\mathbf{K}\{\phi(i)\} = \omega_i^2 \mathbf{M}\{\phi^{(i)}\} \quad (11.16)$$

$$\mathbf{K}\{\phi^{(j)}\} = \omega_j^2 \mathbf{M}\{\phi^{(j)}\} \quad (11.17)$$

Pre-multiplying Equation (11.16) by $\{\phi^{(j)}\}^T$ and Equation (11.17) by $\{\phi^{(i)}\}^T$, we get,

$$\{\phi^{(j)}\}^T \mathbf{K}\{\phi^{(i)}\} = \omega_i^2 \{\phi^{(j)}\}^T \mathbf{M}\{\phi^{(i)}\} \quad (11.18)$$

$$\{\phi^{(i)}\}^T \mathbf{K}\{\phi^{(j)}\} = \omega_j^2 \{\phi^{(i)}\}^T \mathbf{M}\{\phi^{(j)}\} \quad (11.19)$$

Subtracting Equation (11.19) from Equation (11.18) and noting $\{\phi^{(j)}\}^T \mathbf{K}\{\phi^{(i)}\} = ((\{\phi^{(i)}\}^T \mathbf{K}^T \{\phi^{(j)}\})^T$ and the fact that \mathbf{K} and \mathbf{M} are symmetric matrices we have,

$$(\omega_i^2 - \omega_j^2) \{\phi^{(j)}\}^T \mathbf{M}\{\phi^{(i)}\} = 0 \quad (11.20)$$

For all modes $i \neq j$ with distinct eigenvalues ($\omega_i \neq \omega_j$), Equation (11.20) can be specified only if the matrix inner product $\{\phi^{(j)}\}^T \mathbf{M}\{\phi^{(i)}\}$ vanishes. This proves the first half of the proposition stated in Equation (11.15). The other half follows by substituting this result in either of Equation (11.18) or (11.19).

Since the computed mode shapes of a N -DOF system form a set of orthogonal vectors, they span the N -dimensional space completely. In other words, these mode shapes can be used as a set of basis vectors in the N -dimensional space and any vector in this space can be represented as a linear combination of these mode-shapes.

The orthogonality property of mode shapes leads to a very powerful theorem, *modal expansion theorem*, which states that any vector \mathbf{x} in N -dimensional vector space can be represented as a linear combination of mode-shape vectors,

$$\mathbf{x} = \sum_{i=1}^N q_i \{\phi^{(i)}\} \quad (11.21)$$

where $\{\phi^{(i)}\}$ represents the i^{th} mode shape and q_i denotes the corresponding modal coordinate. For a given vector \mathbf{x} , the modal coordinates q_i may be computed by using the property of orthogonality of mode-shapes as,

$$q_i = \frac{\{\phi^{(i)}\}^T \mathbf{M} \mathbf{x}}{\{\phi^{(i)}\}^T \mathbf{M} \{\phi^{(i)}\}}. \quad (11.22)$$

11.5 DETERMINATION OF FUNDAMENTAL FREQUENCY

The determination of the eigenspectrum of a system is an important part of the dynamic analysis of the system. Since the response of MDOF system is usually contained in the lower modes of vibration, determination of the characteristics of the fundamental mode is of primary interest.

11.5.1 Rayleigh Quotient

For any arbitrary vector, $\{\mathbf{u}\}$, representing a displacement configuration of a N -DOF system, the Rayleigh quotient is defined as the ratio

$$\rho = \frac{\mathbf{u}^T \mathbf{K} \mathbf{u}}{\mathbf{u}^T \mathbf{M} \mathbf{u}} \quad (11.23)$$

For a particular case when the vector \mathbf{u} represents the amplitudes of the harmonic oscillations of the N -DOF system or the Rayleigh quotient, ρ , corresponds to square of the frequency of harmonic oscillations. This result follows from the principle of conservation of energy by equating the maximum potential energy stored in the system to the maximum kinetic energy. Further, the Rayleigh quotient has the property of being stationary in the neighbourhood of the natural modes of the system. It is a global minimum for the fundamental mode and global maximum for the highest mode of vibration—also known as the *minimax* property of Rayleigh quotient.

11.5.2 Stodola Method

By transforming the generalised eigenvalue problem to the standard eigenvalue problem,

$$\mathbf{D}\{\phi\} = \lambda\{\phi\} \quad (11.24)$$

where $\mathbf{D} = \mathbf{K}^{-1}\mathbf{M}$ is known as the *dynamical matrix of the system* and $\lambda = \frac{1}{\omega^2}$. Stodola method starts with the choice of a trial vector, say, $\{\hat{\phi}^{(0)}\}$. Pre-multiplying $\{\hat{\phi}^{(0)}\}$ by the dynamical matrix, \mathbf{D} yields another vector $\{\bar{\phi}^{(1)}\}$, which is an improved estimate of the eigenvector. An estimate of the eigenvalue is obtained by taking the ratio of any element of new vector $\{\bar{\phi}^{(1)}\}$ to the corresponding element of the trial vector, *i.e.*,

$$\bar{\lambda}^{(1)} = \frac{\bar{\phi}_j^{(1)}}{\hat{\phi}_j^{(0)}} \quad (11.25)$$

If $\{\hat{\phi}^{(1)}\}$ were a true eigenvector, this ratio would be constant for any choice of the element of these vectors. In general, however, this ratio will be different for different choice of elements of these vectors. In the special case of symmetric coefficient matrices, the minimum and the maximum values of this ratio provide the upper and lower bounds on the eigenvalue. The

iteration resumes with the new trial vector of $\{\hat{\phi}^{(1)}\} = \frac{1}{\bar{\lambda}^{(1)}}\{\bar{\phi}^{(1)}\}$. Thus the equation for i^{th} iteration is given as,

$$\mathbf{D}\{\hat{\phi}^{(i)}\} = \bar{\lambda}^{(i+1)}\{\hat{\phi}^{(i+1)}\} \quad (11.26)$$

The Stodola method can be viewed as an iterative solution of a system of simultaneous equations to arrive at that configuration of generalised displacements for which the inertia forces are exactly balanced by the elastic forces in the structural members.

Why should iterative procedure converge to the first mode always?

To answer this natural query, let us take recourse to the modal expansion theorem and expand an arbitrary trial vector $\{\hat{\phi}\}$ as,

$$\{\hat{\phi}\} = q_1\{\phi^{(1)}\} + q_2\{\phi^{(2)}\} + \cdots + q_N\{\phi^{(N)}\} \quad (11.27)$$

where $\{\phi^{(1)}\}, \{\phi^{(2)}\}, \dots, \{\phi^{(N)}\}$ denote the eigenvectors of the dynamical system. The first iteration results in,

$$\mathbf{D}\{\hat{\phi}\} = \frac{q_1}{\omega_1^2}\{\phi^{(1)}\} + \frac{q_2}{\omega_2^2}\{\phi^{(2)}\} + \cdots + \frac{q_N}{\omega_N^2}\{\phi^{(N)}\} \quad (11.28)$$

Thus each iteration results in amplification of the i^{th} term in the modal expansion by a factor $1/\omega_i^2$. So that after p successive iterations,

$$\mathbf{D}^p\{\hat{\phi}\} = \frac{q_1}{\omega_1^{2p}}\{\phi^{(1)}\} + \frac{q_2}{\omega_2^{2p}}\{\phi^{(2)}\} + \cdots + \frac{q_N}{\omega_N^{2p}}\{\phi^{(N)}\} \quad (11.29)$$

Assuming that the natural frequencies (ω_i) are all distinct and are numbered in the ascending order *i.e.* $\omega_1 < \omega_2 < \cdots < \omega_N$, it follows that after sufficient number of cycles $\frac{1}{\omega_1^{2p}} \gg \frac{1}{\omega_2^{2p}} \gg \cdots \gg \frac{1}{\omega_N^{2p}}$. Therefore the first term in the modal expansion becomes progressively more dominant with each iteration and eventually converges to the first mode $\{\phi^{(1)}\}$.

11.5.3 Converging to Higher Modes

The iteration method described earlier will always converge to the lowest mode, unless the chosen trial vector exactly resembles a higher natural mode. Therefore to determine the higher modes using iteration procedure, it is necessary to *sweep out* all the lower modes. For example, let us assume that the first mode shape has already been determined and has been mass orthonormalized (such that $\{\phi^{(1)}\}^T \mathbf{M} \{\phi^{(1)}\} = 1.0$). Considering any arbitrary trial vector $\{\hat{\phi}\}$ and pre-multiplying it by $\{\phi^{(1)}\}^T \mathbf{M}$ and invoking the orthogonality of mode shapes,

$$\begin{aligned} \{\phi^{(1)}\}^T \mathbf{M} \{\hat{\phi}\} &= \{\phi^{(1)}\}^T \mathbf{M} \{\phi^{(1)}\} q_1 + \{\phi^{(1)}\}^T \mathbf{M} \{\phi^{(2)}\} q_2 + \cdots + \{\phi^{(1)}\}^T \mathbf{M} \{\phi^{(N)}\} q_N \\ &= q_1 \{\phi^{(1)}\}^T \mathbf{M} \{\phi^{(1)}\} \end{aligned} \quad (11.30)$$

where, use has been made of the modal expansion theorem (Equation (11.27)). The coefficient q_1 so determined, gives the extent of representation of the mode-shape $\{\phi^{(1)}\}$ in the trial vector $\{\hat{\phi}\}$. Let us define a new trial vector $\{\hat{\psi}\} = \{\hat{\phi}\} - q_1\{\phi^{(1)}\}$ by sweeping out the traces of known eigen vector $\{\phi^{(1)}\}$. Using this *purified* trial vector in the iteration procedure we would converge to the next lowest mode *i.e.* 2nd mode, $\{\phi^{(2)}\}$. This process can be repeated to compute any desired eigenvector by sweeping out the traces of all the previous lower mode eigenvectors from the trial vector. A geometrical interpretation of the process of sweeping is to determine a trial vector which is orthogonal to all the previously determined eigenvectors and this approach is known as *vector purification/deflation*.

In theory, though it is possible to sweep out completely the traces of a known eigenvector from an assumed trial vector, in practice, however, it is necessary to sweep out the known eigenvectors from trial function before the beginning of each iteration. This precaution is necessary because the round off errors due to finite precision arithmetic, on a computer always leave some small traces of swept out eigenvector(s) in the trial vector at the end of the iteration. It is possible to automate the process of sweeping in each iteration by *sweeping out* the traces of known modes from the coefficient matrix. Let us consider that first $n (< N)$ modes are known and it is required to converge to the $n+1^{\text{th}}$ mode via iteration. Since the need for sweeping the traces of known modes from trial vector at each iteration may be computationally expensive, it is worthwhile to look for the possibility of a more elegant formulation for this procedure. Let us consider that $\{\tilde{\psi}\}$ be the trial vector from which the traces of first $n (< N)$ modes are to be removed. We have, by modal expansion theorem,

$$\{\tilde{\psi}\} = \sum_{j=1}^N \{\phi^{(j)}\} q_j$$

For first n modes, which are known, the coefficients q_j can be computed by using the orthogonality property. The purified trial vector $\{\hat{\psi}\}$ can then be given as,

$$\begin{aligned} \{\hat{\psi}\} &= \{\tilde{\psi}\} - \sum_{j=1}^N \{\phi^{(j)}\} q_j \\ &= \left(\mathbf{I} - \sum_{j=1}^n \frac{1}{\{\phi^{(j)}\}^T \mathbf{M} \{\phi^{(j)}\}} \{\phi^{(j)}\} \{\phi^{(j)}\}^T \mathbf{M} \right) \{\tilde{\psi}\} \\ &= \mathbf{S} \{\tilde{\psi}\} \end{aligned} \quad (11.31)$$

where \mathbf{S} is known as the *sweeping matrix* and the entire process of sweeping out the known modes from a trial vector has been reduced to a simple matrix multiplication. In practice, the coefficient matrix of the eigenvalue problem is post-multiplied by the sweeping matrix and the resulting updated coefficient matrix is used in the iteration procedure to converge to the $n + 1^{\text{th}}$ mode. The sweeping matrix is then updated to sweep out the first $n + 1$ modes by extending the summation in Equation (11.31) to include the $n + 1^{\text{th}}$ mode.

For the demonstration of the procedure, let us consider a three-storey shear building shown in Figure 11.5. The system parameters are given as $m = 3500 \text{ kg}$, $k_1 = k = 1500 \text{ kN/m}$, $k_2 = 1.5k$, and $k_3 = 2.0k$. The mass and stiffness matrices can be written as,

$$\mathbf{M} = m \begin{bmatrix} 1 & 0 & 0 \\ 0 & 1 & 0 \\ 0 & 0 & 1 \end{bmatrix} \quad \mathbf{K} = k \begin{bmatrix} 1 & -1 & 0 \\ -1 & 2.5 & -1.5 \\ 0 & -1.5 & 3.5 \end{bmatrix}$$

For inverse iteration, the system coefficient matrix for the standard form of eigenvalue problem is given as,

$$\mathbf{D} = \mathbf{K}^{-1}\mathbf{M} = \frac{m}{k} \begin{bmatrix} 2.167 & 1.167 & 0.5 \\ 1.167 & 1.167 & 0.5 \\ 0.5 & 0.5 & 0.5 \end{bmatrix}$$

TABLE 11.1 Iteration for the first mode

$\frac{k}{m}\mathbf{D}$			$\{\psi^{(0)}\}$	$\{\hat{\psi}^{(1)}\}$	$\{\psi^{(1)}\}$	$\{\hat{\psi}^{(2)}\}$	$\{\psi^{(2)}\}$	$\{\hat{\psi}^{(3)}\}$	$\{\psi^{(3)}\}$	$\{\hat{\psi}^{(4)}\}$	$\{\psi^{(4)}\}$
2.167	1.167	0.500	1.00	2.875	1.00	3.075	1.00	3.109	1.00	3.12	1.00
1.167	1.167	0.500	0.50	1.875	0.65	2.075	0.67	2.109	0.68	2.12	0.68
0.500	0.500	0.500	0.25	0.875	0.30	0.975	0.32	0.995	0.32	1.00	0.32

Thus, the iteration procedure converges to the first eigenvalue $\lambda_1 = 3.12m/k$ and the corresponding eigenvector is $\{\phi^{(1)}\} = [1.00, 0.68, 0.32]^T$. Table 11.1 shows the iteration for the first mode and accordingly, the natural frequency of the first mode of the structural system is given by $\omega_1^2 = 0.32 \frac{k}{m}$.

Sweeping

The sweeping matrix for removing the first mode is given by,

$$\begin{aligned} \mathbf{S}_1 &= \mathbf{I} - \frac{1}{\{\phi^{(1)}\}^T \mathbf{M} \{\phi^{(1)}\}} \{\phi^{(1)}\} \{\phi^{(1)}\}^T \mathbf{M} \\ &= \begin{bmatrix} 0.361 & -0.435 & -0.204 \\ -0.435 & 0.705 & -0.139 \\ -0.204 & -0.139 & 0.935 \end{bmatrix} \end{aligned} \quad (11.32)$$

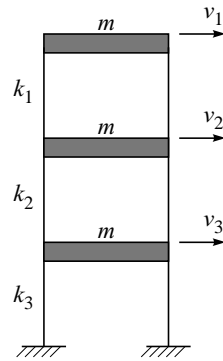


FIGURE 11.5 A 3-storey shear building.

Table 11.2 shows iteration for second mode and the coefficient matrix for the iteration for second mode is given by,

$$\mathbf{D}_1 = \mathbf{DS}_1 = \frac{m}{k} \begin{bmatrix} 0.173 & -0.189 & -0.137 \\ -0.189 & 0.246 & 0.067 \\ -0.137 & 0.067 & 0.296 \end{bmatrix}$$

TABLE 11.2 Iterations for second mode

$\frac{k}{m}\mathbf{D}_1$	$\{\psi^{(0)}\}$	$\{\hat{\psi}^{(1)}\}$	$\{\psi^{(1)}\}$	$\{\hat{\psi}^{(2)}\}$	$\{\psi^{(2)}\}$	$\{\hat{\psi}^{(3)}\}$	$\{\psi^{(3)}\}$	$\{\hat{\psi}^{(4)}\}$	$\{\psi^{(4)}\}$	$\{\hat{\psi}^{(5)}\}$
0.173	-0.189	-0.137	1.00	0.302	1.00	0.49	1.00	0.496	1.0	0.498
-0.189	0.246	0.067	-0.50	-0.329	-1.09	-0.51	-1.04	-0.506	-1.02	-0.505
-0.137	0.067	0.296	-0.25	-0.245	-0.81	-0.45	-0.92	-0.479	-0.966	-0.49

The approximation to eigenvector after 5th iteration is $\{\psi^{(5)}\}^T = [1.000, -1.008, -0.996]$.

Thus, as the iterations proceed, the iteration procedure converges to the second eigenvalue $\lambda_2 = 0.5m/k$ and the corresponding eigenvector is $\{\phi^{(2)}\} = [1.00, -1.00, -1.00]^T$. Accordingly, the natural frequency of the second mode of the structural system is given by $\omega_2^2 = 2.0 \frac{k}{m}$. From the elementary linear algebra, it is known that the trace of a square matrix is equal to the sum of its eigenvalues. Thus, it follows that,

$$\text{Tr}(\mathbf{D}) = \sum_{j=1}^3 \lambda_j$$

and $\lambda_3 = 0.214 \frac{m}{k}$, or $\omega_3^2 = 4.68 \frac{k}{m}$. The corresponding eigenvector can be computed as $\{\phi^{(3)}\} = [1.0, -3.68, 4.68]^T$. Alternatively, the third eigenpair could have been computed by first constructing a new sweeping matrix as

$$\mathbf{S}_2 = \mathbf{I} \sum_{j=1}^2 \frac{1}{\{\phi^{(j)}\}^T \mathbf{M} \{\phi^{(j)}\}} \{\phi^{(j)}\} \{\phi^{(j)}\}^T \quad (11.33)$$

and then deriving the coefficient matrix for iteration for the third mode (\mathbf{D}_2) by pre-multiplying the new sweeping matrix by \mathbf{D} , i.e.,

$$\mathbf{D}_2 = \mathbf{DS}_2$$

The remaining eigenpair may then be computed via iterations.

11.6 FORCED VIBRATION ANALYSIS

The forced vibrations of an MDOF system are described as a set of N coupled, non-homogeneous differential equations in \mathbf{v} as,

$$\mathbf{M}\ddot{\mathbf{v}} + \mathbf{C}\dot{\mathbf{v}} + \mathbf{K}\mathbf{v} = \mathbf{f} \quad (11.34)$$

These equations, in coupled form, are extremely cumbersome, and we shall look for some suitable transformation of the unknowns \mathbf{v} to reduce the system of N coupled differential equations to a set of N uncoupled differential equations. This method of solution is known as mode-superposition method.

11.6.1 Mode-superposition Method

We know by modal expansion theorem that any arbitrary vector \mathbf{v} in an N -dimensional space can be represented as a linear combination of mode-shapes. Thus,

$$\mathbf{v} = \sum_{r=1}^N q_r(t) \{\phi^{(r)}\} = \Phi \mathbf{q} \quad (11.35)$$

where, Φ is the modal matrix with each of its columns representing a mode-shape of the MDOF system and \mathbf{q} is a vector of modal coordinates related to the system coordinate vector \mathbf{v} through a linear transformation given by Equation (11.35). Substituting this transformation in Equation (11.34) and pre-multiplying it by Φ^T , we have,

$$\Phi^T \mathbf{M} \Phi \ddot{\mathbf{q}} + \Phi^T \mathbf{C} \Phi \dot{\mathbf{q}} + \Phi^T \mathbf{K} \Phi \mathbf{q} = \Phi^T \mathbf{f} \quad (11.36)$$

Since the mode shapes Φ are orthogonal with respect to \mathbf{M} and \mathbf{K} matrices, the matrix triple products involving \mathbf{M} and \mathbf{K} in Equation (11.36) both yield diagonal matrices. The damping matrix \mathbf{C} is not in general amenable to such diagonalization procedure. However, for a specific class of damping matrices—called *classical damping*—such a diagonalization using (undamped) mode shapes is indeed possible. A sufficient condition for a damping matrix \mathbf{C} to be diagonalized using undamped mode shapes is to have the following series expansion:

$$\mathbf{C} = \mathbf{M} \sum_n a_n [\mathbf{M}^{-1} \mathbf{K}]^n \quad (11.37)$$

A special case of Equation (11.37) obtained by retaining only two terms of the series for $n = 0$ and $n = 1$ and is known as Rayleigh damping and is very widely used in structural dynamics applications. It is also known as *proportional damping* as the damping matrix is proportional to stiffness and mass matrices in this case. Since the matrices \mathbf{M} and \mathbf{K} are known for a given structural system, a classical damping matrix \mathbf{C} can be completely specified if the coefficients a_n in the series of Equation (11.37) are specified. These coefficients can also be determined so as to have desired damping values in different modes of vibrations. If we assume that the \mathbf{C} in Equation (11.36) is a classical damping matrix, then the system of coupled equations reduces to a set of N uncoupled differential equations in q_r , $r = 1, 2, \dots, N$, as:

$$m_r^* \ddot{q}_r + c_r^* \dot{q}_r + k_r^* q_r = f_r^*, \quad \forall r = 1, 2, \dots, N \quad (11.38)$$

where, $\{\phi^{(r)}\}^T \mathbf{M} \{\phi^{(r)}\} = m_r^*$ represents the modal mass for mode r , $\{\phi^{(r)}\}^T \mathbf{C} \{\phi^{(r)}\} = c_r^*$ is the coefficient of viscous damping in r^{th} mode, $\{\phi^{(r)}\}^T \mathbf{K} \{\phi^{(r)}\} = k_r^*$ denotes the modal stiffness for r^{th} mode, and $\{\phi^{(r)}\}^T \mathbf{f} = f_r^*$, the modal force in mode r . It may be noted that if the mode shapes have been mass-orthonormalized, then these modal parameters reduce to $m_r^* = 1.0$, $c_r^* = 2\zeta_r \omega_r$, and $k_r^* = \omega_r^2$ (note the similarity of form with the equation of motion for SDOF system in

Equation (7.5)). The Equations (11.38) can now be solved for unknowns q_r , independent of each other, by using the solution methods developed for single degree of freedom systems. Once the solution for modal coordinates q_r is available, the response in system coordinates can be obtained by using the linear transformation of Equation (11.35).

11.6.2 Excitation by Support Motion

The forced vibration of MDOF system excited by support motions is described by the coupled system of differential equations as

$$\mathbf{M}\ddot{\mathbf{v}} + \mathbf{C}\dot{\mathbf{v}} + \mathbf{K}\mathbf{v} = -\mathbf{M}\mathbf{r}\ddot{\mathbf{v}}_g \quad (11.39)$$

where $\ddot{\mathbf{v}}_g$ denotes ground acceleration, \mathbf{v} is the vector of structural displacements *relative* to the ground displacements, and \mathbf{r} is a vector of influence coefficients. The i^{th} element of vector \mathbf{r} represents the displacement of i^{th} degree of freedom due to a unit displacement of the base. The nature of this equation is similar to that of standard forced vibration problem as given by Equation (11.34) and hence the method of solution (using mode-superposition) is also similar. Thus the equation can be decoupled as

$$\ddot{q}_r + 2\zeta_r\omega_r\dot{q}_r + \omega_r^2 q_r = -\Gamma_r \ddot{v}_g, \quad \forall r = 1, 2, \dots, N \quad (11.40)$$

where, $\Gamma_r = \frac{\{\phi^{(r)}\}^T \mathbf{M} \mathbf{r}}{\{\phi^{(r)}\}^T \mathbf{M} \{\phi^{(r)}\}}$ is known as the *mode-participation factor* for the r^{th} mode.

Note, however, that the Equation (11.40) differs from the equation of motion of a SDOF system excited by support acceleration \ddot{v}_g by a scaling factor for the excitation. Since the maximum response of SDOF system to ground acceleration is generally available in the form of response spectra, it follows that the maximum value of the r^{th} modal coordinate q_r can be determined directly from the response spectra without solving the differential equation of motion. Therefore, assuming that the spectral displacement ordinate for frequency ω_r and damping ζ_r is given as $S_d(\omega_r, \zeta_r)$, the maximum response for r^{th} modal coordinate $q_{r,\max}$ is given as,

$$q_{r,\max} = \Gamma_r S_d(\omega_r, \zeta_r); \quad \forall r = 1, 2, \dots, N$$

This information about the maximum response in modal coordinates is, however, not very useful for structural design, which is concerned with the maximum response in physical coordinates \mathbf{v} . It is possible to estimate probable maximum response values in physical coordinates from the knowledge of maximum response in modal coordinates by using modal combination rules. Two of the most commonly used modal combination rules are:

Absolute sum method

Assuming that the maximum of each modal coordinate occurs at the same instant of time, the maximum response in physical coordinates at i^{th} DOF is given by,

$$v_{i,\max} \approx \sum_{r=1}^N q_{r,\max} \phi_i^{(r)} \quad (11.41)$$

The absolute sum method of modal combination provides a very conservative estimate of the maximum response in physical coordinates since the time of occurrence of maxima in each mode in general, is different.

Square root of sum of squares (SRSS) method

If we relax the assumption regarding simultaneous occurrence of peak response in all modes, and assuming that the natural frequencies are not very closely spaced then the maximum response in physical coordinate system can be estimated as,

$$v_{i,\max} \approx \left[\sum_{r=1}^N \left(q_{r,\max} \phi_i^{(r)} \right)^2 \right]^{1/2} \quad (11.42)$$

It must be emphasized here that these modal combination rules are approximate procedures for combining the maximum modal responses to get a probable estimate of the maximum response of physical system. These modal combination rules may be used to estimate the probable maximum value for any response quantity of interest such as, shear force, bending moment, drifts, etc. However, care should be taken to ensure that the maximum of each desired response parameter is first calculated for each mode and then these modal maxima are combined according to a modal combination rule. An example which illustrates this procedure is given below.

Example 1 Consider a 3-storey shear building shown in Figure 11.5 with the following properties:

$$\mathbf{M} = \begin{bmatrix} 30.0 & 0.0 & 0.0 \\ 0.0 & 30.0 & 0.0 \\ 0.0 & 0.0 & 30.0 \end{bmatrix} \text{ tonnes}, \quad \boldsymbol{\Phi} = \begin{bmatrix} 1.000 & 1.000 & 1.000 \\ 0.548 & -1.522 & -6.260 \\ 0.198 & -0.872 & 12.10 \end{bmatrix}, \quad \omega_n = \begin{pmatrix} 3.88 \\ 9.15 \\ 15.31 \end{pmatrix} \text{ rad/s}$$

Compute the floor displacements, inter-storey drifts, storey shears and overturning moments of this building when excited by an earthquake. The pseudo-spectral acceleration ordinates of the earthquake ground acceleration for the three modes are given as $S_a = 2.94, 1.57$, and 3.93 m/s^2 . Assume the storey heights to be 3.0 m and use SRSS rule for combining modal responses.

Solution The modal mass in the r^{th} mode of vibration can be computed as $m_r^* = \{\phi^{(r)}\}^T \mathbf{M} \{\phi^{(r)}\}$. For this problem, the modal masses are $m_1^* = 40.185$, $m_2^* = 122.306$, and $m_3^* = 5597.928$. The mode participation factors $\left(\Gamma_r = \frac{1}{m_r^*} \{\phi^{(r)}\}^T \mathbf{M} \mathbf{r} \right)$ can be computed as $\Gamma_1 = 1.303$, $\Gamma_2 = -0.342$, and $\Gamma_3 = 0.037$.

The maximum floor displacements are given by,

$$v_{i,\max} \approx \left[\sum_{r=1}^3 \{\phi_j^{(r)} \Gamma_r (S_{ar}/\omega_r^2)\}^2 \right]^{0.5}$$

which, for the current problem are given by

$$\begin{aligned}\mathbf{v}_{\max} &\approx \left(\begin{array}{l} [\{1.303 \times (2.94 / 3.88^2)\}^2 + \{-0.342 \times (1.57 / 9.15^2)\}^2 + \{0.037 \times (3.93 / 15.31^2)\}^2]^{0.5} \\ [\{0.714 \times (2.94 / 3.88^2)\}^2 + \{0.520 \times (1.57 / 9.15^2)\}^2 + \{-0.232 \times (3.93 / 15.31^2)\}^2]^{0.5} \\ [\{0.258 \times (2.94 / 3.88^2)\}^2 + \{0.298 \times (1.57 / 9.15^2)\}^2 + \{-0.448 \times (3.93 / 15.31^2)\}^2]^{0.5} \end{array} \right) \\ &= \begin{pmatrix} 0.255 \\ 0.139 \\ 0.159 \end{pmatrix} \text{m}\end{aligned}$$

The maximum inter-storey drifts are given by,

$$\Delta_{ij,\max} \approx \left[\sum_{r=1}^3 \left\{ (\phi_i^{(r)} - \phi_j^{(r)}) \Gamma_r S_{ar} / \omega_r^2 \right\}^2 \right]^{0.5}$$

which, in case of current problem leads to,

$$\begin{aligned}\Delta_{\max} &\approx \left(\begin{array}{l} \left[\left\{ (1 - 0.548) \times 1.303 \times \frac{2.940}{3.88^2} \right\}^2 + \left\{ (1 + 1.522) \times -0.342 \times \frac{1.57}{9.15^2} \right\}^2 \right. \\ \quad \left. + \left\{ (1 + 6.260) \times 0.037 \times \frac{3.93}{15.31^2} \right\}^2 \right]^{0.5} \\ \left[\left\{ (0.548 - 0.198) \times 1.303 \times \frac{2.940}{3.88^2} \right\}^2 + \left\{ (-1.522 + 0.872) \times 0.342 \times \frac{1.57}{9.15^2} \right\}^2 \right. \\ \quad \left. + \left\{ (-6.260 - 12.100) \times 0.037 \times \frac{3.93}{15.31^2} \right\}^2 \right]^{0.5} \\ \left[\left\{ (0.198) \times 1.303 \times \frac{2.940}{3.88^2} \right\}^2 + \left\{ (-0.872) \times -0.342 \times \frac{1.57}{9.15^2} \right\}^2 \right. \\ \quad \left. + \left\{ (12.100) \times 0.037 \times \frac{3.93}{15.31^2} \right\}^2 \right]^{0.5} \end{array} \right) \\ &= \begin{pmatrix} 0.116 \\ 0.089 \\ 0.051 \end{pmatrix} \text{m}\end{aligned}$$

The maximum storey shears are given by,

$$V_{j,\max} \approx \left[\sum_{r=1}^3 \left\{ \Gamma_r S_{ar} \sum_{i=1}^j m_{ii} \phi_i^{(r)} \right\}^2 \right]^{0.5}$$

or, in vector form

$$V_{\max} \approx \left(\begin{array}{l} [\{30.0 \times 1.0 \times 1.303 \times 2.94\}^2 + \{30.0 \times 1.0 \times -0.342 \times 1.57\}^2 \\ \quad + \{30.0 \times 1.0 \times 0.037 \times 3.93\}^2]^{0.5} \\ [\{30.0 \times (1 + 0.548) \times 1.303 \times 2.94\}^2 \\ \quad + \{30.0 \times (1 - 1.522) \times -0.342 \times 1.57\}^2 \\ \quad + \{30.0 \times (1 - 6.260) \times 0.037 \times 3.93\}^2]^{0.5} \\ [\{30.0 \times (1 + 0.548 + 0.198) \times 1.303 \times 2.94\}^2 \\ \quad + \{30.0 \times (1 - 1.522 - 0.872) \times -0.342 \times 1.57\}^2 \\ \quad + \{30.0 \times (1 - 6.260 + 12.100) \times 0.037 \times 3.93\}^2]^{0.5} \end{array} \right)$$

$$= \begin{pmatrix} 116.13 \\ 179.57 \\ 204.10 \end{pmatrix} \text{kN}$$

The maximum overturning moments are given by,

$$M_{j,\max} \approx \left[\sum_{r=1}^3 \left\{ \Gamma_r S_{ar} \sum_{i=1}^j (h_i - h_j) m_{ii} \phi_i^{(r)} \right\}^2 \right]^{0.5}$$

or, in vector form,

$$M_{\max} \approx \left(\begin{array}{l} [\{30.0 \times 0.0 \times 1.0 \times 1.303 \times 2.94\}^2 + \{30.0 \times 0.0 \times 1.0 \times -0.342 \times 1.57\}^2 \\ \quad + \{30.0 \times 0.0 \times 1.0 \times 0.037 \times 3.93\}^2]^{0.5} \\ [\{30.0 \times (1 \times (9.0 - 6.0) + 0.548 \times 0.0) \times 1.303 \times 2.94\}^2 \\ \quad + \{30.0 \times (1 \times (9.0 - 6.0) - 1.522 \times 0.0) \times -0.342 \times 1.57\}^2 \\ \quad + \{30.0 \times (1 \times (9.0 - 6.0) - 6.260 \times 0.0) \times 0.037 \times 3.93\}^2]^{0.5} \\ [\{30.0 \times (1 \times (9.0 - 3.0) + 0.548 \times (6.0 - 3.0) + 0.198 \times 0.0) \times 1.303 \times 2.94\}^2 \\ \quad + \{30.0 \times (1 \times (9.0 - 3.0) - 1.522 \times (6.0 - 3.0) - 0.872 \times 0.0) \times -0.342 \times 1.57\}^2 \\ \quad + \{30.0 \times (1 \times (9.0 - 3.0) - 6.260 \times (6.0 - 3.0) + 12.100 \times 0.0) \times 0.037 \times 3.93\}^2]^{0.5} \end{array} \right)$$

$$= \begin{pmatrix} 0.0 \\ 348.39 \\ 880.55 \end{pmatrix} \text{kN.m}$$

Similarly, the calculations for maximum overturning moment at the base can also be performed.

In the above-mentioned example, only one component of ground acceleration was considered for excitation. In general, the structure would be subjected to three mutually orthogonal

translational components of ground motions simultaneously at a support point. Computations for any response quantity of interest for simultaneous excitation by multiple components would, in general, yield different estimates than for any single ground motion component acting alone. It is not adequate, for design purpose, to consider the maximum response out of the three estimates obtained for different ground motion components independently. To find the response parameters for use in design, the response estimates for excitation by individual components may be combined together by SRSS rule. For any generic response quantity of interest, say, R , the value to be adopted for design calculations R_{des} can be obtained as,

$$R_{\text{des}} = \sqrt{R_x^2 + R_y^2 + R_z^2}$$

where, R_x , R_y , and R_z represent the estimate of response R due to excitation by ground motion in x , y , and z directions, respectively.

11.6.3 Mode Truncation

Generally, the mathematical models for real civil engineering structural systems may involve millions of degrees of freedoms, implying that the total number of equations to be solved for modal coordinates (Equations (11.38)) could be of the same order—a formidable task even for the powerful desktop computers available today. Fortunately, it is not necessary to include response in all the modes to get a rational estimate of the total response. Since most of the energy of the dynamic loads of civil engineering structures (such as earthquake ground motions, wind forces, ocean waves, etc.) is concentrated in low frequencies (typically < 35 Hz for earthquakes) the higher modes (with larger natural frequencies) are not excited by these low-frequency forces.² Thus it is possible to truncate the modal summation in Equation (11.35) to the sum of only a few of the lower modes. The total number of terms in such truncated modal summation seldom exceeds a few hundreds, even in very complex structural systems. Thus the response vector \mathbf{v} can be approximately determined as,

$$\mathbf{v} = \sum_{r=1}^{\hat{N}} q_r(t) \{ \phi^{(r)} \} \quad (11.43)$$

where, $\hat{N} << N$. The decision about the number of modes to be included in the response computations may be based on the following two criteria:

- (i) All modes having natural frequencies less than or equal to the highest frequency in the excitation should be included in the modal summation.
- (ii) At least 90% of the total mass of the structural system should be included in the dynamic response computation. This criterion is assessed by considering the cumulative *effective modal mass* ($= \sum_r m_r^* \Gamma_r^2$) for all modes included in the summation, which should be more than 90% of the total mass of the system.

²This inference can be drawn by considering the nature of response of SDOF systems to harmonic excitations. The dynamic amplification factor for the oscillator response approaches unity as the ratio of frequency of excitation to natural frequency (ω/ω_n) decreases and the response approaches that for a static case (see Figure 7.5).

The truncation of the modal summation after a few modes undoubtedly introduces some errors due to neglecting the contribution of higher modes to total response. However, if the above-mentioned two criteria are adhered to, the error resulting from neglecting the higher mode contribution is not likely to be significant to affect the design, except for very rare situations encountered in special structures such as pipings, etc. In such special cases, it is possible to improve on the accuracy of the solution by including the contribution of higher modes as a static correction to the computed dynamic response.

11.6.4 Static Correction for Higher Mode Response

Let us consider the modal contribution to total response as the sum of two parts:

$$\mathbf{v} = \sum_{r=1}^{\hat{N}} \{\phi^{(r)}\} q_r(t) + \sum_{s=\hat{N}+1}^N \{\phi^{(s)}\} q_s(t) \quad (11.44)$$

where, the second term of the modal summation represents the error term due to truncation of modal summation (assuming that only \hat{N} lower modes are being considered for dynamic response computation. Let us now consider the equation for the response of s^{th} modal coordinate

$$m_s \ddot{q}_s(t) + c_s \dot{q}_s(t) + k_s q_s(t) = f_s$$

which can be rearranged as,

$$q_s(t) = \frac{f_s}{k_s} - \frac{\ddot{q}_s(t)}{\omega_s^2} - \frac{2\zeta_s \dot{q}_s(t)}{\omega_s}$$

where, the first term represents the response in s mode if the load were applied statically; the other two terms represent the dynamic correction to the static response in s^{th} mode. The inertia term is inversely proportional to the square of the natural frequency, while the damping term (which is generally very small in magnitude in comparison to elastic and inertia terms) is inversely proportional to the natural frequency. Therefore for higher modes, the contribution from dynamic response terms becomes insignificant in comparison with the static response term and the response in higher modes can be reasonably approximated by considering only the static response. The total response can now be given (after substituting for the modal force $f_s = \{\phi^{(s)}\}^T \mathbf{f}$) as,

$$\begin{aligned} \mathbf{v} &= \sum_{r=1}^{\hat{N}} \{\phi^{(r)}\} q_r(t) + \sum_{s=\hat{N}+1}^N \frac{1}{k_s} \{\phi^{(s)}\} \{\phi^{(s)}\}^T \mathbf{f} \\ &= \sum_{r=1}^{\hat{N}} \{\phi^{(r)}\} q_r(t) + \sum_{s=\hat{N}+1}^N \mathbf{F}_s \mathbf{f} \end{aligned} \quad (11.45)$$

where, $\frac{1}{k_s} \{\phi^{(s)}\} \{\phi^{(s)}\}^T = \mathbf{F}_s$ represents the contribution of s^{th} mode toward the flexibility matrix of the structural system.

It should be noted that although the response of higher modes can be approximated by considering the static response only, the formulation presented above requires that all mode shapes for the system have to be computed in order to compute the contribution of higher modes to the structural flexibility. It is worthwhile to investigate if it is possible to estimate the contribution to structural flexibility from higher modes in terms of lower modes which are being considered for dynamic response. It turns out that it is indeed possible to reformulate the expression of structural flexibility as,

$$\begin{aligned} \sum_{s=\hat{N}+1}^N \frac{1}{k_s} \{\phi^{(s)}\} \{\phi^{(s)}\}^T &= \mathbf{K}^{-1} - \sum_{r=1}^{\hat{N}} \frac{1}{k_r} \{\phi^{(r)}\} \{\phi^{(r)}\}^T \\ &= \mathbf{K}^{-1} - \sum_{r=1}^{\hat{N}} \mathbf{F}_r \end{aligned} \quad (11.46)$$

where, higher mode contribution to structural flexibility has been computed by subtracting the contribution of lower modes to structural flexibility from the total structural flexibility (\mathbf{K}^{-1}). Thus the total response \mathbf{v} can be computed as

$$\mathbf{v} = \sum_{r=1}^{\hat{N}} \{\phi^{(r)}\} q_r(t) + \left(\mathbf{K}^{-1} - \sum_{r=1}^{\hat{N}} \mathbf{F}_r \right) \mathbf{f} \quad (11.47)$$

where, the second term on the right hand side represents the static correction term to account for higher mode response. This correction for higher mode response is also known as *the missing mass correction*.

11.7 MODEL ORDER REDUCTION IN STRUCTURAL DYNAMICS

Since only a few lower modes contribute to the dynamic response of any structural system, it is not necessary to compute all eigenvalues and eigenvectors for a given system. Further, a major portion of the total time for the solution of a structural dynamics problem goes into the solution of eigenvalue problem. Hence, it is beneficial to explore the ways to minimise the time spent in the eigensolution phase which directly results in reduced solution times. A convenient way of achieving this end is by reducing the problem size itself by the use of the concept of generalised coordinates. Let us consider a (N -dimensional) vector \mathbf{v} , which can be represented as

$$\begin{aligned} \mathbf{v} &\approx \sum_{r=1}^p z_r \{\psi^{(r)}\} \\ &= \boldsymbol{\Psi} \mathbf{z} \end{aligned} \quad (11.48)$$

where, $\{\psi^{(r)}\}$ represents a set of orthogonal vectors, called as the *Ritz base vectors*, z_r denote the r^{th} generalised coordinate associated with the r^{th} Ritz vector, and $p \ll N$. Substituting

for \mathbf{v} from Equation (11.48) in the Equation (11.7) for free vibration, we get,

$$\mathbf{M}\Psi\ddot{\mathbf{z}} + \mathbf{K}\Psi\mathbf{z} = \mathbf{0} \quad (11.49)$$

Pre-multiplying by Ψ^T on both sides of the equation, we get,

$$\tilde{\mathbf{M}}\ddot{\mathbf{z}} + \tilde{\mathbf{K}}\mathbf{z} = \mathbf{0} \quad (11.50)$$

where, $\tilde{\mathbf{M}} = \Psi^T \mathbf{M} \Psi$ and $\tilde{\mathbf{K}} = \Psi^T \mathbf{K} \Psi$ are the reduced ($p \times p$) generalised mass and stiffness matrices respectively. Equation (11.50) represents an eigenvalue problem which is much smaller in size in comparison with the original eigenvalue problem given by Equation (11.7). The eigenvectors of this reduced eigenvalue may be substituted back in Equation (11.48) to get the eigenvectors (mode shapes) for the actual structure for further use in the mode superposition analysis. For example, let us assume that Φ_z denotes the modal matrix containing all p eigenvectors of the reduced eigenvalue problem of Equation (11.50). The required mode shapes (for lower modes) of the actual structure can then be obtained as,

$$\Phi = \Psi\Phi_z$$

The frequencies obtained by solving the reduced eigenvalue problem are approximations to the frequencies of the actual structural system. The agreement between the two set of frequencies is generally excellent for the lower modes but is relatively poor for higher modes. The quality of approximation and number of Ritz base vectors required for accurate estimation of desired number of mode shapes of actual structure depends on the choice of Ritz base vectors. Generally, it is necessary that $p = 2 \hat{N}$ in order to estimate accurately the frequencies and mode shapes for \hat{N} lower modes. Further, a good choice for the first Ritz vector ($\{\psi^{(1)}\}$) is the static displacement response vector (in accordance with Rayleigh's method). Other additional Ritz vectors can be estimated by making an arbitrary vector orthogonal to the previously determined Ritz vectors by using a procedure similar to the sweeping of lower modes as discussed earlier. The Rayleigh–Ritz method, as this procedure of model reduction is called, can be a very powerful tool to quickly estimate the frequencies and mode shapes of lower modes and is invariably used in all commercial structural analysis softwares.

11.8 ANALYSIS FOR MULTI-SUPPORT EXCITATION

The issue of spatial variation of ground motions was discussed earlier in the first part on *Earthquake Ground Motions*. Although the implications of this important physical phenomenon are not quite obvious when the plan dimensions of the structure under consideration are very small in comparison with the wavelengths of the seismic waves propagating through the soil. However, if the plan dimensions of the structural system are very large, or are comparable to seismic wavelengths, the spatial variation of ground motions can be a very important modelling consideration. Figure 11.6 shows two different structural systems: (i) an elevated reservoir, and (ii) a continuous girder bridge structure, or a pipeline subjected to earthquake excitation. In the

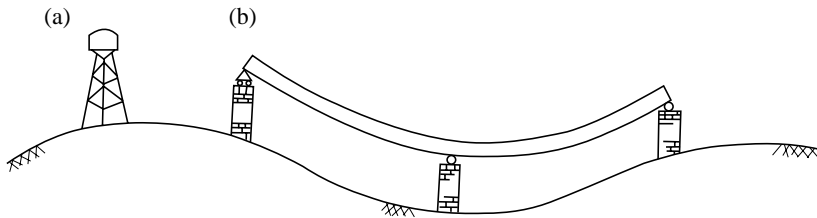


FIGURE 11.6 Effect of spatial variation of ground motions: (a) inconsequential in the case of structures with small plan dimensions, (b) a major consideration in the case of structures with large plan dimensions.

case of elevated reservoir, the spatial variation of earthquake ground motion is inconsequential and the motion can be assumed to be uniform at all points on the foundation base for all practical purposes. However, for the long-span structure, the variation of ground motion from one point to the other is significant, causing differential support motions. The structure should be designed to withstand this additional distress, which is caused entirely due to non-uniform nature of earthquake ground motions. In addition to the generation of quasi-static stresses, the spatial variation of earthquake ground motions can also lead to failure of bridge spans due to inadequacy of the bearing seating lengths to accommodate the out-of-phase motions between different support points. Failure to consider this aspect while designing the seating lengths/widths of the bearing pads has led to numerous collapses of bridge spans in past earthquake. Figure 11.7 shows one such example of failure during the 1999 Kocaeli, Turkey earthquake.

As discussed above, the dynamic behaviour of large structural systems to multiple-support excitation by differential ground motions, has important implications for design of such systems and these effects should be investigated analytically during the design process. The equation of motion for the case of multiple excitation can be given as,

$$[\mathbf{M} \ \mathbf{M}_g] \begin{pmatrix} \ddot{\mathbf{v}}^t \\ \ddot{\mathbf{v}}_g \end{pmatrix} + [\mathbf{C} \ \mathbf{C}_g] \begin{pmatrix} \dot{\mathbf{v}}^t \\ \dot{\mathbf{v}}_g \end{pmatrix} + [\mathbf{K} \ \mathbf{K}_g] \begin{pmatrix} \mathbf{v}^t \\ \mathbf{v}_g \end{pmatrix} = \mathbf{0} \quad (11.51)$$

where, the system property matrices have been partitioned such that the vector \mathbf{v}^t contains total displacement of all *free* degrees of freedom, and \mathbf{v}_g represents the displacement of support degrees of freedom. The Equation (11.51) can be rewritten, after some algebraic manipulation, as,

$$\mathbf{M}\ddot{\mathbf{v}}^t + \mathbf{C}\dot{\mathbf{v}}^t + \mathbf{K}\mathbf{v}^t = -\mathbf{M}_g\ddot{\mathbf{v}}_g - \mathbf{C}_g\dot{\mathbf{v}}_g - \mathbf{K}_g\mathbf{v}_g \quad (11.52)$$

Equation (11.52) can be solved by using method of mode superposition (or, by using step-by-



FIGURE 11.7 Failure of bridge spans due to inadequate seating length (after [2]).

step integration) if the terms on the right hand side are considered to constitute an *effective* force acting on the structural system. However, the ground displacement and velocity time histories also have to be specified in addition to the ground acceleration time histories at all support points. The ground velocity and displacement time histories are generally not available. Sometimes when those time histories are available, the reliability of those time histories is questionable due to several assumptions necessitated by the strong motion data processing algorithms for deriving velocity and displacement time histories from the recorded acceleration data. It is, therefore, beneficial to explore the possibility of reformulating the equation of motion so that the excitation can be specified in terms of ground acceleration only.

For this purpose, let us consider the total displacement response be given by the sum of two components: (i) a quasi-static component (\mathbf{v}^s) which would result if the support displacements were applied statically, and (ii) a dynamic component (\mathbf{v}) oscillating about the quasi-static displacement profile.

$$\mathbf{v}^t(t) = \mathbf{v}^s(t) + \mathbf{v}(t) \quad (11.53)$$

The quasi-static part of the solution is obtained by ignoring the time derivative terms (velocities and accelerations) of Equation (11.52) and noting that the total displacements (\mathbf{v}^t) are, in this case, same as the quasi-static displacements (\mathbf{v}^s). Thus,

$$\begin{aligned} \mathbf{v}^s(t) &= -\mathbf{K}^{-1}\mathbf{K}_g \mathbf{v}_g(t) \\ &= \mathbf{R}\mathbf{v}_g(t) \end{aligned} \quad (11.54)$$

where, \mathbf{R} represents the *influence coefficient matrix* containing the response in all degrees of freedom due to a unit displacement of a support point and is given by,

$$\mathbf{R} = -\mathbf{K}^{-1}\mathbf{K}_g$$

Substituting from Equations (11.53) and (11.52), in Equation (11.52), we get after some rearrangement of terms,

$$\mathbf{M}\ddot{\mathbf{v}} + \mathbf{C}\ddot{\mathbf{v}} + \mathbf{K}\mathbf{v} = -[\mathbf{M}\mathbf{r} + \mathbf{M}_g]\ddot{\mathbf{v}}_g - [\mathbf{C}\mathbf{R} + \mathbf{C}_g]\dot{\mathbf{v}}_g \quad (11.55)$$

As we had discussed earlier, the magnitude of damping forces in structural systems is generally quite small in comparison with the inertia and elastic force terms. In such cases, there will be no appreciable change in the computed dynamic response if the damping term is neglected from the right hand side of Equation (11.55). Thus the equation of motion for multi-support excitation can be reduced to,

$$\mathbf{M}\ddot{\mathbf{v}} + \mathbf{C}\ddot{\mathbf{v}} + \mathbf{K}\mathbf{v} = -[\mathbf{M}\mathbf{r} + \mathbf{M}_g]\ddot{\mathbf{v}}_g \quad (11.56)$$

which contains only ground acceleration term in the excitation. Equation (11.56) can be solved for dynamic component of the response by any standard procedure of dynamic analysis, such as the mode superposition method. It must be mentioned here that the effect of spatial variability of ground motion on seismic response of multiple supported structure is strongly dependent on

the type of model used to describe the ground motion variation. It is desirable to analyse the effects of spatial variation of ground motion by using several suites of ground motions at supports which have been generated artificially to conform to different alternate models postulated to be applicable for the project site [7].

11.9 SOIL-STRUCTURE INTERACTION EFFECTS

All discussion till this point has been based on a tacit assumption that the foundations of structures transfer the loads by direct bearing on firm rocky strata and hence the support conditions could be assumed to correspond to the fixed-base condition. This is, no doubt, a simplifying assumption and is generally valid if the super-structure is much more flexible/compliant than the underlying soil strata upon which the foundations rest. However, when the reverse is true *i.e.*, the super-structure is much more stiff in comparison with the soil strata, the structural response can be significantly influenced by the flexibility of soil.

There are two primary issues involved in the phenomenon of soil–structure interaction. First, as the seismic waves propagate through soil during an earthquake, a discontinuity in the medium of wave propagation is encountered at the interface of soil and structural foundations. The change in the material properties leads to scattering, diffraction, reflection, and refraction of the seismic waves at this soil–foundation interface thereby changing the nature of ground motion at that point from what would have otherwise been observed in the absence of structure and foundation. Further, the seismic wave propagation takes place by deformations in the medium. Since the foundation can be considered to be very rigid in comparison to the soil deposits, the deformations of the soil at the soil–foundation interface are constrained as the foundation cannot deform by the same amount as the soil. This further leads to slippage across the soil–foundation interface—a nonlinear phenomenon—which is very difficult to account for in the mathematical models for practical vibration analysis. Moreover, the rigid foundation acts like a low-pass filter by averaging out the high frequency components in seismic motions due to the kinematic constraint imposed by the rigid foundation. It should be noted that the above-mentioned effects are only due to the wave propagation in elastic medium. The dynamic behaviour of the structure has no role to play in this aspect. Therefore, these effects arising out of the wave propagation considerations are known as *kinematic interaction* effects. The actual seismic input motion to the structural foundation is the result of kinematic interaction analysis considering only the geometry and stiffness properties of the structural foundation and soil. The second aspect of the soil–structure interaction analysis involves the deformations and stresses in supporting soil, induced due to the base shears and moments generated in the vibrating structure. The soil deformations further lead to a modification of the dynamic response of structural system and thereby creating a dynamically interacting system. This second aspect of soil–structure interaction problem which results from the dynamic response of structural system is known as the *inertial interaction*. Figure 11.8 shows a schematic representation of these two issues involved in any soil–structure interaction (SSI) analysis [5].

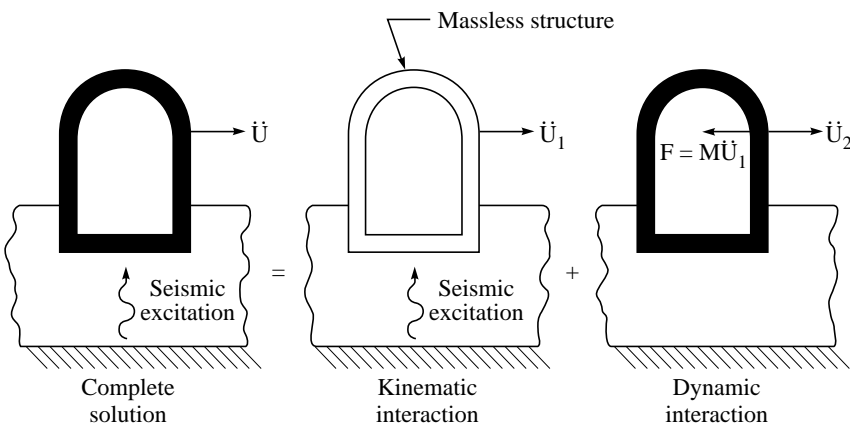


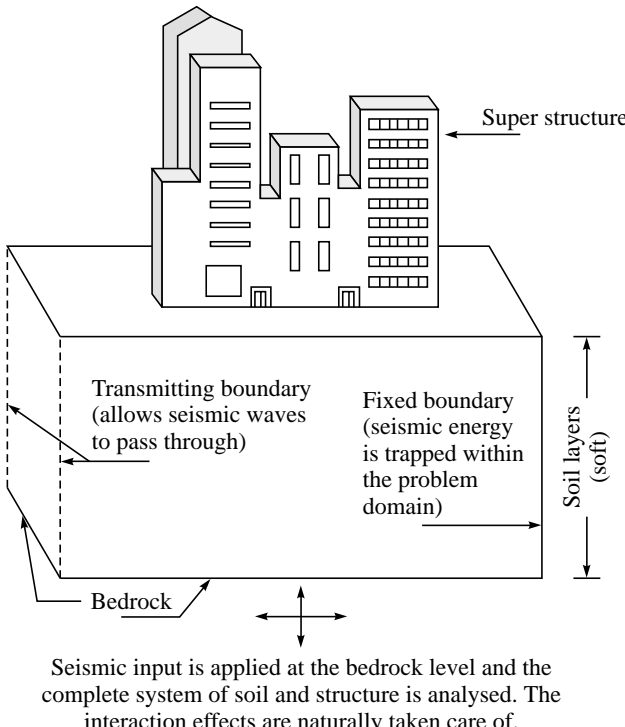
FIGURE 11.8 Soil-structure interaction analysis.

11.9.1 Dynamic Analysis including SSI Effects

Two different approaches have been adopted in the past to investigate the problem of soil-structure interaction and incorporate the effect of soil compliance in the dynamic analysis: (i) the direct approach, and (ii) the substructure approach.

The direct approach

It is based on including the soil medium in the mathematical model developed for dynamic analysis. This is typically done by using finite element discretisation of the domain with appropriate *absorbing/transmitting* boundaries. These special boundary elements are necessary to simulate the effect of unbounded soil medium which requires that the seismic energy should radiate away from the vibration source. The use of absorbing/transmitting boundaries prevent the seismic energy being reflected back into the problem domain. The essential features of this approach can be understood from Figure 11.9. Although the method is quite simple in concept, its implementation for analysis of practical problems presents a formidable computational task. The requirement of including the soil strata in the mathematical model for dynamic analysis leads to a very large system of equations to be solved. Further, the development of absorbing/transmitting boundaries is based on the assumption of the presence of soil layer that is bounded by a rocky strata at the base. The computed results could be erroneous if the site has deep soil deposits and the bottom boundary of the finite element model is placed at a shallow depth instead of the bedrock level. Further, the lower modes of the complete soil-structural system will be dominated by soil deformation modes with the superstructure riding on top of soil mass as a rigid body owing to the more flexible nature of soil in comparison with the structural system. Since the deformations and stresses in structural system are of primary interest for the purpose of design, huge computational effort and storage is required to compute and store the eigen-pairs required for inclusion of all modes, ensuring more that the cumulative effective modal mass is more than 90% of the total vibrating mass. A common numerical trick to force the lower modes of the combined soil-structure system to correspond to the deformations in structural system,



Seismic input is applied at the bedrock level and the complete system of soil and structure is analysed. The interaction effects are naturally taken care of.

FIGURE 11.9 Modelling for analysis of soil–structure interaction effect by direct method.

is to consider the soil medium to be massless. This forces the modes for soil deformation to move to the higher end of the eigen spectrum, thereby providing structural modes at the lower end of the eigen spectrum.

The substructure approach

In the substructure approach the SSI problem is divided into three distinct parts as shown in Figure 11.10, which also demonstrates the basic concept of substructure method of soil–structure interaction analysis [5]. The three-step solution for SSI problems consists of:

- (i) determination of foundation input motion by solving the kinematic interaction problem,
- (ii) determination of the frequency dependent impedance functions describing the stiffness and damping characteristics of the soil-foundation interacting system. This step should account for the geometric and material properties of foundation and soil deposits and is generally computed using equivalent linear elastic properties for soil appropriate for the in-situ dynamic shear strains. This step yields the so-called *soil springs*.
- (iii) computation of response of the real structure supported on frequency dependent soil springs and subjected at the base of these springs to the foundation input motion computed in (i).

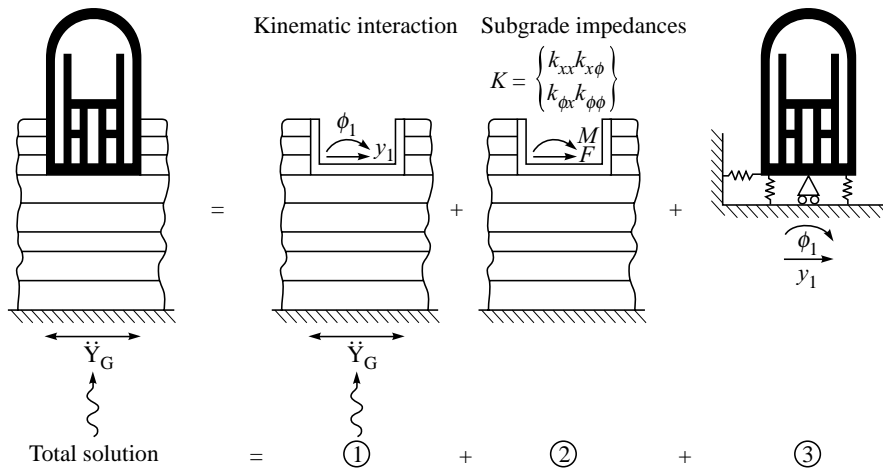


FIGURE 11.10 Soil-structure interaction analysis by substructure method.

It should be noted that if the structural foundations were perfectly rigid, the solution by substructure approach would be identical to the solution by the direct method. Further, the superposition principle is valid for linear systems only. Since the shear modulus and damping properties of soil are strain dependent, the use of the principle of superposition can be questioned. However, it has been observed that most of the nonlinearity in soil behaviour occurs as a result of the earthquake motion, and not as a result of soil-structure interaction itself. Therefore, the soil properties estimated for the same strain levels as expected during a postulated design earthquake may be used in the steps (i) and (ii) without any further modification. Reasonable approximations can be obtained on the basis of one-dimensional wave propagation theory for the solution of step (i), and by using some correction factors for modifying the springs for a surface footing on a layered soil deposits to account for the embedment of foundation as a solution to step (ii) of the problem. Several investigators have provided expressions/curves/charts for the impedance functions for different parameters of the soil-foundation systems. A concise summary of available impedance functions and approximate analytical expressions has been presented by Pais and Kausel [6].

Generally, the foundation input motion is assumed to be the same as free-field motion, i.e. the effects of kinematic interaction are neglected in SSI analysis for most of the common constructions. Kinematic interaction should invariably be considered if the structure and foundations to be constructed are very massive, rigid, and very large. Figure 11.11 shows a simplified model normally used in the analysis of inertial interaction effects. The model consists of a single degree of freedom structure of height h , mass m , stiffness k , and viscous damping coefficient c . The base of the structure is free to translate relative to the ground u_f and also to rotate by amount θ . The impedance functions are represented by the linear and rotational soil springs with complex stiffnesses \bar{k}_u and \bar{k}_θ , respectively. The damping of soil deposits is

contained in the imaginary component of the impedance functions. The simple system shown in Figure 11.11 can be assumed to represent the response of a multi-storeied building which is dominated by the first mode response and the height parameter h is interpreted as the distance from base of the centroid of the inertial force distribution for the first mode [8]. The dynamic stiffness coefficients for a rigid circular disk resting on halfspace can be given as,

$$K^d = K^s(k + ia_0c)$$

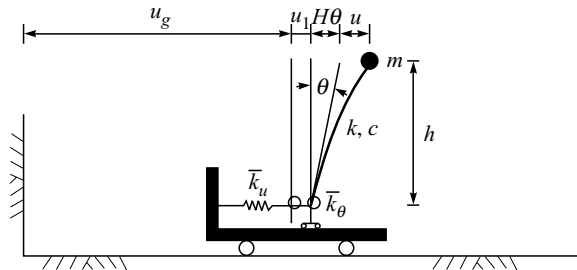


FIGURE 11.11 A simplified model for the analysis of inertial interaction [after (8)].

where, K^d represents the dynamic stiffness (impedance), K^s denotes the appropriate static stiffness, a_0 is a dimensionless measure of frequency defined as $a_0 = \omega R/V_s$, ω is the angular frequency in rad/s, R is the radius of foundation, V_s is the shear wave velocity, and v is Poisson's ratio for soil, k and c are functions of a_0 , v and E/R the embedment ratio. The static stiffness of a rigid circular foundation on a homogeneous half-space are given in Table 11.3. The dynamic stiffnesses for rigid circular cylindrical foundations for different modes of deformation are given in Tables 11.4 and 11.5.

TABLE 11.3 Static stiffness coefficients for rigid, circular cylindrical foundation

Mode	Without embedment	With embedment
Vertical	$K_V^0 = \frac{4GR}{1-v}$	$K_V^s = K_V^0 (1 + 0.54E/R)$
Horizontal	$K_H^0 = \frac{8GR}{2-v}$	$K_H^s = K_H^0 (1 + E/R)$
Rocking	$K_R^0 = \frac{8GR^3}{3(1-v)}$	$K_R^s = K_R^0 (1 + 2.3E/R + 0.58(E/R)^3)$
Torsion	$K_t^0 = \frac{16GR^3}{3}$	$K_t^s = K_t^0 (1 + 2.67E/R)$
Coupling		$K_{RH}^s = (0.4E/R - 0.03)K_H^s$

R = radius of foundation, G = shear modulus, and v = Poisson's ratio of homogeneous half-space, E/R = embedment ratio (E being the depth of foundation).

TABLE 11.4 Dynamic stiffness for rigid, circular cylindrical foundation: vertical and torsion

<i>Vertical</i>	<i>Torsion</i>
$K_V^d = K_V^s (k + ia_0 c)$	$K_t^d = K_t^s (k + ia_0 c)$
$k = 1.0$	$k = 1.0 - \frac{0.35a_0^2}{1.0 + a_0^2}$
$c = \frac{\pi(\alpha + 2.0E/R)}{K_V^s/(GR)}$	$c = \frac{\frac{\pi}{2}(1+4.0E/R) \frac{a_0^2}{b+a_0^2}}{K_t^s/(GR^3)}$
$\alpha = V_p/V_s$	$b = \frac{1}{0.37 + 0.87(E/R)^{2/3}}$

V_p = Velocity of primary (longitudinal) waves in the soil, V_s = velocity of shear waves in the soil

TABLE 11.5 Dynamic stiffness for rigid, circular cylindrical foundation: horizontal and rocking

<i>Horizontal</i>	<i>Rocking</i>
$K_H^d = K_H^s (k + ia_0 c)$	$K_R^d = K_R^s (k + ia_0 c)$
$k = 1.0$	$k = 1.0 - \frac{0.35a_0^2}{1.0 + a_0^2}$
$c = \frac{\pi[1.0 + (1.0 + \alpha)E/R]}{K_H^s/(GR)}$	$c = \frac{\pi \left[\frac{\alpha}{4} + E/R + \left(\frac{1+\alpha}{2} \right) \frac{2}{3} \left(\frac{E}{R} \right)^3 \right] \frac{a_0^2}{b+a_0^2} + 0.84(1+\alpha) \left(\frac{E}{R} \right)^{2.5} \frac{b}{b+a_0^2}}{K_R^s/(GR^3)}$
$\alpha = V_p/V_s$	$b = \frac{2}{1.0 + E/R}$

V_p = Velocity of primary (longitudinal) waves in the soil, V_s = velocity of shear waves in soil, and $K_{RH}^d = K_H^d (0.4E/R - 0.03)$.

It was demonstrated by Velestos and Meek [9] that the seismic response of the system shown in Figure 11.11 can be accurately predicted by an equivalent single degree of freedom oscillator with period \tilde{T} and damping $\tilde{\zeta}$ which represent modifications to the first mode period and damping of structural system to account for the effect of compliant soil. These parameters are known as the *flexible base* parameters as they represent the properties of an oscillator which is free to translate and rotate at its base. The flexible base period can be given as,

$$\frac{\tilde{T}}{T} = \sqrt{1 + \frac{k_1}{K_H^d} + \frac{k_1 h^2}{K_R^d}} \quad (11.57)$$

where T is the period of the (fixed-base) structure in its first mode, and k_1 represents the modal stiffness for the first mode of (fixed-base) structure. The equivalent viscous damping ratio can be defined in terms of the viscous damping of the structure and the radiation and hysteretic damping of the soil–foundation system. The flexible base damping can be given as [10],

$$\tilde{\zeta} = \tilde{\zeta}_0 + \frac{\zeta}{(\tilde{T}/T)^3} \quad (11.58)$$

where $\tilde{\zeta}_0$ represents the damping contributions (radiation and hysteretic) from the soil–foundation system. A closed form expression for $\tilde{\zeta}_0$ can be found in the article by Velestos and Nair [10]. It can be inferred from Equations (11.57) and (11.58) that the primary effect of inertial interaction is the lengthening of natural period and increase in the damping ratio of the dynamical system.

SUMMARY

Different issues in the study of dynamics of a complex system are described in this chapter. Starting from the basic formulation and terminology of the problem, through the discussion of free vibration, forced vibration, the concept of tuned-mass dampers, response spectrum method of seismic analysis, multi-support excitation, to the discussion and analytical modeling of the dynamic soil-structure interaction effects, a wide range of topics are covered. This will help demystify the seismic design codes and promote a better understanding and correct implementation of their commendations of seismic design codes of practice.

REFERENCES

- [1] Clough, R.W. and Penzien J., *Dynamics of Structures*, 2nd ed., McGraw-Hill, New York, 1993.
- [2] Learning from Earthquakes Series Volume IV. “The 1999 Turkey Earthquakes: Bridge Performance and Remedial Actions”, Earthquake Engineering Research Institute, USA 2003.
- [3] Meirovitch, L., *Analytical Methods in Vibrations*, The Macmillan Company, New York, 1967.
- [4] Meirovitch, L., *Computation Methods in Structural Dynamics*, Sijthoff and Noordhoff, Alphen aan den Rijn, The Netherlands, 1980.
- [5] Kausel, E., Whitman, R.V., Morray, J.P., and Elsabee F., “The Spring Method for Embedded Foundations”, *Nuclear Engineering and Design*, 48: 377–392, 1978.
- [6] Pais, A. and Kausel, E., “Approximate Formulas for Dynamic Stiffnesses of Rigid Foundations”, *Soil Dynamics and Earthquake Engineering*, 7: 213–226, 1998.
- [7] Shrikhande, M. and Gupta, V.K., “Synthesizing Ensembles of Spatially Correlated Accelerograms”, *Journal of Engineering Mechanics*, ASCE, 124: 1185–1192, 1998.

- [8] Stewart, J.P., Seed, R.B. and Fenves, G.L., "Empirical Evaluation of Inertial Soil Structure, Interaction and Effects", *Technical Report No. PEER 1998/07*, Pacific Earthquake Engineering Research Centre, University of California, Berkeley.
- [9] Velestos, A.S. and Meek, J.W., "Dynamic Behaviour of Building Foundation Systems", *Earthquake Engineering and Structural Dynamics*, 3: 121–138, 1974.
- [10] Velestos, A.S. and Nair, V.V., "Seismic Interaction of Structures on Hysteretic Foundations", *Journal of Structural Engineering*, ASCE, 101: 109–129, 1975.

PART III

Concepts of Earthquake Resistant Design of Reinforced Concrete Building

Chapter 12

Earthquake and Vibration Effect on Structures: Basic Elements of Earthquake Resistant Design

12.1 INTRODUCTION

Structures on the earth are generally subjected to two types of load: *Static and Dynamic*. Static loads are constant with time while dynamic loads are time-varying. These loads can further be subdivided as shown in Figure 12.1. In general, the majority of Civil Engineering structures are designed with the assumption that all applied loads are static. The effect of dynamic load is not

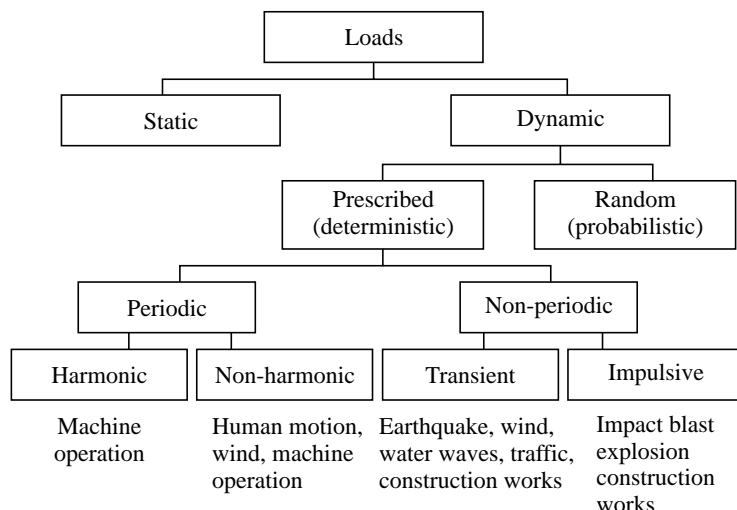


FIGURE 12.1 Various types of static-dynamic loads (Syrmakwzis and Sophocleous, 2001).

considered because the structure is rarely subjected to dynamic loads; more so, its consideration in analysis makes the solution more complicated and time consuming. This feature of neglecting the dynamic forces may sometimes become the cause of disaster, particularly, in case of earthquake. The recent example of this category is Bhuj earthquake of January 26, 2001. Nowadays, there is a growing interest in the process of designing Civil Engineering structures capable to withstand dynamic loads, particularly, earthquake-induced load. The present chapter describes the effect of earthquake load, which is one of the most important dynamic loads alongwith its consideration during the analysis, and design of the structure.

12.2 STATIC AND DYNAMIC EQUILIBRIUM

The basic equation of static equilibrium under displacement method of analysis is given by,

$$F(\text{ext}) = ky \quad (12.1)$$

where, $F(\text{ext})$ is the external applied static force, k is the stiffness resistance, and y is the resulting displacement. The restoring force (ky) resists the applied force, $F(\text{ext})$.

Now, if the applied static force changes to dynamic force or time varying force the equation of static equilibrium becomes one of the dynamic equilibrium and has the form

$$F(t) = m\ddot{y} + c\dot{y} + ky \quad (12.2)$$

If we do a direct comparison of Equations 12.1 and 12.2, we shall find the two additional forces that resist the applied forces with the restoring forces. These additional forces are called *inertia force* ($m\ddot{y}$) and *damping force* ($c\dot{y}$) resulting from the induced acceleration and velocities in the structure. The appearance of inertia and damping forces in the structure during a dynamic loading is the most characteristic distinction between static loading and dynamic loading effects.

The dynamic force may be an earthquake force resulting from rapid movement along the plane of faults within the earth crust. This sudden movement of faults releases great energy in the form of seismic waves, which are transmitted to the structure through their foundations, and causes motion in the structure. These motions are complex in nature and induce abrupt horizontal and vertical oscillations in structures, which result accelerations, velocities and displacement in the structure. The induced accelerations generate *inertial forces* in the structure, which are proportional to acceleration of the mass and acting opposite to the ground motion (Figure 12.2).

The energy produced in the structure by the ground motion is dissipated through internal friction within the structural and non-structural members. This dissipation of energy is called *damping*. The structures always possess some intrinsic damping, which diminishes with time once the seismic excitation stops. These dissipative or damping forces are represented by viscous damping forces, which are proportional to the velocity induced in the structure. The constant of proportionality is called as linear *viscous damping*.

The restoring force in the structures is proportional to the deformation induced in the structure during the seismic excitation. The constant of proportionality is referred as *stiffness* of structure. Stiffness greatly affects the structure's uptake of earthquake-generated forces. On the basis of stiffness, the structure may be classified as brittle or ductile. Brittle structure having

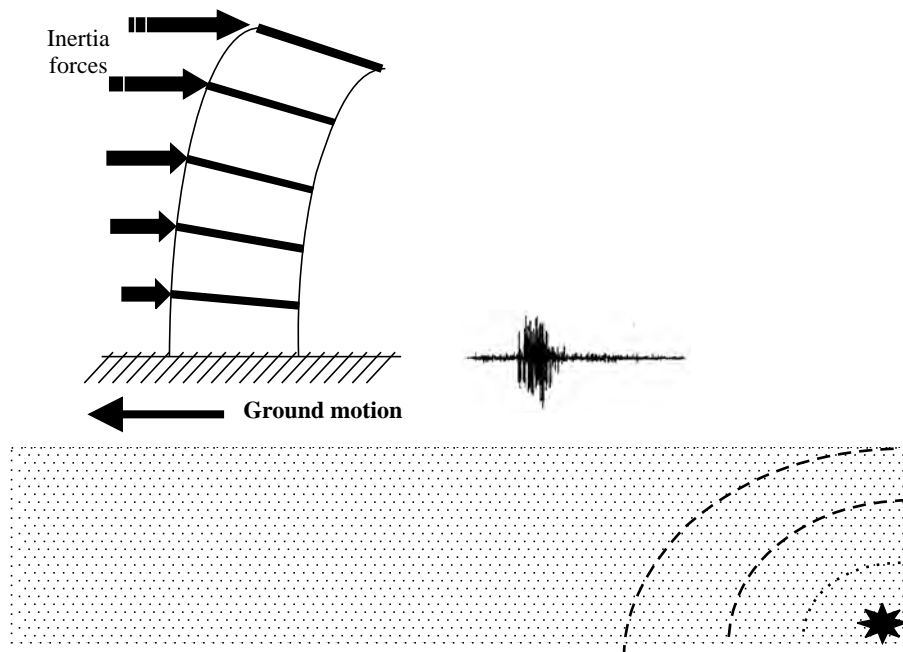


FIGURE 12.2 Structure subjected to earthquake excitation (Syrmakwzis and Sophocleous, 2001).

greater stiffness proves to be less durable during earthquake while ductile structure performs well in earthquakes. This behaviour of structure evokes an additional desirable characteristic called *ductility*. Ductility is the ability of the structure to undergo distortion or deformation without damage or failure.

Therefore, the equation of dynamic equilibrium for earthquake force has the form in which, inertia, damping and restoring forces balance the applied force,

$$F(t) = m\ddot{y}(t) + c\dot{y}(t) + k(t) y(t) \quad (12.3)$$

Where, $m\ddot{y}(t)$ is the inertia forces acting in a direction opposite to that of the seismic motion applied to the base of structure, whose magnitude is the mass of the structure times its acceleration, m is the mass (kg) and $\ddot{y}(t)$ the acceleration (m/sec^2). Inertia forces are the most significant which depend upon the characteristics of the ground motion and the structural characteristics of structure. The basic characteristic of the structure and ground is its *fundamental or natural period*. The fundamental periods of structures may range from 0.05 second for a well-anchored piece of equipments, 0.1 second for a one-storey frame, 0.5 second for a low structure up to about 4 stories, and between 1–2 seconds for a tall building of 10–20 stories. Natural periods of ground are usually in the range of 0.5–2 seconds, so that it is possible for the building and the ground to have the same fundamental period and, therefore, there is a high probability for the structure to approach a state of *partial resonance (quasi-resonance)*. Hence in developing a design strategy for a building, it is desirable to estimate the fundamental periods both of the structure and of the site so that a comparison can be made to see the existence of the probability of quasi-resonance.

$c\ddot{y}(t)$ is the damping force acting in a direction opposite to that of the seismic motion, c is the damping coefficient (N-sec/m) and $y(t)$ the velocity (m/sec). The value of damping in a structure depends on its components, component connections, materials etc. The amount of damping in structural system cannot be analytically ascertained, it must be determined experimentally. In practice this damping effect is expressed as a percentage of the critical damping which is the greatest damping value that allows vibratory movement to develop. Experience has made it possible to estimate the degree of damping in various types of structures, and some of common types of structures are reinforced concrete 5–10%, metal frame 1–5%, masonry 8–15%, Wood structures 15–20%.

$k(t)y(t)$ is the restoring force $k(t)$ is the stiffness (N/m) or resistance is a function of the yield condition in the structure, which in turn is a function of time. The stiffness parameter k is a potential source of discrepancy, and is affected by quality of material, age, cracking, support condition etc. $y(t)$ is the displacement (m).

$F(t)$ is the externally applied force (N). The forcing function is often difficult to estimate accurately, particularly in the case of earthquake.

The Equation (12.3) is a second order differential equation that needs to be solved for the displacement $y(t)$. The number of displacement components required for specifying the position of mass points is called the number of *degrees-of-freedom* required to obtain an adequate solution. This depends upon the complexity of the structural system. For some structures a *single degree-of-freedom* may be sufficient, whereas, for others several hundred degrees of freedom may be required (Anderson, 2001). Depending upon the degree of freedom, a number of *structural models* can be proposed for analyzing the structure. A structure can be analyzed by different models depending upon the objective of the particular analysis.

12.3 STRUCTURAL MODELLING

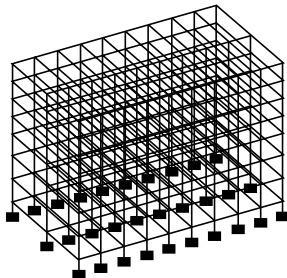
Earthquake response analysis is an art to simulate the behaviour of a structure subjected to an earthquake ground motion based on dynamics and a *mathematical model* of the structure. The correct analysis will depend upon the proper modelling of the behaviour of materials, elements, connection and structure. Models may be classified mainly by essential difference in the degree-of-freedom. The model, or the number of degree of freedom, should be selected carefully considering the objective of the analysis. Sometimes sophistication or complicated models are not only useless but also create misunderstanding to interpret the results in practical problems. Therefore, it is important to select an appropriate and simple model to match the purpose of the analysis. Analytical models should also be based on physical observations and its behaviour under dynamic load. Different types of structural model are described as below to simulate the behaviour of a frame building (Kadeysawa, 2001; Gioncu and Mazzolani, 2002).

12.3.1 Structural Models for Frame Building

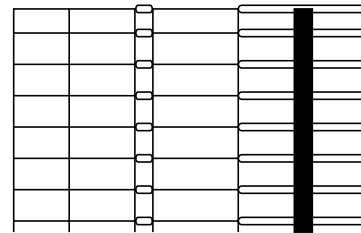
A *three-dimensional model* has independent displacements at each node and can simulate any type of behaviour. Because of the difficulties in modelling, verification and numerical calculation, the three-dimensional model has not yet been used even in the most sophisticated

design practices. Figure 12.3(a) shows three-dimensional frame model which is especially useful to simulate the responses of three-dimensional effects such as

- (i) buildings with irregular geometric configuration,
- (ii) torsional response in the structures with eccentric distributions of stiffness or mass, and
- (iii) earthquake motion in two directions or in skewed direction etc.



(a) Three-dimensional frame model



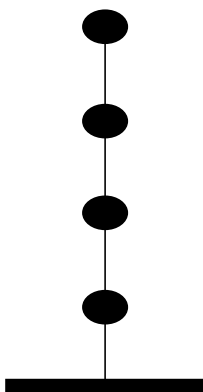
(b) Two-dimensional frame model

FIGURE 12.3 Three-dimensional and two-dimensional structural models.

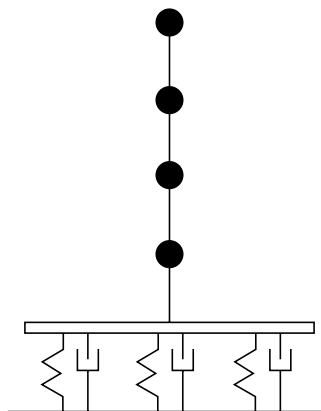
A *two-dimensional plane frame model* shown in Fig 12.3(b) has been used for buildings having symmetric plan and torsional responses are expected to be small. The model connects all the plane frames in one principal direction by assuming the identical horizontal displacement in a floor. In two-dimensional plane frame modelling the number of degree of freedom can be reduced about one-fourth compared to the three-dimensional model.

A *lumped mass model* is simple as shown in Fig. 12.4(a) and most frequently used in early times for practical design of multi-storey buildings. It reduced the substantial amount of calculation and storage in comparison to two-dimensional frame model.

The *soil–structure interaction model* as shown in Fig. 12.4(b) takes into account the possibility of having different horizontal and vertical motions of supports, modification of the natural period of structure due to interaction with the soil, changing of the base motion in



(a) Lumped mass model



(b) Soil–structure interaction models

FIGURE 12.4 Lumped mass model with soil-structure interaction effect.

comparison to the motions in free field, increasing the effective damping due to difference between the tendency of regular structure motions and the chaotic motion of soil.

12.4 SEISMIC METHODS OF ANALYSIS

Once the structural model has been selected, it is possible to perform analysis to determine the seismically induced forces in the structures. There are different methods of analysis which provide different degrees of accuracy. The analysis process can be categorized on the basis of three factors: the type of the externally applied loads, the behaviour of structure/or structural materials, and the type of structural model selected (Figure 12.5). Based on the type of external action and behaviour of structure, the analysis can be further classified as linear static analysis, linear dynamic analysis, nonlinear static analysis, or non-linear dynamic analysis (Beskos and Anagnostoulos, 1997).

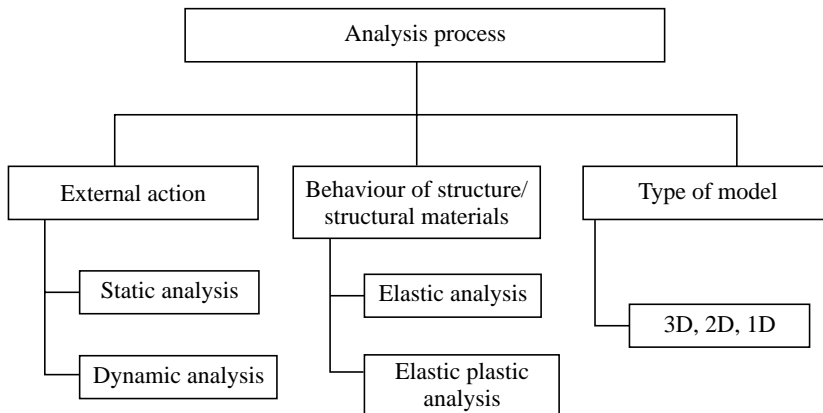


FIGURE 12.5 Method of analysis process (Syrmakezis, 1996).

Linear static analysis or equivalent static analysis can only be used for regular structure with limited height. *Linear dynamic analysis* can be performed in two ways either by *mode superposition method* or *response spectrum method* and *elastic time history method*. This analysis will produce the effect of the higher modes of vibration and the actual distribution of forces in the elastic range in a better way. They represent an improvement over linear static analysis. The significant difference between linear static and dynamic analysis is the level of force and their distribution along the height of the structure. *Non-linear static analysis* is an improvement over the linear static or dynamic analysis in the sense that it allows the inelastic behaviour of the structure. The methods still assume a set of static incremental lateral load over the height of structure. The method is relatively simple to be implemented, and provides information on the strength, deformation and ductility of the structure and the distribution of demands. This permits to identify critical members likely to reach limit states during the earthquake, for which attention should be given during the design and detailing process. But this method contains many

limited assumptions, which neglect the variation of loading patterns, the influence of higher modes, and the effect of resonance. This method, under the name of *push over analysis* has acquired a great deal of popularity nowadays and in spite of these deficiencies this method provides reasonable estimation of the global deformation capacity, especially for structures which primarily respond according to the first mode. A *non-linear dynamic analysis* or *inelastic time history analysis* is the only method to describe the actual behaviour of the structure during an earthquake. The method is based on the direct numerical integration of the motion differential equations by considering the elasto-plastic deformation of the structure element. This method captures the effect of amplification due to resonance, the variation of displacements at diverse levels of a frame, an increase of motion duration and a tendency of regularization of movements result as far as the level increases from bottom to top.

12.4.1 Code-based Procedure for Seismic Analysis

Main features of seismic method of analysis (Riddell and Llera, 1996) based on Indian Standard 1893 (Part 1): 2002 are described as follows:

Equivalent lateral force

Seismic analysis of most of the structures are still carried out on the basis of lateral (horizontal) force assumed to be equivalent to the actual (dynamic) loading. The base shear which is the total horizontal force on the structure is calculated on the basis of structure mass and fundamental period of vibration and corresponding mode shape. The base shear is distributed along the height of structures in terms of lateral forces according to Code formula. This method is usually conservative for low to medium height buildings with a regular conformation.

Response spectrum analysis

This method is applicable for those structures where modes other than the fundamental one affect significantly the response of the structure. In this method the response of Multi-Degree-of-Freedom (MDOF) system is expressed as the superposition of modal response, each modal response being determined from the spectral analysis of single-degree-of-freedom (SDOF) system, which are then combined to compute the total response. Modal analysis leads to the response history of the structure to a specified ground motion; however, the method is usually used in conjunction with a response spectrum.

Elastic time history analysis

A linear time history analysis overcomes all the disadvantages of modal response spectrum analysis, provided non-linear behaviour is not involved. This method requires greater computational efforts for calculating the response at discrete times. One interesting advantage of such procedure is that the relative signs of response quantities are preserved in the response histories. This is important when interaction effects are considered in design among stress resultants.

12.5 SEISMIC DESIGN METHODS

Conventional Civil engineering structures are designed on the basis of two main criteria that are *strength* and *rigidity*. The strength is related to damageability or ultimate limit state, assuring that the force level developed in structures remains in the elastic range, or some limited plastic deformation. The rigidity is related to serviceability limit state, for which the structural displacements must remain in some limits. This assures that no damage occurs in non-structural elements. In case of earthquake resistant design, a new demand must be added to the above-mentioned ones, that is the ductility demand. *Ductility* is an essential attribute of a structure that must respond to strong ground motions. Ductility serves as the shock absorber in a building, for it reduces the transmitted force to one that is sustainable. The resultant sustainable force has traditionally been used to design a hypothetically elastic representation of the building. Therefore, the survivability of a structure under strong seismic actions relies on the capacity to deform beyond the elastic range, and to dissipate seismic energy through plastic deformations. So, the ductility check is related to the control of whether the structure is able to dissipate the given quantity of seismic energy considered in structural analysis or not. Based on three criteria rigidity (serviceability), strength (damageability) and ductility (survivability), the methods of seismic design are described in Figure 12.6 as follows.

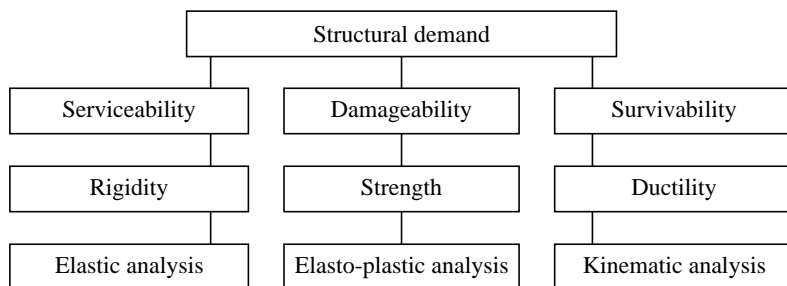


FIGURE 12.6 Design criteria for three performance levels (Gioncu and Mazzolani, 2002).

12.5.1 Code-based Methods for Seismic Design

Lateral strength-based design

This is the most common seismic design approach used today and the IS: 13920: 1993 code is based on this approach. It is based on providing the structure with the minimum lateral strength to resist seismic loads, assuming that the structure will behave adequately in the non-linear range. For this reason only some simple constructional detail rules are to be satisfied—as material ductility, member slenderness, cross-sectional clauses, etc.

Displacement or ductility-based design

It is very well recognized now that because of economic reasons the structure is not designed to have sufficient strength to remain elastic in severe earthquakes. The structure is designed to possess adequate ductility so that it can dissipate energy by yielding and survive the shock. This

method operates directly with deformation quantities and therefore gives better insight on expected performance of structures, rather than simply providing strength in the above-mentioned lateral strength design approach. The ductility-based design has been adopted by the seismic codes of many countries.

Capacity-based design

It is a design approach in which the structures are designed in such a way that hinges can only form in predetermined positions and sequences. It is a procedure of the design process in which strengths and ductilities are allocated and the analysis are interdependent. The capacity design procedure stipulates the margin of strength that is necessary for elements to ensure that their behaviour remains elastic. The reason to name the capacity design is that, in the yielding condition, the strength developed in weaker member is related to the capacity of the stronger member.

Energy-based design

One of the promising approaches for earthquake resistant design in future is energy approach. In this approach, it is recognized that the total energy input, E_I can be resisted by the sum of the kinetic energy E_K , the elastic strain energy E_{ES} , energy dissipated through plastic deformations (hysteretic damping) E_H , and the equivalent viscous damping E_ζ .

The energy equation for a single mass vibrating system is the energy balance between total input energy and the energies dissipated by viscous damping and inelastic deformations and can be written as,

$$E_I = E_K + E_{ES} + E_H + E_\zeta$$

12.6 RESPONSE CONTROL CONCEPTS

Structural response control for seismic loads is a rapidly expanding field of control systems, also known as *earthquake protection system*. The aim of this system is the modification of the dynamic interaction between structure and earthquake ground motion, in order to minimize the structure damage and to control the structural response. The family of earthquake protective systems has grown to include passive, active and hybrid (semi-active) systems as shown in Figure 12.7. The control is based on two different approaches, either the modification of the dynamic characteristics or the modification of the energy absorption capacity of the structure. In the first case, the structural period is shifted away from the predominant periods of the seismic input, thus avoiding the risk of resonance occurrence. It is clear here that the isolation is effective only for a limited range of frequencies of structures (Figure 12.8). The acceleration responses in the structure for some earthquakes can be reduced at the same time; for the other type of earthquake the responses have proved to be much worse. Thus the effectiveness of isolation depends upon the effectiveness of knowing in advance the kind of frequency content that the earthquake will have. In the second case, the capacity of the structure to absorb energy is enhanced through appropriate devices, which reduces damage to the structure. Both the approaches are used in the earthquake protection system. Brief discussions of earthquake protection system are as follows:

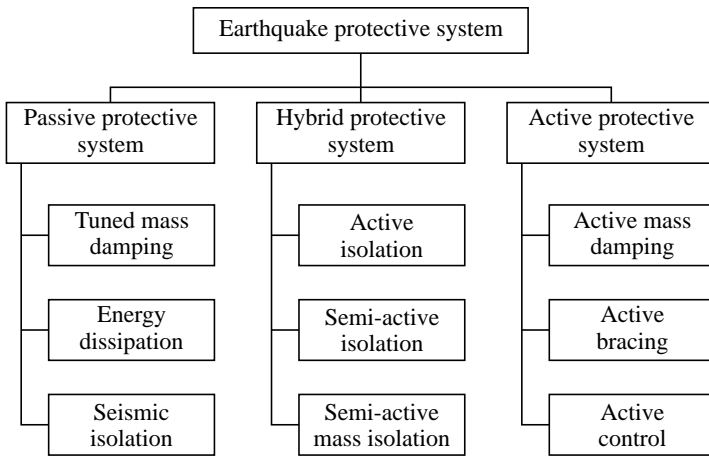


FIGURE 12.7 Family of earthquake protective system (Buckle, 2000).

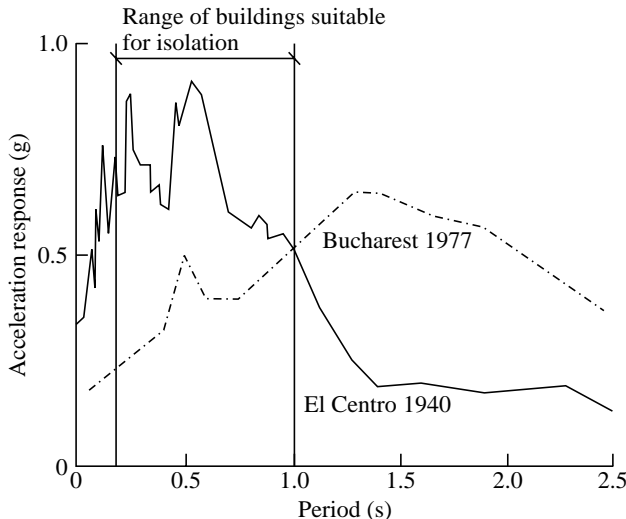


FIGURE 12.8 Earthquake response spectra and isolation (Key, 1988).

12.6.1 Earthquake Protective Systems

Passive control systems

Passive control system includes tuned mass dampers, seismic (base) isolation systems, mechanical dissipaters, and the like. These systems have significant application to buildings, bridges, and industrial plants. Seismic base isolation is the most developed system at the present time. The basic concept of seismic isolation (Williams, 2003) is to reduce the response to earthquake motion by (i) reducing the stiffness, (ii) increasing the natural period of system, and (iii) provision of increased damping to increase the energy dissipation in the system. The principle of seismic base isolation is based on decoupling of structure by introducing low

horizontal stiffness bearing between the structure and foundation. The isolation bearing decreases the frequency of overall building-isolation system to about 0.5 Hz. This low frequency system does not permit transmission of high frequency of earthquake motion to the structure (Figure 12.9).

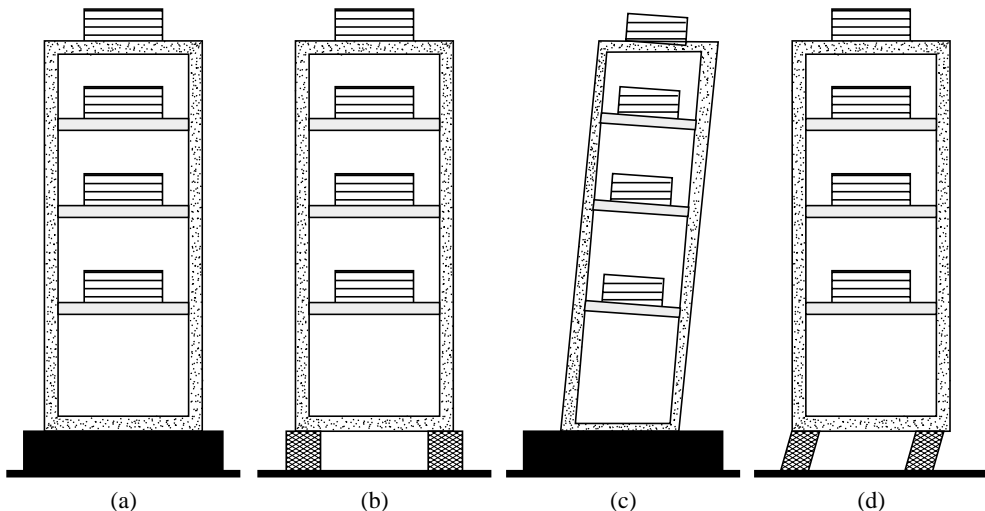


FIGURE 12.9 Base isolation concepts (a) Fixed base building, (b) Base isolated building, (c) Response of fixed base building under earthquake excitation, (d) Response of base isolated building under earthquake excitation.

Active protective systems

In these systems mechanical devices are incorporated into the building, which actively participate in the dynamic behaviour of the building in response to the measurements of its behaviour during the earthquake ground motion. Thus, in these systems, the structure's characteristics are modified according to seismic input to the building. The goals of active systems are to keep forces, displacements and accelerations of structure below specific bounds, in order to reduce the damage in case of a strong earthquake.

Hybrid (semi-active) protective systems

Hybrid systems are systems implying the combined use of passive and active control systems. For example, a base isolated structure is equipped with actuators, which actively control the enhancement of its performance (Gioncu and Mazzolani, 2002).

12.7 SEISMIC EVALUATION AND RETROFITTING

Many of the existing buildings are lacking in adequate earthquake resistance because these are not designed according to modern codes and prevalent earthquake resistant design practice. Also many buildings that are damaged in earthquakes may need not only be repaired but also

upgraded of their strength in order to make them seismically resistant. The seismic evaluation and their retrofitting is one of the most challenging tasks for the structural engineers. The aim of *seismic evaluation* is to assess the possible seismic response of buildings, which may be seismically deficient or earthquake damaged, for its possible future use. The evaluation is also helpful for adopting the retrofitting of structure. The means of *retrofitting* is to upgrade the strength and structural capacity of an existing structure to enable it to safely withstand the effect of strong earthquakes in future. Retrofitting of existing buildings and related issues of their structural safety have not received adequate attention in India. There are at present no guidelines or codes of practice available in the country for retrofitting. The methods of seismic evaluation of existing buildings are not adequately developed. In developed countries research on seismic evaluation and retrofitting have been undertaken during the last two decades.

The methods available for seismic evaluation of existing buildings can be broadly divided into two categories: (i) qualitative methods, and (ii) analytical methods, as shown in Figure 12.10. The qualitative methods are based on the available background information of the structures, past performance of similar structures under severe earthquakes, visual inspection report, some non-destructive test results etc. However, analytical methods are based on considering the capacity and ductility of the buildings, which are based on detailed dynamic analysis of buildings. The methods in this category are capacity/demand method, pushover analysis, inelastic time history analysis etc. Brief discussions on the method of evaluation are as follows.

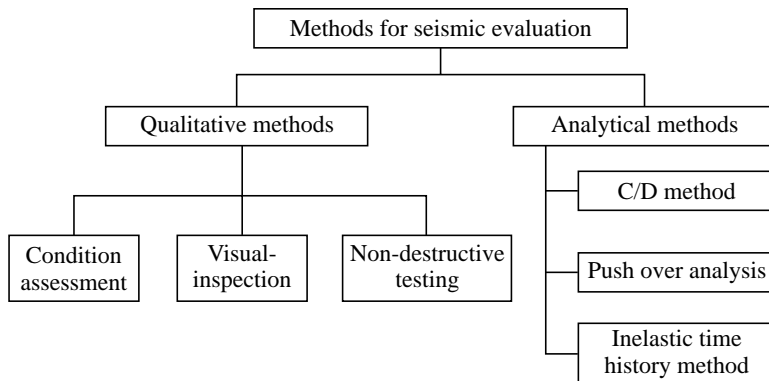


FIGURE 12.10 Methods for seismic evaluation.

12.7.1 Methods for Seismic Evaluation

Capacity/demand (C/D) method

The method has been initially presented by ATC (1983). The forces and displacements resulting from an elastic analysis for design earthquake are called demand. These are compared with the capacity of different members to resist these forces and displacements. A (C/D) ratio less than one indicates member failure and thus needs retrofitting. When the ductility is considered in the section the demand capacity ratio can be equated to section ductility demand of 2 or 3. The

C/D procedures have been subjected to more detailed examination in the light of recent advances in earthquake response studies. The main difficulty encountered in using this method is that there is no relationship between member and structure ductility factor because of non-linear behaviour.

Push Over analysis

The push over analysis of a structure is a static non-linear analysis under permanent vertical loads and gradually increasing lateral loads. The equivalent static lateral loads approximately represent earthquake-induced forces. A plot of total base shear versus top displacement in a structure is obtained by this analysis that would indicate any premature failure or weakness. The analysis is carried out upto failure, thus it enables determination of collapse load and ductility capacity. On a building frame, load/displacement is applied incrementally, the formation of plastic hinges, stiffness degradation, and plastic rotation is monitored, and lateral inelastic force versus displacement response for the complete structure is analytically computed. This type of analysis enables weakness in the structure to be identified. The decision to retrofit can be taken on the basis of such studies.

Inelastic time-history analysis

A seismically deficient building will be subjected to inelastic action during design earthquake motion. The inelastic time history analysis of the building under strong ground motion brings out the regions of weakness and ductility demand in the structure. This is the most rational method available for assessing building performance. There are computer programs available to perform this type of analysis. However there are complexities with regard to biaxial inelastic response of columns, modelling of joints behaviour, interaction of flexural and shear strength and modeling of degrading characteristics of member. The methodology is used to ascertain deficiency and post-elastic response under strong ground shaking.

12.7.2 Methods for Seismic Retrofitting

Retrofit technique employed for a structure can be categorized as (i) structural/global, and (ii) member/local. The techniques employed for seismic retrofitting are illustrated in Figure 12.11.

Structural or global retrofitting

Generally structural level retrofitting are applied when the entire structural lateral load resisting system is deemed to be deficient. Common approaches in this regard are employed to increase stiffness and strength with limited ductility.

Member or local retrofitting

Member or local retrofitting deals with an increase of the ductility of the components with adequate capacities to satisfy their specific limit states.

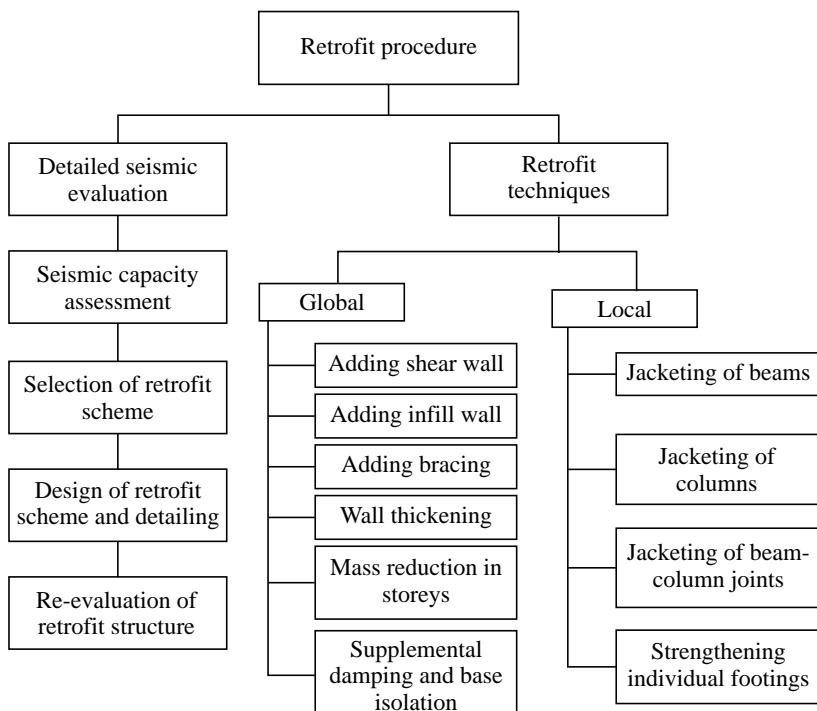


FIGURE 12.11 Methods for seismic retrofitting.

12.8 SEISMIC TEST METHODS

Earthquake-resistant design techniques for structures are often based on rational method of seismic analytical studies. In view of the complexity of the seismic response of structures, heterogeneous natures of construction as well as the strain dependent elastic properties do not allow full justification of the application of analytical methods. A sound quantitative basis on experimental studies may also be an alternative method of earthquake resistant design of structures. The last three decades have bestowed on us a great knowledge of earthquake engineering regarding experimental testing facility. Various offshoots of this technology have emerged and developed over the years while advances in servo-hydraulic technology and computer simulation are making actual shaking more feasible in earthquake engineering. Three types of experimental tests are commonly conducted to evaluate seismic performance of structures namely shaking table test, pseudo-dynamic test, and quasi-static test. Brief descriptions of all seismic test methods are described as follows.

12.8.1 Methods for Seismic Testing

Shaking table test

The shaking table test is the most realistic experimental method for determining dynamic response of the structure. In this the test structure is subjected to a load history which is usually

a ground motion recorded during an earthquake is simulated. A recent trend in shaking table systems is total six-degree of freedom motion ability. The capital equipment cost of shake table is a power function of specific weight and dimension, so only models of the real structures may be tested (Clark, 1990).

Pseudo-dynamic test

In the pseudo-dynamic test dynamic conditions are simulated. This testing is done with on-line computer simulation techniques. The load or deformation is applied quasi-statically at various positions of the test structure, depending on the restoring force directly measured during the test. The test structure is idealised into a discrete parameter system for which the equations of motion are written and integrated and the restoring forces for the system are applied at various floor levels.

Quasi-static test

The quasi-static test is not a dynamic test, in which the rate of application of the load is very low so that the material strain-rate effects do not influence the structural behaviour and inertia forces are not developed. The loading pattern and history must be carefully chosen to be general enough to provide the full range of deformations that the structure will experience under the earthquake excitation. This method adequately captures the important dynamic characteristics of the structure: hysteresis behaviour, energy dissipation capacity, stiffness degradation, ductility, hysteretic damping, the most distressed zones, and lateral strength and deformation capacity. This data is also utilized to make the hysteretic model of component for the dynamic analysis of structure

SUMMARY

The chapter deals with an introduction to the main attributes of earthquake resistant design of structures with a special emphasis on related additional features in comparison to civil engineering design. It introduces briefly the available methods of seismic analysis, seismic design, seismic response control, alongwith current techniques of seismic evaluation and retrofitting. The relevant experimental studies to earthquake engineering practice have also been underlined.

REFERENCES

- [1] Anderson, J.C., "Dynamic Response of Structures", *The Seismic Design Handbook*, 2nd ed., Farzad Naeim (Ed.), Kluwer Academic Publisher, The Netherlands, 2001.
- [2] Buckle, I.G., "Passive Control of Structures for Seismic Loads", *Twelfth World Conference on Earthquake Engineering*, New Zealand, 2000.
- [3] Beskos, D.E. and Anagnostoulos, S.A., *Advances in Earthquake Engineering—Computer Analysis and Design of Earthquake Resistant Structures: A Handbook*, Computational Mechanics Publications, Southampton, UK, 1997.

- [4] Clark, A. "Earthquake Testing Methods for Structures—Examples of Current Practice and Future Directions", *Earthquake Resistant Construction and Design*, Savidis (Ed.), Balkema, Rotterdam, 1990.
- [5] Gioncu, V. and Mazzolani, F.M., *Ductility of Seismic Resistant Steel Structures*, Spon Press, New York, 2002.
- [6] IS 1893, "Criteria for Earthquake Resistant Design of Buildings—Part 1", Bureau of Indian Standards, New Delhi, (2002).
- [7] Kabeyasawa Toshimi, "Earthquake Response Analysis", *Series on Innovation in Structures and Construction*: Vol. 3, Design of Modern High-rise Reinforced Concrete Structures, Hiroyuki Aoyama (Ed.), Imperial College Press, London, 2001.
- [8] Key David., *Earthquake Design Practice for Buildings*, Thomas Telford, London, 1988.
- [9] Riddell, R. and Llera, J.C.D.L., "Seismic Analysis and Design: Current Practice and Future Trends", *Eleventh World Conference on Earthquake Engineering*, Mexico, 1996.
- [10] Syrmakezis, C.A. and Sophocleous, A.A., "Earthquake and Vibration Effect", *Computational Modeling of Masonry, Brickwork and Brickwork Structures*, John W. Bull (Ed.), Saxe-Coburg Publication, Stirling, UK, pp. 1–21, 2001.
- [11] Syrmakezis, C.A., "Tentative Guidelines for Protection and Rehabilitations", *CISM Course on Protection of the Architectural Heritage against Earthquakes*, V. Petrini and M. Save (Eds.), Springer Wien, New York, 1996.
- [12] Williams, A., *Seismic Design of Buildings and Bridges*, Oxford University Press Oxford, New York, 2003.

Chapter 13

Identification of Seismic Damages in RC Buildings during Bhuj Earthquake

13.1 INTRODUCTION

A massive earthquake of magnitude ($M_L = 6.9$ on Richter scale, $M_b = 7.0$, $M_S = 7.6$ and $M_W = 7.7$) occurred on the morning of 51st Republic Day of India (January 26, 2001, Friday) at 08:46:42.9 hours (Indian standard time) as reported by Indian Meteorological Department (IMD), New Delhi. The epicentre of this earthquake was located near Bhachau (latitude 23.40°N and longitude 70.28°E), focal depth 25 km (Srivastav, 2001) with radius of fault area as 23 km. As per USGS NEIC the source parameters are latitude 23.41°N and longitude 70.23°E, $M_W = 7.7$ and focal depth 16 km.

The earthquake is subsequently referred to as Bhuj earthquake or Kutch earthquake. The earthquake ranks as one of the most destructive events recorded so far in India in terms of death toll, damage to infrastructure and devastation in the last fifty years. The major cities affected by the earthquake are Bhuj, Anjar, Bhachau, Gandhidham, Kandla Port, Morbi, Ahmedabad, Rajkot, Sundernagar etc., where majority of the casualties and damages occurred (Figure 13.1). Every earthquake leaves a trail of miseries by the of loss of life and destruction, but it also provides lessons to the human society particularly engineers, architects, builders and administrators for improving design and construction practices. Various types of structures reveal weakness in the form of design and planning practices, inadequate analysis, design deficiency and even poor quality of construction.

Reinforced concrete multi-storeyed buildings in India, for the first time, have been subjected to a strong ground motion shaking in Bhuj earthquake (January 26, 2001). It has been observed that the principal reasons of failure may be accounted to soft stories, floating columns, mass irregularities, poor quality of construction material and faulty construction practices, inconsistent earthquake response, soil and foundation effect and pounding of adjacent structures. This chapter presents description of types of construction, types of damage and causes of damage in selected multi-storeyed reinforced concrete buildings. The majority of the RC buildings

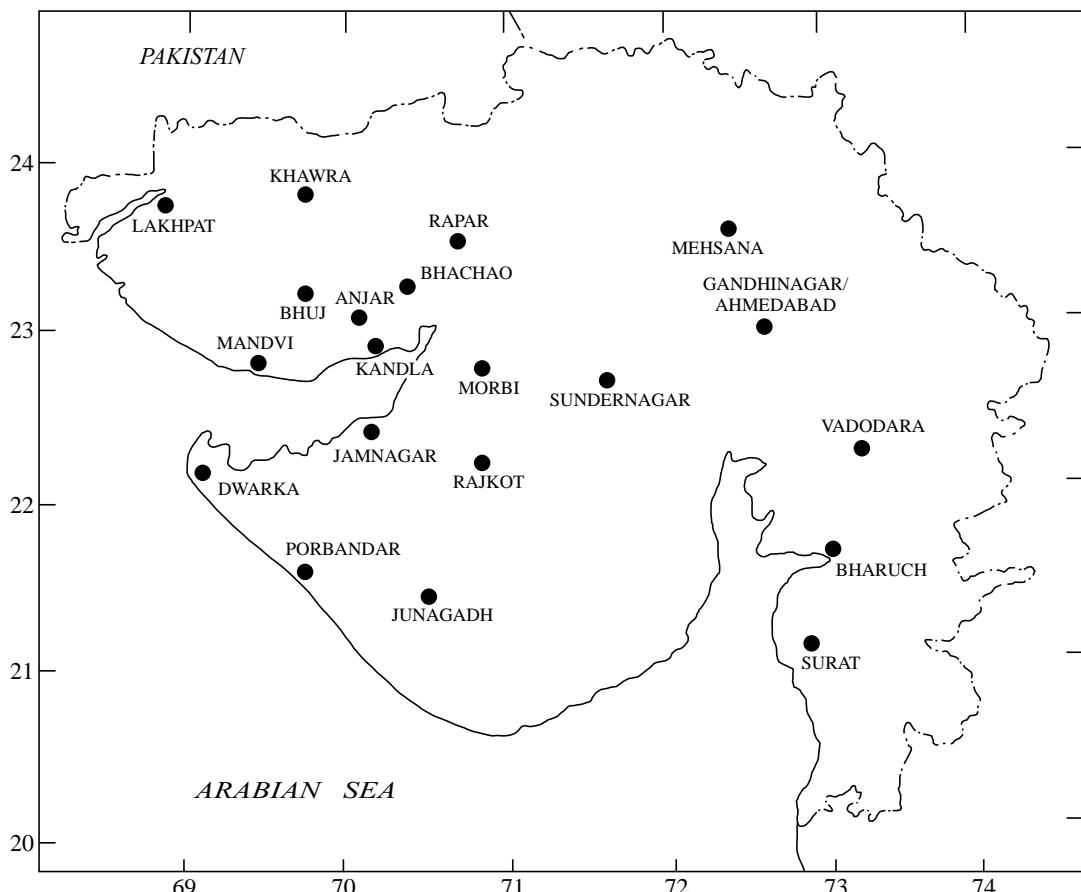


FIGURE 13.1 Map showing the major cities of Gujarat affected by Bhuj earthquake.

surveyed by the team are in Ahmedabad, Bhuj, Gandhidham, Anjar and Bhachau. In Ahmedabad there are approximately 750 high-rise buildings out of which three G+10 buildings collapsed and 88 buildings of varying heights upto G+4 have significantly been found damaged. In Bhuj itself innumerable structures collapsed and many have led to cave in and tilting.

13.2 REINFORCED CONCRETE BUILDING CONSTRUCTION PRACTICES

Reinforced concrete construction is the most common type of construction in the major cities of Gujarat and most of the damages have occurred to these buildings. The buildings are in the range of G+4 to G+10 storey height. The building framing system is generally moment resisting, consisting of reinforced concrete slabs cast monolithically with beams and columns on shallow isolated footing. The upper floors are generally constructed with infill walls made of unreinforced bricks, cut stones or cement concrete blocks. In major commercial cities, the ground floor/basement is often used for commercial and parking purposes, where the infill walls

are omitted, resulting in soft or weak stories. Most of the buildings have overhanging covered balconies of about 1.5 m span on higher floors. The architects often erect a heavy beam from the exterior columns of the building to the end of the balcony on the first floor onwards. A peripheral beam is provided at the end of the erected girder to create more parking spaces at the ground floor and allowing more space on the upper floors. The upper floor balconies or other constructions are constructed on the peripheral beams. The infill walls, which are present in upper floors and absent in the ground floor, create a floating box type situation (Figure 13.2). The dynamic analysis of a G+4 storey RC building on floating column shows that these buildings vibrate in torsional mode, which is undesirable.

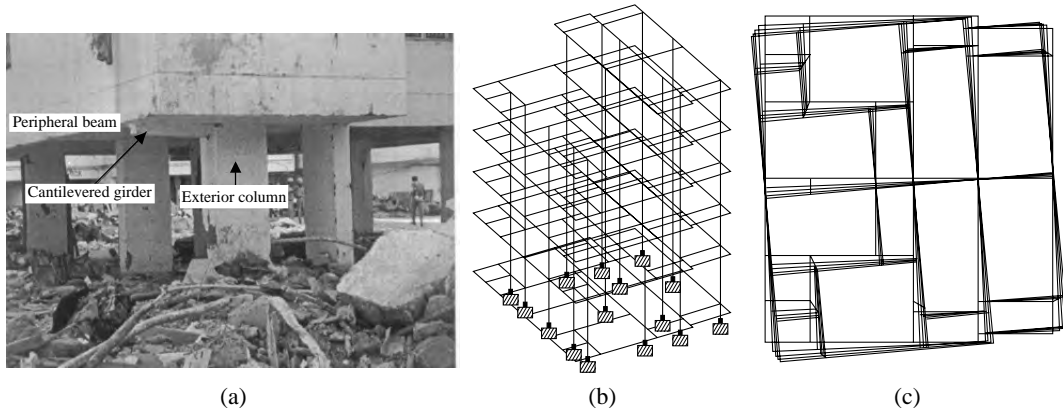


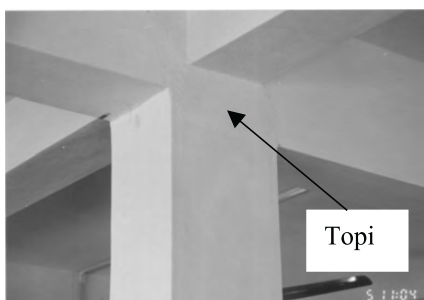
FIGURE 13.2 (a) Floating box construction in Ahmedabad, (Goel, 2001); (b) 3-D mathematical model of a floating type RC building; (c) First mode shape of the building in plan—a torsional mode.

The plan dimensions of building vary considerably ranging from 10 m × 25 m or more in Ahmedabad. Storey heights remain typically between 2.7 m and 3 m, except the lowest storey, which may be as high as 3.5 m to 4.5 m. The lift cores in the multi-storeyed buildings are generally provided in central portion of the building.

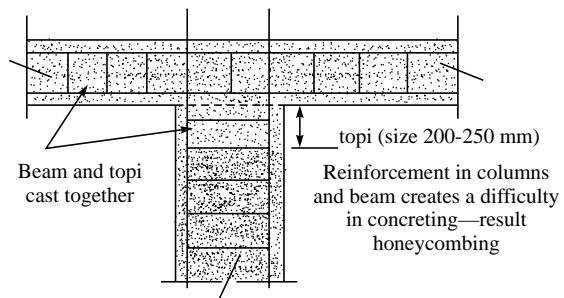
Beam spans generally vary from 2 to 5 m, owing to irregular column spacing. In many buildings, beam reinforcement consists of three to four longitudinal bars of 12 to 16 mm in diameter. Transverse stirrups are usually 6 to 8 mm in diameter placed at a spacing of 20 to 25 cm and ends of the stirrups are usually terminated with 90° hooks.

Columns in most of the buildings are of uniform size along the height of the buildings, with marginal change in the grade of concrete and reinforcement at ground floor. It is apparent that the columns are designed only for axial load, without considering the effect of framing action and lateral loads. The ground floor columns are not cast upto the bottom of the beam and a gap of 200 mm to 250 mm is left called as “*topi*” to accommodate the beam reinforcement, which makes the construction more vulnerable (Figure 13.3a). Due to the congestion of reinforcement in this region, the compaction of concrete is not properly done which results in poor quality of concrete and honeycombing (Figure 13.3b).

Columns often have rectangular cross sections, with typical dimensions *i.e.* 25 cm wide and 60 cm to 80 cm long. Longitudinal reinforcements consist of two rows of four to six bars of 12 to 18 mm diameter. The longitudinal reinforcement ratio is generally between 1 and 2%



(a)



(b)

FIGURE 13.3 (a) Typical construction of 'topi'; (b) Construction detail of 'topi'.

of gross cross-sectional area. Transverse reinforcements consist of a single hoop of 6 mm to 8 mm diameter having 90° hooks spaced at 20 to 25 cm and terminated at the joints. The longitudinal reinforcement is often lap-spliced just above the floor slab. The spacing of transverse reinforcement over the lap splice is same as elsewhere in the column rather being closely spaced. There is no sign of special confinement reinforcement and ductile detailing in the columns. This is a faulty design practice from seismic point of view.

Roofs usually consist of horizontal reinforced concrete slab of 10 to 12 cm thickness resting on beam, which are 50 to 60 cm deep (including the slab) and 20 to 25 cm wide. In some cases, slab is directly cast on columns. The main reinforcement in slab is of 8 mm diameter at a spacing of 10 cm c/c and distribution steel is of 6 mm diameter @ 15 cm to 20 cm c/c.

Elevator cores are made of RC structural walls of thickness varying from 125–250 mm. The advantage of strength and stiffness of these RC walls was not been properly exploited during earthquake because of improper connection between RC walls and slab, and the presence of stair case around the elevator core.

The foundations in private buildings generally consist of an isolated footing with a depth of about 1.5 m for G+4 buildings and 2.7 to 3.5 m for G+10 buildings. The plan sizes of footing are usually 1.2 m × 1.2 m, 1.8 m × 1.8 m or 2.4 m × 2.4 m. There are no tie beams interconnecting the footing, and plinth beams connecting the column at the ground storey level (EERI, 2002). The isolated foundations have been designed assuming bearing capacity of soil as 250 kN/m² (Goyal et al., 2001) though the investigations after the collapse show lower value at the foundation level (200 kN/m²). The majority of the damaged buildings was founded on deep alluvium where amplification of motion in soil seems to have caused large forces in the buildings. In some government buildings, raft foundation has been provided.

It has been observed that most buildings are designed only for gravity loads and a few buildings are designed considering earthquake forces with ductile detailing practices. The materials used in the construction are M15 grade concrete for G+4 storeyed buildings and M 20 grade concrete for G+10 storeyed buildings with Fe 415 reinforcement.

13.3 IDENTIFICATION OF DAMAGE IN RC BUILDINGS

Reinforced concrete buildings have been damaged on a very large scale in Bhuj earthquake of January 26, 2001. These buildings have been damaged due to various reasons. Identification of

a single cause of damage to buildings is not possible. There are combined reasons, which are responsible for multiple damages. It is difficult to classify the damage, and even more difficult to relate it in quantitative manner. This is because of the dynamic character of the seismic action and the inelastic response of the structures. The principal causes of damage to buildings are soft stories, floating columns, mass irregularities, poor quality of material, faulty construction practices, inconsistent seismic performance, soil and foundation effect, pounding of adjacent structures and inadequate ductile detailing in structural components, which have been described in detail subsequently.

13.3.1 Soft Storey Failure

In general, multi-storeyed buildings in metropolitan cities require open taller first storey for parking of vehicles and/or for retail shopping, large space for meeting room or a banking hall owing to lack of horizontal space and high cost. Due to this functional requirement, the first storey has lesser strength and stiffness as compared to upper stories, which are stiffened by masonry infill walls. This characteristic of building construction creates “weak” or “soft” storey problems in multi-storey buildings. Increased flexibility of first storey results in extreme deflections, which in turn, leads to concentration of forces at the second storey connections accompanied by large plastic deformations. In addition, most of the energy developed during the earthquake is dissipated by the columns of the soft stories. In this process the plastic hinges are formed at the ends of columns, which transform the soft storey into a mechanism. In such cases the collapse is unavoidable. Therefore, the soft stories deserve a special consideration in analysis and design.

It has been observed from the survey that the damage is due to collapse and buckling of columns especially where parking places are not covered appropriately. On the contrary, the damage is reduced considerably where the parking places are covered adequately. It is recognised that this type of failure results from the combination of several other unfavourable reasons, such as torsion, excessive mass on upper floors, P-Δ effects and lack of ductility in the bottom storey. Figure 13.4 shows some of the examples of soft/flexible stories and/ or weak



(a)



(b)

FIGURE 13.4 Soft storey failures in reinforced concrete buildings (a) Apollo Apartment at Ahmedabad, ground floor was completely collapsed; (b) G+6 RC framed building at Bhuj, intermediate weak-storey failure.

storey failure in Bhuj earthquake. The Apollo Apartment (Figure 13.4a) in Ahmedabad nearly 15–20 years old where ground floor is used for parking purposes got significantly damaged. The two blocks of this apartment at the entrance have completely collapsed and the upper floors are resting on ground in significantly tilted condition. Figure 13.4b shows the example of intermediate weak storey failure in a G+6 reinforced concrete framed building in Bhuj.

13.3.2 Floating Columns

Most of the buildings in Ahmedabad and Gandhidham, are covering the maximum possible area on a plot within the available bylaws. Since balconies are not counted in Floor Space Index (FSI), buildings have balconies overhanging in the upper stories beyond the column footprint area at the ground storey, overhangs upto 1.2 m to 1.5 m in plan are usually provided on each side of the building. In the upper stories, the perimeter columns of the ground storey are discontinued, and floating columns are provided along the overhanging perimeter of the building. These floating columns rest at the tip of the taper overhanging beams without considering the increased vulnerability of lateral load resisting system due to vertical discontinuity. This type of construction does not create any problem under vertical loading conditions. But during an earthquake a clear load path is not available for transferring the lateral forces to the foundation. Lateral forces accumulated in upper floors during the earthquake have to be transmitted by the projected cantilever beams. Overturning forces thus developed overwhelm the columns of the ground floor. Under this situation the columns begin to deform and buckle, resulting in total collapse. This is because of primary deficiency in the strength of ground floor columns, projected cantilever beam and ductile detailing of beam-column joints. Ductile connection at the exterior beam-column joint is indispensable for transferring these forces.

Figure 13.5 shows damage in reinforced concrete residential buildings (G+4) due to floating columns. This is the second most notable and spectacular cause of failure of buildings. The 15th August Apartment and Nilima Park Apartment buildings at Ahmedabad are the typical examples of failure in which, infill walls present in upper floors are discontinued in the lower floors.



(a)



(b)

FIGURE 13.5 Failure of reinforced concrete buildings with floating columns (a) 15th August Apartment, Ahmedabad, collapse of building on floating columns; (b) Nilima Park Apartment, Ahmedabad, large scale damage in the upper floors.

13.3.3 Plan and Mass Irregularity

Figure 13.6 shows the failure of two most famous multi-storeyed buildings, i.e., Mansi Complex (Figure 13.6a) and Shikhar Apartment (Figure 13.6b) during Bhuj earthquake with their exposed isolated footings (Figure 13.6c and 13.6d). Mansi Complex is a residential building in Vastrapura village consisting of two blocks A and B with 40 units in each block. Shikhar Apartment is also a newly constructed residential complex approximately one year old in Vezalpur under Ahmedabad Urban Development Authority (AUDA) consisting of four blocks with 40 flats in each. Both the buildings are G+10 and are located in the satellite town of Ahmedabad. The plans of both the buildings are irregular. The Mansi Complex has C shaped plan while the Shikhar Apartment has U shaped plan with no expansion or separation joint as reported (Sinvhal et. al. 2001). In A-Block of Mansi Complex the staircase was in the central



(a)



(b)



(c)



(d)

FIGURE 13.6 Failure in reinforced concrete buildings due to structural irregularity: (a) Total collapse of half portion of A-Block of Mansi Complex; (b) Collapse of D-Block of Shikhar Apartment; (c) Oblong isolated footing of a column, A-Block of Mansi Complex; (d) Exposed isolated footing of a column of Shikhar Apartment.

portion of the building while in the D-Block of Shikhar Apartment the staircase was located at the extreme end. Irregularities in plan (C and U shape), mass, stiffness and strength result in significant torsional response. These associated torsional effects may be attributed to collapse of buildings. Presence of a massive swimming pool at 10th floor, a fancy penthouse and some rooms that were not mentioned in original plan are also believed to be the cause of failure of Mansi Complex. Excess mass leads to increase in lateral inertia forces, reduced ductility of vertical load resisting elements and increased propensity towards collapse due to P-Δ effect. Irregularity of mass distribution results in irregular response and complex dynamics. It may be inferred from the characteristic-sway mode of a building that the excessive mass on higher floors produce more unfavourable effects than those at lower floors. The other reasons that contribute to failure are: effect of soft stories, position of service core between the two wings, wall and staircase separation, inadequate connection with slabs at each floor and improper framing system. The column dimension in one direction is relatively high as compared to other direction. The typical size of the column of Mansi Complex in A-block is 80 cm × 27.5 cm and 80 cm × 25 cm in B-Block. The exposed foundation of one column of collapsed portion of the building shows the isolated footing of approximate size of 2 m × 2 m in plan and 60 cm deep with no tie beams. The failure of Shikhar apartment occurred because of column shear failure, poor quality of construction material, and unsymmetrical location of lift, leading to the torsional effect.

13.3.4 Poor Quality of Construction Material and Corrosion of Reinforcement

Figure 13.7 shows some typical examples of building failure due to poor quality of construction material. The failure of Mehta Chambers, G+3, housing morning daily newspaper *Karnvati Express* (Figure 13.7a) and an RC building (Figure 13.7b) at Ahmedabad was due to poor quality of material and corrosion of reinforcement. Figures 13.8a and 13.8b show typical examples of damage due to corrosion of reinforcement at beam column joint, slab of staircase and column face.



(a)



(b)

FIGURE 13.7 Damage of RC buildings due to poor quality of construction (a) Old construction, corroded reinforcement prior to earthquake, Mehta Chambers, Ahmedabad; (b) Poor quality of material, corrosion of reinforcement.



(a)



(b)

FIGURE 13.8 Damage due to corrosion of steel in reinforced concrete buildings (a) Damage due to corrosion of steel at beam column joint; (b) Damage due to corrosion of steel at column face.

There are numerous instances in which faulty construction practices and lack of quality control contributed to the damage. In the cement-sand ratio, the ratio of sand was dangerously high. It also appeared that recycled steel was used as reinforcement. Himgiri Apartment is now a pile of rubble as a result of poor quality of construction materials. Many buildings are damaged due to spalling of concrete by the corrosion of embedded reinforcing bars. The corrosion is related to insufficient concrete cover, poor concrete placement and porous concrete. Several buildings constructed about 5 to 10 years ago were damaged due to lack of quality control. It is reported that the water supply in the outer part of the city is through ground water, which is salty in taste and the same water is used in preparing the concrete mix for construction. The presence of salts may also have affected the quality of concrete (Goel, 2001).

13.3.5 Pounding of Buildings

Although the number of buildings damaged by pounding is small, yet there are few examples in which the primary cause of damage in buildings is due to hammering of adjacent buildings. Anand building, G+5, (Figure 13.9) at Bhuj is an example of pounding failure.

Pounding is the result of irregular response of adjacent buildings of different heights and of different dynamic characteristics. When the floors of adjacent buildings are at different elevations, the floor of each building acts like rams, battering the columns of the other building. When one of the buildings is higher than the other, the building of lower height acts as a base for the upper part of the adjacent taller building. The low height building receives an unexpected load while the taller building suffers from a major stiffness discontinuity at the level of the top of the lower building. Pounding may also occur because of non-compliance of codal provisions particularly for lateral and torsional stiffness and cumulative tilting due to foundation movement.



FIGURE 13.9 Anand building, Bhuj, damage resulting from pounding.

Damage due to pounding can be minimized by drift control, building separation, and aligning floor in adjacent buildings.

13.3.6 Inconsistent Seismic Performance of Buildings

It is evident that the earthquake did not affect all the structures uniformly. The dynamic characteristics of buildings are one of the predominant factors. The severity of damage varied dramatically, with total collapse of buildings in some cases to minor damage in nearby buildings. Swaminarayan Higher Secondary School in Mani Nagar at Ahmedabad, a four-storey RC building, collapsed (Figure 13.10a), while nearby buildings suffered minor damage. Similarly B-Block of Mansi Complex in satellite town sustained only minor damage while the adjacent half portion of the A-Block completely collapsed (Figure 13.10b).

A multi-storeyed RC building, under construction, across the road from Shikhar Apartment escaped damage, while D-Block of Shikhar Apartment collapsed. In some cases the buildings appeared to be identical but the degree of damage varied significantly. Possible explanations for such behaviour could be workmanship, detailing practices, quality of material, design, etc.

More than two-thirds of reinforced concrete buildings, which got collapsed, were recently constructed. Shradha Apartment, a housing society in Ahmedabad's posh Fatehpura area barely six months old, came down. Other buildings in the same area, of less than two years vintage, have also collapsed. It has also been observed that most of the buildings that collapsed lie along the old path of Sabarmati river passing through the city. The south part of city, especially the Mani Nagar area, where majority of damages were observed falls between two lakes, indicating the presence of either poor soil strata or possible construction on reclaimed land.



(a)



(b)

FIGURE 13.10 Failure of reinforced concrete buildings due to different earthquake response
 (a) Swaminarayan school building collapsed while the adjacent building suffered minor damages;
 (b) Collapse of A-Block of Mansi Complex while B-block suffered minor damage.

13.4 DAMAGE TO STRUCTURAL ELEMENTS

Figure 13.11 shows failure in reinforced concrete columns in reinforced concrete buildings. Oblong cross section, a space left at the top of column called '*topi*' during casting and relatively slender column sections compared with beam sections are the main structural defects in columns. These columns are neither designed nor detailed for ductility. Lack of confinement due to large tie spacing, insufficient development length, inadequate splicing of all column bars at the same section, hook configurations of reinforcement do not comply with ductile detailing practices. Figures 13.11a and 13.11b show the failure at the top and bottom of the column due to poor quality of concrete, the inadequate spacing of ties in the critical areas and the presence of strong beams.

Crushing of the compression zone is manifested first by spalling of the concrete cover to the reinforcement; subsequently the concrete core expands and crushes. This phenomenon is



(a)



(b)

FIGURE 13.11 Typical failure of columns in reinforced concrete buildings (a) Cracking and spalling of concrete in first storey column; (b) Base of first storey column with widely spaced ties and spalled concrete.

usually accompanied by buckling of bars in compression and by hoop fracture. The opening of the ties and the disintegration of concrete lead to shortening of the column under the action of axial force. This type of damage is serious as the column not only loses its stiffness but also loses its ability to carry vertical loads (Penelis and Kappos, 1997).

Buildings, which were inspected during the team's visit, have been found with little evidence of failure of beams. There are numerous cases in which the beam-column joints of multi-storeyed buildings have damaged. Figure 13.12(a) shows an example of damage at beam-column joint in a reinforced concrete building. One typical feature of joints constructed in an RC building is shown in Figure 13.12(b), where beams of different cross sections meet at the column faces at the same floor level. Inadequacy of reinforcement in beam-column joints, absence of confining hoop reinforcement, inappropriate location of bar splices in columns are common causes of failure of beam-column joints.



(a)



(b)

FIGURE 13.12 Beam-column joints in reinforced concrete buildings (a) Minor damage at beam column joint; (b) Detail of beam column joint.

Figures 13.13(a) and 13.13(b) show cracking of reinforced concrete slab and beam slab joints in buildings. It is mainly due to widening of existing micro cracks, which are formed



(a)



(b)

Figure 13.13 Damage to RC slab in reinforced concrete buildings (a) Cracks at ceiling—existing micro cracks; (b) Cracks at slab-beam junction.

either because of bending action or temperature/shrinkage. These cracks are further widened and visible due to strong ground shaking. Damage in slab is generally not considered to be dangerous for the stability of the structure. However, it creates serious functional and aesthetic problems.

13.5 DAMAGE TO NON-STRUCTURAL PANEL ELEMENTS

13.5.1 Damage to Infill Walls

Masonry infill walls are used as interior partitions and as exterior walls to form a part of the building envelope in multi-storeyed buildings. In general design practices in India, the strength and stiffness of infill walls are ignored with the assumption of conservative design. In actual, infill walls add considerably to the strength and rigidity of the structures and their negligence will cause failure of many of multi-storeyed buildings. The failure is basically due to stiffening effect of infill panels which is cause of (i) unequal distribution of lateral forces in the different frames and overstressing of some of the building frames; (ii) soft storey or weak storey; (iii) short column or captive column effect; (iv) torsional forces; (v) cracking of the infill walls.

During the excitation of the structure, the reinforced concrete frame begins to deform, and initially the first cracks appear on the plaster along the line of contact of the masonry infill with the frame. As the deformation of the frame becomes larger, the cracks penetrate into the masonry, and are manifested by the detachment of the masonry infill from the frame. Subsequently, diagonal cracks (X shaped) appear because of the strut action of the infill. Figure 13.14(a) shows an example of cracking of infill wall in a residential building of Oil and Natural Gas Corporation (ONGC) at Ahmedabad. To avoid this type of failure, either interaction of infill wall with the frame should be considered in design or a movable joint between infill and frame should be provided.

Sometimes perimeter infill walls are pierced with many closely spaced windows. The columns in between these piers may be called captive columns like a short column. A captive



(a)



(b)

FIGURE 13.14 Failure of infill wall and panel in reinforced concrete buildings (a) Shear (X) cracking of masonry infill; (b) Shear failure in “captive column”.

column is full storey slender column whose clear height is reduced by its part-height contact with a relatively stiff non-structural element, such as a masonry infill wall, which constrains its lateral deformation over the height of contact (CEB, 1996). The shear required to develop flexural yield in the effectively shortened column is substantially higher than shear required developing flexural yield of full-length column. If the designer has not considered this effect of the infill, shear failure may occur before flexural yield and often fail in brittle manner (Figure 13.14b). The cracking in ‘captive’ column generally initiates from window headers and sill levels (Moehle and Mahin, 1991).

13.5.2 Damage to Exterior Walls

Figures 13.15(a) and 13.15(b) illustrate characteristic examples of damage to exterior walls that are poorly connected with the RC frame. These walls are subjected to out-of-plane vibrations. This form of construction of large exterior walls creates a weak plane around the perimeter. When subjected to intense shaking, these large un-reinforced masonry panels confined by stiff frame members have a tendency to resist large out-of-plane vibrations with little sign of distress. When the flexure strength of these panels becomes insufficient to resist these forces, the entire infill panels fail. The magnitude of damage is found to be dependent on the quality of materials and method of construction.



(a)



(b)

FIGURE 13.15 Failure of exterior walls in non-ductile concrete frame (a) Collapse of exterior wall due to restricted ductility of concrete frame; (b) Damage to walls of ground and first floors.

13.6 DAMAGE TO WATER TANK AND PARAPETS

Figure 13.16(a) shows a reinforced concrete building, Prabhu Kripa at Bhuj, in which failure of water tank at the roof of the building was observed. Figure 13.16(b) shows the failure of the top portion of a bare framed reinforced concrete building under construction. Water tanks constructed at the roof level of buildings experience large inertia forces due to amplification of the ground acceleration along the height of the building. Un-reinforced concrete parapets with large height-to-thickness ratio and not improper anchoring to the roof diaphragm may also constitute a hazard. The hazard posed by a parapet increases in direct proportion to its height above building base, which has been observed at several places.



(a)



(b)

FIGURE 13.16 Amplification effects of acceleration in RC frame buildings (a) Failure of water tank in a RC frame building; (b) Top portion of the bare framed RC building under construction collapsed.

13.7 DAMAGE TO VERTICAL CIRCULATION SYSTEMS

Staircases and lifts are the only means of vertical movement in building and the staircases also serve as escape routes during an earthquake. Figures 13.17 and 13.18 show the failure of staircases and a lift core in reinforced concrete buildings.

13.7.1 Damage to Staircase

Figures 13.17(a) and 13.17(b) are typical examples of failure of staircases in Vishram Flat, G+5, in Navarangpura, Ahmedabad and in an RC building at Bhuj due to out-of-phase vibration of



(a)



(b)

FIGURE 13.17 Failure of staircase in reinforced concrete framed buildings (a) Strut action of staircase during out of phase vibration of two blocks; (b) Damage to staircase in reinforced concrete frame building.

two blocks. In quite a few multi-storey complexes, failure of staircase is a major cause of damage. Staircases and corridors are found to have been blocked by the failure of the unreinforced masonry enclosure walls. Many exit doors are found to be jammed due to racking of doorframes. Stairs can start acting as diagonal-bracing elements during earthquake induced motion, and therefore, should be used with sliding joints in the seismic design of buildings. Isolation of stairs from the primary structural system may also minimise the damage to the stair system.

13.7.2 Damage to Elevator

Figure 13.18 shows the undamaged lift core of a building during the earthquake at Gandhidham. Elevators constitute an integral part of the building, and are vulnerable to earthquake. It is important to prevent damage to the elevators for the following reasons: (i) danger to the passengers trapped during the occurrence and difficulties in rescue operations; (ii) undetected damage can cause substantial danger in elevators used after the earthquake; (iii) vertical circulation systems (elevators and stairs) are essential in hospitals which deliver crucial health services after an earthquake.



FIGURE 13.18 Undamaged lift core of a reinforced concrete building.

13.8 EFFECT OF EARTHQUAKE ON CODE DESIGNED STRUCTURES

The Bureau of Indian Standards (BIS) has published two codes IS 1893 (Part 1): 2002 and IS 13920: 1993 for earthquake resistant design of reinforced concrete buildings. The former code deals with the determination of forces and general considerations for design of buildings while the latter code deals with the detailing of reinforced concrete structures for ductility. The government buildings follow the design codes as a mandatory requirement. Therefore, the

performance of governmental buildings in this earthquake has been relatively better on account of code compliance (Thakkar et al., 2001). Figures 13.19(a) and 13.19(b) show a multi-storeyed (G+9) reinforced concrete building, residential quarters for regional passport office and Ayakar Bhawan (G+3) RC building with part basement at Ahmedabad. These buildings were constructed by Central Public Works Department (CPWD) in the years 2000 and 1954 respectively. These two buildings sustained minor damage in the form of cracking of infill brick wall and non-functioning of lift. Both the buildings were in working condition after the earthquake and were not required to be vacated.



(a)



(b)

FIGURE 13.19 Damage in Government constructed Reinforced Concrete buildings (a) Residential quarters for Regional Pass Port Office (G+9), Ahmedabad, minor cracking in filler walls; (b) Ayakar Bhawan (G+3), a RC building, Ahmedabad, diagonal and junction cracks in filler brick wall.

13.9 LESSONS LEARNT FROM DAMAGES OF RC BUILDINGS

The occurrence of Bhuj earthquake has caused significant damage to multi-storeyed reinforced concrete buildings. The lessons learnt from damages are presented below:

- (i) The design of buildings should be based on seismic codes IS 1893 (Part 1): 2002 and IS: 13920: 1993.
- (ii) The multi-storeyed reinforced concrete buildings with vertical irregularities like soft storey construction and buildings with mass irregularities such as massive swimming pool on the roof of the building and the buildings with floating columns should be designed on the basis of dynamic analysis and inelastic design. The ductility provisions are most important in such situations.

- (iii) More care is necessary at the time of planning. The torsional effects in a building can be minimised by proper location of vertical resisting elements and mass distribution. Building design with strong-column weak beam can be achieved at the planning stage. The soft storey stiffness can also be controlled by appropriate design procedure.
- (iv) The infill construction in RC buildings should be duly accounted for structural analysis. The staircase connection with buildings should be made using sliding joints.
- (v) Shear walls should be employed for increasing stiffness and are uniformly distributed in both principal directions.
- (vi) There should be a greater emphasis on the quality of construction.

SUMMARY

Reinforced concrete multi-storeyed buildings in India, for the first time, have been subjected to a strong ground motion shaking during Bhuj earthquake of January 26, 2001 resulting in a considerable damage. It has been observed that the principal reasons of failure are due to soft storeys, floating columns, mass irregularities, poor quality of construction material and faulty construction practices, inconsistent earthquake response, soil and foundation effect and pounding of adjacent structures. This chapter presents description of types of construction, types of damage and causes of damage in selected multi-storeyed reinforced concrete buildings and lessons learnt from the failure. Modifications needed in the design practices to minimize earthquake damages have also been proposed.

REFERENCES

- [1] CEB., *RC Frame under Earthquake Loading—State of the Art Report*, Thomas Telford, 1996.
- [2] Goel, R.K., “Performance of Buildings during the January 26, 2001 Bhuj Earthquake”, *Earthquake Engineering Research Institute*, California.
- [3] Goyal, A., Sinha, R., Chaudhari, M. and Jaiswal, K., “Performance of Reinforced Concrete Buildings in Ahmedabad during Bhuj Earthquake January 26, 2001”, *Workshop on Recent Earthquakes of Chamoli and Bhuj: Volume I*, Roorkee, India, May 24–26, 2001.
- [4] IS 13920, “Ductile Detailing of Reinforced Concrete Structures Subjected to Seismic Forces—Code of Practice”, Bureau of Indian Standards, 1993.
- [5] IS 1893, “Criteria for Earthquake Resistant Design of Structures (Part 1) General Provisions and Buildings (Fifth Revision)”, Bureau of Indian Standards, 2002.
- [6] Moehle, J.P. and Mahin, S.A., “Observation of the Behaviour of Reinforced Concrete Buildings during Earthquake”, SP-127, *Earthquake Resistant Concrete Structures—Inelastic Response and Design*, American Concrete Institute Publication, S.K. Ghosh, (Ed.), 1991.
- [7] Penelis, G.G. and Kappos, A.J., “Earthquake-Resistant Concrete Structures”, *E & FN SPON*, an imprint of Chapman & Hall, 1997.

- [8] Sinhal, A., Bose, P.R., Bose, A., and Prakash, V. "Destruction of Multi-storeyed Buildings in Kutch Earthquake of January 26, 2001", *Workshop on Recent Earthquakes of Chamoli and Bhuj*: Volume II, Roorkee, India, May 24–26, 2001.
- [9] Srivastav, S.K., "Bhuj Earthquake of January 26, 2001—Some Pertinent Questions", *International Conference on Seismic Hazard with Particular Reference to Bhuj Earthquake of January 26, 2001*, New Delhi, October 3–5, 2001.
- [10] Thakkar, S.K., Dubey, R.N., and Agarwal, P., "Behaviour of Buildings, Bridges and Dams in Bhuj Earthquake of January 26, 2001", *Proceedings of 17th US-Japan Bridge Engineering Workshop*, Tsukuba City, Japan, Nov. 12–14, 2001.

Chapter 14

Effect of Structural Irregularities on the Performance of RC Buildings during Earthquakes

14.1 INTRODUCTION

Earthquake resistant design of reinforced concrete buildings is a continuing area of research since the earthquake engineering has started not only in India but in other developed countries also. The buildings still damage due to some one or the other reason during earthquakes. In spite of all the weaknesses in the structure, either code imperfections or error in analysis and design, the structural configuration system has played a vital role in catastrophe. The IS: 1893 (Part 1): 2002 has recommended building configuration system in **Section 7** for the better performance of RC buildings during earthquakes. The building configuration has been described as regular or irregular in terms of size and shape of the building, arrangement of structural elements and mass. Regular building configurations are almost symmetrical (in plan and elevation) about the axis and have uniform distribution of the lateral force-resisting structure such that, it provides a continuous load path for both gravity and lateral loads. A building that lacks symmetry and has discontinuity in geometry, mass, or load resisting elements is called irregular. These irregularities may cause interruption of force flow and stress concentrations. Asymmetrical arrangements of mass and stiffness of elements may cause a large torsional force (where the centre of mass does not coincide with the centre of rigidity).

The section 7 of IS 1893 (Part 1): 2002 enlists the irregularity in building configuration system. These irregularities are categorised in two types (i) vertical irregularities referring to sudden change of strength, stiffness, geometry and mass results in irregular distribution of forces and/or deformation over the height of building and (ii) horizontal irregularities which refer to

asymmetrical plan shapes (e.g. L-, T-, U-, F-) or discontinuities in the horizontal resisting elements (diaphragms) such as cut-outs, large openings, re-entrant corners and other abrupt changes resulting in torsion, diaphragm deformations and stress concentration.

There are numerous examples enlisted in the damage report of past earthquakes in which the cause of failure of multi-storeyed reinforced concrete buildings is irregularities in configurations. This chapter describes the irregularities, performance of irregular buildings in the past earthquakes and possible causes of damage with some recommendations.

14.2 VERTICAL IRREGULARITIES

14.2.1 Vertical Discontinuities in Load Path

One of the major contributors to structural damage in structures during strong earthquake is the discontinuities/irregularities in the load path or load transfer. The structure should contain a continuous load path for transfer of the seismic force, which develops due to accelerations of individual elements, to the ground. Failure to provide adequate strength and toughness of individual elements in the system, or failure to tie individual elements together can result in distress or complete collapse of the system. Therefore, all the structural and non-structural elements must be adequately tied to the structural system. The load path must be complete and sufficiently strong.

The general load path is as follows: earthquake forces, which originate in all the elements of the building are delivered through structural connections to horizontal diaphragms. The diaphragms distribute these forces to vertical resisting components such as columns, shear walls, frames and other vertical elements in the structural system which transfer the forces into the foundation (Figure 14.1). The diaphragms must have adequate stiffness to transmitting these forces.

The examples of load path irregularities are, discontinuous columns, shear walls, bracing, frames, that arise a floating box type situation (Figures 14.2(a) and 14.2(b)). In the case of columns or shear walls that do not continue upto the ground but end at an upper level, shear is induced to overturning forces to another resisting element of a lower level. This imposition of overturning forces overwhelms the columns of lower level through connecting elements. Therefore, the most critical region of damage is the connecting element (link between discontinuous column to lower level column) and lower level columns. Therefore, the primary concern in load path irregularities is regarding the strength of lower level columns and strength of the connecting beams that support the load of discontinuous frame.

The failure due to discontinuity of vertical elements of the lateral load resisting system has been among the most notable and spectacular. One common example of this type of discontinuity occurs in Bhuj earthquake in which, infill walls that are present in upper floors are discontinued in the lower floor (floating columns concept). Another example of discontinuous shear wall is the Olive View Hospital, which nearly collapsed due to excessive deformation in the first two stories during the 1972 San Fernando earthquake and was subsequently demolished (Figure 14.3).

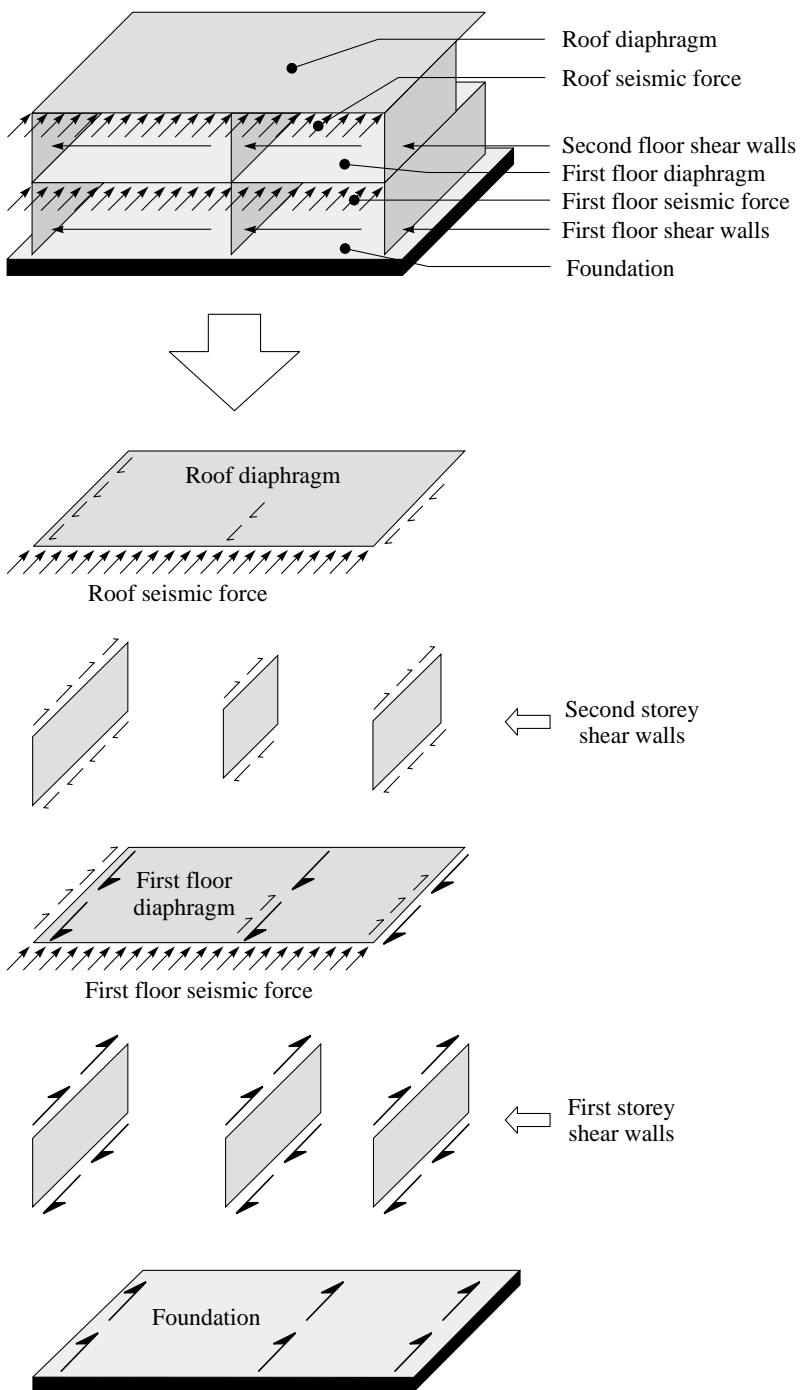


FIGURE 14.1 Seismic forces on the elements of shear wall building system (Vukazich, 1998).

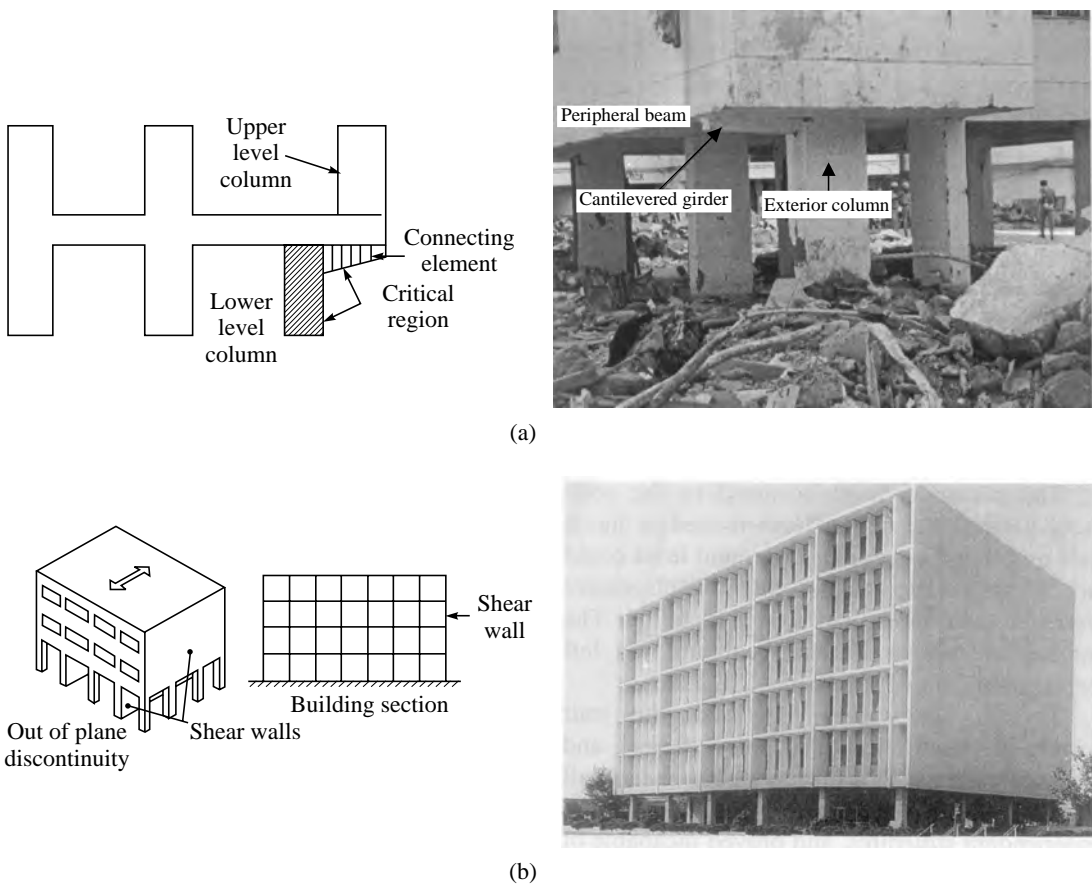


FIGURE 14.2 (a) Floating box construction in residential building in Ahmedabad, India;
(b) Discontinuous shear wall.



FIGURE 14.3 Collapse of building due to excessive deformation in San Fernando earthquake, 1972.

14.2.2 Irregularity in Strength and Stiffness

A “weak” storey is defined as one in which the storey’s lateral strength is less than 80 percent of that in the storey above. The storey’s lateral strength is the total strength of all seismic resisting elements sharing the storey shear for the direction under consideration i.e. the shear capacity of the column or the shear walls or the horizontal component of the axial capacity of the diagonal braces. The deficiency that usually makes a storey weak is inadequate strength of frame columns. A “soft storey is one in which the lateral stiffness is less than 70% of that in the storey immediately above, or less than 80% of the combined stiffness of the three stories above” (Figure 14.4). The essential characteristic of a “weak” or “soft” storey consists of a discontinuity of strength or stiffness, which occurs at the second storey connections. This discontinuity is caused by lesser strength, or increased flexibility, the structure results in extreme deflections in the first storey of the structure, which in turn results in concentration of forces at the second storey connections. The result is a concentration of inelastic action.

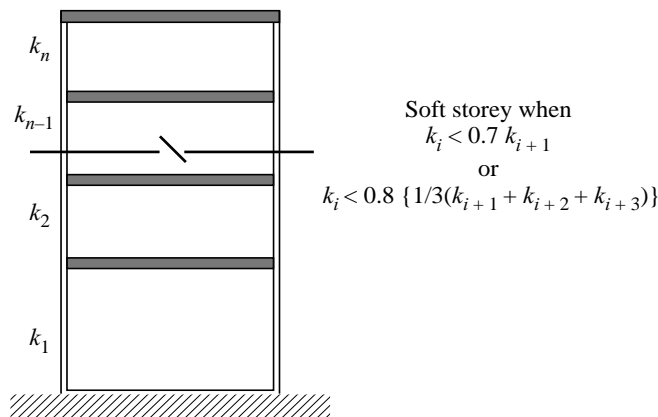


FIGURE 14.4 Stiffness irregularities—soft storey.

The soft storey concept has technical and functional advantages over the conventional construction. First, is the reduction in spectral acceleration and base shear due to increase of natural period of vibration of structure as in a base isolated structure. However, the price of this force reduction is paid in the form of an increase in structural displacement and inter-storey drift, thus entailing a significant P-Δ effect, which is a threat to the stability of the structure (Figure 14.5).

Secondly, a taller first storey is sometimes necessitated for parking of vehicles and/ or retail shopping, large space for meeting room or a banking hall, Figure 14.6. Due to this functional requirement, the first storey has lesser stiffness of columns as compared to stiff upper floor frames, which are generally constructed with masonry infill walls.

The failures of reinforced concrete buildings due to soft stories have remained the main reason in past earthquakes. In the Mexico City earthquake of 1985, researchers determined that soft first stories were a major contribution to 8% of serious failure. A number of cases of soft storey failure have also been reported in Algeria earthquake, 1980, San Salvador earthquake,

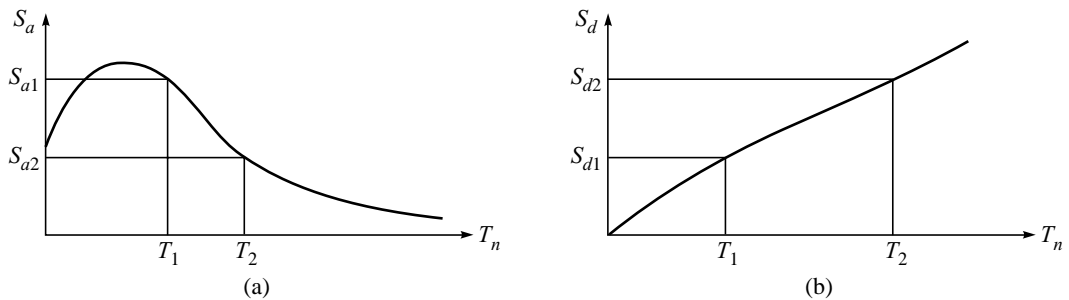


FIGURE 14.5 (a) Design earthquake spectra acceleration (S_a) versus period (T_n); (b) Design earthquake spectral displacement (S_d) versus time period (T_n) (Hart and Wong, 2000).

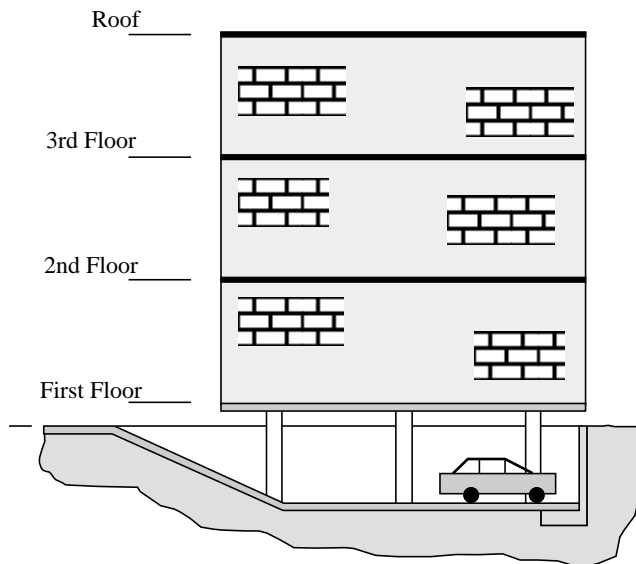


FIGURE 14.6 Soft stories type construction (Vukazich, 1998).

1986, North ridge earthquake, 1994. Bhuj earthquake, 2001 India, also reveals that the soft first storey is the main victim of damage to reinforced concrete building. Figure 14.7 shows two examples of failure of reinforced concrete buildings due to soft stories. It is recognised that this type of failure results from the combination of several other unfavourable reasons, such as torsion, excessive mass on upper floors, P- Δ effects and lack of ductility in the bottom storey. These factors lead to local stress concentrations accompanied by large plastic deformations. Therefore, the soft stories deserve a special consideration in analysis and design. It is not always necessary that all the first tall stories of the buildings are soft stories, if the columns of first storey have been designed on the basis of capacity or ductility.



(a)



(b)

FIGURE 14.7 (a) Collapse of lower storey of a four-storey building in Loma Prieta earthquake, 1989 (EERI, 1990); (b) A weak-storey mechanism developed in the bottom storey of five-storey building under construction during Kocaeli, Turkey earthquake, 1999 (EERI, 1999).

14.2.3 Mass Irregularities

Mass irregularities are considered to exist where the effective mass of any storey is more than 200% of the effective mass of an adjacent storey (Figure 14.8). The effective mass is the real mass consisting of the dead weight of the floor plus the actual weight of partition and equipment. Excess mass can lead to increase in lateral inertial forces, reduced ductility of vertical load resisting elements, and increased tendency towards collapse due to P-Δ effect. Irregularity of mass distribution in vertical and horizontal planes can result in irregular responses and complex dynamics. The characteristic-swaying mode of a building during an earthquake implies that masses placed in the upper stories of building produce considerably more unfavourable effects than masses placed lower down. The centre of gravity of lateral forces is shifted above the base in the case of heavy masses in upper floors resulting in large bending moments. Massive roofs and heavy plant rooms

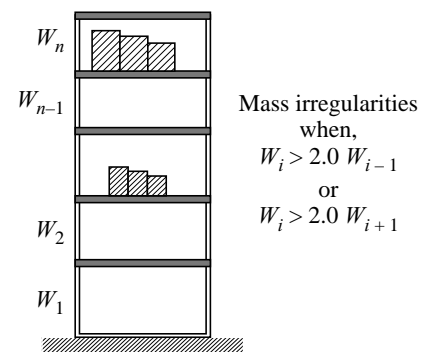


FIGURE 14.8 Mass irregularity in building.

at high level are therefore to be discouraged where possible. Where mass irregularities exist, check the lateral-force resisting elements using a dynamic analysis for a more realistic lateral load distribution of the base shear.

Numerous examples of buildings that collapse due to the presence of excessive vertical load have been identified in Mexico earthquake, 1985. It is believed that the Mansi complex, a multi-storeyed building has failed in Bhuj earthquake due to a massive swimming pool at the upper floor.

14.2.4 Vertical Geometric Irregularity

A vertical setback is a geometric irregularity in a vertical plane. It is considered, when the horizontal dimension of the lateral force resisting system in any storey is more than 150% of that in an adjacent storey (Figure 14.9). The setback can also be visualised as a vertical re-entrant corner. The general solution of a setback problem is the total seismic separation in plan through separation section, so that portions of the building are free to vibrate independently. When the building is not separated, check the lateral-force-resisting elements using a dynamic analysis.

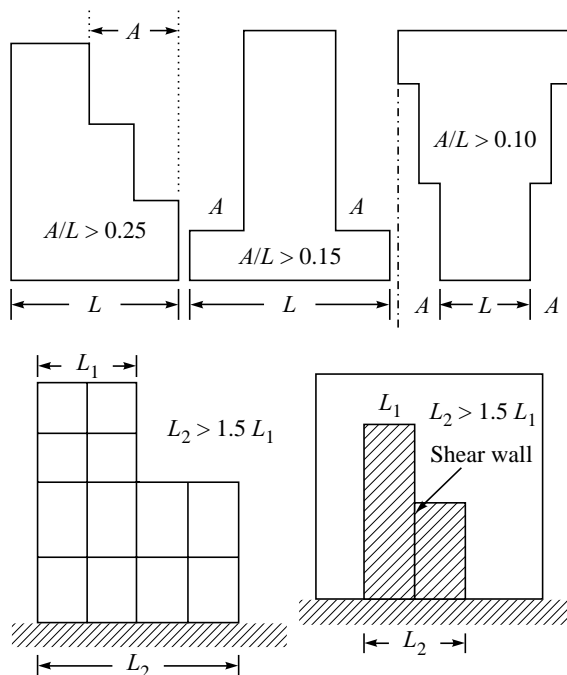


FIGURE 14.9 Vertical geometric irregularity.

14.2.5 Proximity of Adjacent Buildings

Pounding damage is caused by hitting of two buildings constructed in close proximity with each other. Pounding may result in irregular response of adjacent buildings of different heights

due to different dynamic characteristics. Several examples of building failure, as shown in Figure 14.10, have been observed due to pounding in Mexico earthquake, 1985, Kobe earthquake, 1995 and Turkey earthquake, 1992. This problem arises when buildings are built without separation right upto property lines in order to make maximum use of the space. When floor of these buildings are constructed of the same height, damage due to pounding usually is not serious. If this is not the case, there are two problems. When the floors of adjacent buildings are at different elevations, the floor of each structure can act like rams, battering the columns of the other building. When one of the buildings is higher than the other, the lower building can act as a base for the upper part of the higher building; the lower building receives an unexpected large lateral load while the higher building suffers from a major stiffness discontinuity at the level of the top of the lower building. Pounding may also be the result of a combination of many other factors such as insufficient separation between adjacent buildings, different dynamic characteristics of adjacent structures, the unexpected severity of the ground motion, non-compliance with code provisions, particularly for lateral and torsional stiffness due to inadequate building configuration and structural framing system, and cumulative tilting due to foundation movement. Damage due to pounding can be minimized by drift control, building separation, and aligning floors in adjacent buildings.



(a)



(b)

FIGURE 14.10 (a) Minor pounding damage between buildings of different heights in Turkey earthquake, 1992 (EERI, 1993); (b) Pounding between a six storey building and a two-storey building in Kocaeli, Turkey earthquake, 1999 (EERI, 1999).

14.3 PLAN CONFIGURATION PROBLEMS

14.3.1 Torsion Irregularities

Torsion irregularity shall be considered when floor diaphragms are rigid in their own plan in relation to the vertical structural elements that resist the lateral forces. Torsion irregularity is considered to exist when the maximum storey drift, computed with design eccentricity, at one

end of the structure transverse to an axis is more than 1.2 times of the average of the storey drifts at the two ends of the structures (Figure 14.11).

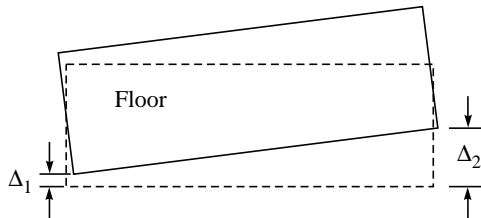


FIGURE 14.11 Torsion irregularities with stiff diaphragm.

The lateral-force-resisting elements should be a well-balanced system that is not subjected to significant torsion. Significant torsion will be taken as the condition where the distance between the storey's centre of rigidity and storey's centre of mass is greater than 20% of the width of the structure in either major plan dimension. Torsion or excessive lateral deflection is generated in asymmetrical buildings, or eccentric and asymmetrical layout of the bracing system that may result in permanent set or even partial collapse. Figures 14.12a and 14.12b show the example of building failure due to torsion in Alaska earthquake, 1964 and Mexico earthquake, 1985 respectively. Torsion is most effectively resisted at point farthest away from the centre of twist, such as at the corners and perimeter of the buildings.



(a)

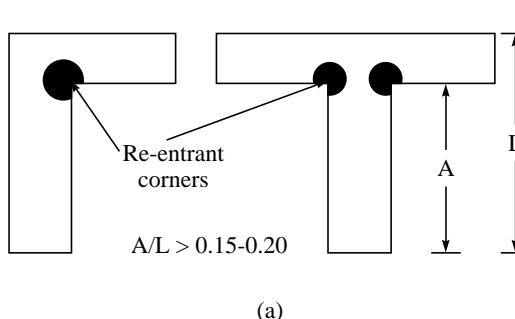


(b)

FIGURE 14.12 (a) Unbalanced location of perimeter wall leading to severe to torsional forces and near collapse in Alaska earthquake, 1964 (Naiem, 2001); (b) Torsional collapse of a building in Mexico city, 1985 (Penelis and Kappos, 1997).

14.3.2 Re-entrant Corners

The re-entrant, lack of continuity or “inside” corner is the common characteristic of overall building configurations that, in plan, assume the shape of an L, T, H, +, or combination of these shapes occurs due to lack of tensile capacity and force concentration (Vukazich, 1998). According to IS 1893 (Part 1): 2002, plan configurations of a structure and its lateral force resisting system contain re-entrant corners, where both projections of the structure beyond the re-entrant corner are greater than 15% of its plan dimension in the given direction. The re-entrant corners of the buildings are subjected to two types of problems. The first is that they tend to produce variations of rigidity, and hence differential motions between different parts of the building, resulting in a local stress concentration at the notch of the re-entrant corner (Figure 14.13a). The second problem is torsion. In Figure 14.13b, an L-shaped building is subjected to a ground motion of Alaska earthquake, 1964 in north-south direction; attempt to move differently at their notch, pulling and pushing each other. So the stress concentrations are high at the notch. The magnitude of the induced forces will depend on mass of building, structural system, length of the wings and their aspect ratios and height of the wings and their height/depth ratios. Examples of damage to re-entrant corner buildings are common and can be identified in Kanto earthquake 1923, Santa Barbara earthquake 1925. To avoid this type of damage, either provide a separation joint between two wings of buildings or tie the building together strongly in the system of stress concentration and locate resistance elements to increase the tensile capacity at re-entrant corner.



(a)



(b)

FIGURE 14.13 (a) Example of buildings with plan irregularities; (b) Damage concentrated at the intersection of two wings of an L-shaped school, Alaska earthquake, 1964.

14.3.3 Non-parallel Systems

The vertical load resisting elements are not parallel or symmetrical about the major orthogonal axis of the lateral-force resisting system (Figure 14.14). These situations are often faced by architects. This condition results in a high probability of torsional forces under a ground motion, because the centre of mass and resistance does not coincide. This problem is often exaggerated in the triangular or wedge shaped buildings resulting from street inter-sections at an

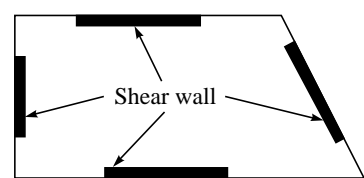


FIGURE 14.14 Non-parallel system.

acute angle. The narrower portion of the building will tend to be more flexible than the wider ones, which will increase the tendency of torsion. To design these types of buildings, special care must be exercised to reduce the effect of torsion or to increase torsional resistance of the narrow parts of the building.

14.3.4 Diaphragm Discontinuity

The diaphragm is a horizontal resistance element that transfer forces between vertical resistance elements. The diaphragm discontinuity may occur with abrupt variations in stiffness, including those having cut-out or open areas greater than 50% of the gross enclosed diaphragm area, or change in effective diaphragm stiffness of more than 50% from one storey to the next (Figure 14.15a). The diaphragm acts as a horizontal beam, and its edge acts as flanges. It is obvious that opening cut in tension flange of a beam will seriously weaken its load carrying capacity. In a number of buildings there has been evidence of roof diaphragms, which is caused by tearing of the diaphragm (Figure 14.15b).

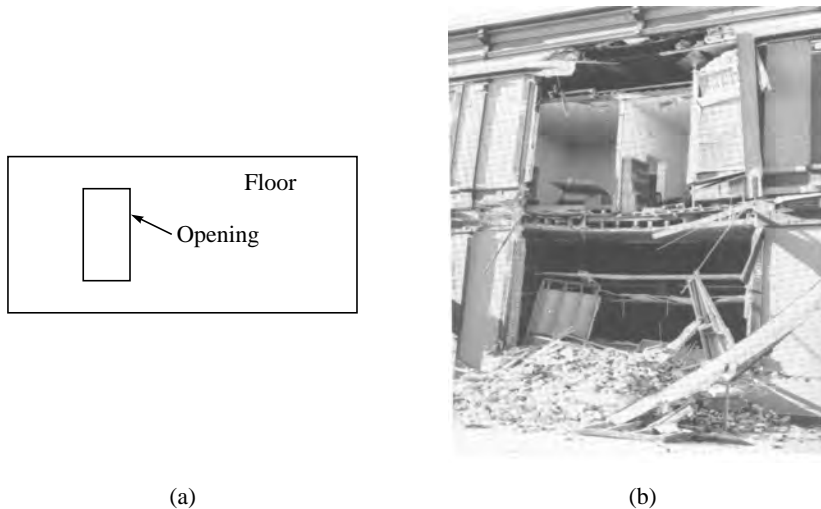


FIGURE 14.15 (a) Diaphragm discontinuity; (b) Failure resulting from diaphragm flexibility in Loma Prieta earthquake, 1989 (EERI, 1990).

14.4 RECOMMENDATIONS

The multi-storeyed reinforced concrete buildings with vertical irregularities like soft storey, mass irregularities, floating box construction should be designed on the basis of dynamic analysis and inelastic design. The proper effect of these irregularities can be accounted by 3-D mathematical modeling of the building and dynamic analysis. The ductility provisions are most important in such situations. More care is necessary at the time of planning for reducing irregularities. The torsional effects in a building can be minimised by proper location of vertical

resisting elements and mass distribution. Shear walls should be employed for increasing stiffness where necessary and be uniformly distributed in both principal directions.

SUMMARY

There are numerous examples cited in the damage reports of past earthquakes in which the cause of failure of reinforced concrete building has been ascribed to irregularities in configurations. IS 1893 (Part 1): 2002 has identified some of the irregularities in elements of load resisting system, which are mainly categorized as horizontal irregularity and vertical irregularity. Vertical irregularities, referring to sudden change of strength, stiffness, geometry and mass, result in irregular distribution of forces and/or deformation over the height of building while horizontal irregularities refer to asymmetrical plan shapes (e.g. L-, T-, U-, F-) or discontinuities in the horizontal resisting elements (diaphragms) such as cut-outs, large openings, re-entrant corners and other abrupt changes resulting in torsion, diaphragm deformations, stress concentration. The chapter presents the influence of irregularity on performance of building during earthquakes. Some recommendations are presented to account for the effects of these irregularities in analysis and design.

REFERENCES

- [1] "Kocaeli, Turkey, Earthquake Reconnaissance Report", *Earthquake Spectra*, Vol. 16, Earthquake Engineering Research Institute, California, December 1999.
- [2] "Erzincan, Turkey, Earthquake Reconnaissance Report", *Earthquake Spectra*, Supplement to Vol. 9, Earthquake Engineering Research Institute, California, July, 1993.
- [3] "Loma Prieta Earthquake Reconnaissance Report", *Earthquake Spectra*, Supplement to Vol. 6, Earthquake Engineering Research Institute, California, July, 1990.
- [4] Hart, G.C. and Wong, K., *Structural Dynamics for Structural Engineers*, John Wiley & Sons, New York, 2001.
- [5] Moehle, J.P. and Mahin, S.A, "Observation of the Behaviour of Reinforced Concrete Buildings during Earthquake", *Earthquake Resistant Concrete Structures—Inelastic Response and Design*, S.K. Ghosh, (Ed.), American Concrete Institute Publication SP-127, 1991.
- [6] Naeim, F., *Seismic Design Handbook*, 2nd ed., Kluwer Academic Publishers, 2001.
- [7] Penelis, G.G. and Kappos, A.J. *Earthquake-Resistant Concrete Structures*, E & FN SPON, an Imprint of Chapman & Hall, 1997.
- [8] *The Mexico Earthquakes—1985*, Michael A. Cassaro and Martinez Romero (Eds.), American Society of Civil Engineers, New York, 1985.
- [9] Vukazich, S.E., *The Apartment Owner's Guide to Earthquake Safety*, San Jose State University, 1998.

Chapter 15

Seismoresistant Building Architecture

15.1 INTRODUCTION

Rational studies along with a knowledge regarding the performance of buildings in earthquakes show that the building architectural design would create maladjustments in building space-forming elements that would not only decrease the seismoresistant capacity of the building but also become the cause of collapse of the building. It is believed that a structural analysis in itself is not sufficient to ensure the seismoresistant stability of the buildings. An integral seismoresistant system must be necessary, in which all components of the buildings can positively interact during the seismic action. A real compatibility between the architectural and the structural design avoids a stepping of the seismoresistant capacity of the building and also provides a positive, efficient and integral seismic resistant system. Several studies and recommendations have been carried out to avoid situations affecting negatively the building's earthquake resistant behaviour. These studies enable architects to develop a systematic study and a methodology to be applied to the architectural design of buildings to optimize earthquake resistant capacity. This study is called seismoresistant building architecture. The main objective of seismoresistant building architecture is to prevent stepping of seismoresistant capacity of building and to optimize seismoresistance. The major aspects involved in seismoresistant building construction are: (i) selection of load resisting system; (ii) its configuration system; (iii) its basic dynamic characteristics and (iv) its construction quality. The present chapter will discuss all these aspects in detail.

15.2 LATERAL LOAD RESISTING SYSTEMS

The first step in architectural planning of a building is to select the lateral load resisting system. The load resisting system must be of closed loops, so that it is able to transfer all the forces acting either vertically or horizontally to the ground. Bureau of Indian Standards (BIS) has approved three major types of lateral force resisting system in the code IS 1893 (Part 1): 2002.

These consist of moment resisting *building frame system*, *bearing wall system* and *dual system*. These systems are further subdivided into types of construction material used. **Table 7 of IS 1893 (Part 1): 2002** lists the different framing system and response reduction factors. Response reduction factor (R) is basically an indicator of the performance of the structure in earthquakes. A low value of R (=1.5) indicates an extremely earthquake prone building *i.e.* unreinforced masonry wall buildings and a high value of R (= 5) indicates an earthquake-resistant type building like special moment resistant reinforced concrete frame or shear wall buildings.

15.2.1 Moment Resisting Frame

In building frame system, the members shown in Figure 15.11(a) (columns and beams) and joints of frame are resisting the earthquake forces, primarily by flexure. This system is generally preferred by architects because they are relatively unobtrusive compared to the shear walls or braced frames, but there may be poor economic risk unless special damage control measures are taken. Slab column frames are not recommended as a lateral load resisting system.

15.2.2 Building with Shear Wall or Bearing Wall System

This system supports all or most of the gravity loads as well as lateral loads. In general, a bearing wall system has a comparably lower value for R since the system lacks redundancy and has a poor inelastic response capacity see Figure 15.1(b). In severe seismic zones, these bearing wall systems are required to be specially detailed as per IS 4326: 1993. This system is not much preferred by the architects.

15.2.3 Building with Dual System

This system consists of shear wall (or braced frame) and moment resisting frame such that (i) the two systems are designed to resist the total design force in proportion to their lateral stiffness considering the interaction of the dual system at all floor levels; and (ii) the moment resisting frames are designed to independently resist at least 25% of design seismic base shear. In general, a dual system comparably has a higher value of R since a secondary lateral support system is available to assist the primary nonbearing lateral support system as shown in Figure 1(c). This system is somewhat less restrictive architecturally.

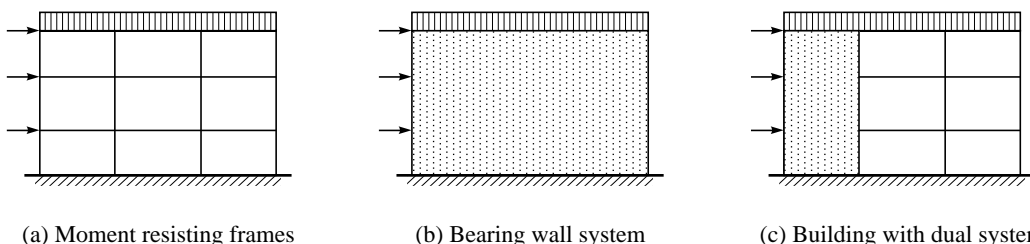
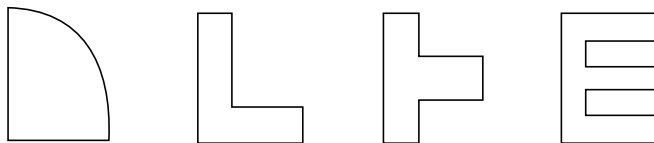


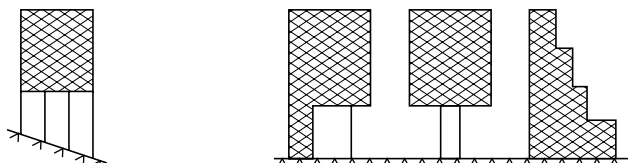
FIGURE 15.1 Different types of building systems.

15.3 BUILDING CONFIGURATION

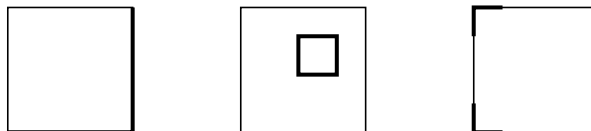
The second step in seismoresistant construction is the configuration of load resisting system of buildings. IS 1893 (Part 1): 2002 has recommended building configuration system in **Section 7** for the better performance of buildings during earthquakes. An important feature in building configuration is its regularity and symmetry in horizontal and vertical plane. Seismic behaviour of irregular shaped plans (Figure 15.2) differs from regular shapes because the first can be subjected to their asymmetry and/or can present local deformations due to the presence of reentrant corners or excessive openings. Both effects give origin to undesired stress concentrations in some resisting members of the building. On the contrary, the ideal rectangular or square plan, structurally symmetric, with enough in-plane stiffness in its diaphragm, presents an ideal behaviour, because it has the same displacement at every point in the slab (Ravan and Lopez, 1996). Therefore, building shaped like a box, such as rectangular, both in plan and elevation, is inherently stronger than one that is L-shaped or U-shaped, that is a building with wings.



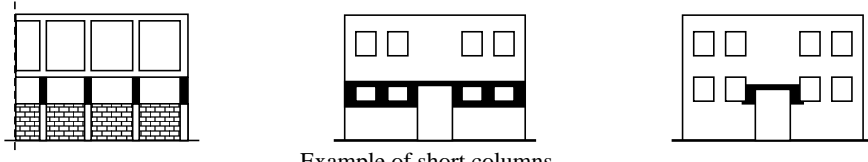
Example of plan irregularity



Example of vertical irregularity



Example of highly torsional configuration



Example of short columns

FIGURE 15.2 General building configuration problems (BIA 1996).

15.3.1 Problems and Solutions

Table 15.1 illustrates the problems associated with the configuration of building and its possible remedial measures (Arnold and Elsesser, 1980).

TABLE 15.1 Building Configurations: Problems and Solutions (Arnold and Elsesser, 1980)

<i>Architectural problems</i>	<i>Structural problems</i>	<i>Remedial measures</i>
Extreme height/depth ratio	High overturning forces, large drift causing non-structural damage, foundation stability	Revise proportion or special structural system
Extreme plan area	Built-up large diaphragm forces	Subdivide building by seismic joints
Extreme length depth ratio	Built-up of large lateral forces in perimeter, large differences in resistance of two axes Experience greater variations in ground movement and soil conditions	Subdivide building by seismic joints
Variation in perimeter strength-stiffness	Torsion caused by extreme variation in strength and stiffness	Add frames and disconnect walls, or use frames and lightweight walls
False symmetry	Torsion caused by stiff asymmetric core	Disconnect core, or use frame with non-structural core walls
Re-entrant corners	Torsion, stress concentrations at the notches	Separate walls, uniform box, centre box, architectural relief, diagonal reinforcement
Mass eccentricities	Torsion, stress concentrations	Reprogram, or add resistance around mass to balance resistance and mass
Vertical setbacks and reverse setbacks	Stress concentration at notch, different periods for different parts of building, high diaphragm forces to transfer at setback	Special structural systems, careful dynamic analysis
Soft storey frame	Causes abrupt changes of stiffness at point of discontinuity	Add bracing, add columns, braced
Variation in column stiffness	Causes abrupt changes of stiffness, much higher forces in stiffer columns	Redesign structural system to balance stiffness
Discontinuous shear wall	Results in discontinuities in load path and stress concentration for most heavily loaded elements	Primary concern over the strength of lower level columns and connecting beams that support the load of discontinuous frame
Weak column-strong beam	Column failure occurs before beam, short column must try and accommodate storey height displacement	Add full walls to reduce column forces, or detach spandrels from columns, or use light weight curtain wall with frame
Modification of primary structure	Most serious when masonry in-fill modifies structural concept, creation	Detach in-fill, or use light-weight materials

Contd.

TABLE 15.1 Contd.

<i>Architectural problems</i>	<i>Structural problems</i>	<i>Remedial measures</i>
Building separation (Pounding)	of short, stiff columns result in stress concentration	Ensure adequate separation, assuming opposite building vibrations
Coupled	Possibility of pounding dependent on building period, height, drift, distance	Design adequate link
Random Openings	Incompatible deformation between walls and links	Careful designing, adequate space for reinforcing design
	Seriously degrade capacity at point of maximum force transfer	

15.4 BUILDING CHARACTERISTICS

The seismic forces exerted on a building are not externally developed forces like wind instead they are the response of cyclic motions at the base of a building causing accelerations and hence inertia force. The response is therefore essentially dynamic in nature. The dynamic properties of the structure such as natural period, damping and mode shape play a crucial role in determining the response of building. Besides, other characteristics of the building system also affect the seismic response such as ductility, building foundation, response of non-structural elements etc. The effects of building's characteristics on its seismic performance are described as follows.

15.4.1 Mode Shapes and Fundamental Period

The elastic properties and mass of building causes to develop a vibratory motion when they are subjected to dynamic action. This vibration is similar to vibration of a violin string, which consists of a fundamental tone and the additional contribution of various harmonics. The vibration of a building likewise consists of a fundamental mode of vibration and the additional contribution of various modes, which vibrates at higher frequencies. In low-rise building (say less than five-storey high) the seismic response depends primarily on the fundamental mode of vibration; accordingly, the period of vibration of this mode, expressed in seconds, is one of the most representative characteristics of the dynamic response of a building. On the basis of time period, building may be classified as rigid ($T < 0.3$ sec), semi-rigid ($0.3 \text{ sec} < T < 1.0$ sec) and flexible structure ($T > 1.0$ sec). Buildings with higher natural frequencies, and a short natural period, tend to suffer higher accelerations but smaller displacement. In the case of buildings with lower natural frequencies, and a long natural period, this is reversed: the buildings will experience lower accelerations but larger displacements. Fundamental period of vibration can be determined by the code based empirical formulas and fundamental modes of the building may be determined by any one of the several methods developed for the dynamic analysis of structures.

15.4.2 Building Frequency and Ground Period

Inertial forces generated in the building depend upon the frequencies of the ground on which the building is standing and the building's natural frequency. When these are near or equal to one another, the building's response reaches a peak level. In some circumstances, this dynamic amplification effect can increase the building acceleration to a value, which may be double or more than that of the ground acceleration at the base of the building. Past studies show that the predominant period at a firm ground site is typically in the range 0.2–0.4 sec while the period can reach 2 sec or more on soft ground. Since building structures have fundamental periods of approximately $0.1 N$ (where N is the number of storeys), it can be concluded that if the foundation soil is firm, rigid structure will have more unfavourable seismic response than flexible structures, whereas the seismic response of flexible structures on soft foundation sites will be less favourable than that of rigid structure. A spectacular example was in Mexico city during 1985 earthquake, which saw enormous damage in medium height buildings of 10–20 storeys, which have periods matching the 2 sec period of the earthquake motions in the city centre, while adjacent low re-rise buildings, with much shorter periods, were proportionately far less damaged. Similar site effects are observed in most damaging earthquakes (Booth, 1994).

15.4.3 Damping

The degree of structural amplification of the ground motion at the base of the building is limited by structural damping. Therefore, damping is the ability of the structural system to dissipate the energy of the earthquake ground shaking. Since the building response is inversely proportional to damping. The more damping a building possesses, the sooner it will stop vibrating—which of course is highly desirable from the standpoint of earthquake performance. There is no numerical method available for determining the damping. It is only obtained by experiments. In a structure, damping is due to internal friction and the absorption of energy by the building's structural and non-structural elements. Today, some of the more advanced techniques of earthquake resistant design and construction employ added damping devices like shock absorbers to increase artificially the intrinsic damping of a building and so improve its earthquake performance.

15.4.4 Ductility

Ductility is defined as the capacity of the building materials, systems, or structures to absorb energy by deforming in the inelastic range. The safety of the building from collapse is on the basis of energy, which must be imparted to the structure in order to make it fail. In such instance, consideration must be given to structure's capacity to absorb energy rather than to its resistance. Therefore ductility of a structure in fact is one of the most important factors affecting its earthquake performance. The primary task of an engineer designing a building to be earthquake resistant is to ensure that the building will possess enough ductility. Although there are as yet no clearly defined methods for determining the ductility of a structure, it is useful to clarify the concept, so that at least a relative appreciation of its importance can be attained. The greater energy is required causing a structure to fail, the greater is its ductility. The ductility of a structure depends on the type of material used and also the structural characteristics of the

assembly. It is possible to build ductile structures with reinforced concrete if care is taken during designing to provide the joints with sufficient abutments that can adequately confine the concrete, thus permitting it to deform plastically without breaking. It is also important for this purpose to ensure that the tension edges of the structure are adequately reinforced and that there are sufficient stirrups to ensure that concrete is properly confined along the compression edge. For example, in columns, due to combined effect of flexure and axial produces a flexural compression failure mode in which failure takes place near the column ends and buckling of longitudinal reinforcement. This can be eliminated by providing the lateral reinforcement in the region of plastic deformation as per IS 13920: 1993.

15.4.5 **Seismic Weight**

Seismic forces are proportional to the building weight and increases along the height of the building. Weight reduction can be obtained by using lighter materials or by relocation of heavy weight such as file racks, libraries, swimming pools etc., at lower levels. For example, if a load P placed at fifth level, the overturning moment becomes 25 times greater than P placed at the first level. Besides, the seismic shear affects from level 1 to 5, whereas, in the second case, only the first level is affected but to a lesser extent (5 times less).

15.4.6 **Hyperstaticity/Redundancy**

In general, hyperstatic (statically indeterminate) structures have advantage because if primary system yields or fails, the lateral force can be redistributed to secondary elements or system to prevent progressive failure (alternate load path). Moreover, hyperstaticity of the structure causes the formation of plastic hinges that can absorb considerable energy without depriving the structure of its stability. Therefore, the redundancy of hyperstatic structure is highly desirable characteristic for earthquake resistant design.

15.4.7 **Non-structural Elements**

The non-structural damage problem is particularly difficult to deal with because the non-structural components that are subjected to seismic forces are not normally within the design scope of the structural engineer, whose responsibility is to provide the seismic safety of the building. In addition, non-structural components—such as partition walls—are often added after the initial building design, and the original architect, or an architect at all, is often not involved. Finally, non-structural components remain uninvolved in the building design and become the source of damage. In general, non-structural damage is caused in two ways. The component may be directly affected by ground motion transmitted by the main structure of the building and be subjected to accelerations and consequent inertial forces in similar way to the building structure. Alternatively, the non-structural components may be affected by the movement or distortion in the structural elements that support or abet the element. These two causes can be summarized as acceleration or drift related damage.

Methods of mitigating the damage to nonstructural components must recognize the probable mode of failure, whether through inertial forces or movement of failure in backing

or abetting structures. For the former, non-structural components must be designed and detailed in a similar way to the building structure, using an analysis of forces to determine bracing support requirements. For the latter, separation from backup or abutting structures is necessary. Mechanical, electrical, and plumbing distribution system must be secured to the building structure, with allowances for differential movement where applicable.

15.4.8 Foundation Soil/Liquefaction

Knowledge of the foundation soil is essential to correct earthquake-resistant design. In some cases a soil behaving well under static loads will pose serious problems under seismic loads. Problems related to foundation soil can be classified mainly in two groups: (i) influence of subsoil on the characteristics of seismic movement, landslides and loss of soil resistance (liquefaction), these problems are not significantly affected by the structures and their foundations and (ii) problems caused by the loads transmitted to the soil by foundations and the settling of the foundations under static and seismic loads. This problem generally arises in loose unsaturated granular soils, which may be compacted as a result of earthquake.

The liquefaction of the soil is most common feature in an earthquake. This phenomenon of loss of resistance is generally occurred in saturated granular soil. At Niigata, Japan, in 1964 subsoil of the loose saturated sand underwent a considerable loss of resistance during an earthquake, as a result, many buildings were damaged, severely undermined and in extreme cases, completely toppled.

15.4.9 Foundations

Foundation of the building is subjected to earthquake stresses; the following major recommendation on structural design must be borne in mind

- (i) Foundation should preferably be designed as continuous (mat or raft) in order to avoid relative horizontal displacement
- (ii) In case of isolated footing, they should be joined to each other by means of foundation beams or ties. These ties should be designed such that it will bear tension and compression forces.
- (iii) It is recommended that parts of building foundations, which rest on soils of different types or are sunk to different depths, should be designed as separate units. In such cases there should also be structural independence in the superstructure.
- (iv) It is recommended that if different parts of the building are to be structurally independent because of the shape of their ground plan; their foundations should also be independent.

15.5 QUALITY OF CONSTRUCTION AND MATERIALS

One of the main factors responsible for stepping of seismoresistant capacity of building is its quality of materials and workmanship of construction. The industrially produced materials used

in construction such as cement, reinforcement, brick etc. should satisfy minimum standards of quality and resistance, which can only be guaranteed by the manufacturers. Besides that, quality of concrete, faulty execution of construction joint, and detailing reinforcement are also affecting the performance of structure. The factors affecting the seismoresistant capacity of building are described as follows. By proper inspection programme their effect could be minimized.

15.5.1 Quality of Concrete

Grade of concrete specified in design documents may not be developed during construction mainly due to

- incorrect proportioning
- insufficient mixing which causes segregation
- aggregates with excessive impurities or improper grading
- excessive high water/cement ratio

15.5.2 Construction Joints

A defective concrete joint, which contributed significantly to causing of failure of many buildings in past earthquakes is due to

- poor execution of the construction joint/discontinuity
- not located at the points specified by the designer
- accumulation of sawdust, dust and loose materials at the surface of joint

15.5.3 General Detailing Requirements

Stepping of seismoresistant capacity of the building is due to

- amount of reinforcement is not placed as specified in design
- insufficient concrete cover to reinforcement results resting in reinforcing bar and cracks in surface concrete
- proper placing of reinforcement during casting
- improper confinement and large tie spacing especially in plastic hinge region
- insufficient confinement and anchorage length at joints
- insufficient splicing length of longitudinal reinforcement in columns or splicing of all bars at the same cross section
- accumulation of splices just above a concrete joint or in plastic hinge zone
- splicing of tension reinforcement in beams and columns in region of tension or reversing stress
- the end of lateral reinforcement should be bent at 135 degree
- use of high resistance steel in relatively low-resistance concrete
- curves in reinforcement cause thrust in concrete when the bar is subjected to tension and compression

SUMMARY

Seismic safety of a building is an interdisciplinary endeavour involving a close cooperation and co-efforts of architects and structural engineers adopting mutually suitable architectural and structural schemes. The seismic analysis and design alone do not ensure good performance of the structure during earthquakes. The building framing system should also conform to the principles of earthquake resistant configuration. The chapter presents structural requirements for building system regarding its selection of load resisting system, configuration system, dynamic characteristics and finally construction quality that are essential for enhancing the seismoresistant capacity of the structure. This will help in eliminating most of the vulnerabilities in the structural system at the conceptual design stage itself.

REFERENCES

- [1] Arnold, Christopher and Elsesser, Eric, "Building Configuration: Problems and Solutions", *Seventh World Conference on Earthquake Engineering*, 1980.
- [2] Arnold, Christopher, "Building Configuration: Characteristics for Seismic Design", *Seventh World Conference on Earthquake Engineering*, 1980.
- [3] Arnold, Christopher, "Architectural Aspects of Seismic Resistant Design", *Eleventh World Conference on Earthquake Engineering*, 1996.
- [4] Arnold, Christopher, "The Seismic Response of Nonstructural Elements in Building", *Bulletin of the New Zealand National Society for Earthquake Engineering*, Vol. 24, No. 4, December, 1991.
- [5] Booth, E., "Concrete Structures in Earthquake Regions", *Longman Scientific and Technical*, Longman Group UK Limited, 1994.
- [6] BIA., "The Assessment and Improvement of the Structural Performance of Earthquake Risk Buildings", *New Zealand National Society for Earthquake Engineering*, June, 1996.
- [7] Giuliani, H., Rodriguez, V.I., Yacante, M.I., Campora, A.M. and Giuliani, H.L., "Seismic Resisting Architecture on Building Scale", *Eleventh World Conference on Earthquake Engineering*, 1996.
- [8] Giuliani, H., "Seismic Resisting Architecture: A Theory for the Architectural Design of Buildings in Seismic Zones", *Twelfth World Conference on Earthquake Engineering*, 2000.
- [9] Raven, E. and Lopez, O.A., "Regular and Irregular Plan Shape Buildings in Seismic Regions: Approaching to an Integral Evaluation", *Eleventh World Conference on Earthquake Engineering*, 1996.

PART IV

Seismic Analysis and Modelling of Reinforced Concrete Building

Chapter 16

Code Based Procedure for Determination of Design Lateral Loads

16.1 INTRODUCTION

Earthquake and its occurrence and measurements, its vibration effect and structural response have been continuously studied for many years in earthquake history and thoroughly documented in literature. Since then the structural engineers have tried hard to examine the procedure, with an aim to counter the complex dynamic effect of seismically induced forces in structures, for designing of earthquake resistant structures in a refined and easy manner. This re-examination and continuous effort has resulted in several revisions of Indian Standard: 1893: (1962, 1966, 1970, 1975, 1984, 2002) code of practice on the “*Criteria for Earthquake Resistant Design of Structures*” by the Bureau of Indian Standards (BIS), New Delhi. In order to properly interpret the codes and their revisions, it has become necessary; that the structural engineers must understand the basic design criteria and procedures for determining the lateral forces. Various approaches to seismic analysis have been developed to determine the lateral forces, ranging from purely linear elastic to non-linear inelastic analysis. Many of the analysis techniques are being used in design and incorporated in codes of practices of many countries. However, this chapter is restricted to the method of analysis described or employed in IS 1893 (Part 1): 2002 of “*Criteria for Earthquake Resistant Design of Structures*” essentially to buildings although in some cases that may be applied to other types of structures as well.

16.2 SEISMIC DESIGN PHILOSOPHY

The philosophy of seismic design can be summarized as:

- (a) The design philosophy adopted in the code is to ensure that structures possess at least a minimum strength to
 - (i) resist minor earthquake (< DBE), which may occur frequently, without damage;

- (ii) resist moderate earthquake (DBE) without significant structural damage through some non-structural damage;
- (iii) resist major earthquake (MCE) without collapse.

"Design Basis Earthquake (DBE) is defined as the maximum earthquake that reasonably can be expected to experience at the site once during lifetime of the structure. The earthquake corresponding to the ultimate safety requirements is often called as Maximum Considered Earthquake (MCE). Generally, the DBE is half of MCE".

- (b) Actual forces that appear on structures during earthquakes are much higher than the design forces specified in the code. It is recognized that the complete protection against earthquakes of all sizes is not economically feasible and design based alone on strength criteria is not justified. The basic criteria of earthquake resistant design should be based on lateral strength as well as deformability and ductility capacity of structure with limited damage, but no collapse. Ductility in the structures will arise from inelastic material, behaviour and detailing of reinforcement in such a manner that brittle failure is avoided and ductile behaviour is induced by allowing steel to yield in controlled manner. Therefore, the gap between the actual and design lateral forces is narrowed down by providing ductility in the structure and additional reserve strength in structures over and above the design strength.
- (c) The design lateral forces specified in the code shall be considered in each of the two orthogonal directions of the structure. For structures, which have lateral force resisting elements in the two orthogonal directions only, the design lateral force shall be considered along one direction at a time, and not in both directions simultaneously. Structures, having lateral force resisting elements in direction other than the two orthogonal directions, shall be analysed considering the load combination as specified in clause 6.3 of IS 1893 (Part 1): 2002.
- (d) Earthquake generated vertical inertia forces are to be considered in design unless it is not significant. Vertical acceleration should be considered in structures with large spans, those in which stability is a criterion for design, or for overall stability analysis of structures. Reduction in gravity force due to vertical component of ground motions can be particularly detrimental in case of pre-stressed horizontal members and of cantilevered members. Hence, special attention should be paid to the effect of vertical component of the ground motion on pre-stressed or cantilevered beams, girders and slab. Where both horizontal and vertical seismic forces are taken into account, load combination specified in the code shall be considered.
- (e) The response of a structure to ground vibrations is a function of the nature of foundation soil; materials, form, size and mode of construction of structures; and the duration and characteristics of ground motion. This code specifies design forces for structures standing on rock or firm soils, which do not liquefy or slide due to loss of strength during ground vibrations.

16.3 DETERMINATION OF DESIGN LATERAL FORCES

The procedures recommended for the determination of lateral force in the code are based on the approximation effects, yielding can be accounted for linear analysis of the building using

the design spectrum. This analysis is carried out by either *modal analysis procedure* or *dynamic analysis procedure* (Clause 7.8 of IS 1893 (Part 1): 2002). A simplified method may also be adopted that will be referred as lateral force procedure (Clause 7.5 of IS 1893 (Part 1): 2002) also recognised as equivalent lateral force procedure or equivalent static procedure in the literature. The main difference between the equivalent lateral force procedure and dynamic analysis procedure lies in the magnitude and distribution of lateral forces over the height of the buildings. In the dynamic analysis procedure the lateral forces are based on the properties of the natural vibration modes of the building, which are determined by the distribution of mass and stiffness over height. In the equivalent lateral force procedures the magnitude of forces is based on an estimation of the fundamental period and on the distribution of forces, as given by simple formulas appropriate for regular buildings. Otherwise the two procedures have similar capabilities and are subject to the same limitation.

16.3.1 Equivalent Lateral Force Procedure

As discussed in the previous section that the equivalent lateral force procedure is the simplest method of analysis and requires less computational effort because, the forces depend on the code based fundamental period of structures with some empirical modifier. The design base shear shall first be computed as a whole, than be distributed along the height of the buildings based on simple formulas appropriate for buildings with regular distribution of mass and stiffness. The design lateral force obtained at each floor level shall then be distributed to individual lateral load resisting elements depending upon floor diaphragm action. In case of rigid diaphragm (reinforced concrete monolithic slab-beam floors or those consisting of prefabricated/precast elements with topping reinforced screed can be taken as rigid diaphragm) action, the total shear in any horizontal plane shall be distributed to the various elements of lateral force resisting system on the basis of relative rigidity (Clause 7.7.2 of IS 1893(Part 1): 2002). The following are the major steps for determining the forces by equivalent static procedures.

Determination of base shear

The total design lateral force or design base shear along any principal direction shall be determined by the following expression, Clause 7.5 of IS 1893 (Part 1): 2002.

$$V_B = A_h W$$

where,

A_h = Design horizontal seismic coefficient for a structure

W = Seismic weight of building

A_h shall be determined by the following expression:

$$A_h = (Z/2)(I/R)(S_a/g)$$

Note: The value of A_h will not be taken less than $Z/2$ whatever the value of (I/R) .

In factor $(Z/2)$, Z is the Zone factor given in **Table 2 of IS 1893 (Part 1): 2002**, for the Maximum Considered Earthquake (MCE) and service life of structure in a Zone. The factor 2 in the denominator of Z is used so as to reduce the Maximum Considered Earthquake (MCE) zone factor to the factor for Design Basis Earthquake (DBE). Z can also be determined from the seismic zone map of India, shown in **Figure 1 of IS 1893 (Part 1): 2002**, which segregates

the country in various areas of similar probable maximum intensity ground motion. The maximum intensity is fixed in such a way that the lifeline/critical structures will remain functional and there is low probability of collapse for structures designed with the provisions provided in the code even for an event of occurrence of earthquake with higher intensity. The values of Z ranges from 0.10 to 0.36 corresponding to Zone II to Zone V. This map has divided the whole country into four zones starting from Zone II to V. The Intensity as per Comprehensive Intensity Scale (MSK 64) broadly associated with the various zones is VI (or less), VII, VIII and IX (and above) for Zones II, III, IV and V respectively. In Zone II, low seismic intensity zone where minor damage could occur has a Z value of 0.10. Zone III ($Z = 0.16$), moderate intensity zone where moderate damage could occur. Zone IV ($Z = 0.24$), severe intensity zone where major property damage could occur and Zone V ($Z = 0.36$), very severe intensity zone that lies in close proximity to certain prescribed major fault systems.

In factor (I/R), I is the *importance factor*, depending upon the functional use of the structures, characterised by hazardous consequences of its failure, post earthquake functional needs, historic value, or economic importance. The **minimum values of importance factor** are given in **Table 6 of IS 1893 (Part 1): 2002**. According to Table 6, buildings are classified in two categories: (i) important service and community buildings and (ii) all other buildings. Important service buildings have an I factor 1.5, and all other buildings are assigned a value of 1.0. The value of I may be more than the assigned value as proposed in Table 6, depending upon economy, strategy considerations like multi-storey buildings, hazardous consequences etc. Essential facilities refer to those buildings of structures that must be safe and usable for emergency purpose after a major earthquake has occurred in order to preserve the peace, health, and safety of general public.

R is the **response reduction factor**, depending on the perceived seismic damage performance of the structure, characterised by ductile or brittle deformations. This characteristic represents the structure's ductility, damping as well as the past seismic performance of structure with various structural framing systems. In actual, the need for incorporation of factor R in base shear formula is an attempt to consider the structure's inelastic characteristics in linear analysis method since it is undesirable as well as uneconomical that a structure will be designed on the basis that it will remain in elastic range for all major earthquakes. A limited inelastic yielding must be allowed to the structure by considering that its vertical load carrying capacity and endangering life safety should not be impairing. The inelastic characteristics include (i) inelastic deformation and its changing pattern as yielding progresses, (ii) the damping characteristics of the yielding elements, and (iii) the variation in stiffness and period of the structure as yielding progresses. In this way, the base shear equation produces force levels that are probably more nearly representative of those occurring in an actual structure. It is achieved by applying those base shears for linear design that are reduced by a factor $1/R$ from those that would be obtained from fully elastic response. Experiments and performance of structure during earthquake have shown that the structure designed for those reduced force level perform adequately, if properly detailed. The value of R increases with the increase of structural ductility and its energy dissipation capacity and degree of redundancy. The factor R is assigned to different types of building structures generally on the basis of empirical or semi-empirical judgement, experience with building performance in past earthquakes, on analytical and experimental studies and on calibration with force levels in codes. The values of R are prescribed in **Table 7 of IS 1893 (Part**

1): 2002 for different types of building systems. Table 7 shows a low value of R approaching 1.5 assigned to an extremely brittle building *i.e.* unreinforced masonry wall buildings and a high value of R (= 5) is assigned to a more ductile structure like special moment resistant frame reinforced concrete or shear wall buildings. The response reduction factor R is also known by the name response modification factor (ATC -3, UBC, NEHRP) or behaviour factor (q -factors) in EC8.

S_a/g is the Average response acceleration coefficient for rock or soil sites as given by **Figure 2 of IS 1893 (Part 1): 2002** and by the equations describe in clause 6.0 for different soil condition based on appropriate natural periods of the structure. These values are given for 5% of damping of the structure; for other value of damping it is modified according to Table 3 of IS 1893 (Part 1): 2002. These curves represent free field ground motion.

The fundamental natural period for buildings are given in **Clause 7.6 of IS 1893 (Part 1): 2002** and it is summarized as:

$T_a = 0.075h^{0.75}$	moment resisting RC frame building without brick infill walls
$T_a = 0.075h^{0.75}$	moment resisting steel frame building without brick infill walls
$T_a = 0.075h/\sqrt{d}$	all other buildings including moment resisting RC frame building with brick infill walls

h is the height of building in m and d is the base dimension of building at plinth level in m, along the considered direction of lateral force.

W is the Seismic weight of building which is the sum of the seismic weight of floors. The seismic weight at any floor level would be equal to dead weight of the floor system plus weight of column and walls in inverse proportion to its distance from the floors plus appropriate amount of imposed load as specified in **Clause 7.3 of IS 1893 (Part 1): 2002**. Imposed load on roof level need not be considered. The basic reasons for considering the percentage of live load as specified in **Table 8 of IS 1893 (Part 1): 2002** are (i) only a part of the maximum live load will probably be existing at the time of earthquake, (ii) non-rigid mounting of the live load absorbs part of the earthquake energy and (iii) specified live load include as part of it, impact effect of the loads which need not be considered since earthquake loads act on the mass only.

Lateral distribution of base shear

The computed base shear is now distributed along the height of the building. The shear force, at any level, depends on the mass at that level and deforms shape of the structure. Earthquake forces deflect a structure into number of shapes, known as the *natural mode shapes*. Number of natural mode shapes depends upon the degree-of-freedom of the system. Generally, a structure has a continuous system with infinite degree-of-freedom. From structural idealisation we convert an infinite degree-of-freedom to finite degree of freedom system. For example, a multi-storeyed building has been idealised into lumped mass model by assuming the mass of the building lumped at each floor level (called node); with one degree of freedom in the direction of lateral displacement in which the structure is being analysed per floor, resulting in as many degree of freedom as the number of floors. Therefore, a multi-storeyed building has a multiple-degree of freedom system with many possible patterns of deformations. The magnitude of the lateral force at a particular floor (node) depends on the mass of that node, the distribution of

stiffness over the height of structure, and the nodal displacements in a given mode. The actual distribution of base shear over the height of the building is obtained as the superposition of all the modes of vibration of the multiple-degree-of-freedom system.

In equivalent lateral force procedure, the magnitude of lateral forces is based on the fundamental period of vibration, the other periods and shapes of natural modes are not required. IS 1893 (Part 1): 2002 uses a parabolic distribution (Paz, 1994) of lateral force along the height of building as per the following expression

$$Q_i = V_B \frac{W_i h_i^2}{\sum_{i=1}^n W_i h_i^2}$$

where,

Q_i = Design lateral force at floor i

W_i = Seismic weight of floor i ,

h_i = Height of floor i measured from base, and

n = Number of stories in the building is the number of levels at which masses are located.

Example 1 A four-storey reinforced concrete frame building as shown, is situated at Roorkee. The height between the floors is 3 m and total height of building is 12 m. The dead load and normal live load is lumped at respective floor. The soil below the foundation is assumed to be hard rock. Assume building is intended to be used as a hospital. Determine the total base shear as per IS 1893 (Part 1): 2002 and compare with the earlier IS: 1893 codes. Distribute the base shear along the height of the building.

Determination of Base Shear as per IS 1893 (Part 1): 2002

The Total Seismic Base Shear is given by

$$V_B = A_h W$$

A_h = Design horizontal acceleration spectrum values and it is determined by the following expression

$$A_h = \frac{Z}{2} \frac{I}{R} \frac{S_a}{g} = \frac{0.24}{2} \frac{1.5}{5} 2.06 = 0.074$$

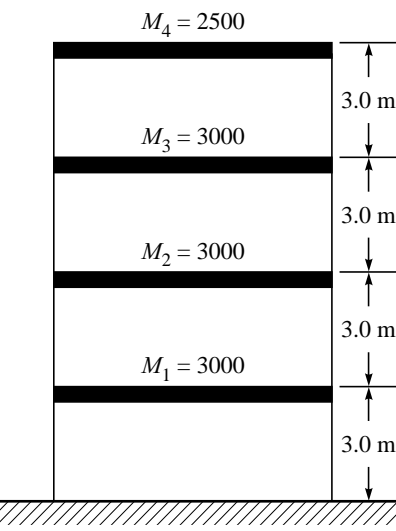
Z (Zone factor) = 0.24 (Roorkee is in Zone IV as per IS 1893 (Part1): 2002)

I (Importance Factor) = 1.5, building is used as a hospital

R (Response Reduction Factor) = 5.0 (Assume Special RC Moment Resisting Frame)

S_a/g (Spectral Acceleration) = 2.06 ($T = 0.075 \text{ } h^{0.75} = 0.075 \text{ } 12^{0.75} = 0.484$, $S_a/g = 1/T$ for hard soil)

The total seismic weight of building (W) = $3 \times 3000 + 2500 = 11,500 \text{ kN}$



Building, for example

Building for example.

Total base shear (V_B) = $0.074 \times 11500 = 851$ kN

Determination of Base Shear as per earlier IS: 1893

Total design base shear for the same building is worked out from the earlier version of IS: 1893 as shown below:

IS: 1893–1962

$$V_B = \alpha_h W$$

α_h = Horizontal seismic coefficient = $\alpha_h = 0.04 \times 0.535 = 0.02$

K factor to allow for the increased flexibility $K = 0.35 S/(N + 0.9)$
($S=8$) = 0.535

S = total number of stories ($\geq 13 = 13$, N = number of stories = 4

(Roorkee is in zone III as per IS: 1893–1962 and soil is hard)

W = Seismic weight of building = 11,500 kN

$$V_B = 0.02 \times 11500 = 230$$
 kN

Total base shear as per IS: 1893–1962 = 230 kN

IS: 1893–1966

$$V_B = C \alpha_h W$$

C = a coefficient defining the flexibility of structure = 1

$C = 9/(n+5)$ not greater than 1, n = number of stories = 4

$C = 9/(4+5) = 1$

α_h = Horizontal seismic coefficient = 0.05

Roorkee is in zone IV as per IS 1893: 1966 and soil type I i.e hard soil

W = Weight of building = 11500 kN

$$V_B = 1 \times 0.05 \times 11500 = 575$$
 kN

Total base shear as per IS: 1893–1966 = 575 kN

IS: 1893–1970

$$V_B = C \alpha_h \beta W$$

C = a coefficient defining the flexibility of structure = $0.5/T^{1/3}$

$T = (0.1 n) = 0.4$ sec, n = number of stories = 4

$C = 0.676$

β = a coefficient depending upon soil foundation system = 1.0

for rock and hard soil and for all types of foundation

α_h = Horizontal seismic coefficient = 0.05

(Roorkee is in zone IV as per IS: 1893: 1970)

W = Weight of building (total dead load + appropriate amount of live load) = 11500 kN

$$V_B = 0.676 \times 0.05 \times 11500 = 388.7$$
 kN

Total base shear as per IS: 1893–1970 = 388.7 kN

IS: 1893–1975

$$V_B = C \alpha_h W$$

C = a coefficient defining the flexibility of structure

$C = 0.9$ for fundamental period ($T = 0.1 \times n = 0.4$ sec)

α_h = Horizontal seismic coefficient = 0.075

$\alpha_h = \beta I \alpha_0$ (In Seismic Coefficient Method) = $1 \times 1.5 \times 0.05 = 0.075$

$\alpha_0 = 0.05$ since Roorkee is in zone IV as per IS: 1893: 1975

$I = 1.5$ (building is used as a hospital)

$\alpha_h = \beta I F_0 S_a/g$ (In Response Spectrum Method) = $1 \times 1.5 \times 0.25 \times 0.1875 = 0.0703$

F_0 = Seismic zone factor for average acceleration spectra = 0.25 for zone IV

$\beta = 1.0$ for rock and hard soil and for all type of foundation

$S_a/g = 0.1875$ correspond to $T = 0.4$ sec and damping 5%

W = Weight of building (total dead load + appropriate amount of live load) = 11500 kN

$$V_B = 0.9 \times 0.075 \times 11500 = 776.25 \text{ kN}$$

Total base shear as per IS: 1893 – 1975 = 776.25 kN

IS: 1893–1984

$$V_B = K C \alpha_h W$$

K = performance factor depending on the structural framing system and brittleness or ductility of construction = 1.0

C = a coefficient defining the flexibility of structure with increase in number of stories depending upon fundamental time period = 0.9 for $T = 0.4$ sec

K (performance factor) = 1.0

α_h = Horizontal seismic coefficient = 0.075

$\alpha_h = \beta I \alpha_0$ (In Seismic Coefficient Method)
 $= 1 \times 1.5 \times 0.05 = 0.075$

$\alpha_h = \beta I F_0 S_a/g$ (In Response Spectrum Method)
 $= 1 \times 1.5 \times 0.25 \times 0.18 = 0.07$

$\beta = 1.0$ for rock and hard soil and for all types of foundation

I = a coefficient depending upon the importance of structures = 1.5 (building is used as a hospital)

$\alpha_0 = 0.05$ since Roorkee is in zone IV as per IS: 1893: 1984

W = Weight of building = 11500 kN

$$V_B = 0.9 \times 0.075 \times 11500 = 776.25 \text{ kN}$$

$F_0 = 0.25$ for zone IV

$S_a/g = 0.18$ correspond to $T = 0.4$ sec and damping 5%

Total base shear as per IS: 1893 – 1984 = 776.25 kN

Vertical Distribution of Base Shear to Different Floor Levels

The design base shear (V_B) computed shall be distributed along the height of the building as per the following expression

$$Q_i = V_B \frac{W_i h_i^2}{\sum_{i=1}^n W_i h_i^2}$$

Using the above equation, base shear is distributed as follows,

$$\begin{aligned} Q_1 &= V_B \left(\frac{W_1 h_1^2}{W_1 h_1^2 + W_2 h_2^2 + W_3 h_3^2 + W_4 h_4^2} \right) \\ &= 851 \left[\frac{3000 \times 3.0^2}{3000 \times 3^2 + 3000 \times 6^2 + 3000 \times 9^2 + 2500 \times 12^2} \right] = 31.13 \text{ kN} \\ Q_2 &= 851 \left[\frac{3000 \times 6.0^2}{3000 \times 3^2 + 3000 \times 6^2 + 3000 \times 9^2 + 2500 \times 12^2} \right] = 124.53 \text{ kN} \\ Q_3 &= 851 \left[\frac{3000 \times 9.0^2}{3000 \times 3^2 + 3000 \times 6^2 + 3000 \times 9^2 + 2500 \times 12^2} \right] = 280.18 \text{ kN} \\ Q_4 &= 851 \left[\frac{3000 \times 12.0^2}{3000 \times 3^2 + 3000 \times 6^2 + 3000 \times 9^2 + 2500 \times 12^2} \right] = 415.08 \text{ kN} \end{aligned}$$

16.3.2 Dynamic Analysis Procedure

IS 1893 (Part 1): 2002 has recommended the method of dynamic analysis of buildings in section 7.8 in the case of (i) regular building—those higher than 40 m in height in Zones IV and V, and those higher than 90 m in height in Zones II and III, (b) Irregular buildings—all framed buildings higher than 12 m in Zones IV and V, and those higher than 40 m in height in Zones II and III. The purpose of dynamic analysis is to obtain the design seismic forces, with its distribution to different levels along the height of the building and to the various lateral load-resisting elements similar to equivalent lateral force method. The procedure of dynamic analysis described in the Code is valid only for regular type of buildings, which are almost symmetrical in plan and elevation about the axis having uniform distribution of the lateral load resisting elements. It is further assumed that all the masses are lumped at the storey level and only sway displacement is permitted at each storey. The procedure of dynamic analysis of irregular type of buildings should be based on 3D modelling of building that will adequately represent its stiffness and mass distribution along the height of the building so that its response to earthquake could be predicted with sufficient accuracy. The dynamic analysis procedure for regular type of building is divided into several distinctive steps, which are as follows:

Determination of eigen-values and eigen-vectors, clause: 7.8.4.1

Let the shear stiffness of i^{th} storey is k_i and the mass is m_i subjected to an external dynamic force $f_i(t)$ and the corresponding displacement $x_i(t)$ as shown in Figure 16.1. Assuming damping in the system is small, so it may be ignored and the system is analyzed as *undamped system*. Using D'Alembert's principle, the dynamic equilibrium equation of mass at each floor is,

$$m_1 \ddot{x}_1 + k_1 (x_1 - x_0) - k_2 (x_2 - x_1) = f_1(t)$$

$$m_2 \ddot{x}_2 + k_2 (x_2 - x_1) - k_3 (x_3 - x_2) = f_2(t)$$

$$m_3 \ddot{x}_3 + k_3 (x_3 - x_2) - k_4 (x_4 - x_3) = f_3(t)$$

$$m_4 \ddot{x}_4 + k_4 (x_4 - x_3) - k_5 (x_5 - x_4) = f_4(t)$$

.....

.....

$$m_{n-1} \ddot{x}_{n-1} + k_{n-1} (x_{n-1} - x_{n-2}) - k_n (x_n - x_{n-1}) = f_{n-1}(t)$$

$$m_n \ddot{x}_n + k_n (x_n - x_{n-1}) = f_n(t)$$

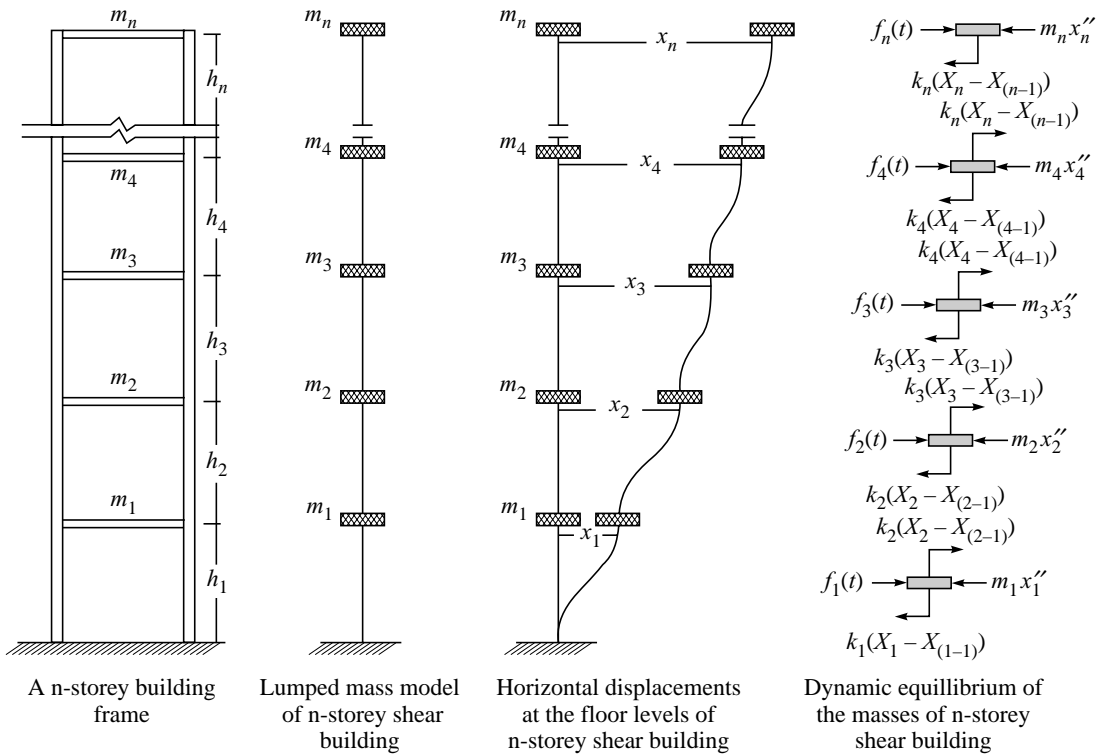


FIGURE 16.1 Dynamic analysis of multi-degree-of-freedom-system (n-storey shear building frame).

Expressing these equations in matrix form

$$\begin{bmatrix} m_1 & 0 & \dots & \dots & \dots & 0 \\ 0 & m_2 & 0 & \dots & \dots & \dots \\ \dots & 0 & m_3 & 0 & \dots & \dots \\ \dots & \dots & 0 & m_4 & 0 & \dots \\ \dots & \dots & \dots & 0 & \dots & 0 \\ 0 & \dots & \dots & \dots & 0 & m_n \end{bmatrix} \begin{bmatrix} \ddot{x}_1 \\ \ddot{x}_2 \\ \ddot{x}_3 \\ \ddot{x}_4 \\ \vdots \\ \ddot{x}_n \end{bmatrix} + \begin{bmatrix} (k_1 + k_2) & -k_2 & 0 & \dots & \dots & 0 \\ -k_2 & (k_2 + k_3) & -k_3 & 0 & \dots & \dots \\ 0 & -k_3 & (k_3 + k_4) & -k_4 & 0 & \dots \\ \dots & 0 & -k_4 & (\dots) & -k_{n-1} & 0 \\ \dots & \dots & 0 & -k_{n-1} & (k_{n-1} + k_n) & -k_n \\ 0 & \dots & \dots & \dots & 0 & -k_n \end{bmatrix} \begin{bmatrix} x_1 \\ x_2 \\ x_3 \\ x_4 \\ \vdots \\ x_n \end{bmatrix} = \begin{bmatrix} f_1 \\ f_2 \\ f_3 \\ f_4 \\ \vdots \\ f_n \end{bmatrix}$$

in which,

$$[M] = \begin{bmatrix} m_1 & 0 & \dots & \dots & \dots & 0 \\ 0 & m_2 & 0 & \dots & \dots & \dots \\ \dots & 0 & m_3 & 0 & \dots & \dots \\ \dots & \dots & 0 & m_4 & 0 & \dots \\ \dots & \dots & \dots & 0 & \dots & 0 \\ 0 & \dots & \dots & \dots & 0 & m_n \end{bmatrix}, [\ddot{X}] = \begin{bmatrix} \ddot{x}_1 \\ \ddot{x}_2 \\ \ddot{x}_3 \\ \ddot{x}_4 \\ \vdots \\ \ddot{x}_n \end{bmatrix}$$

$$[K] = \begin{bmatrix} (k_1 + k_2) & -k_2 & 0 & \dots & \dots & 0 \\ -k_2 & (k_2 + k_3) & -k_3 & 0 & \dots & \dots \\ 0 & -k_3 & (k_3 + k_4) & -k_4 & 0 & \dots \\ \dots & 0 & -k_4 & (\dots) & -k_{n-1} & 0 \\ \dots & \dots & 0 & -k_{n-1} & (k_{n-1} + k_n) & -k_n \\ 0 & \dots & \dots & \dots & 0 & -k_n \end{bmatrix}, [X] = \begin{bmatrix} x_1 \\ x_2 \\ x_3 \\ x_4 \\ \vdots \\ x_n \end{bmatrix}, [F] = \begin{bmatrix} f_1 \\ f_2 \\ f_3 \\ f_4 \\ \vdots \\ f_n \end{bmatrix}$$

The equilibrium equations can be expressed in matrix form as,

$$M\ddot{X} + KX = F$$

where, M and K are called mass and stiffness matrices respectively, which are symmetrical. \ddot{X} , X and F are called acceleration, displacement and force vectors respectively, and all are functions of time (t).

If the structure is allowed to freely vibrate with no external force (vector F is equal to zero) and no damping in simple harmonic motion, then the system represents ***undamped free vibration (Clause 7.8.4.1 of IS 1893 (Part 1): 2002)***. In that case, displacement x can be defined at time t is,

$$x(t) = x \sin(\omega t + \phi)$$

where,

x = amplitude of vibration,

ω = natural circular frequency of vibration

ϕ = phase difference, which depends on the displacement and velocity at time $t = 0$.

Differentiating $x(t)$ twice with respect to time enables the relationship between acceleration and displacement

$$\ddot{x}(t) = -\omega^2 x \sin(\omega t + \phi) = -\omega^2 x(t)$$

Substituting, Equation for free undamped vibration of the MDOF system becomes

$$KX = \omega^2 M X$$

where ω^2 is known as the eigen-value or natural frequencies of the system, defined as,

$$[\omega^2] = \begin{bmatrix} \omega_1^2 & & & \\ & \omega_2^2 & & \\ & & .. & \\ & & & \omega_n^2 \end{bmatrix}$$

This is known as an eigen-value or characteristic value problem.

From the relation that, natural time period, $T = \frac{2\pi}{\omega}$

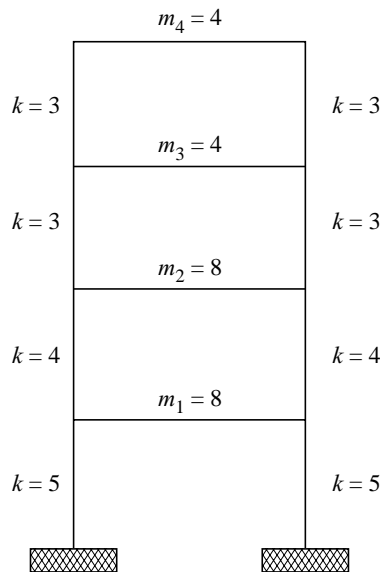
Natural time periods, T are (clause 7.8.4.1)

$$T = \begin{bmatrix} T_1 & 0 & 0 & 0 \\ 0 & T_2 & 0 & 0 \\ 0 & 0 & .. & 0 \\ 0 & 0 & 0 & T_n \end{bmatrix} \text{s}$$

X is known as an eigen-vector/modal vector or mode shape (Clause 7.8.4.1), represented as

$$\{\Phi\} = \{\Phi_1 \Phi_2 \Phi_3 \Phi_4 \dots \Phi_n\}$$

Example 2 Let us consider a one bay four-storey shear building. Taking the masses and columns stiffness of each storey as shown. The summed shear stiffness ($2 \times k_i$) of columns. The stiffness and mass matrix of the entire system are



Stiffness and Mass matrix for the plane frame

$$[K] = \begin{bmatrix} 18 & -8 & 0 & 0 \\ -8 & 14 & -6 & 0 \\ 0 & -6 & 12 & -6 \\ 0 & 0 & -6 & 6 \end{bmatrix}, \quad [M] = \begin{bmatrix} 8 & 0 & 0 & 0 \\ 0 & 8 & 0 & 0 \\ 0 & 0 & 4 & 0 \\ 0 & 0 & 0 & 4 \end{bmatrix}$$

Eigen-values of $[K - \omega^2 M]$, clause: 7.8.4.1

$$[K - \omega^2 M] = \begin{bmatrix} (18 - \omega^2 8) & -8 & 0 & 0 \\ -8 & (14 - \omega^2 8) & -6 & 0 \\ 0 & -6 & (12 - \omega^2 4) & -6 \\ 0 & 0 & -6 & (6 - \omega^2 4) \end{bmatrix}$$

$$[K - \omega^2 M] = (-1)^{(1+1)} (18 - \omega^2 8) \begin{bmatrix} (14 - \omega^2 8) & -6 & 0 & 0 \\ -6 & (12 - \omega^2 4) & -6 & 0 \\ 0 & -6 & (6 - \omega^2 4) & 0 \\ 0 & 0 & 0 & (6 - \omega^2 4) \end{bmatrix}$$

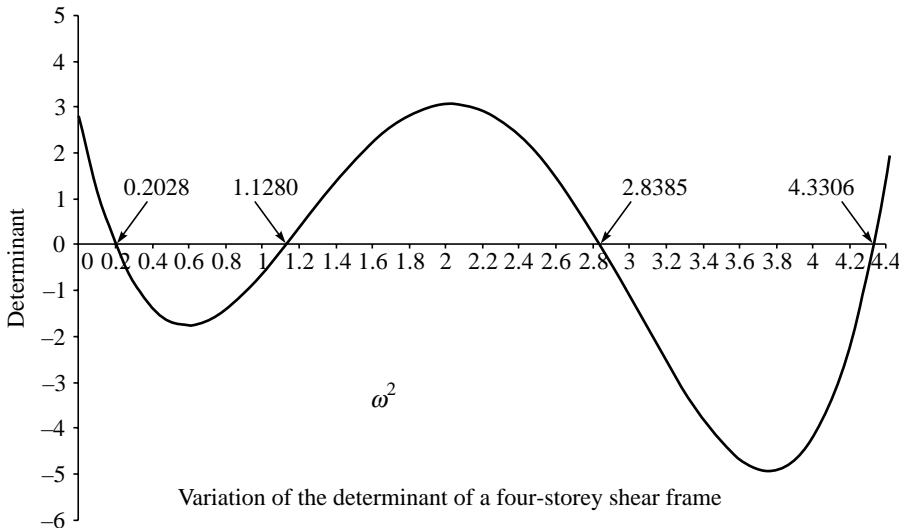
$$+ (-1)^{(1+2)} (-8) \begin{bmatrix} -8 & -6 & 0 & 0 \\ 0 & (12 - \omega^2 4) & -6 & 0 \\ 0 & -6 & (6 - \omega^2 4) & 0 \\ 0 & 0 & 0 & (6 - \omega^2 4) \end{bmatrix}$$

$$[K - \omega^2 M] = \omega^8 - 8.5 \omega^6 + 22.0625 \omega^4 - 18\omega^2 + 2.8125$$

The determinant is a quadratic equation in ω^2 . There are four values of ω^2 for which the determinant $[K - \omega^2 M]$ is zero, they are:

$$\omega_1^2 = 0.2028, \omega_2^2 = 1.1280, \omega_3^2 = 2.8385, \omega_4^2 = 4.3306$$

Therefore, the structure has four eigen-values, which are the natural frequencies of the system.



Eigen-vectors of $[K - \omega^2 M]$, clause: 7.8.4.1

After obtaining the eigen-values of the system, the next step is to calculate the eigen-vectors (mode shape) corresponding to each eigen-value. The characteristics equation governs the undamped free vibration of the MDOF system. There are no external forces acting on the system. The displacement of the structure results from giving initial conditions *i.e.* initial displacement and velocity at a particular storey level. The initial displacement is perfectly arbitrary. Therefore, one can determine the relative rather than absolute displacements (Bhatt, 2002). In this example eigen-vectors corresponding to eigen-values are obtained from the cofactors of any row of the characteristics equation.

The shape of each mode of free vibration is unique but the amplitude of the mode shape is undefined. The mode shape is usually normalized such that the largest term in the vector is 1.0 or the sum of the squares of the terms in the vector is 1.0 or the vectors are normalized so the generalized mass M^* is 1.0 (Carr, 1994), *i.e.*

$$M^* = \{\phi_i\}^T [M] \{\phi_i\} = 1.0$$

$$[K - \omega^2 M] = \begin{bmatrix} (18 - \omega^2 8) & -8 & 0 & 0 \\ -8 & (14 - \omega^2 8) & -6 & 0 \\ 0 & -6 & (12 - \omega^2 4) & -6 \\ 0 & 0 & -6 & (6 - \omega^2 4) \end{bmatrix}$$

$$\omega^2 = 0.2028, 1.1280, 2.8385 \text{ and } 4.3306$$

Eigen-vector for $\omega^2 = 0.2028$

$$[K - \omega^2 M] = \begin{bmatrix} 16.3776 & -8 & 0 & 0 \\ -8 & 12.3776 & -6 & 0 \\ 0 & -6 & 11.1888 & -6 \\ 0 & 0 & -6 & 5.1888 \end{bmatrix}$$

Assume, $x_1 = 1.0$, then

Row 1 gives: $16.3776 - 8 x_2 = 0$, $x_2 = 2.0472$

Row 2 gives: $-8 x_1 + 12.3776 x_2 - 6 x_3 = 0$, $x_3 = 2.8899$

Row 3 gives: $-6 x_2 + 11.1888 x_3 - 6 x_4 = 0$, $x_4 = 3.3418$

$$X = \begin{bmatrix} 1.0 \\ 2.0472 \\ 2.8899 \\ 3.3418 \end{bmatrix}$$

$$X^T M X = [1.0 \quad 2.0472 \quad 2.8899 \quad 3.3418] \begin{bmatrix} 8 & 0 & 0 & 0 \\ 0 & 8 & 0 & 0 \\ 0 & 0 & 4 & 0 \\ 0 & 0 & 0 & 4 \end{bmatrix} \begin{bmatrix} 1.0 \\ 2.0472 \\ 2.8899 \\ 3.3418 \end{bmatrix} = 119.5983$$

$$X = \frac{1}{\sqrt{119.5983}} \begin{bmatrix} 1.0 \\ 2.0472 \\ 2.8899 \\ 3.3418 \end{bmatrix} = \begin{bmatrix} 0.0914 \\ 1.1872 \\ 0.2643 \\ 0.3056 \end{bmatrix}$$

Eigen-vector for $\omega^2 = 1.1280$

$$[K - \omega^2 M] = \begin{bmatrix} 8.9760 & -8 & 0 & 0 \\ -8 & 4.9760 & -6 & 0 \\ 0 & -6 & 7.4880 & -6 \\ 0 & 0 & -6 & 1.4880 \end{bmatrix}$$

Assume, $x_1 = 1.0$, then

Row 1 gives: $8.9760 - 8x_2 = 0$, $x_2 = 1.1220$

Row 2 gives: $-8x_1 + 4.9760x_2 - 6x_3 = 0$, $x_3 = -0.4028$

Row 3 gives: $-6x_2 + 7.488x_3 - 6x_4 = 0$, $x_4 = -1.6242$

$$X = \begin{bmatrix} 1.0 \\ 1.1220 \\ -0.4028 \\ -1.6242 \end{bmatrix}$$

$$X^T MX = [1.0 \quad 1.1220 \quad -0.4028 \quad -1.6242] \begin{bmatrix} 8 & 0 & 0 & 0 \\ 0 & 8 & 0 & 0 \\ 0 & 0 & 4 & 0 \\ 0 & 0 & 0 & 4 \end{bmatrix} \begin{bmatrix} 1.0 \\ 1.1220 \\ -0.4028 \\ -1.6242 \end{bmatrix} = 29.2722$$

$$X = \frac{1}{\sqrt{29.2722}} \begin{bmatrix} 1.0 \\ 1.1220 \\ -0.4028 \\ -1.6242 \end{bmatrix} = \begin{bmatrix} 0.1848 \\ 0.2074 \\ -0.0744 \\ -0.3002 \end{bmatrix}$$

Eigen-vector for $\omega^2 = 2.8385$

$$[K - \omega^2 M] = \begin{bmatrix} -4.7080 & -8 & 0 & 0 \\ -8 & -8.7080 & -6 & 0 \\ 0 & -6 & 0.6460 & -6 \\ 0 & 0 & -6 & -5.3540 \end{bmatrix}$$

Assume, $x_1 = 1.0$, then

Row 1 gives: $-4.7080 - 8x_2 = 0$, $x_2 = -0.5885$

Row 2 gives: $-8x_1 - 8.7080x_2 - 6x_3 = 0$, $x_3 = -0.4792$

Row 3 gives: $-6x_2 - 0.6460x_3 - 6x_4 = 0$, $x_4 = 0.5370$

$$X = \begin{bmatrix} 1.0 \\ -0.5885 \\ -0.4792 \\ 0.5370 \end{bmatrix}$$

$$X^T MX = [1.0 \ -0.5885 \ -0.4792 \ 0.5370] \begin{bmatrix} 8 & 0 & 0 & 0 \\ 0 & 8 & 0 & 0 \\ 0 & 0 & 4 & 0 \\ 0 & 0 & 0 & 4 \end{bmatrix} \begin{bmatrix} 1.0 \\ -0.5885 \\ -0.4792 \\ 0.5370 \end{bmatrix} = 12.8429$$

$$X = \frac{1}{\sqrt{12.8429}} \begin{bmatrix} 1.0 \\ -0.5885 \\ -0.4792 \\ 0.5370 \end{bmatrix} = \begin{bmatrix} 0.2790 \\ -0.1642 \\ -0.1337 \\ 0.1498 \end{bmatrix}$$

Eigen-vector for $\omega^2 = 4.3306$

$$[K - \omega^2 M] = \begin{bmatrix} -16.6448 & -8 & - & 0 \\ -8 & -20.6448 & -6 & 0 \\ 0 & -6 & -5.3224 & -6 \\ 0 & 0 & -6 & -11.3234 \end{bmatrix}$$

Assume, $x_1 = 1.0$, then

Row 1 gives: $16.6448 - 8 x_2 = 0$, $x_2 = -2.0806$

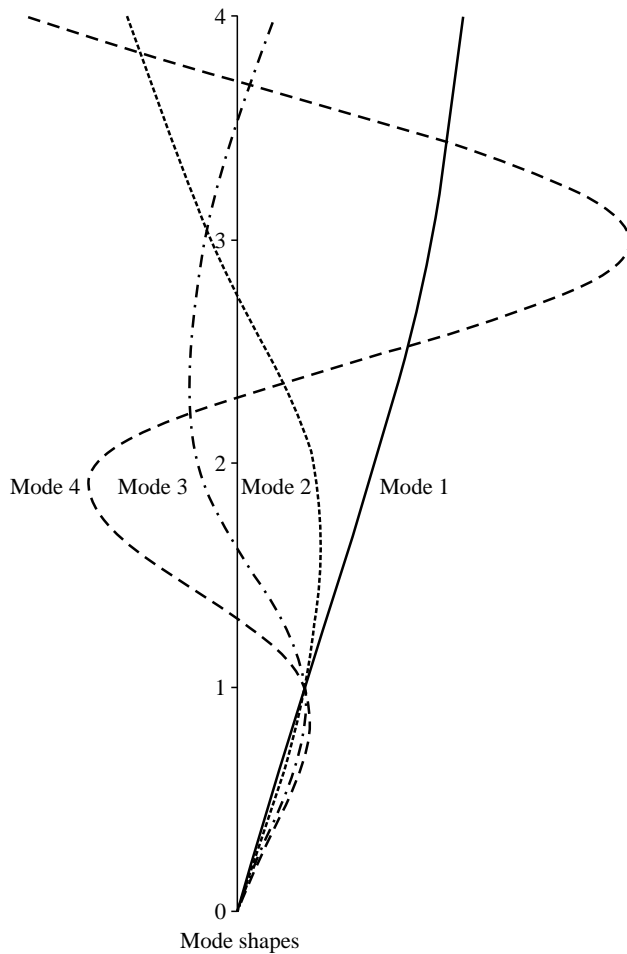
Row 2 gives: $-8 x_1 - 20.6448 x_2 - 6 x_3 = 0$, $x_3 = 5.8256$

Row 3 gives: $-6 x_2 - 5.3224 x_3 - 6 x_4 = 0$, $x_4 = -3.0871$

$$X = \begin{bmatrix} 1.0 \\ -2.0806 \\ 5.8256 \\ -3.0871 \end{bmatrix}$$

$$X^T MX = [1.0 \ -2.0806 \ 5.8256 \ -3.0871] \begin{bmatrix} 8 & 0 & 0 & 0 \\ 0 & 8 & 0 & 0 \\ 0 & 0 & 4 & 0 \\ 0 & 0 & 0 & 4 \end{bmatrix} \begin{bmatrix} 1.0 \\ -2.0806 \\ 5.8256 \\ -3.0871 \end{bmatrix} = 216.501$$

$$X = \frac{1}{\sqrt{216.501}} \begin{bmatrix} 1.0 \\ -2.0806 \\ 5.8256 \\ -3.0871 \end{bmatrix} = \begin{bmatrix} 0.0680 \\ -0.1414 \\ 0.3959 \\ -0.2098 \end{bmatrix}$$



Determination of modal participation factors, clause: 7.8.4.5 (b)

Using the eigen-vectors determined for the four-storey shear frame, modal participation factors and effective masses for all the four modes can be calculated as,

$$[M] = \begin{bmatrix} 8 & 0 & 0 & 0 \\ 0 & 8 & 0 & 0 \\ 0 & 0 & 4 & 0 \\ 0 & 0 & 0 & 4 \end{bmatrix}, M_{\text{Total}} = 8 + 8 + 4 + 4 = 24$$

$$\phi_1 = \begin{bmatrix} 0.0914 \\ 0.1872 \\ 0.2643 \\ 0.3056 \end{bmatrix}, \phi_2 = \begin{bmatrix} 0.1848 \\ 0.2074 \\ -0.0744 \\ -0.3002 \end{bmatrix}, \phi_3 = \begin{bmatrix} 0.2790 \\ -0.1642 \\ -0.1337 \\ 0.1498 \end{bmatrix}, \phi_4 = \begin{bmatrix} 0.0680 \\ -0.1414 \\ 0.3959 \\ -0.2098 \end{bmatrix}$$

The modal participation factor (p_k) of mode k is,

$$p_k = \frac{\sum_{i=1}^n W_i \Phi_{ik}}{\sum_{i=1}^n W_i (\Phi_{ik})^2}$$

$$p_1 = \frac{\sum_{i=1}^4 W_i \Phi_{i1}}{\sum_{i=1}^4 W_i (\Phi_{i1})^2} = \frac{(W_1 \Phi_{11} + W_2 \Phi_{21} + W_3 \Phi_{31} + W_4 \Phi_{41})}{(W_1 (\Phi_{11})^2 + W_2 (\Phi_{21})^2 + W_3 (\Phi_{31})^2 + W_4 (\Phi_{41})^2)}$$

$$= \frac{8 \times 0.0914 + 8 \times 0.1872 + 4 \times 0.2643 + 4 \times 0.3056}{8 \times (0.0914)^2 + 8 \times (0.1872)^2 + 4 \times (0.2643)^2 + 4 \times (0.3056)^2} = 4.5084$$

$$p_2 = \frac{\sum_{i=1}^4 W_i \Phi_{i2}}{\sum_{i=1}^4 W_i (\Phi_{i2})^2} = \frac{(W_1 \Phi_{12} + W_2 \Phi_{22} + W_3 \Phi_{32} + W_4 \Phi_{42})}{(W_1 (\Phi_{12})^2 + W_2 (\Phi_{22})^2 + W_3 (\Phi_{32})^2 + W_4 (\Phi_{42})^2)} = -1.6383$$

Similarly, $p_3 = -0.9831$, $p_4 = 0.1569$

Determination of modal mass, clause: 7.8.4.5 (a)

The modal mass (M_k) of mode k is given by,

$$M_k = \frac{\left[\sum_{i=1}^n W_i \Phi_{ik} \right]^2}{g \left[\sum_{i=1}^n W_i (\Phi_{ik})^2 \right]}$$

Where,

g = Acceleration due to gravity,

Φ_{ik} = Mode shape coefficient at floor i in mode k , and

W_i = Seismic weight of floors i ,

$$M_1 = \frac{\left[\sum_{i=1}^4 W_i \Phi_{i1} \right]^2}{g \left[\sum_{i=1}^4 W_i (\Phi_{i1})^2 \right]} = \frac{[9.81(8(0.0914) + 8(0.1872) + 4(0.2643) + 4(0.3056))]^2}{9.81[9.81(8(0.0914)^2 + 8(0.1872)^2 + 4(0.2643)^2 + 4(0.3056)^2)]}$$

$$= 20.3249$$

$$M_2 = \frac{\left[\sum_{i=1}^4 W_i \Phi_{i2} \right]^2}{g \left[\sum_{i=1}^4 W_i (\Phi_{i2})^2 \right]} = 2.6841,$$

Similarly, $M_3 = 0.9664$, $M_4 = 0.0246$.

Modal Contributions of Various Modes, Clause: 7.8.4.2

$$\text{For mode 1, } \frac{M_1}{M} = \frac{20.3249}{24} = 0.8468 = 84.68\%$$

$$\text{For mode 2, } \frac{M_2}{M} = \frac{2.6841}{24} = 0.1120 = 11.20\%$$

$$\text{For mode 3, } \frac{M_3}{M} = \frac{0.9664}{24} = 0.0402 = 4.02\%$$

$$\text{For mode 4, } \frac{M_4}{M} = \frac{0.0246}{24} = 0.0010 = 0.10\%$$

The effective mass for all modes considered will be $84.68 + 11.20 + 4.02 + 0.1 = 100\%$.

It is clear from the values of the participation factors and effective mass, their value decreases as the mode number increases. The practical significance of this fact is that, in general it is not necessary to include all the modes in a calculation. Only a few significant modes need to be included in order to obtain reasonable results for practical problems. Therefore, the *Clause 7.8.4.2 of IS 1893 (Part I): 2002* states that “*The number of modes to be used in the analysis should be such that the sum total of modal masses of all modes considered is at least 90% of the total seismic mass and missing mass correction beyond 33 Hz are to be considered, modal combination shall be carried out only for modes upto 33 Hz*”.

Design lateral force at each floor in each mode, clause: 7.8.4.5 (c)

The design lateral force (Q_{ik}) at floor i in mode k is given by,

$$Q_{ik} = A_k \Phi_{ik} P_k W_i$$

where A_k is design horizontal acceleration spectrum value as per 6.4.2 using the natural period of vibration (T_k) of mode k .

The design horizontal seismic coefficient A_k for various modes are worked out using

$$A_h = \frac{Z}{2} \frac{I}{R} \frac{S_a}{g}.$$

Design Lateral Force in Each Mode

$$Q_{il} = (A_l P_l \Phi_{il} W_l) Q_{il} = \begin{bmatrix} (A_1 P_1 \Phi_{11} W_1) \\ (A_1 P_1 \Phi_{21} W_1) \\ \dots \\ (A_1 P_1 \Phi_{..1} W_1) \\ (A_1 P_1 \Phi_{n1} W_1) \end{bmatrix} \text{ kN}$$

Similarly, $Q_{i2}, Q_{i3}, Q_{i4} \dots Q_{in}$.

Storey shear forces in each mode, clause 7.8.4.5 (d)

The peak shear force (V_{ik}) acting in storey i in mode k is given by,

$$V_{ik} = \sum_{j=i+1}^n Q_{ik}$$

The storey shear force for the first mode is,

$$V_{i1} = \sum_{j=i+1}^n Q_{il} = \begin{bmatrix} V_{11} \\ V_{21} \\ V_{(n-1)1} \\ V_{n1} \end{bmatrix} = \begin{bmatrix} (Q_{11} + Q_{21} + Q_{..1} + Q_{n1}) \\ (Q_{21} + Q_{(n-1)1} + Q_{n1}) \\ (Q_{(n-1)1} + Q_{n1}) \\ (Q_{n1}) \end{bmatrix} \text{ kN}$$

$$\text{Similarly, } V_{i2} = \begin{bmatrix} V_{12} \\ V_{22} \\ V_{32} \\ V_{42} \end{bmatrix}, V_{i3} = \begin{bmatrix} V_{13} \\ V_{23} \\ V_{33} \\ V_{43} \end{bmatrix}, V_{i4} = \begin{bmatrix} V_{14} \\ V_{24} \\ V_{34} \\ V_{44} \end{bmatrix}$$

Storey shear force due to all modes considered, clause 7.8.4.5 (e)

The peak storey shear force (V_i) in storey i due to all modes considered is obtained by combining those due to each mode in accordance with modal combination as per clause 7.8.4.4. The combinations are usually achieved by using statistical methods.

The design values for the total base shear are obtained by combining the corresponding modal responses. In general these modal maximum values will not occur simultaneously. To overcome this difficulty, it is necessary to use an approximate method.

An upper limit for the maximum response may be obtained by Sum of the ABSolute values (ABS) of the maximum modal contributions. This is very conservative and is very seldom used except in some codes for say two or three modes for very short period structures. If the system does not have closely spaced modes, another estimate of the maximum response, which is widely accepted and which usually provides a reasonable estimate is the Square Root of the Sum of

Squares (SRSS). Application of the **SRSS** method for combining modal responses generally provides an acceptable estimation of the total maximum response. However, when some of the modes are closely spaced *i.e.* the difference between two natural frequencies is within 10% of the smallest of the two frequencies, the use of the SRSS method may either grossly underestimate or overestimate the maximum response. A formulation known as the **Complete Quadratic Combination (CQC)**, based on the theory of random vibration and is also considered as an extension of the SRSS method. For an undamped structure CQC estimate is identical to the SRSS estimate.

Maximum Absolute Response (ABS), Clause 7.8.4.4 (b)

The Maximum Absolute Response (ABS) for any system response quantity is obtained by assuming that the maximum response in each mode occurs at the same instant of time. Thus the maximum value of the response quantity is the sum of the maximum absolute value of the response associated with each mode. Therefore using ABS, maximum storey shear for all modes shall be obtained as

$$\lambda^* = \sum_c^r \lambda_c$$

where the summation is for the closely-spaced modes only. The peak response quantity due to the closely spaced modes (λ^*) is then combined with those of the remaining well-separated modes by the method of SRSS.

Square Root of Sum of Squares (SRSS), Clause 7.8.4.4 (a)

A more reasonable method of combining modal maxima for two-dimensional structural system exhibiting well-separated vibration frequencies is the square-root-of-the-squares (SRSS). The peak response quantity (λ) due to all modes considered shall be obtained as,

$$\lambda = \sqrt{\sum_{k=1}^r (\lambda_k)^2}$$

where λ_k is the absolute value of quantity in mode ' k ', and r is the numbers of modes being considered.

Using the above method, the storey shears are as follows,

$$V_1 = [(V_{11})^2 + (V_{12})^2 + \dots + (V_{1(n-1)})^2 + (V_{1n})^2]^{1/2} \text{ kN}$$

$$V_2 = [(V_{21})^2 + (V_{22})^2 + \dots + (V_{2(n-2)})^2 + (V_{2n})^2]^{1/2} \text{ kN}$$

$$V_3 = [(V_{31})^2 + (V_{32})^2 + \dots + (V_{3(n-1)})^2 + (V_{3n})^2]^{1/2} \text{ kN}$$

...

...

$$V_n = [(V_{n1})^2 + (V_{n2})^2 + \dots + (V_{n(n-1)})^2 + (V_{nn})^2]^{1/2} \text{ kN}$$

Complete Quadratic Combination (CQC), Clause 7.8.4.4

For three-dimensional structural systems exhibiting well-separated vibration frequencies, the peak response quantities shall be combined as per *Complete Quadratic Combination (CQC)* method

$$\lambda = \sqrt{\sum_{i=1}^r \sum_{j=1}^r \lambda_i \rho_{ij} \lambda_j}$$

where,

r = Number of modes being considered,

λ_i = Response quantity in mode i (including sign),

λ_j = Response quantity in mode j (including sign),

ρ_{ij} = Cross modal coefficient,

$$\rho_{ij} = \frac{8\zeta^2(1+\beta_{ij})\beta^{1.5}}{(1-\beta_{ij})^2 + 4\zeta^2\beta_{ij}(1+\beta_{ij})^2}$$

where,

ζ = Modal damping ratio (in fraction),

β_{ij} = Frequency ratio ω_j/ω_i ,

ω_i = Circular frequency in i^{th} mode, and

ω_j = Circular frequency in j^{th} mode.

Therefore all the frequency ratios and cross modal components can be represented in matrix form as shown below,

$$\beta_{ij} = \begin{bmatrix} \beta_{11} & \beta_{12} & \beta_{13} & \beta_{14} \\ \beta_{21} & \beta_{22} & \beta_{23} & \beta_{24} \\ \beta_{31} & \beta_{32} & \beta_{33} & \beta_{34} \\ \beta_{41} & \beta_{42} & \beta_{43} & \beta_{44} \end{bmatrix} = \begin{bmatrix} \omega_1/\omega_1 & \omega_2/\omega_1 & \dots & \omega_{n-1}/\omega_1 & \omega_n/\omega_1 \\ \omega_1/\omega_2 & \omega_2/\omega_2 & \dots & \omega_{n-1}/\omega_2 & \omega_n/\omega_2 \\ \dots & & & & \\ \omega_1/\omega_{n-1} & \omega_2/\omega_{n-1} & \dots & \omega_{n-1}/\omega_{n-1} & \omega_n/\omega_{n-1} \\ \omega_1/\omega_n & \omega_2/\omega_n & \dots & \omega_3/\omega_n & \omega_n/\omega_n \end{bmatrix}$$

$$\rho_{ij} = \begin{bmatrix} \rho_{11} & \rho_{12} & \rho_{13} & \rho_{14} \\ \rho_{21} & \rho_{22} & \rho_{23} & \rho_{24} \\ \rho_{31} & \rho_{32} & \rho_{33} & \rho_{34} \\ \rho_{41} & \rho_{42} & \rho_{43} & \rho_{44} \end{bmatrix}$$

The above quadratic combination i.e. $\lambda = \sqrt{\sum_{i=1}^r \sum_{j=1}^r \lambda_i \rho_{ij} \lambda_j}$ can also be written in matrix form as,

$$[\lambda_1 \lambda_2 \lambda_3 \lambda_4] \begin{bmatrix} \rho_{11} & \rho_{12} & \rho_{13} & \rho_{14} \\ \rho_{21} & \rho_{22} & \rho_{23} & \rho_{24} \\ \rho_{31} & \rho_{32} & \rho_{33} & \rho_{34} \\ \rho_{41} & \rho_{42} & \rho_{43} & \rho_{44} \end{bmatrix} \begin{bmatrix} \lambda_1 \\ \lambda_2 \\ \lambda_3 \\ \lambda_4 \end{bmatrix}$$

Here the terms λ_i and λ_j represent the response of different modes of a certain storey level.

Using the matrix notation the storey shears are worked out

$V_1, V_2, V_3 \dots V_n$ respectively.

Lateral forces at each storey due to all modes, clause 7.8.4.5 (f)

The design lateral forces F_{roof} and F_i , at roof and at i^{th} floor, are calculated as,

$$F_{\text{roof}} = V_{\text{roof}}, \quad \text{and} \quad F_i = V_i - V_{i+1}$$

$$F_4 = V_4 \text{ kN},$$

$$F_3 = (V_3 - V_4) \text{ kN}$$

$$F_2 = (V_2 - V_3) \text{ kN}$$

$$F_1 = (V_1 - V_2) \text{ kN}$$

Example 3 Consider a mass and stiffness matrix for the undamped free vibration of the system as below. Determine the lateral force at each storey.

$$[K] = \begin{bmatrix} 1800 & -800 & 0 & 0 \\ -800 & 1400 & -600 & 0 \\ 0 & -600 & 1200 & -600 \\ 0 & 0 & -600 & 600 \end{bmatrix} \text{ kN}, [M] = \begin{bmatrix} 8 & 0 & 0 & 0 \\ 0 & 8 & 0 & 0 \\ 0 & 0 & 4 & 0 \\ 0 & 0 & 0 & 4 \end{bmatrix} \text{ t},$$

Natural frequencies

$$\omega_1 = 4.5036, \omega_2 = 10.6209, \omega_3 = 16.8479 \text{ and } \omega_4 = 20.8101$$

Eigen-vectors

$$\phi_1 = \begin{bmatrix} 0.0914 \\ 0.1872 \\ 0.2642 \\ 0.3056 \end{bmatrix}, \phi_2 = \begin{bmatrix} -0.1848 \\ -0.2073 \\ 0.0744 \\ 0.3002 \end{bmatrix}, \phi_3 = \begin{bmatrix} -0.2790 \\ 0.1642 \\ 0.1337 \\ -0.1498 \end{bmatrix}, \phi_4 = \begin{bmatrix} 0.0680 \\ -0.1414 \\ 0.3959 \\ -0.2098 \end{bmatrix}$$

Time Periods

$$T = \begin{bmatrix} 1.3951 & 0 & 0 & 0 \\ 0 & 0.5916 & 0 & 0 \\ 0 & 0 & 0.3729 & 0 \\ 0 & 0 & 0 & 0.3019 \end{bmatrix} \text{ s}$$

Modal Participation Factors

$$p_1 = 4.5084, p_2 = -1.6383, p_3 = -0.9831, p_4 = 0.1569$$

Modal Mass

$$M_1 = 20.3249, M_2 = 2.6841, M_3 = 0.9664, M_4 = 0.0246$$

Design Lateral Force at Each Floor in Each Mode

The design lateral force (Q_{ik}) at floor i in mode k is given by,

$$Q_{ik} = A_k \Phi_{ik} P_k W_i$$

$$\text{For } T_1 = 1.3951 \Rightarrow \frac{S_{a1}}{g} = 0.7169, \text{ From Figure 2 of IS 1893 (Part 1): 2002}$$

$$\text{For } T_2 = 0.5916 \Rightarrow \frac{S_{a2}}{g} = 1.6903, \text{ From Figure 2 of IS 1893 (Part 1): 2002}$$

$$\text{For } T_3 = 0.3729 \Rightarrow \frac{S_{a3}}{g} = 2.5, \text{ From Figure 2 of IS 1893 (Part 1): 2002}$$

$$\text{For } T_4 = 0.3019 \Rightarrow \frac{S_{a4}}{g} = 2.5, \text{ From Figure 2 of IS 1893 (Part 1): 2002}$$

The design horizontal seismic coefficient A_h for various modes are worked out using $A_h = \frac{Z}{2} \frac{I}{R} \frac{S_a}{g}$,

$$A_1 = \frac{Z}{2} \frac{I}{R} \frac{S_{a1}}{g} = \frac{0.24}{2} \frac{1}{5} 0.7169 = 0.0172$$

$$A_2 = \frac{Z}{2} \frac{I}{R} \frac{S_{a1}}{g} = \frac{0.24}{2} \frac{1}{5} 1.6903 = 0.0405$$

Similarly,

$$A_3 = 0.060,$$

$$A_4 = 0.060.$$

Design Lateral Force

$$[Q_{il}] = (A_1 P_1 \Phi_{i1} W_i)$$

$$\begin{aligned}
 [Q_{i1}] &= \begin{bmatrix} (A_1 P_1 \Phi_{11} W_1) \\ (A_1 P_1 \Phi_{21} W_2) \\ (A_1 P_1 \Phi_{31} W_3) \\ (A_1 P_1 \Phi_{41} W_4) \end{bmatrix} = \begin{bmatrix} ((0.0172)(4.5084)(0.0914)(8 \times 9.81)) \\ ((0.0172)(4.5084)(0.1872)(8 \times 9.81)) \\ ((0.0172)(4.5084)(0.2646)(4 \times 9.81)) \\ ((0.0172)(4.5084)(0.3056)(4 \times 9.81)) \end{bmatrix} = \begin{bmatrix} (0.5567) \\ (1.1396) \\ (0.8043) \\ (0.9301) \end{bmatrix} \text{kN} \\
 [Q_{i2}] &= \begin{bmatrix} (A_2 P_2 \Phi_{12} W_1) \\ (A_2 P_2 \Phi_{22} W_2) \\ (A_2 P_2 \Phi_{32} W_3) \\ (A_2 P_2 \Phi_{42} W_4) \end{bmatrix} = \begin{bmatrix} ((0.0405)(-1.6383)(-0.1848)(8 \times 9.81)) \\ ((0.0405)(-1.6383)(-0.2073)(8 \times 9.81)) \\ ((0.0405)(-1.6383)(0.0744)(4 \times 9.81)) \\ ((0.0405)(-1.6383)(0.3002)(4 \times 9.81)) \end{bmatrix} = \begin{bmatrix} (0.9623) \\ (1.0794) \\ (-0.1930) \\ (0.7816) \end{bmatrix} \text{kN} \\
 [Q_{i3}] &= \begin{bmatrix} (A_3 P_3 \Phi_{13} W_1) \\ (A_3 P_3 \Phi_{23} W_2) \\ (A_3 P_3 \Phi_{33} W_3) \\ (A_3 P_3 \Phi_{43} W_4) \end{bmatrix} = \begin{bmatrix} ((0.060)(-0.9831)(-0.2790)(8 \times 9.81)) \\ ((0.060)(-0.9831)(0.1642)(8 \times 9.81)) \\ ((0.060)(-0.9831)(0.1337)(4 \times 9.81)) \\ ((0.060)(-0.9831)(-0.1498)(4 \times 9.81)) \end{bmatrix} = \begin{bmatrix} (1.2915) \\ (-0.7601) \\ (-0.3095) \\ (0.3467) \end{bmatrix} \text{kN} \\
 [Q_{i4}] &= \begin{bmatrix} (A_4 P_4 \Phi_{14} W_1) \\ (A_4 P_4 \Phi_{24} W_2) \\ (A_4 P_4 \Phi_{34} W_3) \\ (A_4 P_4 \Phi_{44} W_4) \end{bmatrix} = \begin{bmatrix} ((0.060)(0.1569)(0.0680)(8 \times 9.81)) \\ ((0.060)(0.1569)(-0.1414)(8 \times 9.81)) \\ ((0.060)(0.1569)(0.3959)(4 \times 9.81)) \\ ((0.060)(0.1569)(-0.2098)(4 \times 9.81)) \end{bmatrix} = \begin{bmatrix} (0.0502) \\ (-0.8433) \\ (0.1462) \\ (-0.0775) \end{bmatrix} \text{kN}
 \end{aligned}$$

Storey Shear Forces in Each Mode

The peak shear force will be obtained by $V_{ik} = \sum_{j=i+1}^n Q_{jk}$

The storey shear forces for the first mode is,

$$[V_{i1}] = \sum_{j=i+1}^n Q_{j1} = \begin{bmatrix} V_{11} \\ V_{21} \\ V_{31} \\ V_{41} \end{bmatrix} = \begin{bmatrix} (Q_{11} + Q_{21} + Q_{31} + Q_{41}) \\ (Q_{21} + Q_{31} + Q_{41}) \\ (Q_{31} + Q_{41}) \\ (Q_{41}) \end{bmatrix} = \begin{bmatrix} 3.4306 \\ 2.8739 \\ 1.7344 \\ 0.9301 \end{bmatrix} \text{kN}$$

Similarly,

$$[V_{i2}] = \begin{bmatrix} V_{12} \\ V_{22} \\ V_{32} \\ V_{42} \end{bmatrix} = \begin{bmatrix} 2.6303 \\ 1.6680 \\ 0.5886 \\ 0.7816 \end{bmatrix}, [V_{i3}] = \begin{bmatrix} V_{13} \\ V_{23} \\ V_{33} \\ V_{43} \end{bmatrix} = \begin{bmatrix} 0.5686 \\ -0.7229 \\ 0.0372 \\ 0.3467 \end{bmatrix}, [V_{i4}] = \begin{bmatrix} V_{14} \\ V_{24} \\ V_{34} \\ V_{44} \end{bmatrix} = \begin{bmatrix} -0.7244 \\ -0.7746 \\ 0.0687 \\ -0.0775 \end{bmatrix}$$

Storey Shear Forces due to All Modes Considered

Maximum Absolute Response (ABS)

$$V_1 = [|V_{11}| + |V_{12}| + |V_{13}| + |V_{14}|] = [|3.4307| + |2.6303| + |0.5686| + |-0.7244|] = 7.3539 \text{ kN}$$

$$V_2 = [|V_{21}| + |V_{22}| + |V_{23}| + |V_{24}|] = [|2.8740| + |1.6680| + |-0.7229| + |-0.7746|] = 6.0394 \text{ kN}$$

$$V_3 = [|V_{31}| + |V_{32}| + |V_{33}| + |V_{34}|] = [|1.7344| + |0.5886| + |0.0372| + |0.0687|] = 2.4289 \text{ kN}$$

$$V_4 = [|V_{41}| + |V_{42}| + |V_{43}| + |V_{44}|] = [|0.9301| + |0.7816| + |0.3467| + |-0.0775|] = 2.1359 \text{ kN}$$

Square Root of Sum of Squares (SRSS)

$$\begin{aligned} V_1 &= [(V_{11})^2 + (V_{12})^2 + (V_{13})^2 + (V_{14})^2]^{1/2} \\ &= [(3.4306)^2 + (2.6303)^2 + (0.5686)^2 + (-0.7244)^2]^{1/2} = 4.4199 \text{ kN} \end{aligned}$$

$$\begin{aligned} V_2 &= [(V_{21})^2 + (V_{22})^2 + (V_{23})^2 + (V_{24})^2]^{1/2} \\ &= [(2.8739)^2 + (1.668)^2 + (-0.7229)^2 + (-0.7746)^2]^{1/2} = 3.4877 \text{ kN} \end{aligned}$$

$$\begin{aligned} V_3 &= [(V_{31})^2 + (V_{32})^2 + (V_{33})^2 + (V_{34})^2]^{1/2} \\ &= [(1.7344)^2 + (0.5886)^2 + (0.0372)^2 + (0.0687)^2]^{1/2} = 1.8332 \text{ kN} \end{aligned}$$

$$\begin{aligned} V_4 &= [(V_{41})^2 + (V_{42})^2 + (V_{43})^2 + (V_{44})^2]^{1/2} \\ &= [(0.9301)^2 + (0.7816)^2 + (0.3467)^2 + (-0.0775)^2]^{1/2} = 1.2657 \text{ kN} \end{aligned}$$

Complete Quadratic Combination (CQC)

$$\lambda = \sqrt{\sum_{i=1}^r \sum_{j=1}^r \lambda_i \rho_{ij} \lambda_j}$$

where

r , Number of modes being considered

ρ_{ij} , Cross modal coefficient

λ_i , Response quantity in mode i (including sign)

λ_j , Response quantity in mode j (including sign)

$$\rho_{ij} = \frac{8\zeta^2(1 + \beta_{ij})\beta_{ij}^{1.5}}{(1 - \beta_{ij}^2)^2 + 4\zeta^2\beta_{ij}(1 + \beta_{ij})^2}$$

where

ζ , Modal damping ratio (in fraction), ω_j/ω_i

β_{ij} , Frequency ratio

ω_i , Circular frequency in i th mode, and

ω_j , Circular frequency in j th mode

Therefore all the frequency ratios and cross modal components can be represented in matrix form as shown below,

$$\beta_{ij} = \begin{bmatrix} \beta_{11} & \beta_{12} & \beta_{13} & \beta_{14} \\ \beta_{21} & \beta_{22} & \beta_{23} & \beta_{24} \\ \beta_{31} & \beta_{32} & \beta_{33} & \beta_{34} \\ \beta_{41} & \beta_{42} & \beta_{43} & \beta_{44} \end{bmatrix} = \begin{bmatrix} \omega_1/\omega_1 & \omega_2/\omega_1 & \omega_3/\omega_1 & \omega_4/\omega_1 \\ \omega_1/\omega_2 & \omega_2/\omega_2 & \omega_3/\omega_2 & \omega_4/\omega_2 \\ \omega_1/\omega_3 & \omega_2/\omega_3 & \omega_3/\omega_3 & \omega_4/\omega_3 \\ \omega_1/\omega_4 & \omega_2/\omega_4 & \omega_3/\omega_4 & \omega_4/\omega_4 \end{bmatrix}$$

$$= \begin{bmatrix} 1 & 2.358 & 3.7409 & 4.6207 \\ 0.4240 & 1 & 1.5863 & 1.9593 \\ 0.2673 & 0.6303 & 1 & 1.2351 \\ 0.2164 & 0.5103 & 0.8096 & 1 \end{bmatrix}$$

$$\rho_{11} = \frac{8 \times (0.05)^2 \times (1+1) \times 1^{1.5}}{(1-1^2)^2 + 4 \times (0.05)^2 \times 1 \times (1+1)^2} = 1$$

$$\rho_{12} = \frac{8 \times (0.05)^2 \times (1+2.358) \times 2.358^{1.5}}{(1-2.358^2)^2 + 4 \times (0.05)^2 \times 2.358 \times (1+2.358)^2} = 0.0115$$

Therefore ρ_{ij} calculated for all $i j$ and represented as given below

$$\rho_{ij} = \begin{bmatrix} \rho_{11} & \rho_{12} & \rho_{13} & \rho_{14} \\ \rho_{21} & \rho_{22} & \rho_{23} & \rho_{24} \\ \rho_{31} & \rho_{32} & \rho_{33} & \rho_{34} \\ \rho_{41} & \rho_{42} & \rho_{43} & \rho_{44} \end{bmatrix} = \begin{bmatrix} 1 & 0.115 & 0.004 & 0.0027 \\ 0.0115 & 1 & 0.0430 & 0.0197 \\ 0.004 & 0.0430 & 1 & 0.1816 \\ 0.0027 & 0.0197 & 0.1816 & 1 \end{bmatrix}$$

The above quadratic combination i.e. $\lambda = \sqrt{\sum_{i=1}^r \sum_{j=1}^r \lambda_i \rho_{ij} \lambda_j}$ can also be written as

$$\sum_{i=1}^4 \sum_{j=1}^4 \lambda_i \rho_{ij} \lambda_j = \lambda_1 \rho_{11} \lambda_1 + \lambda_1 \rho_{12} \lambda_2 + \lambda_1 \rho_{13} \lambda_3 + \lambda_1 \rho_{14} \lambda_4 + \lambda_2 \rho_{21} \lambda_1 + \lambda_1 \rho_{22} \lambda_2 + \lambda_1 \rho_{23} \lambda_3 + \lambda_1 \rho_{24} \lambda_4 + \lambda_1 \rho_{31} \lambda_1 + \lambda_1 \rho_{32} \lambda_2 + \lambda_1 \rho_{33} \lambda_3 + \lambda_1 \rho_{34} \lambda_4 + \lambda_1 \rho_{41} \lambda_1 + \lambda_1 \rho_{42} \lambda_2 + \lambda_1 \rho_{43} \lambda_3 + \lambda_1 \rho_{44} \lambda_4$$

In matrix form, it can be represented as

$$[\lambda_1 \ \lambda_2 \ \lambda_3 \ \lambda_4] \begin{bmatrix} \rho_{11} & \rho_{12} & \rho_{13} & \rho_{14} \\ \rho_{21} & \rho_{22} & \rho_{23} & \rho_{24} \\ \rho_{31} & \rho_{32} & \rho_{33} & \rho_{34} \\ \rho_{41} & \rho_{42} & \rho_{43} & \rho_{44} \end{bmatrix} \begin{bmatrix} \lambda_1 \\ \lambda_2 \\ \lambda_3 \\ \lambda_4 \end{bmatrix}$$

Here the terms λ_i or λ_j represent the response of different modes of a certain storey level.

Using the matrix notation the storey shears are worked out as follows:

$$V_1 = \begin{vmatrix} & \left[\begin{matrix} 1 & 0.0115 & 0.004 & 0.0027 \\ 0.0115 & 1 & 0.0430 & 0.0197 \\ 0.004 & 0.0430 & 1 & 0.1816 \\ 0.0027 & 0.0197 & 0.1816 & 1 \end{matrix} \right] & \begin{matrix} 3.4307 \\ 2.6303 \\ 0.5686 \\ -0.7244 \end{matrix} \end{vmatrix}$$

$$= [4.4328]$$

$$V_2 = \begin{vmatrix} & \left[\begin{matrix} 1 & 0.0115 & 0.004 & 0.0027 \\ 0.0115 & 1 & 0.0430 & 0.0197 \\ 0.004 & 0.0430 & 1 & 0.1816 \\ 0.0027 & 0.0197 & 0.1816 & 1 \end{matrix} \right] & \begin{matrix} 2.8740 \\ 1.6680 \\ -0.7229 \\ -0.7746 \end{matrix} \end{vmatrix}$$

$$= [3.5064]$$

$$V_3 = \begin{vmatrix} & \left[\begin{matrix} 1 & 0.0115 & 0.004 & 0.0027 \\ 0.0115 & 1 & 0.0430 & 0.0197 \\ 0.004 & 0.0430 & 1 & 0.1816 \\ 0.0027 & 0.0197 & 0.1816 & 1 \end{matrix} \right] & \begin{matrix} 1.7344 \\ 0.5886 \\ 0.0372 \\ 0.0687 \end{matrix} \end{vmatrix}$$

$$= [1.8411]$$

$$V_4 = \begin{vmatrix} & \left[\begin{matrix} 1 & 0.0115 & 0.004 & 0.0027 \\ 0.0115 & 1 & 0.0430 & 0.0197 \\ 0.004 & 0.0430 & 1 & 0.1816 \\ 0.0027 & 0.0197 & 0.1816 & 1 \end{matrix} \right] & \begin{matrix} 0.9301 \\ 0.7816 \\ 0.3467 \\ -0.0775 \end{matrix} \end{vmatrix}$$

$$= [1.2776]$$

Lateral Forces at Each Storey due to All Modes Considered

Maximum Absolute Response (ABS)

$$F_{\text{roof}} = F_4 = V_4 = 2.1359 \text{ kN}$$

$$F_3 = V_3 - V_4 = 2.4289 - 2.1359 = 0.2930 \text{ kN}$$

$$F_2 = V_2 - V_3 = 6.0394 - 2.4289 = 3.6105 \text{ kN}$$

$$F_1 = V_1 - V_2 = 7.3539 - 6.0394 = 1.3145 \text{ kN}$$

Square Root of Sum of Squares (SRSS)

$$F_{\text{roof}} = F_4 = V_4 = 1.2657$$

$$F_3 = V_3 - V_4 = 1.8332 - 1.2657 = 0.5674 \text{ kN}$$

$$F_2 = V_2 - V_3 = 3.4877 - 1.8332 = 1.6544 \text{ kN}$$

$$F_1 = V_1 - V_2 = 4.4199 - 3.4877 = 0.9322 \text{ kN}$$

Complete Quadratic Combination (CQC)

$$F_{\text{roof}} = F_4 = V_4 = 1.2776 \text{ kN}$$

$$F_3 = V_3 - V_4 = 1.8411 - 1.2776 = 0.5635 \text{ kN}$$

$$F_2 = V_2 - V_3 = 3.5064 - 1.8411 = 1.6653 \text{ kN}$$

$$F_1 = V_1 - V_2 = 4.4432 - 3.5064 = 0.9368 \text{ kN}$$

Comparison of ABS, SRSS and CQC Results

Method of Modal Combination	Base Shear in kN
ABS	7.3539
SRSS	4.4199
CQC	4.4432

SUMMARY

Determination of design lateral forces is the primary requirement of seismic analysis and design of a structure. The design lateral forces are often carried out by equivalent static lateral force procedure and dynamic analysis of structures. Dynamic analysis is carried out either by response spectrum method or by time history method. The aim of this chapter is to present a *clause wise* approach for determination of lateral forces as per IS 1893 (Part 1): 2002 with the help of worked out examples. Equivalent static and response spectrum method has been used in this chapter for determining the design lateral forces. Determination of lateral forces from earlier version of IS 1893 has also been worked out to know the impact of change of code. Seismic design philosophy for earthquake resistant design of structures has also been explained in brief.

REFERENCES

- [1] BIS 1893, *Criteria for Earthquake Resistant Design of Structures—Part 1: General Provisions and Buildings* (fifth revision), Bureau of Indian Standards, New Delhi, 2002.
- [2] Bhatt, P., *Programming the Dynamic Analysis of Structures*, Spon Press, 2002.
- [3] Carr, A.J., “Dynamic Analysis of Structures”, *Bulletin of the New Zealand National Society for Earthquake Engineering*, Vol. 27, No. 2, June, 1994.

- [4] IS 1893, *Indian Standard Recommendations for Earthquake Resistance of Structure*, Indian Standard Institute, New Delhi, 1962.
- [5] IS 1893, *Indian Standard Recommendations for Earthquake Resistance of Structure* (First Revision), Indian Standard Institute, New Delhi, 1966.
- [6] IS 1893, *Indian Standard Criteria for Earthquake Resistance of Structure* (second revision), Indian Standard Institute, New Delhi, 1970.
- [7] IS 1893, *Indian Standard Criteria for Earthquake Resistance of Structure* (third revision), Indian Standard Institute, New Delhi, 1975.
- [8] IS 1893, *Indian Standard Criteria for Earthquake Resistance of Structure* (fourth revision), Indian Standard Institute, New Delhi, 1984.
- [9] Newmark, N.M. and Hall, W.J., "Earthquake Spectra and Design", *Engineering Monographs on Earthquake Criteria, Structural Design, and Strong Motion Records*, Earthquake Engineering Research Institute, 1982.
- [10] Paz, M., *International Handbook of Earthquake Engineering—Codes, Programmes and Examples*, Chapman & Hall, 1994.

Chapter 17

Consideration of Infill Wall in Seismic Analysis of RC Buildings

17.1 INTRODUCTION

A large number of reinforced concrete and steel buildings are constructed with masonry infills. Masonry infills are often used to fill the void between the vertical and horizontal resisting elements of the building frames with the assumption that these infills will not take part in resisting any kind of load either axial or lateral; hence its significance in the analysis of frame is generally neglected. Moreover, non-availability of realistic and simple analytical models of infill becomes another hurdle for its consideration in analysis. In fact, an infill wall enhances considerably the strength and rigidity of the structure. It has been recognised that frames with infills have more strength and rigidity in comparison to the bared frames and their ignorance has become the cause of failure of many of the multi-storeyed buildings. The recent example in this category is the Bhuj earthquake on 26 January, 2001. The main reason of failure is the stiffening effect of infilled frame that changes the basic behaviour of buildings during earthquake and creates new failure mechanism. This chapter will discuss the structural action of infill panel and failure modes and modelling of infill walls with and without openings.

17.2 STRUCTURAL AND CONSTRUCTIONAL ASPECTS OF INFILLS

The presence of masonry infills is the cause of (i) unequal distribution of lateral forces in the different frames of a building—overstressing of some frames; (ii) vertical irregularities in strength and stiffness—soft storey or weak storey as a result higher interstorey drifts and higher ductility demands of RC elements of the soft storey in comparison to remaining stories; (iii) horizontal irregularities—significant amount of unexpected torsional forces since the centre of rigidity is moved towards the stiffer infilled frames of increased stiffness and as a result

occurrence of very large rotation and large displacements in the extreme bare frames; (iv) inducing the effect of short column or captive column in infilled frame—a captive column is full storey slender column whose clear height is reduced by its part-height contact with a relatively stiff masonry infill wall, which constraints its lateral deformation over the height of contact (CEB, 1996) resulting in premature brittle failure of columns and (v) failure of masonry infills—out-of-plane and in-plane failure results which become the cause of casualties.

A significant amount of research work has been carried out on the consideration of stiffening effect of infill panels and its constructional details. A clear decision has to be taken by the structural engineers, whether the infill walls will be made to participate in resisting the load or not. Depending upon its load resisting mechanism of infills the construction details will be followed as:

- (i) only axial load—fill walls tight to the under side of the floor system – arching action is the dominant mechanism,
- (ii) axial and lateral load—friction or mechanical anchorage along the top to transfer lateral load to the wall—connection must be able to transfer reaction,
- (iii) Only lateral load—wall built tight to the columns and a movement joint at the top of wall, and no axial and lateral movement joints along all the sides of walls and must be sufficiently thick to isolate the effects of inter-storey drift, floor deflection and differential movement—this type of wall is called **partition wall** (Drydale, Hamid and Baker, 1994).

17.3 FAILURE MECHANISM OF INFILLED FRAME

The failure mechanism of an infilled frame is quite complex and depends upon a number of factors such as relative strength and stiffness properties of infill and frame, frame wall interface gaps, openings, shear connectors, and such other characteristics. Figure 17.1 shows the five most

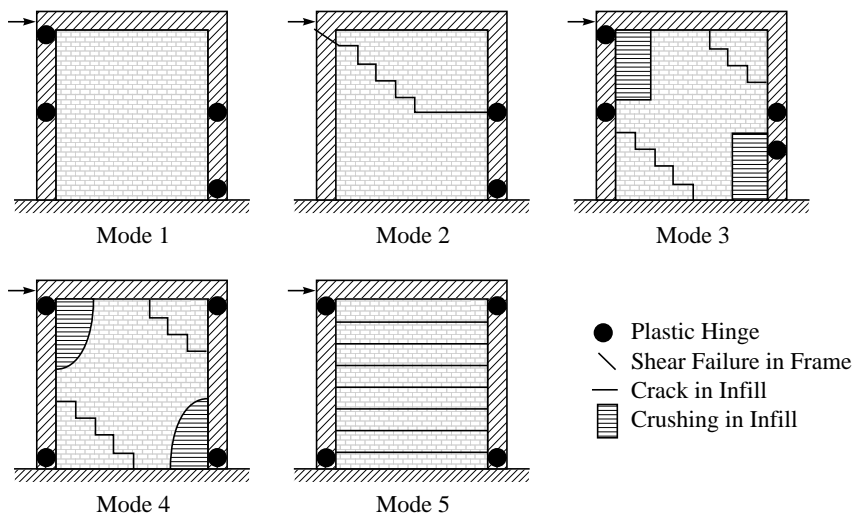


FIGURE 17.1 Infilled frame failure modes (Buonopane et al., 1999).

common modes of failure of masonry infilled frame under increasing intensity of lateral loads (Buonopane et al., 1999). In principle, failure mechanism of an infilled frame depends to a great extent on the relative strength of the frame and the infill (El-Dakhakhni et al., 2003, Mehrabi et al., 1996).

Mode 1: Sliding shear failure through bed joint of a masonry infill – associated with infill with weak joints and strong members. This formation of the shear crack separates the panel into two parts, which reduces the effective column height approximately to half. At this cracked condition, the system will behave as a knee-braced system.

Mode 2: Shear failure at the loaded side columns or beam-column joints – associated with strong infill and a weak frame. The diagonal/sliding cracks in the infills have been first noticed followed by shear failure of the loaded sided columns.

Mode 3: Corner Crushing in the infill at least one of its loaded corners – associated with strong infill surrounded by a strong frame.

Mode 4: Diagonal shear cracking in the form of a crack connecting the two loaded corners and columns yielding in flexure-associated with strong infill surrounded by a weak frame or a frame with weak joints and strong members. Cracking of the walls occur from one corner to the diagonally opposite corner and the masonry wall fails in shear or diagonal tension.

Mode 5: Frame Failure in the form of plastic hinges in the columns or the beam column connection – also associated with strong infill surrounded by a weak frame or frame with weak joints and strong members.

Most of the studies are focused on the corner crushing mode of failure i.e. *mode 3* in which, the diagonal compression strut mechanism is fully developed that converts the frame system into the truss (Figure 17.2), increasing the lateral stiffness of the frame manifold. In fact, one may expect an initial lateral stiffness of the infilled frame 5 to 40 times of the respective bare frame. Nowadays, the diagonal strut model is widely accepted as a simple and rational way to describe the influence of the frame-panel interaction.

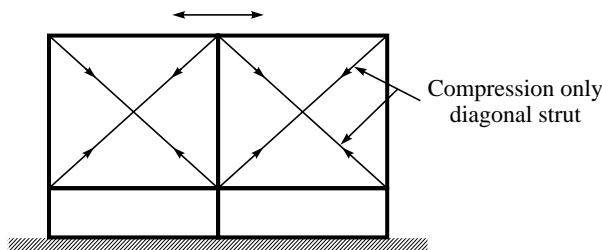


FIGURE 17.2 Diagonal compression strut mechanism.

17.4 ANALYSIS OF INFILLED FRAMES

It has already been discussed in the previous sections that the presence of infill affects the distribution of lateral load in the frames of building because of the increase of stiffness of some

of the frames. The distribution of lateral forces in the frames of building basically depends upon the center of rigidity of the building and the resultant of the applied lateral loads. If both nearly coincide, distribution of lateral load remains straightforward *i.e.* in the ratio of their relative stiffness. If it is not the case, large torsional forces are introduced in the building. These type of structures can be better analysed on the basis of 3D analysis of building after considering the increased stiffness of the infilled frames.

The study of interaction of infill with frames has been attempted by using sophisticated analysis like finite element analysis or theory of elasticity. But due to uncertainty in defining the interface conditions between the infilled with the frames, an approximate analysis method may be better acceptable. One of the most common approximation of infilled walls is on the basis of equivalent diagonal strut *i.e.* the system is modeled as a braced frame and infill walls as web element. The main problem in this approach is to find the effective width for the equivalent diagonal strut. Various investigators have suggested different values of width of equivalent diagonal strut.

17.4.1 Equivalent Diagonal Strut

Infill wall without openings

The geometric and material properties of the equivalent diagonal strut are required for conventional braced frame analysis to determine the increased stiffness of the infilled frame. The geometric properties are of effective width and thickness of the strut. The thickness and material properties of strut are similar to the infill wall. Many investigators have proposed various approximations for the width of equivalent diagonal strut. Originally proposed by Polyakov (1956) and subsequently developed by many investigators, the width of strut depends on the length of contact between the wall and the columns, α_h , and between the wall and beams, α_L shown in Figure 17.3. The proposed range of contact length is between one-fourth and one-tenth of the length of panel. Stafford Smith (1966) developed the formulations for α_h and α_L on the basis of beam on an elastic foundation. The following equations are proposed

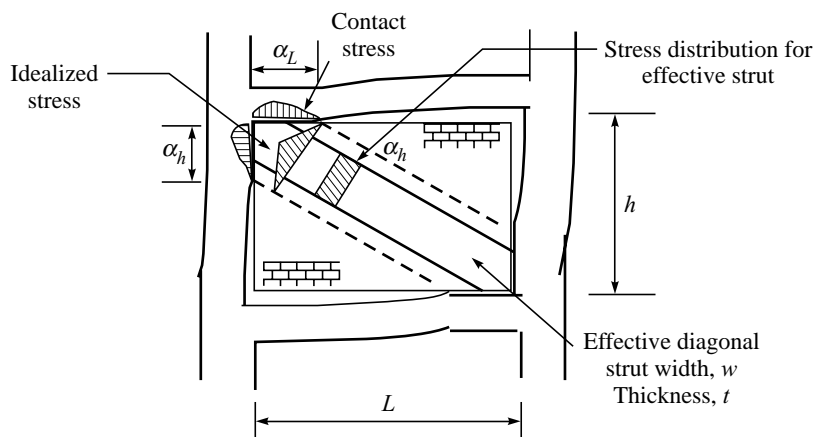


FIGURE 17.3 Equivalent diagonal strut (Drydale, Hamid and Baker, 1994).

to determine α_h and α_L , which depend on the relative stiffness of the frame and infill, and on the geometry of the panel.

$$\alpha_h = \frac{\pi}{2} \sqrt[4]{\frac{4E_f I_c h}{E_m t \sin 2\theta}}$$

$$\alpha_L = \pi \sqrt[4]{\frac{4E_f I_b L}{E_m t \sin 2\theta}}$$

where,

E_m and E_f = Elastic modulus of the masonry wall and frame material, respectively

t, h, L = Thickness, height, and length of the infill wall, respectively

I_c, I_b = Moment of inertia of the column and the beam of the frame, respectively

$$\theta = \tan^{-1}(h/L)$$

Hendry (1998) has proposed the following equation to determine the equivalent or effective strut width w , where the strut is assumed to be subjected to uniform compressive stress

$$w = \frac{1}{2} \sqrt{\alpha_h^2 + \alpha_L^2}$$

Holmes (1963) recommended a width of the diagonal strut equal to one-third of the diagonal length of the panel, whereas New Zealand Code (NZS 4230) specifies a width equal to one quarter of its length.

Example 1 Determine the increase in stiffness of the frame as shown in the given figure, when the brick infill walls are included in the analysis of frame. The infills are provided in the top two stories and the properties of frame and infill are given as

Frame properties:

$$E_f = 5000 \sqrt{f_{ck}}$$

$$f_{ck} = 20 \text{ MPa}$$

Width of beam and column (b) = 0.30 m

Depth of beam and column (d) = 0.45 m

I_c = Moment of inertia of the column

I_b = Moment of inertia of beam

$$I_c = I_b = 0.002278125 \text{ m}^4$$

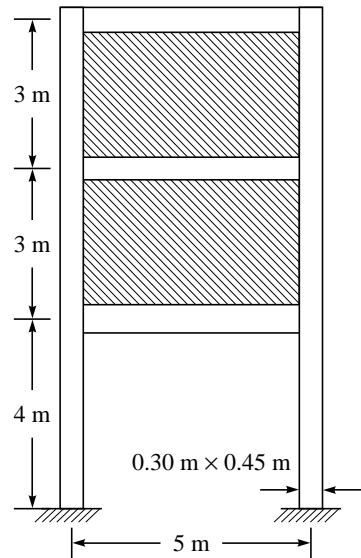
Infill properties

$$E_m = \text{Elastic modulus of masonry wall} \\ = 13800 \text{ MPa}$$

t = thickness of the infill wall = 0.23 m

h = height of the infill wall = 2.55 m

L = length of the infill wall = 4.55 m



(a) Calculating the width of equivalent diagonal strut

Infills in second and third stories are modelled as equivalent diagonal struts and its equivalent width of a strut is given as,

$$W = \frac{1}{2} \sqrt{\alpha_h^2 + \alpha_L^2}$$

where,

$$\alpha_h = \frac{\pi}{2} \left[\frac{E_f I_c h}{2E_m t \sin 2\theta} \right]^{1/4} \quad \text{and} \quad \alpha_L = \pi \left[\frac{E_f I_b L}{2E_m t \sin 2\theta} \right]^{1/4}$$

$$\theta = \tan^{-1} (h/L)$$

$$\theta = \tan^{-1} (2.55/4.55) = 29.267^\circ$$

L_d , A_d = length and area of equivalent strut

$$\alpha_h = 0.618 \text{ m}$$

$$\alpha_L = 1.7 \text{ m}$$

$$W = 0.904 \text{ m}$$

$$L_d = \sqrt{(h^2 + L^2)} = 5.2158 \text{ m}$$

$$A_d = tW = 0.2079 \text{ m}^2$$

(b) Analysis of Frame with Strut

The frame has been analysed with diagonal pin-jointed strut using a plane frame computer programme. Stiffness is calculated by assuming that the supports are fixed and load is applied at the floor level. Horizontal deflection is measured at the floor level and lateral stiffness is calculated by dividing horizontal deflection to unit load. The stiffness of all three stories are presented in Table 17.1.

TABLE 17.1 Calculation of storey stiffness in building frame

Storey 1	Storey 2	Storey 3
<p>$\delta = 0.071 \text{ m}$</p> <p>$K_1 = 14.084 \text{ MN/m}$</p>	<p>$\delta = 0.003 \text{ m}$</p> <p>$K_2 = 333.333 \text{ MN/m}$</p>	<p>$\delta = 0.003 \text{ m}$</p> <p>$K_3 = 333.333 \text{ MN/m}$</p>

The ratio of stiffness of first storey without infill to second storey with infill is

$$K_{\text{without infill}}/K_{\text{with infill}} = 0.042$$

Infill wall with openings

Infill walls in the frame are frequently contained in door and window openings at the different locations, which reduces stiffness and load carrying capacity of the diagonal strut depending upon the size of opening and its locations. If openings are small, and outside the one of the diagonal strut, its effect may be negligible in stiffness calculation *i.e.* full effect of equivalent diagonal strut will be taken into consideration (as discussed above) because the other diagonals of the panel become strut when the load is reversed. If the openings are large and centrally located, it may interfere the diagonal bracing action, thereby causing premature shear failure of the sections on the either side of the opening. Experimental and analytical studies show that centrally located openings may reduce the stiffness and strength of diagonal strut about 75% and 40% respectively.

Simple analytical method for calculating the stiffness of infill panels with opening is not easily available so far. However, Kadir (1974) has suggested an approximation method for analysing infilled panels with openings in which the panel is replaced by a diagonal member of the equivalent stiffness, and the stiffness of this diagonal can be calculated by considering the infill as a frame action from the relationship

$$K_w = \frac{48E_w}{h_w(h_w + h_f)} \left(\frac{J_1 J_h}{J_1 h_w + J_h l_w} \right)$$

where, J_1 and J_h are the moments of inertia of the vertical and horizontal sections of the infill frame as shown in Figure 17.4.

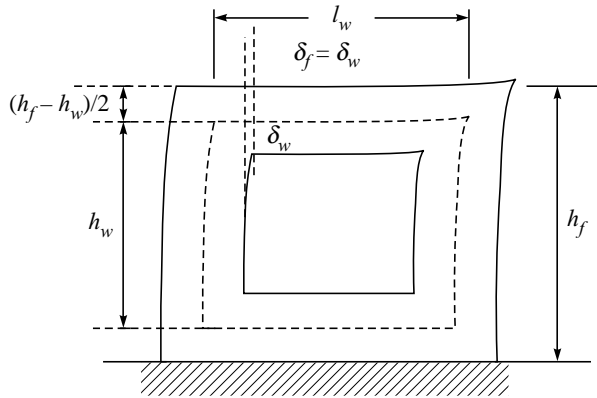


FIGURE 17.4 Dimensions of equivalent brickwork frame (Hendry, 1998).

Liaus and Lee (1977) have also put forward a method of the calculation of the stiffness and strength of infilled frames with openings using a stain energy method to establish the area of the equivalent diagonal strut. Rigid arms (Figure 17.5), which store no strain energy, are

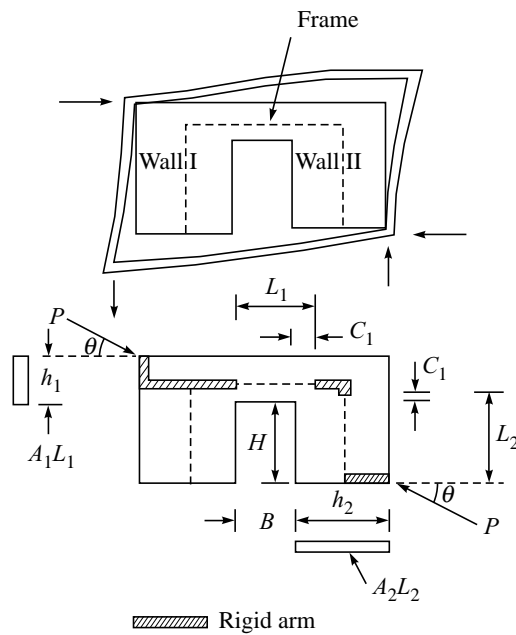


FIGURE 17.5 Analysis of infilled frame with opening (Liaus and Lee, 1977).

introduced to account for the finite width of walls and finite depth of the beam. The effective length of the beam and height of the walls are given respectively by,

$$\begin{aligned} L_1 &= B + C_1 \\ L_2 &= H + C_2 \leq L'_2 \end{aligned}$$

where L'_2 is the distance from the bottom of the wall to the centroid axis of the beam. It is recommended that the value of C_1 should be half the depth of beam.

The total strain energy of an infill subjected to diagonal load $P = 1$ is minimised to give the deflection in the direction of load

$$\Delta = \frac{1}{3E} \left\{ \frac{\sin^2 \theta}{I_1} [(L_1 - m_1)^3 - m_1^3] + \frac{\cos^2 \theta}{I_2} [(L_2 - m_2)^3 + m_2^3] + \frac{1.2E}{G} \left[\frac{L_1 \sin^2 \theta}{A_1} + \frac{L_2 \cos^2 \theta}{A_2} \right] \right. \\ \left. + \frac{L_1 \cos^2 \theta}{A_1} + \frac{L_2 \sin^2 \theta}{A_2} \right\}$$

where,

$$m_1 = \frac{h_1}{2} \cot \theta$$

$$m_2 = \frac{h_2}{2} \tan \theta$$

The diagonal stiffness k of the infill is equal to the reciprocal of the deflection when $P = 1$. If an equivalent diagonal strut of length L_d replaces the infill, the stiffness of the strut is given by,

$$k = EA_e/L_d$$

Hence the cross-sectional area of the equivalent diagonal strut is,

$$A_e = L_d/E\Delta$$

The infilled frame can then be converted into the frame with the equivalent diagonal struts, and analysed by usual method of frame analysis.

SUMMARY

Multi-storeyed buildings are often analysed without considering the effect of infill wall panels on the assumption that these infill panel will not resist any kind of load. However, these infill panels increase the strength and stiffness of frame considerably and are responsible for unequal distribution of forces in buildings. The aim of the chapter is to focus on structural and constructional aspect of infill along with its failure mechanism. It also presents how to consider an infill wall in seismic analysis of frame. A solved example has also been presented for modeling the infill as an equivalent diagonal strut. An approximate solution of infill wall with opening has also been discussed.

REFERENCES

- [1] IS 1893, *Criteria for Earthquake Resistant Design of Structures—Part 1, General Provisions and Buildings* (fifth revision), Bureau of Indian Standards, New Delhi, 2002.
- [2] CEB, *RC Frames under Earthquake Loading—State of the Art Report*, Thomas Telford, 1996.
- [3] Drysdale, R.G., Hamid, A.A., and Baker, L.R., *Masonry Structures—Behaviour and Design*, Prentice Hall, Englewood Cliffs, New Jersey, 1994.
- [4] Hendry, A.W. *Structural Masonry*, 2nd ed., Macmillan Press, 1998.
- [5] Holmes, M., “Combined Loading on Infilled Frames”, *Proceedings of the Institute of Civil Engineers*, 25: 31–38, 1963.
- [6] Kadir, M.R.A., “The Structural Behaviour of Masonry Infill Panels in Framed Structures”, *Ph.D. Thesis*, University of Edinburgh, 1974.
- [7] Liauw, T.C. and Lee, S.W., “On the Behaviour and the Analysis of Multi-storey Infilled Frames Subject to Lateral Loading”, *Proceedings of Institute of Civil Engineers*, 1977.
- [8] Liauw, T.C., “An Approximate Method of Analysis for Infilled Frame with or without Openings”, *Building Science*, 7: 223–238, Pergamon Press, 1972.
- [9] NZS 4230, “Code of Practice for the Design of Masonry Structures (Part 1)”, Standard Association of New Zealand, Wellington, 1990.

- [10] Polyakov, S.V., "Masonry in Framed Buildings, Gosudalst—Vennoe' stvo Literature po Straitel' stuv i Arkitekture, Moskva, Trans. G.L. Cairns", Building Research Station, Watford, Herts, 1956.
- [11] Parducci, A. and Mezzi, M., "Repeated Horizontal Displacements of Infilled Frames having Different Stiffness and Connection Systems—Experimental Analysis", *Proceedings of 7th World Conference on Earthquake Engineering*, 7: 193–196, Istanbul, 1980.
- [12] Stafford-Smith, B., "Behaviour of Square Infilled Frames", *Journal of the Structural Division*, Proceedings of ASCE, Vol. 91, No. ST1, pp. 381–403, 1966.

Chapter 18

Step-by-Step Procedure for Seismic Analysis of a Four-storeyed RC Building as per IS 1893 (Part 1): 2002

18.1 INTRODUCTION

A four-storeyed RC building has been analyzed by the equivalent static method, response spectrum method and time-history method as per IS 1893 (Part 1): 2002. The example illustrates the step-by-step procedure for determination of forces. One of the plane frames in transverse direction has been considered for the purpose of illustration by assuming that the building is symmetric in elevation and planned as shown in Figure 18.1. The preliminary

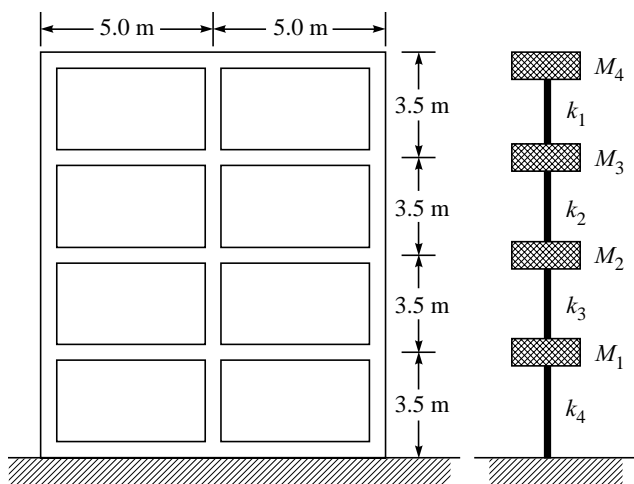


FIGURE 18.1(a) Plane frame structure and its lumped mass model.

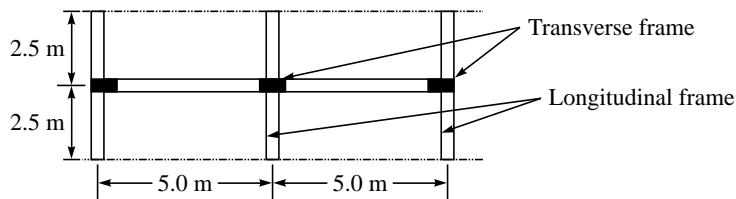


FIGURE 18.1(b) Plan showing the column and beams at floor levels of the plane frame.

building data required for analysis are assumed in Table 18.1.

TABLE 18.1 Assumed preliminary data required for analysis of frame

1.	Type of structure	Multi-storey rigid jointed plane frame (Special RC moment resisting frame)
2.	Seismic zone	IV (Table 2, IS 1893 (Part 1): 2002)
3.	Number of stories	Four, (G+3)
4.	Floor height	3.5 m
5.	Infill wall	250 mm thick including plaster in longitudinal and 150 mm in transverse direction
6.	Imposed load	3.5 kN/m ²
7.	Materials	Concrete (M 20) and Reinforcement (Fe415)
8.	Size of columns	250 mm × 450 mm
9.	Size of beams	250 mm × 400 mm in longitudinal and 250 mm × 350 mm in transverse direction
10.	Depth of slab	100 mm thick
11.	Specific weight of RCC	25 kN/m ³
12.	Specific weight of infill	20 kN/m ³
13.	Type of soil	Rock
14.	Response spectra	As per IS 1893 (Part 1): 2002
15.	Time history	Compatible to IS 1893 (Part 1): 2002 spectra at rocky site for 5% damping

18.2 EQUIVALENT STATIC LATERAL FORCE METHOD

A step-by-step procedure for analysis of the frame by equivalent static lateral force method is as follows:

18.2.1 Step 1: Calculation of Lumped Masses to Various Floor Levels

The earthquake forces shall be calculated for the full dead load plus the per centage of imposed load as given in Table 8 of IS 1893 (Part 1): 2002. The imposed load on roof is assumed to be zero. The lumped masses of each floor are worked out as follows:

Roof

Mass of infill + Mass of columns + Mass of beams in longitudinal and transverse direction of that floor + Mass of slab + Imposed load of that floor if permissible.

$$\begin{aligned} &= \{(0.25 \times 10 \times (3.5/2) + 0.15 \times 15 \times (3.5/2)) 20\} + \{(0.25 \times 10 \times 0.40 + 0.25 \times 15 \\ &\quad \times 0.35) 25\} + \{0.10 \times 5 \times 10 \times 25\} + \{(0.25 \times 0.45 \times (3.5/2) \times 3) \times 25\} + 0^* \\ &= 363.82 \text{ kN (weight)} = 37.087 \text{ ton (mass)} \end{aligned}$$

3rd, 2nd, 1st Floors

$$\begin{aligned} &= \{(0.25 \times 10 \times 3.5) + (0.15 \times 15 \times 3.5)\} 20\} + \{(0.25 \times 10 \times 0.40 + 0.25 \times 15 \times 0.35) 25\} \\ &\quad + \{0.10 \times 5 \times 10 \times 25\} + \{0.25 \times 0.45 \times 3.5 \times 3 \times 25\} + \{5 \times 10 \times 3.5 \times 0.5^{**}\} \\ &= 632.43 \text{ kN (weight)} = 64.45 \text{ ton (mass)} \end{aligned}$$

* Imposed load on roof not considered.

** 50% of imposed load, if imposed load is greater than 3 kN/m²

Seismic weight of building

$$\begin{aligned} &= \text{Seismic weight of all floors} = M_1 + M_2 + M_3 + M_4 \\ &= 64.45 + 64.45 + 64.45 + 37.08 = 230.43 \text{ ton} \end{aligned}$$

Note: The seismic weight of each floor is its full dead load plus appropriate amount of imposed load, as specified in Clause 7.3.1 and 7.3.2 of IS 1893 (Part1): 2002. Any weight supported in between stories shall be distributed to the floors above and below in inverse proportion to its distance from the floors.

18.2.2 Step 2: Determination of Fundamental Natural Period

The approximate fundamental natural period of a vibration (T_a), in seconds, of a moment resisting frame building without brick infill panels may be estimated by the empirical expression

$$T_a = 0.075 \times h^{0.75} = 0.075 \times 14^{0.75} = 0.5423 \text{ s}$$

where h is the height of the building, in metres.

18.2.3 Step 3: Determination of Design Base Shear

Design seismic base shear, $V_B = A_h W$

$$A_h = \frac{Z}{2} \frac{I}{R} \frac{S_a}{g} = \frac{0.24}{2} \frac{1}{5} 1.842 = 0.0443$$

For $T_a = 0.5423 \Rightarrow \frac{S_a}{g} = \frac{1}{T_a} = 1.842$, for rock site from **Figure 2 of IS 1893 (Part 1): 2002**

Design seismic base shear, $V_B = 0.0443 \times (230.43 \times 9.81) = 99.933 \text{ kN}$

18.2.4 Step 4: Vertical Distribution of Base Shear

The design base shear (V_B) computed shall be distributed along the height of the building as per the expression,

$$Q_i = V_B \frac{W_i h_i^2}{\sum_{i=1}^n W_i h_i^2} \quad (18.1)$$

where,

Q_i = Design lateral forces at floor i ,

W_i = Seismic weights of the floor i ,

h_i = Height of the floor i , measured from base, and

n = Number of stories

Using the Equation 18.1, base shear is distributed as follows:

$$\begin{aligned} Q_1 &= V_B \left(\frac{W_1 h_1^2}{W_1 h_1^2 + W_2 h_2^2 + W_3 h_3^2 + W_4 h_4^2} \right) \\ &= 99.933 \left[\frac{632.25 \times 3.5^2}{632.25 \times 3.5^2 + 632.25 \times 7^2 + 632.25 \times 10.5^2 + 363.82 \times 14^2} \right] = 4.306 \text{ kN} \end{aligned}$$

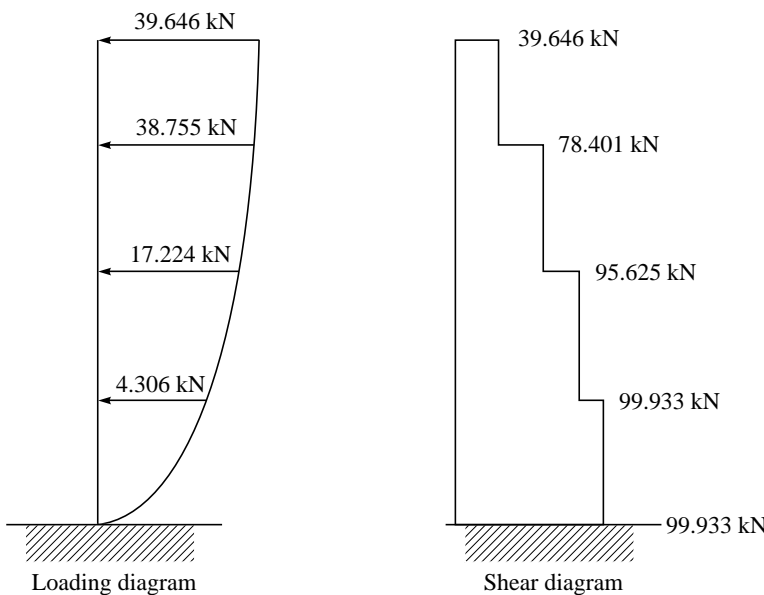
Similarly,

$$Q_2 = 0.1724 \times 99.933 = 17.224 \text{ kN}$$

$$Q_3 = 0.3872 \times 99.933 = 38.733 \text{ kN}$$

$$Q_4 = 0.3967 \times 99.933 = 39.646 \text{ kN}$$

Lateral force distribution at various floor levels



18.3 RESPONSE SPECTRUM METHOD

A: Frame without Considering the Stiffness of Infills

A step-by-step procedure for analysis of the frame by response spectrum method is as follows:

18.3.1 Step 1: Determination of Eigenvalues and Eigenvectors

Mass matrice, M and stiffness matrice, K of the plane frame lumped mass model are,

$$M = \begin{bmatrix} M_1 & 0 & 0 & 0 \\ 0 & M_2 & 0 & 0 \\ 0 & 0 & M_3 & 0 \\ 0 & 0 & 0 & M_4 \end{bmatrix} = \begin{bmatrix} 64.65 & 0 & 0 & 0 \\ 0 & 64.45 & 0 & 0 \\ 0 & 0 & 64.45 & 0 \\ 0 & 0 & 0 & 37.08 \end{bmatrix} \text{ton}$$

Column stiffness of storey,

$$k = \frac{12EI}{L^3} = \frac{12 \times 22360 \times 10^3 \left(\frac{0.25 \times 0.45^3}{12} \right)}{3.5^3} = 11880.78 \text{ kN/m}$$

Total lateral stiffness of each storey,

$$k_1 = k_2 = k_3 = k_4 = 3 \times 11880.78 = 35642.36 \text{ kN/m}$$

Stiffness of lumped mass modelled structure

$$K = \begin{bmatrix} k_1 + k_2 & -k_2 & 0 & 0 \\ -k_2 & k_2 + k_3 & -k_3 & 0 \\ 0 & -k_3 & k_3 + k_4 & -k_4 \\ 0 & 0 & -k_4 & k_4 \end{bmatrix} = \begin{bmatrix} 71284.72 & -3564.36 & 0 & 0 \\ -3564.36 & 71284.72 & -3564.36 & 0 \\ 0 & -3564.36 & 71284.72 & -35642.36 \\ 0 & 0 & -35642.36 & 35642.36 \end{bmatrix} \text{kN/m}$$

For the above stiffness and mass matrices, eigenvalues and eigenvectors are worked out as follows:

$$|K - \omega^2 m| = \begin{vmatrix} 2k - \omega^2 m & -k_2 & 0 & 0 \\ -k_2 & 2k - \omega^2 m & -k_3 & 0 \\ 0 & -k_3 & 2k - \omega^2 m & -k_4 \\ 0 & 0 & -k_4 & k - \omega^2 0.575 m \end{vmatrix} = 0$$

Taking $k/m = \omega_n^2$

Therefore,

$$(\omega_n^2)^4 - 8.3(\omega_n^2)^3 (\omega^2) + 10.75(\omega_n^2)^2 (\omega^2)^2 - 4.45(\omega_n^2)(\omega^2)^3 + 0.575(\omega^2)^4 = 0$$

By solving the above equation, natural frequencies (eigenvalues) of various modes are

Eigenvalues

$$[\omega^2] = \begin{bmatrix} 81 & & & \\ & 657 & & \\ & & 1475 & \\ & & & 2065 \end{bmatrix}$$

$$\omega_1^2 = 81, \omega_2^2 = 657, \omega_3^2 = 1475, \omega_4^2 = 2065$$

The quantity of ω_i^2 , is called the i^{th} eigenvalue of the matrix $[-M\omega_i^2 + K]\phi_i$. Each natural frequency (ω_i) of the system has a corresponding eigenvector (mode shape), which is denoted by ϕ_i . The mode shape corresponding to each natural frequency is determined from the equations

$$[-M\omega_1^2 + K]\phi_1 = 0$$

$$[-M\omega_2^2 + K]\phi_2 = 0$$

$$[-M\omega_3^2 + K]\phi_3 = 0$$

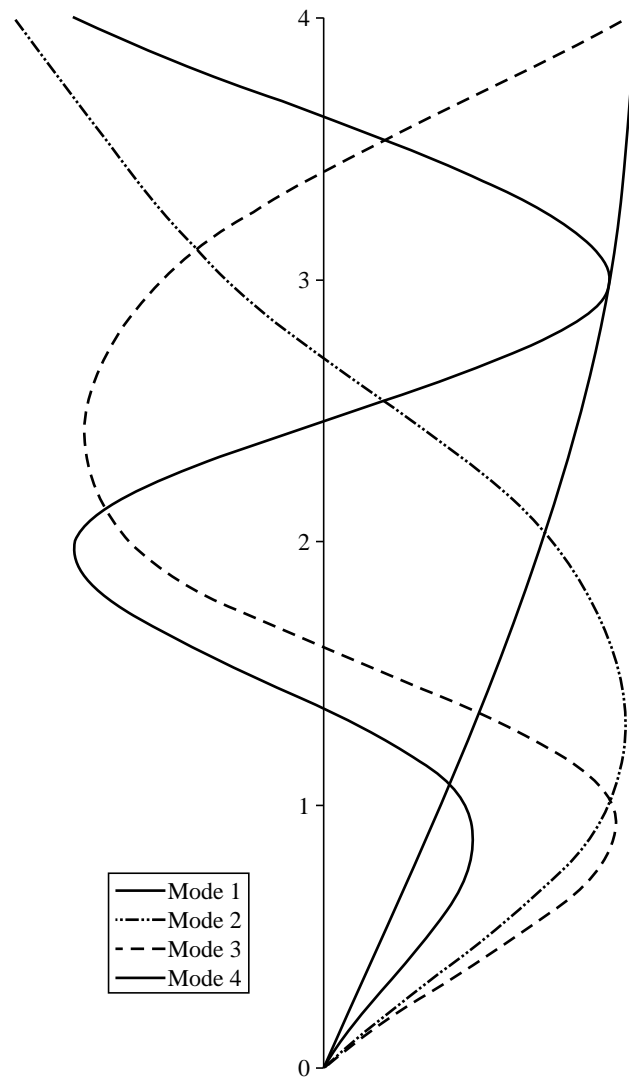
$$[-M\omega_4^2 + K]\phi_4 = 0$$

Solving the above equation, modal vector (eigenvectors), mode shapes and natural periods under different modes are

Eigenvectors $\{\phi\}$

$$\{\Phi\} = \{\Phi_1 \ \Phi_2 \ \Phi_3 \ \Phi_4\} = \begin{bmatrix} -0.0328 & 0.0795 & 0.0808 & -0.0397 \\ -0.0608 & 0.0644 & -0.0540 & 0.0690 \\ -0.0798 & -0.0273 & -0.0448 & -0.0799 \\ -0.0872 & -0.0865 & 0.0839 & 0.0696 \end{bmatrix}$$

Mode shapes



Natural time period

$$T = \begin{bmatrix} 0.6977 & 0 & 0 & 0 \\ 0 & 0.2450 & 0 & 0 \\ 0 & 0 & 0.1636 & 0 \\ 0 & 0 & 0 & 0.1383 \end{bmatrix} \text{ s}$$

18.3.2 Step 2: Determination of Modal Participation Factors

The modal participation factor (p_k) of mode k is,

$$p_k = \frac{\sum_{i=1}^n W_i \Phi_{ik}}{\sum_{i=1}^n W_i (\Phi_{ik})^2}$$

$$p_1 = \frac{\sum_{i=1}^4 W_i \Phi_{i1}}{\sum_{i=1}^4 W_i (\Phi_{i1})^2} = \frac{(W_1 \Phi_{11} + W_2 \Phi_{21} + W_3 \Phi_{31} + W_4 \Phi_{41})}{(W_1 (\Phi_{11})^2 + W_2 (\Phi_{21})^2 + W_3 (\Phi_{31})^2 + W_4 (\Phi_{41})^2)} = -14.40$$

$$p_2 = \frac{\sum_{i=1}^4 W_i \Phi_{i2}}{\sum_{i=1}^4 W_i (\Phi_{i2})^2} = \frac{(W_1 \Phi_{12} + W_2 \Phi_{22} + W_3 \Phi_{32} + W_4 \Phi_{42})}{(W_1 (\Phi_{12})^2 + W_2 (\Phi_{22})^2 + W_3 (\Phi_{32})^2 + W_4 (\Phi_{42})^2)} = 4.30$$

Similarly,

$$p_3 = 1.95, p_4 = -0.68$$

18.3.3 Step 3: Determination of Modal Mass

The modal mass (M_k) of mode k is given by,

$$M_k = \frac{\left[\sum_{i=1}^n W_i \Phi_{ik} \right]^2}{g \left[\sum_{i=1}^n W_i (\Phi_{ik})^2 \right]}$$

where,

g = Acceleration due to gravity,

Φ_{ik} = Mode shape coefficient at floor i in mode k , and

W_i = Seismic weight of floor i ,

$$M_1 = \frac{\left[\sum_{i=1}^4 W_i \Phi_{i1} \right]^2}{g \left[\sum_{i=1}^4 W_i (\Phi_{i1})^2 \right]}$$

$$M_1 = \frac{[9.81(64.45(-0.0328) + 64.45(-0.0608) + 64.45(-0.0798) + 37.08(-0.0872))]^2}{9.81[9.81(64.45(-0.0328)^2 + 64.45(-0.0608)^2 + 64.45(-0.0798)^2 + 37.08(-0.0872)^2)]} \\ = 207.60$$

$$M_2 = \frac{\left[\sum_{i=1}^4 W_i \Phi_{i2} \right]^2}{g \left[\sum_{i=1}^4 W_i (\Phi_{i2})^2 \right]}, \text{ similarly, } M_2 = 18.54, M_3 = 3.82, M_4 = 0.47.$$

Modal contributions of various modes

For mode 1, $\frac{M_1}{M} = \frac{207.60}{230.43} = 0.90 = 90\%$

For mode 2, $\frac{M_2}{M} = \frac{18.54}{230.43} = 0.0804 = 8.04\%$

For mode 3, $\frac{M_3}{M} = \frac{3.82}{230.43} = 0.0165 = 1.65\%$

For mode 4, $\frac{M_4}{M} = \frac{0.47}{230.43} = 0.0020 = 0.20\%$

18.3.4 Step 4: Determination of Lateral Force at Each Floor in Each Mode

The design lateral force (Q_{ik}) at floor i in mode k is given by,

$$Q_{ik} = A_k \Phi_{ik} P_k W_i$$

where,

A_k = Design horizontal acceleration spectrum value as per clause 6.4.2 of IS 1893 (Part 1): 2002 using the natural period of vibration (T_k) of mode k .

The design horizontal seismic coefficient A_h for various modes are,

$$A_{hk} = \frac{Z}{2} \frac{I}{R} \frac{S_{ak}}{g}$$

$$A_{h1} = \frac{Z}{2} \frac{I}{R} \frac{S_{a1}}{g} = \frac{0.24}{2} \frac{1}{5} 1.433 = 0.0343$$

$$A_{h2} = \frac{Z}{2} \frac{I}{R} \frac{S_{a2}}{g} = \frac{0.24}{2} \frac{1}{5} 2.5 = 0.060$$

Similarly $A_{h3} = 0.060$, $A_{h4} = 0.060$.

The average response acceleration coefficient for rock sites as per **IS 1893 (Part 1): 2002** is calculated as follows:

For rocky, or hard soil sites

$$\frac{S_a}{g} = \begin{cases} 1 + 15T; & 0.00 \leq T \leq 0.10 \\ 2.5; & 0.10 \leq T \leq 0.40 \\ 1.00/T; & 0.40 \leq T \leq 4.0 \end{cases}$$

$$\text{For } T_1 = 0.6978 \Rightarrow \frac{S_{a1}}{g} = 1.433$$

$$\text{For } T_2 = 0.2450 \Rightarrow \frac{S_{a2}}{g} = 2.5$$

$$\text{For } T_3 = 0.1636 \Rightarrow \frac{S_{a3}}{g} = 2.5$$

$$\text{For } T_4 = 0.1382 \Rightarrow \frac{S_{a4}}{g} = 2.5$$

Design lateral force in each mode

$$Q_{i1} = (A_1 \ P_1 \ \Phi_{i1} \ W_i)$$

$$[Q_{i1}] = \begin{bmatrix} (A_{h1} \ P_1 \ \Phi_{11} \ W_1) \\ (A_{h1} \ P_1 \ \Phi_{21} \ W_2) \\ (A_{h1} \ P_1 \ \Phi_{31} \ W_3) \\ (A_{h1} \ P_1 \ \Phi_{41} \ W_4) \end{bmatrix} = \begin{bmatrix} ((0.0343)(-14.40)(-0.0328)(64.45 \times 9.81)) \\ ((0.0343)(-14.40)(-0.0608)(64.45 \times 9.81)) \\ ((0.0343)(-14.40)(-0.0798)(64.45 \times 9.81)) \\ ((0.0343)(-14.40)(-0.0872)(37.08 \times 9.81)) \end{bmatrix} = \begin{bmatrix} (10.275) \\ (19.043) \\ (25.018) \\ (15.720) \end{bmatrix} \text{ kN}$$

$$\text{Similarly, } [Q_{i2}] = \begin{bmatrix} -43.44 \\ -35.199 \\ 14.920 \\ 27.207 \end{bmatrix}, [Q_{i3}] = \begin{bmatrix} -44.204 \\ 29.499 \\ 24.517 \\ -26.385 \end{bmatrix}, [Q_{i4}] = \begin{bmatrix} 21.749 \\ -37.722 \\ 43.675 \\ -21.878 \end{bmatrix}.$$

18.3.5 Step 5: Determination of Storey Shear Forces in Each Mode

The peak shear force is given by,

$$V_{ik} = \sum_{j=i+1}^n Q_{ik}$$

The storey shear forces for the first mode is,

$$V_{i1} = \sum_{j=i+1}^n Q_{i1} = \begin{bmatrix} V_{11} \\ V_{21} \\ V_{31} \\ V_{41} \end{bmatrix} = \begin{bmatrix} (Q_{11} + Q_{21} + Q_{31} + Q_{41}) \\ (Q_{21} + Q_{31} + Q_{41}) \\ (Q_{31} + Q_{41}) \\ (Q_{41}) \end{bmatrix} = \begin{bmatrix} 70.056 \\ 59.781 \\ 40.738 \\ 15.720 \end{bmatrix} \text{ kN}$$

Similarly,

$$V_{i2} = \begin{bmatrix} V_{12} \\ V_{22} \\ V_{32} \\ V_{42} \end{bmatrix} = \begin{bmatrix} -36.514 \\ 6.927 \\ 42.127 \\ 27.207 \end{bmatrix}, V_{i3} = \begin{bmatrix} V_{13} \\ V_{23} \\ V_{33} \\ V_{43} \end{bmatrix} = \begin{bmatrix} -16.572 \\ 27.632 \\ -1.867 \\ -26.385 \end{bmatrix}, V_{i4} = \begin{bmatrix} V_{14} \\ V_{24} \\ V_{34} \\ V_{44} \end{bmatrix} = \begin{bmatrix} 5.824 \\ -15.925 \\ 21.796 \\ -21.878 \end{bmatrix}$$

18.3.6 Step 6: Determination of Storey Shear Force due to All Modes

The peak storey shear force (V_i) in storey i due to all modes considered is obtained by combining those due to each mode in accordance with modal combination i.e. SRSS (Square Root of Sum of Squares) or CQC (Complete Quadratic Combination) methods.

Square root of sum of squares (SRSS)

If the building does not have closely spaced modes, the peak response quantity (λ) due to all modes considered shall be obtained as,

$$\lambda = \sqrt{\sum_{k=1}^r (\lambda_k)^2},$$

where,

λ_k = Absolute value of quantity in mode ' k ', and r is the numbers of modes being considered.

Using the above method, the storey shears are,

$$\begin{aligned} V_1 &= [(V_{11})^2 + (V_{12})^2 + (V_{13})^2 + (V_{14})^2]^{1/2} \\ &= [(70.056)^2 + (-36.514)^2 + (-16.572)^2 + (5.824)^2]^{1/2} = 80.930 \text{ kN} \\ V_2 &= [(V_{21})^2 + (V_{22})^2 + (V_{23})^2 + (V_{24})^2]^{1/2} \\ &= [(59.781)^2 + (6.927)^2 + (27.632)^2 + (-15.925)^2]^{1/2} = 68.110 \text{ kN} \\ V_3 &= [(V_{31})^2 + (V_{32})^2 + (V_{33})^2 + (V_{34})^2]^{1/2} \\ &= [(40.738)^2 + (42.127)^2 + (-1.867)^2 + (21.796)^2]^{1/2} = 62.553 \text{ kN} \\ V_4 &= [(V_{41})^2 + (V_{42})^2 + (V_{43})^2 + (V_{44})^2]^{1/2} \\ &= [(15.720)^2 + (27.207)^2 + (-26.385)^2 + (-21.878)^2]^{1/2} = 48.499 \text{ kN} \end{aligned}$$

Complete quadratic combination (CQC)

$$\lambda = \sqrt{\sum_{i=1}^r \sum_{j=1}^r \lambda_i \rho_{ij} \lambda_j}$$

where,

r = Number of modes being considered,

ρ_{ij} = Cross modal coefficient,

λ_i = Response quantity in mode i (including sign),

λ_j = Response quantity in mode j (including sign),

$$\rho_{ij} = \frac{8\zeta^2(1 + \beta_{ij})\beta^{1.5}}{(1 + \beta_{ij})^2 + 4\zeta^2\beta_{ij}(1 + \beta_{ij})^2}$$

where,

ζ = Modal damping ratio (in fraction),

β_{ij} = Frequency ratio ω_j/ω_i ,

ω_i = Circular frequency in i^{th} mode, and

ω_j = Circular frequency in j^{th} mode.

Therefore all the frequency ratios and cross modal components can be represented in matrix form as,

$$\beta_{ij} = \begin{bmatrix} \beta_{11} & \beta_{12} & \beta_{13} & \beta_{14} \\ \beta_{21} & \beta_{22} & \beta_{23} & \beta_{24} \\ \beta_{31} & \beta_{32} & \beta_{33} & \beta_{34} \\ \beta_{41} & \beta_{42} & \beta_{43} & \beta_{44} \end{bmatrix} = \begin{bmatrix} \omega_1/\omega_1 & \omega_2/\omega_1 & \omega_3/\omega_1 & \omega_4/\omega_1 \\ \omega_1/\omega_2 & \omega_2/\omega_2 & \omega_3/\omega_2 & \omega_4/\omega_2 \\ \omega_1/\omega_3 & \omega_2/\omega_3 & \omega_3/\omega_3 & \omega_4/\omega_3 \\ \omega_1/\omega_4 & \omega_2/\omega_4 & \omega_3/\omega_4 & \omega_4/\omega_4 \end{bmatrix}$$

$$= \begin{bmatrix} 1 & 2.84 & 4.26 & 5.04 \\ 0.35 & 1 & 1.49 & 1.77 \\ 0.23 & 0.66 & 1 & 1.18 \\ 0.19 & 0.56 & 0.84 & 1 \end{bmatrix}$$

$$\rho_{ij} = \begin{bmatrix} \rho_{11} & \rho_{12} & \rho_{13} & \rho_{14} \\ \rho_{21} & \rho_{22} & \rho_{23} & \rho_{24} \\ \rho_{31} & \rho_{32} & \rho_{33} & \rho_{34} \\ \rho_{41} & \rho_{42} & \rho_{43} & \rho_{44} \end{bmatrix} = \begin{bmatrix} 1 & 0.0073 & 0.0031 & 0.0023 \\ 0.0073 & 1 & 0.0559 & 0.0278 \\ 0.0031 & 0.0559 & 1 & 0.2597 \\ 0.0023 & 0.0278 & 0.2597 & 1 \end{bmatrix}$$

The above quadratic combination i.e. $\lambda = \sqrt{\sum_{i=1}^r \sum_{j=1}^r \lambda_i \rho_{ij} \lambda_j}$ can also be written in matrix form

as,

$$[\lambda_1 \lambda_2 \lambda_3 \lambda_4] \begin{bmatrix} \rho_{11} & \rho_{12} & \rho_{13} & \rho_{14} \\ \rho_{21} & \rho_{22} & \rho_{23} & \rho_{24} \\ \rho_{31} & \rho_{32} & \rho_{33} & \rho_{34} \\ \rho_{41} & \rho_{42} & \rho_{43} & \rho_{44} \end{bmatrix} \begin{bmatrix} \lambda_1 \\ \lambda_2 \\ \lambda_3 \\ \lambda_4 \end{bmatrix}$$

Here the terms λ_i or λ_j represent the response of different modes of a certain storey level.

Using the matrix notation the storey shears are,

$$V_1 = \sqrt{\begin{bmatrix} [70.05 & -36.51 & -16.57 & 5.82] \end{bmatrix} \begin{bmatrix} 1 & 0.0073 & 0.0031 & 0.0023 \\ 0.0073 & 1 & 0.0559 & 0.0278 \\ 0.0031 & 0.0559 & 1 & 0.2597 \\ 0.0023 & 0.0278 & 0.2597 & 1 \end{bmatrix} \begin{bmatrix} 70.05 \\ -36.51 \\ -16.57 \\ 5.82 \end{bmatrix}} = [80.70]$$

$$V_2 = \sqrt{\begin{bmatrix} [59.78 & 6.92 & 27.63 & -15.92] \end{bmatrix} \begin{bmatrix} 1 & 0.0073 & 0.0031 & 0.0023 \\ 0.0073 & 1 & 0.0559 & 0.0278 \\ 0.0031 & 0.0559 & 1 & 0.2597 \\ 0.0023 & 0.0278 & 0.2597 & 1 \end{bmatrix} \begin{bmatrix} 59.78 \\ 6.92 \\ 27.63 \\ -15.92 \end{bmatrix}} = [66.61]$$

$$V_3 = \sqrt{\begin{bmatrix} [40.73 & 42.12 & -1.86 & 21.79] \end{bmatrix} \begin{bmatrix} 1 & 0.0073 & 0.0031 & 0.0023 \\ 0.0073 & 1 & 0.0559 & 0.0278 \\ 0.0031 & 0.0559 & 1 & 0.2597 \\ 0.0023 & 0.0278 & 0.2597 & 1 \end{bmatrix} \begin{bmatrix} 40.73 \\ 42.12 \\ -1.86 \\ 21.79 \end{bmatrix}} = [62.95]$$

$$V_4 = \sqrt{\begin{bmatrix} [15.72 & 27.20 & -26.38 & -21.87] \end{bmatrix} \begin{bmatrix} 1 & 0.0073 & 0.0031 & 0.0023 \\ 0.0073 & 1 & 0.0559 & 0.0278 \\ 0.0031 & 0.0559 & 1 & 0.2597 \\ 0.0023 & 0.0278 & 0.2597 & 1 \end{bmatrix} \begin{bmatrix} 15.72 \\ 27.20 \\ -26.38 \\ -21.87 \end{bmatrix}} = [48.48]$$

18.3.7 Step 7: Determination of Lateral Forces at Each Storey

The design lateral forces F_{roof} and F_i , at roof and at i^{th} floor, are calculated as,

$$F_{roof} = V_{roof} \text{ and } F_i = V_i - V_{i+1}$$

Square root of sum of squares (SRSS)

$$F_{roof} = F_4 = V_4 = 46.499 \text{ kN}$$

$$F_{\text{floor 3}} = F_3 = V_3 - V_4 = 62.553 - 46.499 = 16.053 \text{ kN}$$

$$F_{\text{floor } 2} = F_2 = V_2 - V_3 = 68.11 - 62.553 = 5.556 \text{ kN}$$

$$F_{\text{floor } 1} = F_1 = V_1 - V_2 = 80.930 - 68.11 = 12.820 \text{ kN}$$

Complete quadratic combination (CQC)

$$F_{\text{roof}} = F_4 = V_4 = 48.48 - 0 = 48.48 \text{ kN}$$

$$F_{\text{floor } 3} = F_3 = V_3 - V_4 = 62.95 - 48.48 = 14.47 \text{ kN}$$

$$F_{\text{floor } 2} = F_2 = V_2 - V_3 = 66.61 - 62.95 = 3.66 \text{ kN}$$

$$F_{\text{floor } 1} = F_1 = V_1 - V_2 = 80.70 - 66.61 = 14.09 \text{ kN}$$

B: Frame Considering the Stiffness of Infills

The frame considered in previous section is again analysed by considering the stiffness of infill walls. The infill is modelled as equivalent diagonal strut.

The mass matrix $[M]$ for the lumped plane frame model is,

$$M = \begin{bmatrix} M_1 & 0 & 0 & 0 \\ 0 & M_2 & 0 & 0 \\ 0 & 0 & M_3 & 0 \\ 0 & 0 & 0 & M_4 \end{bmatrix} = \begin{bmatrix} 64.45 & 0 & 0 & 0 \\ 0 & 64.45 & 0 & 0 \\ 0 & 0 & 64.45 & 0 \\ 0 & 0 & 0 & 37.08 \end{bmatrix} \text{ ton}$$

Column stiffness of storey

$$k = \frac{12EI}{L^3} = \frac{12 \times 22360 \times 10^3 (0.001893)}{3.5^3} = 11846.758 \text{ kN/m}$$

Stiffness of infill is determined by modeling the infill as an equivalent diagonal strut, in which,

$$\text{Width of strut, } W = \frac{1}{2} \sqrt{\alpha_h^2 + \alpha_l^2}$$

α_h and α_l are given as,

$$\alpha_h = \frac{\pi}{2} \left[\frac{E_f I_c h}{2 E_m t \sin 2\theta} \right]^{1/4}, \quad \alpha_l = \frac{\pi}{2} \left[\frac{E_f I_b l}{E_m t \sin 2\theta} \right]^{1/4}, \quad \theta = \tan^{-1} \frac{h}{l}$$

where,

E_f = Elastic modulus of frame material = 22360 N/m²

E_m = Elastic modulus of masonry wall = 13,800 N/m²

t = Thickness of infill wall = 250 mm

h = Height of infill wall = 3.5 m

l = Length of infill wall = 5.0 m

$$I_c = \text{Moment of inertia of columns} = \frac{1}{12} (0.25 \times 0.45^3) = 0.001893 \text{ m}^4$$

$$I_c = \text{Moment of inertia of columns} = \frac{1}{12} (0.25 \times 0.40^3) = 0.001333 \text{ m}^4$$

$$\alpha_h = \frac{\pi}{2} \left[\frac{22360 \times 0.001893 \times 3.5}{2 \times 13800 \times 0.25 \times \sin 2 \times 35} \right]^{1/4} = 0.611 \text{ m}$$

$$\alpha_l = \pi \left[\frac{22360 \times 0.001333 \times 5.0}{13800 \times 0.25 \times \sin 2 \times 35} \right]^{1/4} = 1.45 \text{ m}$$

$$W = \frac{1}{2} \sqrt{\alpha_h^2 + \alpha_l^2} = 0.7885 \text{ m}$$

$$A = \text{Cross-sectional area of diagonal stiffness} = W \times t = 0.7885 \times 0.25 = 0.1972 \text{ m}^2$$

$$l_d = \text{Diagonal length of strut} = \sqrt{h^2 + l^2} = 6.103 \text{ m}$$

Therefore, stiffness of infill is

$$\frac{AE_m}{l_d} \cos^2 \theta = \frac{0.1972 \times 13800 \times 10^6}{6.103} 0.819^2 = 299086.078 \times 10^3 \text{ N/m}$$

For the frame with two bays there are two struts participating in one direction, total lateral stiffness of each storey

$$k_1 = k_2 = k_3 = k_4 = 3 \times 11846.758 + 2 \times 299086078 = 633712.430 \text{ kN/m}$$

Stiffness matrix $[K]$ of lumped mass model is,

$$K = \begin{bmatrix} k_1 + k_2 & -k_2 & 0 & 0 \\ -k_2 & k_2 + k_3 & -k_3 & 0 \\ 0 & -k_3 & k_3 + k_4 & -k_4 \\ 0 & 0 & -k_4 & k_4 \end{bmatrix} = \begin{bmatrix} 1.2674 & -0.6337 & 0 & 0 \\ -0.6337 & 1.2674 & -0.6337 & 0 \\ 0 & -0.6337 & 1.2674 & -0.6337 \\ 0 & 0 & -0.6337 & 0.6337 \end{bmatrix} \times 10^6 \text{ kN/m}$$

For the above stiffness and mass matrices, eigenvalues and eigenvectors are,

$$|K - \omega^2 M| = \begin{bmatrix} 2k - \omega^2 m & -k_2 & 0 & 0 \\ -k_2 & 2k - \omega^2 m & -k_3 & 0 \\ 0 & -k_3 & 2k - \omega^2 m & -k_4 \\ 0 & 0 & -k_4 & k - \omega^2 0.575m \end{bmatrix} = 0, k/m = \omega_n^2$$

Therefore, quadratic equation in ω is,

$$(\omega_n^2)^4 - 8.3(\omega_n^2)^3 (\omega^2) + 10.75(\omega_n^2)^2 (\omega^2)^2 - 4.45(\omega_n^2)(\omega^2)^3 + 0.575(\omega^2)^4 = 0$$

Eigenvalues

$$[\omega^2] = \begin{bmatrix} 1442 & & & \\ & 11698 & & \\ & & 26227 & \\ & & & 36719 \end{bmatrix},$$

$$\omega_1^2 = 1442, \omega_2^2 = 11698, \omega_3^2 = 26227, \omega_4^2 = 36719$$

Eigenvectors $\{\phi\}$

$$\{\Phi\} = \{\Phi_1 \ \Phi_2 \ \Phi_3 \ \Phi_4\} = \begin{bmatrix} -0.0328 & 0.0795 & 0.0808 & -0.0397 \\ -0.0608 & 0.0644 & -0.0540 & 0.0690 \\ -0.0798 & -0.0273 & -0.0448 & -0.0799 \\ -0.0872 & -0.0865 & 0.0839 & 0.0696 \end{bmatrix}$$

Natural frequency in various modes

$$[\omega] = \begin{bmatrix} 37.975 & 0 & 0 & 0 \\ 0 & 108.157 & 0 & 0 \\ 0 & 0 & 161.947 & 0 \\ 0 & 0 & 0 & 191.621 \end{bmatrix} \text{ rad/s}$$

Natural time period

$$T = \begin{bmatrix} 0.1655 & 0 & 0 & 0 \\ 0 & 0.0581 & 0 & 0 \\ 0 & 0 & 0.0388 & 0 \\ 0 & 0 & 0 & 0.0328 \end{bmatrix}$$

Modal participation factors

$$p_1 = \frac{\sum_{i=1}^4 W_i \Phi_{i1}}{\sum_{i=1}^4 W_i (\Phi_{i1})^2} = \frac{(W_1 \Phi_{11} + W_2 \Phi_{21} + W_3 \Phi_{31} + W_4 \Phi_{41})}{(W_1 (\Phi_{11})^2 + W_2 (\Phi_{21})^2 + W_3 (\Phi_{31})^2 + W_4 (\Phi_{41})^2)} = -14.40$$

$$p_2 = \frac{\sum_{i=1}^4 W_i \Phi_{i2}}{\sum_{i=1}^4 W_i (\Phi_{i2})^2} = \frac{(W_1 \Phi_{12} + W_2 \Phi_{22} + W_3 \Phi_{32} + W_4 \Phi_{42})}{(W_1 (\Phi_{12})^2 + W_2 (\Phi_{22})^2 + W_3 (\Phi_{32})^2 + W_4 (\Phi_{42})^2)} = 4.30$$

Similarly, $p_3 = 1.95$, $p_4 = -0.68$

Modal mass

$$M_1 = \frac{\left[\sum_{i=1}^4 W_i \Phi_{i1} \right]^2}{g \left[\sum_{i=1}^4 W_i (\Phi_{i1})^2 \right]}$$

$$M_1 = \frac{[9.81(64.45(-0.0328) + 64.45(-0.0608) + 64.45(0.0798) + 37.08(-0.0872))]^2}{9.81[9.81(64.45(-0.0328)^2 + 64.45(-0.0608)^2 + 64.45(0.0798)^2 + 37.08(-0.0872)^2)]} \\ = 207.60$$

Similarly, $M_2 = 18.54$, $M_3 = 3.82$, $M_4 = 0.47$.

Modal contributions of various modes

$$\text{For mode 1, } \frac{M_1}{M} = \frac{207.60}{230.43} = 0.90 = 90\%$$

$$\text{For mode 2, } \frac{M_2}{M} = \frac{18.54}{230.43} = 0.0804 = 8.04\%$$

$$\text{For mode 3, } \frac{M_3}{M} = \frac{3.82}{230.43} = 0.0165 = 1.65\%$$

$$\text{For mode 4, } \frac{M_4}{M} = \frac{0.47}{230.43} = 0.0020 = 0.20\%$$

Design lateral force at each floor in each mode

The design lateral force (Q_{ik}) at floor i in mode k is given by,

$$Q_{ik} = A_k \Phi_{ik} P_k W_i$$

The design horizontal seismic coefficient A_h for various modes are,

$$A_{h1} = \frac{Z}{2} \frac{I}{R} \frac{S_{a1}}{g} = \frac{0.24}{2} \frac{1}{5} 2.5 = 0.060$$

$$A_{h2} = \frac{Z}{2} \frac{I}{R} \frac{S_{a2}}{g} = \frac{0.24}{2} \frac{1}{5} 1.871 = 0.045$$

Similarly,

$$A_{h3} = 0.037, A_{h4} = 0.035$$

For rocky, or hard soil sites

$$\frac{S_a}{g} = \begin{cases} 1 + 15T; & 0.00 \leq T \leq 0.10 \\ 2.5; & 0.10 \leq T \leq 0.40 \\ 1.00/T; & 0.40 \leq T \leq 4.0 \end{cases}$$

$$\text{For } T_1 = 0.1655 \Rightarrow \frac{S_{a1}}{g} = 2.5$$

$$\text{For } T_2 = 0.0581 \Rightarrow \frac{S_{a2}}{g} = 1 + 15T = 1.871$$

$$\text{For } T_3 = 0.0388 \Rightarrow \frac{S_{a3}}{g} = 1 + 15T = 1.582$$

$$\text{For } T_4 = 0.0382 \Rightarrow \frac{S_{a4}}{g} = 1 + 15T = 1.492$$

Design lateral force

$$Q_{i1} = (A_1 P_1 \Phi_{i1} W_i)$$

$$[Q_{i1}] = \begin{bmatrix} (A_{h1} P_1 \Phi_{11} W_1) \\ (A_{h2} P_1 \Phi_{21} W_2) \\ (A_{h3} P_1 \Phi_{31} W_3) \\ (A_{h4} P_1 \Phi_{41} W_4) \end{bmatrix} = \begin{bmatrix} ((0.060)(-14.40)(-0.0328)(64.45 \times 9.81)) \\ ((0.060)(-14.40)(-0.0608)(64.45 \times 9.81)) \\ ((0.060)(-14.40)(-0.0798)(64.45 \times 9.81)) \\ ((0.060)(-14.40)(-0.0872)(37.08 \times 9.81)) \end{bmatrix} = \begin{bmatrix} (17.922) \\ (33.215) \\ (43.637) \\ (27.419) \end{bmatrix} \text{kN}$$

Similarly,

$$[Q_{i2}] = \begin{bmatrix} -32.512 \\ -26.343 \\ 11.166 \\ 20.361 \end{bmatrix}, [Q_{i3}] = \begin{bmatrix} -27.972 \\ 18.667 \\ 15.514 \\ -16.696 \end{bmatrix}, [Q_{i4}] = \begin{bmatrix} 12.980 \\ -22.512 \\ 26.065 \\ -13.057 \end{bmatrix}$$

Storey shear forces in each mode

The peak shear force will be obtained by,

$$V_{ik} = \sum_{j=i+1}^n Q_{ik}$$

The storey shear forces for the first mode is,

$$V_{i1} = \sum_{j=i+1}^n Q_{il} = \begin{bmatrix} V_{11} \\ V_{21} \\ V_{31} \\ V_{41} \end{bmatrix} = \begin{bmatrix} (Q_{11} + Q_{21} + Q_{31} + Q_{41}) \\ (Q_{21} + Q_{31} + Q_{41}) \\ (Q_{31} + Q_{41}) \\ (Q_{41}) \end{bmatrix} = \begin{bmatrix} 122.194 \\ 104.272 \\ 71.057 \\ 27.419 \end{bmatrix} \text{ kN}$$

Similarly,

$$V_{i2} = \begin{bmatrix} V_{12} \\ V_{22} \\ V_{32} \\ V_{42} \end{bmatrix} = \begin{bmatrix} -27.327 \\ 5.184 \\ 31.528 \\ 20.361 \end{bmatrix}, V_{i3} = \begin{bmatrix} V_{13} \\ V_{23} \\ V_{33} \\ V_{43} \end{bmatrix} = \begin{bmatrix} -10.487 \\ 17.485 \\ -1.182 \\ -16.696 \end{bmatrix}, V_{i4} = \begin{bmatrix} V_{14} \\ V_{24} \\ V_{34} \\ V_{44} \end{bmatrix} = \begin{bmatrix} 3.476 \\ -9.5042 \\ 13.008 \\ -13.057 \end{bmatrix}$$

Storey shear force due to all modes

Square Root of Sum of Squares (SRSS)

$$V_1 = [(V_{11})^2 + (V_{12})^2 + (V_{13})^2 + (V_{14})^2]^{1/2} \\ = [(122.194)^2 + (-27.327)^2 + (-10.487)^2 + (3.475)^2]^{1/2} = 125.699 \text{ kN}$$

$$V_2 = [(V_{21})^2 + (V_{22})^2 + (V_{23})^2 + (V_{24})^2]^{1/2} \\ = [(104.272)^2 + (5.185)^2 + (17.485)^2 + (-9.504)^2]^{1/2} = 106.281 \text{ kN}$$

$$V_3 = [(V_{31})^2 + (V_{32})^2 + (V_{33})^2 + (V_{34})^2]^{1/2} \\ = [(71.057)^2 + (31.528)^2 + (-1.182)^2 + (13.008)^2]^{1/2} = 78.827 \text{ kN}$$

$$V_4 = [(V_{41})^2 + (V_{42})^2 + (V_{43})^2 + (V_{44})^2]^{1/2} \\ = [(27.419)^2 + (20.362)^2 + (-16.696)^2 + (-13.057)^2]^{1/2} = 40.196 \text{ kN}$$

Complete Quadratic Combination (CQC)

$$V_1 = \sqrt{\begin{pmatrix} 1 & 0.0073 & 0.0031 & 0.0023 \\ 0.0073 & 1 & 0.0559 & 0.0278 \\ 0.0031 & 0.0559 & 1 & 0.2597 \\ 0.0023 & 0.0278 & 0.2597 & 1 \end{pmatrix} \begin{bmatrix} 122.194 \\ -27.327 \\ -10.487 \\ 3.475 \end{bmatrix}} \\ = [125.512]$$

$$V_2 = \sqrt{\begin{pmatrix} 1 & 0.0073 & 0.0031 & 0.0023 \\ 0.0073 & 1 & 0.0559 & 0.0278 \\ 0.0031 & 0.0559 & 1 & 0.2597 \\ 0.0023 & 0.0278 & 0.2597 & 1 \end{pmatrix} \begin{bmatrix} 104.272 \\ 5.184 \\ 17.485 \\ -9.504 \end{bmatrix}} \\ = [105.977]$$

$$V_3 = \sqrt{\begin{bmatrix} 71.057 & 31.528 & -1.182 & 13.008 \end{bmatrix} \begin{bmatrix} 1 & 0.0073 & 0.0031 & 0.0023 \\ 0.0073 & 1 & 0.0559 & 0.0278 \\ 0.0031 & 0.0559 & 1 & 0.2597 \\ 0.0023 & 0.0278 & 0.2597 & 1 \end{bmatrix} \begin{bmatrix} 71.057 \\ 31.528 \\ -1.182 \\ 13.008 \end{bmatrix}}$$

$$= [79.125]$$

$$V_4 = \sqrt{\begin{bmatrix} 27.419 & 20.362 & -16.696 & -13.057 \end{bmatrix} \begin{bmatrix} 1 & 0.0073 & 0.0031 & 0.0023 \\ 0.0073 & 1 & 0.0559 & 0.0278 \\ 0.0031 & 0.0559 & 1 & 0.2597 \\ 0.0023 & 0.0278 & 0.2597 & 1 \end{bmatrix} \begin{bmatrix} 27.419 \\ 20.362 \\ -16.696 \\ -13.057 \end{bmatrix}}$$

$$= [40.964]$$

Lateral forces at each storey due to all modes

Square Root of Sum of Squares (SRSS)

$$F_{rooF} = F_4 = V_4 = 40.196 \text{ kN}$$

$$F_{floor3} = F_3 = V_3 - V_4 = 78.827 - 40.196 = 38.631 \text{ kN}$$

$$F_{floor2} = F_2 = V_2 - V_3 = 106.281 - 78.827 = 27.454 \text{ kN}$$

$$F_{floor1} = F_1 = V_1 - V_2 = 125.699 - 106.281 = 19.418 \text{ kN}$$

Complete Quadratic Combination (CQC)

$$F_{rooF} = F_4 = V_4 = 40.964 - 0 = 40.964 \text{ kN}$$

$$F_{floor3} = F_3 = V_3 - V_4 = 79.125 - 40.964 = 38.161 \text{ kN}$$

$$F_{floor2} = F_2 = V_2 - V_3 = 105.977 - 79.125 = 26.852 \text{ kN}$$

$$F_{floor1} = F_1 = V_1 - V_2 = 125.512 - 105.977 = 19.535 \text{ kN}$$

Comparison of Base Shear with and without Infills

Ratio of Base shear with infill to without infill (SRSS) = $125.699/80.930 = 1.553$

18.4 TIME HISTORY METHOD

Dynamic response of the plane frame model with infills to a specified time history compatible to IS code spectrum for 5% damping at rocky hard soil has been evaluated using mode superposition method. A step-by-step procedure for analysis of the frame by time history method is as follows (Tedesco et. al., 1999).

18.4.1 Step 1: Calculation of Modal Matrix

The equation of motion for a multi-degree-of-freedom system in matrix form can be expressed as

$$[m]\{\ddot{x}\} + [c]\{\dot{x}\} + [k]\{x\} = -\ddot{x}_g(t) [m]\{I\}$$

where,

$[m]$ = mass matrix

$[k]$ = stiffness matrix

$[c]$ = damping matrix

$\{I\}$ = unit vector

$\ddot{x}_g(t)$ = ground acceleration

The solution of equation of motion for any specified forces is difficult to obtain, mainly due to coupling of the variables $\{x\}$ in the physical coordinates. In mode superposition analysis or a modal analysis a set of normal coordinates *i.e.* principal coordinates is defined, such that, when expressed in those coordinates, the equations of motion become uncoupled. The physical coordinates $\{x\}$ may be related with normal or principal coordinates $\{q\}$ from the transformation expression as,

$$\{x\} = [\Phi]\{q\} \quad [\Phi] \text{ is the modal matrix,}$$

Time derivatives of $\{x\}$ are,

$$\{\dot{x}\} = [\Phi]\{\dot{q}\}$$

$$\{\ddot{x}\} = [\Phi]\{\ddot{q}\}$$

Substituting the time derivatives in the equation of motion, and pre-multiplying by $[\Phi]^T$ results in,

$$[\Phi]^T[m][\Phi]\{\ddot{q}\} + [\Phi]^T[c][\Phi]\{\dot{q}\} + [\Phi]^T[k][\Phi]\{q\} = (-\ddot{x}_g(t) [\Phi]^T[m]\{I\})$$

More clearly it can be represented as follows:

$$[M]\{\ddot{q}\} + [C]\{\dot{q}\} + [K]\{q\} = \{P_{\text{eff}}(t)\}$$

where,

$$[M] = [\Phi]^T[m][\Phi]$$

$$[C] = [\Phi]^T[c][\Phi]$$

$$[K] = [\Phi]^T[k][\Phi]$$

$$\{P_{\text{eff}}(t)\} = (-\ddot{x}_g(t)[\Phi]^T[m]\{I\})$$

$[M]$, $[C]$ and $[K]$ are the *diagonalized modal mass matrix*, *modal damping matrix*, and *modal stiffness matrix*, respectively, and $\{P_{\text{eff}}(t)\}$ is the *effective modal force vector*.

Mass and stiffness matrices for the plane frame model with infills are

$$K = \begin{bmatrix} k_1 + k_2 & -k_2 & 0 & 0 \\ -k_2 & k_2 + k_3 & -k_3 & 0 \\ 0 & -k_3 & k_3 + k_4 & -k_4 \\ 0 & 0 & -k_4 & k_4 \end{bmatrix} = \begin{bmatrix} 1.2674 & -0.6337 & 0 & 0 \\ -0.6337 & 1.2674 & -0.6337 & 0 \\ 0 & -0.6337 & 1.2674 & -0.6337 \\ 0 & 0 & -0.6337 & 0.6337 \end{bmatrix} \times 10^6 \text{ kN/m}$$

$$M = \begin{bmatrix} M_1 & 0 & 0 & 0 \\ 0 & M_2 & 0 & 0 \\ 0 & 0 & M_3 & 0 \\ 0 & 0 & 0 & M_4 \end{bmatrix} = \begin{bmatrix} 64.45 & 0 & 0 & 0 \\ 0 & 64.45 & 0 & 0 \\ 0 & 0 & 64.45 & 0 \\ 0 & 0 & 0 & 37.08 \end{bmatrix} \text{ ton}$$

Natural frequencies and mode shape for the plane frame model

$$[\omega] = \begin{bmatrix} 37.975 & 0 & 0 & 0 \\ 0 & 108.157 & 0 & 0 \\ 0 & 0 & 161.947 & 0 \\ 0 & 0 & 0 & 191.621 \end{bmatrix} \text{ rad/s}, T = \begin{bmatrix} 0.1655 & 0 & 0 & 0 \\ 0 & 0.0581 & 0 & 0 \\ 0 & 0 & 0.0388 & 0 \\ 0 & 0 & 0 & 0.0328 \end{bmatrix} \text{ s}$$

$$\phi_1 = \begin{bmatrix} -0.0328 \\ -0.0608 \\ -0.0798 \\ -0.0872 \end{bmatrix}, \phi_2 = \begin{bmatrix} 0.0795 \\ 0.0644 \\ -0.0273 \\ -0.0865 \end{bmatrix}, \phi_3 = \begin{bmatrix} 0.0808 \\ -0.0540 \\ -0.0448 \\ 0.0839 \end{bmatrix}, \phi_4 = \begin{bmatrix} -0.0397 \\ 0.0690 \\ -0.0799 \\ 0.0696 \end{bmatrix}$$

Therefore, $[M]$, $[K]$ and $[C]$ are,

$$[M] = [\Phi]^T [m] [\Phi] = \begin{bmatrix} 1 & 0 & 0 & 0 \\ 0 & 1 & 0 & 0 \\ 0 & 0 & 1 & 0 \\ 0 & 0 & 0 & 1 \end{bmatrix}$$

$$[K] = [\Phi]^T [k] [\Phi] = \begin{bmatrix} 1442 & 0 & 0 & 0 \\ 0 & 11698 & 0 & 0 \\ 0 & 0 & 26227 & 0 \\ 0 & 0 & 0 & 36719 \end{bmatrix}$$

$$[C] = \text{diag}(2M_r \zeta_r \omega_r) = \begin{bmatrix} 3.7975 & 0 & 0 & 0 \\ 0 & 10.815 & 0 & 0 \\ 0 & 0 & 16.1947 & 0 \\ 0 & 0 & 0 & 19.1621 \end{bmatrix}$$

18.4.2 Step 2: Calculation of Effective Force Vector

The excitation function is,

$$\{P_{\text{eff}}(t)\} = (-\ddot{x}_g(t)[\Phi]^T[m]\{I\}) \quad \text{or} \quad (-\ddot{x}_g(t)\Gamma_r)$$

$$\Gamma_r = \frac{\{\Phi\}_r^T[m]\{I\}}{\{\Phi\}_r^T[m]\{\Phi\}_r} = \frac{\{\Phi\}_r^T[m]\{I\}}{M_r}$$

Modal participation factors for the plane frame are $\Gamma_r = \begin{bmatrix} -14.40 \\ 4.30 \\ 1.95 \\ -0.68 \end{bmatrix}$,

$$\{P_{\text{eff}}(t)\} = (-\ddot{x}_g(t) [\Phi]^T[m]\{I\}) = \begin{Bmatrix} -14.40 \\ 4.30 \\ 1.95 \\ -0.68 \end{Bmatrix} (-\ddot{x}_g(t))$$

The compatible time history $\{\ddot{x}_g(t)\}$ as per spectra of IS 1893 (Part 1): 2002 for 5% damping at rocky soil strata is given in Figure 18.2.

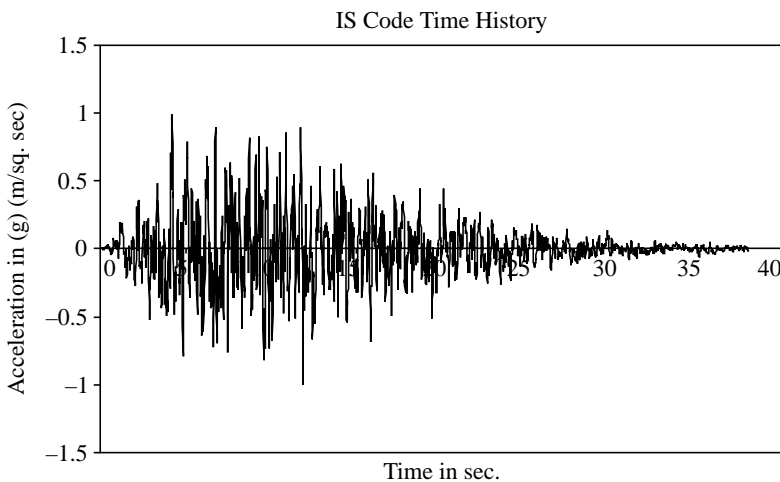


FIGURE 18.2 Compatible time history as per spectra of IS 1893 (Part 1): 2002 for 5% damping at rocky soil.

18.4.3 Step 3: Calculation of Displacement Response in Normal Coordinate

The uncoupled equations in the normal coordinates are,

$$\ddot{q}_1 + 3.9795 \dot{q}_1 + 1442q_1 = 14.40 \ddot{x}_g(t)$$

$$\ddot{q}_2 + 10.815 \dot{q}_2 + 11698q_2 = -4.30 \ddot{x}_g(t)$$

$$\ddot{q}_3 + 16.1947 \dot{q}_3 + 26227q_3 = -1.95 \ddot{x}_g(t)$$

$$\ddot{q}_4 + 19.1621 \dot{q}_4 + 36719q_4 = 0.68 \ddot{x}_g(t)$$

The displacement response q_r in normal coordinates can be evaluated by any of the numerical methods. Here, *Piecewise-linear interpolation* method has been used for evaluating the response of linear system (Appendix 1). For the given time history as shown in Figure 18.2, the response time history q in the principal coordinates or normal coordinates are shown in Figures 18.3 to 18.6.

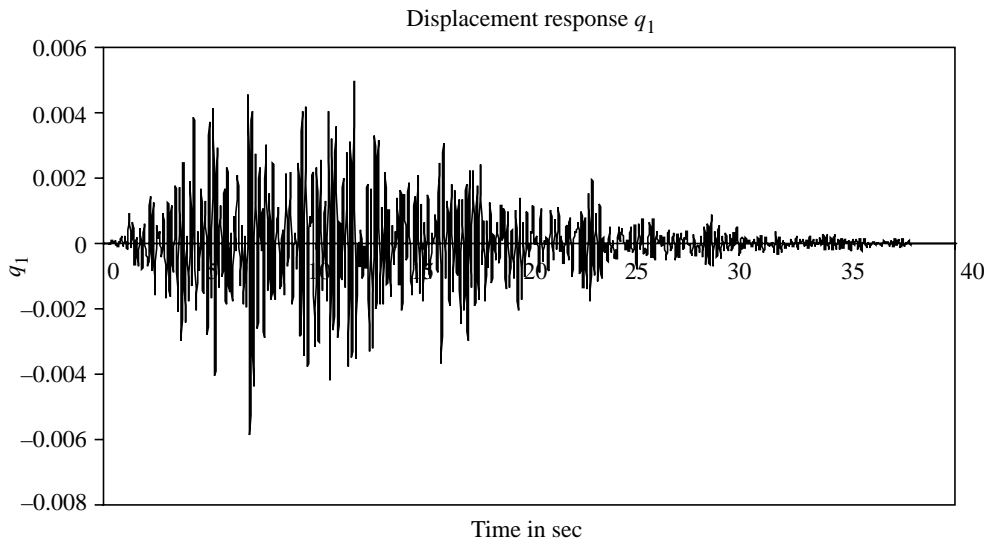


FIGURE 18.3 Response history q_1 in normal coordinates.

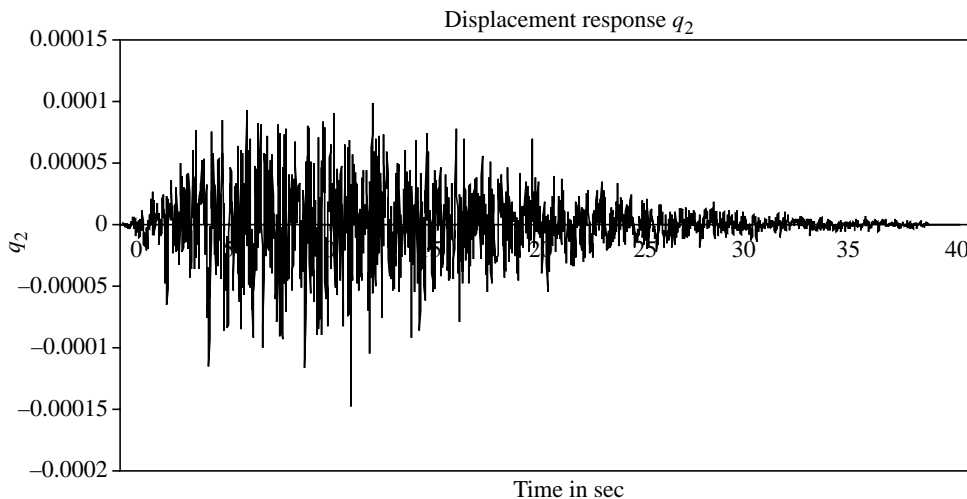


FIGURE 18.4 Response history q_2 in normal coordinates.

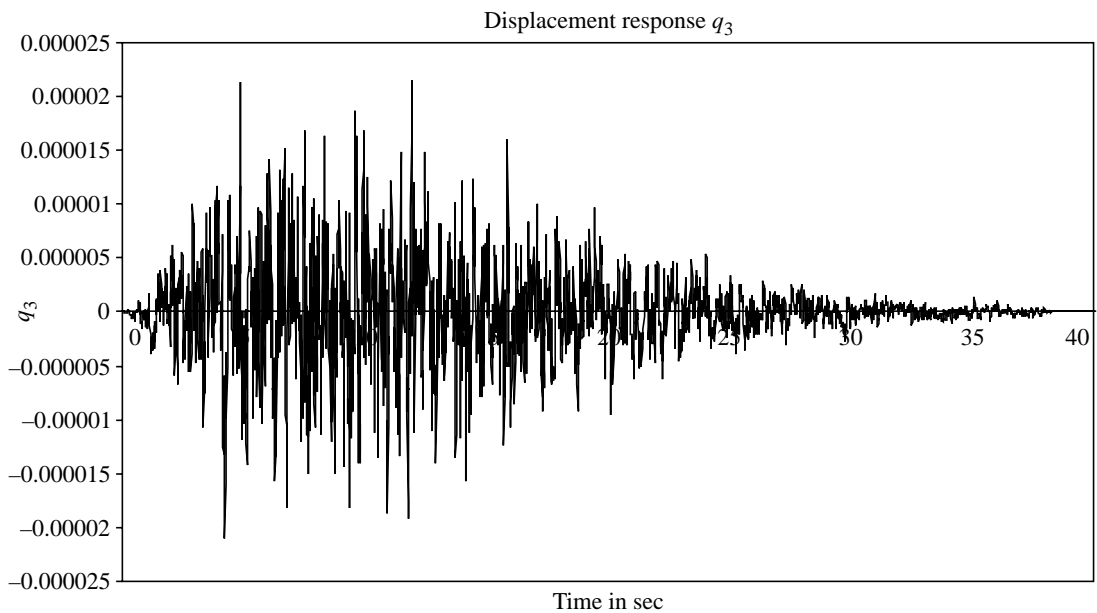


FIGURE 18.5 Response history q_3 in normal coordinates.

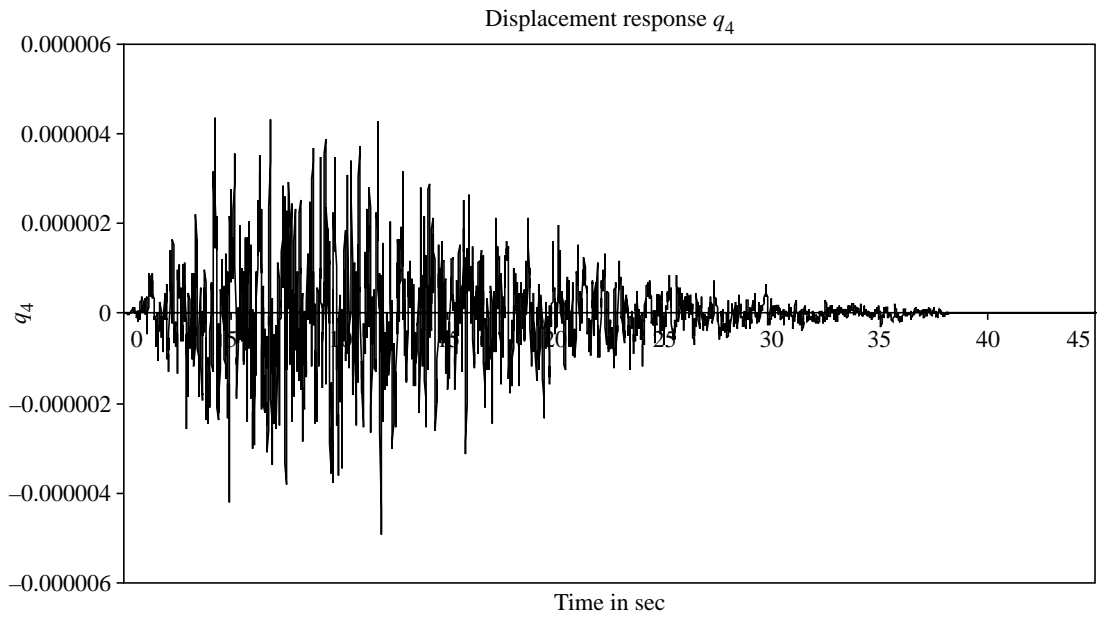


FIGURE 18.6 Response history q_4 in normal coordinates.

18.4.4 Step 4: Displacement Response in Physical Coordinates

Displacement response in physical coordinates $\{x\}$ is calculated from the transformation

expression.

$$\{x(t)\} = \sum_{r=1}^n \{\Phi\}_r q_r(t)$$

$$\{x(t)\} = \sum_{r=1}^n \{\Phi\}_r q_r(t) = \{\Phi\}_1 q_1(t) + \{\Phi\}_2 q_2(t) + \{\Phi\}_3 q_3(t) + \{\Phi\}_4 q_4(t)$$

$$= \begin{pmatrix} -0.0328 \\ -0.0608 \\ -0.0798 \\ -0.0872 \end{pmatrix} q_1(t) + \begin{pmatrix} 0.0795 \\ 0.0644 \\ -0.0273 \\ -0.0865 \end{pmatrix} q_2(t) + \begin{pmatrix} 0.0808 \\ -0.0540 \\ -0.0448 \\ 0.0839 \end{pmatrix} q_3(t) + \begin{pmatrix} -0.0397 \\ 0.0690 \\ -0.0799 \\ 0.0696 \end{pmatrix} q_4(t)$$

$$= \left\{ \begin{array}{l} (-0.0328) q_1(t) + (0.0795) q_2(t) + (0.0808) q_3(t) + (-0.0397) q_4(t) \\ (-0.0608) q_1(t) + (0.0644) q_2(t) + (-0.0540) q_3(t) + (0.0690) q_4(t) \\ (-0.0798) q_1(t) + (-0.0273) q_2(t) + (-0.0448) q_3(t) + (-0.0799) q_4(t) \\ (-0.0872) q_1(t) + (-0.0865) q_2(t) + (0.0839) q_3(t) + (0.0696) q_4(t) \end{array} \right\}$$

Therefore the response of masses at various floor levels in the physical coordinates $\{x\}$ are obtained as shown in Figures 18.7–18.10.

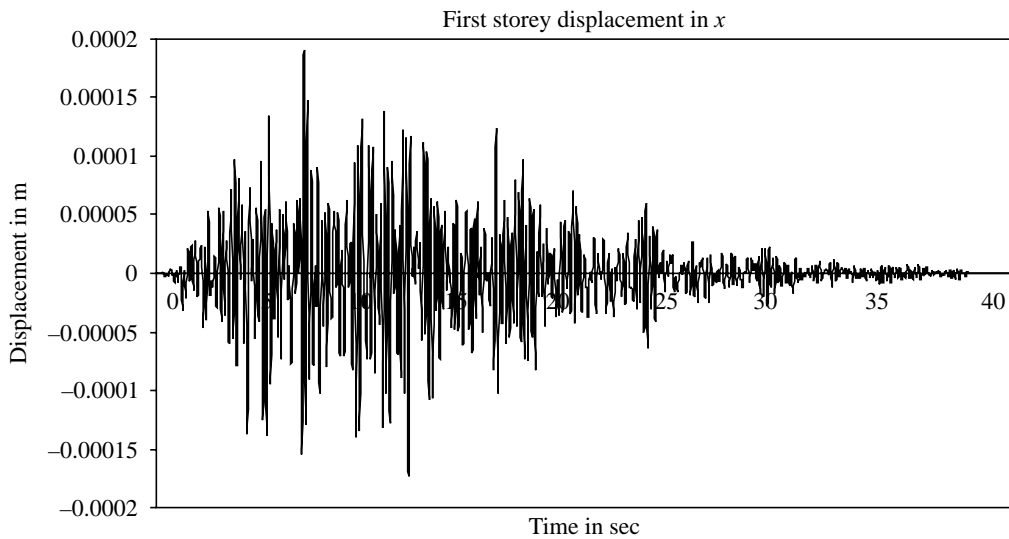


FIGURE 18.7 First storey displacement response history in physical coordinates.

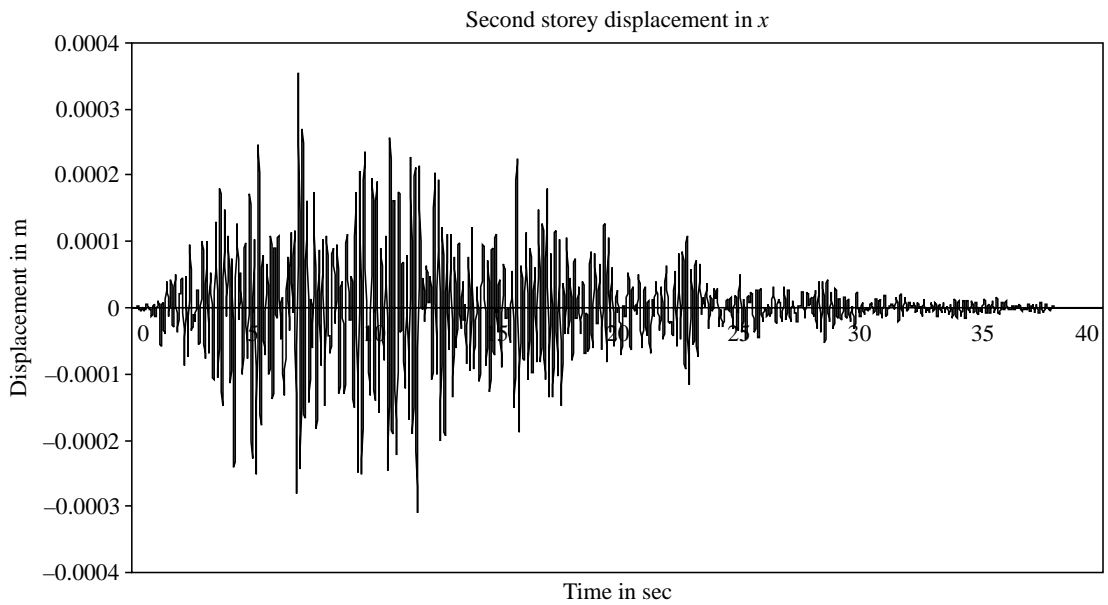


FIGURE 18.8 Second storey displacement response history in physical coordinates.

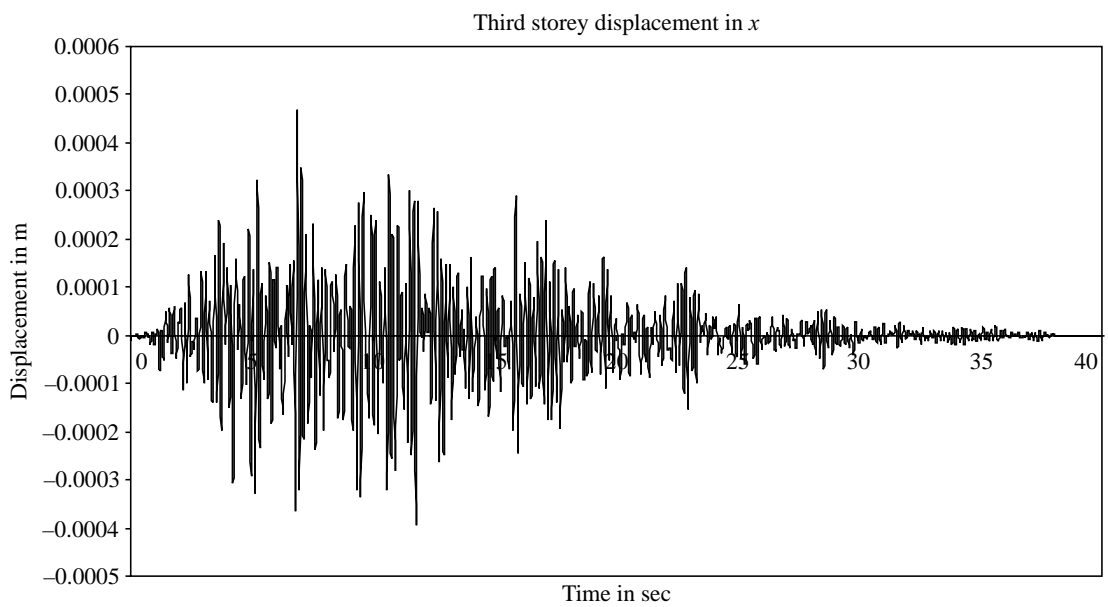


FIGURE 18.9 Third storey displacement response history in physical coordinates.

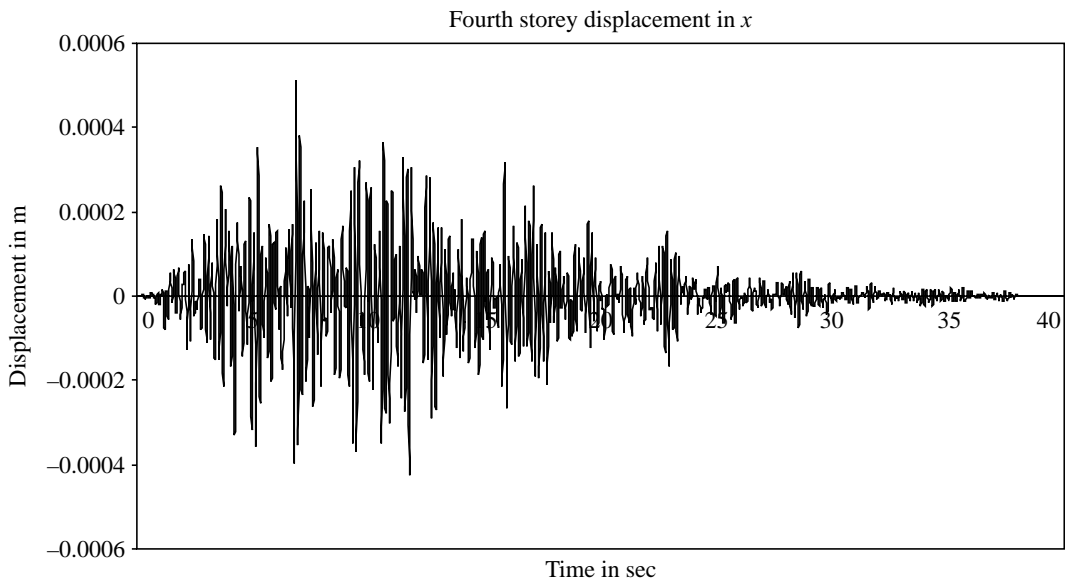


FIGURE 18.10 Fourth storey displacement response history in physical coordinates.

18.4.5 Step 5: Calculation of Effective Earthquake Response Forces at Each Storey

When the relative displacements of the masses $\{x(t)\}$ have been established, the effective earthquake forces or the elastic restoring forces $F_s(t)$ acting at each mass m_i are determined from,

$$\{F_s(t) = [k]\{x(t)\}\}$$

$$\begin{aligned}
 &= \begin{bmatrix} 1.2674 & -0.6337 & 0 & 0 \\ -0.6337 & 1.2674 & -0.6337 & 0 \\ 0 & -0.6337 & 1.2674 & -0.6337 \\ 0 & 0 & -0.6337 & 0.6337 \end{bmatrix} \times 10^6 \begin{Bmatrix} x_1(t) \\ x_2(t) \\ x_3(t) \\ x_4(t) \end{Bmatrix} \\
 &= \begin{bmatrix} 1267424 x_1(t) - 633712 x_2(t) \\ -633712 x_1(t) + 1267424 x_2(t) - 633712 x_3(t) \\ -633712 x_2(t) + 1267424 x_3(t) - 633712 x_4(t) \\ -633712 x_3(t) + 633712 x_4(t) \end{bmatrix}
 \end{aligned}$$

The obtained elastic restoring forces at various floor levels are shown in the Figures 18.11 to 18.14.

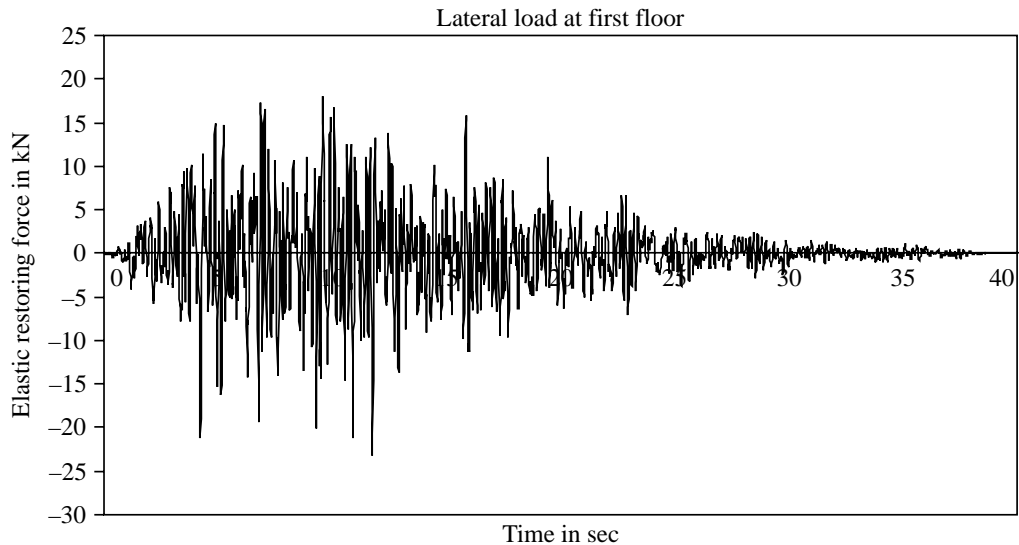


FIGURE 18.11 First storey lateral load response history in kN.

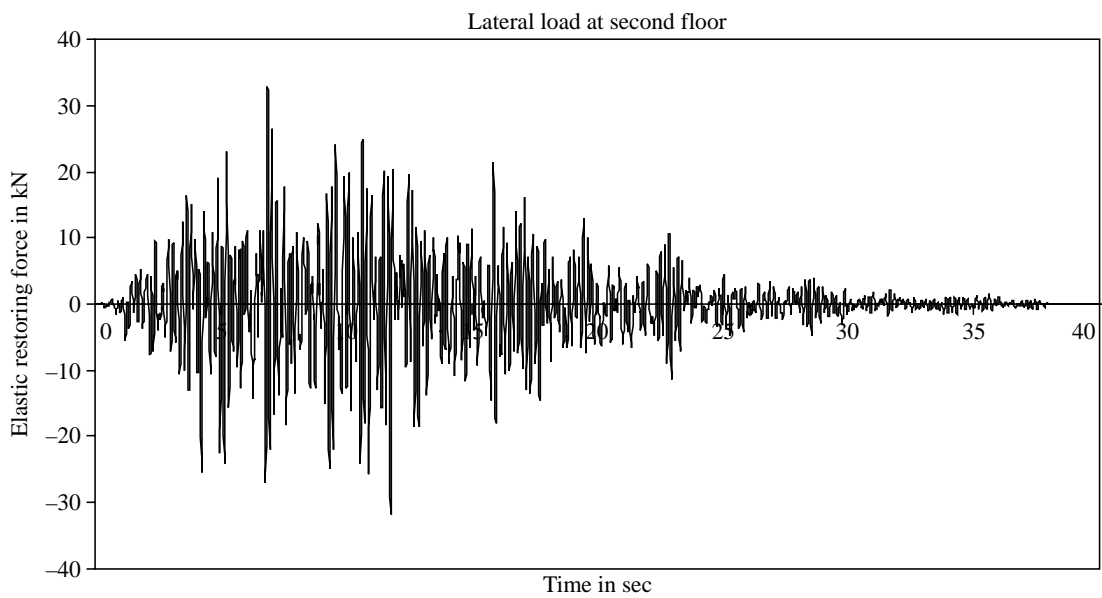


FIGURE 18.12 Second storey lateral load response history in kN.

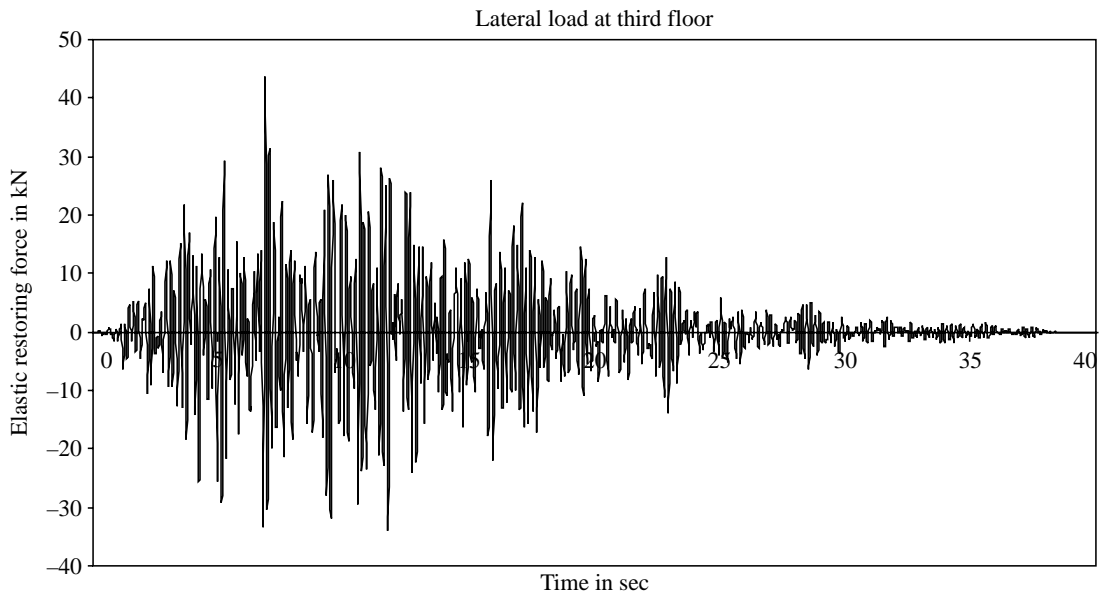


FIGURE 18.13 Third storey lateral load response history in kN.

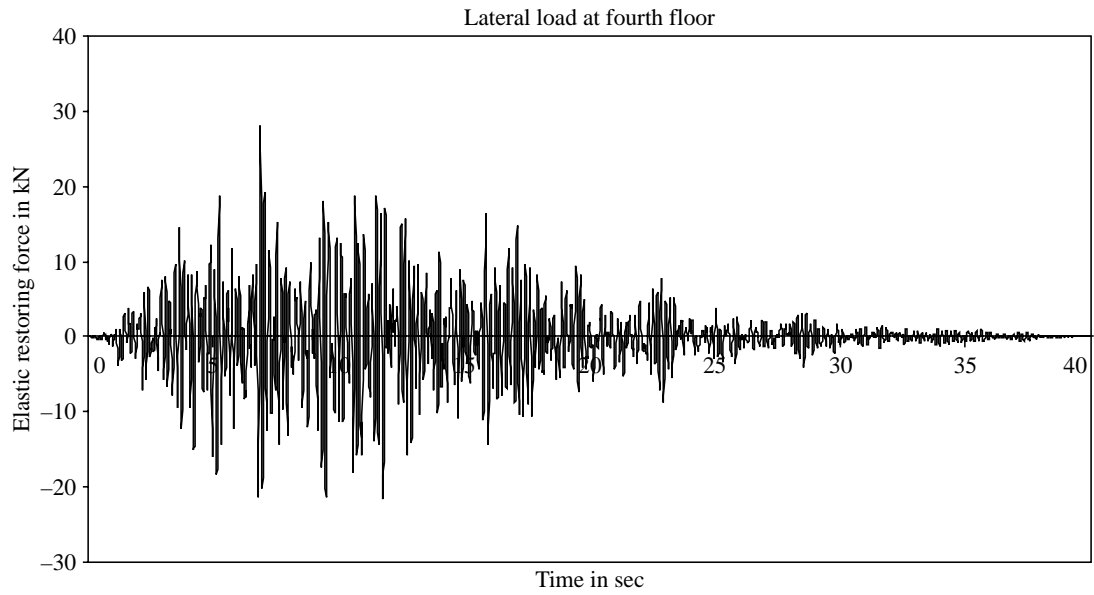


FIGURE 18.14 Fourth storey lateral load response history in kN.

18.4.6 Step 6: Calculation of Storey Shear

The storey shears are calculated as,

$$\{V(t)\} = [S][k]\{x(t)\}$$

where $[S]$ is the $(n \times n)$ upper triangular matrix given as,

$$[S] = \begin{bmatrix} 1 & 1 & 1 & \dots & 1 \\ 0 & 1 & 1 & \dots & 1 \\ 0 & 0 & 1 & \dots & 1 \\ \vdots & \vdots & \vdots & \ddots & \vdots \\ \vdots & \vdots & \vdots & \ddots & \vdots \\ 0 & 0 & 0 & \dots & 1 \end{bmatrix}$$

$$\{V(t)\} = \begin{bmatrix} 1 & 1 & 1 & 1 \\ 0 & 1 & 1 & 1 \\ 0 & 0 & 1 & 1 \\ 0 & 0 & 0 & 1 \end{bmatrix} \begin{bmatrix} 1.2674 & -0.6337 & 0 & 0 \\ -0.6337 & 1.2674 & -0.6337 & 0 \\ 0 & -0.6337 & 1.2674 & -0.6337 \\ 0 & 0 & -0.6337 & 0.6337 \end{bmatrix} \times 10^6 \begin{bmatrix} x_1(t) \\ x_2(t) \\ x_3(t) \\ x_4(t) \end{bmatrix}$$

$$\therefore \begin{bmatrix} V_1(t) \\ V_2(t) \\ V_3(t) \\ V_4(t) \end{bmatrix} = \begin{bmatrix} 633712x_1(t) \\ -633712x_1(t) + 633712x_2(t) \\ -633712x_2(t) + 633712x_3(t) \\ -633712x_3(t) + 633712x_4(t) \end{bmatrix}$$

The storey shears at each storey are shown in Figures 18.15 to 18.18.

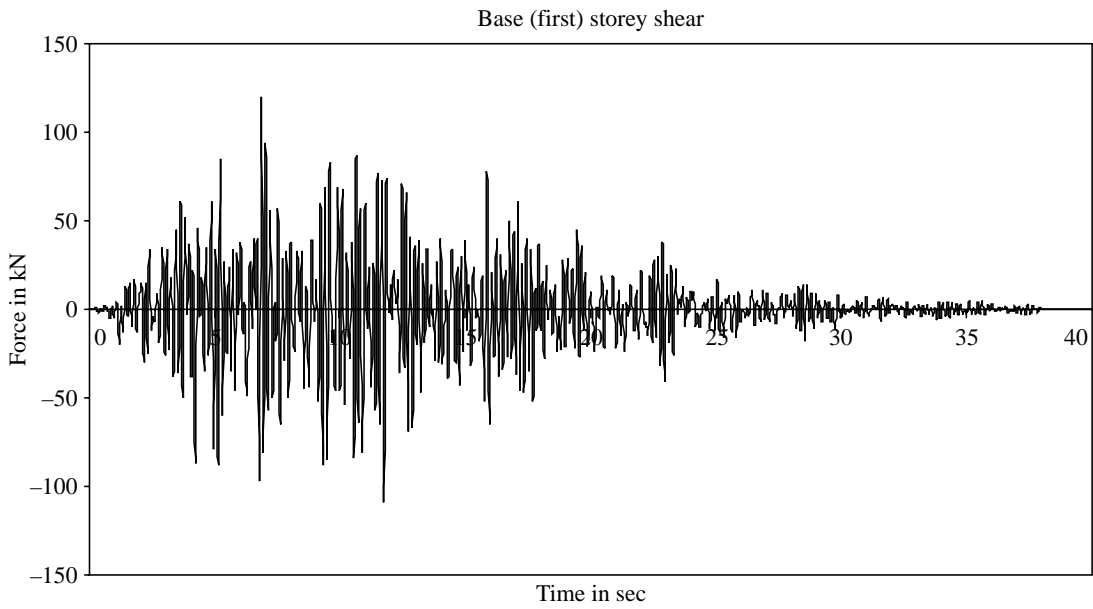


FIGURE 18.15 First storey (base) shear response history $V_1(t)$ (kN).

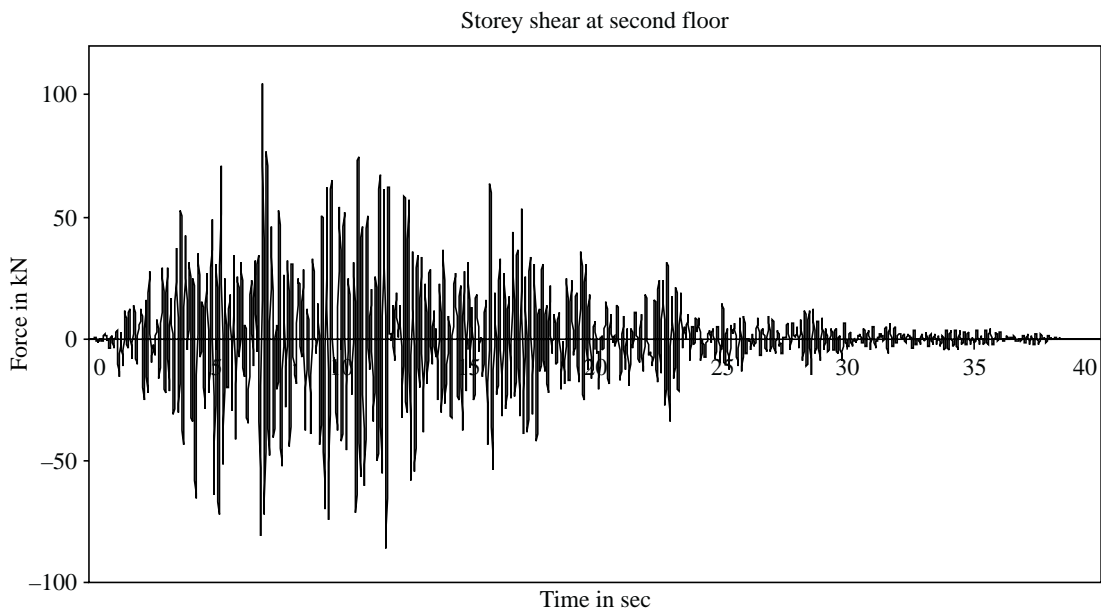


FIGURE 18.16 Second storey-storey shear response history $V_2(t)$ (kN).

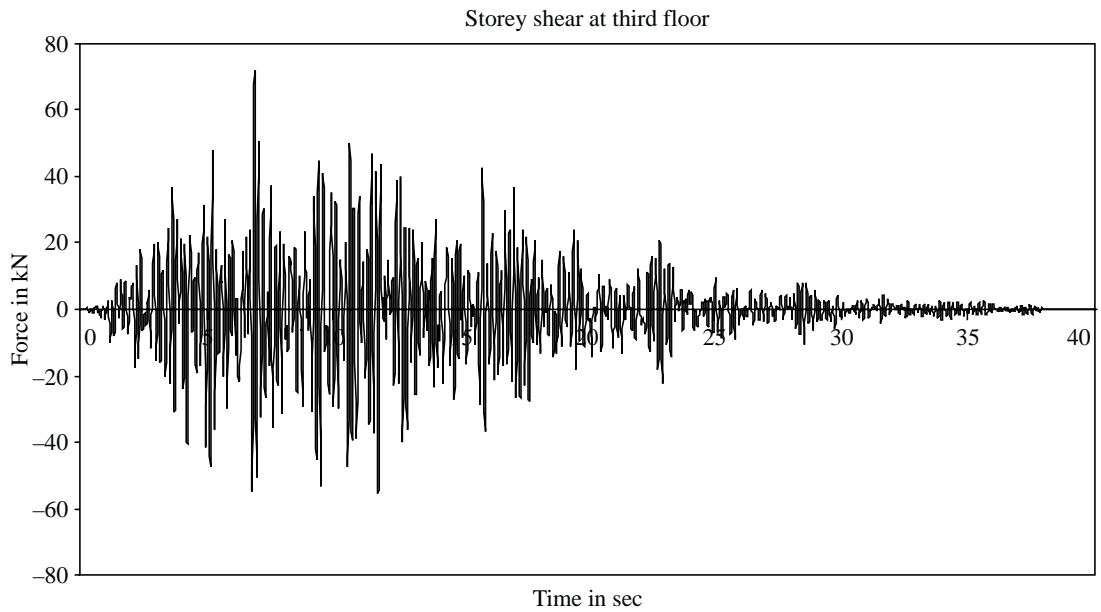


FIGURE 18.17 Third storey-storey shear response history $V_3(t)$ (kN).

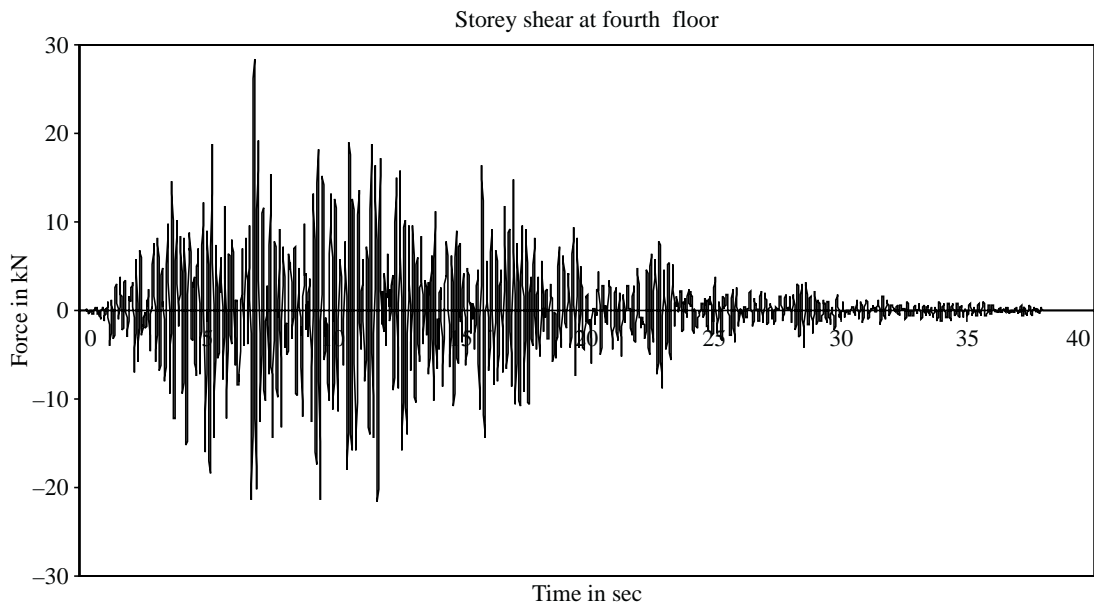


FIGURE 18.18 Fourth storey-storey shear response history $V_4(t)$ (kN).

18.4.7 Step 7: Calculation of Maximum Response

Maximum response of relative displacement, elastic restoring forces, storey shears at each storey in plane frame has been summarized in Table 18.2.

TABLE 18.2 Summary of maximum response for the example structure

Location	X_{\max} (m)	$(F_s)_{\max}$ (kN)	V_{\max}
x_1	1.899×10^{-4}	23.300	120.390
x_2	3.54×10^{-4}	32.870	104.460
x_3	4.68×10^{-4}	43.855	72.090
x_4	5.13×10^{-4}	28.236	28.236

The total base shears $V_1(t)$ obtained from time history method is presented in Figure 18.15. The maximum base shear obtained from time history analysis is 120.39 kN, while from response spectrum analysis is 125.69 kN.

APPENDIX 1: LINEAR INTERPOLATION OF EXCITATION

The recurrence formulas written to obtain the response in a single degree of freedom system based on the interpolation of the excitation function are given below:

$$\begin{aligned} u_{i+1} &= Au_i + B\dot{u}_i + Cp_i + Dp_{i+1} \\ \dot{u}_{i+1} &= A'u_i + B'\dot{u}_i + C'p_i + D'p_{i+1} \end{aligned}$$

The coefficients $A, B, C, D, A', B', C', D'$ depend on the system parameters ω_n , k and ζ , and on the time interval $\Delta t = \Delta t_i$

$$A = e^{-\zeta\omega_n\Delta t} \left(\frac{\zeta}{\sqrt{1-\zeta^2}} \sin \omega_D \Delta t + \cos \omega_D \Delta t \right)$$

$$B = e^{-\zeta\omega_n\Delta t} \left(\frac{1}{\omega D} \sin \omega D \Delta t \right)$$

$$C = \frac{1}{k} \left\{ \frac{2\zeta}{\omega_n \Delta t} + e^{-\zeta\omega_n\Delta t} \left[\left(\frac{1-2\zeta^2}{\omega_D \Delta t} - \frac{\zeta}{\sqrt{1-\zeta^2}} \right) \sin \omega_D \Delta t - \left(1 + \frac{2\zeta}{\omega_n \Delta t} \right) \cos \omega_D \Delta t \right] \right\},$$

$$D = \frac{1}{k} \left\{ 1 - \frac{2\zeta}{\omega_n \Delta t} + e^{-\zeta\omega_n\Delta t} \left[\frac{2\zeta^2-1}{\omega_D \Delta t} \sin \omega_D \Delta t + \frac{2\zeta}{\omega_n \Delta t} \cos \omega_D \Delta t \right] \right\}$$

$$A' = e^{-\zeta\omega_n\Delta t} \left(\frac{\omega_n}{\sqrt{1-\zeta^2}} \sin \omega D \Delta t \right)$$

$$B' = e^{-\zeta\omega_n\Delta t} \left(\cos \omega D \Delta t - \frac{\zeta}{\sqrt{1-\zeta^2}} \sin \omega D \Delta t \right)$$

$$C' = \frac{1}{k} \left\{ -\frac{1}{\Delta t} + e^{-\zeta\omega_n\Delta t} \left[\left(\frac{\omega_n}{\sqrt{1-\zeta^2}} + \frac{\zeta}{\Delta t \sqrt{1-\zeta^2}} \right) \sin \omega_D \Delta t + \frac{1}{\Delta t} \cos \omega_D \Delta t \right] \right\}$$

$$D' = \frac{1}{k \Delta t} \left[1 - e^{-\zeta\omega_n\Delta t} \left(\frac{\zeta}{\sqrt{1-\zeta^2}} \sin \omega_D \Delta t + \cos \omega_D \Delta t \right) \right]$$

The numerical solution for the equation (A1) is obtained as follows after determining the values

$$\omega_{n1} = \sqrt{k_1/m_1} = \sqrt{\frac{1442}{1}} = 37.975 \text{ rad/sec}$$

The time step is taken as the time step of the time history i.e $\Delta t = 0.01$ sec
The coefficients obtained for equation (A1) are

$$A = 0.9296, B = 0.009597, C = 0.0000324, D = 0.0000164$$

$$A' = -13.812, B' = 0.8932, C' = 0.0047, D' = 0.004878$$

Substituting the coefficients obtained in the recurrence formulas for displacement and velocity, we get the response of the uncoupled equation in normal coordinates (q).

SUMMARY

The chapter illustrates the procedure of seismic analysis of a real frame as per IS 1893 (Part 1): 2002 with and without considering the effect of infill. Equivalent static, response spectrum and time history methods have been used to analyse the frame and a comparison for all the methods has also been made. A step-by -step approach has been employed to illustrate the procedures. In the equivalent static force procedure, the inertia forces are determined based on empirical formulas as specified in IS 1893 (Part 1): 2002 and are distributed along the height of the building by assuming parabolic distribution (applicable only for regular structures with limited height). The forces determined by the response spectrum method and time history method account for the effect of higher modes of vibration and actual distribution of forces in the elastic range.

REFERENCES

- [1] BIS 1893, *Criteria for Earthquake Resistant Design of Structures—Part 1: General Provisions and Buildings* (fifth revision), Bureau of Indian Standards, New Delhi, 2002.
- [2] Tedesco, J.W., McDougal, W.G., and Ross, C.A. *Structural Dynamics—Theory and Application*, Addison-Wesley Longman, 1999.

Chapter 19

Mathematical Modelling of Multi-storeyed RC Buildings

19.1 INTRODUCTION

Mathematical model of a structure is its idealization by a suitable form amenable to structural analysis by a standard procedure. The most important step in the design process of a building is to create an appropriate mathematical model that will adequately represent its stiffness, mass distribution and energy dissipation so that its response to earthquake could be predicted with sufficient accuracy. The model and its degree of sophistication are dependent upon the analysis and design requirements specified in the code. Some of the common types of models employed for buildings are *2D plane frame model*, *3D space frame model*, and *reduced 3D model with three degree of freedom per storey*. A practice commonly followed is to employ 3D space frame models for static solution and reduced 3D model for dynamic solution. If the main purpose of analysis is to calculate seismic actions for proportioning and designing of RC members, a member-by-member type of model is most suitable. In such a model, beams, columns and walls between successive floors are represented as 3D beam element. The degrees of freedom considered are 3 translations and 3 rotations at each joint of these elements. Masses can be lumped at nodal points with all 6 DOFs there. The principal issues in mathematical modelling of a building system are: (i) assumptions in modelling (ii) modelling of beams and columns, floor diaphragms, shear walls, infill walls, staircases and soil and foundation. The idealisation of an RC structure for seismic response analysis should capture all-important features of structural behaviour under design earthquake forces. The detailed finite element analysis of a building is usually not required, as accurate predictions of displacements and point-by-point determination of elastic stresses are not necessary to be determined for seismic design.

19.2 PLANAR MODELS

Majority of typical buildings are structured on the basis of frames, shear walls and box type of elements like staircases and elevator shafts to transmit vertical and horizontal loads. These elements are tied together by beams and slabs, which are supposed to act as rigid or flexible

diaphragm diaphragms in their planes. Frames and shear walls are assumed to have stiffness in their own plane. When the frames and walls in a building are located along two orthogonal directions, much of the action can be represented by plane frame idealization. Therefore plane-frame idealization of buildings is a natural choice of structural model. The various types of plane-frame models employed are as follows:

19.2.1 Shear Beam Model

A **shear beam model** is one in which the shear force acting on any mass depends only on relative displacements of adjacent masses. The shear beam model represented by close-coupled system is shown in Figure 19.1. This model assumes that girders are infinitely stiff and axial deformations of columns are ignored. The columns behave as shear springs with its stiffness equal to $12EI/h^3$, where EI is the flexural rigidity and h is the storey height. This assumption restricts the coupling between stories and results in a simple model. The building can thus be represented as a lumped mass system connected by shear springs as shown in Figure 19.1(b). The masses are lumped at each floor level; the interstorey spring stiffness is equal to the sum of the stiffness of columns in that storey. Holzer's method is normally employed for determining natural frequencies and modes. Because of simplicity, the shear beam model has often been used for low-rise framed buildings. The effect of assuming no joint rotation can result in significant errors in both mode shapes and frequencies of low frequency structures, while neglect of axial deformation in columns may also result in error in frequencies of the order of 10%. Analytical formulations are also available for shear beam model.

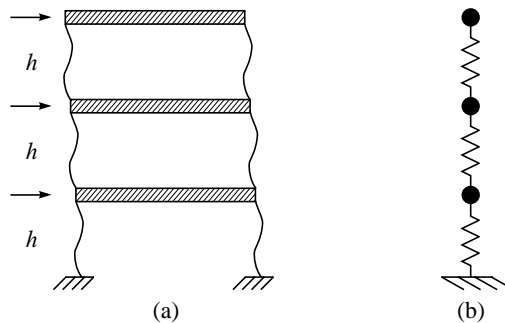


FIGURE 19.1 (a) Deflection of a frame under lateral load; (b) shear beam model (close-coupled system).

19.2.2 Flexure Beam Model

A **flexure beam model** (Figure 19.2) corresponds to a typical cantilever beam with masses lumped at discrete points. This represents an example of a far-coupled system. The force acting on any mass depends on displacement relative to all other masses of the system. An analytical model of a multi-storeyed building, that considers joint rotations as well as axial deformation in columns correspond to a flexural beam model. A plane frame idealization considered as an assemblage of beam and column elements, assuming primarily flexural deformation in its members will lead to such model.

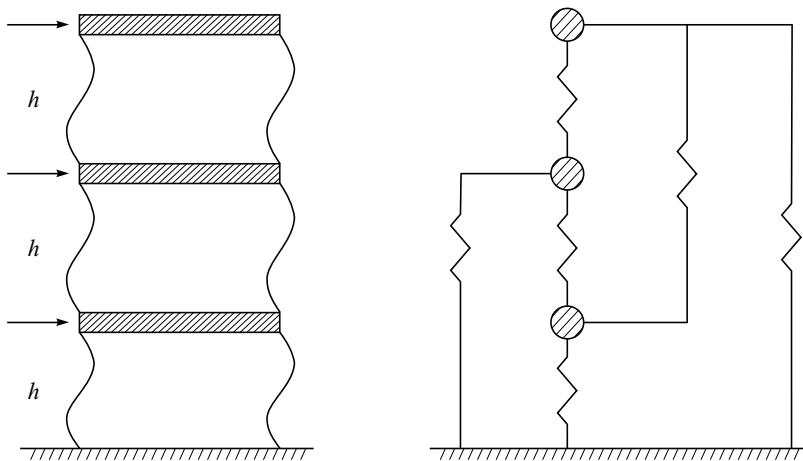


FIGURE 19.2 Flexure beam model (far coupled system).

19.2.3 Idealized Plane Frame Model

When the plan consists of combination of parallel frames and frame-shear walls, then single idealized plane frame model of all such frames can be represented as shown in Figure 19.3. Different units, such as frame 1, frame 2, etc., represent the lateral resisting frame along each line. These units are then connected at storey levels by rigid links, which simulate the inplane rigidity of floors. The finite width of core and wall are taken into account as represented by beam with rigid ends. This type of plane frame model can be analyzed by a standard plane frame programme.

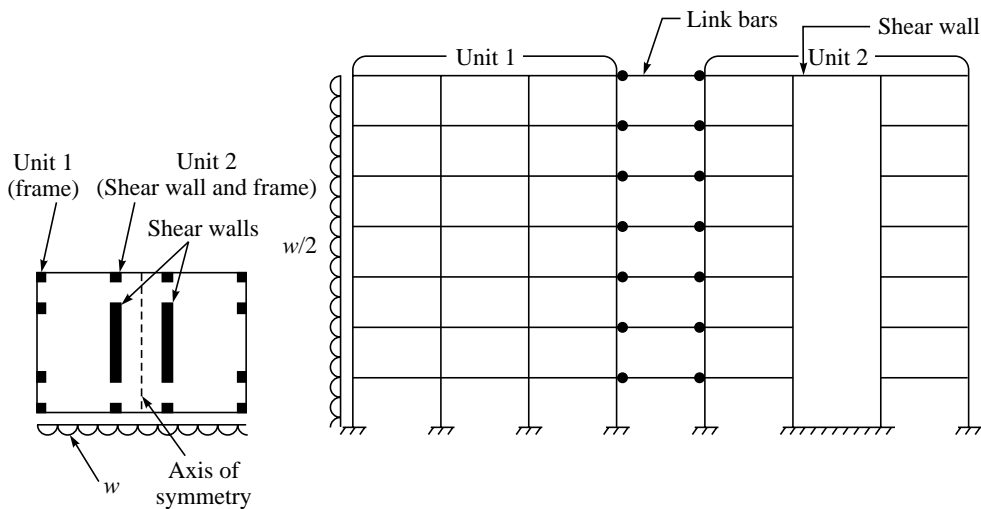


FIGURE 19.3 Idealization of plane frame (link model).

19.2.4 Equivalent Shear Wall Frame Model

In order to analyze the building with parallel frames in plan as shown in Figure 19.4, an equivalent shear wall-frame model is established (Khan-Sbarounis, 1964). The equivalent frame is obtained by lumping together all the frames into one bay equivalent frame, and combining all shear walls into an equivalent shear wall. This equivalent frame-shear wall system is analyzed for total lateral loads on the building in the particular direction. Subsequently the forces computed in the equivalent frame are distributed to the component elements from which the equivalent frame was composed in proportion to the lateral stiffness.

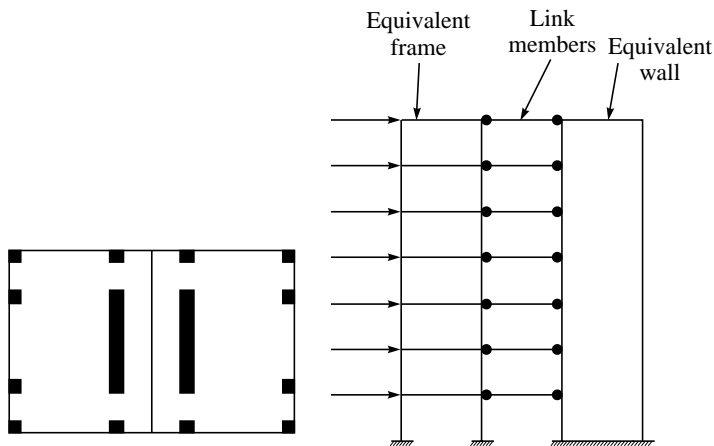


FIGURE 19.4 Equivalent shear wall frame (block frame model) (Khan-Sbarounis, 1964).

19.2.5 Plane Frame Model of Coupled Shear Walls

The multi-storeyed shear walls with openings are called *coupled shear walls*, these can be idealized by a frame with finite joints. The coupled wall is thus represented as a frame except that the finite width of the columns in comparison with the beam is recognized. A typical representation of coupled wall by a frame model is shown in Figure 19.5.

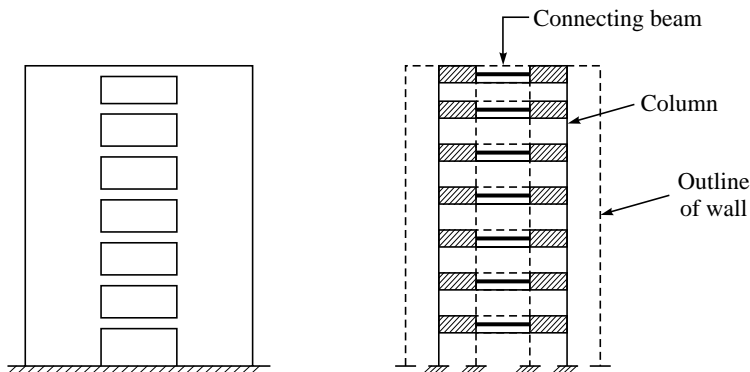


FIGURE 19.5 Modelling of coupled shear wall by a plane frame.

19.3 3D SPACE FRAME MODEL

If the layout of the building is unsymmetrical, the building can be best analyzed by a 3D space frame model. Any combination of frame and walls can be idealized as a space frame consisting of assemblage of beam and column elements. Each element of a model in space frame consists of a beam element with six degree of freedom at each joint. The stiffness matrix of this beam element is 12×12 . Any torsional effects are automatically considered in this model. The ground motions can be applied in one, two or three directions, individually or simultaneously. The analysis is best suited for non-rectangular units, building with unsymmetry in plan or elevation and complex frame with missing beam/column and building with floating columns. The main issues in 3D modelling are as follows:

- (i) structural idealization of building by 3D beam element,
- (ii) modelling of floor diaphragms,
- (iii) finite size of joints between members, and
- (iv) modelling of non-structural elements such as staircases and infill walls.

19.4 REDUCED 3D MODEL

The majority of buildings in which floor diaphragms are sufficiently rigid in their planes, the dynamic analysis can be carried out by using reduced 3D model. This is based on following assumptions.

- (i) the floors are rigid in their planes having 3 DOFs, two horizontal translations and a single rotation about a vertical axis,
- (ii) the masses of the building and mass moments of inertia are lumped at the floor levels at the corresponding degrees of freedom,
- (iii) the vertical component of the earthquake motion is ignored, and
- (iv) the inertia forces or moments due to vertical or rotational components of joint motions are negligible, therefore ignored.

The simplified model with above assumptions is shown in Figure 19.6. The dynamic degrees of freedom are drastically reduced by static condensation and yet it produces quite accurate results. In case the floor diaphragms are not adequately rigid in buildings with very stiff vertically resisting elements such as elevator cores, and diaphragms having large openings, irregular shapes etc., the in-plane rigid assumption is not valid. In such cases a more complex model with additional degrees of freedom is considered to properly represent in-plane flexibility. The floor slabs in such cases can be idealized as an assemblage of finite elements.

19.5 SOME IMPORTANT ISSUES IN MODELLING

19.5.1 *Modelling of Floor Diaphragms*

Typically slabs are considered to be supported on rigid supports, these are analysed and designed for gravity loads separately from the frame system. The floor slabs should be adequately

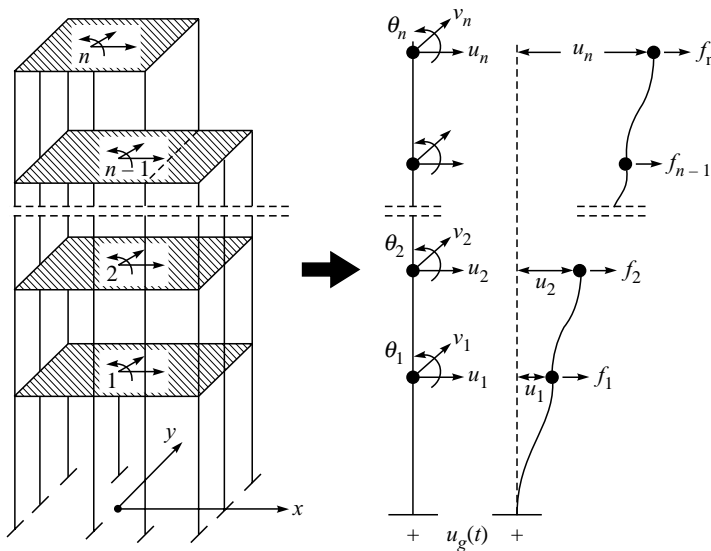


FIGURE 19.6 Building model with 3 DOFs per floor (Beskos, 1997).

represented in 3D model of the structure so that their dead loads and live loads are properly accounted for. Under seismic action floor, slabs play an important role of transmitting inertial loads to the frame and tying together elements of the later into a 3D entity. To perform these roles, slabs should be adequately connected with their supporting beams, walls and columns. The slabs are modelled in two ways: (i) rigid diaphragms; (ii) flexible floor diaphragms.

Modelling of rigid diaphragms

The in-plane stiffness of floor should be properly recognised and included in the model. The most convenient way of doing this is by introducing at each floor level an additional node termed '*master*' node with 3 DOFs: two translation and a rotation about normal to the plane of floor (Beskos, 1997). The master node is placed close to the centroid of the plan of floor and should not coincide with other floor nodes. The other corresponding 3 DOFs of all floor nodes, called *slaves* are related to those of the master node through a 3×3 transfer matrix. If the floor is horizontal, all these master and slave DOFs refer to global co-ordinate system and the slave DOFs can be condensed and only master node DOFs is left.

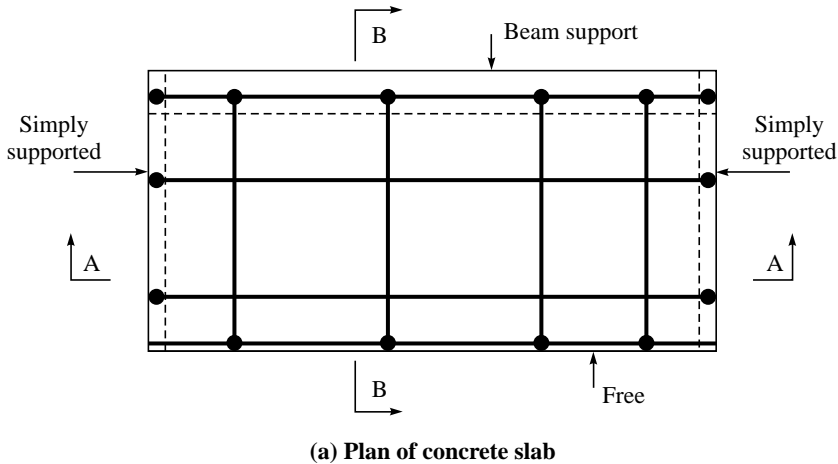
Modelling of flexible diaphragms

The in-plane flexibility of floor needs to be modelled under following conditions:

- when floor flexibility can significantly affect distribution of forces to the lateral force resisting elements,
- when in-plane stress field in the floor diaphragm needs to be computed for design of diaphragm, and
- some of the floor beams are prestressed and the same model of the floor-frame system can be used for calculation of the effects of prestressing force on the various structural members.

Modelling of floor diaphragm by grillage elements

The concrete slabs/diaphragms can be idealized by grillage elements in both the directions, Figure 19.7(a). The grillage element is a beam element in which combined bending and torsion effects are included (Figure 19.7(b)) (Macleod, 1990). Four to five grillage elements in each orthogonal direction can reasonably represent the flexibility of floor slab.



(a) Plan of concrete slab

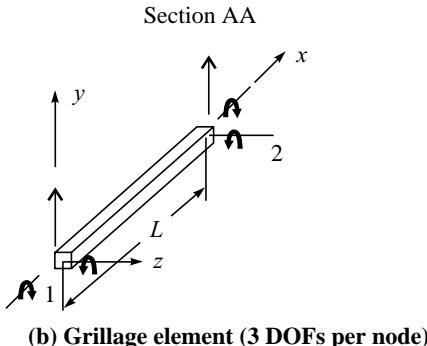
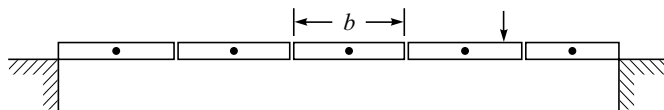


FIGURE 19.7 Modelling of floor diagram by grillage elements (Macleod, 1990).

Modelling of floor slab by finite element

Another method of modelling flexibility of floor is the use of **Finite Element (FE)**. This can take care of situations (ii) and (iii) as discussed earlier. A single FE is usually not sufficient for representing a slab, a few finite elements may be required for proper modelling of slab, then a care is to be exercised in accounting for compatibility of slab DOFs with supporting beams.

If there is no pressing need to use FE for floor slab, the in-plane flexibility of the latter can be approximated through proper selection of the moment of inertia I_y of the supporting beams about normal to the plane of floor with or without adding bi-diagonal bracing to each slab panel (Beskos, 1997).

19.5.2 Modelling of Soil-Foundation

The flexibility of soil is usually modelled by inserting discrete spring-dashpot elements between the foundation members, footings, grade beams or piles, and the soil medium. The spring and dashpot constants are determined from elastic half-space solution. In case of stiff, massive foundation, the effects of soil–structure interaction are important. Today's hardware capabilities allow incorporation of the entire system of building superstructure, the foundation elements and the underlying soil into a single model for the purpose of a seismic response analysis. This is very rarely done for multistoreyed buildings unless the significant effect of soil–structure interaction is envisaged in soft soils. Seismic design standards still do not include full incorporation of soil–structure interaction effects in seismic analysis and design, especially as these effects are mostly favourable. Practically all modern codes for earthquake resistant design of normal structures are based on the assumption that the structure is completely fixed to the ground. The soil–structure interaction should include the effects of both **kinematics** and **inertial interaction**.

The consideration of soil flexibility by elastic springs considers SSI effects only partially due to lengthening of time period of structure that usually results in the reduction of base shears and moments, but this does not take into account the change in input motion as a result of energy feedback from vibrating structure and radiation damping which can be included by considering kinematics interaction. Another important effect in soil modelling is the **soil damping**. Certain amount of energy of a vibrating structure is dissipated in soil through radiation damping. There are two components of radiation damping: (i) translational damping; (ii) rocking damping. The translation damping is of the order of 30%–35%. While rocking damping could vary between 5% and 7%. In the modal analysis of structures supported on soil medium the effect of soil damping is considered on the basis of equivalent modal damping. The equivalent modal damping is worked out on the basis of strain energy in each component of structure and soil in a particular mode of vibration.

19.5.3 Foundation Models

The foundation modelling would depend on the type of foundation. The types of foundation commonly employed for buildings are: (i) isolated footing and wall footing; (ii) raft; and (iii) pile. The foundation modelling (Macleod, 1990) for each type is described below:

Isolated footing and wall footing

A column on isolated footing along with foundation beam could be modelled as beam elements as shown in Figure 19.8(a). Wall as strip footing could be modelled by beam elements as shown in Figure 19.8(b).

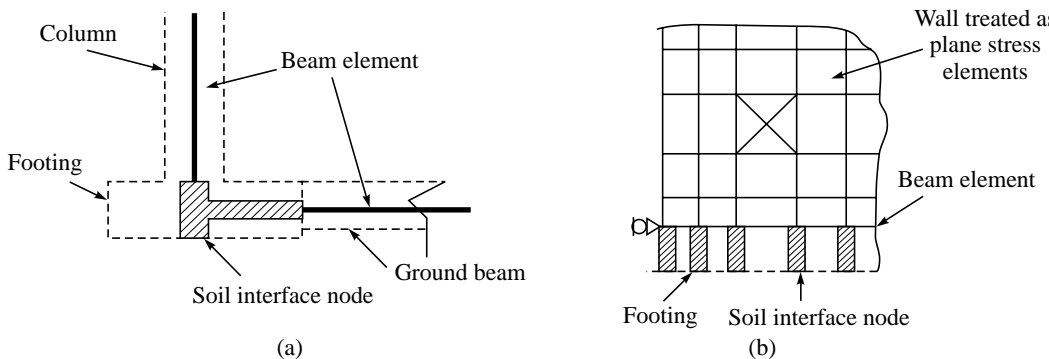


FIGURE 19.8 (a) Beam with footing; (b) Wall on strip footing (Macleod, 1990).

Raft foundation

The raft foundation can be used as grillage model. The deep raft should be modelled considering effect of shear deformation using Mindlin plate element. For greater accuracy, plate bending or flat shell elements can be employed for modelling raft foundation.

Pile foundation

A column may be resting on pile cap supported by group of piles. The lateral stiffness of pile group would be represented by linear and rotational springs on top of the pile. The choice of springs depends on pile geometry, E-value of pile, soil characteristics, whether or not the pile is end bearing, the interaction of pile in a group. This is a complex problem. The representation of pile group by springs may require a finite element study.

19.5.4 Soil Models

The commonly used models of soil (Macleod, 1990) are described below:

Winkler model

The elasticity of soil can be represented by a simple linear spring. Typical Winkler deformation is shown in Figure 19.9(a). A pressure q over an area A caused deformation δ , the load deformation relation of Winkler spring is expressed as $q = k_x \delta$, where k_x is the spring stiffness or modules of subgrade reaction and δ is deformation of soil surface. Values of k_x are based on plate-bearing tests. This type of soil model is highly approximate because soil behaviour is not

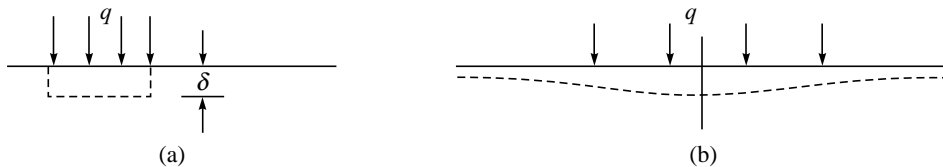


FIGURE 19.9 (a) Winkler model; (b) Elastic half space deformation (Macleod, 1990).

linear. The merit of Winkler model is to include flexibility of soil, which can be used to study relative effect of soil movements on structural behaviour, rather than as a means of predicting these movements.

Elastic half space model

In this model, soil is considered as a linear elastic medium requiring conventional elastic spring constants to define its properties. Elastic half space deformation is shown in Figure 19.9(b). Typical values of elastic constants in elastic half space are available in closed form expression (Clough and Penzien, 1986).

19.5.5 Modelling of Staircases

The staircases connect the successive levels or stories of a structure and thus contribute to its lateral stiffness. If the lateral-load-resisting frame is relatively flexible such as in low-rise frame structures and the location of staircase in plan affects significantly the torsional rigidity and response, it may be proper to include staircase in the structural model. In this way the effect of participation of staircase on seismic effect can be modelled as: (i) inclined truss member (ii) inclined beam member. Only monolithic connections of the staircase and its supporting beams to the rest of structure are included in the model as the nodes between the elements.

19.5.6 Modelling of Infills

The consideration of stiffening effect of infill panel on the frame is often important as it can considerably alter the behaviour of building in elastic range. The effect of infill from elastic to inelastic behaviour of a building can be quite complex. Yet its effect can be fairly well represented by a diagonal strut (Figure 19.10), having the same thickness as panel one, effective width may depend upon number of factors. Empirical expressions are available for stiffness of strut on the basis of studies conducted by various investigators.

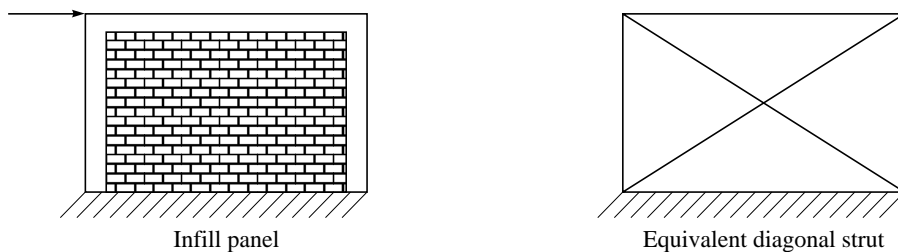


FIGURE 19.10 Diagonal strut model of infill.

SUMMARY

The process of development of suitable mathematical model for building system is described. Various models with their underlying assumptions and limitations are presented. A clear

understanding of these modelling issues will greatly facilitate an automated design of structural systems by the use of an appropriate computer software.

REFERENCES

- [1] Beskos, D.E. and Anagnostopoulos, S.A., *Computer Analysis and Design of Earthquake Resistant Structures—A Handbook*, Principles of Earthquake Resistant Design by J.M. Røeset, (ch. 7, p. 333), Buildings by S.A. Anagnostopoulos, (ch. 8, 369), Reinforced Concrete Structures by M.N. Fardis, (ch. 9, p. 441), Computational Mechanics Publications, 1997.
- [2] Clough and Penzien, *Dynamics of Structures*, McGraw-Hill, International Editions, 1986.
- [3] Fintel, Mark, *Handbook of Concrete Engineering*, Multi-storey Structures (ch. 10) by Mark Fintel Earthquake Resistant Structures (ch. 12), by Aranaldo T. Derecho and Mark Fintel, Van Nostrand Reinhold Company.
- [4] Farzad Naim, *The Seismic Design Handbook*, 2nd ed., Van Nostrand Reinhold Company, New York, 2001.
- [5] Macleod, I.A., *Analytical Modelling of Structural Systems*, Ellis Horwood, England, 1990.
- [6] Khan, F.R. and Sbarounis, J.A., “Interaction of Shear Wall and Frames”, *Proceedings of ASCE*, 90 (St 3). 285–335, June, 1964.

PART V

Earthquake Resistant Design (ERD) of Reinforced Concrete Buildings

Chapter 20

Ductility Considerations in Earthquake Resistant Design of RC Buildings

20.1 INTRODUCTION

As per IS 1893 (Part 1): 2002, Clause 6.1.3, “*Actual forces that appear on structures during earthquakes are much higher than the design forces specified in the code.*” It is recognized that neither the complete protection against earthquakes of all sizes is economically feasible nor design alone based on strength criteria is justified. The basic approach of earthquake resistant design should be based on lateral strength as well as deformability and ductility capacity of structure with limited damage but no collapse. The code IS 13920: 1993 entitled “*Ductile Detailing of Reinforced Concrete Structures Subjected to Seismic Forces—Code of Practice*” is based on this approach. This standard covers the requirements of lateral strength designing and detailing of monolithic reinforced concrete buildings so as to give them adequate toughness and ductility to resist severe earthquake shock without collapse. Thus, the ductility of a structure is in fact one of the most important factors affecting its seismic performance and it has been clearly observed that the well-designed and detailed reinforced structures behave well during earthquakes and “*the gap between the actual and design lateral forces is narrowed down by providing ductility in the structure.*”

Ductility in the structures will arise from inelastic material behaviour and detailing of reinforcement in such a manner that brittle failure is avoided and ductile behaviour is induced by allowing steel to yield in controlled manner. Therefore, one of the primary tasks of an engineer designing an earthquake resistant building is to ensure that the building will possess enough ductility to withstand the size and types of earthquakes, which it is likely to experience during its lifetime.

20.2 IMPACT OF DUCTILITY

The structural engineer must have to understand the impact of ductility on the building response when it is subjected to earthquake force. For example consider a single degree freedom system consisting of a metal rod and a weight, as shown in Figure 20.1. As the ground moves or displaces, the characteristics of the ground to weight connection will play a vital role. If this connection is very rigid, the weight will experience the same or larger forces as compared to ground force but if the connection is very flexible as is in case of a metal rod, it will bend or deform and the weight will subject to lesser forces because some of the energy will be consumed to displace the system. Most of the building responses under earthquake are within these two extremes.

From this simple example we can easily conclude that ductility, properly induced in the building system, will improve the behaviour of the building—primarily by reducing the forces in the structure. *Therefore, ductility is an essential attribute of an earthquake resistant design of structure that serves as a shock absorber in a structure and reduces the transmitted force to one that is sustainable.*

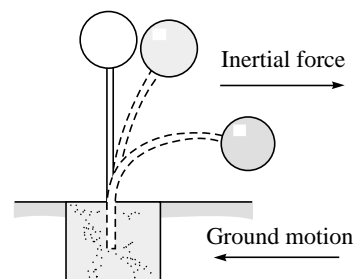


FIGURE 20.1 Ductility of a metal rod (MCEER web site).

20.3 REQUIREMENTS FOR DUCTILITY

In order to achieve a ductile structure we must give stress on three key areas during the design process. Firstly, the overall design concept for the building configuration must be sound. Secondly, individual members must be designed for ductility, and finally connection and other structural details need careful attention. It is well recognized and accepted analysis of experimental results and analytical studies, that in earthquake resistant design of structures, all structural members and their connections and supports *i.e.*, all critical regions whose yielding strength may be reached and exceeded by a severe earthquake, should be designed (sized and detailed) with large ductility and stable hysteresis behaviour so that the entire structure will remain ductile displaying stable hysteresis behaviour. There are two main reasons for this ductility requirement: first, it allows the structure as a whole, to develop its maximum potential strength, through distribution of internal forces, which is given by the combination of maximum strengths of all components; and second, large structural ductility allows the structure to move as a mechanism under its maximum potential strength, resulting in the dissipation of large amount of energy (Bertero, 1991).

20.4 ASSESSMENT OF DUCTILITY

Ductility is the capability of a material, structural component, or entire structure to undergo deformation after its initial yield without any significant reduction in yield strength. Ductility is generally measured in terms of ductility ratio or ductility factor, which is the ratio of the

maximum deformation that a structure or element can undergo without significant loss of initial yielding resistance to the initial yield deformation.

20.4.1 Member/Element Ductility

Displacement ductility

In order to determine the ductility ratio of an element, yield displacement and ultimate displacement must be defined clearly. *Yield load* is defined as the load when the reinforcement at the center of the resultant of tensile forces in the reinforcement yields, (Figure 20.2(a)). Some iterative calculations are needed to determine the yield load, but if the yield load is defined as described, the yield displacement can be computed as the displacement when the load reaches the yield load. At the same time, the ultimate displacement can be defined as the maximum displacement where the load does not become lower to the yield load, (Figure 20.2(b)).

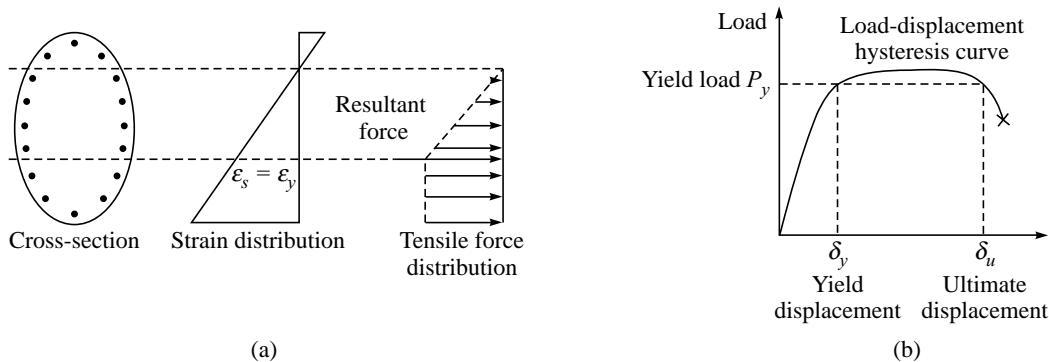


FIGURE 20.2 (a) Yield criterion; (b) Definition of ductility ratio (Machida, 1999).

Ductility ratio is influenced by various factors, and must be evaluated properly considering all of these factors according to designed structures and members. The ductility ratio becomes around 10 when the axial compressive stress, compressive strength of concrete and yield strength of reinforcement are in the range of 1 MPa, 20–30 MPa, 300–400 MPa, respectively.

Rotational and curvature ductility

In order to evaluate the ductility of a structure, curvature ductility ratio or rotation angle ductility ratio of each element is needed.

The rotational ductility factor is often expressed on the basis of plastic hinge idealization: $\mu_r = 1 + (\theta_h/\theta_y)$, where, θ_h = maximum plastic hinge rotation, θ_y = yield rotation (*in case of a beam loaded by two anti-symmetric end moments, $\theta_y = \frac{M_y L}{6EI}$, where, M_y , L , I and E are yield moment, length, moment of inertia and modulus of elasticity of the beam respectively*). There is no unique yield rotation that could be used in the definition of ductility factor. This definition applies for anti-symmetric deformation of beam members that occurs in beams of laterally loaded frames.

Curvature ductility is the ratio of curvature at the ultimate strength of the section to the curvature at first yield of tension steel in the section. It is defined for bilinear moment-curvature relationships as:

$$\mu_c = \frac{\phi_{\max}}{\phi_y} = 1 + \frac{\phi_p}{\phi_y}$$

where, ϕ_p = plastic portion of maximum curvature and ϕ_y = yield curvature (Figure 20.3).

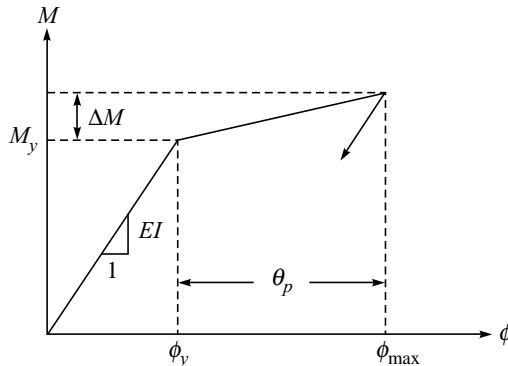


FIGURE 20.3 Bilinear moment-curvature relationship for beams (Machida, 1999).

The rotational ductilities are better measures of flexural damage than curvature ductilities. It is the simple index to characterize the severity of inelastic flexural deformation. True curvature ductilities are substantially larger than rotational ductilities. Comparing the member rotational ductility factor μ_r in a building with global ductility μ_b , the former is typically larger. This is due to the possibility for substantial localized yielding while the building can still be elastic.

The JSCE code, the EC 8 and the NZ code are proposing methods to calculate ductility factor of member or to express the relation between the amount of shear reinforcement in the plastic hinge region and the ductility factor as summarized in Table 20.1.

TABLE 20.1 Ductility calculations (Machida, 1999)

Codes	Calculation methods
JSCE Code	<p>Evaluation of ductility factor (μ_d) of member</p> $\mu_d = [\mu_0 + (1-\mu_0)(\sigma_0/\sigma_b)]/\gamma_b$ <p>where, $\mu_0 = 12(0.5V_{cd} + V_{sd})/V_{mu} - 3$, σ_0 : normal compressive stress σ_b: normal compression stress at balanced failure, V_{cd} : shear capacity from concrete, V_{sd} : shear capacity from shear reinforcement,</p> <p>γ_b = a partial safety factor (may be assumed as 1.5)</p> <p>V_{mu} = shear force acting on every section of the element when the element reaches its flexural capacity M_u</p>
EC8	<p>The following equation is proposed to obtain the minimum amount of confining reinforcement corresponding to the ductility factor</p> $\omega_{ad,r} > 1.74(A_c/A_{cc})(0.009\mu_c + 0.17)\eta_k - 0.07 > \omega_{w,min}$

Contd.

TABLE 20.1 Contd.

<i>Codes</i>	<i>Calculation methods</i>
NZ Code	<p>where, $\omega_{od,r}$: minimum amount of reinforcement, A_c: gross concrete area of section, A_{cc}: confined concrete area of section, $\omega_{w,min}$: 0.12 for ductile and 0.08 for limited ductile structures,</p> <p>μ_c = required curvature ductility,</p> <p>η_k = normalized axial force</p> <p>The following equation is derived for rectangular column</p> $\frac{A_{sh}}{s_h \cdot h''} = \left\{ \frac{A_g}{A_c} \frac{(\phi_u / \phi_y) - 33p_t \cdot m + 22}{111} \frac{f'_c}{f_{vt}} \cdot \phi \frac{N^*}{f'_c \cdot A_g} \right\} - 0.006$ <p>where, A_{sh}: total effective area of transverse bars in the direction under consideration within centre to center spacing of hoops sets s_h, h'': dimension of core of rectangular or square column at right angles to the direction of transverse bars under consideration measured to the center line of the perimeter hoop, A_g: gross area of column, A_c: core area of column, ϕ_u/ϕ_y: curvature ductility factor, $p_t = A_{st}/A_g$, A_{st}: total area of longitudinal steel, $m = f_{vt}/0.85f'_c$, f_{vt}: lower characteristics strength yield strength of transverse steel, f'_c: concrete compressive cylinder strength, N^*: axial compressive load on column, ϕ: strength reduction factor</p> <p>A_{sh} may be controlled by other requirement on transverse reinforcement.</p>

20.4.2 Structural Ductility

Structure ductility in a global sense depends on the displacement ductility of its members because response displacement of each member can be evaluated even with static analysis. Its quantification requires a relationship between lateral loads and displacement of whole building. This may be obtained by a pushover analysis by plotting total base shear versus the top storey displacement or preferably, versus the displacement at the level where the resultant force $Q_b = \sum F_i$ is applied (Figure 20.4). The u_b is determined from the work of lateral forces F_i as follows:

$$u_b = \frac{\sum_{i=1}^n F_i u_i}{Q_b}$$

where F_i is the lateral force at floor i and u_i its lateral displacement. The code defined that lateral force distribution can be used for analysis. The ductility of a building may be quantified by the factor

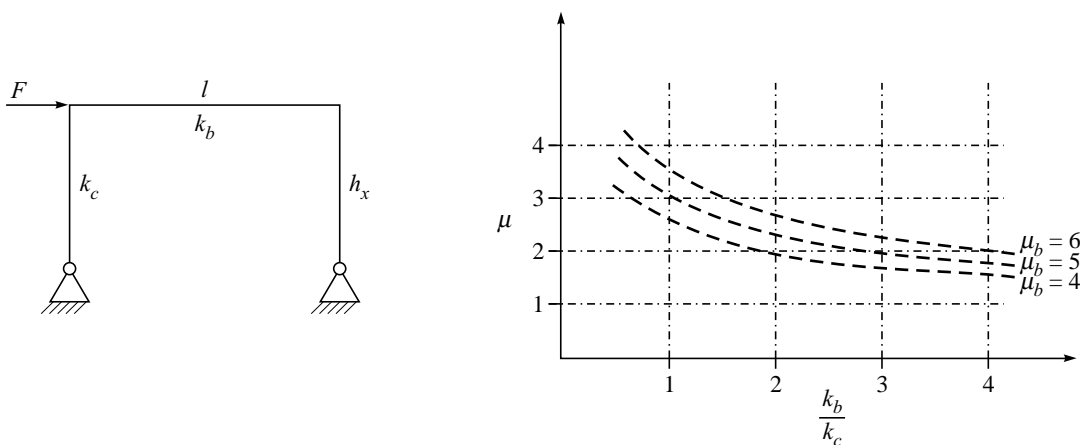
$$\mu_b = \frac{u_{\max}}{u_y}$$

For a single storey frame the relationship between the beam ductility (μ_m) and system ductility (μ_b) is,

$$\mu_b = \frac{k_b/k_c + \mu_m}{k_b/k_c + 1}$$

FIGURE 20.4 Pushover (or overload) analysis.

k_b/k_c = ratio of member stiffness, beam and column. This ratio is described graphically in Figure 20.5.

**FIGURE 20.5 Relationship between member ductility (μ_m) and system ductility (μ) (Englekirk, 2003).**

20.5 FACTORS AFFECTING DUCTILITY

Some important factors on which the ductility will depend are:

- (i) Ductility increases linearly with an increase in the shear strength carried by concrete for small value of axial compressive stress ($0 \leq \sigma_0 \leq 1$ MPa), (Machida, 1999).
- (ii) Ductility linearly reduces upto the point where axial compressive stress becomes equal to the axial compressive stress at balanced failure.

- (iii) With the increase of ultimate strain of concrete, the ductility factor increases. Thus confining of concrete increases the ductility appreciably.
- (iv) An increase in yield strength of steel with all other variables constantly decreases ductility. The ductility increases with the increase in concrete strength.
- (v) The lateral reinforcement tends to improve ductility by preventing shear failures, restraining the compression steel against buckling. The lateral reinforcement in the form of closed stirrups is effective in binding the compression zone thereby confining the concrete and increasing the ductility of section.
- (vi) Shear failure occurs at a smaller deflection than the flexural failure and hence absorbs much less energy. Members should be designed and detailed by providing web reinforcement so that their strength in shear exceeds the strength in flexure. Therefore, ductility increases as the stirrups in the specimen increases.
- (vii) Bond failures and anchorage failures are sudden and brittle. Special attention must be given in details to prevent them from occurring in structures, which must behave in a ductile manner.

20.6 DUCTILITY FACTORS

The displacement ductility ratio or *ductility factors* (μ) are used in the reduction of the required linear elastic strength of structure. In actual, the need for incorporation of *response reduction factor* (R) in base shear formula in IS 1893 (Part 1): 2002 is an attempt to consider the structural ductility in addition to over strength, energy dissipating capacity, the stability of vertical load carrying system at maximum induced inelastic deformations. The value of R is prescribed in **Table 7 of IS 1893 (Part 1): 2002** for different types of building systems. It shows a low value of R approaching 1.5 assigned to an extremely brittle building *i.e.* unreinforced masonry wall building and a high value of R ($= 5$) is assigned to a more ductile structure like special moment resistant frame reinforced concrete or shear wall buildings.

The response reduction factor may be same as ductility factor (μ) in the case of structures with a very long period with respect to the period of the predominant frequency content of the earthquake ground motion. Sometimes the response reduction factor may be equal to $R = \sqrt{2\mu - 1}$ which is only applicable if the structure is subjected to relatively very short acceleration pulse (with respect to its fundamental period) and the input energy for the linear elastic structure is the same as that for the inelastic (perfectly-plastic) structure (Bertero, 1986).

The NZ Code is proposing the relation of the maximum values of the design ductility factor and structural types which correspond to structural action is summarized in Table 20.2.

TABLE 20.2 Categories of structural/member actions (Machida, 1999)

S.No.	Categories	Applicable ductility factors (μ)
1.	Ductile structure	$\mu = 3 \sim 6$
2.	Partially ductile	$\mu = 3.3 \sim 6$
3.	Structure of limited ductility demand	$\mu < 6$
4.	Structure of limited ductility capacity	$\mu < 6$

Contd.

TABLE 20.2 Contd.

S.No.	Categories	Applicable ductility factors (μ)
5.	Elastic structure	$\mu = 1$
6.	Structure incorporating mechanical energy dissipating devices	
7.	Structure locked into the ground	$\mu = 1$

20.7 DUCTILE DETAILING CONSIDERATIONS AS PER IS 13920: 1993

Provision for ductile detailing in the members of reinforced concrete buildings are given in IS 13920: 1993. These provisions are for the anchorage and splices of longitudinal reinforcement, spacing, anchorage and splices of lateral reinforcement, and joint of member. It is often observed in past earthquakes that the problems in structural detailing may also be a significant cause of damage. The discussions herein focus on the provision of ductile detailing provision for RC buildings and its possible reasons for providing structure, which will be helpful to understand the importance of the ductile detailing for earthquake resistant design of structure.

5.0 General Specifications

5.1 *The design and construction of reinforced concrete buildings shall be governed by the provision of IS 456: 1978 (now IS: 456: 2000), except as modified by the provisions of this code.*

5.2 *For all buildings which are more than 3 stories in height, the minimum grade of concrete shall be M 20 ($f_{ck} = 20 \text{ MPa}$)*

Possible Explanations:

- The concrete strength below M 20 may not have the requisite strength in bond or shear to take full advantage of the design provisions
- Bending strength of a reinforced concrete member is relatively insensitive to concrete compressive, tensile and shear strength and durability, which are adversely affected by weak concrete

5.3 *Steel reinforcements of grade Fe 415 or less shall be used*

Possible Explanations:

- For reinforcement, the provisions, firstly, of adequate ductility and secondly, of an upper limit on the yield stress or characteristic strength, are essential. It is a general practice to limit the yield stress of reinforcement to 415 MPa
- Strong steel is not preferable to low strength steel in earthquake prone region because typical stress strain curve of low steel shows the following advantages: (a) a long yield plateau; (b) a greater breaking strain; and (c) less strength gain after first yield

- Mild steel is more ductile and its reduced post yield strength gain is advantageous. Provided that the yield strength is confined to specified limits, design can determine section maximum flexure strengths in order to design other areas of the structure to prevent premature brittle shear failure (capacity design approach)
- Mild steel should be used, as primarily reinforcement in areas where earthquake damage is expected, such as beam in moment resisting frames Higher strength steel (with a yield strength > 300 MPa) is appropriate for other structural elements where flexural yielding can't occur under earthquake load

6.0 Flexural Members

6.1 General

These requirements apply to frame members resisting earthquake-induced forces and designed to resist flexure. These members shall satisfy the following requirements.

6.1.1 *The factored axial stress on the member under earthquake loading shall not exceed $0.1f_{ck}$.*

Possible Explanation:

- Generally, axial force in the flexural member is relatively very less but if factored axial compressive stress in the frame member exceeds to $0.1f_{ck}$, axial force will also be considered besides bending and member will be designed as per clause 7.0

6.1.2 *The member shall preferably have a width to depth ratio of more than 0.3.*

Possible Explanations:

- To provide more uniform design approach
- To minimize the risk of lateral instability
- Experience gained from past

6.1.3 *The width of the member shall not be less than 200 mm.*

Possible Explanations:

- To decrease the sensitivity to geometric error
- Experience gained from practice with RC frames resisting earthquake induced forces

6.1.4 *The depth D of the member shall preferably be not more than one-fourth of the clear span.*

Possible Explanations:

- To take into account the non-linearity of strain distribution and lateral buckling
- Experimental evidence indicates that under load reversals or displacement into nonlinear range, the behaviour of continuous members having length to depth ratios of less than four is significantly different from the behaviour of relatively slender members

6.2 Longitudinal Reinforcement

6.2.1 (a) *The top as well as bottom reinforcement shall consist of at least two bars throughout the member length.*

Possible Explanations:

- To ensure integrity of the member under reversed loading
- It is a construction requirement rather than behavioral requirement

6.2.1 (b) *The tension steel ratio on any face, at any section, shall not be less than $\rho_{min} = 0.24\sqrt{f_{ck}/f_y}$, where f_{ck} and f_y are in MPa.*

Possible Explanation:

- To provide necessary ductility or to avoid brittle failure upon cracking

6.2.2 *The maximum steel ratio on any face at any section shall not exceed $p_{max} = 0.025$.*

Possible Explanations:

- To avoid steel congestion and limit shear stresses in beams of typical proportions
- Practically, low steel ratio should be used whenever possible

6.2.3 *The positive steel at a joint face must be at least equal to half of the negative steel at that face.*

Possible Explanations:

- To ensure adequate ductility at potential plastic hinge regions, and to ensure that minimum tension reinforcement is present for moment reversal
- To allow the possibility of the positive moment at the end of a beam due to earthquake induced lateral displacements exceeding the negative moments due to gravity loads
- To produce balanced conditions and limit the incorrect assumption such as linear strain distribution, well defined yield point for the steel, limiting compressive strain in concrete of 0.003 and compressive stress in the shell concrete

6.2.4 *The steel provided at each of the top and bottom face of the member at any section along its length shall be at least equal to one-fourth of the maximum negative moment steel provided at the face of either joint. It may be clarified that redistribution of moments permitted in IS 456:1978 (clause 36.1) will be used only for vertical load moments and not for lateral load moments*

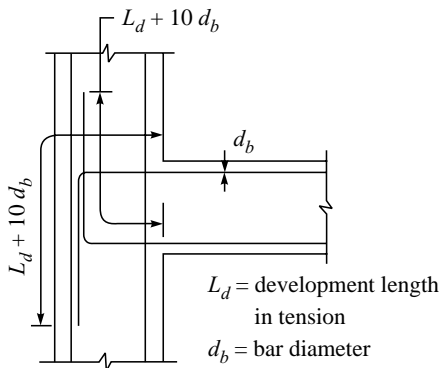
Possible Explanations:

- This is to ensure some positive and negative moment capacity throughout the beam in order to allow unexpected deformations and moment distribution from severe earthquake action
- To allow the possibility of the positive moment at the end of a beam due to earthquake induced lateral displacements exceeding the negative moments due to gravity loads
- To produce balanced conditions and limit the incorrect assumption such as linear strain distribution, well defined yield point for the steel, limiting compressive strain in concrete of 0.003 and compressive stress in the shell concrete

6.2.5 *In an external joint, both the top and the bottom bars of the beam shall be provided with anchorage length, beyond the inner face of the column, equal to the development length in tension plus 10 times the bar diameter minus the allowance for 90 degrees bend(s). In an internal joint, both face bars of the beam shall be taken continuously through the column.*

Possible Explanations:

- Such arrangement will make a ductile junction and provide adequate anchorage of beam reinforcement into columns
- The capacity of the beam is developed by embedment in the column and within the compression zone of the beam on the far side of the connection
- The length available for the development of the strength of a beam bars is gradually reduced during cyclic reversals of earthquake actions because of the yield penetration from the face of a column

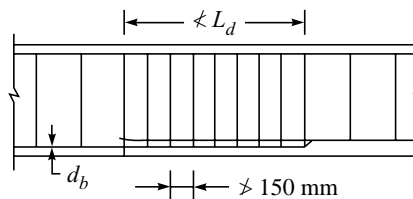


Anchorage of beam bars in an external joint.

6.2.6 *The longitudinal bars shall be spliced, only if hoops are provided over the entire splice length, at spacing not exceeding 150 mm. The lap length shall not be less than the bar development length in tension. Lap splices shall not be provided (a) within a joint, (b) within a quarter length of the member where flexural yielding may generally occur under the effect of earthquake forces. Not more than 50 per cent of the bars shall be spliced at one section.*

Possible Explanations:

- Lap splices of reinforcement are prohibited at regions where flexural yielding is anticipated because such splices are not reliable under conditions of cyclic loading into the inelastic range
- Transverse reinforcement for lap splices at any location is mandatory because of the possibility of loss of concrete cover



$L_d = \text{development length in tension}$

$d_b = \text{bar diameter}$

Lap splice in beams.

6.2.7 Use of welded spliced and mechanical connections may also be made, as per 25.2.5.2 of IS 456:1978. However, not more than half the reinforcement shall be spliced at a section where flexural yielding may take place. The location of splices shall be governed by 6.2.6.

Possible Explanations:

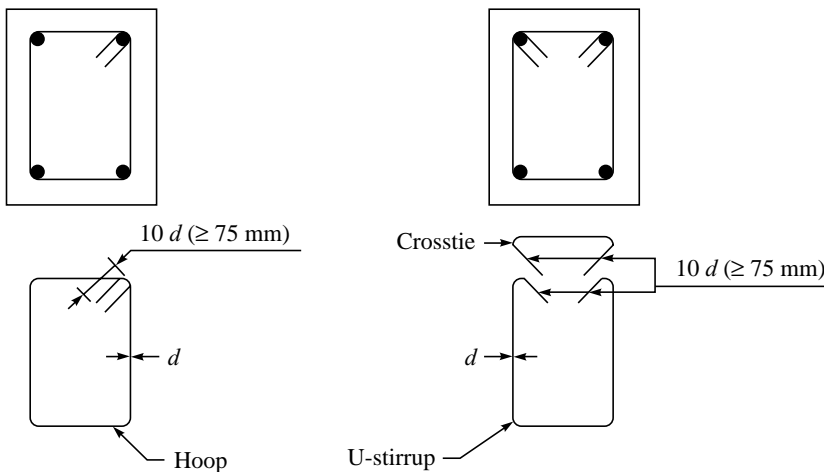
- Welded splices are one in which the bars are lap welded or butt-welded to develop the breaking strength of the bar
- A mechanical connection is a connection which relies on mechanical interlock with the bar deformations to develop the connection capacity
- In a structure undergoing inelastic deformations during an earthquake, tensile stresses in reinforcement may approach the tensile strength of the reinforcement. The requirement of welded spliced and mechanical connections is intended to avoid a splice failure when the reinforcement is subjected to expected stress levels in yielding regions
- The location of welding splices is restricted because tensile stresses in reinforcement in yielding regions cannot exceed the strength requirement

6.3 Web Reinforcement

6.3.1 Web reinforcement shall consist of vertical hoops. A vertical hoop is a closed stirrup having a 135° hook with a 10-diameter extension (but not < 75 mm) at each end that is embedded in the confined core. In compelling circumstances, it may also be made up of two pieces of reinforcement: A U stirrup with a 135° hook and a 10-diameter extension (but not < 75 mm) at each end, embedded in the confined core and cross tie. A crosstie is a bar having a 135° hook with a 10 diameter extension (but not < 75 mm) at each end. The hooks shall engage peripheral longitudinal bars.

Possible Explanations:

- Stirrups are required to prevent the compression bar from buckling
- Transverse reinforcement is required to confine the concrete in the regions where yielding is expected so as to minimize strength degradation
- To provide shear strength for full flexural capacity of the member



Beam web reinforcement.

6.3.2 The minimum diameter of the bar forming a hoop shall be 6 mm. However, in beams with clear span exceeding 5 m, the minimum bar diameter shall be 8 mm.

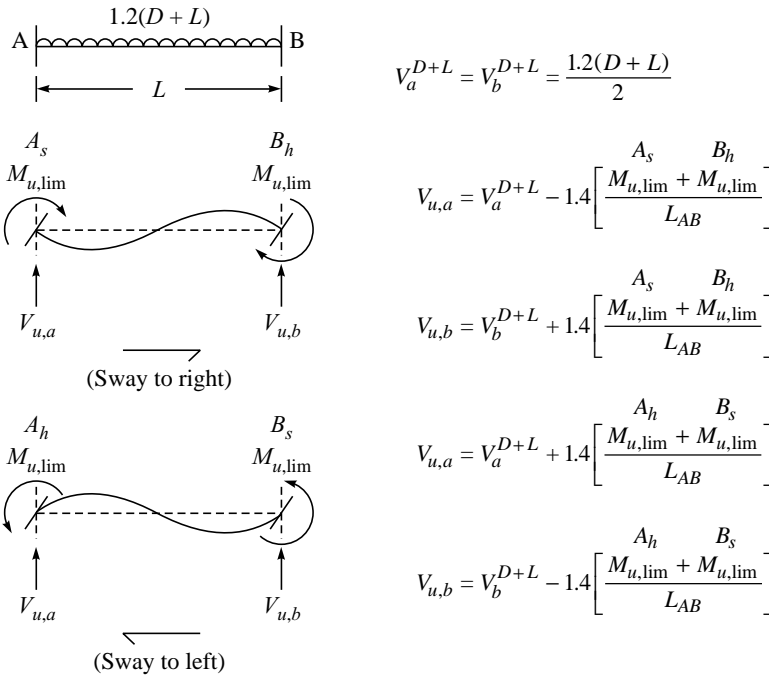
Possible Explanation:

- This refers to construction and durability (corrosion of reinforcement) rather than behavioral requirements

6.3.3 The shear force to be resisted by the vertical hoops shall be the maximum of: (a) calculated factored shear force as per analysis, and (b) shear force due to formation of plastic hinges at both ends of the beam plus the factored gravity load on the span.

Possible Explanations:

- Actual forces that appear on structures during earthquakes are much higher than the design forces specified in the code, it is assumed that frame members will dissipate energy in the nonlinear range response, unless a frame member possesses a strength that is a multiple on the order of 3 or 4 of the design forces. It is desirable that the beams should yield in flexure before failure in shear
- The design shear force should be a good approximation of the maximum shear that may develop in a member at any event. Therefore, required shear strength for frame members is related to flexural strength of the designed member rather than factored shear forces indicated by lateral load analysis



Calculation of design shear force for beam.

6.3.4 The contribution of bent up bars and inclined hoops to shear resistance of the section shall not be considered.

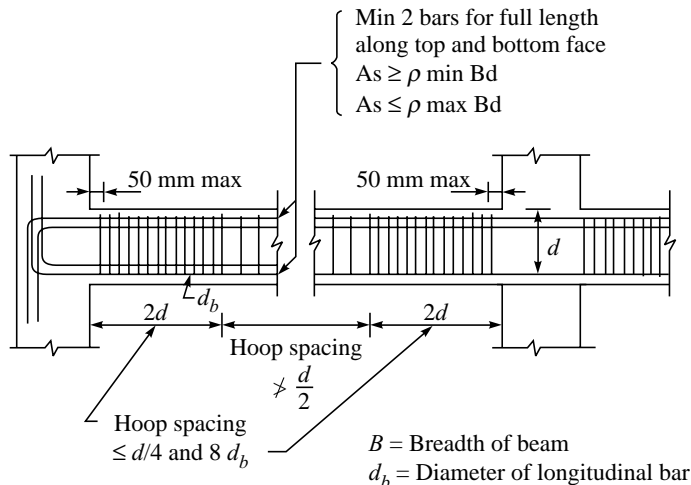
Possible Explanation:

- Spalling of the concrete shell is anticipated during strong motion, especially at and near regions of flexural yielding, all web reinforcement should be provided in the form of closed hoops

6.3.5 *The spacing of hoops over a length of $2d$ at either end of a beam shall not exceed (a) $d/4$, and (b) 8 times the diameter of the smallest longitudinal bar; however it need not be less than 100 mm. The first hoop shall be at a distance not exceeding 50 mm from the joint face. Vertical hoops at the same spacing as above shall also be provided over a length equal to $2d$ on either side of a section where flexural yielding may occur under the effect of earthquake forces. Elsewhere the beam shall have vertical hoops at a spacing not exceeding $d/2$.*

Possible Explanations:

- Potential plastic hinge regions in beams require special detailing where a plastic hinge develops. It serves three main purposes (i) prevents buckling of longitudinal bars in compression; (ii) provides some confinement of the concrete; and (iii) acts as shear reinforcement
- In the case of members with varying strength along the span or member for which the permanent load represents a large proportion of the total design load, concentration of inelastic rotation may occur within the span. If such a condition is anticipated, transverse reinforcement should also be provided in regions where yielding is expected



Beam reinforcement.

7.0 Columns and Frame Members subjected to Bending and Axial load

7.1 General

7.1.1 *These requirements apply to frame members, which have a factored axial stress in excess of $0.1 f_{ck}$ under the effect of earthquake forces.*

Possible Explanation:

- the member subjected to axial forces greater than a specified limit shall take both the load bending and axial

7.1.2 *The minimum dimension of the member shall not be less than 200 mm. However, in frames, which have beams with center-to-center span exceeding 5 m or columns of unsupported length exceeding 4 m, the shortest dimension of the column shall not be less than 300 mm.*

Possible Explanations:

- to avoid very slender columns
- to avoid column failure before beams (strong column weak beam concept)
- experience from practice with reinforced concrete frames resisting earthquake-induced forces

7.1.3 *The ratio of the shortest cross sectional dimension to the perpendicular dimension shall preferably be not less than 0.4.*

Possible Explanation:

- Experience from practice with reinforced concrete frames resisting earthquake-induced forces

7.2 Longitudinal Reinforcement

7.2.1 *Lap splices shall be provided only in the central half of the member length. It should be proportioned as a tension splice. Hoops shall be provided over the entire splice length at spacing not exceeding 150 mm from centre-to-centre. Not more than 50 per cent of the bars shall be spliced at one section.*

Possible Explanations:

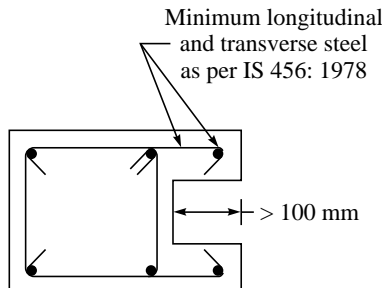
- Lap splices of inadequate length may lead to column distress and even failure. It should be enclosed with transverse reinforcement because of the uncertainty in moment distributions along the height and the need for confinement of lap splices subjected to stress reversals
- Longitudinal bars in potential plastic hinge regions should be distributed reasonably and uniformly around the perimeter of the section in order to assist the confinement of concrete

7.2.2 *Any area of a column that extends more than 100 mm beyond the confined core due to architectural requirements shall be detailed in the following manner. In case the contribution of this area to strength has been considered, then it will have minimum longitudinal and transverse reinforcement as per this code. However if this area has been treated as non-structural, the minimum reinforcement requirements shall be governed by IS 456:1978 provisions minimum longitudinal and transverse reinforcement, as per IS 456:1978.*

Possible Explanation:

- The unreinforced shell may spall as the column deforms to resist earthquake effects. Separation of portions of the shell from the core caused by local spalling creates a

falling hazard. The additional reinforcement is required to reduce the risk of portions of the shell falling away from the column



Reinforcement requirement for column with more than 100 mm projection beyond core.

7.3 Transverse Reinforcement

7.3.1 *Transverse reinforcement for circular columns shall consist of spiral or circular hoops. In rectangular columns rectangular hoops may be used. A rectangular hoop is a closed stirrup, having a 135° hook with 10-diameter extension (but not < 75 mm) at each end that is embedded in the confined core.*

Possible Explanation:

- Columns of building subjected to seismic loading often carry large flexure and shear load, when diagonal tension cracks are possible, shear reinforcement will be required. Therefore, the anchorage and the shape of tie must be such that tensile forces resulting from truss action can be transversed from one face of the column to the other

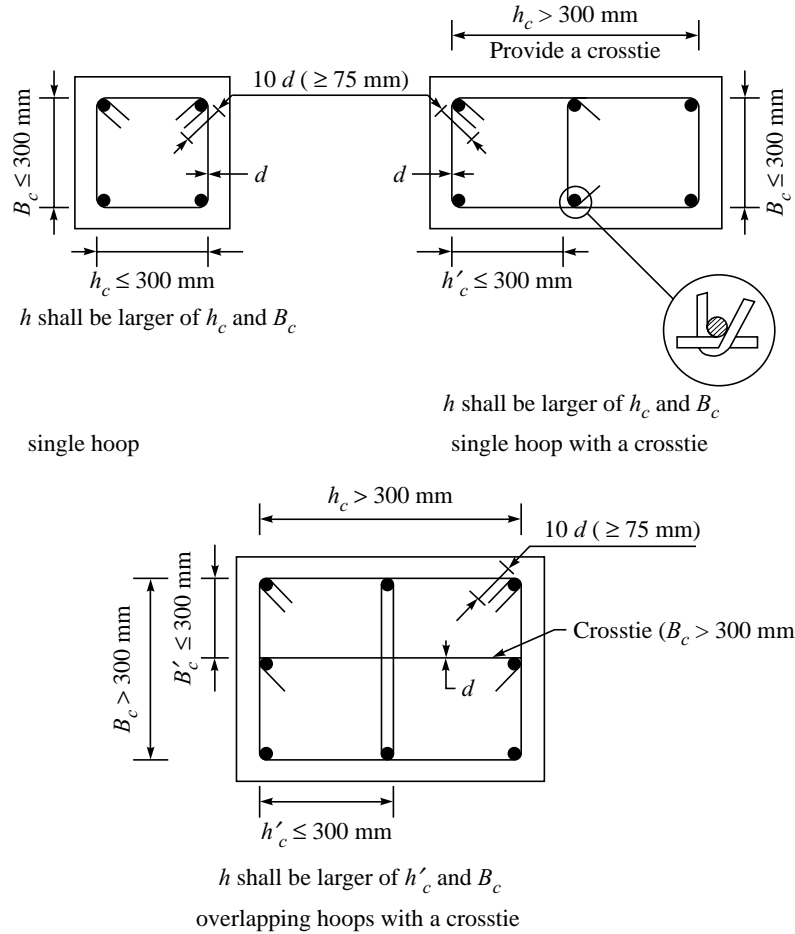
7.3.2 *The parallel legs of rectangular hoop shall be spaced not more than 300 mm centre-to-centre. If the length of any side of the hoop exceeds 300 mm, a crosstie shall be provided. Alternatively, a pair of overlapping hoops may be provided within the column. The hooks shall engage peripheral longitudinal bars.*

7.3.3 *The spacing of hoops shall not exceed half the least lateral dimension of the column, except where special confining reinforcement is provided as 7.4.*

Possible Explanations:

- The maximum centre-to-centre spacing of the transverse reinforcement is considered necessary to restrain buckling of longitudinal steel and for adequate confinement of the concrete. Too much spacing would not provide adequate lateral restraint or confinement; too small a spacing would not allow aggregate particles to pass between the transverse bars when concrete is being placed
- Observations after earthquakes have shown significant damage to columns in the non-confined region, and the minimum ties or spirals required should provide more uniform toughness of the column along its length
- Column bars carrying compression are liable to buckle under large strain. When yielding takes place in steel approach, the lateral restrain provided the cover cannot

rely upon concrete. Therefore, transverse ties must provide lateral support to each column bar to prevent stability due to outward buckling



Transverse reinforcement in columns.

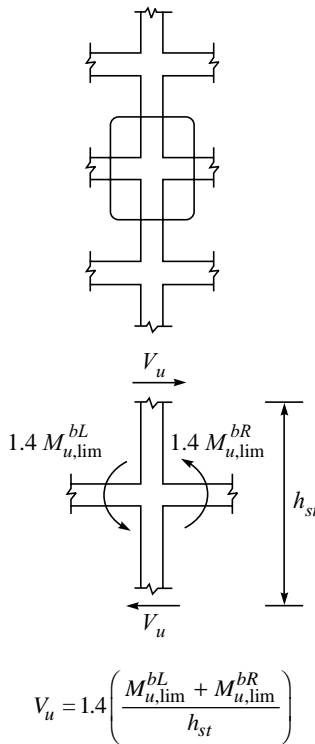
7.3.4 The design shear force for columns shall be the maximum of: a) calculated factored shear force as per analysis and b) a factored shear force given by

$$V_U = 1.4 \left[\frac{M_{u,\lim}^{bL} + M_{u,\lim}^{bR}}{h_{st}} \right]$$

where $M_{u,\lim}^{bL}$ and $M_{u,\lim}^{bR}$ are moment of resistance, of opposite sign of beams framing into the column from opposite faces and h_{st} is the storey height. The beam moment capacity is to be calculated as per IS 456:1978.

Possible Explanation:

- The moment capacity of a joint may be limited by the flexural strength of the beams framing into the joint. Where beams frame into opposite sides of a joint, the combined strength may be sum of the negative moment strength of the beam on one side of the joint and the positive moment strength of the beam on the other side of the joint



Calculations of design shear force for column.

7.4 Special Confining Reinforcement

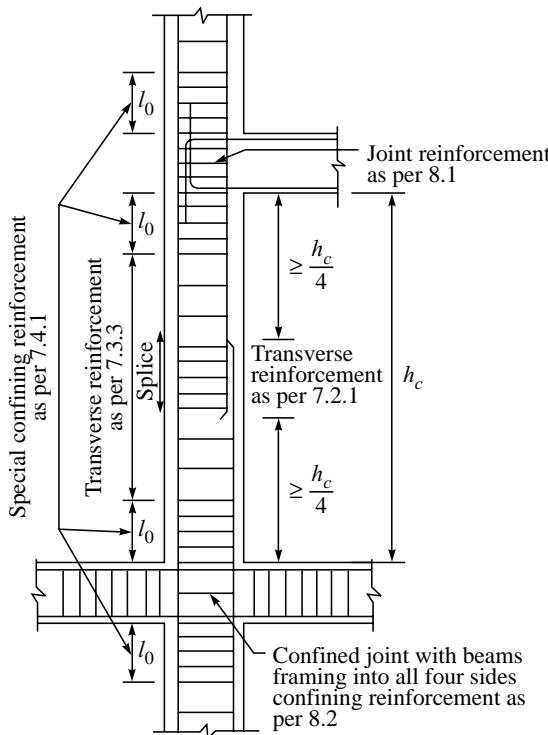
This requirement shall be met with, unless a larger amount of transverse reinforcement is required from shear strength considerations.

- 7.4.1 Special confining reinforcement shall be provided over a length l_0 from each joint face, towards midspan, and on either side of any section, where flexural yielding may occur under the effect of earthquake forces. The length ' l_0 ' shall not be less than (a) larger lateral dimension of the member at the section where yielding occurs, (b) 1/6 of clear span of the member, and (c) 450 mm.

Possible Explanations:

- Potential plastic hinge regions in columns shall be considered to be end regions adjacent to moment resisting connections over a minimum length from the connection

- This stipulates a minimum length which provides closely spaced transverse reinforcement at the member ends, where flexural yielding normally occurs
- This is provided to confine the concrete core, to support the longitudinal compressive reinforcement against inelastic buckling and for resistance in conjunction with the confined concrete, against shear

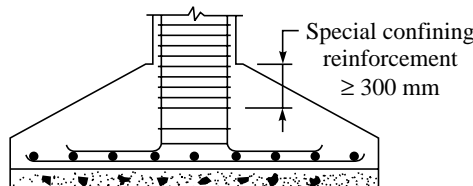


Column and joint detailing.

7.4.2 When a column terminates into a footing or mat, special confining reinforcement shall extend at least 300 mm into the footing or mat.

Possible Explanations:

- yield penetration
- due to very high axial loads and flexural demands at the base, special confining reinforcement shall extend at least 300 mm into the footing or mat of building



Provision of special confining reinforcement in footings.

7.4.3 When the calculated point of contra-flexure, under the effect of gravity and earthquake loads, is not within the middle half of the member clear height, special confining reinforcement shall be provided over the full height of the column.

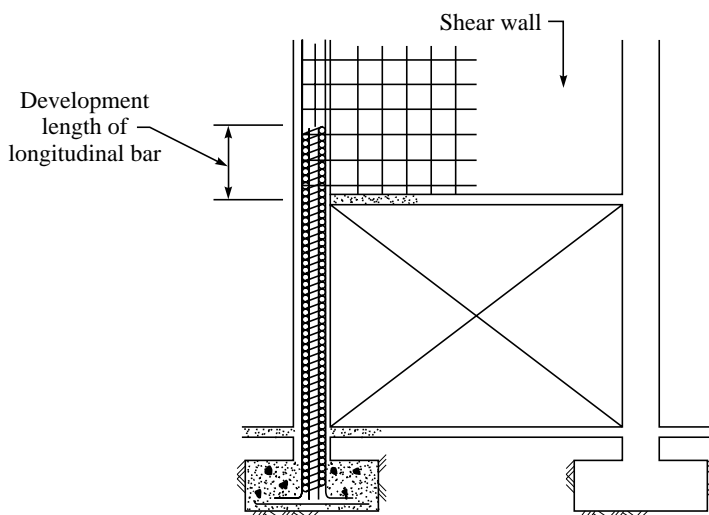
Possible Explanations:

- This provision was added to provide reasonable protection and ductility to the mid height of columns between transverse reinforcement. Post-earthquake observations have shown significant damage to columns in the non confined region, with the minimum required ties or spirals providing a more uniform toughness of the column along its length
- The eccentricity in the point of contra-flexure would result in additional shear load, as the normal confining reinforcement shall be based on the calculation of point of contra flexure being within the middle half of the members clear height

7.4.4 Columns supporting reactions from discontinued stiff members, such as walls, shall be provided with special confining reinforcement over their full height. This reinforcement shall also be placed above the discontinuity for at least the development length of the largest longitudinal bar in the column. Where the column is supported on a wall, this reinforcement shall be provided over the full height of the column; it shall also be provided below the discontinuity for the same development length.

Possible Explanations:

- Columns supporting discontinued stiff members, such as walls or trusses, may develop considerable inelastic response. Therefore, it is required that these columns have special transverse reinforcement throughout their length
- This covers all columns beneath the level at which the stiff member has been discontinued, unless the factored forces corresponding to earthquake effect are low

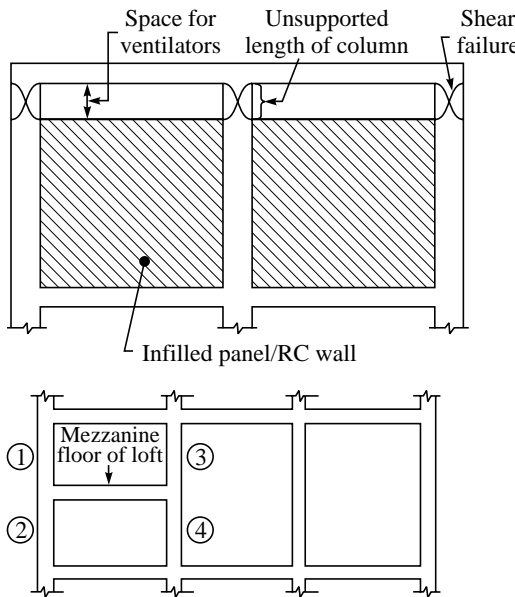


Special confining reinforcement requirement for column under discontinued walls.

7.4.5 Special confining reinforcement shall be provided over the full height of a column, which has significant variation in stiffness along its height. This variation in stiffness may result due to the presence of bracing, a mezzanine floor or a R.C.C. wall on either side of the column that extends only over a part of the column height.

Possible Explanation:

- Due to presence of bracing, a mezzanine floor or a R.C.C. or infill wall on either side of the column, the effective height of the column has reduced. The shear required to develop flexural yield in the effectively shortened column is substantially higher than shear required developing flexural yield of full-length column. If the designer has not considered this effect, shear failure may occur before flexural yield resulting in fail in brittle manner



(1), (2), (3) and (4) relatively stiff columns—they attract large seismic shear force.

Column with varying stiffness.

7.4.6 The spacing of hoops used as special confining reinforcement shall not exceed 1/4 of minimum member dimension but need not be less than 75 mm nor more than 100 mm.

Possible Explanations:

- The requirement of minimum spacing is to obtain adequate concrete confinement and the requirement, the spacing does not exceed 100 mm is intended to restrain longitudinal reinforcement buckling after spalling
- The limitation has been guided by tests to provide adequately uniform confining stress to the column core

7.4.7 The area of cross section, A_{sh} , of the bar forming circular hoops or spiral, to be used as special confining reinforcement shall not be less than

$$A_{sh} = 0.09 SD_k \frac{f_{ck}}{f_y} \left\{ \frac{A_g}{A_k} - 1 \right\}$$

where, A_{sh} = area of the bar cross section, S = pitch of spiral or spacing of hoops, D_k = diameter of core measured to the outside of the spiral or hoop, f_{ck} = characteristic compressive strength of concrete cube, f_y = yield stress of steel (of circular hoop or spiral), A_g = gross area of the column cross section, and A_k = area of concrete core = $\pi D_k^2 / 4$

Possible Explanations:

- For working out the amount of lateral hoops for necessary confinement, a criterion may be adopted that the load carrying the cross section of the column may be made equal to that of the column without shell concrete. Using this criterion, the cross-sectional area of the bar forming circular hoops or a spiral used for confinement of concrete is given in code
- Test and experience show that columns containing the amount of spiral reinforcement exhibit considerable toughness and ductility

7.4.8 The area of cross section, A_{sh} of the bar forming rectangular hoop, to be used as special confining reinforcement shall not be less than

$$A_{sh} = 0.18 Sh \frac{f_{ck}}{f_y} \left\{ \frac{A_g}{A_k} - 1 \right\}$$

where, h = longer dimension of the rectangular confining hoop measured to its outer face. It shall not exceed 300 mm and A_k = area of confined concrete core in the rectangular hoop measured to its outside dimensions

Possible Explanations:

- The limitation has been guided by the experience and various tests to achieve high flexural ductility capacity and to confine the concrete
- Rectangular hoops are less effective in confining the column core hence 0.18 multiplying factor in place of 0.09 in circular hoops, is introduced

8.0 Joints of Frames

8.1 The special confining reinforcement as required at the end of column shall be provided through the joint, unless the joint is confined as specified by 8.2

Possible Explanations:

- This also helps resist the shear force transmitted by the framing members and improves the bond between steel and concrete within the joint
- This helps maintain the vertical load carrying capacity of the joint even after spalling of the outer shell

8.2 A joint, which has beams framing into all vertical faces of it and where each beam width is at least 3/4 of the column width, may be provided with half the special confining

reinforcement required at the end of the column. The spacing of hoops shall not exceed 150 mm.

Possible Explanation:

- The minimum transverse reinforcement required in the joint is the same as the confinement reinforcement specified for the column ends immediately above or below the joint, except that where the joint is confined by elastic beams on all 4 sides, these requirements may be relaxed. This is because the rest half of the confinement is provided by the rigid beams framing into the vertical faces of the joint

9.0 Shear Walls

9.1 General Requirements

9.1.1 *The requirements of this section apply to the shear walls, which are part of the lateral force resisting system of the structure.*

Possible Explanation:

- Wall being relative stiff elements, will in general resist all earthquake forces

9.1.2 *The thickness of any part of the wall shall preferably be not less than 150 mm.*

Possible Explanations:

- To avoid very thin section, because these sections are susceptible to lateral instability in zones where inelastic cyclic loading may have to be sustained
- To safeguard against premature out-of-plane buckling in the potential plastic hinge region of walls

9.1.3 *The effective flange width to be used in the design of flanged wall sections, shall be assumed to extend beyond the face of the web for a distance which shall be the smaller of (a) half the distance to an adjacent shear wall web, and (b) 1/10th of the total wall height.*

Possible Explanation:

- Tests show that effective flange width increases with increasing drift level and the effectiveness of a flange in compression differs from that of a flange in tension. The value used for the effective compression flange width has little impact on the strength and deformation capacity of the wall therefore to simplify design a single value of effective flange width based on an estimate of the effective tension flange width is used in both tension and compression

9.1.4 *Shear walls shall be provided with reinforcement in the longitudinal and transverse directions in the plane of the wall. The minimum reinforcement ratio shall be 0.0025 of the gross area in each direction. This reinforcement shall be distributed uniformly across the cross section of the wall.*

Possible Explanations:

- The uniform distribution requirement of the shear reinforcement is related to the intent to control the width of inclined cracks

9.1.5 If the factored shear stress in the wall exceeds $0.25\sqrt{f_{ck}}$ or if the wall thickness exceeds 200 mm, reinforcement shall be provided in two curtains, each having bars running in the longitudinal and transverse directions in the plane of the wall.

Possible Explanations:

- The use of two curtains of reinforcement will reduce fragmentation and premature deterioration of the concrete under cyclic loading into the inelastic range
- The requirement of two layers of reinforcement in walls carrying substantial design shears is based on the observation that under ordinary construction conditions, the probability of maintaining a single layer of reinforcement near middle of the wall section is quite low. Furthermore, presence of reinforcement close to the surface tends to inhibit fragmentation of the concrete in the event of severe cracking during an earthquake

9.1.6 The diameter of the bars to be used in any part of the wall shall not exceed $1/10^{th}$ of the thickness of that part.

Possible Explanations:

- This is to prevent the use of very large diameter bars in thin wall sections
- The maximum diameter of bars is restricted to avoid the use of large bars in thin walls

9.1.7 The maximum spacing of reinforcement in either direction shall not exceed the smaller of $l_w/5$, $3t_w$, and 450 mm, where l_w is the horizontal length of the wall, and t_w is the thickness of the wall web

Possible Explanation:

- This limitation has been guided by the experience and various tests to confine the concrete

9.2 Shear Strength

9.2.1 The nominal shear stress τ_v , shall be calculated as: $\tau_v = \frac{V_u}{t_w d_w}$

where, V_u = factored shear force, t_w = thickness of the web, and d_w = effective depth of wall section. This may be taken as 0.8 l_w for rectangular sections.

Possible Explanation:

- The nominal shear strength of the section is computed with the nominal shear strength provided by concrete and shear reinforcement

9.2.2 The design shear strength of concrete τ_c shall be calculated as per **Table 13 of IS 456: 1978**.

Possible Explanation:

- The shear carried by the concrete is affected primarily by the concrete tensile strength and the ratio of the longitudinal steel

9.2.3 The nominal shear stress in the wall τ_v shall not exceed $\tau_{c,max}$ as per **Table 14 of IS 456: 1978**.

9.2.4 When τ_v is less than τ_c shear reinforcement shall be provided in accordance with 9.1.4, 9.1.5 and 9.1.7.

9.2.5 When τ_v is greater than τ_c , the area of horizontal shear reinforcement, A_h , to be provided within a vertical spacing, S_v , is given by

$$V_{us} = \frac{0.87 f_y A_h d_w}{S_v}$$

where, $V_{us} = (V_u - \tau_c t_w d_w)$, is the shear force to be resisted by the horizontal reinforcement. However, the amount of horizontal reinforcement provided shall not be less than the minimum as per 9.1.4.

Possible Explanation:

- Research has shown that shear behaviour of wide beams with substantial flexural reinforcement is improved if the transverse spacing of stirrup legs across the section is reduced

9.2.6 The vertical reinforcement that is uniformly distributed in the wall shall not be less than the horizontal reinforcement calculated as per 9.2.5.

Possible Explanation:

- Uniform distribution of the reinforcement across the height and width of the wall helps control the width of inclined cracks

9.3 Flexural strength

9.3.1 The moment of resistance, M_{uv} , of the wall section may be calculated as for columns subjected to combined bending and axial load as per IS 456 1978. The moment of resistance of slender rectangular shear wall section with uniformly distributed vertical reinforcement is given in Annex A.

Possible Explanations:

- These equations were derived assuming a rectangular wall section of depth l_w and thickness t_w that is subjected to combine uniaxial bending and axial compression
- Two equations are given for calculating the flexure strength of the section. Their use depends on whether the section fails in flexure tension or in flexure compression (Medhekar and Jain, 1993)

9.3.2 The cracked flexural strength of the wall section should be greater than its uncracked flexural strength.

Possible Explanations:

- Applicable to those wall sections which, for architectural or other reasons, are much larger in cross section than required from strength consideration alone
- To prevent a brittle failure involving sudden fracture of the tension reinforcement

9.3.3 In walls that do not have boundary elements, vertical reinforcement shall be concentrated at the end of the wall. Each concentration shall consist of a minimum of 4 bars of 12 mm diameter arranged in at least 2 layers.

Possible Explanation:

- Concentrated vertical reinforcement near the edges of the wall is more effective in resisting bending moment

9.4 Boundary Element

Boundary elements are portions along the wall edges that are strengthened by longitudinal and transverse reinforcement. Though they may have the same thickness as that of the wall web, it is advantageous to provide them with greater thickness.

Possible Explanations:

- To consider the factor of safety as these boundary element carry all the vertical forces at the critical wall section, when the maximum horizontal earthquake force act on the wall
- Wall sections having stiff and well confined boundary elements which develop substantial flexural strength, are less susceptible to lateral buckling, and have better shear strength and ductility in comparison to plane rectangular walls not having stiff and well confined boundary elements

9.4.1 Where the extreme fibre compressive stress in the wall due to factored gravity loads plus factored earthquake force exceeds $0.2f_{ck}$, boundary elements shall be provided along the vertical boundary of walls. The boundary elements may be discontinued where the calculated compressive stress becomes less than $0.15f_{ck}$. The compressive stress shall be calculated using a linearly elastic model and gross section properties.

Possible Explanation:

- During severe earthquake, the flanges of a wall are subjected to high compressive and tensile stress reversals. Hence, the concrete needs to be well confined so as to sustain the load reversals without a large degradation in strength

9.4.2 A boundary element shall have adequate axial load carrying capacity, assuming short column action, so as to enable it to carry an axial compression equal to the sum of factored gravity load on it and the additional compressive load induced by the seismic force. The latter may be calculated as: $\frac{(M_u - M_{uv})}{C_w}$

where, M_u = factored design moment on the entire wall section. M_{uv} = moment of resistance provided by distributed vertical reinforcement across the wall section. C_w = center to center distance between the boundary elements along the two vertical edges of the wall.

Possible Explanation:

- The boundary element is assumed to be effective in resisting the design moment due to earthquake induced forces along with the web of the wall. The axial compression

that is required to be developed in the boundary element for this purpose, is given by $\frac{(M_u - M_{uv})}{C_w}$. Thus, the boundary element should be designed as a short column for an axial load equal to the sum of the above axial compression and the gravity load on it

9.4.3 If the gravity load adds to the strength of the wall, its load factor shall be taken as 0.8.

Possible Explanation:

- Moderate axial compression results in higher moment capacity of the wall. Hence, the beneficial effect of axial compression by gravity loads should not be fully relied upon in design due to the possible reduction in its magnitudes by vertical accelerations

9.4.4 The percentage of vertical reinforcement in the boundary elements shall not be less than 0.8 per cent, nor greater than 6 per cent. In order to avoid congestion, the practical upper limit would be 4 per cent.

9.4.5 Boundary elements, where required, as per 9.4.1 shall be provided throughout their height, with special confining reinforcement, as per 7.4

9.4.6 Boundary elements need not be provided, if the entire wall section is provided, with special confining reinforcement as per 7.4.

Possible Explanation:

- The load reversals impose severe demand compression on the concrete in boundary element hence the confining reinforcement shall be required

9.5 Coupled Shear Walls

9.5.1 Coupled shear walls shall be connected by ductile coupling beams. If the earthquake induced shear stress in the coupling beam exceeds: $\frac{0.1l_s \sqrt{f_{ck}}}{D}$, where l_s is the clear span of the coupling beam and D is its overall depth, the entire earthquake induced shear and flexure shall, preferably, be resisted by diagonal reinforcement

Possible Explanation:

- Coupled shearwall of limited ductility shall be connected by ductile coupling beams. Coupling beams must have large ductility as they are subjected to extensive inelastic deformations at their ends. In such coupling beams the entire earthquake induced shear and flexure shall be resisted by diagonal reinforcement unless the earthquake

$$\text{induced shear stress is less than } \frac{0.1l_s \sqrt{f_{ck}}}{D}$$

9.5.2 The area of reinforcement to be provided along each diagonal in a diagonally reinforced coupling beam shall be: $A_{sd} = \frac{V_u}{1.74 f_y \sin \alpha}$, where, V_u is the factored shear force, and α

is the angle made by the diagonal reinforcement with the horizontal. At least 4 bars of 8 mm diameter shall be provided along each diagonal. The reinforcement along each diagonal shall be enclosed by special confining reinforcement, as per 7.4. The pitch of spiral or spacing of ties shall not exceed 100 mm.

Possible Explanation:

- The design of a diagonally reinforced coupling beam is based on the assumption that the shear force resolves itself into diagonal compression and tension force, these forces intersect each other at midspan where no moment is to be resisted. Thus, the shear force will be equal to $(2T_u \sin\alpha)$, where $T_u = 0.87 f_y A_{sd}$. The diagonal bars that are in compression need to be restrained against buckling. Hence, special confining reinforcement has to be provided all along their length

9.5.3 *The diagonal or horizontal bars of a coupling beam shall be anchored in the adjacent walls with an anchorage in the adjacent walls with an anchorage length of 1.5 times the development length in tension*

Possible Explanation:

- This increase in development length is to consider the adverse effect of reversed cyclic loading on the anchorage of a group of bars

9.6 *Openings in Walls*

9.6.1 *The shear strength of a wall with openings should be checked along critical planes that pass through openings.*

Possible Explanation:

- An opening in a shear wall causes high shear stresses in the region of the wall adjacent to it. Hence, it is necessary to check such regions for adequacy of horizontal shear reinforcement in order to prevent diagonal tension failure due to shear

9.6.2 *Reinforcement shall be provided along the edges of openings in walls. The area of the vertical and horizontal bars should be such as it is equal to that of the respective interrupted bars. The vertical bars should extend for the full storey height. The horizontal bars should be provided with development length in tension beyond the sides of the opening.*

Possible Explanation:

- Reinforcement shall prevent crack propagation

9.7 *Discontinuous Walls*

Columns supporting discontinuous walls shall be provided with special confining reinforcement as per 7.4.4.

Possible Explanation:

- Column supporting discontinued shear walls may be subjected to significant axial compression and may have to undergo extensive inelastic deformations. Hence they need to be adequately confined over their full height to ensure good ductility

9.8 Construction Joints

The vertical reinforcement ratio across a horizontal construction joint shall not be less than, $\frac{0.92}{f_y} \left(\tau_v - \frac{P_u}{A_g} \right)$ where, τ_v is the factored shear stress at the joint, P_u is the factored axial force (positive for compression), and A_g is the gross cross sectional area of the joint.

Possible Explanation:

- The design shear force at the joint must be less than the shear force that can be safely transferred across the joint, V_j . The calculated shear friction concept is given by $V_j = \mu(0.8P_u + 0.87f_y A_v)$, where, μ is the coefficient of friction at the joint ($\mu = 1.0$), and A_v is the area of vertical reinforcement available. To account for the possible effects of vertical acceleration, the axial load is taken as $0.8P_u$ instead of P_u itself

9.9 Development, Splice and Anchorage Requirement

9.9.1 Horizontal reinforcement shall be anchored near the edges of the wall or in the confined core of the boundary elements.

Possible Explanations:

- Horizontal reinforcement acts as web reinforcement for resisting the shear force. Hence it should be well anchored
- The capacity of the beam is developed by embedment in the column and within the compression zone of the beam on the far side of the connection

9.9.2 Splicing of vertical flexural reinforcement should be avoided, as far as possible, in regions where yielding may take place. This zone of flexural yielding may be considered to extend for a distance of l_w above the base of the wall or one sixth of the wall height, whichever is more. However, this distance need not be greater than $2l_w$. Not more than one third of this vertical reinforcement shall be spliced at such a section. Splices in adjacent bars should be staggered by a minimum of 600 mm.

9.9.3 Lateral ties shall be provided around lapped spliced bars that are larger than 16 mm in diameter. The diameter of the tie shall not be less than one fourth of the spliced bar nor less than 6 mm. The spacing of ties shall not exceed 150 mm center to centre.

Possible Explanation:

- The splicing is not allowed in regions of potential plastic hinging since such splices are not considered to be reliable under reversed inelastic cycles of deformation unless each spliced bar is confined by stirrup ties

9.9.4 Welded splices and mechanical connections shall confirm to 25.2.5.2 of IS 456:1978. However, not more than half the reinforcement shall be spliced at a section, where flexural yielding may take place.

Possible Explanation:

- The location of welding splices is restricted because tensile stresses in reinforcement in yielding regions cannot exceed the strength requirement

SUMMARY

Ductility is one of the main attributes for earthquake resistant design of structures. To make reinforced concrete structures sufficiently ductile, various provisions are stipulated in the code IS 13920: 1993 entitled “*Ductile Detailing of Reinforced Concrete Structures Subjected to Seismic Forces*”. These provisions are related to the anchorage and splices of longitudinal reinforcement, spacing, anchorage, and splicing of lateral reinforcement, special confining reinforcement at the potential plastic hinge region, minimum size requirements for flexural, axial member etc. The ductile detailing requirement in shear wall is also discussed. The chapter deals with the importance of ductility and a clause - by - clause explanation of IS 13920: 1993 so that one can understand and appreciate its importance.

REFERENCES

- [1] ACI 318M–99/318RM–99, “Building Code Requirements for Structural Concrete (318M-99) and Commentary (318RM-99)”, American Concrete Institute, Farmington Hills, Michigan.
- [2] Bertero, V.V., Anderson, J.C., Krawinkler, H., Miranda, E., et al., “Design Guidelines for Ductility and Drift Limits”, *Report No. UCB/EERC-91/15*, Earthquake Engineering Research Center, University of California, 1991.
- [3] Bertero, V.V., “Implication of Recent Earthquakes and Research on Earthquake Resistant Design and Construction of Buildings”, *Report No. UCB/EERC-86/03*, Earthquake Engineering Research Center, University of California, 1986.
- [4] Eurocode 8, “Design of Structures for Earthquake Resistance—Part 1: General Rules, Seismic Actions and Rules for Buildings”, *CEN*, (2002).
- [5] Englekirk, R.E., *Seismic Design of Reinforced and Precast Concrete Buildings*, John Wiley & Sons, 2003.
- [6] IS 13920, “Ductile Detailing of Reinforced Concrete Structures Subjected to Seismic Forces”, Edition 1.2, Bureau of Indian Standards, New Delhi, 2002-03.
- [7] Machida, A., Moehle, J., Pinto, P. and Matsumoto, N., “Ductility Consideration for Single Element and for Frame Structures”, *Proceedings of Comparative Performance of Seismic Design Codes for Concrete Structures*, Vol. 1, T. Tanabe (Ed.), Elsevier Science, 1999.
- [8] Machida, A., Moehle, J., Pinto, P., Park, R. and Niwa, J., “Detailing Consideration”, *Proceedings of Comparative Performance of Seismic Design Codes for Concrete Structures*, Vol. 1, T. Tanabe (Ed.), Elsevier Science, 1999.
- [9] Medhekar, M.S. and Jain, S.K., “Seismic Behaviour Design and Detailing of RC Shear Walls, Part 1: Behaviour and Strength”, *Indian Concrete Journal*, Vol. 67, No. 7, pp. 311–318, 1993.
- [10] Medhekar, M.S. and Jain, S.K., “Seismic Behaviour Design and Detailing of RC Shear Walls, Part II: Design and Detailing”, *Indian Concrete Journal*, Vol. 67, No. 9, pp. 451–457, 1993.

- [11] Naeim, Farzad, *The Seismic Design Handbook*, 2nd ed. Kluwer Academic Publisher, The Netherlands, 2001.
- [12] NZS 3101, *Concrete Structures Standard Part 1—The Design of Concrete Structures*, Standards New Zealand, Paerewa Aotearoa, 1995.

Chapter 21

Earthquake Resistant Design of a Four-storey RC Building Based on IS 13920: 1993

21.1 INTRODUCTION

In this chapter, a detailed design of a four-storeyed office building having a regular layout, which can be divided into a number of similar vertical frames, has been considered to illustrate the analysis and design of a frame. Only one frame in transverse direction has been considered for analysis and design. A standard computer program on a personnel computer has been carried out for the analysis. The design is carried out according to IS 13920: 1993 following the IS 456: 2000 and SP 16: 1980. The detailing of reinforcement at level 2 in the frame considered has been presented.

21.2 PRELIMINARY DATA FOR EXAMPLE FRAME

The floor plan of a typical public-cum-office building is shown in Figure 21.1. The plan is regular in nature in the sense that it has all columns equally placed. Thus, entire building space frame can be divided into a number of vertical frames. An interior frame 4-4 as shown in Figure 21.2 is considered for analysis and design. Following are some of the salient features of the frame

- | | |
|--------------------------|--------------------------------------|
| 1. Type of structure | Multi-storey rigid jointed frame |
| 2. Zone | IV |
| 3. Layout | As shown in Figure 21.1 |
| 4. Number of stories | Four (G + 3) as shown in Figure 21.2 |
| 5. Ground storey height | 4.0 m |
| 6. Floor-to-floor height | 3.35 m |

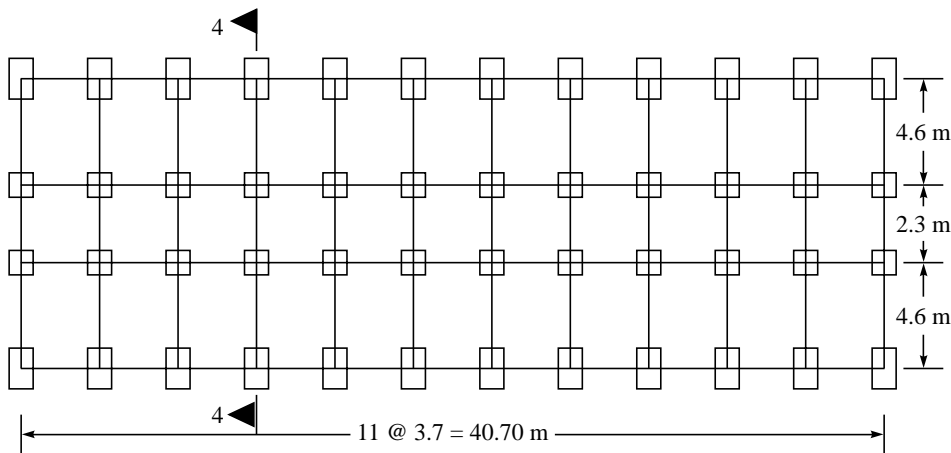


FIGURE 21.1 Typical plan of the building.

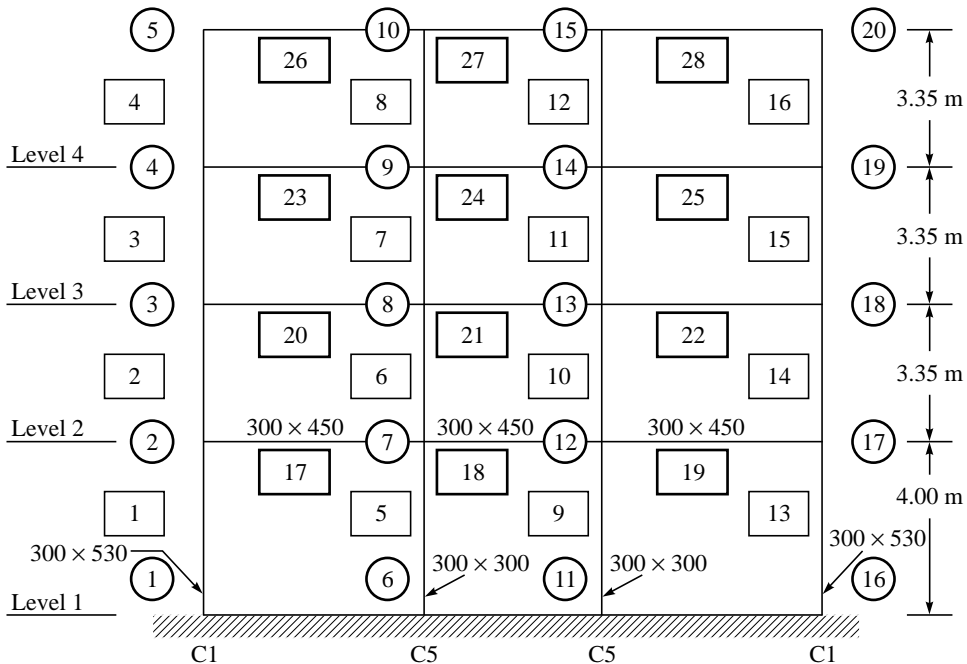


FIGURE 21.2 Detail of frame 4-4.

- | | |
|-----------------------|---|
| 7. External walls | 250 mm thick including plaster |
| 8. Internal walls | 150 mm thick including plaster |
| 9. Live load | 3.5 kN/m^2 |
| 10. Materials | M 20 and Fe 415 |
| 11. Seismic analysis | Equivalent static method (IS 1893 (Part 1): 2002) |
| 12. Design philosophy | Limit state method conforming to IS 456: 1978 |
| 13. Ductility design | IS 13920: 1993 |

14. Size of exterior column	300×500 mm
15. Size of interior column	300×300 mm
16. Size of beams in longitudinal and transverse direction	300×450 mm
17. Depth of slab	120 mm

21.3 LOADING DATA

Dead Load (DL)

Terrace water proofing (TWF) = 1.5 kN/m²
Floor Finish (FF) = 0.5 kN/m²

Weight of slab

$25 D$ kN/m², where D is total depth of slab

(Assume total depth of slab = 120 mm)

Weight of walls

External walls (250 mm thick)
= 5 kN/m/meter height (20 @ 0.25)
Internal walls 150 mm thick
= 3 kN/m/meter height (20 @ 0.15)

Live Load (LL)

Roof = 1.5 kN/m²
Live load on floor
= 3.5 kN/m²

Earthquake Load (EQ)

$$\alpha_h = (Z/2) (S_a/g)(I/R)$$

$$Z = 0.24 \text{ (Zone IV)}$$

$$S_a/g = 2.5^*, I = 1.0,$$

$$R = 5.0 \text{ (SMRF)}$$

$$\alpha_h = (0.24/2) \times (2.5) \times (1.0/5.0) = 0.06$$

$$T = 0.09 h/\sqrt{d}$$

$$= 0.09 (14.05)/\sqrt{11.50}$$

$$= 0.372$$

For $T = 0.372$
 $S_a/g = 2.5^*$ (from IS
1893 (Part 1): 2002)

21.4 ANALYSIS OF SUB-FRAME 4-4

21.4.1 Dead Load Analysis

DL at roof level

Weight of slab
= $25 D = 25 \times 0.12 = 3.0$ kN/m²
Weight of finishes = F.F + T.W.F.
= $0.5 + 1.5 = 2.0$ kN/m²
Total weight = 5.0 kN/m²

Total weight on beam C1-C5

Tributary floor area on beam C1-C5
= $0.5 \times (0.9 + 4.6) \times 1.85 \times 2 = 10.175$ m²
Slab weight on beam C1-C5
= $5 \times 10.175 = 50.875$ kN
Weight on beam C1-C5 per meter
= $50.875/4.6 = 11.05$ kN/m
Self-weight of beam
= $25 \times 0.30 \times (0.45 - 0.10) = 2.625$ kN/m

DL at floor level

Weight of slab
= $25 D = 25 \times 0.12 = 3.0$ kN/m²
Weight of finishes (F.F) = 0.5 kN/m²
Total weight = 3.5 kN/m²

Total weight on beam C1-C5

Tributary floor area on beam C1-C5
= $0.5 \times (0.9 + 4.6) \times 1.85 \times 2 = 10.175$ m²
Slab weight on beam C1-C5
= $3.5 \times 10.175 = 35.62$ kN
Weight on beam C1-C5 per meter
= $35.62/4.6 = 7.74$ kN/m
Self-weight of beam
= $25 \times 0.30 \times (0.45 - 0.10) = 2.625$ kN/m

Total weight on beam C1-C5

$$= 11.05 + 2.625 = 13.684 \text{ kN/m}$$

Total weight on beam C5-C5

Tributary floor area on beam C5-C5

$$= 0.5 \times 2.3 \times 1.15 \times 2 = 2.645 \text{ m}^2$$

Total weight on beam C5-C5

$$= 5 \times 2.645 = 13.225 \text{ kN}$$

Weight on beam C5-C5

$$= 13.225/2.3 = 5.75 \text{ kN/m}$$

Self-weight of beam

$$= 25 \times 0.30 \times (0.45 - 0.10) = 2.625 \text{ kN/m}$$

Total weight on beam C5-C5

$$= 5.75 + 2.625 = 8.375 \text{ kN/m}$$

Weight of walls

$$= 20 \times 0.15 \times (3.35 - 0.45) = 14.50 \text{ kN/m}$$

Total weight on beam C1-C5

$$= 7.74 + 14.50 + 2.625 = 24.86 \text{ kN/m}$$

Total weight on beam C5-C5

Tributary floor area on beam C5-C5

$$= 0.5 \times 2.3 \times 1.15 \times 2 = 2.645 \text{ m}^2$$

Total weight on beam C5-C5

$$= 3.5 \times 2.645 = 9.2575 \text{ kN}$$

Weight on beam C5-C5

$$= 9.2575/2.3 = 4.025 \text{ kN/m}$$

Self-weight of beam

$$= 25 \times 0.30 \times (0.45 - 0.10) = 2.625 \text{ kN/m}$$

Weight of walls

$$= 20 \times 0.15 \times (3.35 - 0.45) = 14.50 \text{ kN/m}$$

Total weight on beam C5-C5

$$= 4.025 + 2.625 + 14.50 = 21.15 \text{ kN/m}$$

The dead loads on various beams and columns in the frame are shown in Figure 21.3.

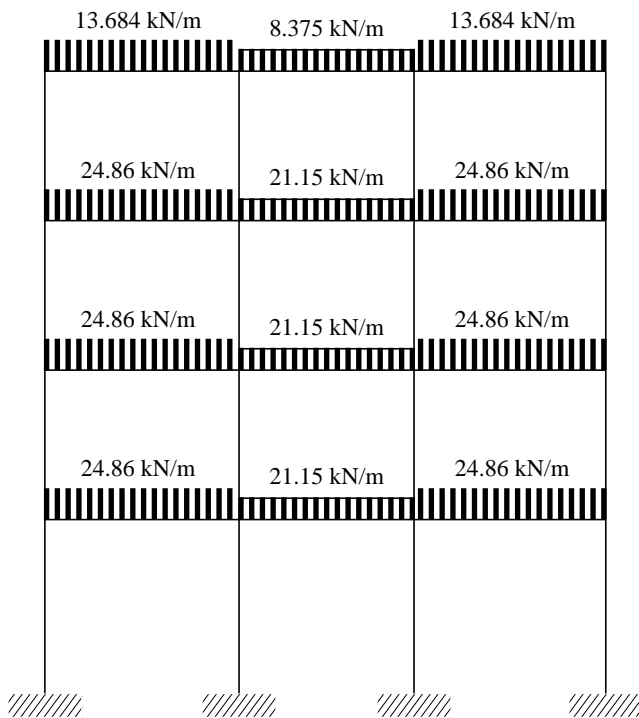


FIGURE 21.3 Dead Load on Frame 4-4 (kN/m).

21.4.2 Live (Imposed) Load Analysis

LL at roof level

Weight of live load = 1.5 kN/m²

Total weight on beam C1-C5

$$\begin{aligned} \text{Tributary floor area on beam C1-C5} \\ = 0.5 \times (0.9 + 4.6) \times 1.85 \times 2 = 10.175 \text{ m}^2 \end{aligned}$$

Total weight on beam C1-C5

$$= 1.5 \times 10.175 = 15.265 \text{ kN}$$

Total weight on beam C1-C5

$$= 15.265/4.6 = 3.32 \text{ kN/m}$$

Total weight on beam C5-C5

Tributary floor area on beam C5-C5

$$= 0.5 \times 2.3 \times 1.15 \times 2 = 2.645 \text{ m}^2$$

Total weight on beam C5-C5

$$= 1.5 \times 2.645 = 3.9675 \text{ kN}$$

Total weight on beam C5-C5

$$= 3.9675/2.3 = 1.725 \text{ kN/m}$$

LL at floor level

Weight of live load = 3.5 kN/m²

Total weight on beam C1-C5

$$\begin{aligned} \text{Tributary floor area on beam C1-C5} \\ = 0.5 \times (0.9 + 4.6) \times 1.85 \times 2 = 10.175 \text{ m}^2 \end{aligned}$$

Total weight on beam C1-C5

$$= 3.5 \times 10.175 = 35.62 \text{ kN}$$

Total weight on beam C1-C5

$$= 35.62/4.6 = 7.74 \text{ kN/m}$$

Total weight on beam C5-C5

Tributary floor area on beam C5-C5

$$= 0.5 \times 2.3 \times 1.15 \times 2 = 2.645 \text{ m}^2$$

Total weight on beam C5-C5

$$= 3.5 \times 2.645 = 9.2575 \text{ kN}$$

Total weight on beam C5-C5

$$= 9.2575/2.3 = 4.025 \text{ kN/m}$$

The live loads on various beams and columns in the frame are shown in Figure 21.4.

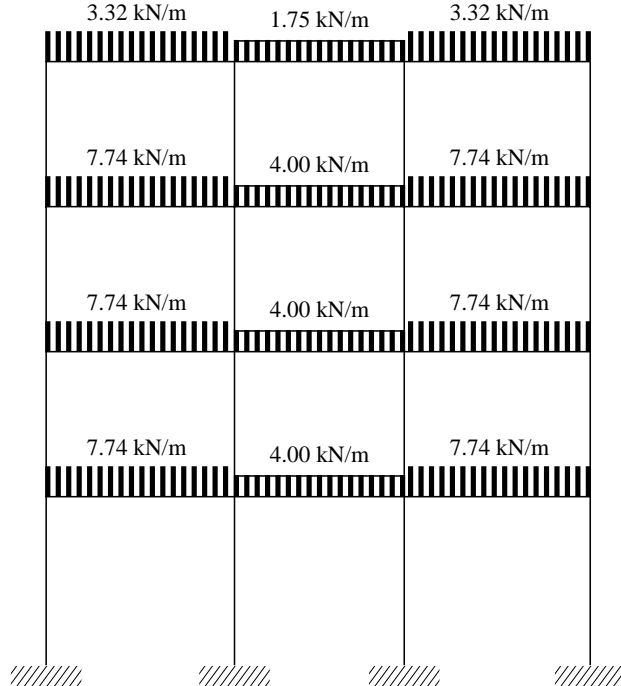


FIGURE 21.4 Live Load on Frame 4-4 (kN/m).

21.4.3 Earthquake Load Analysis

Determination of total base shear

Dead load

- (a) Weight of floor i.e. ($W_s + FF$)
 $= 40.70 \times 11.50 \times (3.0 + 0.5) = 1638.175 \text{ kN}$
- (b) Weight of roof i.e. ($W_s + TWF + FF$)
 $= 40.70 \times 11.50 \times (3.0 + 1.5 + 0.5)$
 $= 2340.25 \text{ kN}$
- (c) Weight of peripheral beams (Transverse)
 $= \{2(4.6 - 0.45/2 - 0.3/2) \times 2.625\} \times 2 +$
 $\{1(2.3 - 0.30/2 - 0.3/2) \times 2.625\} \times 2 = 54.86 \text{ kN}$
- (d) Weight of peripheral beams (Longitudinal)
 $= \{11(3.7 - 0.30/2 - 0.3/2) \times 2.625\} \times 2$
 $= 196.35 \text{ kN}$
- (e) Weight of parapet wall (1.0 m height,
150 mm thick)
 $= 2 \times (40.70 + 11.50) \times 1.0 \times 3 = 313.20 \text{ kN}$
- (f) Weight of external wall (thickness
of wall 250 mm)
 $= 20 \times 0.25 \times (20.9 + 74.8) \times (3.35 - 0.45)$
 $= 1387.65 \text{ kN}$
- (g) Interior beams (Transverse)
 $= \{(2 \times 4.225 + 2.0) \times 2.625\} \times 11$
 $= 274.32 \text{ kN}$
- (h) Interior beams (Longitudinal)
 $= \{(3.7 - 0.3) \times 2.625 \times 11\} \times 2 = 196.35 \text{ kN}$
- (i) Weight of interior wall (thickness = 150 mm),
Length (Transverse)
 $= \{(4.6 - 0.45/2 - 0.3/2) \times 2 + (2.3 - 0.3)\} \times 10$
 $= 104.5 \text{ m}$
Length (Longitudinal)
 $= \{(3.7 - 0.3) \times 11 \times 2\} = 74.8 \text{ m}$
Height = $3.35 - 0.45 = 2.90 \text{ m}$
Weight = $20 \times 0.15 \times (104.5 + 74.8) \times 2.90$
 $= 1559.91 \text{ kN}$
- (j) Weight of exterior column/height
 $= 2 \times 12 \times 0.30 \times 0.45 \times 25 = 81 \text{ kN/m}$
- (k) Weight of interior column/height
 $= 2 \times 12 \times 0.30 \times 0.30 \times 25 = 54 \text{ kN/m}$

Live load

- Live load on roof = Zero
- Live load on floors
 $= 50\% \text{ of } 3.5 \text{ kN/m}^2 = 1.75 \text{ kN/m}^2$
- Total live load on each floor
 $= 40.70 \times 11.50 \times 1.75 = 819.08 \text{ kN}$

Concentrated mass

- At roof = $(b + c + d + e + f/2 + g + h + i/2 + j \times 3.35/2 + k \times 3.35/2) + 0.0$
 $= 5074.98 \text{ kN}$

At 2nd and 3rd floor =
 $(a + c + d + f + g + h + i + (j + k) 3.35) + 819.08 = 6578.95 \text{ kN}$

At 1st floor = $(a + c + d + f + g + h + i + (j + k) (3.35 + 4.0) 0.5) + 819.08$
 $= 6622.80 \text{ kN}$

Total weight = $5074.98 + 2 \times 6578.95 + 6622.80 = 24855.69 \text{ kN}$

Total base shear

$$\begin{aligned} &= \alpha_h \times W = 0.6 \times 24855.69 \\ &= 1491.34 \text{ kN} \end{aligned}$$

Base shear in each frame

$$= 1491.34/12 = 125 \text{ kN}$$

Determination of Design Lateral Loads at Each Floor

Level	W_i (MN)	h_i (meter)	$W_i h_i^2$	$W_i h_i^2 / \sum W_i h_i^2$	Q_i (kN)
(1)	(2)	(3)	(4)	(5)	(6)
Roof (Level 5)	5.074	14.05	1001.62	0.452	56.50
Third Floor (Level 4)	6.578	10.70	753.16	0.34	42.50
Second Floor (Level 3)	6.578	7.35	355.36	0.16	20.00
First Floor (Level 2)	6.622	4.00	105.95	0.048	6.00
Ground floor (Level 1)	—	0.00			
			$\Sigma = 2216.04$	$\Sigma = 1.0$	$\Sigma = 125$

The seismic loads (sway to left) and (sway to right) on the considered frame are shown in Figures 21.5 and 21.6 respectively.

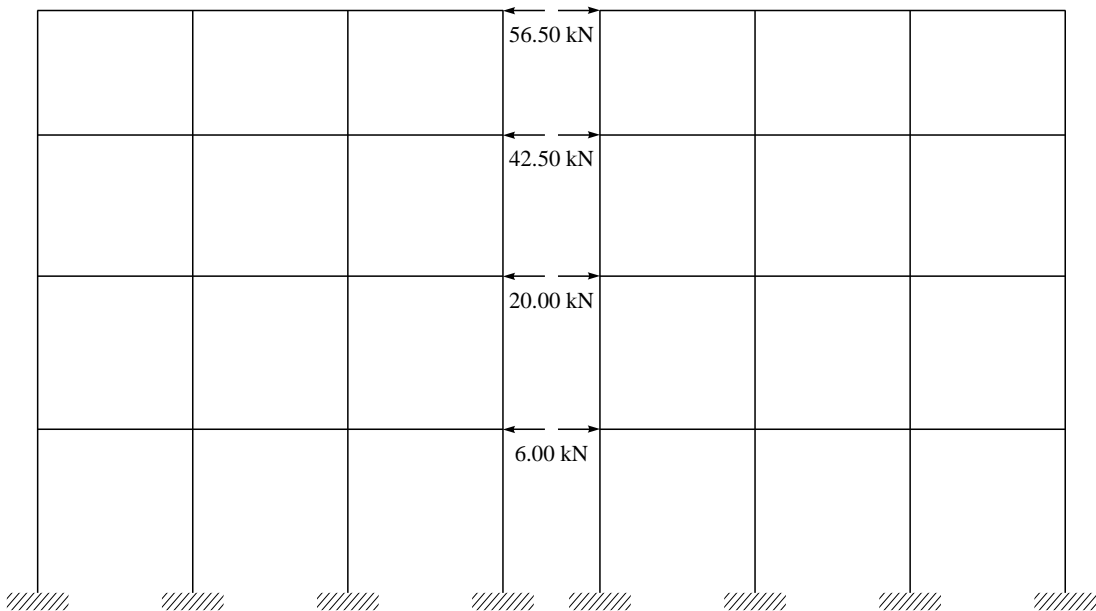


FIGURE 21.5 Equivalent static lateral load (sway to left) on Frame 4-4 in kN.

Figure 21.6 Equivalent static lateral load (sway to right) on Frame 4-4 in kN.

21.5 LOAD COMBINATIONS

The analysis has been carried out for Dead Load (DL), Live Load or Imposed Load (IL) and Earthquake Load (EL) in both the directions i.e. sway to left (+EL) and sway to right (-EL) by a standard computer program. The combination of the above cases has been made according to Clause 6.3 of IS 1893 (Part 1): 2002 as given in Table 21.1. The member forces for the above load combinations are given in Table 21.2.

TABLE 21.1 Load combinations

<i>Load case</i>	<i>Details of load cases</i>
1	1.5 (DL + IL)
2	1.2 (DL + IL + EL)
3	1.2 (DL + IL - EL)
4	1.5 (DL + EL)
5	1.5 (DL - EL)
6	0.9 DL + 1.5 EL
7	0.9 DL - 1.5 EL

TABLE 21.2 Results of analysis under various load combinations

<i>Member no.</i>	<i>Node no.</i>	<i>Forces</i>	<i>Load case 1</i>	<i>Load case 2</i>	<i>Load case 3</i>	<i>Load case 4</i>	<i>Load case 5</i>	<i>Load case 6</i>	<i>Load case 7</i>
1	1	Axial Shear Moment	425.40 -12.89 -17.45	221.8 44.16 138.2	458.3 -64.74 -165.9	180.1 58.26 176.8	475.6 -77.88 -203.3	48.70 62.19 182.2	344.3 -73.94 -197.9
	2	Axial Shear Moment	-425.4 +12.89 -34.10	-221.8 -44.16 38.49	-458.3 64.74 -93.07	-180.1 -58.26 56.19	-475.6 77.88 -108.2	-48.70 -62.19 66.61	-344.3 73.94 -97.84
	2	Axial Shear Moment	+306.7 -30.59 -53.61	168.1 12.53 13.29	322.1 -61.40 -98.82	141.1 22.85 29.26	333.6 -69.56 -110.9	45.93 32.25 45.69	238.4 -60.17 -94.45
2	3	Axial Shear Moment	-306.7 +30.59 -48.87	-168.1 -12.53 28.69	-322.1 61.4 -106.9	-141.1 -22.85 47.28	-333.6 69.56 -122.2	-45.93 -32.25 62.34	-238.4 60.17 -107.1
	3	Axial Shear Moment	+185.50 -28.63 -47.18	108.7 8.92 3.378	187.9 -54.45 -78.40	95.56 17.99 15.35	194.5 -61.23 -86.88	37.36 26.76 29.87	136.3 -52.45 -72.35
3	4	Axial Shear Moment	-185.50 +28.63 -48.74	-108.7 -8.92 26.49	-187.9 54.45 -104.0	-95.56 -17.99 44.90	-194.5 61.23 -118.2	-37.36 -26.76 59.78	-136.3 52.45 -103.4
	4	Axial Shear Moment	+63.51 -29.51 -48.97	37.74 -7.73 -26.67	63.71 -39.38 -51.65	35.70 -3.65 -22.57	68.16 -43.21 -53.80	14.83 5.86 -7.13	47.30 -33.70 -38.37
4	5	Axial Shear Moment	-63.51 +29.51 -49.88	-37.74 7.73 0.76	-63.71 39.38 -80.27	-35.70 3.65 10.33	-68.16 43.21 -90.96	-14.83 -5.86 26.77	-47.30 33.70 -74.52
	6	Axial Shear Moment	+512.20 +2.82 +3.75	428.8 22.81 44.85	390.7 -18.29 -38.83	428.9 27.77 55.08	381.3 -23.6 -49.53	258.9 26.99 54.03	211.2 -24.38 -50.57
5	7	Axial Shear Moment	-512.2 -2.82 +7.52	-428.8 -22.81 46.38	-390.7 18.29 -34.32	-428.9 -27.77 56.00	-381.3 23.6 -44.88	-258.9 -26.99 53.91	-211.2 24.38 -46.97

Contd.

TABLE 21.2 Contd.

Member no.	Node no.	Forces	Load case 1	Load case 2	Load case 3	Load case 4	Load case 5	Load case 6	Load case 7
6	7	Axial	+362.6	294.4	285.7	293.0	282.1	172.4	161.5
		Shear	+7.24	40.25	-28.62	48.39	-37.70	46.40	-39.69
		Moment	+12.60	68.1	-47.86	81.79	-63.15	78.32	-66.63
7	8	Axial	-362.6	-294.4	-285.7	-293.0	-282.1	-172.4	-161.5
		Shear	-7.24	-40.25	28.62	-48.39	37.70	-46.40	39.69
		Moment	+11.64	66.74	-48.02	80.32	-63.13	77.13	-66.32
8	8	Axial	+215.4	174.1	170.4	174.1	169.5	102.2	97.60
		Shear	+6.36	32.82	-22.60	39.29	-30.00	37.6	-31.69
		Moment	+10.64	54.69	-37.55	65.45	-49.85	62.6	-52.70
9	9	Axial	-215.4	-174.1	-170.4	-174.1	-169.5	-102.2	-97.60
		Shear	-6.36	-32.82	22.60	-39.29	30.00	-37.6	31.69
		Moment	+10.65	55.30	-38.14	66.17	-50.64	63.34	-53.46
10	9	Axial	+69.04	57.98	52.45	60.39	53.48	36.77	29.86
		Shear	+4.82	21.95	-14.20	26.30	-18.89	24.96	-20.23
		Moment	+8.97	36.79	-22.37	43.71	-30.24	41.27	-32.68
11	10	Axial	-69.04	-57.98	-52.45	-60.39	-53.48	-36.77	-29.86
		Shear	-4.82	-21.95	14.20	-26.30	18.89	-24.96	20.23
		Moment	+7.18	36.75	-25.20	44.39	-33.04	42.35	-35.08
12	11	Axial	+512.2	390.7	428.8	381.3	428.9	211.2	258.9
		Shear	-2.82	18.29	-22.81	23.60	-27.77	24.38	-26.99
		Moment	-3.75	38.83	-44.85	49.53	-55.08	50.57	-54.03
13	12	Axial	-512.2	-390.7	-428.8	-381.3	-428.9	-211.2	-258.9
		Shear	+2.82	-18.29	22.81	-23.60	27.77	-24.38	26.99
		Moment	-7.52	34.32	-46.38	44.80	-56.00	46.97	-53.91
14	12	Axial	+362.6	285.7	294.4	282.1	293.0	161.5	172.4
		Shear	-7.24	28.62	-40.25	37.70	-48.39	39.69	-46.40
		Moment	-12.6	47.86	-68.10	63.10	-81.79	66.63	-78.32
15	13	Axial	-362.6	-285.7	-294.4	-282.1	-293.0	-161.5	-172.4
		Shear	+7.24	-28.62	40.25	-37.70	48.39	-39.69	46.40
		Moment	-11.64	48.02	-66.74	63.13	-80.32	66.32	-77.13
16	13	Axial	+215.4	170.4	174.1	169.5	174.1	97.60	102.2
		Shear	-6.36	22.6	-32.83	30.00	-39.29	31.69	-37.6
		Moment	-10.64	37.55	-54.69	49.85	-65.45	52.70	-62.6
17	14	Axial	-215.4	-170.4	-174.1	-169.5	-174.1	-97.60	-102.2
		Shear	+6.36	-22.6	32.83	-30.00	39.29	-31.69	37.6
		Moment	-10.65	38.14	-55.30	50.64	-66.17	53.46	-63.34
18	14	Axial	+69.04	52.45	57.98	53.48	60.39	29.86	36.77
		Shear	-4.82	14.20	-21.95	18.89	-26.30	20.23	-24.96
		Moment	-8.97	22.37	-36.79	30.24	-43.70	32.68	-41.27
19	15	Axial	-69.04	-52.45	-57.98	-53.48	-60.39	-29.86	-36.77
		Shear	+4.82	-14.20	21.95	-18.89	26.30	-20.23	24.96
		Moment	-7.18	25.20	-36.75	33.04	-44.39	35.08	-42.35

Contd.

TABLE 21.2 Contd.

<i>Member no.</i>	<i>Node no.</i>	<i>Forces</i>	<i>Load case 1</i>	<i>Load case 2</i>	<i>Load case 3</i>	<i>Load case 4</i>	<i>Load case 5</i>	<i>Load case 6</i>	<i>Load case 7</i>
13	16	Axial Shear Moment	+425.4 +12.89 +17.45	458.3 64.74 165.9	221.8 -44.16 -138.2	475.6 77.88 203.3	180.1 -58.26 -176.8	344.3 73.94 197.9	48.70 -62.19 -182.2
	17	Axial Shear Moment	-425.4 -12.89 +34.10	-458.3 -64.74 93.07	-221.8 44.16 -38.49	-475.6 -77.88 108.2	-180.1 58.26 -56.19	-344.3 -73.94 97.84	-48.70 62.19 -66.61
14	17	Axial Shear Moment	+306.7 +30.59 +53.61	322.1 61.40 98.82	168.1 -12.53 -132.9	333.6 69.56 110.9	141.1 -22.85 -29.26	238.4 60.17 94.45	45.93 -32.25 -45.69
	18	Axial Shear Moment	-306.7 -30.59 +48.87	-322.1 -61.40 106.9	-168.1 12.53 -28.69	-333.6 -69.56 122.2	-141.1 22.85 -47.28	-238.4 -60.17 107.1	-45.93 32.25 -62.34
15	18	Axial Shear Moment	+185.5 +28.63 +47.18	187.9 54.45 78.40	108.7 -8.92 -3.37	194.5 61.23 86.88	95.56 -17.99 -15.35	136.3 52.45 72.35	37.36 -26.76 -29.87
	19	Axial Shear Moment	-185.5 -28.63 +48.74	-187.9 -54.45 104	-108.7 8.92 -26.49	-194.5 -61.23 118.2	-95.56 17.99 -44.90	-136.3 -52.45 103.4	-37.36 26.76 -59.78
16	19	Axial Shear Moment	+63.51 +29.51 +48.97	63.71 39.38 51.65	37.74 7.73 26.67	68.16 43.21 53.80	35.70 3.65 22.57	47.3 33.7 38.37	14.83 -5.86 7.13
	20	Axial Shear Moment	-63.51 -29.51 +49.88	-63.71 -39.38 80.27	-37.74 -7.73 -0.76	-68.16 -43.21 90.96	-35.70 -3.65 -10.33	-47.3 -33.7 74.52	-14.83 5.86 -26.77
17	2	Axial Shear Moment	-17.71 +118.7 +87.71	-24.43 53.73 -51.78	3.35 136.2 191.9	-26.41 38.94 -85.45	8.31 142.0 219.1	-20.95 2.76 -112.3	13.77 105.8 192.3
	7	Axial Shear Moment	+17.71 +106.2 -58.84	24.43 126.2 -114.9	-3.35 43.76 20.72	26.41 132.6 -130.0	-8.31 29.52 39.62	20.95 100.2 -111.7	-13.77 -2.92 57.86
18	7	Axial Shear Moment	-13.28 +43.42 +38.72	-6.985 8.14 0.46	-6.98 61.18 61.46	-5.78 3.34 -7.82	-5.78 69.63 68.41	-1.53 -13.69 -20.50	-1.53 52.61 55.74
	12	Axial Shear Moment	+13.28 +43.42 -38.72	6.985 61.18 -61.46	6.98 8.14 -46.41	5.78 69.6 -68.41	5.78 3.35 7.83	1.53 52.61 -55.74	1.53 -13.69 20.50
19	12	Axial Shear Moment	-17.71 +106.2 +58.84	3.35 43.76 -20.72	-24.43 126.2 114.9	8.31 29.52 -39.62	-26.41 132.6 130.0	13.77 -2.92 -57.86	-20.95 100.2 111.7
	17	Axial Shear Moment	+17.71 +118.7 -87.71	-3.35 136.2 -191.9	24.43 53.73 51.78	-8.31 142.0 -219.1	26.41 38.94 85.45	-13.77 105.8 -192.3	20.95 2.76 112.3

Contd.

TABLE 21.2 Contd.

<i>Member no.</i>	<i>Node no.</i>	<i>Forces</i>	<i>Load case 1</i>	<i>Load case 2</i>	<i>Load case 3</i>	<i>Load case 4</i>	<i>Load case 5</i>	<i>Load case 6</i>	<i>Load case 7</i>
20	3	Axial Shear Moment	+1.96 +121.1 +96.05	20.38 59.42 -32.07	6.94 134.2 185.3	25.14 45.56 -62.63	8.34 139.1 209.0	24.52 8.58 -92.2	7.72 102.1 179.5
	8	Axial Shear Moment	-1.96 +103.8 -56.31	-20.38 120.50 -108.5	-6.94 45.74 18.23	-25.14 126.0 -122.3	-8.34 32.47 36.11	-24.52 94.35 -105.1	-7.72 0.85 53.36
21	8	Axial Shear Moment	+1.08 +43.42 +34.02	12.97 -0.24 -12.92	12.97 69.56 67.35	16.04 -7.14 -23.46	16.04 80.11 76.88	15.71 -24.16 -34.67	15.71 63.08 65.66
	13	Axial Shear Moment	-1.08 +43.42 -34.02	-12.97 69.56 -67.35	-12.97 -0.23 12.92	-16.04 80.10 -76.8	-16.04 -7.14 23.46	-15.71 63.08 -65.66	-15.71 -24.16 34.67
22	13	Axial Shear Moment	+1.96 +103.8 +56.31	6.94 45.74 -18.23	20.38 120.5 108.5	8.34 32.47 -36.11	25.14 126.0 122.3	7.72 0.85 -53.36	24.52 94.35 105.1
	18	Axial Shear Moment	-1.96 +121.1 -96.05	-6.94 134.2 -18.53	-20.38 59.42 32.07	-8.34 139.1 -209.0	-25.14 45.56 62.63	-7.72 102.1 -179.5	-24.52 8.58 92.20
23	4	Axial Shear Moment	-0.88 +122.0 +97.71	34.35 70.95 0.18	15.07 124.2 155.7	42.10 59.86 -22.33	18.01 126.4 172.0	42.85 22.52 -52.65	18.75 89.04 141.7
	9	Axial Shear Moment	+0.88 +102.9 -53.70	-34.45 109.0 -87.70	-15.07 55.78 1.60	-42.10 111.7 -96.85	-18.01 45.16 14.78	-42.85 80.40 -80.48	-18.75 13.88 31.15
24	9	Axial Shear Moment	-2.41 +43.42 +34.08	23.47 7.14 -4.39	23.47 62.19 58.91	29.12 2.07 -13.03	29.12 70.89 66.11	30.22 -14.95 -24.14	30.22 53.86 55.00
	14	Axial Shear Moment	+2.41 +43.42 -34.08	-23.47 62.19 -58.91	-23.47 7.13 4.39	-29.12 70.89 -66.10	-29.12 2.07 13.03	-30.22 53.86 -55.00	-30.22 -14.95 24.14
25	14	Axial Shear Moment	-0.88 +102.9 +53.70	15.07 55.78 -1.60	34.35 109.00 87.70	18.01 45.16 -14.78	42.11 111.7 96.85	18.75 13.88 -31.15	42.85 80.40 80.48
	19	Axial Shear Moment	+0.88 +122.0 -97.71	-15.07 124.2 -155.7	-34.35 70.95 -0.18	-18.01 126.4 -172.0	-42.11 59.86 22.33	-18.75 89.04 -141.7	-42.85 22.52 52.65
26	5	Axial Shear Moment	+29.51 +63.51 +49.88	75.53 37.74 -0.76	39.38 63.71 80.27	88.40 35.70 -10.30	43.21 68.16 90.96	78.89 14.83 -26.77	33.70 47.30 74.52

Contd.

TABLE 21.2 Contd.

<i>Member no.</i>	<i>Node no.</i>	<i>Forces</i>	<i>Load case 1</i>	<i>Load case 2</i>	<i>Load case 3</i>	<i>Load case 4</i>	<i>Load case 5</i>	<i>Load case 6</i>	<i>Load case 7</i>
27	10	Axial Shear Moment	-29.51 +51.61 -22.52	-75.53 54.26 -37.26	-39.38 28.29 1.18	-88.40 58.72 -42.62	-43.21 26.26 5.42	-78.89 41.84 -34.34	-33.70 9.37 12.70
	10	Axial Shear Moment	+24.69 +17.42 +15.34	53.58 3.72 0.51	53.58 24.16 24.02	62.10 1.67 -1.78	62.10 27.22 27.61	53.93 -5.07 -7.00	53.93 20.48 22.38
	15	Axial Shear Moment	-24.69 +17.42 -15.34	-53.58 24.16 -24.02	-53.58 3.72 -0.51	-62.10 27.22 -27.61	-62.10 1.66 1.78	-53.93 20.48 -22.38	-53.93 -5.07 7.00
28	15	Axial Shear Moment	+29.51 +51.61 +22.52	39.38 28.29 -1.17	75.53 54.26 37.26	43.21 26.26 -5.42	88.40 58.72 42.62	33.70 9.37 -12.70	78.89 41.84 35.34
	20	Axial Shear Moment	-29.51 +63.51 -49.88	-39.38 63.71 -80.27	-75.53 37.74 0.76	-43.21 68.16 -90.96	-88.40 35.70 10.33	-33.7 47.30 -74.52	-78.89 14.83 26.77

21.6 DESIGN OF SUB-FRAME 4-4

A detailed design of a sub-frame 4-4 at level 2 has been carried out with the design aid of 456: 1978 and IS 13920: 1993.

21.6.1 Design of a Flexure Member

To illustrate the design procedure a flexure member 17 has been considered. The design forces have been taken as the **maximum values** from the combined load cases tabulated in Table 21.2.

5.0 General specification

- 5.1 Member shall be designed according to IS 456: 1978 OK
- 5.2 Buildings >3 storey height, minimum grade of concrete M 20 OK
- 5.3 Steel reinforcement of grade Fe 415 or less shall be used OK

6.0 Design of flexural member

- 6.1 General
 - 6.1.1 Factored axial stress less than $0.1 f_{ck}$ NA
 - 6.1.2 The member shall preferably have a width-to-depth ratio of more than 0.3
Width/Depth = $300/450 = 0.67 > 0.3$ OK
 - 6.1.3 Width ≤ 200 mm = 300 mm OK
 - 6.1.4 Depth $\geq \frac{1}{4}$ (Clear Span) i.e. $\frac{1}{4} (4600 - 300) = 1075$ mm OK

6.2 Longitudinal reinforcement

Reinforcement at section 2 due to hogging moment 219.1 kN-m

Assuming 25 mm dia bars with 25 mm clear cover

Effective depth (d) = $450 - 25 - 25/2 = 412.5$ mm

From **Table D, SP 16: 1980**

$$M_{u,\text{lim}}/bd^2 = 2.76 \text{ (For M 20 and Fe = 415)}$$

$$M_{u,\text{lim}} = 2.76 \times 300 \times 412.5^2 = 140.88 \text{ kN-m}$$

Actual moment 219.1 kN-m is greater than $M_{u,\text{lim}}$, So section is doubly reinforced.

Reinforcement from **Table 50, SP 16: 1980**

$$M_u/bd^2 = (219.1 \times 10^6)/(300 \times 412.5^2) = 4.29 \approx 4.30$$

$$d'/d = (25 + 12.5)/41.25 = 0.091 \approx 0.10$$

Referring to **Table 50, SP 16: 1980**

$$P_{1(\text{top})} = 1.429 \text{ and } P_{1(\text{bottom})} = 0.498 \quad (1)$$

corresponding to $M_u/bd^2 = 4.30$ and $d'/d = 0.10$

Reinforcement at section 2 due to sagging moment

$$M_{u,\text{lim}} = 2.76 \times 300 \times 412.5^2 = 140.88 \text{ kN-m}$$

Actual moment 112.3 kN-m is smaller than $M_{u,\text{lim}}$, so section is singly reinforced.

Reinforcement from **Table 2, SP 16: 1980**

$$M_u/bd^2 = (112.3 \times 10^6)/(300 \times 412.5^2) = 2.54$$

$$P_{2(\text{bottom})} = 0.857 \quad (2)$$

Required reinforcement maximum of equation (1) and (2), i.e.

$$P_{(\text{top})} = 1.429 \text{ and } P_{(\text{bottom})} = 0.857$$

Reinforcement at top (A_t) = $1.429 \times 300 \times 412.5^2 = 1768.38 \text{ mm}^2$ (2 @ $16\phi + 4$ @ $22\phi = 1922 \text{ mm}^2$)

Reinforcement at bottom (A_b) = $0.857 \times 300 \times 412.5^2 = 1060.54 \text{ mm}^2$ (2 @ $16\phi + 2$ @ $22\phi = 1162 \text{ mm}^2$)

- 6.2.1 (a) Top and bottom reinforcement shall consist at least 2 bars throughout the member length OK
- 6.2.1 (b) Tension steel ratio $\rho_{\min} \leq 0.24\sqrt{f_{ck}/f_y}$, i.e. 0.258 given 0.857 OK
- 6.2.2 Maximum steel ratio at any section, not exceed $\rho_{\max} = 2.5$ given 1.429 OK

6.2 Longitudinal reinforcement

Reinforcement at section 7 due to hogging moment 130 kN-m

$$M_{u,\text{lim}}/bd^2 = 2.76 \text{ (For M 20 and Fe = 415)}$$

$$M_{u,\text{lim}} = 2.76 \times 300 \times 412.5^2 = 140.88 \text{ kN-m}$$

Actual moment 130 kN-m is less than $M_{u,\text{lim}}$, so section is singly reinforced.

Reinforcement from **Table 2, SP 16: 1980**

$$M_u/bd^2 = (130 \times 10^6)/(300 \times 412.5^2) = 2.54$$

Referring to **Table 2, SP 16: 1980** corresponding to $M_u/bd^2 = 2.54$ and M 20

$$P_{(\text{top})} = 0.858 \quad (3)$$

Reinforcement at section 7 due to sagging moment 57.86 kN-m

Actual moment 57.86 kN-m is less than $M_{u,\text{lim}}$, so section is singly reinforced.

Reinforcement from **Table 2, SP 16: 1980**

$$M_u/bd^2 = (57.86 \times 10^6)/(300 \times 412.5^2) = 1.113$$

Referring to **Table 2, SP 16: 1980** corresponding to $M_u/bd^2 = 1.113$ and M 20

$$P_{(\text{bottom})} = 0.337 \quad (4)$$

Required reinforcement of equations (3) and (4) i.e.

$$P_{(\text{top})} = 0.858 \text{ and } P_{(\text{bottom})} = 0.337$$

Reinforcement at top (A_t) = $(0.858/100) \times 300 \times 412.5 = 1061.7 \text{ mm}^2$ (2 @ $16\phi + 2$ @ $22\phi = 1162 \text{ mm}^2$)

Reinforcement at bottom (A_b) = $(0.337/100) \times 300 \times 412.5 = 417 \text{ mm}^2$ (which is greater than minimum reinforcement requirement of 0.258%) (2 @ $16\phi + 1$ @ $12\phi = 515 \text{ mm}^2$)

- | | | |
|--|--|----|
| 6.2.1 | (a) Top and bottom reinforcement shall consist of at least 2 bars throughout the member length | OK |
| 6.2.1 | (b) Tension steel ratio $\rho_{\min} \leq 0.24\sqrt{f_{ck}}/f_y$, i.e. 0.258 given 0.857 | OK |
| 6.2.2 | Maximum steel ratio at any section, not exceed $\rho_{\max} = 2.5$ given 0.857 | OK |
| 6.3 Shear reinforcement requirement | | |
| 6.3.1 | Details of web reinforcement | OK |
| 6.3.2 | Minimum diameter of hoop 6 mm and in case of beam with clear span > 5 m
hoop diameter 8 mm | OK |
| 6.3.3 | Shear force maximum of
(a) Calculated factored shear force as given in Table 21.2, i.e. 142 kN
(b) Shear force due to formation of plastic hinges at both ends of the beam | |

At Section 2

$$P_t = 1922/(300 \times 412.5) = 0.0155 \approx 1.55$$

% at top

$$P_b = 1162/(300 \times 412.5) = 0.00938 \approx 0.938$$

% at bottom

Referring **Table 50, SP 16: 1980**

$$M_{u,\text{lim}}/bd^2 = 4.7 \text{ (} P_t = 1.55 \text{ and } d'/d = 0.10 \text{)}$$

$M_{u,\text{lim}}$ (Hogging moment capacity)

$$= 4.70 \times 300 \times 412.5^2 = 239.92 \text{ kN-m}$$

$$M_{u,\text{lim}}/bd^2 = 2.72 \text{ (} P_t = 0.938 \text{ and } f_{ck} 20,$$

Table 2, SP 16: 1980

$M_{u,\text{lim}}$ (Sagging moment capacity)

$$= 2.72 \times 300 \times 412.5^2 = 138.84 \text{ kN-m}$$

At Section 7

$$P_t = 1162/(300 \times 412.5) = 0.00938 \approx 0.938\% \text{ at top}$$

$$V_a^{D+L} = V_b^{D+L} = 1.2 \times 32.6 \times 4.6/2 = 90 \text{ kN}$$

For sway to right

$$V_{u,a} = 90 - 1.4(139 + 139)/4.6 = 5.39 \text{ kN}$$

$$V_{u,b} = 90 + 1.4(139 + 139)/4.6 = 174.60 \text{ kN}$$

For sway to left

$$V_{u,a} = 90 + 1.4(240 + 69)/4.6 = 184.04 \text{ kN}$$

$$V_{u,b} = 90 - 1.4(240 + 69)/4.6 = -4.04 \text{ kN}$$

Determination of shear reinforcement

$$\rho = 100 \times 515/300 \times 412.50 = 0.416\%$$

$$\tau_c = 0.44 \text{ N/mm}^2 (\rho = 0.416\%, \text{ M 20})$$

$$\tau_v = 184.04/300 \times 412.50 = 1.487 \text{ N/mm}^2$$

$$\tau_{c,\text{max}} \text{ for M 20} = 2.8 \text{ N/mm}^2$$

$$V_{us} = V_u - \tau_c bd = 184.04 - 0.44 \times 300 \times 412.5 \times 10^{-3} = 129.59 \text{ kN}$$

Adopt 8 mm two legged vertical stirrups

$$A_{sv} = 100.50 \text{ mm}^2$$

$$P_b = 515/(300 \times 412.5) = 0.00416 \approx 0.416\% \\ \text{at bottom}$$

Referring **Table 2, SP 16: 1980**

$$M_{u,\text{lim}}/bd^2 = 2.72 \quad (P_t = 0.938 \text{ and } f_{ck} 20)$$

$M_{u,\text{lim}}$ (Hogging moment capacity),

$$= 2.72 \times 300 \times 412.5^2 = 138.84 \text{ kN-m}$$

$$M_{u,\text{lim}}/bd^2 = 1.35 \quad (P_t = 0.416 \text{ and } f_{ck} 20)$$

$M_{u,\text{lim}}$ (Sagging moment capacity)

$$= 1.35 \times 300 \times 412.5^2 = 68.91 \text{ kN-m}$$

$$S_{\max} > \begin{cases} d/4 = 412.5/4 = 103.125 \text{ mm} \\ 8d_{\min} = 8 \times 22 = 176 \text{ mm} \leq 100 \text{ mm} \\ s = 0.87 \times 415 \times 100.50 \times \\ \quad 412.50/(129.59 \times 1000) \\ \quad = 115.53 \text{ mm} \end{cases}$$

Adopt 8 mm bar at a spacing of 100 mm and beyond distance 2 d from support, maximum spacing of stirrups $S_{\max} = d/2$ i.e. $412.5/2 = 206.25$ i.e. 200 mm c/c.

21.6.2 Design of Exterior Columns

In this example, the columns at ground floor are designed for illustration. The exterior columns 1 and 13 (Figure 21.1) are designed for the forces as tabulated in Table 21.2 based on **maximum interaction ratio**.

Assume size of column	300 mm × 530 mm
Concrete mix	M 20
Vertical reinforcement	Fe 415
Axial load from load case 5	475.6 kN
Moment from load case 5	203.3 kN

The general requirement of the column for ductility will follow IS 13920: 1993 and vertical reinforcement of the column is designed according to 456: 2000. The transverse and special confinement reinforcement will be determined by following the IS 13920: 1993 and IS 456: 2000.

7.0 Column subjected to bending and axial load

7.1 General

- 7.1.1 IS 13920:1993 specification will be applicable if axial stress $> 0.1 f_{ck}$
i.e. $475.6 \times 1000/300 \times 530 = 2.99 \text{ N/mm}^2 > 0.1 \times 20 = 2 \text{ N/mm}^2$ OK
- 7.1.2 Minimum dimension of the member $< 250 \text{ mm}$ (300 mm) OK
- 7.1.3 Shortest cross-section dimension/perpendicular dimension < 0.4 i.e. $300/530 = 0.56$ OK

7.2 Vertical (longitudinal) reinforcement

Assume 20 mm ϕ with 40 mm cover ($d' = 40 + 10 = 50 \text{ mm}$, $d'/D = 50/530 = 0.094 \approx 0.10$)

From Chart 45, **SP 16: 1980** ($d'/D = 0.10$, 415 N/mm^2)

$$P_u/f_{ck}bD = 475.6 \times 10^3/(20 \times 300 \times 530) = 0.15$$

$$M_u/f_{ck}bD^2 = 203.30 \times 10^6/(20 \times 300 \times 530^2) = 0.12$$

Reinforcement on four sides from Chart 45, **SP 16: 1980**

$$P/f_{ck} = 0.08, \text{ reinforcement in \%} = 0.08 \times 20 = 1.6\%$$

$$A_s = pbd/100 = 1.6 \times 300 \times 530/100 = 2544 \text{ mm}^2 (8@ 20\phi = 2513 \text{ mm}^2)$$

- 7.2.1 Lap splices only in central half portion of the member
Hoops over the entire splice length at a spacing < 150 mm
Not more than 50% bar shall be spliced at one section
- 7.2.2 Any area of column that extends more than 100 mm should be detailed as per **Figure 6 in IS 13920: 1993.**
- 7.3 *Transverse reinforcement*
- 7.3.1 Hoop requirement as per **Figure 7A in IS 13920: 1993**
- 7.3.2 If the length of hoop > 300 mm a cross tie shall be provided as shown in Figure 7B or detailed as Figure 7C.
- 7.3.3 Hoop spacing shall not be exceeded half the least lateral dimension of column i.e. $300/2 = 150 \text{ mm}$
- 7.3.4 The design shear force for column shall be maximum of (a) and (b).
 - (a) Calculated factored shear force as per analysis i.e. 77.88 kN (Table 21.2)
 - (b) A factored shear force given by

$$V_u = 1.4[M_{u,\lim}^{bL} + M_{u,\lim}^{bR}]/h_{st}]$$

where, $M_{u,\lim}^{bL}$ and $M_{u,\lim}^{bR}$ are moment of resistance, of opposite sign, of beams and h_{st} is the storey height.

Moment of resistance of beam at section 2 is

$$P_t = 1922/(300 \times 412.5) = 0.0155 \approx 1.55\% \text{ at top}$$

$$P_b = 1162/(300 \times 412.5) = 0.00938 \approx 0.938\% \text{ at bottom}$$

Referring **Table 50, SP 16: 1980**

$$M_{u,\lim}/bd^2 = 4.7 \quad (P_t = 1.55 \text{ and } d'/d = 0.10)$$

$$M_{u,\lim} \text{ (Hogging moment capacity)} = 4.70 \times 300 \times 412.5^2 = 239.92 \text{ kN-m}$$

$$M_{u,\lim}/bd^2 = 2.72 \quad (P_t = 0.938 \text{ and } f_{ck} 20, \text{ Table 2, SP 16: 1980})$$

$$M_{u,\lim} \text{ (Sagging moment capacity)} = 2.72 \times 300 \times 412.5^2 = 138.84 \text{ kN-m}$$

$$V_u = 1.4 (239.92)/3.675 = 91.42 \text{ kN}$$

$$V_c = \tau_c bd = 0.898 \times 300 \times (530 - 50) = 129.338 \text{ kN} \quad (\tau_c = 0.62 \times 1.448 \quad (A_{st} = 2512/2 = 1256 \text{ mm}^2 \text{ and } \delta = 1 + 3 P_u/A_g f_{ck} = 1.448))$$

Therefore, nominal shear reinforcement shall be provided in accordance with 26.5.1.6 of IS 456: 2000.

Use 8 mm diameter two-legged stirrups ($A_{sv} = 2 \times 50.26 = 100.52 \text{ mm}^2$)

For minimum stirrups

$$S_v \leq A_{sv} 0.87 f_y/0.4 b \quad i.e. 100.52 \times 0.87 \times 415/0.4 \times 300 \leq 302 \text{ mm}$$

The spacing shall be lesser of

$$(a) 0.75 d = 0.75 \times 480 = 360 \text{ mm}$$

$$(b) 300 \text{ mm (7.3.3)}$$

$$(c) 302 \text{ as calculated}$$

Provide 8 mm ϕ two-legged stirrups about 300 mm c/c

7.4 Special confining reinforcement

- 7.4.1 Special confining reinforcement will provide over a length of l_0 towards the mid-span of column

$$l_0 \leq \begin{cases} \text{depth of member} = 530 \text{ mm} \\ 1/6 (\text{clear span}) = (4.0 - 0.45)/6 = 591 \text{ mm} \Rightarrow 450 \text{ mm} \\ 450 \text{ mm} \end{cases}$$

- 7.4.6 The spacing of hoop shall not exceed

$$S_{\max} \geq \begin{cases} 1/4 (\text{minimum member dimensions}) = 1/4 \times 300 = 75 \text{ mm} \\ \text{should not be less than } 75 \text{ mm} \\ \text{should not be greater than } 100 \text{ mm} \end{cases} \Rightarrow 75 \text{ mm}$$

- 7.4.8 Minimum area of cross section of the bar forming hoop is,

$$A_{sh} = 0.18 Sh f_{ck}/f_y (A_g/A_k - 1.0)$$

$$A_{sh} = 0.18 \times 75 \times 235 \times 20/415 ((530 \times 300)/(470 \times 240) - 1.0)) = 62.62 \text{ mm}^2$$

Use 10 mm dia bar (78.53 mm^2) at a spacing of $75 \times 78.53/62.62 = 94 \text{ mm c/c.}$

21.6.3 Design of Interior Columns

The interior columns 5 and 9 are designed for the forces as tabulated in Table 21.2 on the basis of **maximum interaction ratio**.

Assume size of column	$300 \text{ mm} \times 300 \text{ mm}$
Concrete mix	M 20
Vertical reinforcement	Fe 415
Axial load from load case 4	428.9 kN
Bending moment from load case 4	56 kN-m

The general requirement of the column for ductility will follow from IS 13920: 1993 and vertical reinforcement of the column is designed according to 456: 2000. The transverse and special confinement reinforcement will be determined by following the IS 13920: 1993 and IS 456: 2000.

7.0 Column subjected to bending and axial load

7.1 General requirement

- 7.1.1 IS 13920:1993 specification will be applicable if axial stress $> 0.1 f_{ck}$
i.e. $428.9 \times 1000/300 \times 300 = 4.76 \text{ N/mm}^2 > 0.1 \times 20 = 2 \text{ N/mm}^2$
- 7.1.2 Minimum dimension of the member should not be less than 200 mm (300 mm) OK
- 7.1.3 Shortest cross-section dimension/perpendicular dimension should not be less than 0.4 *i.e.* $300/300 = 1.0$ OK

7.2 Vertical (longitudinal) reinforcement

Assume 20 mm ϕ with 40 mm cover ($d' = 40 + 10 = 50$ mm, $d'/D = 50/300 = 0.16$)
From **Chart 45, SP 16: 1980** ($d'/D = 0.15$, 415 N/mm 2)

$$P_u/f_{ck}bd = 428.9 \times 10^3 / (20 \times 300 \times 300) = 0.238$$

$$M_u/f_{ck}bd^2 = 56 \times 10^6 / (20 \times 300 \times 300^2) = 0.104$$

Reinforcement on four sides from Chart 45, SP 16: 1980

$$P/f_{ck} = 0.095, \text{ reinforcement in \%} = 0.095 \times 20 = 1.9\%$$

$$A_s = pbd/100 = 1.9 \times 300 \times 300/100 = 1710 \text{ mm}^2$$

Provide 6@ 20 mm ϕ i.e. 1884 mm 2

7.2.1 Lap splices only in central half portion of the member

Hoops over the entire splice length at a spacing < 150 mm

Not more than 50% bar shall be spliced at one section

7.2.2 Any area of column that extends more than 100 mm should be detailed as per **Figure 6 of IS 13920: 1993.**

7.3 Transverse reinforcement

7.3.1 Hoop requirement as per **Figure 7A in IS 13920: 1993** OK

7.3.2 If the length of hoop > 300 mm a cross tie shall be provided as shown in **Figure 7B or detailed as Figure 7C in IS 13920: 1993.** OK

7.3.3 Hoop spacing should not be greater than half the least lateral dimension of column i.e. $300/2 = 150$ mm

7.3.4 The design shear force for column shall be maximum of (a) and (b).

(a) Calculated factored shear force as per analysis i.e. 27.77 kN (Table 21.2)

(b) Factored shear force given by

$$V_u = 1.4[M_{u,\lim}^{bL} + M_{u,\lim}^{bR}]/h_{st}]$$

where, $M_{u,\lim}^{bL}$ and $M_{u,\lim}^{bR}$ are moment of resistance, of opposite sign, of beams and h_{st} is the storey height.

Moment of resistance of beam at section 7 is,

$$P_t = 1162/(300 \times 412.5) = 0.00938 \approx 0.938\% \text{ at top}$$

$$P_b = 515/(300 \times 412.5) = 0.00416 \approx 0.416\% \text{ at bottom}$$

Referring **Table 2, SP 16: 1980**

$$M_{u,\lim}/bd^2 = 2.72 \quad (P_t = 0.938 \text{ and } f_{ck} 20)$$

$$M_{u,\lim} \text{ (Hogging moment capacity)} = 2.72 \times 300 \times 412.5^2 = 138.84 \text{ kN-m}$$

$$M_{u,\lim}/bd^2 = 1.35 \quad (P_t = 0.416 \text{ and } f_{ck} 20)$$

$$M_{u,\lim} \text{ (Sagging moment capacity)} = 1.35 \times 300 \times 412.5^2 = 68.91 \text{ kN-m}$$

$$V_u = 1.4(69 + 139)/3.675 = 79.23 \text{ kN}$$

$$V_c = \tau_c bd = 0.53 \times 300 \times (300 - 50) = 83.91 \text{ kN} \quad (\tau_c = 0.67 \times 1.67 = 1.118)$$

$$(A_s = 942 \text{ mm}^2 \text{ and } \delta = 1 + 3 P_u/A_g f_{ck} = 1.67))$$

Therefore, nominal shear reinforcement shall be provided in accordance with 26.5.1.6 of IS 456: 2000.

Use 8 mm diameter two-legged stirrups ($A_{sv} = 2 \times 50.26 = 100.52 \text{ mm}^2$)

For minimum stirrups

$$s_v \leq A_{sv} \cdot 0.87 f_y / 0.4 b \text{ i.e. } 100.52 \times 0.87 \times 415 / 0.4 \times 300 \leq 302 \text{ mm}$$

The spacing shall be lesser of

$$(a) 0.75 d = 0.75 \times 250 = 187.5 \text{ mm}$$

$$(b) 300 \text{ mm (7.3.3)}$$

$$(c) 302 \text{ mm as calculated}$$

Provide 8 mm ϕ two-legged stirrups about 187.5 mm c/c. But hoop spacing should not be greater than half the least lateral dimension i.e. $300/2 = 150 \text{ mm c/c}$

7.4 Special confining reinforcement

- 7.4.1 Special confining reinforcement will provide over a length of l_0 towards the mid-span of column

$$l_0 \leq \begin{cases} \text{depth of member} = 300 \text{ mm} \\ 1/6 (\text{clear span}) = (4.0 - 0.45)/6 = 591 \text{ mm} \Rightarrow 300 \text{ mm} \\ 450 \text{ mm} \end{cases}$$

- 7.4.6 The spacing of hoop shall not exceed

$$S_{\max} \geq \begin{cases} 1/4 (\text{minimum member dimensions}) = 1/4 \times 300 = 75 \text{ mm} \\ \text{should not be less than } 75 \text{ mm} \\ \text{should not be greater than } 100 \text{ mm} \end{cases} \Rightarrow 75 \text{ mm}$$

- 7.4.8 Minimum area of cross section of the bar forming hoop is

$$A_{sh} = 0.18 S_h f_{ck} / f_y (A_g / A_k - 1.0)$$

$$A_{sh} = 0.18 \times 75 \times 250 \times 20 / 415 ((300 \times 300) / (250 \times 250) - 1.0)) = 71.56 \text{ mm}^2$$

Use 10 mm dia bar (78.53 mm^2) at a spacing of $75 \times 78.53 / 71.56 = 82.30 \text{ mm c/c}$ i.e. 80 mm c/c.

8.0 Joints of frames

- 8.1 The special confining reinforcement as required at the end of column shall be provided through the joint as well, unless the joint is confined by 8.2

- 8.2 A joint which has beams framing into all vertical faces of it and beam width, is at least $\frac{3}{4}$ of the column width, may be provided with half the special confining reinforcement required at the end of the column. The spacing of hoop shall not exceed 150 mm. Therefore, $A_{sh} = 78.53/2 = 39.26 \text{ mm}^2$. Use 8 mm dia bar (50.26 mm^2) at a spacing of $82.3 \times 50.26 / 35.52 = 105 \text{ mm c/c}$.

21.6.4 Detailing of Reinforcements

Details of reinforcement at level 2 of subframe 4-4 shown in Figure 21.7.

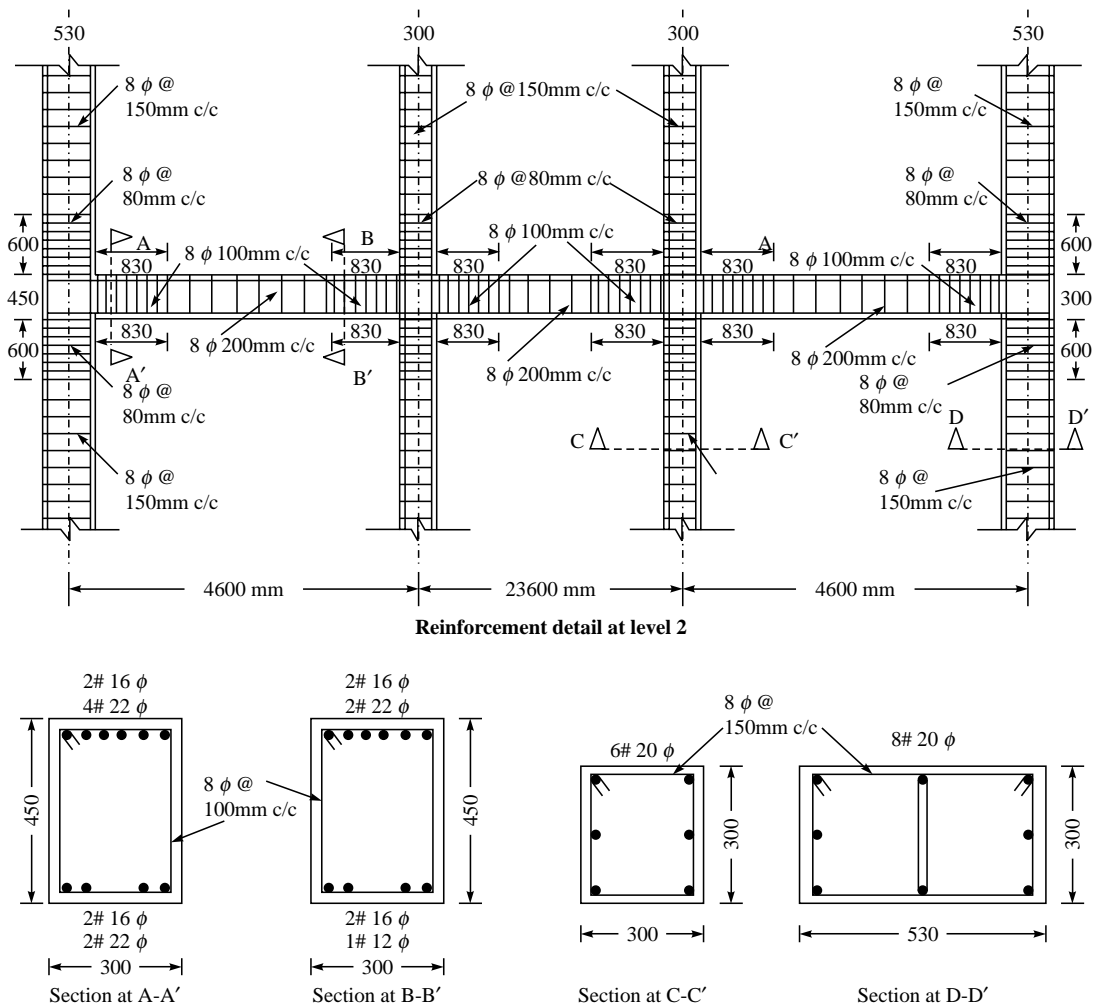


FIGURE 21.7 Detailing of reinforcements at level 2 of sub-frame 4-4.

SUMMARY

The earthquake resistant design of a *real* building frame is an ideal way to demonstrate to structural engineers the difference between conventional civil engineering practices and concepts of earthquake resistant design. The aim of this chapter is to illustrate a detailed worked out example on seismic analysis and design of four-storey RC frame building. The seismic analysis is carried out by equivalent static method using a plane frame programme alongwith dead and live load analysis. Design forces have been worked out by considering all the load combinations as per IS 1893 (Part 1): 2002. Seismic design has been carried out by lateral strength design method following the ductile detailing as per IS 13920: 1993.

REFERENCES

- [1] IS 1893, *Criteria for Earthquake Resistant Design of Structures—Part 1, General Provisions and Buildings* (Fifth Revision), Bureau of Indian Standards, New Delhi, 2002.
- [2] IS 13920, *Ductile Detailing of Reinforced Concrete Structures Subjected to Seismic Force*, Bureau of Indian Standards, New Delhi, 1993.
- [3] IS 456, *Plain and Reinforced Concrete—Code of Practice*, Bureau of Indian Standards, New Delhi, 2000.
- [4] Paulay T. and Priestley, M.J.N., *Seismic Design of Reinforced Concrete and Masonry Buildings*, John Wiley & Sons, New York, 1992.
- [5] SP 16, *Design Aids for Reinforced Concrete to IS: 456–1978*, Bureau of Indian Standards, New Delhi, 1980.

Chapter 22

Earthquake Resistant Design of Shear Wall as per IS 13920: 1993

22.1 INTRODUCTION

A 14-storeyed reinforced concrete building with shear wall in zone IV has been considered for the illustration of design of shear wall. The lateral forces have been resisted by a dual system consisting of Special Moment Resisting Frames (SMRF) and reinforced concrete shear walls. The main emphasis in this chapter is on (i) distribution of design lateral force in SMRF with shear wall and SMRF without shear wall and (ii) design of shear wall and reinforcement requirement, through practical example.

22.2 DESCRIPTION OF BUILDING

The building considered for this study is assumed to be a hospital building ($I = 1.5$) situated in zone IV ($Z = 0.24$) consisting of five blocks out of which the central block with shear wall has been considered for the study. The building has a dual system; the response reduction factor ($R = 5$) has been opted for two reasons (a) the shear wall and the SMRF systems are designed to resist the total design lateral forces in proportion to their relative rigidities considering the interaction of the dual system at all floor levels; and (b) the SMRF are designed to independently resist not less than 25% of the design seismic base shear. The typical plan and elevation of the central block and its elevation is shown in Figure 22.1.

The X-direction of the block consists of 4 bay of SMRF @ 6.5 m each and in Z-direction 3 bay of frames @ 6 m each. The building is 14 storeyed and floor-to-floor heights are 3.1 m. The columns and structural walls have same cross-sections throughout the height of the building. The floor beams and slabs also have the universal dimensions at all floor levels. A shear wall of 250 mm thickness is centrally located at the exterior frames in X-direction of the block. It

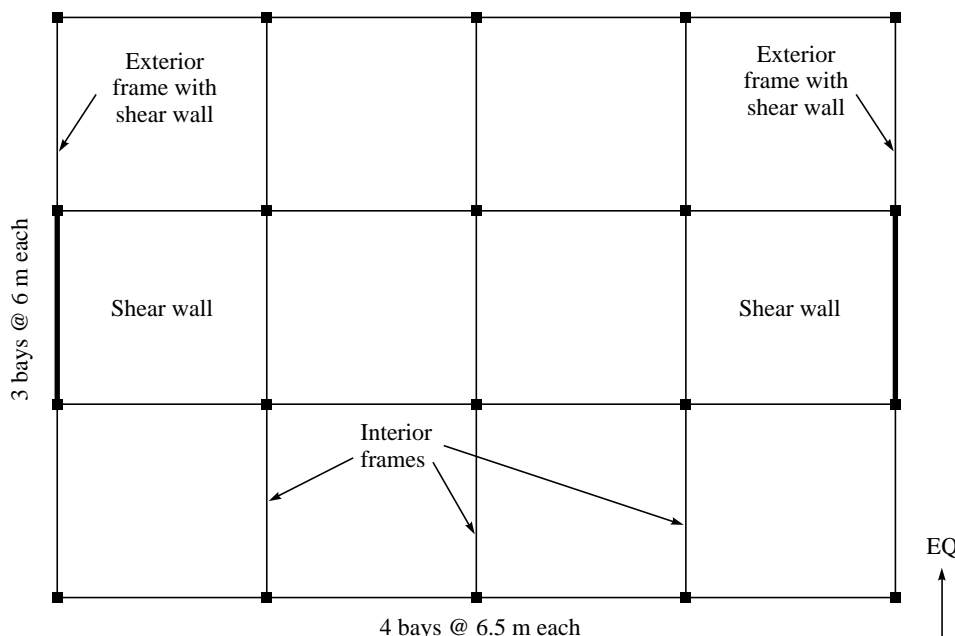


FIGURE 22.1 Typical plan of the building with shear wall.

is assumed that the thickness of roof and floor slab is 200 mm. The dimension of all beams of frames are 500 mm × 500 mm and the columns size is 700 mm × 700 mm. The structure is assumed to be fixed at base. The grade of concrete is M 20 and steel used is Fe 415. On the basis of the above data and the dimensions, the weight of typical floor and the roof has been estimated in Table 22.1. The calculation of base shear corresponding to the whole structure in the X-direction is calculated in Table 22.2 as per IS 1893 (Part 1): 2002. The distribution of total base shear along the height of the building at each floor is given in Table 22.3 and corresponding shear are given in Table 22.4.

22.3 DETERMINATION OF DESIGN LATERAL FORCES

The building considered consists of parallel arrangements of three identical interior frames and two exterior frames with shear walls in the direction of motion (X-direction). A **two-dimensional plane frame model** has been used for the determination of lateral forces in the SMRF with and without shear wall assuming no torsional effect. The mathematical model connects all the plane frames in the direction of motion by assuming the same horizontal displacement in a floor. In the example, two exterior frames with shear wall may be modelled as single frame (say frame X-1) with double stiffness, strength and weight. Here the shear wall is modelled as a wide column connected to the adjacent columns of the SMRF with rigid link. Three identical interior SMRF are again modelled as a single lumped frame (say frame X-2) with triple stiffness, strength and weight. The modelled frame X-1 and X-2 are connected with hinged rigid bars at each floor level as shown in Figure 22.2 and the prescribed lateral forces

TABLE 22.1 Seismic weight calculation of the building

	<i>Slab</i> (kN)	<i>Beam</i> (kN)	<i>Column</i> (kN)	<i>Shear</i> wall (kN)	<i>Live</i> load (kN)	<i>Total</i> <i>load</i> (kN)
14	2340	1212.5	379.75	116.25	—	4048.5
13	2340 ⁽¹⁾	1212.5 ⁽²⁾	759.5 ⁽³⁾	232.5 ⁽⁴⁾	175.5 ⁽⁵⁾	4720.0
12	2340	1212.5	759.5	232.5	175.5	4720.0
11	2340	1212.5	759.5	232.5	175.5	4720.0
10	2340	1212.5	759.5	232.5	175.5	4720.0
9	2340	1212.5	759.5	232.5	175.5	4720.0
8	2340	1212.5	759.5	232.5	175.5	4720.0
7	2340	1212.5	759.5	232.5	175.5	4720.0
6	2340	1212.5	759.5	232.5	175.5	4720.0
5	2340	1212.5	759.5	232.5	175.5	4720.0
4	2340	1212.5	759.5	232.5	175.5	4720.0
3	2340	1212.5	759.5	232.5	175.5	4720.0
2	2340	1212.5	759.5	232.5	175.5	4720.0
1	2340	1212.5	759.5	232.5	175.5	4720.0
						Σ65408.5

(1) Weight of slab = $26 \times 18 \times 0.2 \times 25 = 2340$ kN(2) Weight of beam = $0.5 \times 0.5 \times (18 \times 5 + 26 \times 4) \times 25 = 1212.5$ kN(3) Weight of column = $0.7 \times 0.7 \times (3.1/2 + 3.1/2) \times 25 \times 2 = 759.5$ kN(4) Weight of shear wall = $6 \times 3.1 \times 0.25 \times 25 = 232.5$ kN(5) Live load on floors = $26 \times 18 \times 1.5 \times (25/100) = 175.5$ kN**TABLE 22.2 Calculation of seismic base shear (V_B) as per IS 1893 (Part 1): 2002**

1.	Fundamental natural time period (T_a) $T_a = 0.075h^{0.75} = 0.075 (43.4)^{0.75} = 1.268$ sec
2.	Design horizontal seismic coefficient (A_h) $A_h = (Z/2) (I/R) (S_a/g)$ $Z = 0.24; I = 1.5; R = 5.0$ (S_a/g) for $T_a = 1.268$ sec, 5% damping = $1.36/T_a = 1.36/1.268 = 1.073$ $A_h = (0.24/2) (1.5/5.0) (1.073) = 0.038628$
3.	Design Base Shear $V_B = A_h \times W$ $= 0.038628 \times 65408.5 = 2526.60$ kN

as calculated in Table 22.3 are applied on combined frame (say frame X). The distribution of lateral forces in frame X-1 and frame X-2 is given in Table 22.5. Table 22.5 indicates that at the top (14th floor level), the lumped frame X-1 takes 108% of the total storey shear. This

TABLE 22.3 Floor-wise distribution of design lateral force

	W_i (kN)	h_i (m)	$W_i \cdot h_i^2$	$(W_i \cdot h_i^2 / \sum W_i \cdot h_i^2)$	Q_i (kN)
14	4048.5	43.4	7625.6×10^3	0.1703	430.30
13	4720.0	40.3	7665.7×10^3	0.1712	432.55
12	4720.0	37.2	6531.7×10^3	0.1459	368.63
11	4720.0	34.1	5488.5×10^3	0.1226	309.76
10	4720.0	31.0	4535.9×10^3	0.1013	255.94
9	4720.0	27.9	3674.1×10^3	0.082	207.18
8	4720.0	24.8	2903.0×10^3	0.065	164.23
7	4720.0	21.7	2222.6×10^3	0.049	123.80
6	4720.0	18.6	1632.9×10^3	0.036	90.96
5	4720.0	15.5	1133.9×10^3	0.025	63.16
4	4720.0	12.4	725.7×10^3	0.016	40.43
3	4720.0	9.3	408.2×10^3	0.009	22.74
2	4720.0	6.2	181.4×10^3	0.004	10.11
1	4720.0	3.1	45.3×10^3	0.001	2.53
			$\Sigma 44774.8 \times 10^3$		$\Sigma 2522.32$

TABLE 22.4 Design lateral forces at each floor in the X-direction corresponding to entire structure and resulting shear

Floor level	Height (m)	Storey weight (kN)	Seismic forces	
			Lateral force F_x (kN)	Storey shear, ΣF_x (kN)
14 (Roof)	43.4	4048.5	430.30	430.30
13	40.3	4720	432.55	862.85
12	37.2	4720	368.63	1231.48
11	34.1	4720	309.76	1541.24
10	31.0	4720	255.94	1797.18
9	27.9	4720	207.18	2004.36
8	24.8	4720	164.23	2168.59
7	21.7	4720	123.80	2292.39
6	18.6	4720	90.96	2383.35
5	15.5	4720	63.16	2446.51
4	12.4	4720	40.43	2486.94
3	9.3	4720	22.74	2509.68
2	6.2	4720	10.11	2519.79
1	3.1	4720	2.53	2522.32

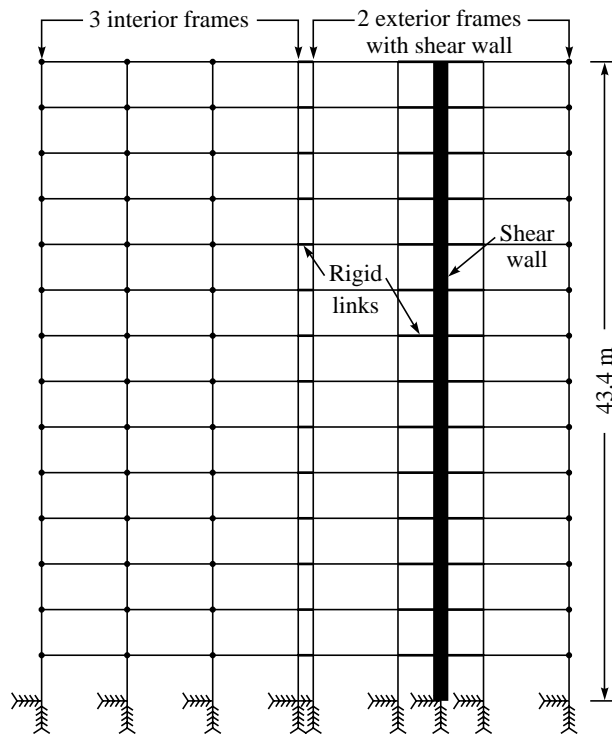


FIGURE 22.2 Two-dimensional plane frame (X-frame) model of shear wall building.

TABLE 22.5 Distribution of seismic storey shears between the frames X-1 and X-2

Storey level	Frame (X-1) (3 interior frames)		Frame (X-2) (2 exterior frames with shear walls)		Total storey shear (kN)
	Storey shear	% of total (kN)	Storey shear	% of total (kN)	
14 (Roof)	466.46	108.40	-36.16	-8.40	430.30
13	566.85	65.70	296.00	34.30	862.85
12	562.30	45.66	669.18	54.34	1231.48
11	550.16	35.70	991.08	64.30	1541.24
10	545.89	30.37	1251.29	69.67	1797.18
9	542.15	27.04	1462.21	72.96	2004.36
8	533.32	24.60	1635.27	75.40	2168.59
7	513.36	22.39	1779.03	77.61	2292.39
6	482.40	20.24	1900.95	79.76	2383.35
5	438.32	17.92	2008.19	82.08	2446.51
4	379.27	15.25	2107.67	84.75	2486.94
3	306.19	12.20	2203.49	87.80	2509.68
2	230.09	9.13	2289.70	90.87	2519.79
1	183.78	7.28	2338.54	92.72	2522.32

reflects the fact that in frame shear wall systems, interaction between frame and wall under lateral loads results in the frame supporting the wall at the top while at the base most of the horizontal shear is resisted by the wall. Table 22.5 also indicates that the two exterior frames with shear wall take about 92% of the base shear and three interior frames take about 8% of base shear in X-direction. Table 22.6 shows the design values for the shear wall under the different load cases as per Clause of IS 1893 (Part 1): 2002. The last column of the table indicates the design axial load for boundary element of shear wall (adjacent columns of shear wall), which include the effect of additional increase of axial loads in columns due to earthquake induced overturning. The SMRF of the building should not be designed less than 25% of the design lateral loads as per IS 1893 (Part 1): 2002. The forces in shear wall under different load combination are given in Table 22.6.

TABLE 22.6 Design forces in shear wall (frame X-1) under different load cases

Load case	Moment (kN-m)	Shear (kN)	Axial force (kN)	Axial load (kN) on boundary elements
1.5(DL+LL)	1747	71.06	10390	2454.5
1.2(DL+LL+EQZ)	17920	2658	8403	4532.5
1.2(DL+LL-EQZ)	20760	2772	8217	5040
1.5(DL+EQZ)	22630	3332	9114	5425
1.5(DL-EQZ)	25710	3456	8881	5970
0.9DL+1.5EQZ	23240	3356	5516	4808
0.9DL-1.5EQZ	25110	3431	5283	5120

22.4 DESIGN OF SHEAR WALL

The design of a shear wall in a 14-storeyed reinforced concrete building has been presented for illustration (AFM 1992, Medhekar and Jain, 1993; Naeim, 2001). The design forces as per IS 1893 (Part 1): 2002 in the shear wall have already been calculated and summarized in Table 22.6. The sectional and reinforcement details fulfilled according to the Clauses of IS 13920: 1993 are presented as under:

Clause as per IS 13920	Design requirement as per IS 1893 (Part 1): 2002	Details provided in the shear walls
9.1	<i>General requirements</i>	
9.1.1	The design of shear wall is based on the assumption that it will be the part of the lateral force resisting system of the structure	Lateral force resisting system in the building is a dual system consisting of SMRF and shear walls. In general, the shear walls will resist all the lateral force being a relatively stiff element. OK

- 9.1.2 In order to safeguard against premature out-of-plane buckling in the potential plastic hinge region of walls, minimum thickness of shear wall should not be less than 150 mm Assumed thickness of shear wall OK 250 mm
- 9.1.3 Shear wall is subjected to combined flexure and axial load therefore; the ends of the wall will be subjected to high axial load. Therefore, it is necessary to thicken the wall in boundary regions. This is readily achieved by providing flange elements with sufficient dimensions so as to provide adequate flexural rigidity at the end of the wall section. This effective flange width to be used in the design of flanged wall sections, shall be assumed to extend beyond the face of the web for a distance which shall be smaller of (a) half the distance to an adjacent shear wall web (b) $1/10^{\text{th}}$ of the total wall height. The shear wall is provided in between the middle two columns of the exterior frames. These columns will act as a flange element or boundary elements for the shear wall. Therefore, there is no need for further thickening of shear wall at the end or boundary regions.
- 9.1.4 To control the width of inclined cracks in the wall, the code recommends the reinforcement in both the direction of walls *i.e.* horizontal and vertical. The minimum reinforcement ratio should be 0.0025 of the gross area in each direction of the wall and should be uniform across the cross section of the wall. Calculated reinforcement in horizontal and vertical direction is greater than the minimum prescribed reinforcement. Provided reinforcement is uniformly distributed in both the directions
- 9.1.5 To reduce fragmentation and premature deterioration of the concrete under load reversal loading in inelastic range, it is preferred that the longitudinal and transverse reinforcement should be provided in two curtains if (a) factored shear stress in the wall exceeds $0.25\sqrt{f_{ck}}$ or (b) wall thickness > 200 mm Since the thickness of shear wall is 250 mm and also the factored shear stress (τ_v) is greater than $0.25\sqrt{f_{ck}}$ the reinforcement is provided in two curtains. (see Clause 9.2.1)
- 9.1.6 To prevent the use of very large diameter of reinforcement, the code restricts the diameter of bar upto $1/10^{\text{th}}$ of the thickness of part. Diameter of bar used in horizontal and vertical reinforcement is 8 mm, which is smaller than $1/10$ (250) = 25 mm.

9.1.7	The maximum spacing of reinforcement in either direction shall not exceed the smallest of $l_w/5$, $3 t_w$, and 450 mm; where l_w is the horizontal length of wall, and t_w is the thickness of the wall web. This limitation has been guided by the experience and various tests to confine the concrete.	Spacing provided in horizontal and vertical direction of reinforcement is 130 mm which is smaller of (a) $l_w/5 = 1160$ mm, (b) $3 t_w = 750$ mm and 450 mm.	OK
9.2	<i>Shear strength requirements</i>		
9.2.1	The nominal shear stress, τ_v , shall be calculated as	The nominal shear stress, $\tau_v = \frac{1728}{250 \times 4800} = 1.44 \text{ N/mm}^2$	OK
	where, V_u = Factored shear force t_w = thickness of web d_w = effective depth of wall section. This may be taken as 0.8 l_w for rectangular sections. l_w = horizontal length of wall	$V_u = 3456/2 = 1728 \text{ kN}$ $t_w = 250 \text{ mm}$ $d_w = 0.8 \times 6000 = 4800 \text{ mm}$ $l_w = 6000 \text{ mm}$	
9.2.2	The design strength of concrete (τ_c) shall be calculated as per <i>Table 13 of IS: 456: 2000</i>	Assume horizontal and vertical reinforcement (A_s) is 0.25% and concrete grade M 20, permissible shear stress in concrete is $\tau_c = 0.36 \text{ N/mm}^2$	OK
9.2.3	The nominal shear stress in the wall, τ_v , shall not exceed $\tau_{c, \text{max}}$ as per <i>Table 14 of IS: 456: 2000</i>	$\tau_{c, \text{max}} = 2.8 \text{ N/mm}^2$ Therefore, $\tau_v (1.44 \text{ N/mm}^2) < \tau_{c, \text{max}} (2.8 \text{ N/mm}^2)$	OK
9.2.4	When τ_v is less than τ_c , shear reinforcement shall be provided in accordance with 9.1.3, 9.1.4, and 9.1.6 of the code	$\tau_v (1.44 \text{ N/mm}^2) > \tau_c (0.36 \text{ N/mm}^2)$	NA
9.2.5	When τ_v is greater than τ_c , the area of horizontal shear reinforcement, A_h , to be provided within a vertical spacing S_v , is given by	Shear force required for horizontal shear reinforcement is $V_{us} = (\tau_v - \tau_c) t_w d_w$ $= (1.44 - 0.36) \times 250 \times 4800$ $= 1296 \text{ kN}$	OK
	where, $V_{us} = (V_u - \tau_c t_w d_w)$ is the shear force to be resisted by the horizontal reinforcement. However, the amount of horizontal reinforcement provided	Spacing required for two legged 8 Φ tor bar is, $S_v = \frac{0.87 \times 415 \times 100 \times 4800}{1296 \times 10^3}$ $= 133.7 \text{ mm}$	

shall not be less than the minimum as per 9.1.3 of the code

This requires the ratio $A_s/S_v = 0.747$
Minimum horizontal reinforcement =
0.0025 of gross area, this requires the
ratio = $0.0025 \times 250 = 0.625$

Hence, provide 8 mm diameter bar at 130 c/c in 2 curtains as horizontal reinforcement

- 9.2.6 The vertical reinforcement that is uniformly distributed in the wall shall not be less than the horizontal reinforcement calculated as per 9.2.5

Hence, provide 8 mm diameter bar at 130 c/c in 2 curtains as vertical reinforcement also. OK

9.3 Flexural strength

- 9.3.1 The moment of resistance, M_{uv} , of the wall section shall be calculated as for columns subjected to combined axial load and uni-axial bending as per IS: 456–1978. The moment of resistance that is provided by uniformly distributed vertical reinforcement in a slender rectangular wall section may be calculated as follows:

(a) For $x_u/l_w \leq x_u^*/l_w$

$$\frac{M_{uv}}{f_{ck}t_w l_w^2} = \phi \left[\left(1 + \frac{\lambda}{\phi} \right) \left(\frac{1}{2} - 0.416 \frac{x_u}{l_w} \right) - \left(\frac{x_u}{l_w} \right)^2 \left(0.168 + \frac{\beta^2}{3} \right) \right]$$

where,

$$\frac{x_u}{l_w} = \left(\frac{\phi + \lambda}{2\phi + 0.36} \right);$$

$$\frac{x_u^*}{l_w} = \left(\frac{0.0035}{0.0035 + 0.87 \frac{f_y}{E_s}} \right)$$

$$\phi = \left(\frac{0.87 f_y \rho}{f_{ck}} \right); \lambda = \left(\frac{P_u}{f_{ck} t_w l_w} \right)$$

$$\rho = \text{Vertical reinforcement ratio} = A_{st}/(t_w l_w)$$

$$\rho = A_{st}/(t_w l_w); A_{st} = A_s l_w / S_v$$

$$\rho = A_{sv}/t_w S_v = 0.747/250 = 0.003$$

$$\phi = \frac{0.87 \times 415 \times 0.003}{20} = 0.054$$

$$\lambda = \frac{5195 \times 10^3}{20 \times 250 \times 6000} = 0.173$$

$$\frac{x_u}{l_w} = \left(\frac{0.054 + 0.173}{2 \times 0.054 + 0.36} \right) = 0.496$$

$$\frac{x_u^*}{l_w} = \left(\frac{0.0035}{0.0035 + 0.87 \frac{415}{2 \times 10^5}} \right) = 0.66$$

Since $x_u/l_w \leq x_u^*/l_w$

$$\frac{M_{uv}}{f_{ck}t_w l_w^2} = 0.054$$

$$\left[\left(1 + \frac{0.173}{0.054} \right) \left(\frac{1}{2} - 0.416 \times 0.496 \right) - (0.496)^2 \left(0.168 + \frac{0.516^2}{3} \right) \right] = 0.063$$

	A_{st} = Area of uniformly distributed vertical reinforcement $\beta = \frac{0.87f_y}{0.0035E_s} = 0.516$ E_s = Elastic modulus of steel P_u = axial compression on wall	$M_{uv} = 20 \times 250 \times 6000^2 \times 0.063 = 11,341 \text{ kN-m}$ The remaining moment i.e. $M_u - M_{uv} = 12855 - 11341 = 1514 \text{ kN-m}$ shall be resisted by reinforcement in boundary elements.
9.3.2	The cracked flexural strength of the wall section should be greater than its uncracked flexural strength.	NA
9.3.3	In walls that do not have boundary elements, vertical reinforcement consisting of at least 4 bars of minimum 12 mm diameter arranged in two layers shall be provided along the edge of the wall.	Concentrated vertical reinforcement near the edges of the wall is more effective in resisting bending moment.
9.4	Boundary elements Boundary elements are portions along the wall edges that are strengthened by longitudinal and transverse reinforcement. Though they may have the same thickness as that of the wall web, it is advantageous to provide them with greater thickness.	NA
9.4.1	Where the extreme fiber compressive stress in the wall due to combined axial load and bending is greater than $0.2 f_{ck}$, boundary elements shall be provided along the vertical boundaries of walls. The boundary elements may be discontinued where the calculated compressive stress becomes less than $0.15 f_{ck}$.	Gross sectional properties $l_w = 6000 \text{ mm}, t_w = 250 \text{ mm}$ $A_g = 1500 \times 10^3 \text{ mm}^2$ $I_y = t_w l_w^3 / 12 = 250 \times 6000^3 / 12 = 4.5 \times 10^{12} \text{ mm}^4$ $f_c = \frac{P_u}{A_g} + \frac{M_u(l_w/2)}{I_y} = \frac{5195 \times 10^3}{1500 \times 10^3} + \frac{12855 \times 10^6 \times 3000}{4.5 \times 10^{12}} = 12.034 \text{ N/mm}^2 > 4.0 (0.2 \times 20)$ Therefore, provide boundary elements
9.4.2	A boundary element shall have adequate axial load carrying capacity, assuming short column action, so as to enable it to carry an axial compression equal to the sum of factored	The adjacent columns of shear wall act as a boundary element. From Table 22.6, the maximum compressive axial load on boundary element column is $P_u = 5970 \text{ kN}$ under different loading conditions.

gravity load on it and the additional compressive load induced by the seismic force. The latter may be calculated as

$$(M_u - M_{uv})/C_w$$

where,

M_u = factored design moment on the entire wall section

M_{uv} = Moment of resistance provided by distributed vertical reinforcement across the wall section

C_w = Center to center distance between the boundary elements along the two vertical edges of the wall.

Let with existing column size having dimension 700 mm \times 700 mm and assume longitudinal reinforcement 2% of the gross area

$$A_g = 700 \times 700 = 49 \times 10^4 \text{ mm}^2$$

$$A_s = 0.02 \times 49 \times 10^4 = 9800 \text{ mm}^2$$

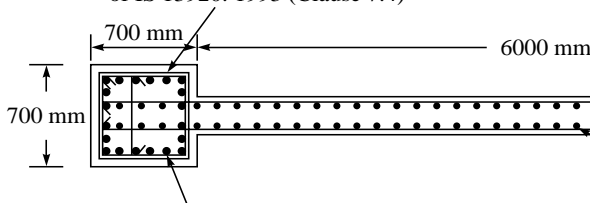
Axial load capacity of boundary element column acting as short column

$$\begin{aligned} P_u &= 0.4 f_{ck} A_g + (0.67 f_y - 0.4 f_{ck}) A_s \\ &= 0.4 \times 20 \times 49 \times 10^4 + (0.67 \times 415 - 0.4 \times 20) \times 9800 \\ &= 6566.49 \text{ kN.} > P_u \text{ (5970 kN)} \end{aligned}$$

- 9.4.3 If the gravity loads add to the strength of the wall, its load factor shall be taken as 0.8. NA
- 9.4.4 The percentage of vertical reinforcement in the boundary elements shall not be less than 0.8 per cent neither greater than 6%. In order to avoid congestion, the practical upper limit would be 4%. Provided vertical reinforcement is 2% of gross area = 9800 mm²
Provide 20 bars of 25 mm diameter equally distributed on the four sides of section.
- 9.4.5 Boundary elements where required as 9.4.1, shall be provided with special confining reinforcement as is required for column in IS 13920: 1993. Detailing in the adjacent columns of OK shear wall or boundary element is accorded to IS 13920: 1993

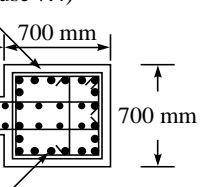
22.5 DETAILING OF REINFORCEMENTS

Details of longitudinal and transverse reinforcement in columns as special confining reinforcement requirements of IS 13920: 1993 (Clause 7.4)



20 longitudinal bar of 25 mm diameter (equally distributed on the four sides of section)

Details of longitudinal and transverse reinforcement in columns as special confining reinforcement requirements of IS 13920: 1993 (Clause 7.4)



8 mm diameter bar at 130 c/c in 2 curtains as horizontal and vertical reinforcement

20 longitudinal bar of 25 mm diameter (equally distributed on the four sides of section)

Reinforcement details in reinforced concrete shear wall

SUMMARY

Multi-storeyed reinforced concrete building frame with shear walls (*dual system*) are now fast becoming as popular as an alternate structural form for resisting the earthquake forces. However, the design of a dual system always requires special consideration for distribution of lateral forces between frames and shear walls. The aim of this chapter is to illustrate a *simple* procedure for the distribution of lateral forces in shear wall and frame. A two-dimensional rigid link model has been discussed in which shear wall is modelled as a wide column connected with frame by rigid link. Seismic design procedure of a shear wall has also been presented by considering each clause as mentioned in IS 13920: 1993 with the help of a worked out example for a 14-storeyed reinforced concrete building.

REFERENCES

- [1] AFM 88-3. "Seismic Design for Buildings", *Technical Manual of Army TM 5-809-10, Navy Navfac P-355 and Air Force*, Department of the Army, the Navy, and the Air Force, Washington, 1992.
- [2] IS 1893, *Criteria for Earthquake Resistant Design of Structures—Part 1: General Provisions and Buildings* (Fifth Revision), Bureau of Indian Standards, New Delhi, 2002.
- [3] IS 13920, *Ductile Detailing of Reinforced Concrete Structures Subjected to Seismic Force*, Bureau of Indian Standards, New Delhi, 1993.
- [4] IS 456, *Plain and Reinforced Concrete—Code of Practice*, Bureau of Indian Standards, New Delhi, 2000.
- [5] Medhekar, M.S. and Jain, S.K., "Seismic Behaviour Design and Detailing of RC Shear Walls, Part 1: Behaviour and Strength", *Indian Concrete Journal*, Vol. 67, No. 7, pp. 311–318, 1993.
- [6] Medhekar, M.S. and Jain, S.K., "Seismic Behaviour Design and Detailing of RC Shear Walls—Part II: Design and Detailing", *Indian Concrete Journal*, Vol. 67, No. 9, pp. 451–457, 1993.
- [7] Naeim Farzad, *The Seismic Design Handbook*, 2nd ed., Kluwer Academic Publisher, The Netherlands, 2001.
- [8] SP 16, *Design Aids for Reinforced Concrete to IS: 456–1978*, Bureau of Indian Standards, New Delhi, 1980.
- [9] SP 34, *Handbook on Concrete Reinforcement and Detailing*, Bureau of Indian Standards, New Delhi, 1987.

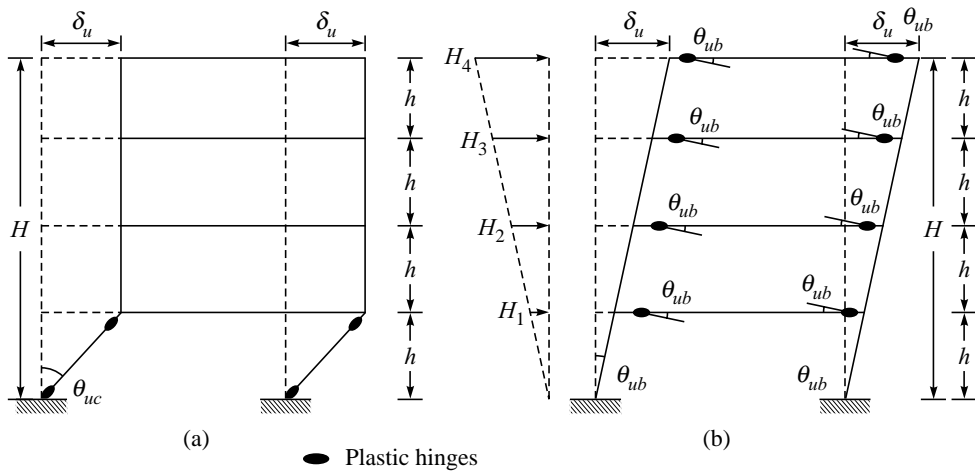
Chapter 23

Capacity Based Design—An Approach for Earthquake Resistant Design of Soft Storey RC Buildings

23.1 INTRODUCTION

The basic concept of *capacity design of structures* is the spreading of inelastic deformation demands throughout the structures in such a way that the formation of plastic hinges takes place at predetermined positions and sequences. *In other words, the capacity design is based on deterministic allocation of strength and ductility in the structural elements for successful response and collapse prevention during a catastrophic earthquake by rationally choosing the successive regions of energy dissipation so that predecided energy dissipation mechanism would hold throughout the seismic action.* The reason to name the capacity design is that, in the yielding condition, the strength developed in weaker member is related to the capacity of the stronger member.

In multi-storey reinforced concrete buildings this can be achieved by formation of plastic hinges at the end regions of nearly all the beams in all stories of the building while vertical members (columns and walls) remain essentially elastic in all stories, with the exception of the base of the bottom storey (Figure 23.1). This will provide a strong column–weak beam structure by eliminating the possibility of column sway mechanism (soft storey) of building and avoiding shear failures in columns and beams (CEB, 1998). This chapter will illustrate the capacity design procedure for a multi-storey building frame with the help of an example.



$$\theta_{ub,req} = \frac{\delta_u}{H} \quad \theta_{uc,req} = \frac{\delta_u}{h} \text{ for same } \delta, \theta_{uc,req} \gg \theta_{ub,req}$$

FIGURE 23.1 Capacity based design concept: change of failure mechanism from (a) Storey mechanism (b) Beam mechanism.

23.2 PRELIMINARY DATA FOR (G+3) PLANE FRAME

A four-storeyed (G+3) reinforced concrete plane frame, as shown in Figure 23.2, has been designed on the concept of capacity based. The assumed data for the analysis of frame are given in Table 23.1.

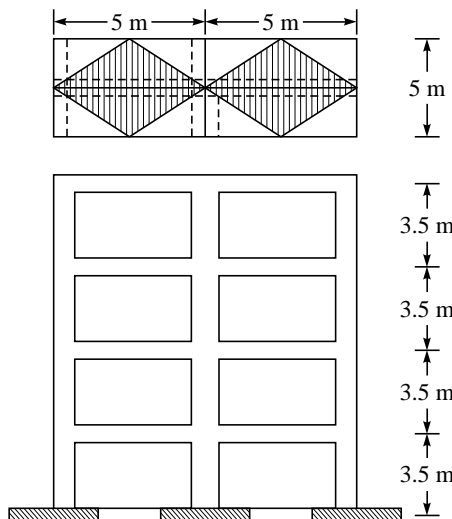


FIGURE 23.2 Plan and elevation of G+3 plane frame.

TABLE 23.1 Preliminary data for G+3 plane frame

1 Type of structure	Multistorey rigid jointed plane frame
2 Zone	V
3 Number of stories	(G+3)
4 Imposed load	2 kN/m ² at roof and 4 kN/m ² at floors
5 Terrace water proofing (TWF)	1.5 kN/m ²
6 Floor finishes	0.5 kN/m ²
7 Depth of slab	120 mm
8 Materials	M 20 concrete and Fe 415 steel
9 Unit weight of RCC	25 kN/m ³
10 Unit weight of masonry	20 kN/m ³
11 Modulus of elasticity of concrete	2.23×10^7 kN/m ²
12 Bay width of plane frame	5 m
13 Total height of building frame	14 m
14 Height of storey	3.5 m
15 Beams	300 × 450 mm
16 Columns	300 × 450 mm (outer) in upper floors 300 × 500 mm (internal) in upper floors 300 × 550 mm (outer) in ground floor 300 × 650 mm (internal) in ground floor
17 Clear cover of beam	25 mm
18 Clear cover of column	40 mm
19 Seismic coefficient A_h	0.09
$Z = 0.36, I = 1, R = 5$ (SMRF)	$A_h = (Z/2) (I/R) (S_a/g)$
$S_a/g = 2.5$ ($T = 0.09h/\sqrt{d} = 0.09 \times 14/\sqrt{10}$ $= 0.3984$ sec)	$A_h = (0.36/2) (1/5) (2.5) = 0.09$

23.2.1 Determination of Loads

Dead load calculations

The dead loads on various beams and columns in the frame are calculated according to yield line theory and shown in Figure 23.3.

Dead load at roof level

Weight of slab

Total intensity of load of slab including floor finish and terrace waterproofing = $(0.12 \times 25 + 1.5 + 0.5) = 5$ kN/m²

Loading on beams

- (a) Slab load on beam = 25 kN/m.
- (b) Self-weight of beam = 2.475 kN/m.

Dead load at floor level

Weight of slab

Total intensity of load of slab including floor finish = $(0.12 \times 25 + 0.5) = 3.5$ kN/m².

Loading on beams

- (a) Slab load on beam = 17.5 kN/m.
- (b) Self-weight of beam = 2.475 kN/m.
- (c) Weight of wall = 14.03 kN/m

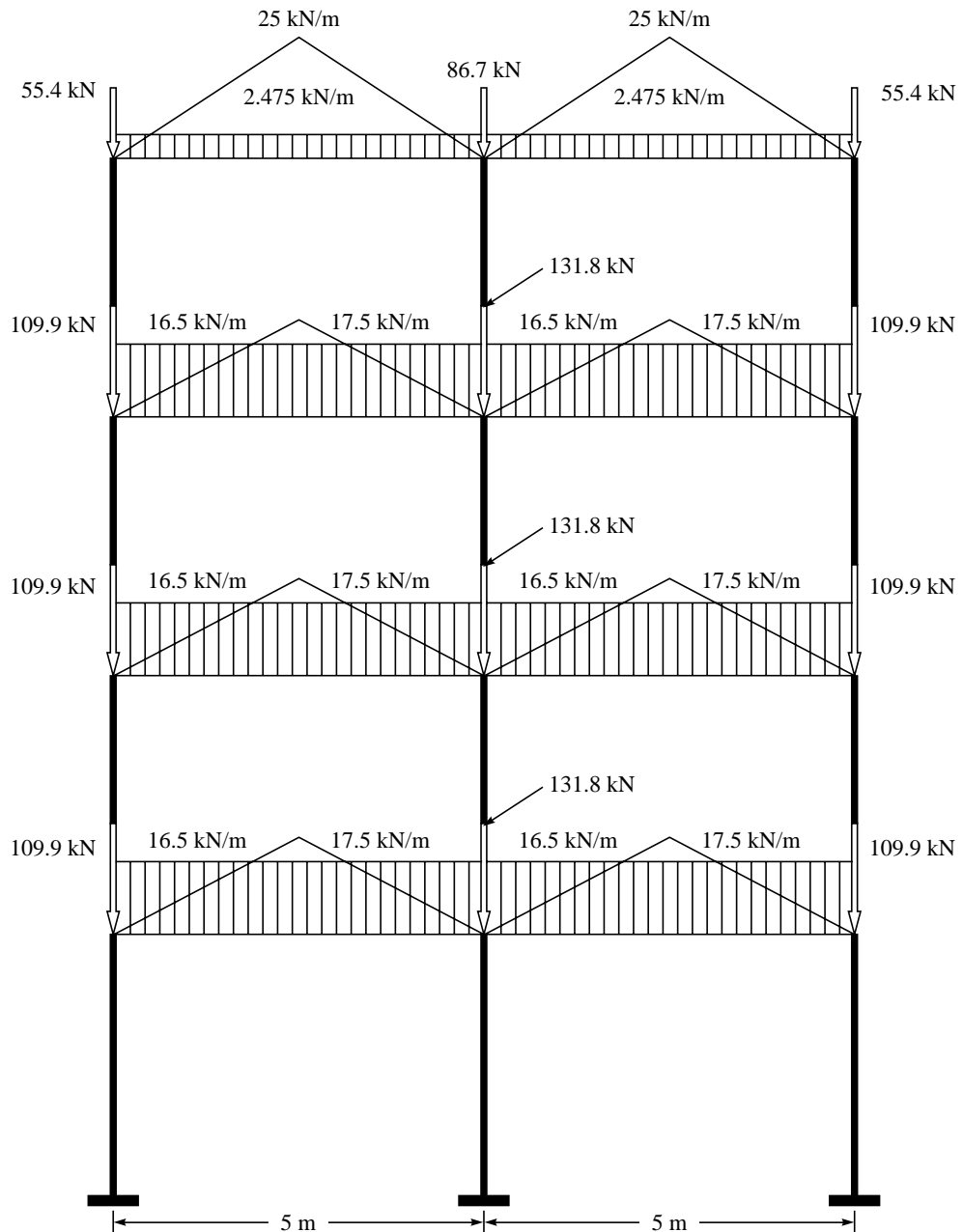


FIGURE 23.3 Dead load on G+3 plane frame.

Loading on columns

(Self-weight of slab as point load on column from transverse beams, self-weight of transverse beams, column self-weight)

Loading on columns

(Self-weight of slab as point load on column from transverse beams, self-weight of transverse beams, column self-weight)

- (a) Slab load of 62.5 kN on middle column and 31.25 on each end column.
- (b) Beam load of 12.375 kN on middle column and end columns.
- (c) Column self-weight 11.8125 kN
- (a) Slab load of 43.75 kN on middle column and 21.875 on each end column.
- (b) Beam self-weight of 12.375 kN on middle column and end columns.
- (c) Column self-weight 11.8125 kN
- (d) Wall load of 63.84 kN on each column

Live load calculations

The live loads on various beams and columns in the frame are calculated according to yield line theory and is shown in Figure 23.4. The intensity of imposed loading (live load) has been considered as per IS 1893 (Part 1): 2002.

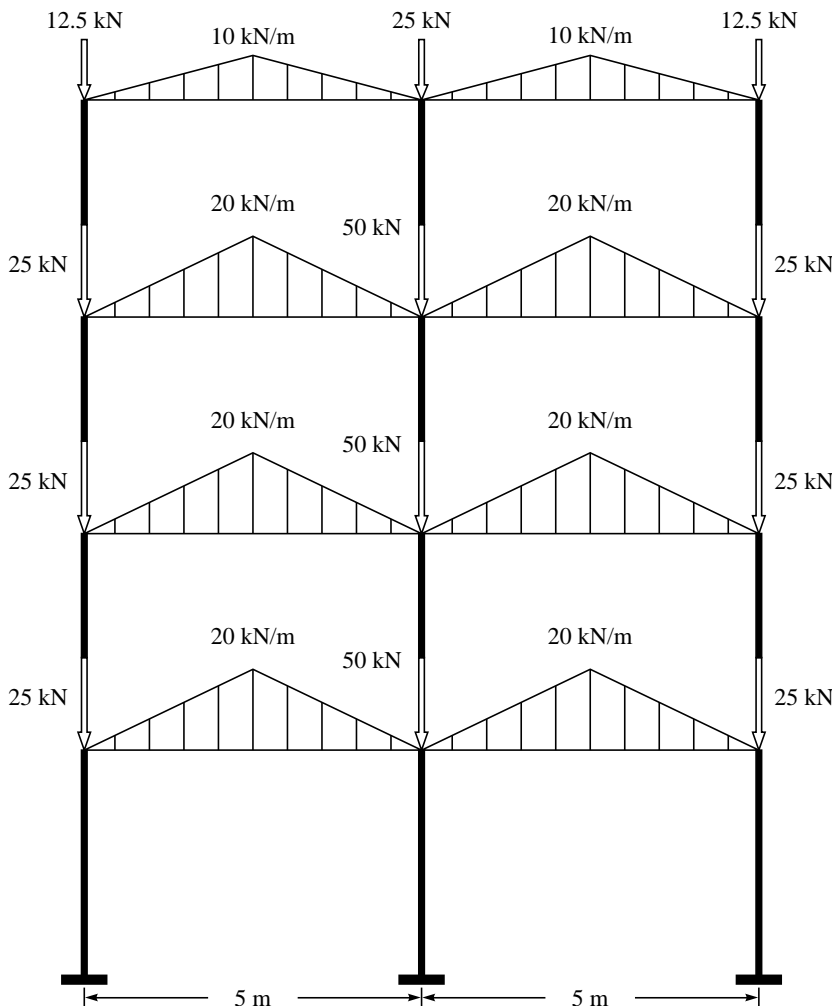


FIGURE 23.4 Live load on G+3 plane frame.

Live load (Imposed) at roof level

Intensity of live load = 2 kN/m²

Loading on beams

Slab live load = 10 kN/m.

Loading on columns

Live load from slab is 25 kN on middle column and 12.5 kN on each end column

Live load (Imposed) at floor level

Intensity of live load = 4 kN/m².

Loading on beams

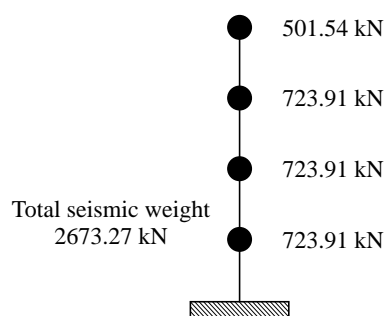
Slab live load on beam = 20 kN/m.

Loading on columns

Live load from slab is 50 kN on middle column and 25 kN on each end column

Earthquake load calculations

Seismic weight lumped at each storey is shown in Figure 23.5. Seismic base shear has been calculated from seismic coefficient method (\bar{V}_B) and response spectrum method (V_B) as per IS 1893 (Part 1): 2002.



	<i>Seismic weight</i>	<i>At roof</i>		<i>At floor</i>	
Imposed load		0	kN	104.5	kN
Dead loads					
Slab weight	261.25	kN		182.75	kN
Beam weight	62.98	kN		62.98	kN
Column weight	17.72	kN		35.437	kN
Wall weight	159.6	kN		338.12	kN
Total weight	501.54	kN		723.912	kN

FIGURE 23.5 Seismic weight lumped to storey levels

Total seismic weight = 2673.27 kN

Base shear from seismic coefficient (\bar{V}_B) = $A_h \cdot W = 0.09 \times 2673.27 = 240.60$ kN

Base shear from response spectrum analysis (V_B) = 162.524 kN

$$\bar{V}_B/V_B = 1.48$$

23.3 STEP-BY-STEP PROCEDURE FOR CAPACITY BASED DESIGN

23.3.1 Step 1: Seismic Analysis of Frame (G+3)

Seismic analysis of the plane frame is carried out with all load combinations as per IS 1893 (Part 1): 2002. The maximum interaction effect for columns and maximum force for beams from all load combinations for each member is considered for design. Design forces in columns and beams are presented in Figures 23.6 and 23.7. In capacity based design, beams are designed similar to normal design procedure for the calculated forces by the linear elastic analysis for different load combinations. Figure 23.8 shows the actual amount of longitudinal reinforcement provided in the beams.

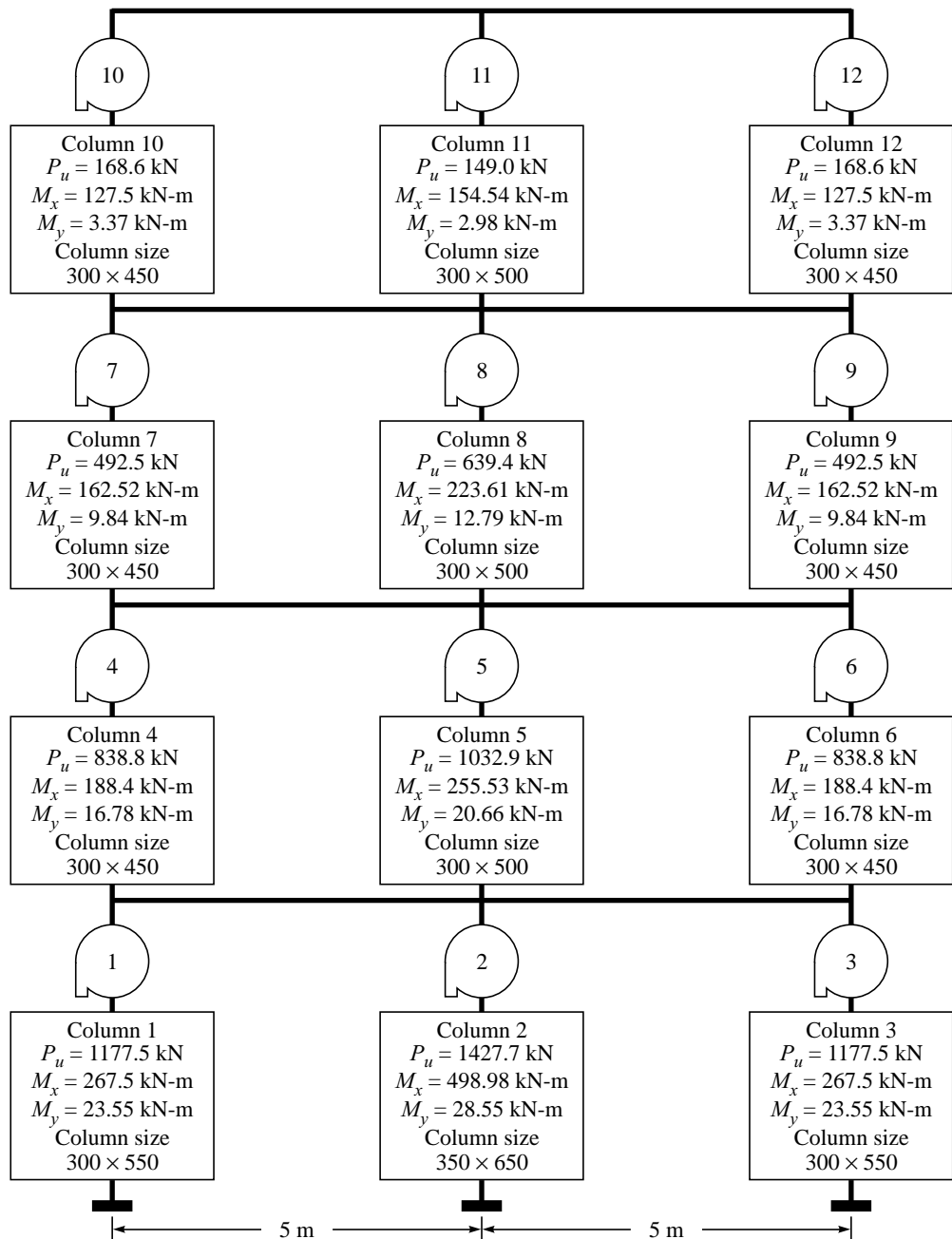


FIGURE 23.6 Design axial and biaxial bending forces for maximum interaction ratio of columns from all load combinations.

The design forces of columns are not completely based on linear elastic analysis, rather they depend upon the actual flexural capacities of the beams framing into the same joint. So

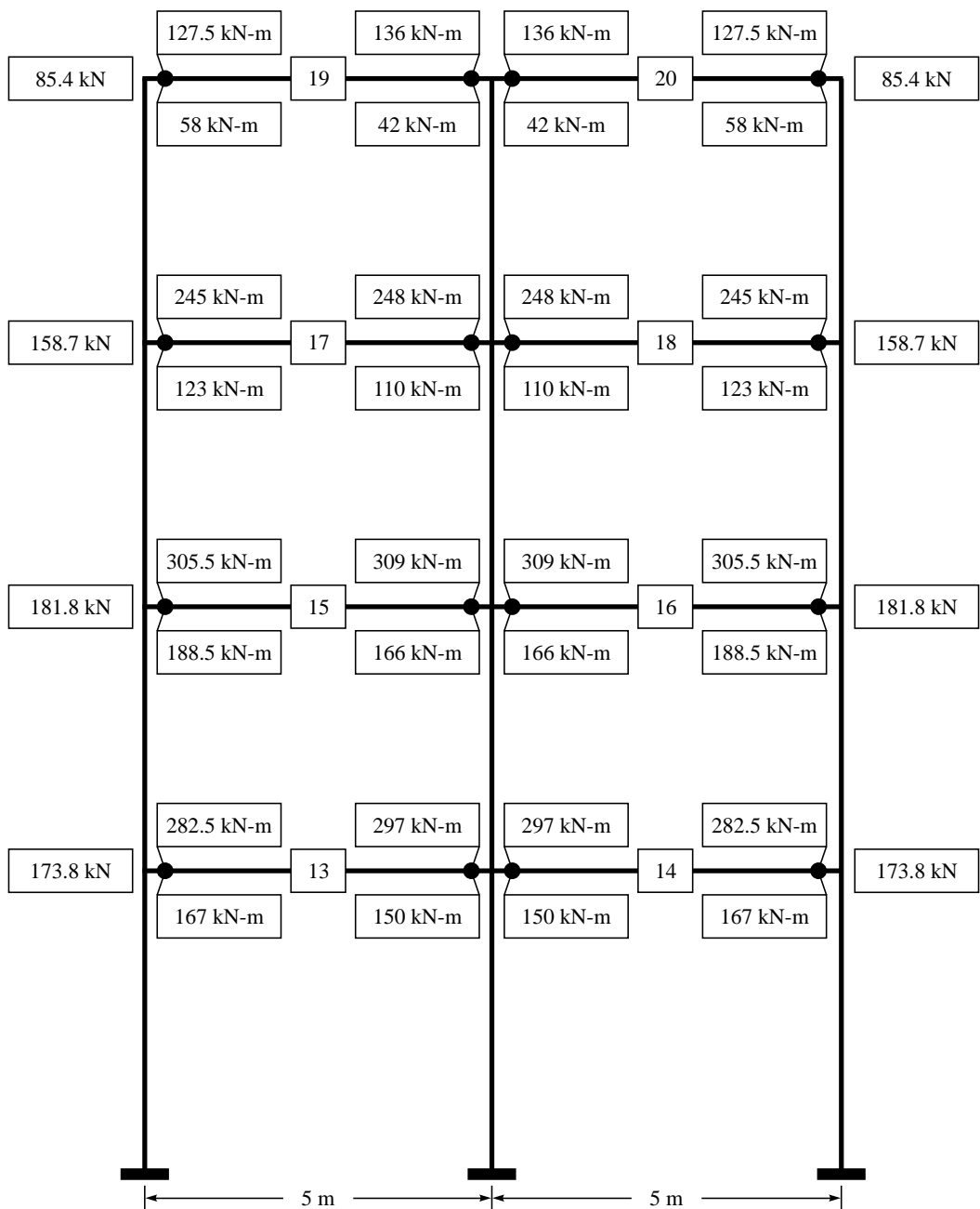


FIGURE 23.7 Maximum design shear, maximum hogging and sagging bending moment of beams in all load combinations.

that plastic hinges may not form at the base of the column above and at the top of the column below the joint (except at the base of the column of a ground storey).

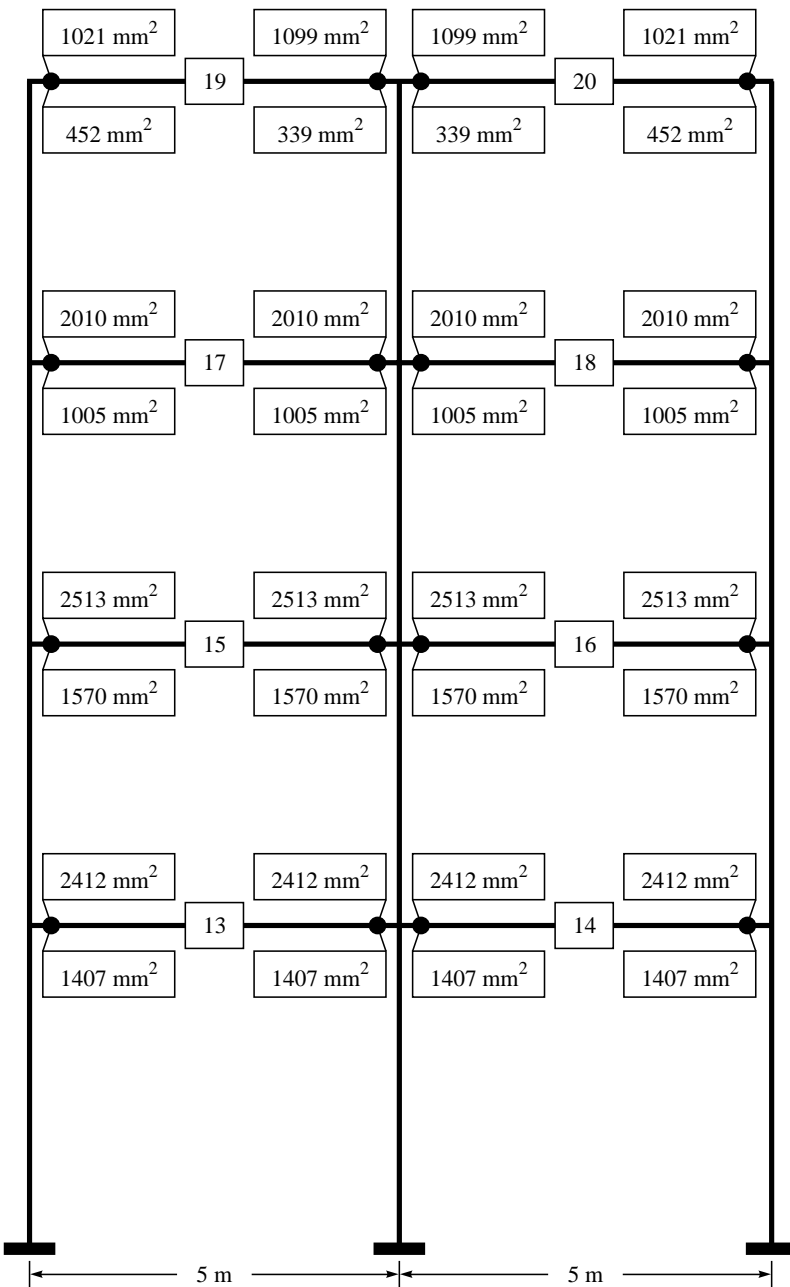


FIGURE 23.8 Provided top and bottom reinforcement in beams for the design forces.

23.3.2 Step 2: Determination of Flexural Capacity of Beams

The flexural capacities of the beams under hogging and sagging condition for the provided

reinforcement are shown in Figure 23.9. An example of calculations for determining the flexural capacities of beam is presented in Appendix 1.

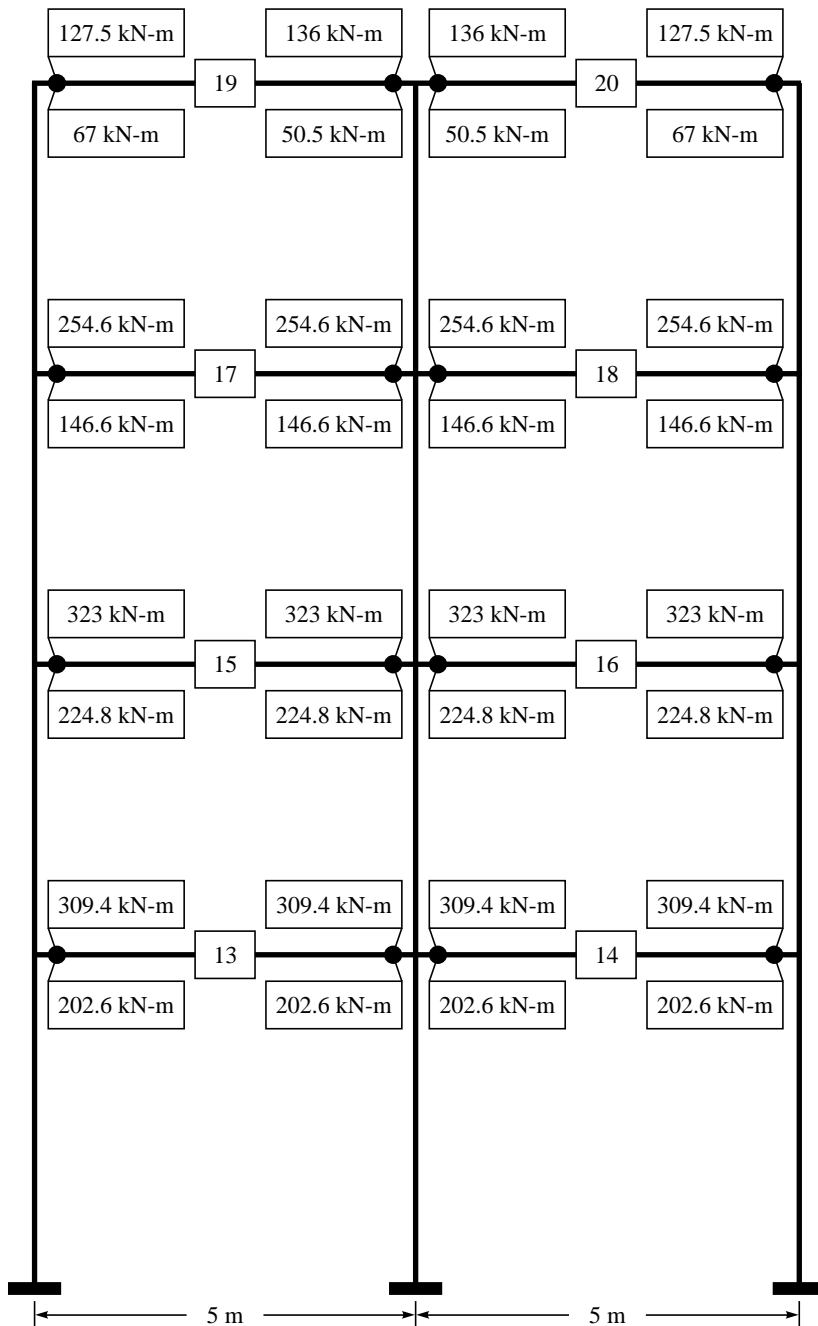


FIGURE 23.9 Flexural capacities of beams as per provided reinforcement, hogging (above) and sagging (below).

23.3.3 Step 3: Establishing a Strong Column–Weak Beam Mechanism

To eliminate the possibility of a column sway mechanism (soft storey) during the earthquake, it is essential that the plastic hinges should be formed in beams (except at the base of the columns of ground storey). This condition can be achieved after moment capacity verification of columns with beams at every joint of the frame with the formation of beam mechanism only. The deformational capacities of beams and the initial design capacities of columns for seismic action in one direction are shown in Figure 23.10. The amount by which the design moments of columns at a joint, to be magnified, is achieved by the determination of the magnification factor at that particular joint. The procedure for determining the moment magnification factor at a joint is illustrated in Appendix 2 and the values of moment magnification factor for each joint is given in Table 23.2.

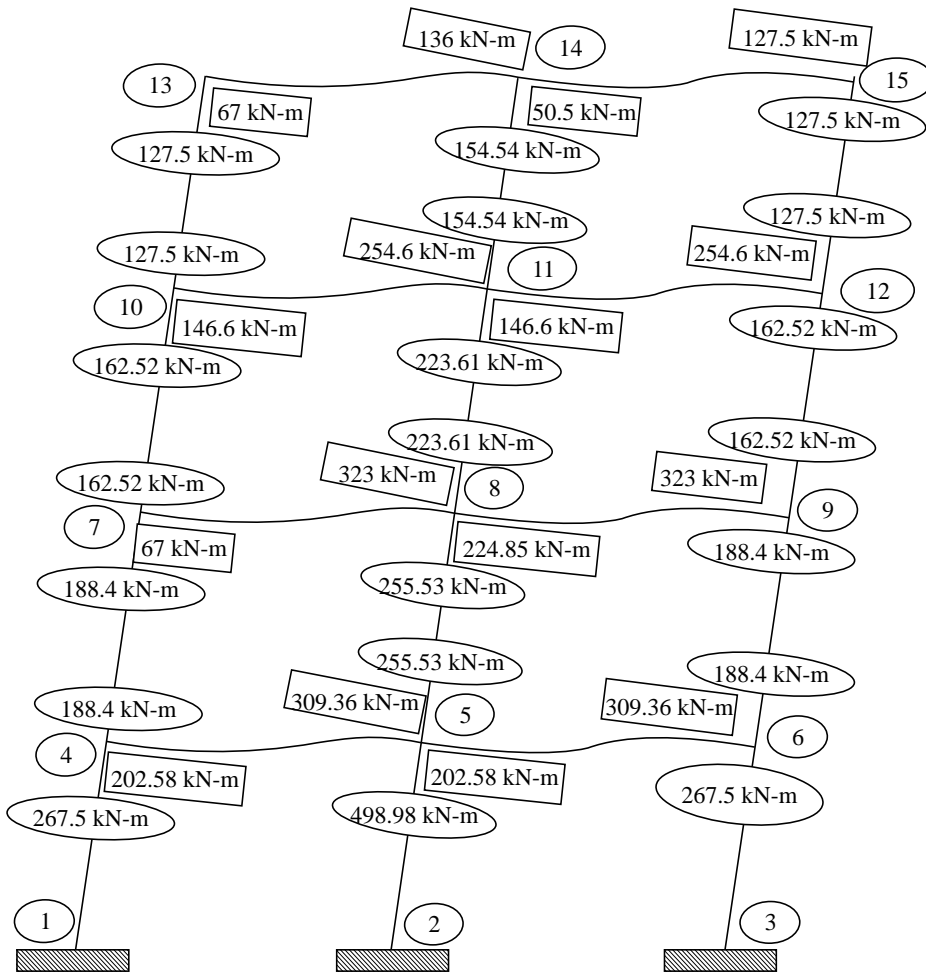


FIGURE 23.10 Deformational capacities of columns and beams at every joint in seismic direction 2.

TABLE 23.2 Determination of moment magnification factors at all joints

Joint no.	Seismic direction	Sum of resisting moments of top and bottom columns at joint (1)	Sum of resisting moments of left and right beams at joint with an overstrength factor of 1.35 (2)	Check for (1) \geq (2)	Moment magnification factor α_{cd}
13,15	1	(0+127.5)=127.5	1.35(0+67.09)=90.57	OK	1
	2	(0+127.5)=127.5	1.35(0+127.5)=172.12	Not OK	1.35
14	1	(0+154.54)=154.54	1.35(136+50.50)=251.77	Not OK	1.63
	2	(0+154.54)=154.54	1.35(136+50.50)=251.77	Not OK	1.63
10,12	1	(127.5+162.52)=290.02	1.35(0+146.59)=197.89	OK	1
	2	(127.5+162.52)=290.02	1.35(0+254.62)=343.73	Not OK	1.185
11	1	(154.54+223.61)=378.15	1.35(254.62+146.59)=541.63	Not OK	1.432
	2	(154.54+223.61)=378.15	1.35(254.62+146.59)=541.63	Not OK	1.432
7,9	1	(162.52+188.4)=350.92	1.35(0+224.85)=303.54	OK	1
	2	(162.52+188.4)=350.92	1.35(0+323)=436.05	OK	1.242
8	1	(223.61+255.53)=479.14	1.35(323+224.85)=739.59	Not OK	1.543
	2	(223.61+255.53)=479.14	1.35(323+224.85)=739.59	Not OK	1.543
4,6	1	(188.4+267.5)=455.9	1.35(0+202.58)=273.48	OK	1.0
	2	(188.4+267.5)=455.9	1.35(0+309.36)=417.63	OK	1.0
5	1	(255.53+498.98)=754.5	1.35(309.36+202.58)=691.12	OK	1.0
	2	(255.53+498.98)=754.5	1.35(309.36+202.58)=691.12	OK	1.0

23.3.4 Step 4: Determination of Moment Magnification Factors for Columns

As per Table 23.2, the moment capacities of columns are to be checked for the sum of the moment capacities of beams at the joint with an over strength factor of 1.35 (adopted from Euro code, EC 8). If the “sum of capacities of columns” is less than the “sum of moment capacities of beams multiplied by over strength factor”, the column moments should be magnified by the factor by which they are lacking in moment capacity over beams. If the sum of column moments is greater than sum of beam moments, there is no need to magnify the column moments. In such cases the multiplying factor is taken as unity. After obtaining the moment magnification factors, the column flexural strengths are to be increased accordingly at every joint and the maximum revised moment from the top and bottom joints to be taken for design. The calculations are shown in Figure 23.11. The column is to be designed for the magnified moment and the axial load coming on to the column from analysis as given in Table 23.3.

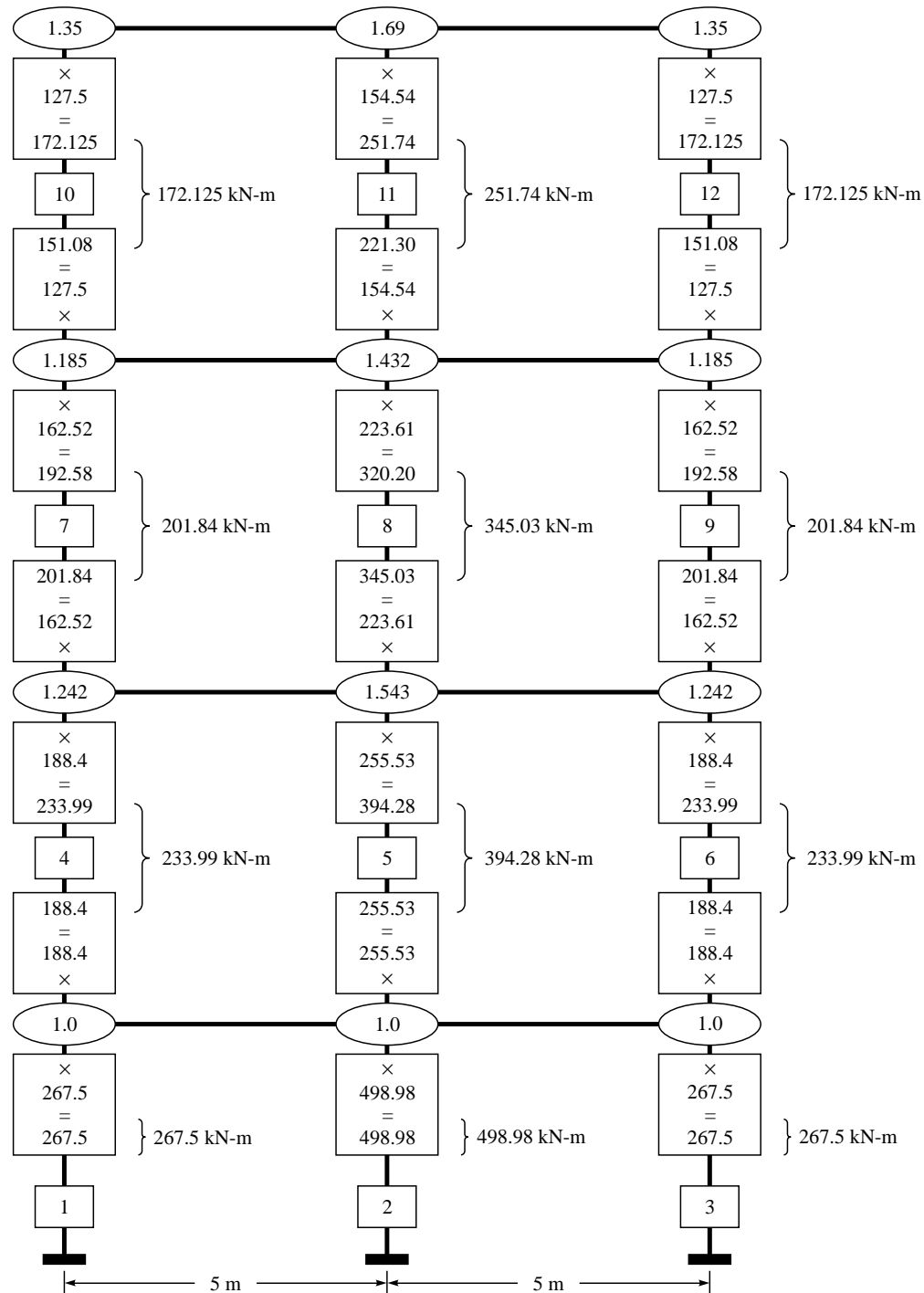


FIGURE 23.11 Revision of column moments according to capacity based design by moment magnification factor.

TABLE 23.3 Revised design capacities of columns

Storey No.	Column No.	Size (mm × mm)	Final Design				%steel interaction ratio
			Axial load P_{uz} (kN)	M_x M_{ux} (kNm)	M_y M_{uy} (kNm)		
4	10, 12	300 × 450	168.6	172.12	3.37	2.327	0.90
4	11	300 × 500	149	251.74	2.98	2.513	0.97
3	7, 9	300 × 450	492.5	210.84	9.84	2.793	0.97
3	8	300 × 500	639.4	345.03	12.79	3.77	1.00
2	4, 6	300 × 450	838.8	233.99	16.78	3.258	1.00
2	5	300 × 500	1032.9	394.28	20.66	4.608	1.00
1	1, 3	300 × 550	1177.5	267.5	23.55	2.437	1.00
1	2	350 × 650	1427.7	498.98	28.55	2.486	1.00

23.3.5 Step 5: Capacity Design for Shear in Beams

The design shear forces in beams are corresponding to the equilibrium condition of the beam under the appropriate gravity load (permanent dead load + % of live load) and to end resisting moments corresponding to the actual reinforcement provided, further multiplied by a factor γ_{Rd} , (Figure 23.12). This γ_{Rd} -factor compensates the partial safety factor γ_s applied to yield strength of steel and to account the strain hardening effects. In the absence of more reliable data, γ_{Rd} may be taken as 1.25.

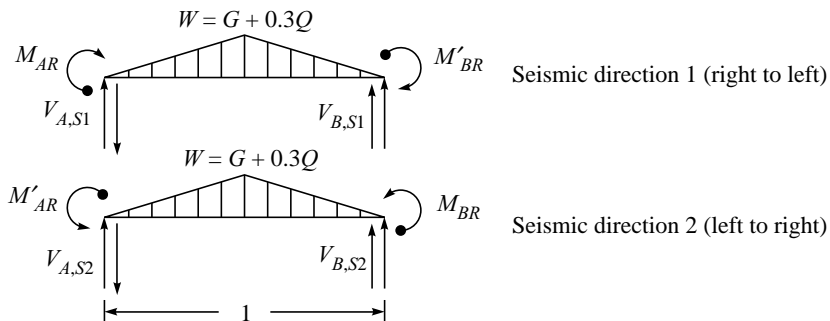


FIGURE 23.12 Equilibrium condition for the determination of shear force (Penelis and Kappos, 1997).

where, M_{AR} , M'_{AR} , M_{BR} , M'_{BR} are the actual resisting moments at the hinges accounting for the actual area of the reinforcing steel (all positive) and γ_{Rd} the amplification factor taking into account the reduced probability that all end cross sections exhibit simultaneously the same overstrength. G , dead load, Q , live load acting on the beam.

$$V_{A,S1} = \frac{wl}{2} - \gamma_{Rd} \left(\frac{M_{AR} + M'_{BR}}{l} \right), V_{B,S1} = \frac{wl}{2} + \gamma_{Rd} \left(\frac{M_{AR} + M'_{BR}}{l} \right) \dots \text{direction 1}$$

$$V_{A,S2} = \frac{wl}{2} + \gamma_{Rd} \left(\frac{M'_{AR} + M_{BR}}{l} \right), V_{B,S2} = \frac{wl}{2} + \gamma_{Rd} \left(\frac{M'_{AR} + M_{BR}}{l} \right) \dots \text{direction 2}$$

Design shear force for **Beams 13 and 14** in seismic directions 1 and 2 are calculated as

$$V_{A,S1} = \frac{141.5}{2} - 1.25 \left(\frac{202.58 + 309.36}{5} \right) = -57.235 \text{ kN}$$

$$V_{B,S1} = \frac{141.5}{2} + 1.25 \left(\frac{202.58 + 309.36}{5} \right) = 198.735 \text{ kN}$$

$$V_{A,S2} = \frac{141.5}{2} + 1.25 \left(\frac{309.36 + 202.58}{5} \right) = 198.735 \text{ kN}$$

$$V_{B,S2} = \frac{141.5}{2} - 1.25 \left(\frac{309.36 + 202.58}{5} \right) = -57.235 \text{ kN}$$

Similarly the capacity design shear forces for other beams and their shear reinforcement are given in Table 23.4.

TABLE 23.4 Capacity based shear and shear reinforcement for beams

Beam No.	Seismic direction 1 kN	Seismic direction 2 kN	Maximum shear kN	Shear reinforcement (IS 13920:1993)
13,14	-57.23	198.735	198.735	8 mm @ 104 mm c/c
	198.735	-57.235		
15,16	-66.21	207.71	207.71	8 mm @ 103 mm c/c
	207.71	-66.21		
17,18	-29.55	-29.55	171.05	8 mm @ 104 mm c/c
	171.05	171.05		
19,20	-9.58	85.68	91.95	6 mm @ 100 mm c/c
	91.957	-3.31		

23.3.6 Step 6: Capacity Design for Shear in Columns

Capacity design shear forces are evaluated by considering the equilibrium of the column under the actual resisting moments at its ends, as shown in Figure 23.13.

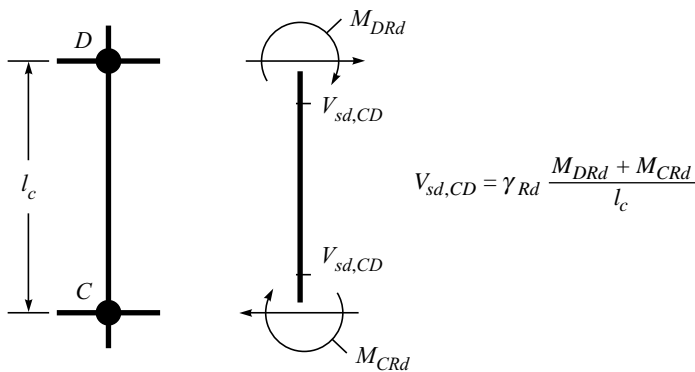


FIGURE 23.13 Capacity design values of shear forces acting on columns (Penelis and Kappos, 1997).

where, M_{DRd} and M_{CRd} are the flexural capacities of the end sections as detailed (the earthquake action has to be considered with both signs), l_c is the clear height of the column and $\gamma_{Rd} = 1.35$

Calculated capacity based design shear forces in the columns of the plane frame are given in Table 23.5.

TABLE 23.5 Capacity based design shear in columns and design of lateral ties

Columns	Capacity based shear (kN)	Specially confining reinforcement
1,3	$1.35 ((267.50+267.5)/3.5) = 206.35$ kN	10 Φ @ 50 mm c/c upto l_o 10 Φ @ 150 mm c/c after l_o
2	$1.35 ((498.98+498.98)/3.5) = 384.92$ kN	10 Φ @ 100 mm c/c upto l_o 10 Φ @ 175 mm c/c after l_o
4,6	$1.35 ((233.99+233.99)/3.5) = 180.50$ kN	10 Φ @ 45 mm c/c upto l_o 10 Φ @ 150 mm c/c after l_o
5	$1.35 ((394.28+394.28)/3.5) = 304.15$ kN	10 Φ @ 45 mm c/c upto l_o 10 Φ @ 150 mm c/c after l_o
7,9	$1.35 ((201.84+201.84)/3.5) = 155.70$ kN	10 Φ @ 45 mm c/c upto l_o 10 Φ @ 150 mm c/c after l_o
8	$1.35 ((345.03+345.03)/3.5) = 266.16$ kN	10 Φ @ 48 mm c/c upto l_o 10 Φ @ 150 mm c/c after l_o
10,12	$1.35 ((172.12+172.12)/3.5) = 132.78$ kN	10 Φ @ 45 mm c/c upto l_o 10 Φ @ 150 mm c/c after l_o
11	$1.35 ((251.74+251.74)/3.5) = 194.20$ kN	10 Φ @ 48 mm c/c upto l_o 10 Φ @ 150 mm c/c after l_o

23.3.7 Step 7: Detailing of Reinforcements

The detailing of shear reinforcement for the whole frame is shown in Figure 23.14, special confining reinforcement requirements as per IS 13920:1993. The details of main reinforcement are not shown.

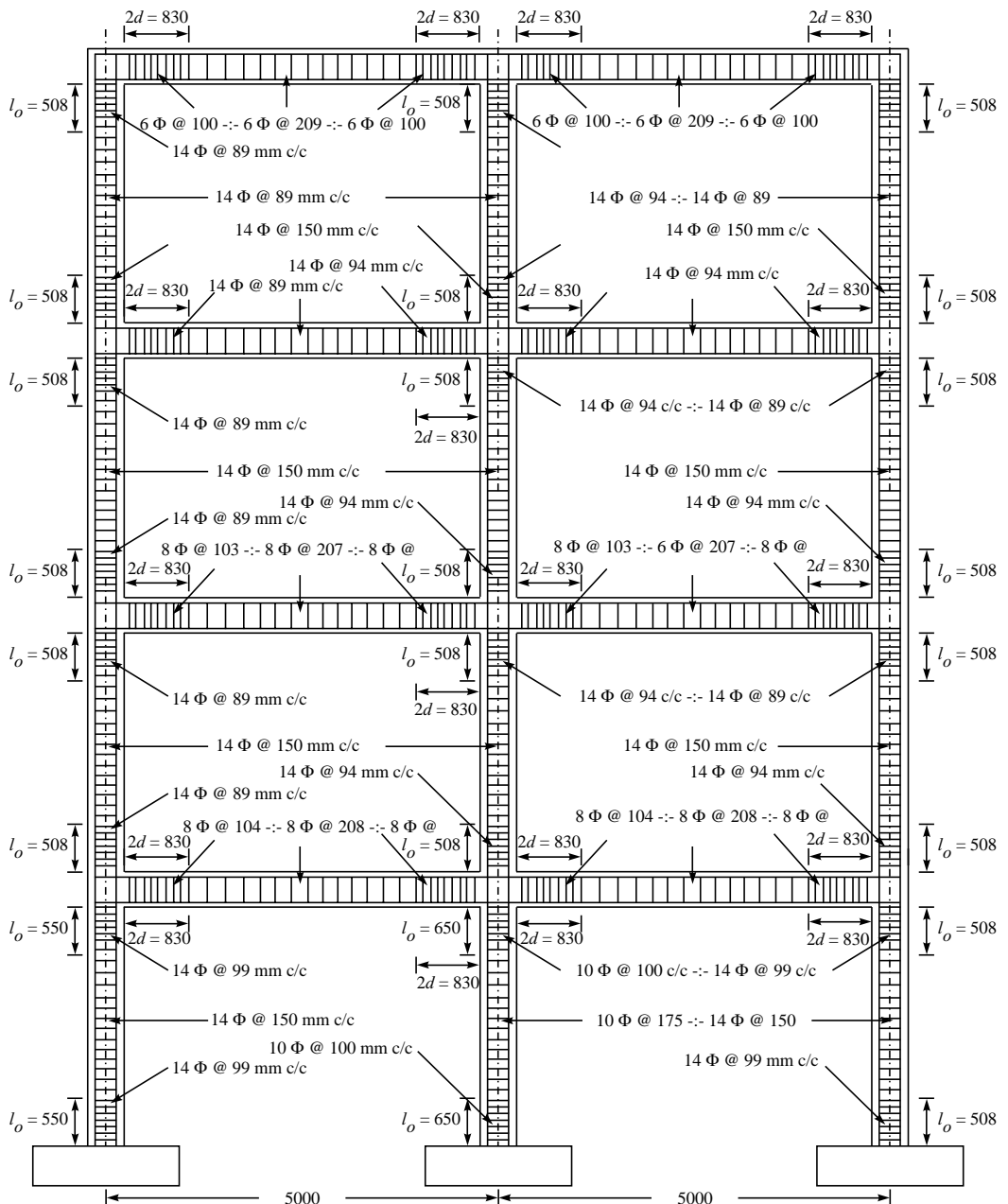


FIGURE 23.14 Detail of special confining reinforcement (shear) for the whole frame according to IS 13920:1993.

Appendix 1: Beam Flexural Capacity Calculation as per Design Aid IS 456: 1978

In hogging moment capacity calculation, the top face reinforcement in tension and bottom face reinforcement in compression, therefore hogging capacity of beam section will be calculated on the basis of rectangular section while in sagging capacity calculation, the top face reinforcement in compression and bottom face reinforcement in tension, flange action of the slab will also be taken into account. Hence sagging capacity of beam section will be calculated on the basis of T-section as shown in Figure A1.

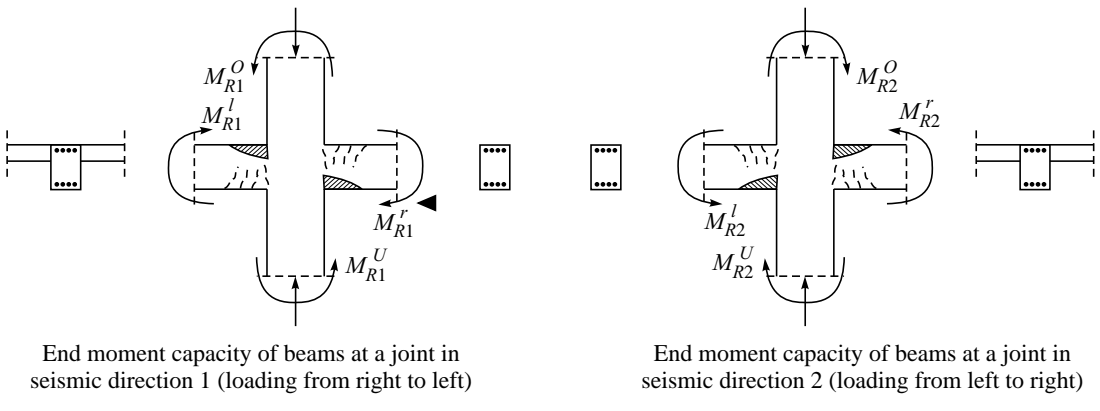


FIGURE A1 Moment capacity verification of columns at any joint in two seismic directions (Penelis and Kappos, 1997).

where, M_{R1}^O , M_{R1}^U , M_{R2}^O , M_{R2}^U are the design moments of the over and under columns at a joint before capacity revision, taking into account the axial load. M_{R1}^l , M_{R1}^r , M_{R2}^l , M_{R2}^r are the resisting moments of left and right beams at a joint in seismic directions 1 and 2.

Flexural capacity calculation of beam 13

Hogging moment capacity calculations

Provided top steel, 2412 mm², and bottom steel, 1407 mm². Beam dimensions: B = 300 mm, D = 450 mm, d = 450–25–8 = 417 mm

$$M_{ulim} = 0.36 \times \frac{X_{u\max}}{d} \left[1 - 0.42 \times \frac{X_{u\max}}{d} \right] bd^2 f_{ck}$$

$$= 143.942 \text{ kN}$$

Steel corresponding to M_{ulim} , is

$$A_{st1} = \frac{0.48 \times 0.36 \times 20 \times 300 \times 417}{0.87 \times 415}$$

$$= 1197.46 \text{ mm}^2$$

Sagging moment capacity calculations

The sagging action of beam near supports will cause the monolithically constructed slab to act as flange of T-beam, contributing additional compressive force, thus increasing the flexural capacity of the beam for the provided reinforcement.

$$A_{st} = 1407 \text{ mm}^2,$$

$$b_f = \frac{l_0}{6} + b_w + 6D_f$$

$$= \frac{0.7 \times 5000}{6} + 300 + 6 \times 120$$

$$= 1603 \text{ mm}$$

$$\text{Available } A_{st2} = A_{st} - A_{st1} = 2412 - 1197.46 \\ = 1215.3 \text{ mm}^2.$$

Additional moment capacity due to available compression steel

$$M_2 = A_{sc} \times f_{sc} (d-d')/10^6 \\ = 1407 \times 353(417-40)/10^6 = 187.24 \text{ kNm}$$

A_{st2} required for provided A_{sc} ,

$$(A_{sc} \times f_{sc})/(0.87 \times 415) \\ = (1407 \times 353)/(0.87 \times 415) \\ = 1375.62 \text{ mm}^2$$

But A_{st2} available is 1215.28 mm².

Therefore flexural moment contribution for 1215.28 mm² A_{st2} is

$$M_2 = 0.87 \times 415 \times A_{st2} \times (417 - 40)/10^6 \\ = 0.87 \times 415 \times 1215.3 \times (417 - 40)/10^6 \\ = 165.42 \text{ kNm}$$

Total hogging capacity of beam

$$M = M_U + M_2 = 143.942 + 165.42 \\ = 309.36 \text{ kNm}$$

For $X_u < D_f$, the moment of resistance of T-beam is given by the equation

$$X_u = \frac{0.87 \times f_y \times A_{st}}{0.36 \times f_{ck} \times b_f} \\ = \frac{0.87 \times 415 \times 1407}{0.36 \times 20 \times 1603} \\ = 44.01 \text{ mm}$$

Therefore $X_u < 120 \text{ mm}$

$$M_u = 0.87 \times 415 \times A_{st2} \times \\ d \left(1 - \frac{A_{st} \times f_y}{b_f \times d \times f_{ck}} \right) / 10^6 \\ = 0.87 \times 415 \times 1407 \times 417 \times \\ \left(1 - \frac{1407 \times 415}{1603 \times 417 \times 20} \right) / 10^6 \\ = 202.58 \text{ kNm}$$

Total sagging capacity of beam
 $M = 202.58 \text{ kNm}$

Appendix 2: Determination of Moment Magnification Factor at Every Joint

The sum of the resisting moments of the columns, taking into account the action of axial load, should be greater than the sum of the resisting moments of all adjacent beams for each (positive or negative) direction of the seismic action (Figure A1).

$$|M_{R1}^O| + |M_{R1}^U| \geq \gamma_{Rd} |M_{R1}^l| + |M_{R1}^r| \\ |M_{R2}^O| + |M_{R2}^U| \geq \gamma_{Rd} |M_{R2}^l| + |M_{R2}^r|$$

where γ_{Rd} is a factor which takes into account the variability of the yield stress f_y and the probability of strain hardening effects in the reinforcement (overstrength factor). It is taken as 1.35 according to EC8 for seismic Ductility Class High. Therefore, the capacity design is satisfied if the columns are designed for the following moments:

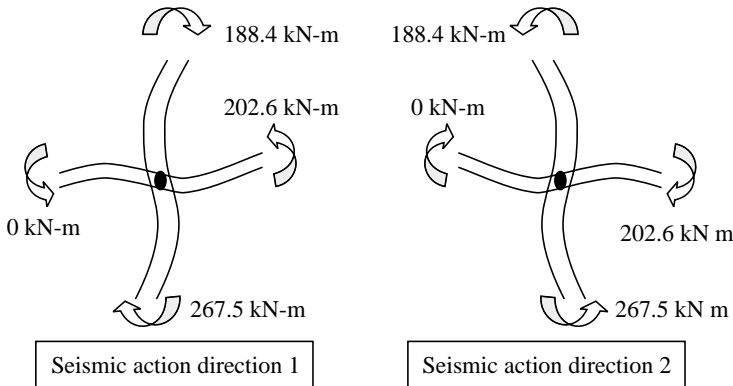
$$M_{S1,CD} = \alpha_{CD,1} M_{S1} \\ M_{S2,CD} = \alpha_{CD,2} M_{S2}$$

where

$$\alpha_{CD1} = \gamma_{Rd} \frac{|M_{R1}^l| + |M_{R1}^r|}{|M_{R1}^O| + |M_{R1}^U|}$$

$$\alpha_{CD2} = \gamma_{Rd} \frac{|M_{R2}^l| + |M_{R2}^r|}{|M_{R2}^o| + |M_{R2}^u|}$$

$M_{R1}^o, M_{R1}^u, M_{R2}^o, M_{R2}^u$ are the design moments of the over and under columns at a joint before capacity revision, taking into account the axial load. $M_{R1}^l, M_{R1}^r, M_{R2}^l, M_{R2}^r$ are the resisting moments of left and right beams at a joint in seismic directions 1 and 2. $\alpha_{CD1}, \alpha_{CD2}$ are the moment magnification factor in seismic directions 1 and 2 respectively. $M_{S1,CD}, M_{S2,CD}$ are the magnified column moments in seismic directions 1 and 2 respectively.



SUMMARY

The main cause of failure of multi-storey reinforced concrete buildings during seismic motion is the soft storey sway mechanism or column sway mechanism. If the structure is designed on strong column–weak beam concept, there are possibilities for eliminating a column sway mechanism. This procedure for design of structure is known as *Capacity Based Design*, which of course would be the future design philosophy for earthquake resistant building designs in India. In this chapter, a G+3 reinforced concrete frame building has been designed on the basis of capacity design by following IS 13920:1993. At present capacity based design concept is applied for the solution of a soft storey problem with a view to avoid the concentration of ductility demand in the soft storey elements by distributing it throughout the structure by proportionate design of strong column and weak beam structure.

REFERENCES

- [1] Armstrong, I.C., "Capacity Design of Reinforced Concrete Frames for Ductile Earthquake Performance", *Bulletin of the New Zealand Society for Earthquake Engineering*, Vol. 5, No. 4, December, 1972.
- [2] CEB, *Seismic Design of Reinforced Concrete Structures for Controlled Inelastic Response*, Thomas Telford, UK, 1998.

- [3] Chapman, H.E., North, P.J. and Park, R., "Capacity Design Principles and Practices", *Bulletin of the New Zealand National Society for Earthquake Engineering*, Vol. 13, No. 3, September, 1980.
- [4] Dadi, V.V.S., Surya Kumar, "Seismic Evaluation of Reinforced Concrete Building with Soft Storey", *M. Tech. Dissertation*, Department of Earthquake Engineering, IIT Roorkee, June 2004.
- [5] Eurocode 8, "Design of Structures for Earthquake Resistance—Part 1: General rules, Seismic actions and rules for Buildings", *CEN*, 2002.
- [6] IS 13920, *Ductile Detailing of Reinforced Concrete Structures Subjected to Seismic Forces—Code of Practice*, Bureau of Indian Standards, New Delhi, 1993.
- [7] IS 1893, *Criteria for Earthquake Resistant Design of Structures—Part 1: General Provisions and Buildings* (Fifth Revision), Bureau of Indian Standards, New Delhi, 2002.
- [8] NZS 3101, *Concrete Structures Standard*, Part 1—*The Design of Concrete Structures*, Standards New Zealand, Paerewa Aotearoa, 1995.
- [9] Paulay, T. and Goodisir, W.J., "The Capacity Design of Reinforced Concrete Hybrid Structures for Multistorey Buildings", *Bulletin of the New Zealand National Society for Earthquake Engineering*, Vol. 19, No. 1, March, 1986.
- [10] Penelis, G.G. and Kappos, A.J., "Earthquake-Resistant Concrete Structures", *E & FN SPON*, an Imprint of Chapman & Hall, 1997.

PART VI

Earthquake Resistant Design (ERD) of Masonay Buildings

Chapter 24

Identification of Damages and Non-damages in Masonry Buildings from Past Indian Earthquakes

24.1 INTRODUCTION

The masonry buildings have proved to be the most vulnerable to earthquake forces and have suffered maximum damage in past earthquakes. A survey of the affected areas in past earthquakes (Bhuj, 2001, Chamoli, 1999, Jabalpur, 1997, Killari, 1993, Uttarkashi, 1991 and Bihar-Nepal, 1988) has clearly demonstrated that the major loss of lives was due to collapse of low strength masonry buildings. The loss of lives could have been minimized upto optimum by making the buildings earthquake resistant. This requires diagnostic analysis of the structural behaviour of the 'As Built' condition of these constructions. Diagnostic studies are best achieved by dynamic testing of stereotyped, prototype buildings, which manifest their structural distress pattern, and verification upto its optimum limit. Each earthquake puts buildings in the affected area to an earthquake withstand test and provides an opportunity to learn lessons for future preparedness to meet the challenge of disaster. Thus, the efforts of post-earthquake damage survey should be directed to arrive at engineering lessons for improving earthquake resistant design and construction practice. This chapter is motivated towards the identification of typical features of damages and non-damages of masonry buildings during recent earthquakes in India. The experience and observations of damages and performance of structures in earthquakes with the results of earthquake engineering research must be utilized in improving earthquake resistant design and construction techniques of masonry buildings for preventing damages in future earthquakes.

24.2 PAST INDIAN EARTHQUAKES

The characteristic of past earthquakes where masonry construction is significantly damaged is described in Table 24.1. The table illustrates some parameters of earthquake and losses in terms

TABLE 24.1 Characteristics and damage statistics of earthquakes

<i>Earthquake parameters</i>	<i>Bhuj earthquake</i>	<i>Chamoli earthquake</i>	<i>Jabalpur earthquake</i>	<i>Killari earthquake</i>	<i>Uttarkashi earthquake</i>	<i>Bihar-Nepal earthquake</i>
<i>Date</i>	Jan. 26, 2001	March 29, 1999	May 22, 1997	Sept. 30, 1993	Oct. 20, 1991	Aug. 21, 1988
<i>Time</i>	08.46 hrs	00.35 hrs	4.21 hrs	3.56 hrs	2.53 hrs	4.54 hrs
<i>Epicentre</i>	23.40 N 70.34 E	30.429 N 79.228 E	23.083 N 80.081 E	18.22 N 76.356 E	30.75 N 78.68 E	26.4 N 86.6 E
<i>Focal depth</i>	18 km	21 km	36 km	5 to 15 km	15 km	20 km
<i>Magnitude</i>	7.7	6.8	6.0	6.4	6.6	6.5
<i>Max. intensity</i>	IX+	VIII+	VIII	VII+	VIII+	VIII+
<i>Duration</i>	17 to 23 sec	6 to 30 sec	15 to 30 sec	30 to 40 sec	45 sec	—
<i>Ground acc.</i>	0.106 g	0.35 g	—	0.2 g	0.52 g	0.10 g
<i>People died</i>	13,800	103	55	10,000	760	1000
<i>People injured</i>	1,67,000	400	1000	20,000	5000	9000
<i>House damage</i>	12,00,000	4500	45,000+	20,000+	80,000+	2,50,000

of life and property. The masonry construction without following the earthquake resistant features has been subjected to massive failure in earthquakes. The occurrence of disaster is dependent upon several parameters like: (i) magnitude of earthquake (ii) closeness of epicentre from urban area (iii) size and distribution of population (iv) provisions of earthquake resistant features (v) type and quality of construction and maintenance.

24.3 FEATURES OF DAMAGES AND NON-DAMAGES

The seismic performance of masonry buildings during the mentioned earthquakes is documented in reconnaissance reports (EERI, 2002; DEQ, 2000; DEQ, 1997, ISET, 1994; GSI, 1992; DEQ, 1988) from which a number of observations are summarized as follows:

24.3.1 Bhuj Earthquake, January 26, 2001

A massive earthquake of magnitude ($M_L = 6.9$ on Richter scale, $M_b = 7.0$, $M_S = 7.6$ and $M_W = 7.7$) occurred on the morning of 51st Republic day of India (January 26, 2001, Friday) at 08:46:42.9 hours (IST) as reported by Indian Meteorological Department (IMD), New Delhi. The epicentre of this earthquake was located near Bhachau (latitude 23.40 °N and longitude 70.28 °E), focal depth 25 km with radius of fault area 23 km. The major cities affected by the earthquake were Bhuj, Anjar, Bhachau, Gandhidham, Kandla Port, Morbi, Ahmedabad, Rajkot, Sardarnagar, etc., (Figure 24.1), where majority of the casualties and damages occurred.

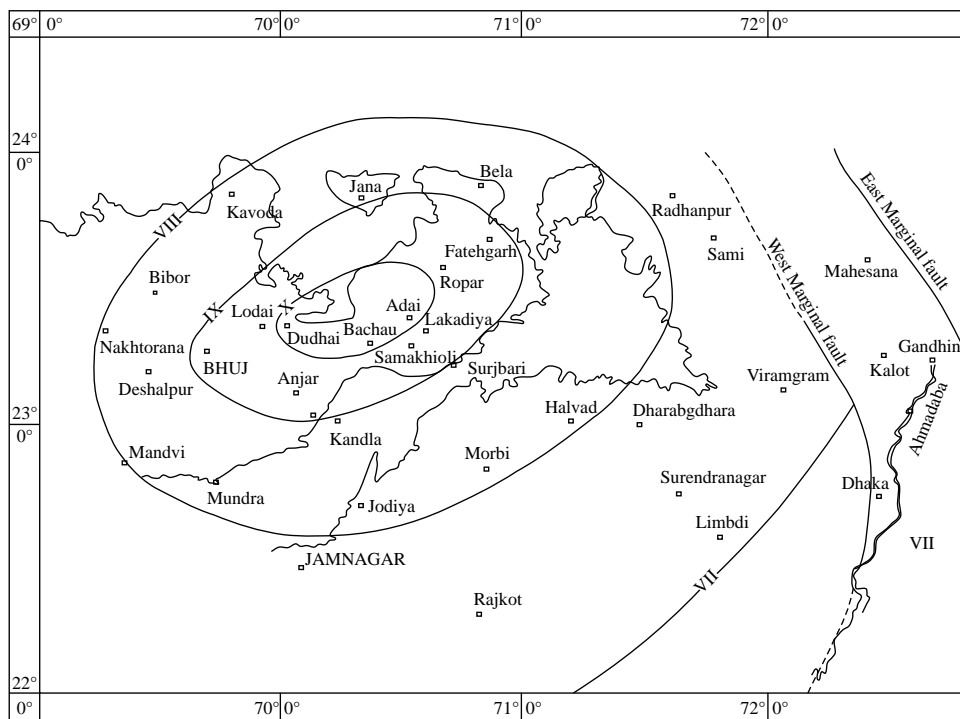


FIGURE 24.1 Isoseismal map of Bhuj Earthquake of January, 2001 (EERI, 2002).

Types of construction

Different types of masonry constructions have been observed in the earthquake-affected areas (Figure 24.2), which can be summarized as

- (a) Traditional earthen houses reinforced with wooden sticks and sun-dried clay brick (adobe) construction. Both the constructions were circular in plan of about 4–8 m diameter, locally called as *bhunga*. The walls were raised on a shallow foundation with a conical roof on top tied with ropes to form a thatch roof.
- (b) Rural village houses made up from random rubble masonry laid in lime/mud/cement mortar. The roof was covered with *Manglore* clay tiles. In urban areas houses were constructed with dressed stones/concrete blocks/sun-burnt clay bricks in cement mortar.



(a)



(b)

FIGURE 24.2 Traditional construction in Bhuj affected area (a) Arch type stone masonry (b) Details of wooden roof with joist and planks.

Types of damages and non-damages

Typical features of damages and non-damages in masonry buildings during Bhuj earthquake, 2001 are highlighted in Figure 24.3 and are summarized as follows:

- (a) Stone masonry houses in mud mortar without any earthquake resistant features as per IS: 4326, is the most common type of construction for economically weaker sections. These houses were mostly damaged during the earthquake due to lack of (i) structural integrity (no bands), (ii) positive mechanism of roofing system (no bottom tie member), (iii) connection between wall to roof (rafter rest directly on the wall), (iv) connection between wall to wall and within the two wythes of wall (no through stone).
- (b) Random rubble masonry in cement mortar with reinforced concrete slab used in the construction of single- or two-storeyed residential units with plinth and lintel band, performed very well. The wall roof interface had nominal sliding and separation, and the walls between plinth and lintel bands sustained shear cracks.
- (c) The seismic performances of clay brick masonry and cement block masonry have depended upon the earthquake resistant features. Bentonite factory building and stone block masonry with lintel bands, near Bhuj, escaped from damages.

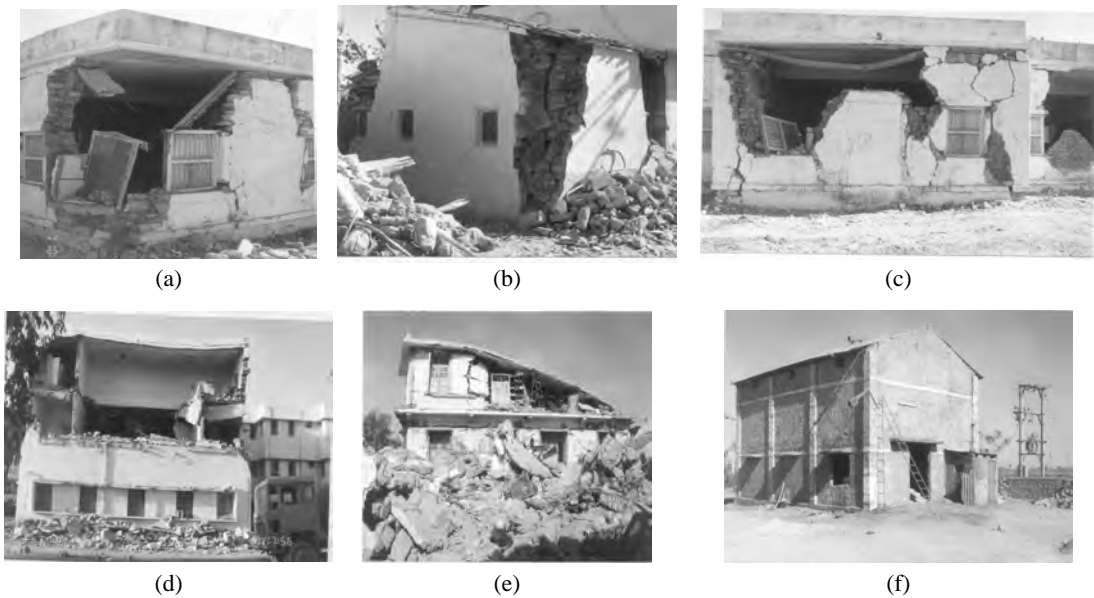


FIGURE 24.3 Typical features of damages and non-damages (a and b) Collapse of the corner zone (c) Out-of-plane collapse of a wall, in presence of an r.c. tie beam and a rigid slab (d) Overturning of the wall (e) Collapse of roof (f) No damage due to horizontal bands.

- (d) Re-cycled construction materials and the structures without earthquake resistant features are the main cause of failure of masonry buildings in Anjar region.

24.3.2 Chamoli Earthquake, March 29, 1999

A moderate earthquake of magnitude 6.8 rocked Chamoli area of Kumaon Garhwal Himalayan region at 00:35 hrs on March 29, 1999. The epicentre of this earthquake was close to Chamoli and the maximum intensity observed was VIII on MSK scale. The most affected area by the earthquake was the Chamoli and Rudraprayag district as depicted from Figure 24.4. The stone masonry houses in mud mortar with slate roofs generally supported on timber or bamboo trusses suffered maximum damage as compared to the other types of construction.

Types of construction

Typical features of masonry construction have been observed in the earthquake-affected areas (Figure 24.5), which can be summarized as:

- (a) Majority of masonry buildings were load bearing box type made up of stone, brick or concrete block. Old stone masonry houses were constructed in mud mortar with large size of stone blocks sandwiched between many thin wafers of (2 to 5 mm thick) slates arranged in layers. The resulting stone masonry is different from typical random rubble masonry. The wall thickness varied about 45 cm to 75 cm consisting of two wythes each of 20 to 30 cm thick separated by filler materials. The filler materials were loosely

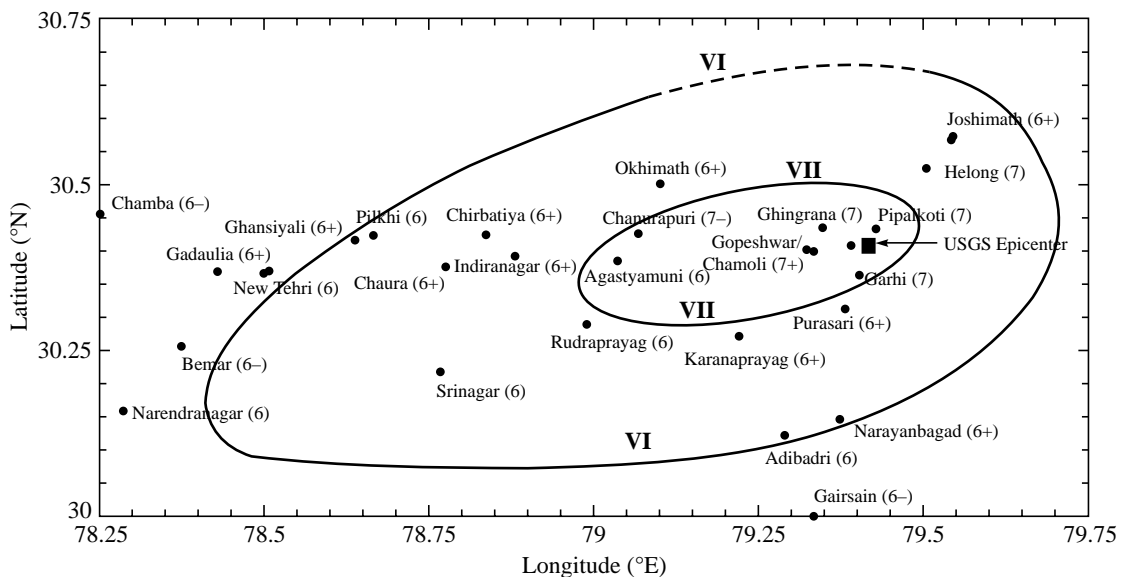


FIGURE 24.4 Isoseismal map of Chamoli earthquake, 1999 (Shrikhande et al., 2000).

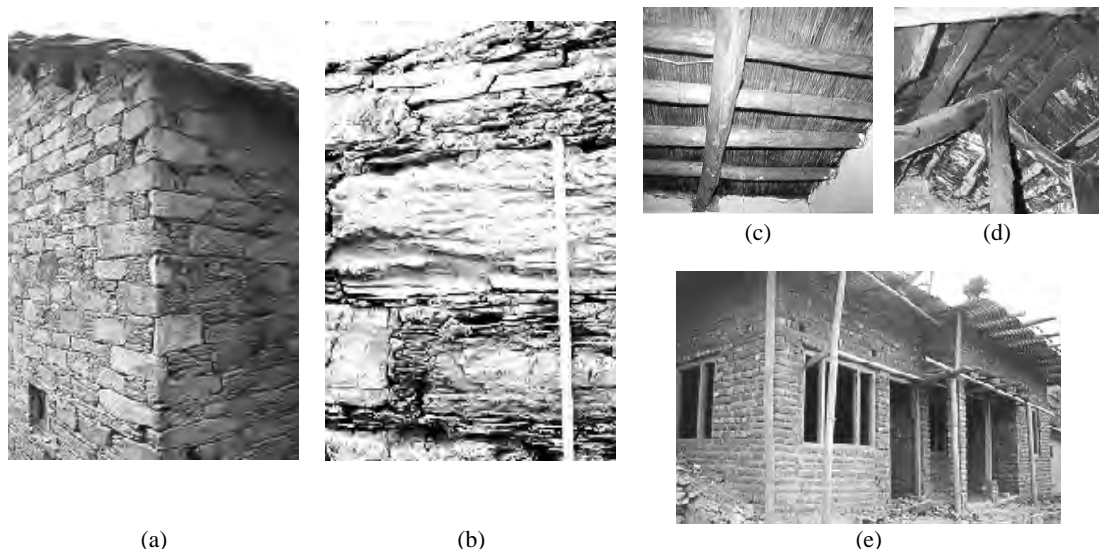


FIGURE 24.5 Typical construction features in earthquake affected areas (a) Traditional stone masonry wall (b) Slate masonry wall (c) and (d) Typical roof constructions (e) New brick construction with lintel band.

packed small stones and slates embedded in mud mortar. In well-constructed houses where quality of workmanship was good, stones were also used frequently to bind both wythes. The roofing system of this type of construction was generally pitched roofs made up of wooden joists and plank or simple wooden truss and rafter.

- (b) Random rubble stone masonry without layers of thin slates were laid in mud mortar and plastered in cement-sand mortar to provide finish surface. The walls were composed of two wythes with total wall thickness varying from 45 to 75 cm. The usage of burnt-clay brick masonry construction in cement sand mortar has also been seen in the recent years after Uttarkashi (1991) and Killari (1993) earthquakes. These constructions have generally lintel and roof band.

Types of damages and non-damages

Typical features of damages and non-damages in masonry buildings during Chamoli earthquake, 1999 have been highlighted in Figure 24.6 and are summarized as follows:

- (a) Random rubble stone masonry without any layer of slates or use of thicker slates has suffered maximum damage in comparison to stone masonry with multi-layers of thin slates in mud mortar. It is mainly due to energy dissipation through friction and material hysteresis.
- (b) Much of the damage may be due to ageing, inferior construction materials, inadequate support of the roof and roof trusses, poor wall-to-wall connections, poor detailing work, weak in-plane wall due to large openings, lack of integrity or robustness and asymmetric floor plans.
- (c) Non-compliance to the earthquake resistant construction features, as well as poor construction practices, use of local available materials were responsible for the majority of structural damage.



FIGURE 24.6 Typical features of damages (a) Overturning of wall (b) & (c) Out-of-plane failures of wall due to lack of connection between wall and floor.

24.3.3 Jabalpur Earthquake, May 22, 1997

A moderate earthquake of magnitude (M_b) 6.0 occurred at 4.21 hrs on May 22, 1997. The epicentre of the earthquake was near to the city of Jabalpur. The maximum intensity VIII on MMI scale was observed around Jabalpur city in a radius of about 15 km (Figure 24.7). The earthquake was felt in the region of Jabalpur, Seoni, Mandla and other towns in the Narmada belt of Madhya Pradesh and adjoining district of Uttar Pradesh and Maharashtra. Majority of houses, which were damaged in the earthquake, were mud houses having thick mud walls with roof constructed of tiles and supported on a bamboo grid.

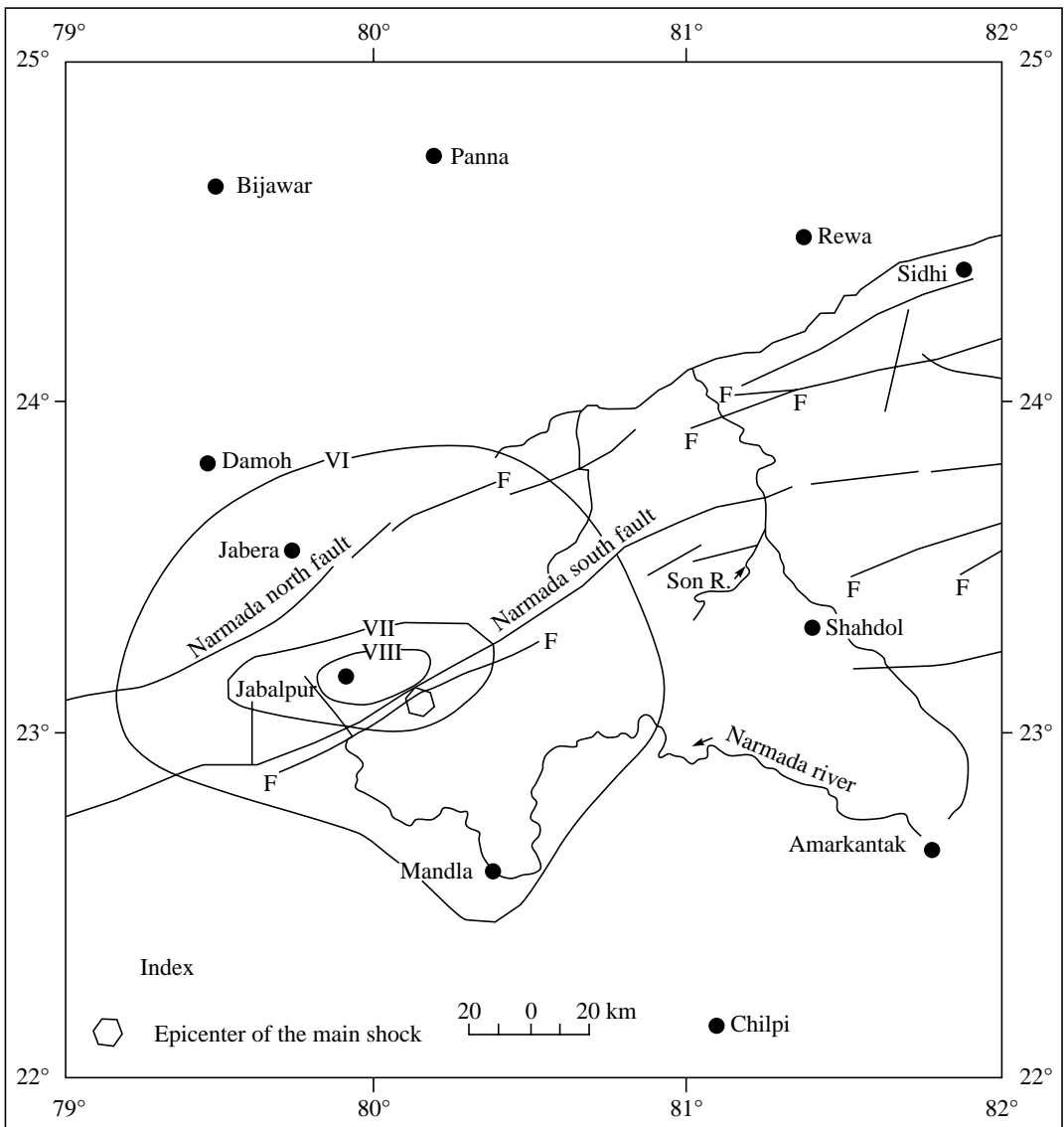


FIGURE 24.7 Isoseismal map of Jabalpur earthquake, May (GSI, 2000).

Types of construction

The non-engineered types of houses, which have suffered maximum damage, were either constructed with mud or burnt-clay brick in lime mortar. Roof consisted of clay tiles or RBC. The houses of 20 to 50 years old used stone and bricks for walls and tiles, stone slab, reinforced concrete (RC) and reinforced brick concrete (RBC) for roof and floor (Figure 24.8).



(a)



(b)

FIGURE 24.8 Traditional construction in earthquake affected areas (a) Brick masonry with flexible roof (b) Brick masonry with RCC slab without any earthquake resistant features.

Types of damages and non-damages

Typical features of damages and non-damages in masonry buildings during Jabalpur earthquake, 1997 have been highlighted in Figure 24.9 and are summarized as follows.

- Heavy damage to a very large number of two- or three-storey brick masonry buildings constructed by different government agencies.
- Unreinforced brick infill walls cracked at relatively small deformations and they would also have suffered flexure failure if their slenderness ratio (height to thickness) would have been large.
- Frequent failures of the walls enclosing the stairs at the roof level.
- Non-engineered buildings suffered heavy damage due to ageing, inferior construction materials, inadequate support of the roof and roof trusses, poor wall-to-wall connections, poor detailing work, out-of-plane instability of walls, lack of integrity.
- One- and two-storey unreinforced masonry buildings performed satisfactorily, especially those, which did not suffer layout or planning deficiencies and where the quality of workmanship and material were good.



(a)



(b)



(c)

FIGURE 24.9 Typical failure of masonry wall (a) Out-of-plane (flexure) failure of wall (b) Diagonal (shear failure), and (c) Failure at connection.

- (f) The extent of damage would have been drastically reduced, if modern earthquake resistant design procedure and construction practice had been followed.

24.3.4 Killari Earthquake, September 30, 1993

An earthquake of magnitude $M_b = 6.3$ occurred on September 30, 1993 with its epicentre close to Killari. The peninsular India has been considered seismically stable. The earthquake caused strong ground shaking in the region of Latur, Osmanabad, Sholapur, Gulbarga and Bidar. There was a heavy damage in the localised area of 15 km close to Killari which is on the northern side of river Tarna. The maximum intensity in the epicentral track was VIII+ on MMI (Figure 24.10). A large number of stone masonry houses collapsed. The reason for large toll of lives was the collapse of residential houses and its time of occurrence, which happened to be in early hours of morning when people were fast asleep.

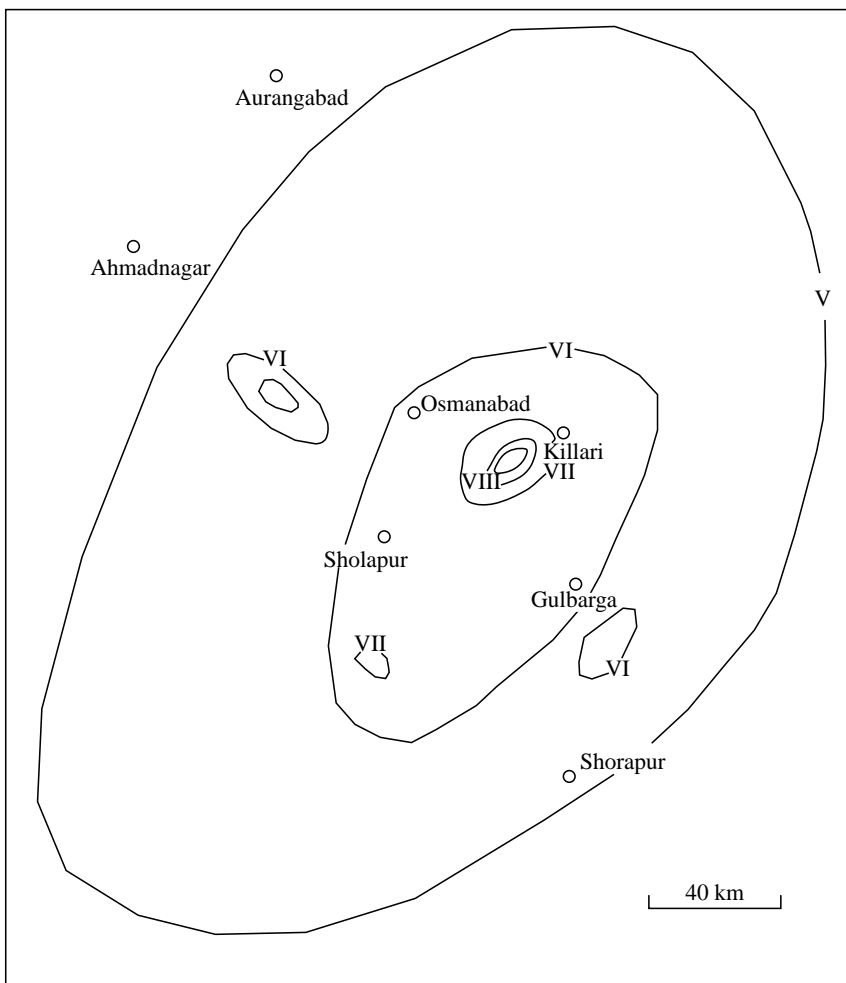


FIGURE 24.10 Isoseismal map of Killari (Latur) earthquake, of Sept., 1993 (GSI, 2000).

Types of construction

Typical features of masonry construction have been observed in the earthquake-affected areas (Figure 24.11), which can be summarized as;

- (a) The locally available heavy deccan trap stones, mostly rounded and smooth were used in building construction. The walls 700 mm to 1800 mm thick were made of random rubble stone masonry laid in mud mortar with small openings for doors and windows. The foundations of these houses are taken to a depth varying from 600 mm to 2500 mm below the top cover of black cotton soil. The roof consisted of timber rafters running in two perpendicular directions over which wooden planks and a thick layer of mud is laid. The compact layer of mud on roof varies between 300 mm and 800 mm making it heavy. Dry pack masonry has also been used in many houses.
- (b) The timber frames and beams bounded by stone walls had been used in many of the old and traditional houses. The vertical posts of wood were provided at a distance of about 1.0 m to 1.5 m. A stone wall was made around this frame. The roofs of such houses were also heavy due to use of thick layer of mud.
- (c) The mixed form of construction, such as storey of brick masonry or stone blocks in cement mortar had been added over storey of traditional random rubble masonry construction. The building of stone masonry employing earthquake resistant measures, though few in number were also existing in the earthquake affected area. The block masonry, adobe building and thatched huts type of construction had also been prevalent in the region.



(a)



(b)

FIGURE 24.11 Typical features of construction (a) Dry pack masonry in rural houses of Karnataka (b) Details of traditional construction of roof.

Types of damages and non-damages

Typical features of damages and non-damages in masonry buildings during Killari earthquake, 1993 have been highlighted in Figure 24.12 and are summarized as follows:

- (a) The majority of damage occurred to stone masonry houses in random rubble construction in mud mortar. The masonry with mud and other organic material used for binding



(a)

(b)

(c)

FIGURE 24.12 Typical features of failure (a) Out of-plane failure (b) Corner failure and (c) Diagonal shear failure.

had deteriorated in strength over the years. The large number of fore shocks had already weakened these structures.

- (b) There were a few cases of collapse of reinforced concrete roofs, which were supported on dressed stone masonry or brick masonry in cement mortar. The failure of masonry walls caused falling of roofs like a sheet.
- (c) The roofs of old stone masonry houses with wooden frames have remained intact resting on posts and beams, though masonry walls failed.
- (d) The buildings made of crushed stone block in cement mortar underwent minor damage. The stone masonry buildings with earthquake resistant features like corner strengthening withstood the shock with minor distress.
- (e) The houses of dry pack masonry with heavy roofs far away from the epicentral regions also performed satisfactorily, mainly because of low intensity of shaking.

24.3.5 Uttarkashi Earthquake, October 20, 1991

In the early hours on October 20, 1991 an earthquake having $M_b = 6.6$ rocked the Garhwal region of Uttar Pradesh (now in Uttarakhand) for 45 seconds and caused enormous destruction of houses and loss of life. The affected area lies in known seismic zones IV and V. The greater loss of life occurred because of its occurrence in the night when people were sleeping and buildings collapsed on them. The epicentre of earthquake was at a place called Agora. The area affected by the earthquake is shown in Figure 24.13, which includes Uttarkashi, Tehri and Chamoli regions. The maximum intensity in epicentral track was VIII+ on Modified Mercalli Intensity Scale. Numerous landslides occurred in these districts. The telecommunication and power supply were completely cutoff due to broken telephone and electric poles. Gwana steel bridge located about 6 km from Uttarkashi on road to Gangotri collapsed, cutting off hundreds of villages. A large number of residential houses, educational and health buildings were damaged. There were some cases of non-damage to buildings, which had earthquake resistant features.

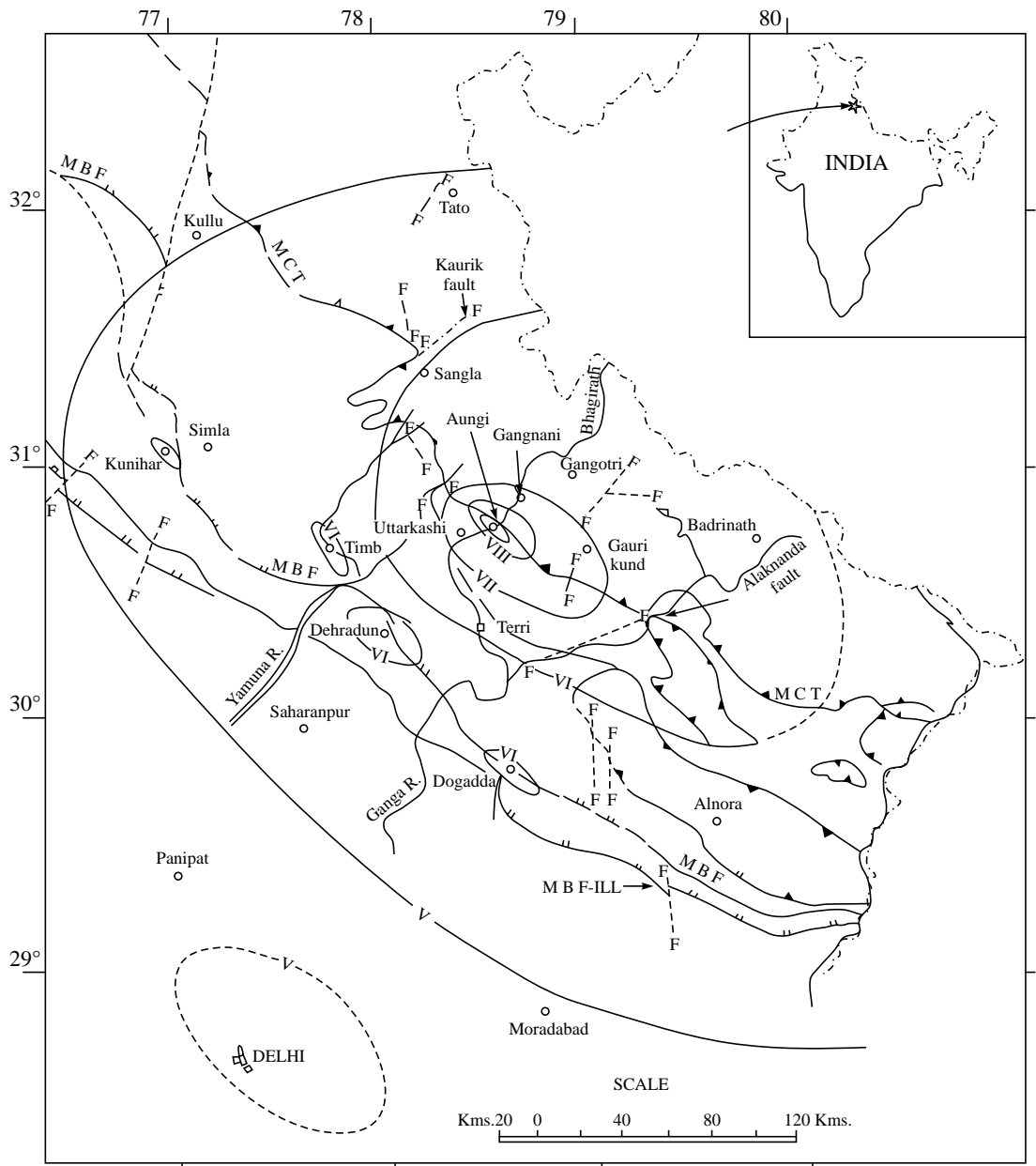


FIGURE 24.13 Isoseismal map of Uttarkashi earthquake of Oct., 1991 (GSI, 1995).

Types of construction

Typical features of masonry construction have been observed in the earthquake-affected areas (Figure 24.14), which can be summarized as:



(a)



(b)

FIGURE 24.14 Conventional construction in Uttarkashi town (a) and (b) Old conventional house with wooden beams and columns (GIS, 1992).

- (a) *Random Rubble Stone Masonry:* Most of the buildings have been constructed using locally available materials such as stone and mud. The walls, pillars and veranda columns were built in random rubble masonry laid in mud mortar. The foundations of the houses were constructed with bigger stones. The door and window lintels were usually made with wood in older construction and reinforced cement concrete in newer construction. The roofing consisted of CGI sheets laid on wooden planks and wooden rafters. The use of wood had rapidly declined due to its non-availability for building construction. The buildings currently built had reinforced cement concrete beam slab for roofing and walls in rubble stone masonry laid in mud/cement mortar. The stone wall thickness ranges from 35 cm to 45 cm. There is normally no interlocking or proper connection between the walls at the corners.
- (b) *Cement Concrete Block Construction:* The buildings using cement concrete blocks of single or double storey load bearing walls, 200 mm thick were also constructed in these districts. These blocks were laid in 1:6 cement sand mortar. Due to heavy snowfall, the roofs were made sloping either with CGI sheets or in RC slab construction. Some of these buildings had earthquake resistant provisions of IS: 4326 in the form of lintel band, roof band and gable band.
- (c) *Earthen Building:* The rural construction mostly consisted of mud, adobe and stone masonry buildings. The adobe in mud buildings was mostly self-made without any earthquake resistance. The houses were plastered with mud from inside and outside. The one- or two-storey houses were generally very old. The live stocks were sheltered in the ground floor while people lived on the first floor.

Types of damages and non-damages

Though the damages have occurred in all types of construction, with varying degrees from cracking of walls to total collapse, but the typical features of damages (Figure 24.15) are:



(a)



(b)



(c)



(d)

FIGURE 24.15 Typical features of damages (a) and (b) Out-of-plane of external walls (c) Out-of-plane collapse of outer leaf (d) Shear failure of walls (GIS, 1992).

- The widespread damage, in most cases resulting in collapse, occurred to old stone masonry buildings of random rubble construction in mud mortar or no mortar. The buildings had thick masonry walls with inadequate interlocking stones and no earthquake resistant features were observed like bands or corner strengthening.
- The damages were more in the houses with undressed or round stones than the houses with half dressed flat stones.
- The wide spread damages were also observed to the cement concrete block construction but no complete collapse was seen. The buildings had no earthquake resistant features.
- The earthen buildings suffered wide cracks in walls, separation of walls at corners and complete collapse of wall, roofs and floors. More than one-storeyed buildings in adobe suffered more damage than single-storeyed buildings.
- The stone masonry houses of traditional construction using wooden beams and planks were not damaged.

24.3.6 Bihar-Nepal Earthquake, August 21, 1988

In early hours 04:40 on August 21, 1988, a strong earthquake of magnitude 6.6 on Richter scale with its epicentre close to Bihar-Nepal border occurred. The maximum in the epicentral track

is estimated to be VI to VII on MMI scale (Figure 24.16). The most affected towns of Nepal were Dharan, Biratnagar, Dhankuta, Sunsari district, Panchthar, Therathum, Ilam while towns of Northern Bihar were Madhubani, Darbhanga, Muzaffarpur, Munghyer, Barauni, Bhagalpur, Bihar Sherif, Nalanda, Saharsa and Patna. Most of the damaged buildings in the earthquake were old brick masonry houses and kuchcha houses without any earthquake resistant features. Large scale liquefaction in the Gangetic plane, landslides in the hilly region and dampness due to excessive rain were the additional reasons for this widespread damage in such a moderate size of earthquake.

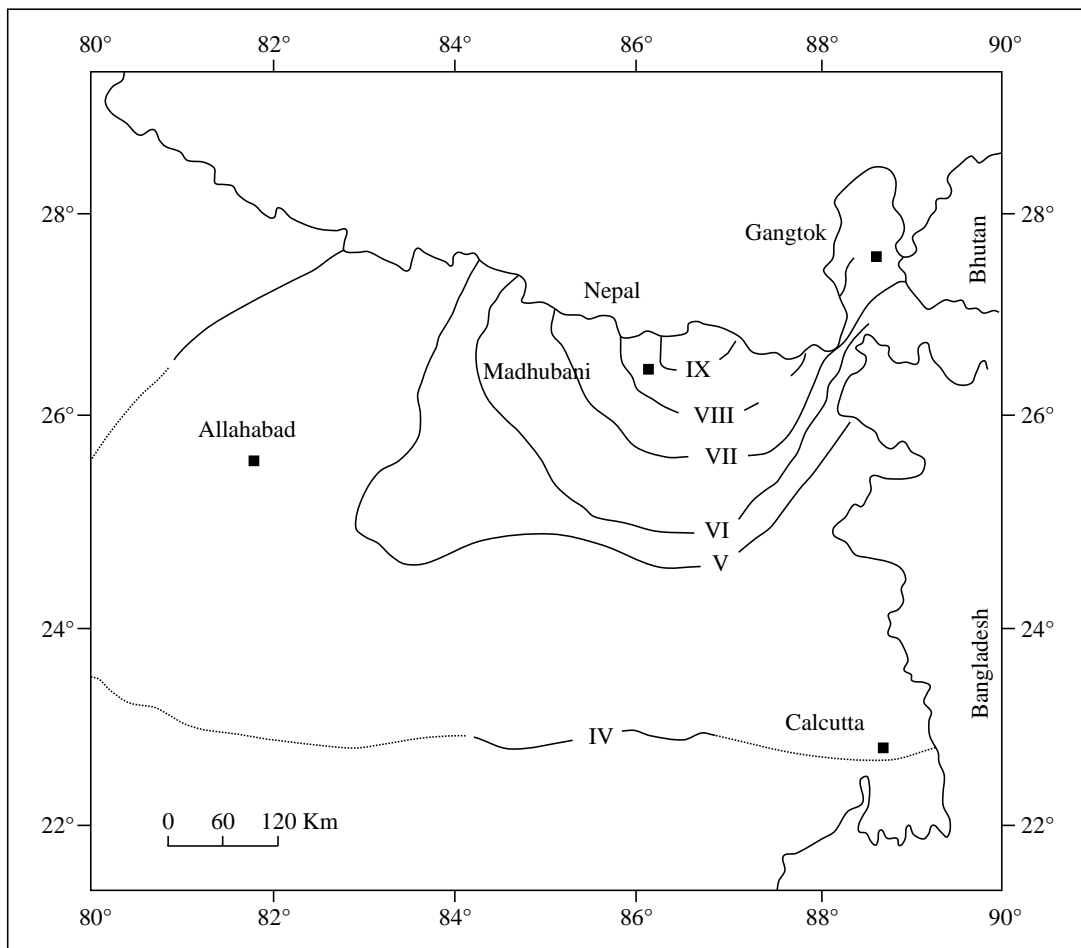


FIGURE 24.16 Isoseismal map of Bihar-Nepal earthquake of Aug. 1988 (GSI, 2000).

Types of construction

The old masonry buildings were constructed in burnt brick in lime-surki mortar. The roof consisted of inclined tile roof on rafter. In case of upper flat slabs or roof, a layer of bricks topped by a layer of mud had been used. The arch constructions were common in door and

window openings (Figure 24.17). The building heights ranged from one to three stories. The foundation soil is of alluvial type.



(a)



(b)

FIGURE 24.17 Traditional construction in earthquake affected areas (a) Masonry with inclined roof (b) Arch type construction.

Types of damages and non-damages

Typical features of damages and non-damages in masonry buildings during Bihar-Nepal earthquake, 1988 have been highlighted in Figure 24.18 and are summarized as follows:

- (a) Spreading of roof rafter had caused separation at corners of wall false ceiling
- (b) Vertical cracking of brick masonry arches near the crown, wedge action
- (c) Failure at the corners of openings
- (d) Horizontal shear cracks due to poor strength of cement-sand ratio
- (e) Absence of horizontal band in brick and stone masonry houses
- (f) Government buildings constructed according to IS codes have performed well



FIGURE 24.18 Typical features of damages (a) and (b) Out-of-plane failure of wall and arches (c) Failure of columns and roof.

- (g) The arch construction has been found to be weak and are failure in most cases
- (h) Some structures were damaged due to liquefaction of soil
- (i) In old buildings, there was a deterioration of strength and poor workmanship has been the cause of failure in many cases
- (j) The framed construction has shown better performance than the load bearing construction

24.4 LESSONS LEARNT

The seismic behaviour of masonry buildings during past earthquakes has provided several lessons. Some of these are presented as under:

- (a) Lack of structural integrity is one of the principal sources of weakness responsible for severe damage leading to collapse. The failure of connection between two walls, between walls and roof as well as between walls and foundation has been observed.
- (b) Damage in walls has consisted of nearly vertical cracking over head of the openings, diagonal tension cracking of piers between adjacent openings, separations of orthogonal walls, and partial out-of-plane collapse of second-storey walls.
- (c) One of the main causes of damage has been the absence of bond between perpendicular walls causing separation from each other at the junction, the consequence of which is the loss of rigid box like action of enclosures.
- (d) Bond elements in walls have remained conspicuous by their absence and separate inner and outer wythes of the walls during shaking.
- (e) The highest rate of damage in buildings has been firstly, due to the failure of first and second floor projections, secondly, due to the failure of ornamental balconies and parapet walls, thirdly, due to the failure of arches over opening, and lastly, due to the collapse of improperly tied gable ends.
- (f) Stone masonry buildings with thick exterior walls have also been severely damaged or

collapsed because of poor construction but survived, and remain intact during major earthquakes when they exhibit excellent workmanship.

- (g) Walls that are inadequately anchored to the floor diaphragm can exhibit large diagonal cracks in the piers due to inplane loads. If the mortar joints are weak, as in lime mortar, the cracks follow the joint.
- (h) Diaphragms that are insufficiently anchored can separate from the masonry wall, causing wall collapse. Unanchored gable ends of masonry walls are susceptible to this problem.
- (i) The provision of vertical steel or elements in the corner of the buildings as well as existence of horizontal tie beams increase resistance to earthquakes.
- (j) Non-structural elements must be given proper design considerations for lateral forces and should be braced or restrained. The collapse of many of these walls clearly illustrates this point.
- (k) The potential out-of-plane failure of non-structural elements (parapet, veneers, gables, and unanchored walls) during earthquakes constitutes the most serious life-safety hazard for this type of construction.
- (l) Inplane failure less common than out-of-plane failures was noted in many strengthened buildings. The typical shear failures occurred in many buildings.
- (m) In general, buildings with irregular plans experienced more damage than rectangular buildings. The damage was often concentrated at corners due to lack of a detailed analysis that included the effects of odd shaped plans.

24.5 RECOMMENDATIONS

In compliance with the past earthquake resistive structures, a number of principles have been formulated which may be summed up as: (i) The weight and rigidity of a structure must be uniformly and symmetrically distributed to the plane of symmetry passing through the centre of gravity; (ii) The proportionality requirements must be met by the building dimensions i.e. the length and height of the building should not be too great; (iii) The structure must be light, as practicable and have its centre of gravity as low as possible; (iv) Desirable tough, light and elastic material be used which have uniform properties; (v) In the vertical and horizontal planes the load carrying elements must be coupled to form closed contours; (vi) The foundations of earthquake resistant buildings must be firm and have enough depth.

SUMMARY

Masonry is widely used for housing construction in India and many countries of the world due to innumerable advantages over both reinforced concrete and steel. However, there are some disadvantages as well, particularly, when it is to be built in seismic environment. The seismic resistance capacity of masonry construction is relatively low in comparison to steel or reinforced concrete constructions. Past earthquakes have revealed that masonry construction is susceptible to damages during earthquakes because of lack of integral action, lack of strong and ductile connections between walls, roof elements and foundation, inadequate strength for out-of-plane

forces, low tensile and shear strength of mortar, high in plane stiffness of wall, low ductility and deformability capacity and heavy mass. This chapter focuses on the behaviour of masonry building during past earthquakes in India, which help to identify the causes of damage and non-damage in masonry buildings.

REFERENCES

- [1] Agarwal, Pankaj., "Experimental Study of Seismic Strengthening and Retrofitting Measures in Masonry Buildings", *Ph.D. Thesis*, Department of Earthquake Engineering, University of Roorkee, Roorkee, June 1999.
- [2] DEQ, *Jabalpur Earthquake of May 22, 1997: Reconnaissance Report*, Department of Earthquake Engineering, University of Roorkee, Roorkee, September, 2000.
- [3] DEQ, *Damage Survey Report on Bihar-Nepal Earthquake of August 21, 1988*, Department of Earthquake Engineering, University of Roorkee, Roorkee, 1988.
- [4] DEQ, *A Report on Chamoli Earthquake of March 29, 1999*, Department of Earthquake Engineering, University of Roorkee, Roorkee, September, 2000.
- [5] Dubey, R.N., Thakkar, S.K., and Agarwal, Pankaj, "Performance of Masonry Building during Bhuj Earthquake", 12th *Symposium on Earthquake Engineering*, IIT Roorkee, December, 2002.
- [6] EERI. "Bhuj, India Earthquake of January 26, 2001: Reconnaissance Report", *Earthquake Spectra*, Supplement to Vol. 18, July, 2002.
- [7] GSI, *Uttarkashi Earthquake, October 20, 1991*, Geological Survey of India, Special Publication No. 30, 1992.
- [8] ISET, "Damage Report of the Latur—Osmanabad Earthquake of September 30, 1993", *Bulletin of Indian Society of Earthquake Technology*, Vol. 31, No. 1, 1994.
- [9] Narayan, J.P., Sharma, M.L., and Kumar Ashwani. "A Seismological Report on the 26 January 2001 Bhuj, India Earthquake", *Seismological Research Letters*, Vol. 73, No. 3, May/June, 2002.
- [10] Shrikhande, M., et al., "The March 29, 1999 Earthquake at Chamoli, India", *12th WCEE*, Auckland, New Zealand, February, 2000.
- [11] Thakkar, S.K., Dubey, R.N., and Agarwal, Pankaj, "Damages and Lessons Learnt from Recent Indian Earthquakes", *Symposium on Earthquake Effects on Structures, Plant and Machinery*, New Delhi, November 13–15, 1996.
- [12] GSI, *Seismotectonic Atlas of India and its Environe*, Geological Survey of India, 2000.
- [13] GSI, *Uttarkashi Earthquake*, Geological Survey of India, 1995.

Chapter 25

Elastic Properties of Structural Masonry

25.1 INTRODUCTION

Structural masonry is a combination of a few or all the constituent masonry materials: masonry unit, mortar, grout and reinforcement. The physical and engineering properties of constituent materials have already been widely discussed in standard undergraduate textbooks and their respective BIS codes. The strength and stiffness properties of integral masonry or masonry assemblage are not very common particularly in India, hence very limited information is available even in the codes. This chapter will deal with the engineering properties of constituent materials in brief and with a detailed discussion on the strength and stiffness properties of masonry assemblage. Information and data given here are valid for respective masonry tests in laboratory. However, a good interpretation can be made for the similar type of masonry in case of absence of sufficient data.

25.2 MATERIALS FOR MASONRY CONSTRUCTION

25.2.1 Unit

A *masonry unit* may be brick, block made from concrete or clay, stone, adobe etc. Depending upon the unit used in the masonry, the construction may be classified as brick masonry, block masonry, stone masonry, adobe masonry, etc. IS 4326: 1993 in Clause 8.1.1 has specified the minimum requirement of masonry unit. The code specifies that well-burnt bricks and solid concrete blocks possessing a compressive/crushing strength not less than 35 MPa shall be used. Moreover for squared stone masonry, stone block masonry or hollow concrete blocks the specification according to IS 1597 (Part 2): 1992 having adequate strength may be used. The *compressive strength* of unit may be defined as the maximum stress to which the unit can be subjected by a gradually increasing load applied in perpendicular either to the bedding plane or normal position. The modulus of elasticity of the individual unit is not generally determined and is therefore not specified in most of the codes. If it is required, the modulus of elasticity

for the units may be obtained by secant modulus of stress-strain curve of unit under compression, which is the slope of a line from zero stress to approximately 33% of the unit compressive strength. The modulus of elasticity of the unit remains somewhat greater than the respective masonry.

The tensile strength of the unit is measured by the modulus of rupture or splitting tension, which increases with the unit's compressive strength, but is generally a smaller fraction of the compressive strength. The ratio of modulus of rupture to compressive strength varies from about 0.10 up to 0.32 (Drydale, Hamid and Baker, 1994).

Another stiffness index may be expressed in terms of Poisson's ratio i.e. the ratio of lateral expansion to longitudinal deformation. Experiments reveal values 0.23 for ungrouted clay masonry to 0.40 for grouted clay masonry (Schneider and Dickey, 1994).

25.2.2 Mortar

Mortar is a plastic mixture of materials used to bind masonry unit into a structural mass. IS 4326: 1993 in Clause 8.1.2 has recommended mortar mixture used in masonry construction in seismic areas for various categories of building. The categories of construction are defined in Clause 7.1 depending upon the design seismic coefficient (α_h) (Category: A ($0.04 < \alpha_h < 0.05$), B ($0.05 < \alpha_h < 0.06$), C ($0.06 < \alpha_h < 0.08$), D ($0.08 < \alpha_h < 0.12$) and E ($0.12 \leq \alpha_h$)). Recommended mortar mixture for A categories of construction type building are M₂ (Cement-sand 1:6) or M₃ (Lime-cinder 1:3) or even richer. For the construction of B and C category type buildings the recommended mortar are M₂ (Cement-lime-sand 1:2:9 or Cement-sand 1:6) or richer and for D and E type of construction, the recommended mortar are H₂ (Cement-sand 1:4) or M₁ (Cement-lime-sand 1:1:6) or richer. Masonry may further be subdivided on the basis of type of mortar used for example brick masonry in cement mortar. The important properties of the hardened mortar that affect masonry construction are bond strength, flexural tensile strength and compressive strength. Bond strength of mortar is usually lesser than the flexural tensile strength of mortar therefore the flexural tensile strength of masonry is governed by the bond strength of mortar to brick. These properties may be determined as (Grimn, 1975),

Bond strength of mortar to brick can be estimated as:

$$f_b = 0.005[1.8 + (F - 105)^{0.5}](40 - A)(124 - t_m)$$

in which,

f_b = bond strength of mortar to brick in psi (1 psi = 6.894 N/m²)

F = initial flow of mortar, as a % { $F = 195[1.72 + \log(C_v/L) [(W/C_w) - 0.05] - 72]$; and
 W/C_w = water-cement ratio by weight where $0.4 < (W/C_w) < 1.0$ }

A = air content in mortar by volume, where $A < 30$, as a %

t_m = mortar exposure time (spreading mortar of laying brick), where $t < 120$, in seconds

Flexural tensile strength of mortar can be approximated as:

$$f_{tm} = 1.47 \times 10^{-5} f_c (11,700 - f_c)$$

in which,

f_{tm} = flexural tensile strength of mortar in psi (1 psi = 6.894 N/m²)

f_c = compressive strength of mortar in psi (1 psi = 6.894 N/m²)

Compressive strength of mortar can be approximated as:

$$f_c = 3.25s\alpha\beta T(554\delta + \gamma(130 - F))$$

f_c = compressive strength of mortar in psi (1 psi = 6.894 N/m²)

s = 1 for 2 in (50 mm) cubes, 0.9 for 2-in × 4-in (50 mm × 100 mm) or 3-in × 6-in (76 mm × 150 mm) cylinders

α = mortar curing factor values 0.7 at 7 days, 0.85 at 14 days, 0.93 at 21 days, and 1.0 at 28 days. For air-dried specimen at 7 days and 28 days, α = 0.8.

β = air content factor [$\beta = 0.021(57.3 - A)$], A = Air content in mortar by volume, where $A < 30$, as a %

T = plastic mortar age factor [$T = 0.029(35 - T_p^2)$]; and T_p = age of plastic mortar i.e., time in mixing to time in use), in hours ($T_p < 4$)

δ = mortar type factor [$\delta = 1 + 1.46 \log(C_v/L)$]

$\gamma = (C_v/L + 3.7)$

25.2.3 Grout

Grout is a mixture of Portland cement, sand, gravel and water. It is generally used for increasing the compressive strength of masonry. It is placed in the cores of hollow masonry units or between the wythe of solid units to bind the reinforcing steel and masonry into a structural system. IS 4326: 1993 has recommended minimum cement concrete of grade M 15 so as to achieve good bond and corrosion resistance. Here masonry is further subdivided on the basis of grouting. Grouted masonry excels in compressive strength.

25.2.4 Reinforcement

Reinforcing steel in masonry has been extensively used in the western countries for revitalising the masonry construction in earthquake prone areas. Reinforcing steel extends the characteristics of ductility, toughness and energy absorption that is very necessary in structures subjected to the dynamic forces of earthquakes. Reinforcing steel also resist the shear and tensile forces generated by the dynamic load. Masonry with reinforcement is further classified as reinforced masonry. Reinforced masonry performs well in earthquake because it has sufficient ductility to sustain the load reversals beyond the capability of plain, unreinforced masonry. In India, reinforcement is provided in the form of various horizontal bands, and vertical reinforcement at the corners and junctions of walls and around the openings. Horizontal bands with vertical reinforcement at corners and junctions of walls are provided to integrate the structure and steel provided around the opening to prevent the diagonal cracks that tend to radiate from the corners of opening. IS 4326: 1993 specifies the requirements and the size of reinforcement in the masonry depending upon the building category.

25.3 ELASTIC PROPERTIES OF MASONRY ASSEMBLAGE

It is difficult to determine the strength and elastic properties of masonry on the basis of known properties of the constituent material *e.g.* masonry units, mortars, grout and reinforcement. The prediction of the behaviour of masonry assemblage on the basis of its constituent material is too complex. Therefore, the strength and elastic properties of integral masonry are determined by making of wall specimens and testing under vertical and cyclic lateral loading (Drysdale, Hamid and Baker, 1994), which are discussed as follows:

25.3.1 Compressive Strength

Compressive strength plays an important role in load bearing structures. Compressive strength of masonry is often used as the basis of assigning design stress and in some cases as a quality control measure. Its importance is realised in relation to other strength characteristics.

Test machine capacity, specimens height limits etc. have made the use of prism necessary as the principal type of compression test specimen rather than full scale specimens. A standard prism according to IS: 1905–1987 usually consists of one masonry unit long, one unit thick and shall be at least 40 cm high and shall have a height to thickness ratio (h/t) between 2 and 5, as per actual construction. For convenience, the stack pattern is commonly used to study the strength, stiffness and deformation capacity of masonry in compression (Figure 25.1a). When masonry prisms with height-to-thickness ratio (h/t) of less than 5 are tested, the ultimate compressive strength must be multiplied by the factor given in Table 25.1 to correct slenderness effects. The ultimate compressive strength of prism is calculated by dividing the maximum compressive load by the cross-sectional area of prism. The ASTM E 447, Method B describes test equipment, test procedures of prism tests in detail.

TABLE 25.1 Prism height to thickness correction factors (IS: 1905–1987)

Prism (h/t)	2.00	2.50	3.00	3.50	4.00	5.00
Correction factor (Brick work)	0.73	0.80	0.86	0.91	0.95	1.00
Correction factor (Block work)	1.00	—	1.20	—	1.30	1.37

Note: Interpolation is veiled for intermediates values.

When prism is subjected to uniaxial compressive force, Figure 25.1(a), the mortar has a tendency to expand laterally more than brick. Since mortar and brick are bound together, the brick confines the mortar laterally. Shear stress at the brick mortar interface results in an internal state of stress which consists of triaxial compression in the mortar and bilateral tension coupled with uniaxial compression in the brick as shown in Figure 25.1(b). The stress-strain curve of the unit, mortar and masonry under axial compression is shown in Figure 25.1(c). The figure clarifies that the masonry has lesser strength compared to its unit. It may also be observed that the mode of failure of prism has been vertical splitting in case of large h/t ratio prism and typical shear failure in low h/t ratio prism.

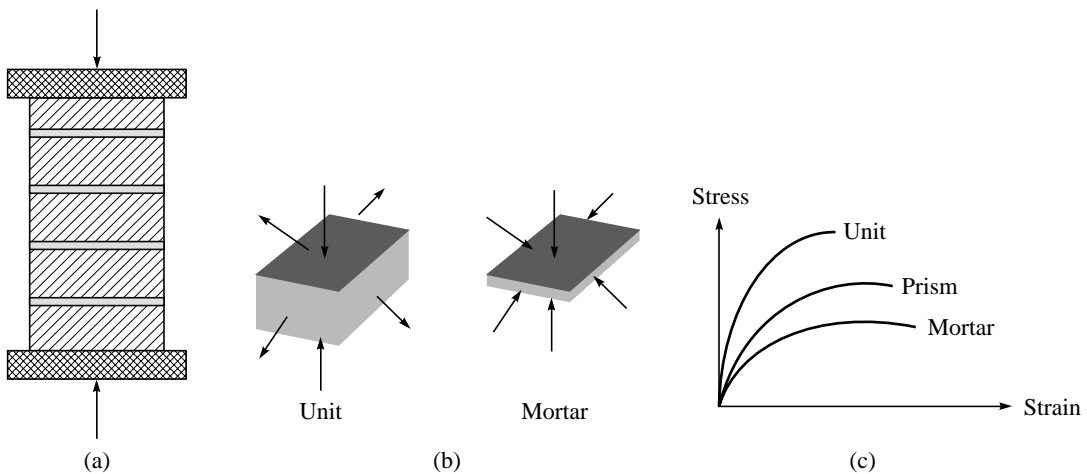


FIGURE 25.1 (a) Prism under axial compression (b) State of stress of units and mortar (c) Stress–strain relationship for materials and prism (McNary and Abrams, 1985).

The stress–strain relationship and the value of Young’s modulus for brickwork in compression are frequently required in structural design. The modulus of masonry may be estimated from the following methods;

Secant method: Powell and Hodgkinson, 1976 (Source: Hendry, 1998) have tested brickwork in compression to failure using four types of bricks having different strength for determining the stress–strain relationship. The mortar strength has been kept the same. The stress–strain curve has been shown in Figure 25.2(a) and the results of these tests are summarized in Table 25.2. By plotting these stress-strain curves on a dimension less basis in Figure 25.2(b), it is found that

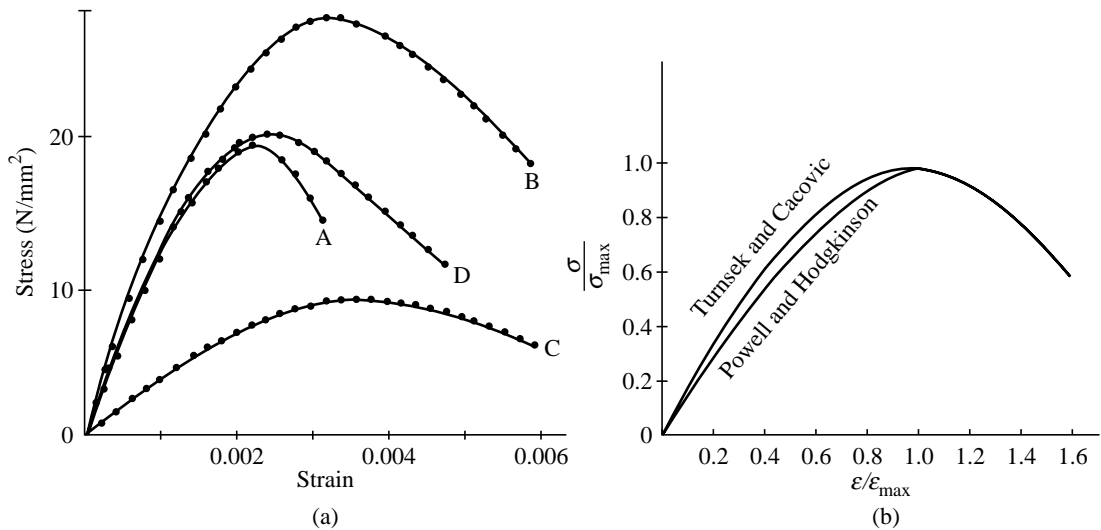


FIGURE 25.2 Stress–strain curves for brickwork in compression: (a) Four types of bricks 1:1/4:3 mortar (b) Dimensionless stress–strain curves (Hendry, 1998).

TABLE 25.2 Stress-strain relationship for brickwork (mortar 1:1/4:3, mean compressive strength 15.24 N/mm²) (Hendry, 1998)

Brick compressive strength (N/mm ²)	Brickwork compressive strength (N/mm ²)	Elastic modulus	
		tangent* (N/mm ²)	secant** (N/mm ²)
25.5	9.33	4960	3740
45.3	20.10	16830	11610
69.6	19.93	18230	11900
71.7	27.65	17370	12930

*Initial tangent modulus

**Secant modulus at 2/3 of maximum stress

the curves for the four types of bricks are in the same form and in good agreement as reported by Turnsek and Cacovic, 1971. The relationship is closely represented by the parabola.

The modulus of elasticity from the stress strain can be determined as,

Chord modulus for a line joining the curve at 5% of f_m to 33% of f_m MIA, 1998

Chord modulus for a line joining the curve at 5% of f_m to 35% of f_m Knutsson and Nielsen, 1995 (Source: Hendry, 1998)

Since this region usually lies well within the reasonable linear part of the curve, the lower part of the curve is ignored because it often represents a relatively flat region associated with closing up of the interface between the mortar and the units.

Empirical basis: A number of authors have correlated the modulus of elasticity of masonry to its compressive strength (f_m) on an empirical basis as below:

$E_m = 750 f_m$, 20.5 Gpa (maximum) MIA, 1998

$E_m = 400 - 1000 f_m$ Sahlin, 1971

$E_m = 2116 \sqrt{f_m}$ Schubert, 1982

$E_m = 1180 f_m^{0.83}$ Sinha and Pedreschi, 1983

$E_m = 1000 f_m$ EC 6 and CIB (Bull, 2001)

Compressive strength of brickwork in different mortar is given in Table 25.3 (SP 20 (S&T): 1991).

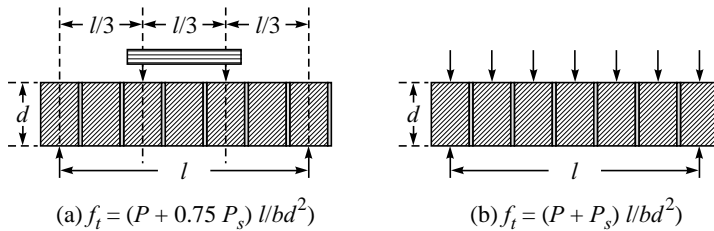
TABLE 25.3 Strength of brickwork in different mortar (using clay brick of strength 32.7 N/mm²) (SP 20 (S&T): 1991)

Mortar mix	Mortar compressive strength (28 days)	Brickwork compressive strength (28 days)	Ratio
Cement:lime:sand	N/mm ² (X)	N/mm ² (Y)	Y/X
1:1/4:3	17.8	8.9	0.50
1:1/2:4½	10.8	9.3	0.86
1:1:6	4.7	8.5	1.82
1:2:9	1.7	4.6	2.69

25.3.2 Flexural Tensile Strength

Masonry walls subjected to lateral load either due to wind, earthquake or eccentric vertical external load/or self-weight produce bending about the vertical axis/horizontal axis or both the axis, depending upon its support condition and geometry. Bending about vertical axis produces flexure tension normal to bed joints (f_{tn}) and bending about horizontal axis produces flexure tension parallel to bed joint (f_{tp}). The flexures tensile strength (modulus of rupture) is, of course, different in bending in a plane normal to bed joints (f_{tn}), than for bending in a plane parallel to bed joint (f_{tp}) in the wall. The ratio of flexural tensile strength parallel to bed joint (f_{tp}) to normal to bed joints (f_{tn}), referred to as the orthogonal strength ratio R which is affected by many factors. It is a measure of the degree of anisotropy of the material and is set at 2.0 in masonry codes. However, the ratio ranges from 1.5 to 8 for clay masonry (Baker, 1977).

ASTM E 72 has defined the method and tested the procedure for determining the flexural tensile strength, which is referred as Wall test. ASTM E 518 provides two methods for performing tests on flexure beams known as *beam test*. Method A uses concentrated loads at 1/3 points of the span and Method B uses a uniform loading over the entire span as shown in Figure 25.3(a) and 25.3(b) respectively.



f_t = modulus of rupture (MPa), P = maximum machine applied load (N), P_s = weight of specimen, (N), l = span, mm, b = average width of specimen, mm, d = average depth of specimen, mm

FIGURE 25.3 (a) Method A set-up (b) Method B set-up (BIA, 1988).

Many investigators (Grimm, 1975) have attempted to establish a relationship between material properties and flexural tensile strength. Flexural tensile strength (modulus of rupture) of brick masonry is a function of tensile bond strength of mortar to brick, mortar cement content, mortar bed joint thickness, and orientation of mortar bed joint with respect to span either normal to joint or parallel to joint. Table 25.4 shows the results of James (Hendry, 1998) in different type of mortar. Test results indicated that the flexural tensile strength parallel to bed

TABLE 25.4 Flexural tensile strength of small specimens (Hendry, 1998)

Mortar	Flexure strength (N/mm ²)			
	Normal to bed joint		Parallel to bed joint	
	Stack prism	3-course specimen	3-course specimen	4-course specimen
1:2:9	0.39		2.08	1.78
1:1:6	0.594		2.40	2.03
1:1/4:3	0.984		2.74	2.29

joint has not been much affected by the type of mortar however a difference was noticeable in the orthogonal direction.

Grimm, 1975 has established a formula for estimating the flexural tensile strength of brick masonry as,

$$f_t = 0.67\theta kf_b (1.1 - t_j) \left[3.8 + \left(\frac{C_v}{L} - 1 \right)^{0.5} \right]$$

in which,

f_t = flexural tensile strength of brick masonry normal to bed joint in psi (1 psi = 6.894 N/m²)

θ = workmanship constant for masonry in flexure (1 for all mortar joint filled and 0.8 joints partly filled)

k = stress orientation factor (1 for normal to bed joint and 2 for parallel to bed joint)

f_b = bond strength of mortar to brick in psi (1 psi = 6.894 N/m²)

t_j = mortar joint thickness, in inch

C_v/L = cement-lime ratio by volume in mortar

Typical values for the flexural tensile strength normal to bed joint of conventional brick masonry range from 50 psi to 500 psi (340 kN/m² to 3,400 kN/m²)

25.3.3 Shear Strength

Load bearing masonry walls are often subjected to axial compression (vertical dead and live loads), flexure (eccentric vertical loading, wind or earthquake loading) and also shear (in-plane lateral loads and the effects of axial load and bending). This combined loading creates a state of complex stress in the wall and becomes one of the causes to its failure. Depending upon the form of construction and the relative value of compressive and shear forces the possible shear failure modes in masonry assemblages are: (i) shear slip failure along bed joint—if shear force is greater than the normal compression force; (ii) diagonal tension cracking—if both shear force and normal compressive force are comparative; and (iii) shear compression failure or splitting failure—if shear force is a small fraction of normal compressive force. First two modes of failure are more commonly observed in the case of failure of masonry walls during earthquakes. Therefore, the shear strength against bed joint failure as well as diagonal tensile (shear) strength against diagonal tension are of considerable concern to structural designer, especially where seismic design is required.

Shear strength along bed joint

The shear strength along the bed joint is the function of bond strength between mortar and units and normal compressive stress. It is best represented by the Mohr–Coulomb type of equation i.e.

$$\tau = \tau_0 + \mu f_n$$

τ = ultimate shear strength of the brickwork in N/mm²

τ_0 = cohesion or bond strength between the mortar to brick in N/mm²

f_n = normal compressive stress in N/mm² and

μ = coefficient of internal friction of brick work

This equation suggests that as an increase in the normal compressive stress is applied to brickwork, the horizontal shear strength of the brickwork also increases. But this phenomenon is perceptible only upto when the normal compressive stress remains under prism compressive strength; afterwards the shear strength starts declining. The decrease in shear strength corresponds to the change in the compression splitting failure mode (Drydale, Hamid and Baker, 1994). Moreover the value of μ also starts to decrease substantially with increasing normal compressive stress and it has been necessary to consider an average value of μ .

A wide range of values of coefficient of internal friction (μ) and the bond shear strength has been reported depending upon the material used and the test specimens and loading arrangements. The coefficient of internal friction (μ) for brick masonry made with solid brick varies from 0.2 to 0.84 and bond strength (τ_0) varies from 0.20 to 0.40 N/mm². Perhaps $\mu = 0.68$ and $\tau_0 = 0.3$ is a reasonable value. Typical value for the shear strength of brick masonry ranges from 410 kN/m² to 4690 kN/m² (Grimm, 1975).

Masonry walls are intended to resist shear force due to in plane lateral load in addition to the effect of compressive load and bending. Experimentally, there is no standardised test for the determination of shear strength of masonry along the bed joint. However, in literature Triplet type test is mentioned for the determination of shear strength, with an intention to minimize bending stresses on the mortar joint and to produce uniform shear deformation along the joint but the variation in the results is very large, as shown in Figure 25.4.

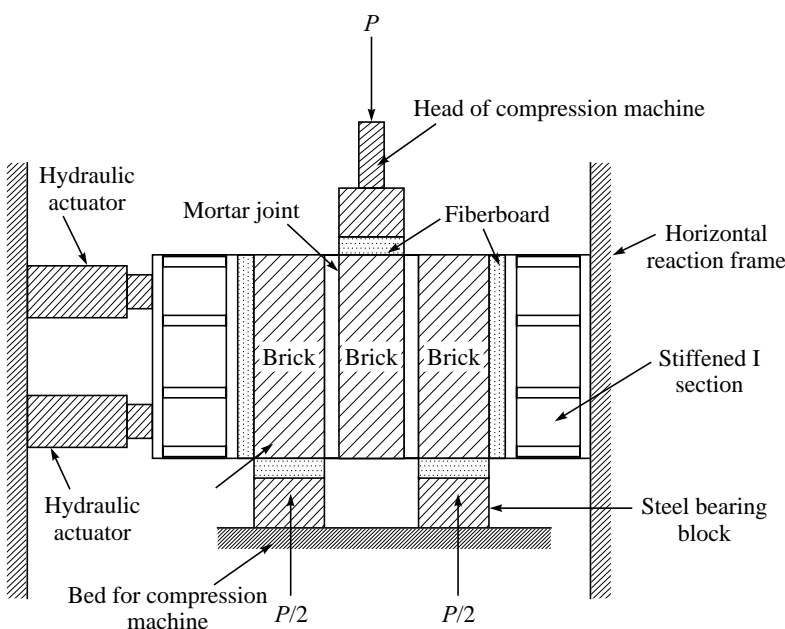


FIGURE 25.4 Diagrammatic representation of Triplet test equipment (Smith and Carter, 1971).

Off-axis compression test is also performed on the specimens constructed with mortar joints at various angles to the loading axis, which produces different combinations of compressive force normal to bed joints and shear force parallel to the bed joint. The modes of failure depending upon the compression and shear stress in the specimen are shown in Figure 25.5.

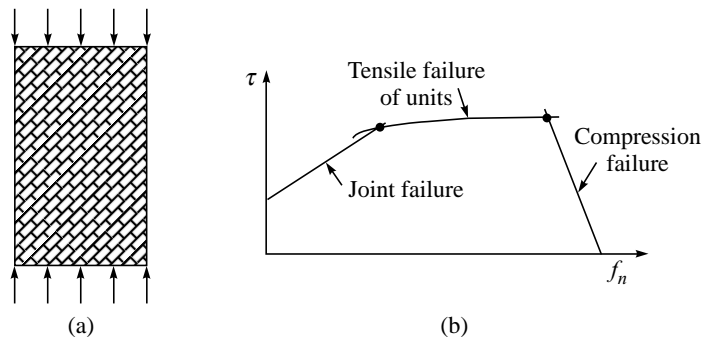


FIGURE 25.5 (a) Off-axis compression test (Drydale, Hamid and Baker, 1994) (b) failure modes of masonry in shear with vertical compression (Hendry, 1998).

Diagonal tensile (shear) strength

The failure of walls during earthquake is caused by combined effect of normal compressive and shear stresses, which is represented by the principal tensile stress and when it exceeds, the diagonal tensile strength of the masonry failure will take place. The ASTM test standards specify two test methods for determining the diagonal tension (shear) strength. ASTM E 519, Standard Test Method for Diagonal Tension (Shear) in Masonry Assemblages and ASTM E 72, Method for Conduction Strength Tests of Panels for Building Construction are generally used for this purpose. The E 72 racking load test may be applied for testing materials and construction of all types, while E 519 applies only for masonry (BIA, 1992).

The diagonal tension test is based on subjecting a $1.2\text{m} \times 1.2\text{m}$ square section of wall by the thickness of the wall type to diagonal compression through loading shoes at two diagonally opposite corners of the specimens, shown in Figure 25.6(a). The failure mode of the test is through formation of diagonal crack parallel to the line of action of the compression force.

The diagonal tensile stress may be calculated from the equation;

$$f_t = 0.707 P/A$$

where,

P = applied load (N) and

A = average of the gross or net area of the cross section along the bed and head joints in mm^2 .

The gross area is used in calculation if the specimens are constructed with solid units, while net area is used in case of specimen with hollow units. Net area of the specimen, mm^2 is calculated as

$$A_n = \left(\frac{w + h}{2} \right) t n$$

where,

w = width of specimen, mm

h = height of specimen, mm

t = total thickness of specimen, mm

n = percent of the gross area of the unit that is solid, expressed as a decimal

The modulus of rigidity or shear modulus (modulus of elasticity in shear) may be calculated as follows (ASTM, 2002);

$$G = f_t / \gamma$$

where,

G = modulus of rigidity, MPa

f_t = diagonal tensile (shear) stress

γ = shear strain calculated as $\frac{\Delta V + \Delta H}{g}$

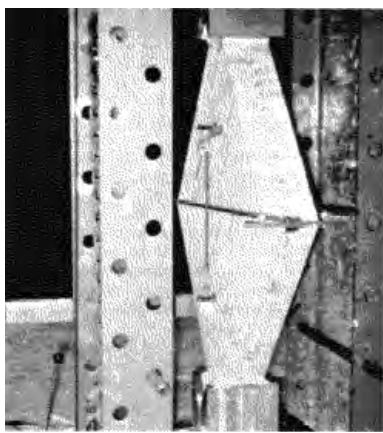
ΔV = vertical shortening, mm

ΔV = horizontal shortening, mm

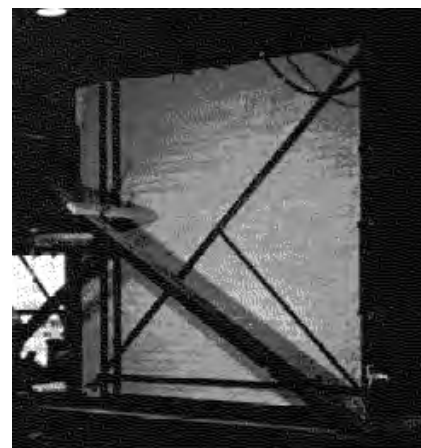
g = vertical gauge length, mm (ΔH must be based on the same gauge length as for ΔV)

In racking test method, compressive stresses are introduced into the specimens through the tie down. This method of test requires a specimen of square wall size by 2.4 m \times 2.4 m, subjected to a horizontal force at the top of the wall. The vertical tie down is also required to prevent rotation of the specimen and overturning of the specimen, Figure 25.6 (b). The results obtained from the racking test are relevant for the particular loading condition and wall geometry used in the test. Walls with no axial load, yield slightly higher results, which remain 25% to 50% greater than the bond strength of brick to mortar.

In the absence of experimental data, the following equation may be used to estimate the diagonal tensile strength (Grimm, 1975) and shear modulus of brick masonry as follows:



(a)



(b)

FIGURE 25.6 Standard shear test (a) Diagonal tension test instrumentation for modulus of rigidity (b) Racking test frame and specimen (BIA, 1987).

Diagonal tensile (shear) strength

$$f_{dt} = k(f'_m)^{0.5}$$

f_{dt} = diagonal tensile strength of brick masonry in diagonal tension, in psi (1 psi = 6.894 N/m²)

k = constant factor, the values of k ranged between 2.5 and 4.5. An average value of 3.5 may be used.

f'_m = Compressive strength of brick masonry prism, in psi (1 psi = 6.894 N/m²)

Shear modulus

The shear modulus of brick masonry G is inversely proportional to the shearing stress and is proportional to the pre compressive stress. For approximate calculation, G might be taken as

$$G = E/2(1 + \nu)$$

where,

E = modulus of elasticity in compression

ν = Poisson's ratio (for brick masonry value varies from 0.11 to 0.20)

MIA, 1998 has assumed the value of $G = 0.4 E$. Typical value for shear modulus of brickwork ranges from 1500–2000 N/mm².

SUMMARY

The properties of masonry are not very well related to its constituent's materials such as unit, mortar, grout and reinforcement. However, for seismic design of masonry structure there is a need to consider strength and elastic characteristics of masonry. The strength characteristics such as compressive strength, tensile and shear strength are often required in checking design of masonry structures. The modulus of elasticity, Poisson's ratio and damping properties are required for carrying out seismic studies. There is a scarcity of data available on strength characteristics and elastic properties of masonry. This chapter deals with the engineering properties of constituent materials in brief with a detailed discussion on the strength and stiffness properties of masonry assemblage. The tests for determining the structural properties have also been discussed.

REFERENCES

- [1] American Society of Testing and Materials, "Compressive Strength of Masonry Assemblages", *ASTM E 447-84*, Philadelphia, PA, 1984.
- [2] American Society of Testing and Materials, "Measurements of Masonry Flexural Bond Strength", *ASTM C 1072-82*, Philadelphia, PA, 1986.
- [3] American Society of Testing and Materials, 'Test Method for Flexural Bond Strength of Masonry", *ASTM E 518-80*, Philadelphia, PA, 1987.

- [4] American Society of Testing and Materials, "Standard Methods for Conducting Strength Tests on Panels for Building Construction", *ASTM E 72*, Philadelphia, PA, 1989.
- [5] Amrhein, J.E., *Reinforced Masonry Engineering Handbook—Clay and Concrete Masonry*, 5th ed., Masonry Institute of America, 1992.
- [6] ASTM, ASTM Standards in Building Codes, *ASTM International*, West Conshohocken, PA, 2002.
- [7] Baker, L.R., "The Lateral Strength of Brickwork—An Overview", *Proceedings of the Sixth International Symposium on Load Bearing Brickwork*, London, 1997.
- [8] BIA., "Testing for Engineered Brick Masonry—Quality Control", *Technical Notes 39B on Brick Construction*, Brick Industry Association, Reston, Virginia, 1988.
- [9] BIA, "Testing of Engineered Brick Masonry—Determination of Allowable Design Stresses", *Technical Notes 39A on Brick Construction*, Brick Industry Association, Reston, Virginia, 1987.
- [10] Bull, J.W., *Computation Modelling of Masonry, Brickwork and Blockwork Structures*, Saxe-Coburg Publications, UK, 2001.
- [11] CIB, "International Recommendations for Design and Erection of Masonry Buildings", 1958.
- [12] Dhanasekar, M., Page, A.W., and Kleeman, P.W., "The Failure of Brick Masonry Under Bi-axial Stresses", *Proceedings of Institution of Civil Engineers*, Part 2, 79, 295–313, June 1985.
- [13] Drydale, R.G., Hamid, A.A., and Baker, L.R., *Masonry Structures—Behaviour and Design*, Prentice Hall, Englewood Cliffs, New Jersey, 1994.
- [14] Eurocode No. 6, 1988. "Common Unified Rules for Masonry Structures", Commission of the European Communities, *Report EUR 9888 EN*, 1988.
- [15] Grimm, C.T., "Strength and Related Properties of Brick Masonry", *Journal of Structural Engineering*, ASCE, Vol. 101, No. ST 1, 217–232, January, 1975.
- [16] Hamid, A.A. and Drydale, R.C. "The Shear Behaviour of Brickwork Bed Joints", *Proceedings of British Ceramic Society*, No. 30, September 1982.
- [17] Hendry, A.W, *Structural Masonry*, 2nd ed., Macmillan Press, 1998.
- [18] Hendry, A.W. and Sinha, B.P. "Shear Test on Full Scale Single Storey Brickwork Structures Subjected to Pre-compression", *Civil Engineering Publications Wks Rev.*, 1339-44, 1971.
- [19] IS 1905:1987 (1985). *Code of Practice for Structural Use of Unreinforced Masonry*, Bureau of Indian Standards, New Delhi, 1985.
- [20] IS 4326:1993, *Earthquake Resistant Design and Construction of Buildings—Code of Practice*, Bureau of Indian Standards, New Delhi. 1993.
- [21] Knutsson, H.H. and Nielson, J. "On the Modulus of Elasticity for Masonry", *Masonry International*, 9(2), 57–61, 1995.
- [22] McNary, W.S. and Abrams, D.P. "Mechanics of Masonry in Compression", *Journal of Structural Engineering*, ASCE, Vol. 111, No. 4, 857–870, April, 1985.
- [23] MIA, *Masonry Codes and Specification*, A Co-publication of the Masonry Institute of America and CRC Press, New York, 1998.

- [24] Page, A.W., "Concentrated Loads on Solid Masonry Walls—A Parametric Study and Design Recommendations", *Proceedings of Institution of Civil Engineers*, Part 2, 85: 271–289, June, 1982.
- [25] Pieper, K. and Trautsch, W., "Shear Tests on Walls", *Proceedings of 2nd International Brick Masonry Conference* (Stoke-on-Trent), H.W.H. West and K.H. Speed (Eds.) British Ceramic Research Association, Stoke-on-Trent, 1971.
- [26] Powell, B. and Hodgkinson, H.R., "The Determination of Stress/Strain Relationship of Brickwork", *Proceedings of Fourth International Brick Masonry Conference, Brugge*, Paper 2.a.5, 1976.
- [27] Sahlin, S., *Structural Masonry*, Prentice Hall, Englewood Cliffs, New Jersey, 1971.
- [28] Schneider, H., "Tests on Shear Resistance of Masonry", *Proceedings of the Fourth International Brick Masonry Conference, Brugge*, 1976.
- [29] Schneider, H. and Schnell, W., "Tests on the Shear Strength of Brickwork", *Betonwerk & Fertigteil-Technik*, 44, 1978.
- [30] Schneider, R.R. and Dickey, W.L., *Reinforced Masonry Design*, 3rd ed., Prentice Hall, New Jersey, 1994.
- [31] Schubert, P., "Modulus of Elasticity of Masonry", *Proceedings of the Fifth International Brick Masonry Conference*, Washington, 1982.
- [32] Sinha, B.P. and Pedreschi, R., "Compressive Strength and Some Elastic Properties of Brickwork", *International Journal of Masonry Construction*, 1983.
- [33] Sinha, B.P. and Hendry, A.W., "Racking Test on Storey Height Shear Wall Structures with Openings Subjected to Pre-compression", *Designing, Engineering and Constructing with Masonry Products*, F.B. Johnson (Ed.), Gulf, Houston, Texas, 1969.
- [34] Smith, B.S. and Carter, C., "Hypothesis for Shear Failure of Brickwork", *Journal of the Structural Division, Proceedings of the American Society of Civil Engineers*, April, 1971.
- [35] SP 20 (S&T), *Handbook on Masonry Design and Construction*, Bureau of Indian Standards, New Delhi, 1991.
- [36] Turnsek, V. and Cacovic, F., "Some Experimental Results on the Strength of Brick Masonry Walls", *Proceedings of 2nd International Brick Masonry Conference*, Stoke-on-Trent, pp. 149–156, 1970.

Chapter 26

Lateral Load Analysis of Masonry Buildings

26.1 INTRODUCTION

Masonry buildings are widely used for housing construction not only in India but in many other countries of the world. There are innumerable advantages of masonry construction over both types of construction *i.e.* reinforced concrete and steel such as, thermal comfort, sound control, possibility of addition and alteration after construction, less formwork, easy and inexpensive repair, use of locally available materials, need of less skilled labour, less engineering intervention etc. However, there are some disadvantages as well, particularly, when it is built in seismic environment. The seismic resistance capacity of masonry construction is relatively low in comparison to engineered constructions. Table 26.1 compares the properties of masonry to the comparable properties of structural steel and reinforced concrete (STP 992, 1988). Therefore, many developed nations have imposed certain restrictions on the use of unreinforced masonry constructions. However, in developing nations unreinforced masonry construction is still being used frequently. In India, masonry constructions are generally made by using locally available materials like stone, brick, timber, adobe, mud etc. and are constructed in a traditional manner with or without the earthquake resistant features mentioned in IS: 4326 and 13927. Therefore, this type of construction is treated as non-engineered construction and most of the casualties are due to collapse of these constructions in earthquakes. Moreover the plight is that even after gaining knowledge of earthquake engineering since the last three decades, neither a proper method has been developed for the seismic analysis and design of masonry buildings nor the topic is fairly covered in the current Indian curriculum in spite of the fact that about 90% population of India lives in masonry buildings. The present and subsequent chapters are a step towards with regard to develop a procedure for seismic analysis and design of masonry buildings. The procedure is divided into several distinctive steps in order to create a solid feeling and confidence that masonry buildings may also be designed as engineered construction.

TABLE 26.1 Properties of masonry, structural steel, and reinforced concrete masonry unit strength and mortar strength (STP 992, 1988)

Bricks	27600 to 110000 kPa (4000 to 16000 psi) compression 2800 to 11000 kPa (400 to 1600 psi) tension	Steel	Reinforced concrete
Mortar	5200 to 20700 kPa (750 to 3000 psi) compression 70 to 2100 kPa (10 to 300 psi) tensile bond		
Stresses (ultimate)	<i>Brick masonry</i>	<i>Steel</i>	<i>Reinforced concrete</i>
Compression	14000 to 32000 kPa (2000 to 4600 psi)	414000 to 690000 kPa (60000 to 100000 psi)	41400 to 70000 kPa (6000 to 10000 psi)
Tension	70 to 2100 kPa (10 to 300 psi)	414000 to 690000 kPa (60000 to 100000 psi)	103400 to 206800 kPa (15000 to 30000 psi)
Flexure	14000 to 32000 kPa (2000 to 4600 psi)	248000 to 414000 kPa (36000 to 60000 psi)	41400 to 70000 kPa (60000 to 10000 psi)
Shear	690 to 1400 kPa (100 to 200 psi)	138000 to 207000 kPa (20000 to 30000 psi)	690 to 2100 kPa (100 to 300 psi)
Torsion	1400 to 2100 kPa (200 to 300 psi)	207000 to 345000 kPa (30000 to 50000 psi)	1380 to 3450 kPa (200 to 500 psi)
Ductility	Brittle	Ductile	Semi-brittle
Coefficients (thermal)	5.4 to 6.3×10^{-6} mm/mm/ $^{\circ}\text{C}$ (3.0 to 3.5×10^{-6} in./in./ $^{\circ}\text{F}$)	11.7×10^{-6} mm/mm/ $^{\circ}\text{C}$ (6.5×10^{-6} in./in./ $^{\circ}\text{F}$)	9.0 to 10.0×10^{-6} mm/mm/ $^{\circ}\text{C}$ (5.0 to 5.5×10^{-6} in./in./ $^{\circ}\text{F}$)
Moisture	0.00018 to 0.00025	— — —	— — —

26.2 PROCEDURE FOR LATERAL LOAD ANALYSIS OF MASONRY BUILDINGS

To understand the proper design procedure for low-rise masonry buildings, this procedure is divided into several distinctive steps. In actual practice, these various steps may not be so clearly delineated nor so distinctly separated, but at this stage, at least, this step-by-step procedure is recommended in order to understand it properly. Figure 26.1 shows masonry building subjected to a lateral load and its resisting mechanism. In load bearing masonry buildings, the walls, which carry gravity loads, also act as shear walls to resist lateral load. The structural walls parallel to lateral force and subjected to in-plane (shear) forces and bending are called *shear walls*. The walls perpendicular to seismic force/lateral force and subjected to out-of-plane bending are called *flexural walls*. Following are the major steps for the lateral load analysis of masonry buildings:

Step 1: Determination of lateral load based on IS 1893 (Part 1): 2002

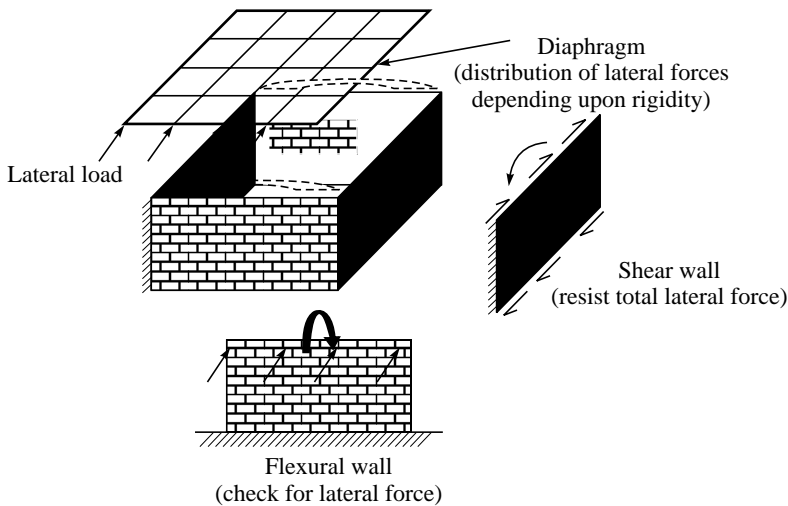


FIGURE 26.1 Force resisting mechanism in masonry buildings.

- Step 2: Distribution of lateral forces on the basis of flexibility of diaphragms
- Step 3: Determination of rigidity of shear wall by considering the openings
- Step 4: Determination of direct shear forces and torsional shear forces in shear walls
- Step 5: Determination of increase in axial load in piers due to overturning
- Step 6: Check the stability of flexural wall for out-of-plane forces

26.2.1 Step 1: Determination of Lateral Loads

Earthquake load

One of the most important lateral loads on a structure is due to earthquake, which arises from inertia (mass) of the structure. These earthquake loads are sudden, dynamic and can be of immense intensity. The magnitude of lateral force mainly depends upon the seismic zone, type of soil or ground condition and fundamental characteristics. The design base shear shall first be computed as a whole, then be distributed along the height of the buildings based on simple formulas appropriate for buildings with regular distribution of mass and stiffness. The design lateral force obtained at each floor level shall then be distributed to individual lateral load resisting element depending upon floor diaphragm action. Following are the major steps for determining the lateral forces

Design seismic base shear

The design seismic base shear force, V_B that acts on the building in a given direction is as follows

$$V_B = \alpha_h W$$

α_h = The design horizontal seismic coefficient for a structure. It is determined by the following expression

$(Z/2) (I/R) (S_a/g)$, provided that for any structure with $T \leq 0.1$ sec the value of α_h will not be taken less than $Z/2$ what ever be the value of I/R .

where,

$(Z/2) = Z$ is the zone factor, based on Maximum Considered Earthquake (MCE) and service life of structure in a zone. Factor 2 in the denominator of Z is used so as to reduce the MCE zone factor to the factor of Design Basis Earthquake (DBE). The country is divided into four zones and the values of Z ranges from 0.10 to 0.36. Zone factors for different zones are given in Table 2 of IS 1893 (Part 1): 2002.

$(I/R) =$ Ratio of importance factor and response reduction factor. The values of importance factor and response reduction factors are given in Table 6 and 7 of IS 1893 (Part 1): 2002. The ratio of (I/R) shall not be greater than 1.0.

$(S_a/g) =$ Average response acceleration coefficient for rock and soil sites based on appropriate natural period and damping of the structures. The equations of (S_a/g) for different type of soil in different ranges of period are given in Clause 6.4.2 of IS 1893 (Part 1): 2002. The value of time period of the building may be determined as follows:

$$T_a = \frac{0.09h}{\sqrt{d}}$$

where,

h = height of building, in m,

d = base dimension of the building at plinth level, in m, along considered direction of the lateral force, and

W = seismic weight of the building.

Vertical distribution of base shear to different floor levels

The design base shear (V_B) computed shall be distributed along the height of the building (Figure 26.2) as per the following expression

$$Q_i = V_B \frac{W_i h_i^2}{\sum_{i=1}^n W_i h_i^2}$$

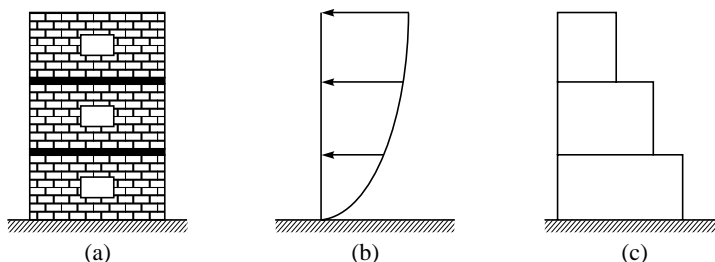


FIGURE 26.2 (a) Seismic shear on building (b) Seismic load (c) Storey shear.

where,

Q_i = design lateral force at floor i ,

W_i = seismic weight of floors i ,

h_i = height of floor i , measured from base, and

n = number of stories in the building is the number of levels at which the masses are located.

Example 1 Determine the lateral forces on two-storey un-reinforced brick masonry building situated at Roorkee

Building data

Plan size = 20 m × 20 m

Total height of building = 6 m

(each storey height = 3.0 m)

Weight of roof = 2.5 kN/m²

Weight of walls = 5.0 kN/m²

Live load at roof = 0

Live load at floors = 1 kN/m²

(25% of imposed load if imposed load is lesser than 3.0 kN/m² as per

Table 8 of IS 1893 (Part 1): 2002

Zone factor (Z) = 0.24

Importance factor (I) = 1.0

Response reduction factor = 1.5

Spectral acceleration (S_a/g) = 2.5

Soil = Type II (Medium soil)

The seismic dead load at roof level (W_f)

Weight of roof

$$= 2.5 \times 20 \times 20 = 1000 \text{ kN}$$

Weight of walls

$$= (5 \times 4 \times 20 \times 3)/2 = 600 \text{ kN}$$

Weight at roof level (W_r)

$$= 1000 + 600 = 1600 \text{ kN}$$

The seismic dead load at second floor level

Weight of second floor

$$= 2.5 \times 20 \times 20 = 1000 \text{ kN}$$

Weight of walls

$$= (5 \times 4 \times 20 \times 3) = 1200 \text{ kN}$$

Weight of live load

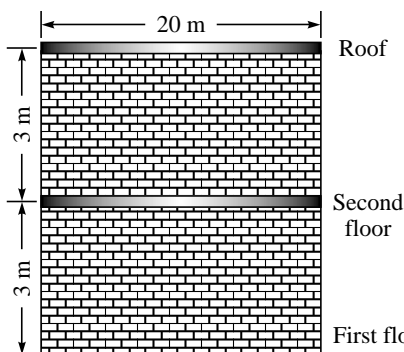
$$= 1 \times 20 \times 20 \times 0.25 = 100 \text{ kN}$$

Total weight at second floor (W_2)

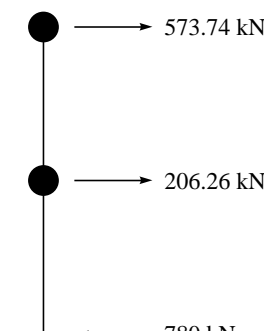
$$= 1000 + 1200 + 100 = 2300 \text{ kN}$$

Total weight of building

$$= 1600 + 2300 = 3900 \text{ kN}$$



(a)



(b)

Elevation of masonry building and lateral force.

The natural period of building as per IS 1893 (Part 1): 2002

$$T = 0.09h/\sqrt{d} = 0.09 \times 6/\sqrt{20} = 0.12, \Rightarrow S_a/g = 2.5$$

The base shear is,

$$V_B = A_h W = [(Z/2)(I/R)(S_a/g)]W = [(0.24/2)(1.0/1.5)(2.5)]3900 = 780 \text{ kN}$$

Vertical distribution of base shear to different floor levels is

At roof level

$$Q_r = 780 \frac{1600 \times 6^2}{(1600 \times 6^2 + 2300 \times 3^2)} = 573.74 \text{ kN}$$

At second floor level

$$Q_2 = 780 \frac{2300 \times 3^2}{(1600 \times 6^2 + 2300 \times 3^2)} = 206.26 \text{ kN}$$

26.2.2 Step 2: Distribution of Lateral Forces

Figure 26.3 shows the distribution of lateral forces in box type shear wall buildings. In order to transfer the seismic forces to the ground, there should be a continuous load path in the building. The general load path is as follows: earthquake forces, which originate in all the elements of the building, are delivered through the transverse wall of the building and it is bent

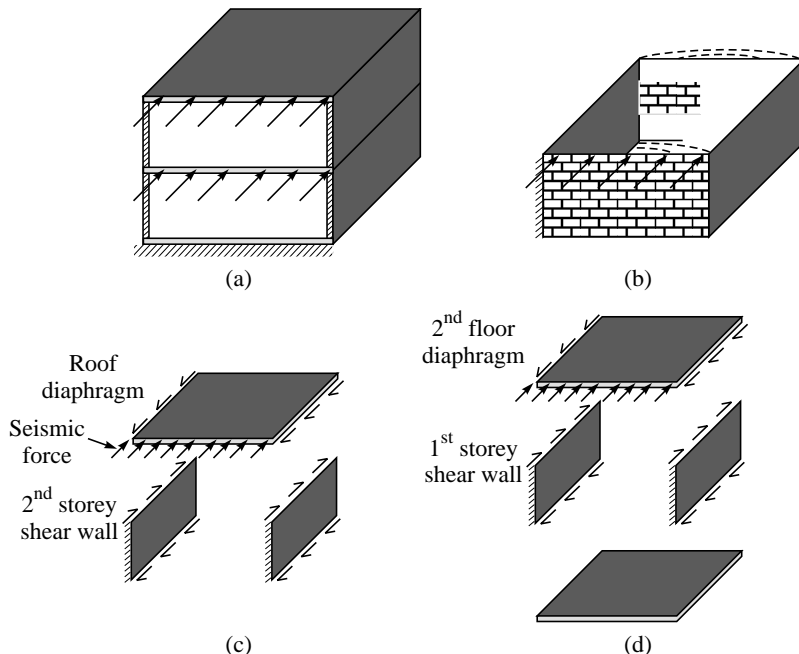


FIGURE 26.3 Lateral force distribution in a box type building (a) Box type masonry building subjected to lateral load (b) Bend of first storey/second storey transverse walls (c) Distribution of lateral forces in second storey (d) Distribution of lateral forces in first storey.

between the floors. The lateral loads are transmitted from these transverse walls to the side shear wall by horizontal floor and roof diaphragms. The diaphragms distribute these forces to vertical resisting components such as shear walls and vertical resisting elements if any, which transfer the forces into the foundation. The diaphragms must have adequate stiffness and strength to transmit these forces. The distribution of lateral forces in the masonry building will depend upon the flexibility of horizontal diaphragm *i.e.* how rigid the walls are as compared to the rigidity of the diaphragm. The rigidity of the diaphragms is classified into two groups on relative flexibility: **rigid** and **flexible diaphragm**.

Rigid diaphragms

A diaphragm may be considered rigid when its midpoint displacement, under lateral load, is less than twice the average displacements at its ends. *Rigid diaphragm distributes the horizontal forces to the vertical resisting elements in direct proportion to the relative rigidities*. It is based on the assumption that the diaphragm does not deform itself and will cause each vertical element to deflect the same amount. Rigid diaphragms capable of transferring torsional and shear deflections and forces are also based on the assumption that the diaphragm and shear walls undergo rigid body rotation and this produces additional shear forces in the shear wall. Rigid diaphragms consist of reinforced concrete diaphragms, precast concrete diaphragms, and composite steel deck.

Flexible diaphragms

A diaphragm is considered flexible, when the midpoint displacement, under lateral load, exceeds twice the average displacement of the end supports. It is assumed here that the relative stiffness of these non-yielding end supports is very great compared to that of the diaphragm. Therefore, diaphragms are often designed as simple beams between end supports, and distribution of the lateral forces to the vertical resisting elements on a tributary width, rather than relative stiffness. Flexible diaphragm is not considered to be capable of distributing torsional and rotational forces. Flexible diaphragms consist of diagonally sheathed wood diaphragms, etc. Figure 26.4 provides a comparison between flexible and rigid diaphragms (Williams, 2003).

Example 2 Distribute a seismic load of 100 kN in end shear walls A, B and C in case of

- (i) rigid diaphragm (ii) flexible diaphragm

Rigid diaphragm

$$\text{Wall A} = (100 \times 5)/(5 + 3 + 2) = 50 \text{ kN}$$

$$\text{Wall B} = (100 \times 3)/(5 + 3 + 2) = 30 \text{ kN}$$

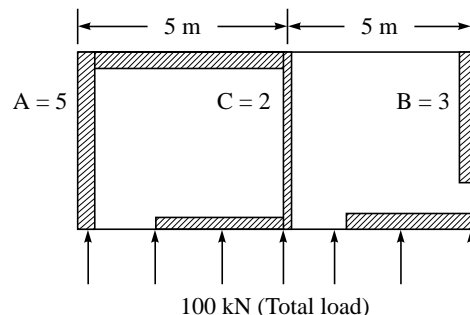
$$\text{Wall C} = (100 \times 2)/(5 + 3 + 2) = 20 \text{ kN}$$

Flexible diaphragm

$$\text{Wall A} = (100 \times 2.5)/(10) = 25 \text{ kN}$$

$$\text{Wall B} = (100 \times 2.5)/(10) = 25 \text{ kN}$$

$$\text{Wall C} = (100 \times (2.5 + 2.5))/(10) = 50 \text{ kN}$$



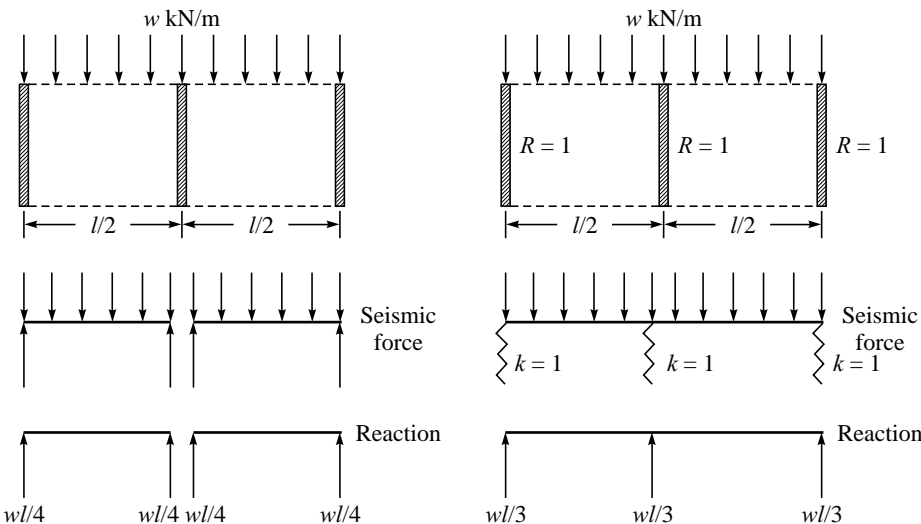


FIGURE 26.4 Comparison between flexible and rigid diaphragm (Williams, 2003).

26.2.3 Step 3: Determination of Rigidity of Shear Wall

The lateral load capacity of shear wall is mainly dependent on the in-plane resistance rather than out-of-plane stiffness. The distribution of lateral load to the shear walls is based on the relative wall rigidities if a rigid diaphragm supports the walls and the segment of wall deflects equally. The rigidity of a shear wall is dependent on its dimensions, modulus of elasticity (E_m), modulus of rigidity (G_m) and the support condition.

Pier analysis

In masonry structures, it is generally assumed that in one- and two-storey buildings the walls may be considered cantilevered and the segment of the walls between adjacent openings are called piers and might be considered fixed at top and bottom, depending on the relative rigidities of the walls versus those of the floor diaphragms. The main assumptions in the analysis are (Schneider and Dickey, 1994):

- Rotational deformations of the portions above and below the openings are much smaller than those of the piers between the openings and are neglected.
- Points of contra flexure are assumed at the mid points of the piers and shears are assumed to be carried among the piers such that their top deflects by equal amount.
- Lateral forces will be transformed to the various parallel resisting elements in direct proportion to their stiffness
 - Large portion of the total lateral force is required to reduce same deflection in a stiffer wall compared to that of a more flexible one
 - Stiffness refers to the lateral force magnitude required to produce a unit deflection
 - Relative, rather than absolute, stiffness can be computed since each wall is only being compared to the combined stiffness of the entire wall system

Cantilever pier or wall

If the pier or wall fixed only at the bottom and top is free to translate and rotate, it is considered a *cantilevered wall*. When a force (P) is applied at the top of a pier, it will produce a deflection, Δ_c that is the sum of the deflections due to bending moment (Δ_m) plus that due to shear (Δ_v) (Figure 26.5).

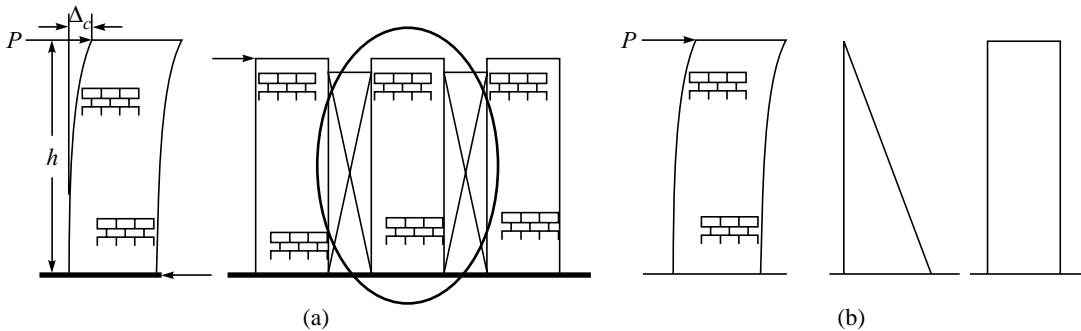


FIGURE 26.5 (a) Wall pier displaced at top and cantilevering from fixed bottom (b) Deflection of walls due to bending and shear deformations (Amrhein, 1998).

$$\begin{aligned}\Delta_c &= \Delta_m + \Delta_v \\ &= Ph^3/3E_m I + 1.2Ph/AG_m\end{aligned}$$

where,

Δ_m = deflection due to flexural bending

Δ_v = deflection due to shear

P = lateral force on pier

h = height of pier

A = cross section of pier

E_m = modulus of elasticity in compression

G_m = modulus of elasticity in shear (shear modulus)

For masonry, $G_m = 0.4 E_m$

$$\Delta_c = \frac{P}{E_m t} \left[4 \left(\frac{h}{d} \right)^3 + 3(h/d) \right]$$

Rigidity of cantilever pier $R_c = 1/\Delta_c = E_m t / (4(h/d)^3 + 3(h/d))$

Fixed pier or wall

For a wall/pier fixed at top and the bottom, the deflection from a force, P (Figure 26.6),

$$\begin{aligned}\Delta_f &= \Delta_m + \Delta_v \\ &= Ph^3/12E_m I + 1.2Ph/AG_m\end{aligned}$$

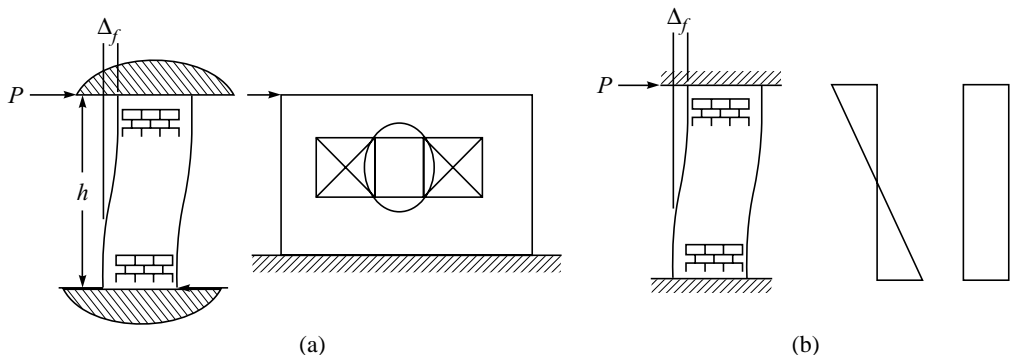


FIGURE 26.6 (a) Wall pier with top displaced and fixed at top and bottom (b) Deflection of walls due to bending and shear deformations (Amrhein, 1998).

For masonry, $G_m = 0.4 E_m$

$$\Delta_f = \frac{P}{E_m t} \left[\left(\frac{h}{d} \right)^3 + 3(h/d) \right]$$

Rigidity of fixed pier

$$R_f = 1/\Delta_f = E_m t / ((h/d)^3 + 3(h/d))$$

Effect of aspect ratio on deflection due to shear

Aspect ratio (h/d)	% deflection due to shear		(i)
	Cantilever wall	Fixed end wall	
0.25	92	98	
1	43	5	
2	16	43	(ii)
4	5	16	
8	1	4.3	(iii)

- (i) Very squat shear wall ($h/d < 0.25$), rigidities based on shear deformation are reasonably accurate
- (ii) For intermediate height of shear wall ($0.25 < h/d < 4.0$), including both the components of deflection
- (iii) For high h/d ratio, the effect of shear deformation is very small and rigidity based on flexural stiffness is reasonably accurate (Drydale, Hamid and Baker, 1994).

Horizontal and vertical combinations

If the shear wall segments are combined horizontally, the combined rigidity $R = R_{c1} + R_{c2} + R_{c3}$, if the segments are combined vertically, the combined rigidity $1/R = 1/R_{c1} + 1/R_{c2} + 1/R_{c3}$ (Figure 26.7).

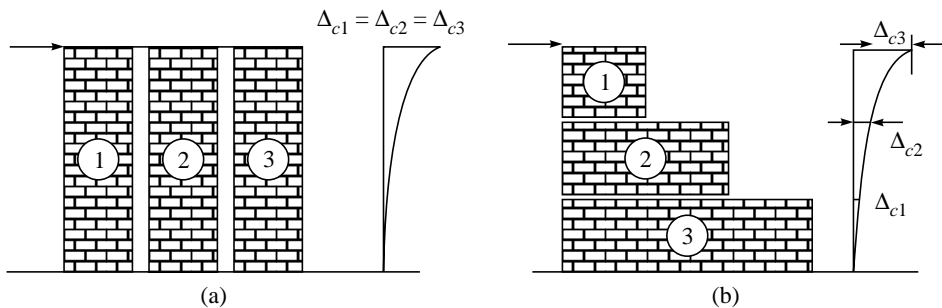


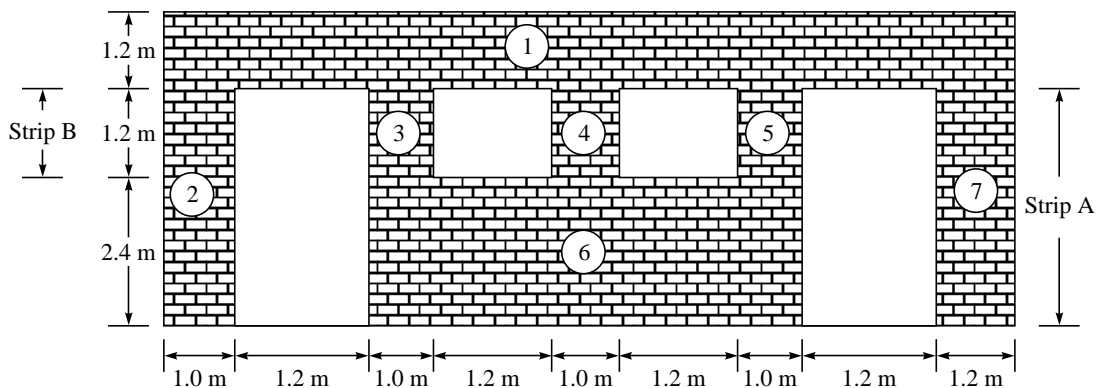
FIGURE 26.7 (a) Horizontal combination of wall segments (b) Parallel combination of wall segments (Drydale, Hamid and Baker, 1994).

Method for calculating the rigidity of wall with opening

The following steps are required for calculating the rigidity of wall with opening (Drydale, Hamid and Baker, 1994).

- (i) Calculate the deflection of the solid wall as a cantilever, $\Delta_{\text{solid}(c)}$ (for one- or two-storey building)
- (ii) Calculate the cantilever deflection of an interior strip, having a height equal to that of the highest opening, is calculated and subtracted from the solid wall deflection. This step removes the entire portion of the wall containing all the openings ($\Delta_{\text{strip of highest opening}(c)}$)
- (iii) Calculate the deflections of all the piers as fixed within that interior strip being determined by their own individual rigidities ($\Delta_{\text{peirs}(f)}$)
- (iv) Add deflection of piers to the modified wall deflection to arrive at the total deflection of the actual wall with openings (Δ_{total})
- (v) The reciprocal of this value becomes the relative rigidity of the wall $\left(R = \frac{1}{\Delta_{\text{total}}} \right)$

Example 3 Determine the rigidity of the shear wall, as shown, in terms of Et



$$\Delta_{\text{wall}} = \Delta_{\text{solid wall}(c)} - \Delta_{\text{strip A}(c)} + \Delta_{2,3,4,5,6,7(f)}$$

$$\Delta_{2,3,4,5,6,7(f)} = 1/(R_{2,3,4,5,6,7(f)})$$

$$R_{2,3,4,5,6,7(f)} = R_{2(f)} + R_{3,4,5,6(f)} + R_{7(f)}$$

$$R_{3,4,5,6(f)} = 1/\Delta_{3,4,5,6(f)}$$

$$\Delta_{3,4,5,6(f)} = \Delta_{\text{solid 3,4,5,6}(f)} - \Delta_{\text{stripB}(f)} + \Delta_{3,4,5(f)}$$

$$\Delta_{3,4,5(f)} = \frac{1}{R_{3(f)} + R_{4(f)} + R_{5(f)}}$$

$$\Delta_{\text{solid}(c)} = \frac{1}{Et} \left[4 \left(\frac{h}{d} \right)^3 + 3 \left(\frac{h}{d} \right) \right] = 1.882/Et \quad \text{For } \frac{h}{d} = \frac{3.6+1.2}{10} = 0.48$$

$$\Delta_{\text{stripA}(c)} = \frac{1}{Et} \left[4 \left(\frac{h}{d} \right)^3 + 3 \left(\frac{h}{d} \right) \right] = 1.266/Et \quad \text{For } \frac{h}{d} = \frac{3.6}{10} = 0.36$$

$$R_{3(f)} = R_{4(f)} = R_{5(f)} = Et \left/ \left[\left(\frac{h}{d} \right)^3 + 3 \left(\frac{h}{d} \right) \right] \right. = 0.187/Et \quad \text{For } \frac{h}{d} = \frac{1.2}{10} = 0.12$$

$$\Delta_{3,4,5(f)} = 1/3(0.187Et) = 1.782/Et$$

$$\Delta_{3,4,5,6(f)} = \frac{1}{Et} \left[\left(\frac{h}{d} \right)^3 + 3 \left(\frac{h}{d} \right) \right] = 2.311/Et \quad \text{For } \frac{h}{d} = \frac{3.6}{5.4} = 0.67$$

$$\Delta_{\text{stripB}(f)} = \frac{1}{Et} \left[\left(\frac{h}{d} \right)^3 + 3 \left(\frac{h}{d} \right) \right] = 0.671/Et \quad \text{For } \frac{h}{d} = \frac{1.2}{5.4} = 0.22$$

$$\Delta_{3,4,5,6(f)} = 2.311/Et - 0.671/Et + 1.782/Et = 3.422/Et$$

$$R_{3,4,5,6(f)} = 0.292 Et$$

$$R_{2(f)} = Et \left/ \left[\left(\frac{h}{d} \right)^3 + 3 \left(\frac{h}{d} \right) \right] \right. = 0.017Et \quad \text{For } \frac{h}{d} = \frac{3.6}{1.0} = 3.6$$

$$R_{7(f)} = Et \left/ \left[\left(\frac{h}{d} \right)^3 + 3 \left(\frac{h}{d} \right) \right] \right. = 0.028Et \quad \text{For } \frac{h}{d} = \frac{3.6}{1.2} = 3.0$$

$$R_{2,3,4,5,6,7(f)} = 0.017Et + 0.292Et + 0.028Et = 0.337Et$$

$$\Delta_{2,3,4,5,6,7(f)} = 2.967/Et$$

$$\Delta_{\text{wall}} = 1.882/Et - 1.266/Et + 2.967/Et = 3.583/Et$$

$$R_{\text{wall}} = 0.279Et$$

26.2.4 Step 4: Determination of Direct Shear Forces and Torsional Shear Forces

Direct shear forces

In case of rigid diaphragm it is assumed that the walls are tied together with the diaphragm, the lateral force (P) will be distributed to the walls in proportion to their relative stiffness.

For any wall i , the relative stiffness is given by,

$$R_i = k_i / \sum_{i=1}^n k_1 + k_2 + \dots + k_n$$

Direct shear forces on parallel walls are equal to $(V_D)_i = R_i P$

Torsional shear forces

When the centre of mass and centre of rigidity do not coincide, torsional shear forces will be induced on the wall in addition to the direct shear force. The horizontal load, P , will be at the centre of mass, thus a torsional moment, M_t , is induced that is equal to $P_y \times e_x$, where e_x equals the distance between the line of force (centre of mass) and the centre of rigidity. Even in symmetrical structure, where $e = 0$, a minimum eccentricity amounting to 5% of the building dimension is assumed which is called *accidental eccentricity* (Figure 26.8).

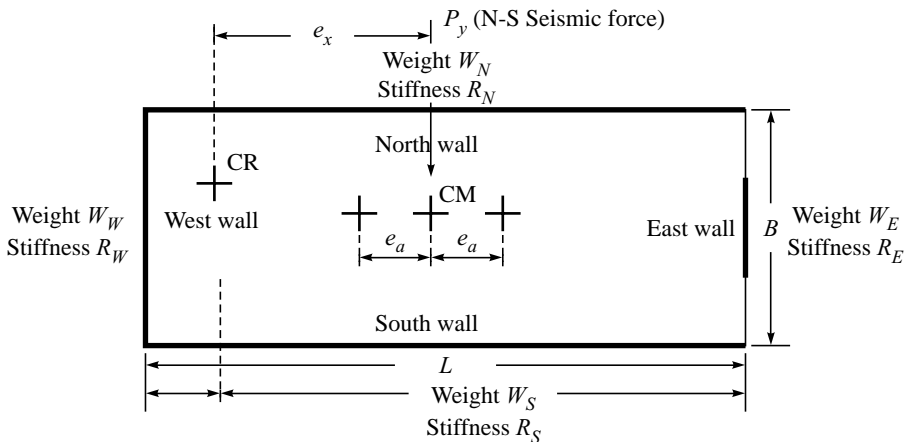


FIGURE 26.8 Torsional shear determination (Williams, 2003).

Centre of mass

Centre of mass \bar{X}_m is found by taking statical moments about a point, say south-west corner, using the respective lumped weights of walls as forces in the moment summation (Figure 26.9).

$$\bar{X}_m = (W_R \times L/2 + W_N \times L/2 + W_S \times L/2 + W_E \times L)/\Sigma W$$

where,

$$\Sigma W = (W_R + W_N + W_S + W_E + W_W),$$

W_R , W_N , W_S , W_E and W_W represent the weight of roof and respective walls
Similarly,

$$\bar{Y}_m = (W_R \times B/2 + W_E \times B/2 + W_W \times B/2 + W_N \times B)/\Sigma W$$

where,

$$\Sigma W = (W_R + W_E + W_W + W_N + W_S),$$

W_R , W_E , W_W , W_N and W_S represent the weight of roof and respective walls.

Centre of rigidity

The centre of rigidity, \bar{X}_{CR} and \bar{Y}_{CR} , is calculated by taking statical moments about a point, say, *south-west corner*, using the relative stiffnesses of the walls parallel to the y -axis as forces in the moment summation (Figure 26.9). The stiffness of slab is not considered in the determination of centre of rigidity.

$$\bar{X}_r = \frac{\Sigma R_y x}{\Sigma R_y} = \frac{(R_W \times 0 + R_E \times L)}{(R_W + R_E)} = \frac{R_E \times L}{(R_W + R_E)} \quad \dots \text{Centre of rigidity}$$

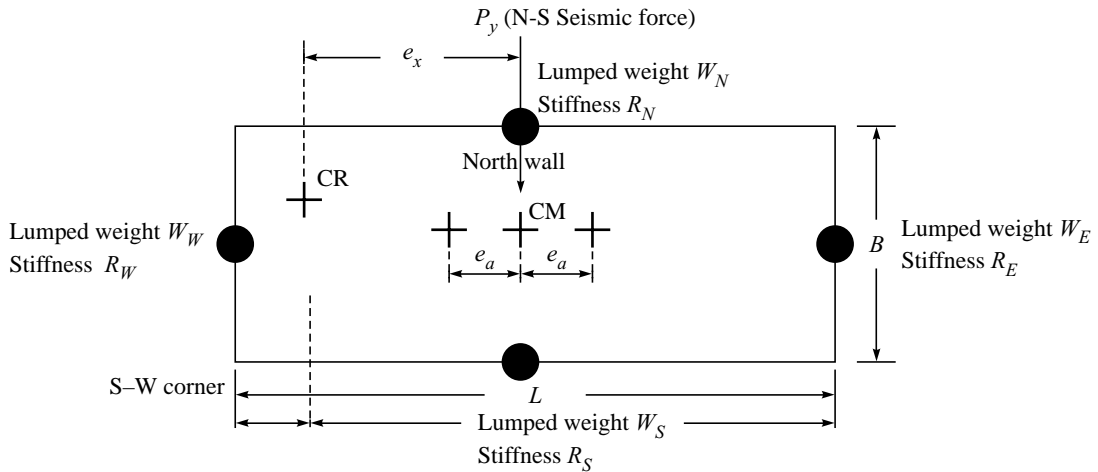


FIGURE 26.9 Lumped model for torsional shear determination.

Since the walls parallel to the x -direction do not contribute significantly to the lateral resistance in the y -direction, these relative rigidity terms do not appear in this summation. On the other hand, the y co-ordinate of the centre of rigidity \bar{Y}_r , entails the use of the R_x terms (in-plane lateral stiffness of the wall in the x -direction) as follows:

$$\bar{Y}_r = \frac{\Sigma R_x y}{\Sigma R_x} = \frac{(R_N \times B + R_S \times 0)}{(R_N + R_S)} = \frac{R_N \times B}{(R_N + R_S)} \quad \dots \text{Centre of rigidity}$$

Torsional eccentricity, $e_x = \bar{X}_m - \bar{X}_r$ and $e_y = \bar{Y}_m - \bar{Y}_r$

Total shear forces on parallel walls

The total horizontal shear, $(P_y)_i$, resisted by a particular wall element, with an axis parallel to the y -direction, due to the applied horizontal load, $(P_y)_i$, may be obtained from the expression

$$(P_y)_i = \frac{R_y}{\sum R_y} P_y \pm \frac{R_y \bar{x}}{J_r} P_y e_x \quad \dots \text{Total wall shear}$$

direct shear torsional shear

where, \bar{x} or \bar{y} = perpendicular distance from the centre of rigidity, CR, to the axis of wall in question

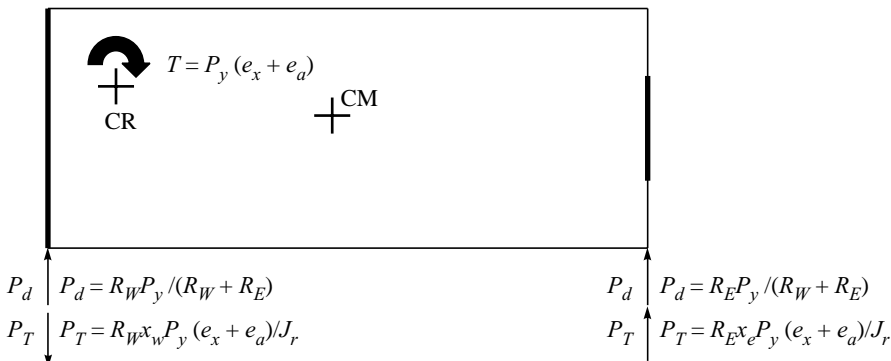
$$\Sigma R_y \text{ or } \Sigma R_x = 1.00$$

Similarly, for an applied horizontal force in the x -direction

$$(P_x)_i = \frac{R_x}{\sum R_x} P + \frac{R_x \bar{y}}{J_r} P_x e_y$$

In the preceding equations, J_r , equals the relative rotational stiffness of all the walls in the storey under consideration. It corresponds to a polar moment of inertia and may be found by the expression

$$J_r = \Sigma (R_x \bar{y}^2 + R_y \bar{x}^2) \dots \quad \text{Polar moment of inertia}$$



Note: The torsional forces have always plus sign. This stems from the fact that, since the horizontal load P is reversible, the code generally states that the effect of torsional moment be considered only when they tend to increase the direct stress.

Example 4 Calculating the torsional shear forces in one-storey shear wall masonry structure with a rigid diaphragm roof. The relative rigidity of each shear wall is given.

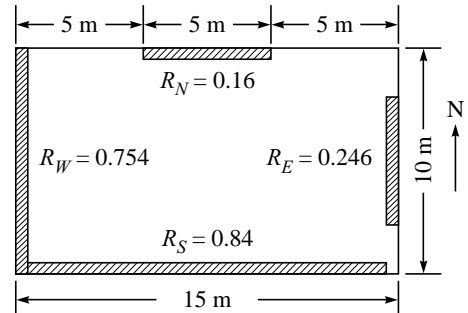
Given:

Building is a one-storey box system;

All walls are a total of 5 m height; 4 m upto roof level and 1 m parapet.

Seismic Zone V,

$$Z = 0.36, I = 1.0, R_W = 1.5, S_a/g = 2.5$$



Weights:

$$\text{Roof} = 3.0 \text{ kN/m}^2, \text{ Wall} = 5 \text{ kN/m}^2$$

$$\text{Base Shear} = 300 \text{ kN}$$

To calculate the shear forces due to torsion, first calculate the locations of the centre of mass and the centre of rigidity.

Location of the centre of mass

Centre of mass, \bar{X}_{CM} and \bar{Y}_{CM} , is calculated by taking statical moments about a point, say, *south west corner*, using the respective weights of walls as forces in the moment summation as shown in Table 26.2.

TABLE 26.2 Calculation of centre of mass

Item	Weight (kN)	X (m)	Y (m)	WX (kN-m)	WY (kN-m)
Roof slab	$10 \times 15 \times 3 = 450$	7.5	5.0	3375	2250
N-Wall	$5 \times 5 \times 5 = 125$	7.5	10.0	937.5	1250
S-Wall	$15 \times 5 \times 5 = 375$	7.5	0.0	2812.5	0
E-Wall	$5 \times 5 \times 5 = 125$	15.0	5.0	1875	625
W-Wall	$10 \times 5 \times 5 = 250$	0.0	5.0	0	1250
$\Sigma W = 1325$		$\Sigma WX = 9000$		$\Sigma WY = 5375$	

$$\bar{X}_{CM} = \Sigma WX / \Sigma W = 6.79 \text{ m from west wall}$$

$$\bar{Y}_{CM} = \Sigma WY / \Sigma W = 4.06 \text{ m from south wall}$$

Location of the centre of rigidity

The centre of rigidity, \bar{X}_{CR} and \bar{Y}_{CR} , is calculated by taking statical moments about a point, say, *south-west corner*, using the relative stiffnesses of the walls as forces in the moment summation. The stiffness of slab and parapet height are not considered in the determination of centre of rigidity. The calculation for the centre of rigidity is shown in Table 26.3.

TABLE 26.3 Calculation of centre of rigidity

Item	R_x	R_y	X (m)	Y (m)	$Y R_x$	$X R_y$
N-Wall	0.16	—	—	10	1.6	—
S-Wall	0.84	—	—	0.0	0	—
E-Wall	—	0.246	15	—	—	3.69
W-Wall	—	0.754	0.0	—	—	0.0
$\Sigma R_x = 1.0$		$\Sigma R_y = 1.0$		$\Sigma Y R_x = 1.6$		$\Sigma X R_y = 3.69$

$$\bar{X}_{CR} = \Sigma X R_y / \Sigma R_y = 3.69 \text{ m from west wall}$$

$$\bar{Y}_{CR} = \Sigma Y R_x / \Sigma R_x = 1.6 \text{ m from south wall}$$

Torsional eccentricity

Torsional eccentricity in y-direction

Eccentricity between centre of mass and centre of rigidity

$$e_y = 4.06 - 1.6 = 2.46 \text{ m}$$

Add minimum 5% accidental eccentricity

$$0.05 \times 10 = 0.50 \text{ m}$$

$$\text{Total eccentricity} = 2.46 + 0.50 = 2.96 \text{ m}$$

Torsional eccentricity in x-direction

Eccentricity between centre of mass and centre of rigidity

$$e_x = 6.79 - 3.69 = 3.10 \text{ m}$$

Add minimum 5% accidental eccentricity

$$0.05 \times 15 = 0.75 \text{ m}$$

$$\text{Total eccentricity} = 3.10 + 0.75 = 3.85 \text{ m}$$

Torsional moment

The torsional moment due to East-West seismic force, rotate the building in y-direction, hence

$$M_{TX} = V_x e_y = 300 \times 2.96 = 888 \text{ kN-m}$$

Similarly, if considered seismic force in N-S direction

$$M_{TY} = V_y e_x = 300 \times 3.85 = 1155 \text{ kN-m}$$

Distribution of direct shear forces and torsional shear forces

If we consider the seismic force only in East-West direction, the walls in North-South direction will resist the forces and the walls in E-W direction may be ignored. Table 26.4 shows the calculation of distribution of direct shear and torsional shear.

Similarly, if we considered seismic force in N-S direction, the walls in E-W direction will resist the forces and the walls in N-S direction may be ignored. Table 26.5 shows the calculation of distribution of direct shear and torsional shear.

26.2.5 Step 5: Determination of Increase in Axial Load due to Overturning

In shear wall analysis, the principal forces are in-plane shear (direct + torsional), in-plane moment (in-plane shear $\times \frac{1}{2}$ of height of pier) and dead and live load carried by the pier. In

TABLE 26.4 Distribution of forces in North and South shear walls

Item	R_x	d_y^* (m)	$R_x d_y$	$R_x d_y^2$	Direct shear forces (kN)	Torsional forces ** (kN)	Total shear (kN)
N-Wall	0.16	8.4	1.344	11.28	48	+89	137
S-Wall	0.84	1.6	1.344	2.15	252	-89	252
$\Sigma 13.40$							

*Distance of considered wall from centre of rigidity ($10 - 1.6 = 8.4$ m)

$$\text{**Torsional forces in N-Wall} = \frac{R_x d_y}{\sum R_x d_y^2} V_x e_y = \frac{1.344}{13.40} \times 888 = 89 \text{ kN}$$

$$\text{Torsional forces in S-Wall} = \frac{R_x d_y}{\sum R_x d_y^2} V_x e_y = \frac{1.344}{13.40} \times 888 = 89 \text{ kN}$$

TABLE 26.5 Distribution of forces in East and West shear walls

Item	R_y	d_x^* (m)	$R_y d_x$	$R_y d_x^2$	Direct shear forces (kN)	Torsional forces ** (kN)	Total shear (kN)
E-Wall	0.246	11.31	2.78	31.46	73.8	-76.96	150.76
W-Wall	0.754	3.69	2.78	10.26	226.2	+76.96	226.20
$\Sigma 41.72$							

* Distance of considered wall from centre of rigidity ($15 - 3.69 = 11.31$ m)

$$\text{** Torsional forces in E-Wall} = \frac{R_y d_x}{\sum R_y d_x^2} V_y e_x = \frac{2.78}{41.72} \times 1155 = 76.96 \text{ kN}$$

$$\text{Torsional forces in W-Wall} = \frac{R_y d_x}{\sum R_y d_x^2} V_y e_x = \frac{2.78}{41.72} \times 1155 = 76.96 \text{ kN}$$

addition to these forces sometimes, the lateral forces from winds or earthquakes create severe overturning moments on buildings. If the overturning moment is great enough, it may overcome the dead weight of the structure and may cause tension at the ends of piers of shear walls. It may also induce high compression forces in the pier of walls that may increase the axial load in addition to dead load and live load. The increase in axial load in piers due to overturning moments may be evaluated in the following manner (Schneider and Dickey, 1994).

Overturning moment at second floor level (Figure 26.10)

$$(M_{ovt})_2 = V_r (h_2 + h_3) + V_3 h_2$$

Total overturning moment on pier in the first storey

$M_{ovt} = (M_{ovt})_2 + \text{total } V \times \text{distance to the second floor level from critical level of the pier in the first storey}$ (Assume, at the sill height of piers h_{cr} , as shown in Figure 26.10).

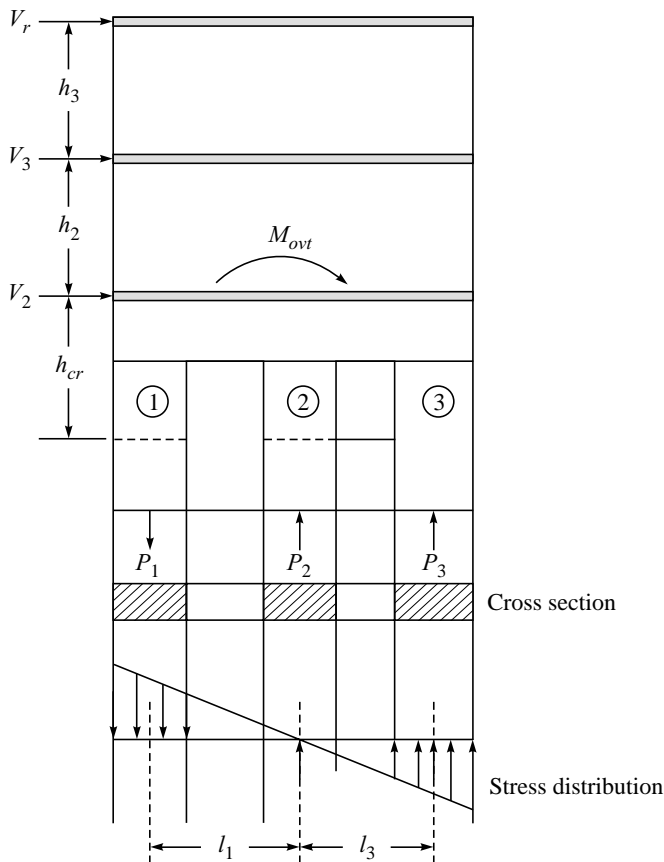


FIGURE 26.10 Axial load on pier due to overturning.

Thus the axial load on a pier due to overturning Change to P_{ovt} is

$$P_{ovt} = (M_{ovt})(l_f A_i)/I_n$$

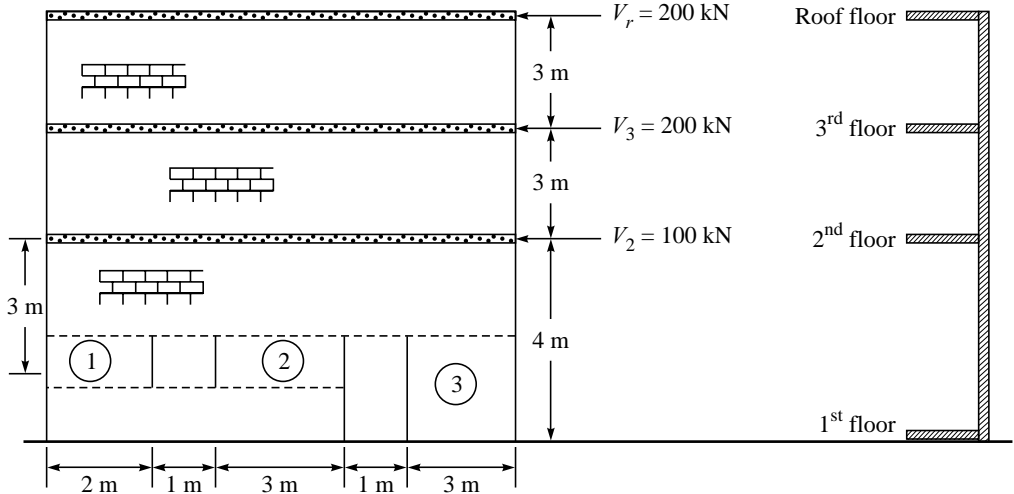
where,

l_i = Distance from the centre of gravity of the net wall section in the first storey to the centroid of the pier in question = $\sum_{i=1}^n l_i A_i / \Sigma A_i$

A_i = Cross-sectional area of pier in question

I_n = moment of inertia of net wall section in first storey = $\sum_{i=1}^n A_i l_i^2$

Example 5 Determine the increase in axial load due to overturning effects of lateral forces in wall as shown.



Taking the sum of moments about the centre line of axis of the vertical load

$$M_{ovt2} = V_r(h_2 + h_3) + V_3 \times h_2 = 200(3 + 3) + 200 \times 3 = 1800 \text{ kN}$$

$$M_{ovt} = (M_{ovt})_2 + \text{total } V \times h = 1800 + 500 \times 3 = 3300 \text{ kN}$$

Centroid of net section of wall

Pier	Area A_i (m^2)	d/s from left edge of wall to centroid of pier (m)	Al (m^3)
1	$2 \times 1/4$	1	0.5
2	$3 \times 1/4$	$2 + 1 + 1.5 = 4.5$	3.375
3	$3 \times 1/4$	8.5	6.375
$\Sigma A_i = 2.0 \text{ m}^2$			$\Sigma Al = 10.25$

$$\text{Distance from left edge to centroid} = \frac{\Sigma Al}{\Sigma A_i} = \frac{10.25}{2.0} = 5.125 \text{ m}$$

Moment of inertia of net section of wall

Increase in axial load on the individual pier in the first storey

$$P_{ovt} = M_{ovt} \cdot \frac{l_i A_i}{I_n} = \frac{3300 l_i A_i}{18.621} = 177.22 l_i A_i$$

26.2.6 Step 6: Walls Subjected to Out-of-plane Bending

In seismic design of masonry building, it is assumed that the total base shear induced by an earthquake will be resisted by the in-plane shear wall and transverse walls or flexural walls which will not resist any shear. However, the flexural wall will be checked for out-of-plane forces with the vertical loads. This action produces combined actions of axial compression and bending forces. Lateral stability of the walls need to be checked for this combined effect.

The relationship between the combined effects of axial load (P) and bending (M) can be related to the virtual eccentricity ($e = M/P$), and for linear elastic behaviour of section it can be expressed as, Figure 26.11(a),

$$F_m = P/A + M/S$$

where

F_m = limiting (allowable) stresses for combined axial compression and bending

A = area of section and,

S = section modulus

This equation can be used to define the linear interaction diagram and represented as shown in Figure 26.11(b).

If $P_0 = F_m \cdot A$ is the section capacity at zero eccentricity and $M_0 = F_m \cdot S$ is the moment that can be carried with zero axial load, the interaction can be represented by the unity equation as,

$$P/P_0 + M/M_0 = 1$$

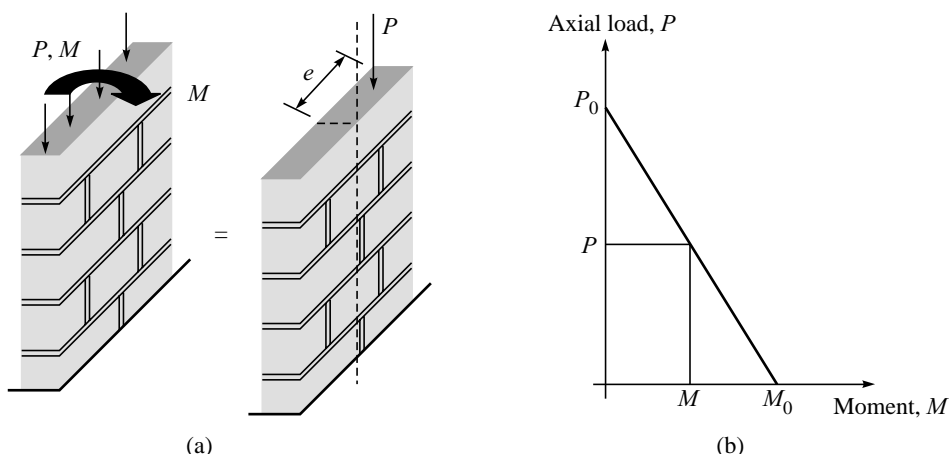


FIGURE 26.11 (a) Wall subjected to axial and out-of-plane loads (b) Linear interaction diagrams (Drysdale, Hamid and Baker, 1994).

The unity equation in some of masonry codes also be present in the form of

$$f_a/F_a + f_b/F_b = 1$$

where,

f_a, f_b = compressive stresses due to applied axial load and bending, respectively

F_a, F_b = allowable axial and bending compressive stresses, respectively

Both these equations are used for describing linear behaviour of section. For masonry, the effects of tensile cracking, non-linear stress-strain behaviour of masonry, the equation is conservative. However, the unity equation can be useful for working stress design of cracked sections, where the limiting compressive stresses under axial compression and bending are not equal. For unreinforced masonry, the allowable compressive stresses, F_a and F_b are given as follows:

$$F_b = 1/3f'_m$$

and

$$\begin{aligned} F_a &= 0.25 f'_m (70r/h)^2 && \text{for } h/r > 99 \\ &= 0.25 f'_m [1 - (h/140r)^2] && \text{for } h/r \leq 99 \end{aligned}$$

where,

h/r = slenderness ratio of the wall and

f'_m = design compressive strength of masonry

Nominal allowable load carrying capacity P_n of the wall in out-of-plane is,

$$P_n = f'_m b t (1/1 + 6e/t)) \quad \text{for } 0 < e < t/6$$

$$P_n = b t f'_m \left(\frac{3}{4} \left(1 - 2 \frac{e}{t} \right) \right) \quad \text{for } e > t/6$$

SUMMARY

Masonry buildings in India are generally designed on the basis of IS 1905. The procedure for seismic analysis and design of masonry buildings has still not received adequate attention in India in spite of the fact that the single-most important factor of contributing maximum damage and casualties in past earthquake is the collapse of masonry buildings. This chapter deals with step-by-step procedure for lateral load analysis of masonry buildings. The analysis includes the determination of lateral loads, distribution of lateral loads in case of rigid and flexible diaphragms, pier analysis of shear walls with torsional effects and increase of axial load in piers of shear wall due to overturning. A number of worked-out examples have been presented to illustrate the procedure properly.

REFERENCES

- [1] Amrhein, J.E., *Reinforced Masonry Engineering Handbook*, Masonry Institute of America, CRC Press, 1998.
- [2] Drydale, R.G., Hamid, A.H., and Baker, L.R., *Masonry Structure: Behaviour and Design*, Prentice Hall, Englewood Cliffs, New Jersey, 1994.
- [3] Schneider, R.R. and Dickey, W.L., *Reinforced Masonry Design*, 3rd ed., Prentice Hall, Englewood Cliffs, New Jersey, 1994.
- [4] Williams, Alan, *Seismic Design of Buildings and Bridges*, Oxford University Press, 2003.
- [5] STP 992, *Masonry: Materials, Design, Construction and Maintenance*, Harry A. Harris (Ed.), ASTM, Philadelphia, PA, 1988.

Chapter 27

Seismic Analysis and Design of Two-storeyed Masonry Buildings

27.1 INTRODUCTION

Masonry buildings in India are generally designed for vertical loads based on IS 1905. It is not confirmed whether the lateral load effects from wind or earthquakes have been considered in analysis or not, particularly when the buildings are constructed in seismic prone areas. In this chapter, an example has been presented to illustrate the design procedure for low rise masonry buildings.

27.2 BUILDING DATA

The plan and elevation of building are shown in Figure 27.1. Assume data for the building as follows:

Material strength

Permissible compressive strength of masonry (f_m) = 2.5 N/mm²

(Assuming unit strength = 35 MPa and mortar H1 type)

Permissible stresses in steel in tension = 0.55 f_y

(Use high strength deformed bar (Fe 415) i.e. f_y = 230 N/mm²)

Live load data

Live load on roof = 1.0 kN/m² (for seismic calculation = 0)

Live load on floor = 1.0 kN/m²

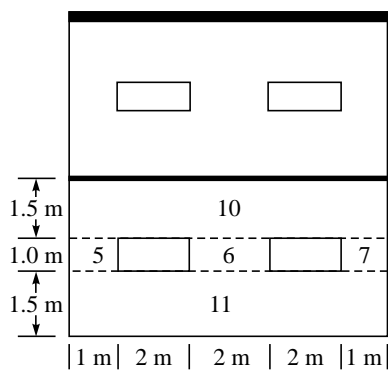
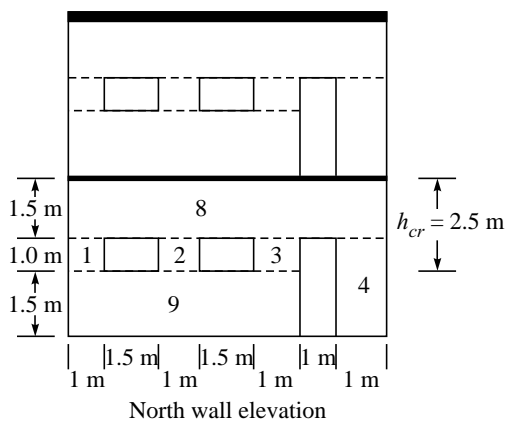
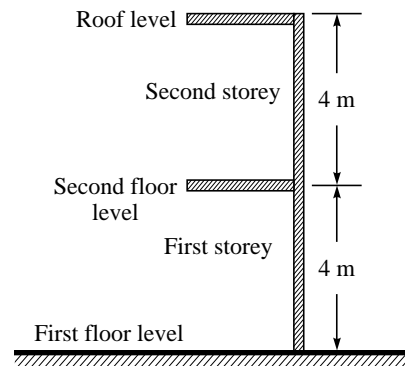
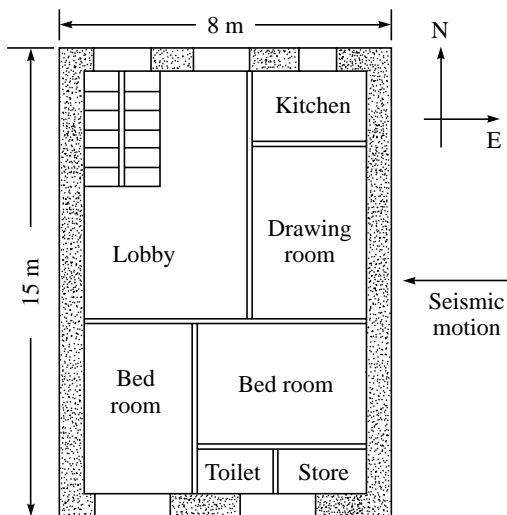


FIGURE 27.1 Example building.

Dead load data

Thickness of floor and roof slab = 120 mm

Weight of slab = 3 kN/m² (Assuming weight density of concrete = 25 kN/m³)

Thickness of wall = 250 mm

Weight of wall = 5 kN/m² (Assuming weight density of masonry = 20 kN/m³)

Seismic data

Seismic zone = V

Zone factor (Z) = 0.36

Importance factor (I) = 1

Response reduction factor (R) = 3.0 (as per IS 1893 (Part 1): 2002)

Soil medium type, for which average response acceleration coefficient are as:

$$\frac{S_a}{g} = \begin{cases} 1 + 15T, & 0.00 \leq T \leq 0.10 \\ 2.50, & 0.10 \leq T \leq 0.55 \\ 1.36/T, & 0.55 \leq T \leq 4.00 \end{cases}$$

Direction of seismic force = E–W direction

27.3 STEP 1: DETERMINATION OF DESIGN LATERAL LOAD

Seismic weight calculations

<i>Description</i>	<i>Load calculations</i>	<i>Total</i>
DL and LL load at roof level		
(i) Weight of roof	3 × 8 × 15	360 kN
(ii) Weight of walls <i>(Assume half weight of walls at second storey is lumped at roof)</i>	1/2{2(8 + 15) × 4 × 5}	460 kN
(iii) Weight of live load (LL) <i>(for seismic calculation, LL on roof is zero)</i>	0 × 8 × 15	0 kN
(W _r) Weight at roof level (i) + (ii) + (iii)	360 + 460 + 0	820 kN
DL and LL load at floor level		
(i) Weight of floor	3 × 8 × 15	360 kN
(ii) Weight of walls <i>(Assume half weight of walls at second storey and half weight of walls at first storey is lumped at roof)</i>	2 × 1/2{2(8 + 15) × 4 × 5}	920 kN
(iii) Weight of live load (LL)	1 × 8 × 15	120 kN
(W _f) Weight at second level (i) + (ii) + (iii)	360 + 920 + 120	1400 kN
Total seismic weight of building (W _r + W _f)	820 + 1400	2220 kN

Time period calculations

The approximate fundamental natural period of a masonry building can be calculated from the Clause 7.6.2 of IS 1893 (Part 1): 2002 as,

$$T_a = 0.09h/\sqrt{d}$$

where,

h = height of building in m, {i.e. 4.0 (first storey) + 4.0 (second storey) = 8.0 m}

d = Base dimension of building at the plinth level, in m, along the considered direction of lateral force (i.e. 8 m, assuming earthquake in E–W direction)

$$T_a = 0.09 \times 8/\sqrt{8} = 0.032 \text{ sec}$$

$$S_a/g = 2.5, \text{ for } T = 0.032$$

$$A_h = \frac{ZIS_a}{2Rg} = \left(\frac{0.36}{2}\right)\left(\frac{1}{3}\right)(2.5) = 0.15$$

The total design lateral base shear (V_B) along the direction of motion is given by,

$$V_B = A_h W = 0.15 \times 2220 = 333 \text{ kN}$$

The design lateral base shear (V_B) is distributed along the height of building as shown in Figure 27.2.

$$\text{Lateral force at roof level} = V_B \frac{\sum_{i=1}^n W_i h_i^2}{\sum_{i=1}^n W_i h_i^2} = 333 \frac{820 \times 8^2}{(820 \times 8^2 + 1400 \times 4^2)} = 233.35 \text{ kN}$$

$$\text{Lateral force at roof level} = V_B \frac{\sum_{i=1}^n W_i h_i^2}{\sum_{i=1}^n W_i h_i^2} = 333 \frac{1400 \times 4^2}{(820 \times 8^2 + 1400 \times 4^2)} = 99.65 \text{ kN}$$

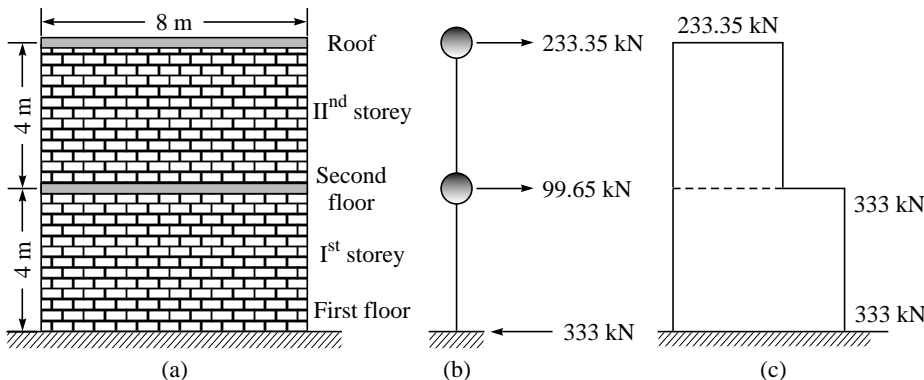


FIGURE 27.2 (a) Elevation of building (b) Seismic load or storey shear (c) Σ Storey shear (shear envelope).

27.4 STEP 2: DETERMINATION OF WALL RIGIDITIES

In the second step, we will calculate the relative stiffness of exterior shear walls. It is assumed here that all the lateral force will be resisted by the exterior shear walls. Therefore, the stiffness and masses of interior wall may be neglected in seismic analysis.

Rigidity of North shear wall

$$\Delta_{wall} = \Delta_{solid\ wall(c)} - \Delta_{strip\ A(c)} + \Delta_{1,2,3,9,4(f)}$$

$$\Delta_{1,2,3,9,4(f)} = \frac{1}{R_{1,2,3,9,4(f)}}$$

$$R_{1,2,3,9,4(f)} = R_{1,2,3,9(f)} + R_{4(f)}$$

$$R_{1,2,3,9(f)} = \frac{1}{\Delta_{1,2,3,9(f)}}$$

$$\Delta_{1,2,3,9(f)} = \Delta_{solid\,1,2,3,9(c)} - \Delta_{stripB(f)} + \Delta_{1,2,3(f)}$$

$$\Delta_{1,2,3(f)} = \frac{1}{R_{1(f)} + R_{2(f)} + R_{3(f)}}$$

Rigidity of cantilever pier is given by $R_C = \frac{Et}{4\left(\frac{h}{d}\right)^3 + 3\left(\frac{h}{d}\right)}$

Rigidity of fixed pier is given by $R_f = \frac{Et}{\left(\frac{h}{d}\right)^3 + 3\left(\frac{h}{d}\right)}$

$$R_{solid(c)} = \frac{Et}{4\left(\frac{4}{8}\right)^3 + 3\left(\frac{4}{8}\right)} = 0.5Et, \Delta_{solid(c)} = 2.0/Et$$

$$R_{stripA(c)} = \frac{Et}{4\left(\frac{2.5}{8}\right)^3 + 3\left(\frac{2.5}{8}\right)} = 0.944 Et$$

$$\Delta_{stripA(c)} = 1.06/Et$$

$$R_{solid\,1,2,3,9(f)} = \frac{Et}{4\left(\frac{2.5}{6}\right)^3 + 3\left(\frac{2.5}{6}\right)} = 0.756 Et$$

$$\Delta_{solid\,1,2,3,9(f)} = 1.322/Et$$

$$R_{stripB(f)} = \frac{Et}{\left(\frac{1}{6}\right)^3 + 3\left(\frac{1}{6}\right)} = 1.98Et$$

$$\Delta_{stripB(f)} = 0.546/Et$$

$$R_{1(f)} = R_{2(f)} = R_{3(f)} = \frac{Et}{\left(\frac{1}{1}\right)^3 + 3\left(\frac{1}{1}\right)} = 0.25Et$$

$$\Delta_{1,2,3(f)} = 1.33/Et$$

$$\Delta_{1,2,3,9(f)} = 1.322/Et - 0.5046/Et + 1.33/Et = 2.15/Et$$

$$R_{1,2,3,9(f)} = Et/2.15 = 0.465Et$$

$$R_{4(f)} = \frac{Et}{\left(\frac{2.5}{1}\right)^3 + 3\left(\frac{2.5}{1}\right)} = 0.043 Et$$

$$\Delta_{1,2,3,9,4(f)} = 1.968/Et$$

$$\Delta_{wall} = 2.0/Et - 1.06/Et + 1.96/Et = 2.908/Et$$

$$R_{wall} = 0.343Et$$

Rigidity of South shear wall

$$\Delta_{wall} = \Delta_{solid\ wall(c)} - \Delta_{strip\ A2(c)} + \Delta_{5,6,7(f)}$$

$$\Delta_{5,6,7(f)} = \frac{1}{R_{5,6,7(f)}}$$

$$R_{5,6,7(f)} = R_{7(f)} + R_{6(f)} + R_{5(f)}$$

$$R_{5(f)} = R_{7(f)} = \frac{Et}{\left(\frac{1}{1}\right)^3 + 3\left(\frac{1}{1}\right)} = 0.25Et$$

$$R_{6(f)} = \frac{Et}{\left(\frac{1}{2}\right)^3 + 3\left(\frac{1}{2}\right)} = 0.615Et$$

$$R_{5,6,7(f)} = 2 \times 0.25Et + 0.615 = 1.115Et$$

$$\Delta_{5,6,7(f)} = \frac{1}{R_{5,6,7(f)}} = 0.896/Et$$

$$R_{solid(c)} = \frac{Et}{4\left(\frac{4}{8}\right)^3 + 3\left(\frac{4}{8}\right)} = 0.5Et$$

$$\Delta_{solid(c)} = 2.0/Et$$

$$R_{stripA2(c)} = \frac{Et}{4\left(\frac{1}{8}\right)^3 + 3\left(\frac{1}{8}\right)} = 2.612Et$$

$$\Delta_{solidA2(c)} = 0.382/Et$$

$$\begin{aligned} \Delta_{wall} &= \Delta_{solid\ wall(c)} - \Delta_{stripA2(c)} + \Delta_{5,6,7(f)} \\ &= 2/Et - 0.382/Et + 0.896/Et = 2.513/Et \end{aligned}$$

$$R_{wall} = 0.398 Et$$

Relative stiffness of walls

$$\text{North shear wall} = 0.343/(0.343 + 0.398) = 0.462$$

$$\text{South shear wall} = 0.398/(0.343 + 0.398) = 0.538$$

27.5 STEP 3: DETERMINATION OF TORSIONAL FORCES

To calculate the shear forces due to torsion, first calculate the locations of the centre of mass and the centre of rigidity.

Location of the centre of mass

Centre of mass, \bar{X}_{CM} and \bar{Y}_{CM} , is calculated by taking statical moments about a point, *say, south west corner*, using the respective weights of walls as forces in the moment summation. Because of symmetrical layout of building, the centre of mass will occur near the centre of building *i.e.* $\bar{X}_{CM} = 4.0$ m, $\bar{Y}_{CM} = 7.5$ m. However for methodology purpose the calculations for the centre of mass is shown in Table 27.1.

TABLE 27.1 Calculation of centre of mass

Item	Weight i (kN)	X (m)	Y (m)	WX (kN-m)	WY (kN-m)
Roof slab	$8 \times 15 \times 3 = 360$	4.0	7.5	1440	2700
N-Wall	$8 \times 4 \times 5 = 160$	4.0	15	640	2400
S-Wall	$8 \times 4 \times 5 = 160$	4.0	0.0	640	0
E-Wall	$15 \times 4 \times 5 = 300$	8.0	7.5	2400	2250
W-Wall	$15 \times 4 \times 5 = 300$	0.0	7.5	0	2250
$\Sigma W = 1280$				$\Sigma WX = 5120$	$\Sigma WY = 9600$

$$\bar{X}_{CM} = \Sigma WX / \Sigma W = 4.0 \text{ m from west wall}$$

$$\bar{Y}_{CM} = \Sigma WY / \Sigma W = 7.5 \text{ m from east wall}$$

Location of the centre of rigidity

The centre of rigidity, \bar{X}_{CR} and \bar{Y}_{CR} , is calculated by taking statical moments about a point, *say, south-west corner*, using the relative stiffnesses of the walls as forces in the moment summation. The stiffness of slab is not considered in the determination of centre of rigidity. The calculation for the centre of rigidity is shown in Table 27.2.

TABLE 27.2 Calculation of centre of rigidity

Item	R_x	R_y	X (m)	Y (m)	$Y R_x$	$X R_y$
N-Wall	0.462	—	—	15	6.93	—
S-Wall	0.538	—	—	0.0	0	—
E-Wall	—	0.5	8.0	—	—	4.0
W-Wall	—	0.5	0.0	—	—	0.0
$\Sigma R_x = 1.0$		$R_y = 1.0$			$\Sigma Y.R_x = 6.93$	$\Sigma X.R_y = 4.0$

$$\bar{X}_{CR} = \Sigma X R_y / \Sigma R_y = 4.0 \text{ m from W-Wall}$$

$$\bar{Y}_{CR} = \Sigma Y R_x / \Sigma R_x = 6.93 \text{ m from S-Wall}$$

Torsional eccentricity

Torsional eccentricity in y-direction

Eccentricity between centre of mass and centre of rigidity

$$e_y = 7.50 - 6.72 = 0.78 \text{ m}$$

Add minimum 5% accidental eccentricity

$$0.05 \times 15 = 0.75 \text{ m}$$

Total eccentricity = $0.78 + 0.75 = 1.53 \text{ m}$

Torsional eccentricity in x-direction

Eccentricity between centre of mass and centre of rigidity

$$e_x = 4.0 - 4.0 = 0.00 \text{ m}$$

Add minimum 5% accidental eccentricity

$$0.05 \times 8 = 0.40 \text{ m}$$

Total eccentricity = $0.00 + 0.40 = 0.40 \text{ m}$

Torsional moment

The torsional moment due to E–W seismic force rotate the building in y-direction, hence

$$M_{TX} = V_x e_y = 333 \times 1.53 = 509.50 \text{ kN-m}$$

Similarly, if considered seismic force in N–S direction

$$M_{TY} = V_y e_x = 333 \times 0.40 = 133.2 \text{ kN-m}$$

($V_y = V_x$, because S_a/g is constant value of 2.5 for the time period $0.11 \leq T \leq 0.55$)

Distribution of direct shear force and torsional shear force

Since, we are considering the seismic force only in E–W direction, the walls in N–S direction will resist the forces and the walls in E–W direction may be ignored. Table 27.3 shows the calculation of distribution of direct shear and torsional shear.

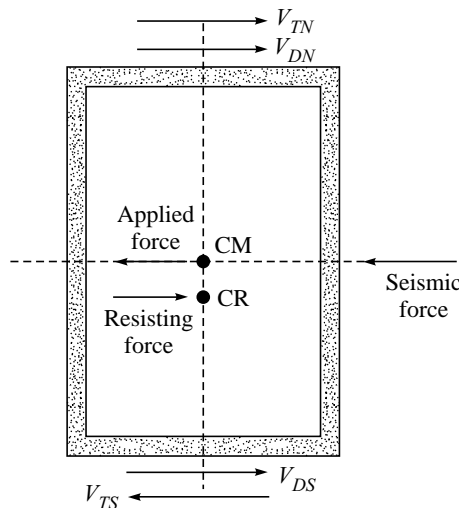
TABLE 27.3 Distribution of forces in North and South shear walls

Item	R_x	d_y^* (m)	$R_x d_y$	$R_x d_y^2$	Direct shear force (kN)	Torsional shear force** (kN)	Total shear (kN)
N-Wall	0.462	8.07	3.728	31.67	153.85	+33.94	187.80
S-Wall	0.538	6.93	3.728	24.30	179.15	-33.94	179.15
$\Sigma = 55.96$							

* Distance of considered wall from centre of rigidity ($15 - 6.93 = 8.07 \text{ m}$)

$$** \text{Torsional forces in N-Wall} = \frac{R_x d_y}{\sum R_x d_y^2} V_x e_y = \frac{3.728}{55.96} \times 509.44 = 33.94 \text{ kN}$$

$$\text{Torsional forces in S-Wall} = \frac{R_x d_y}{\sum R_x d_y^2} V_x e_y = \frac{3.728}{55.96} \times 509.44 = 33.94 \text{ kN}$$



The torsional forces are additive on the north wall and subtractive on the south wall as shown, since the code directs that negative torsional shear shall be neglected. Hence the total shear acting on the south wall is simply direct shear only.

Distribution of the total shear to individual piers within the wall

The shear carried by the north and south shear wall is now distributed to individual piers on the basis of their respective stiffness.

North shear wall

Piers	Shear (kN)		Stiffness (R)	Relative stiffness	Shear force
1	56.70	Pier group 1, 2, 3, 9	0.465	0.915	171.80 kN
2	56.70	Pier 4	0.043	0.085	15.96 kN
3	56.70	Shear 171.8 kN in pier group 1, 2, 3, 9 is further divided in vertical piers 1, 2, and 3 in proportion to their stiffness. The stiffness of pier 1, 2, and 3 are 0.25 each so the shear force carried by each pier is			
4	15.96	Pier 1, 2, and 3	0.25 each	0.33	56.70 in each pier

South shear wall

Piers	Shear (kN)		Stiffness (R)	Relative stiffness	Shear force
5	40.30	Pier 5	0.25	0.225	40.30 kN
6	98.53	Pier 6	0.615	0.55	98.53 kN
7	40.30	Pier 7	0.25	0.225	40.30 kN

27.6 STEP 4: DETERMINATION INCREASE IN AXIAL LOAD DUE TO OVERTURNING

Total overturning moment due to lateral force acting on the building is,

M_{ovt} = Total shear (V_x) \times vertical distance between second floor level to critical plane of weakness, assuming at the level of sill + applied overturning moment at second floor level

Assume the stiffness of second storey walls is the same as first storey, the total direct shear in E-W direction of seismic load i.e. in x-direction is divided in North and South shear wall in the proportion to their stiffness (see Table 27.3)

Direct Shear in North wall (V_{NX}) = 153.85 kN

Direct Shear in South wall (V_{SX}) = 179.15 kN

Distribution of lateral force along the height of North and South wall is:

North shear wall

$$\text{Lateral force at roof level} = V_{NX} \times \frac{W_r h_r^2}{\sum_{i=1}^n W_i h_i^2} = 107.78 \text{ kN}$$

$$\text{Lateral force at second floor level} = V_{NX} \times \frac{W_2 h_2^2}{\sum_{i=1}^n W_i h_i^2} = 46.07 \text{ kN}$$

South shear wall

$$\text{Lateral force at roof level} = V_{SX} \times \frac{W_r h_r^2}{\sum_{i=1}^n W_i h_i^2} = 125.56 \text{ kN}$$

$$\text{Lateral force at second floor level} = V_{SX} \times \frac{W_2 h_2^2}{\sum_{i=1}^n W_i h_i^2} = 53.59 \text{ kN}$$

Increase in axial load in piers of North shear wall

Overshielding moment in North wall (M_{ovt}) is

M_{ovt} = total shear at second floor ($V_{NX} = 153.85$ kN) \times critical height ($h_{cr} = 1.5 + 1 = 2.5$ m)
+ lateral load at roof level $Q_r = 107.78$ kN) \times storey height ($h = 4.0$ m)

$$M_{ovt} = 153.85 \times 2.5 + 107.78 \times 4.0 = 815.75 \text{ kN-m}$$

Increase in axial load due to overturning moment

$$P_{ovt} = M_{ovt} \frac{l_i A_i}{I_n}$$

where,

$l_i A_i$ = Centroid of net section of wall is calculated as shown in Table 27.4.

I_n = Moment of inertia of net section of wall is calculated as shown in Table 27.5.

TABLE 27.4 Calculation of centroid of net section of wall

Pier	Area (A_i) m^2	l (distance from left edge of wall to centroid of piers) m	$A_i l (\text{m}^3)$
1	$1 \times 0.25 = 0.25$	0.5 m	0.125
2	$1 \times 0.25 = 0.25$	3.0 m	0.750
3	$1 \times 0.25 = 0.25$	5.5 m	1.375
4	$1 \times 0.25 = 0.25$	7.5 m	1.875
$\Sigma = 1.0$			$\Sigma = 4.125$

Distance from left edge to centroid of net section of wall = $4.125/1.0 = 4.125$ m

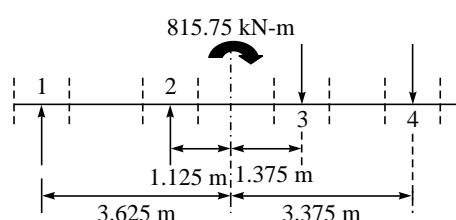
TABLE 27.5 Calculation of moment of inertia of net section of wall

Pier	(A_i) m^2	I_i (m)	$A_i l_i (\text{m}^3)$	$A_i l_i^2 (\text{m}^4)$	$I = t d^3 / 12$	$I_n = I + A_i l_i^2$
1	0.25	3.625	0.906	3.285	$0.25 \times 1^3 / 12 = 0.02$	3.305
2	0.25	1.125	0.281	0.316	$0.25 \times 1^3 / 12 = 0.02$	0.326
3	0.25	1.375	0.344	0.472	$0.25 \times 1^3 / 12 = 0.02$	0.492
4	0.25	3.375	0.844	2.848	$0.25 \times 1^3 / 12 = 0.02$	2.868
$\Sigma = 1.0$					$\Sigma = 6.99 = 7 \text{ m}^4$	

Increase in axial load in individual piers of North wall is determined in Table 27.6.

TABLE 27.6 Increase in axial load in the pier of North wall

Pier	$A_i l_i (\text{m}^3)$	$P_{ovt} = M_{ovt} \frac{l_i A_i}{I_n}$ (kN)
1	0.906	105.58
2	0.281	32.75
3	0.344	40.09
4	0.844	98.36



$$M_{ovt} = 815.75 \text{ kN-m}$$

$$I_n = 7.0 \text{ m}^4$$

Increase in axial load in piers of South shear wall

Overshooting moment in South wall (M_{ovt}) is,

M_{ovt} = total shear at second floor ($V_{SX} = 179.15 \text{ kN}$) \times critical height ($h_{cr} = 1.5 + 1 = 2.5 \text{ m}$)
+ lateral load at roof level ($Q_r = 125.56 \text{ kN}$) \times storey height ($h = 4.0 \text{ m}$)

$$M_{ovt} = 179.15 \times 2.5 + 125.56 \times 4.0 = 950.12 \text{ kN-m}$$

Increase in axial load due to overshooting moment

$$P_{ovt} = M_{ovt} \frac{l_i A_i}{I_n}$$

where,

$l_i A_i$ = centroid of net section of wall is calculated as shown in Table 27.7.

I_n = Moment of inertia of net section of wall is calculated as shown in Table 27.8.

TABLE 27.7 Calculation of centroid of net section of wall

Pier	Area (A_i) m^2	l (distance from left edge of wall to centroid of piers) m	$A_i l (\text{m}^3)$
5	$1 \times 0.25 = 0.25$	0.50 m	0.125
6	$2 \times 0.25 = 0.50$	4.0 m	2.00
7	$1 \times 0.25 = 0.25$	7.5 m	1.875
$\Sigma = 1.0$			$\Sigma = 4.0$

Distance from left edge to centroid = $4.0/1.0 = 4.0 \text{ m}$

TABLE 27.8 Calculation of moment of inertia of net section of wall

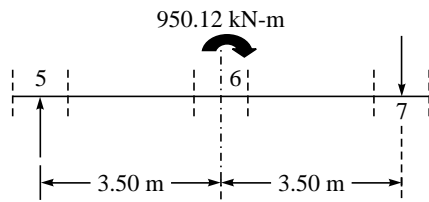
Pier	$(A_i) \text{ m}^2$	l_i (m)	$A_i l_i (\text{m}^3)$	$A_i l_i^2 (\text{m}^4)$	$I = td^3/12$	$I_n = I + A_i l_i^2$
5	0.25	3.50	0.875	3.06	$0.25 \times 1^3/12 = 0.02$	3.08
6	0.50	0.00	0	0	$0.50 \times 1^3/12 = 0.04$	0.04
7	0.25	3.50	0.875	3.06	$0.25 \times 1^3/12 = 0.02$	3.08
$\Sigma = 1.0$			$\Sigma = 6.20 \text{ m}^4$			

Increase in axial load in individual piers of south shear wall is determined as in Table 27.9.

$$M_{ovt} = 950.12 \text{ kN-m}, I_n = 6.20 \text{ m}^4$$

TABLE 27.9 Increase in axial load in the pier of South shear wall

Pier	$A_i l_i$ (m ³)	$P_{ovt} = M_{ovt} \frac{l_i A_i}{I_n}$ (kN)
5	0.875	134.08
6	0	0.0
7	0.875	134.08



27.7 STEP 5: DETERMINATION OF PIER LOADS, MOMENTS AND SHEAR

The total axial load (due to dead load, live load and overturning), shear and moment in the individual piers of both the shear walls are calculated in Tables 27.10 and 27.11 as below:

TABLE 27.10 Axial load, moment, shear in piers of North shear wall

North wall: First storey

Pier	Effective width of pier (m)	P_d^1 (kN)	P_L^2 (kN)	P_{ovt} (kN)	Shear V_E for moment (kN)	Moment (kN-m) = $V_E \times h/2$
1	1.75	135.62	26.25	105.58	56.70	$56.70 \times 1/2 = 28.35$
2	2.5	193.75	37.50	32.75	56.70	$56.70 \times 1/2 = 28.35$
3	2.25	174.37	33.75	40.09	56.70	$56.70 \times 1/2 = 28.35$
4	1.5	116.25	22.50	98.36	15.96	$15.96 \times 2.5/2 = 19.95$

TABLE 27.11 Axial load, moment, shear in piers of South shear wall

South wall: First storey

Pier	Effective width of pier (m)	P_d^1 (kN)	P_L^2 (kN)	P_{ovt} (kN)	Shear V_E for moment (kN)	Moment (kN-m) = $V_E \times h/2$
5	2	155	30	134.08	40.30	$40.30 \times 1/2 = 20.15$
6	4	310	60	0.0	98.53	$98.53 \times 1/2 = 49.27$
7	2	155	30	134.08	40.30	$40.30 \times 1/2 = 20.15$

1. P_d = effective loading width of pier \times deal load intensity in kN/m

Effective loading width of pier = width of pier + 1/2 of each adjacent opening of pier

Dead load intensity is calculated as (per metre length of wall)

North wall: First storey

- Weight of first storey (from level of IInd floor to sill level) = $2.5 \times 0.25 \times 20 = 12.5$ kN/m

2. Weight of second storey	$= 4 \times 0.25 \times 20$	$= 20 \text{ kN/m}$
3. Weight of floor at II nd storey level (Assume North and South shear wall will take equal amount of load)	$= 1/2(0.12 \times 15 \times 25)$	$= 22.5 \text{ kN/m}$
4. Weight of roof	$= 1/2(0.12 \times 15 \times 25)$	$= 22.5 \text{ kN/m}$

Total load $= 77.5 \text{ kN/m}$

South wall: First storey

1. Weight of first storey (from level of II nd floor to sill level)	$= 2.5 \times 0.25 \times 20$	$= 12.5 \text{ kN/m}$
2. Weight of second storey	$= 4 \times 0.25 \times 20$	$= 20 \text{ kN/m}$
3. Weight of floor at II nd storey level (Assume North and South shear wall will take equal amount of load)	$= 1/2(0.12 \times 15 \times 25)$	$= 22.5 \text{ kN/m}$
4. Weight of roof	$= 1/2(0.12 \times 15 \times 25)$	$= 22.5 \text{ kN/m}$

Total load $= 77.5 \text{ kN/m}$

2. P_L = effective loading width of pier \times live load intensity in kN/m

Effective loading width of pier = width of pier + 1/2 of each adjacent opening of pier

Live load intensity (per metre length of wall) calculated as

North wall: First storey

1. Live load on floor (1 kN/m^2) (Assume North and South shear wall will take equal amount of load)	$= 1/2(1 \times 15)$	$= 7.5 \text{ kN/m}$
2. Live load on roof (1 kN/m^2) (Assume North and South shear wall will take equal amount of load)	$= 1/2(1 \times 15)$	$= 7.5 \text{ kN/m}$
	Total load	$= 15 \text{ kN/m}$

South wall: First storey

1. Live load on floor (1 kN/m^2) (Assume North and South shear wall will take equal amount of load)	$= 1/2(1 \times 15)$	$= 7.5 \text{ kN/m}$
2. Live load on roof (1 kN/m^2) (Assume North and South shear wall will take equal amount of load)	$= 1/2(1 \times 15)$	$= 7.5 \text{ kN/m}$
	Total load	$= 15 \text{ kN/m}$

27.8 STEP 6: DESIGN OF SHEAR WALLS FOR AXIAL LOAD AND MOMENTS

Determination of jamb steel at the pier boundary

North shear wall

Pier	Moment (kN-m)	Effective depth (mm ²)	Area of jamb steel A_s^* (mm ²)	No. of bars	Check for adequacy** of piers						
					P (kN) (total)	d (m)	t (m)	f_a/F_a	f_b/F_b	$\frac{f_a}{F_a} + \frac{f_b}{F_b}$	
1	28.35	900	152.17	2@ 10Φ	267.45	1	0.25	0.427	0.217	0.644	OK
2	28.35	900	152.17	2@ 10Φ	264	1	0.25	0.422	0.217	0.639	OK
3	28.35	900	152.17	2@ 10Φ	248.21	1	0.25	0.397	0.217	0.614	OK
4	19.95	900	107.08	2@ 10Φ	237.11	1	0.25	0.379	0.153	0.532	OK

South shear wall

Pier	Moment (kN-m)	Effective depth (mm ²)	Area of jamb steel A_s^* (mm ²)	No. of bars	Check for adequacy** of piers						
					P (kN) (total)	d (m)	t (m)	f_a/F_a	f_b/F_b	$\frac{f_a}{F_a} + \frac{f_b}{F_b}$	
5	20.15	900	108.15	2@ 10Φ	309.08	1	0.25	0.494	0.154	0.648	OK
6	49.27	1800	132.23	2@ 10Φ	370.00	2	0.25	0.296	0.094	0.390	OK
7	20.15	900	108.15	2@ 10Φ	319.08	1	0.25	0.456	0.154	0.610	OK

* Jamb steel at the pier boundary is given by,

$$A_s = \frac{M}{f_s \times 0.9 \times d_{\text{effective}}}$$

$$f_s = 0.55Fe = 0.55 \times 415 = 230 \text{ N/mm}^2$$

$$d_{\text{effective}} = d_{\text{total}} - \text{Cover}$$

** Adequacy of individual piers under compression and moment is checked by interaction formula i.e.

$$\frac{f_a}{F_a} + \frac{f_b}{F_b} \leq 1.33$$

$$f_a = \frac{\text{P}_{\text{total}} \text{ i.e. } (\text{P}_d + \text{P}_L + \text{P}_{\text{overt}})}{\text{width of pier (d) } xt}$$

$$f_b = M/(td^2/6)$$

F_a = Permissible compressive stress = 2.5 N/mm² (as per IS: 1905)

F_b = Permissible bending stress = $2.5 + 0.25 \times 2.5 = 3.125 \text{ N/mm}^2$ (as per IS: 1905)

27.9 STEP 7: DESIGN OF SHEAR WALLS FOR SHEAR

Shear in building may be resisted by providing the bands or bond beams. The bands represent a horizontal framing system, which transfer the horizontal shear induced by the earthquakes from the floors to shear (structural) walls. It also connects all the structural walls to improve

the integral action. In combination with vertical reinforcement, it improves the strength, ductility and energy dissipation capacity of masonry walls. Depending upon its location in the building it may be termed as roof, lintel, and plinth band at lintel level. In case of flexible diaphragm, both roof and lintel band is required however in case of rigid diaphragm, a band at lintel level is sufficient. Plinth band is useful in sustaining differential settlements, particularly, when foundation soil is soft or has uneven properties.

Design of bond beam

Total seismic shear in E-W direction = 333 kN

Moment produced (M)

$$= V \times L/8 = 333 \times 15/8$$

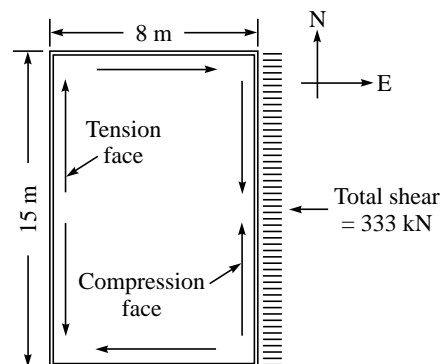
$$= 624.37 \text{ kN-m}$$

$$T = M/d = 624.37/8 = 78.04 \text{ kN}$$

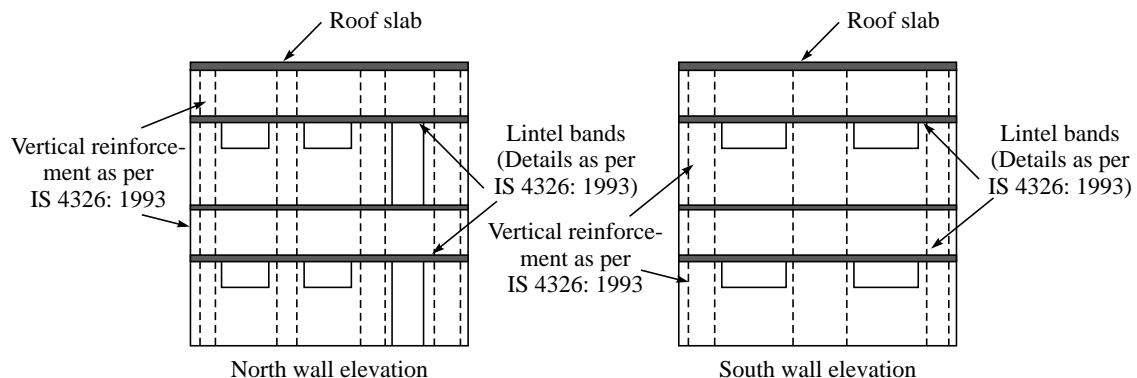
$$A_s = T/f_s = 78.04 \times 1000/230$$

$$= 339.33 \text{ mm}^2$$

Use 2 @ 16 Φ (= 402 mm 2)



27.10 STEP 8: STRUCTURAL DETAILS



SUMMARY

A state-of-the-art example for seismic analysis and design of a masonry building has been presented in this chapter. A two-storey masonry building situated in Zone IV has been analysed and designed. The seismic analysis has been carried out by considering earthquake only in one direction. The design forces are determined by considering direct and torsional forces due to lateral loads, axial load due to overturning in addition to dead and live loads. The seismic design includes the determination of vertical steel at corners and openings of shear wall for resisting

the compression and flexure forces and design of lintel band for resisting the shear forces in piers of shear walls.

REFERENCES

- [1] Amrhein, J.E., *Reinforced Masonry Engineering Handbook*, Masonry Institute of America, CRC Press, 1998.
- [2] Drysdale, R.G., Hamid, A.H., and Baker, L.R., *Masonry Structure: Behaviour and Design*, Prentice Hall, Englewood Cliffs, New Jersey, 1994.
- [3] Schneider, R.R. and Dickey, W.L., *Reinforced Masonry Design*, 3rd ed., Prentice Hall, New Jersey, 1994.
- [4] Tally, N., *Design of Reinforced Masonry Structures*, McGraw-Hill, 2001.
- [5] Tomazevic, M., *Earthquake-Resistant Design of Masonry Buildings*, Imperial Colleges Press, London, 2000.
- [6] Williams, Alan, *Seismic Design of Buildings and Bridges*, Oxford University Press, 2003.

PART VII

Seismic Evaluation and Retrofitting of Reinforced Concrete and Masonry Buildings

Chapter 28

Seismic Evaluation of Reinforced Concrete Buildings: A Practical Approach

28.1 INTRODUCTION

Most of the existing buildings, which do not fulfil the current seismic requirements, may suffer extensive damage or even collapse if shaken by a severe ground motion. The aim of evaluation is to assess the seismic capacity of earthquake vulnerable buildings or earthquake damaged buildings for the future use. The evaluation may also prove helpful for degree of intervention required in seismically deficient structures. The methodologies available so far for the evaluation of existing buildings can be broadly divided into two categories: (i) **qualitative methods** (ii) **analytical methods**. The qualitative methods are based on the background information available of the building and its construction site, which require some or few documents like architectural and structural drawings, past performance of similar buildings under severe earthquakes, visual inspection report, some non-destructive test results. The methods under this category are Field Evaluation Method, Rapid Visual Screening Method, ATC-14 methodology etc. The analytical methods are based on the consideration of the capacity and ductility of buildings on the basis of available drawings. The methods in this category are Capacity/Demand (C/D) method, Screening method, Pushover analysis, Nonlinear inelastic analysis etc. It is often seen that the drawings of buildings are generally not available due to one or more reasons. Moreover, the evaluation of the capacity and ductility of a building is also a cumbersome task, which is difficult for a field engineer and may not be practical in the present Indian scenario. It is important to underline that the methods of evaluation procedure should be very simple and immediate based on synthetic information that can prove suitable for risk evaluation on large populations. Therefore, qualitative evaluation of the buildings is generally being carried out.

The aim of these methods is to direct the evaluating engineer to identify the weak links in the structure that could precipitate the structural or component failure. Traditionally, a qualitative evaluation of a structure is conducted by a visual examination of the structure alongwith some testing of materials. Over the last decade or more, other valuable and practical non-destructive evaluation methods have been developed for relatively rapid inspection of damage and deterioration of structures. The objective of this chapter is to present a general methodology for evaluation of buildings based on the condition assessment, visual inspection and some non-destructive test. This methodology should be treated as a guide to that decision making process and not as the absolute method of evaluation.

28.2 COMPONENTS OF SEISMIC EVALUATION METHODOLOGY

The evaluation of any building is a difficult task, which requires a wide knowledge about the structures, cause and nature of damage in structures and its components, material strength etc. The proposed methodology is divided into three components:

1. *Condition Assessment* based on (i) data collection or information gathering of structures from architectural and structural drawings (ii) performance characteristics of similar type of buildings in past earthquakes, (iii) rapid evaluation of strength, drift, materials, structural components and structural details. This component of methodology is primarily based on ATC-14 project and is used basically for undamaged existing structures.
2. *Visual Inspection/Field Evaluation* based on observed distress and damage in structures. Visual inspection is more useful for damaged structures however it may also be conducted for undamaged structures.
3. *Non-Destructive Evaluation (NDE)* is generally carried out for quick estimation of materials strength, determination of the extent of deterioration and to establish causes remain out of reach from visual inspection and determination of reinforcement and its location. NDT may also be used for preparation of drawing in case of non-availability.

28.2.1 Condition Assessment for Evaluation

The aim of **condition assessment** of the structure is the collection of information about the structure and its past performance characteristics to similar type of structure during past earthquakes and the qualitative evaluation of structure for decision-making purpose. More information can be included, if necessary as per requirement.

Data collection/information gathering

Collection of the data is an important portion for the seismic evaluation of any existing building. The information required for the evaluated building can be divided as follows:

Building data

- architectural, structural and construction drawings

- vulnerability parameters: number of stories, year of construction, and total floor area
- specifications, soil reports, and design calculations
- seismicity of the site

Construction data

- identifications of gravity load resisting system
- identifications of lateral load resisting system
- maintenance, addition, alteration, or modifications in structures
- field surveys of the structure's existing condition

Structural data

- materials
- structural concept: vertical and horizontal irregularities, torsional eccentricity, pounding, short column and others
- detailing concept: ductile detailing, special confinement reinforcement
- foundations
- non-structural elements

Past performance data

Past performance of similar type of structure during the earthquake provides considerable amount of information for the building, which is under evaluation process. Following are the areas of concerns, which are responsible for poor performance of buildings during earthquake

Materials concerns

- low grade on concrete
- deterioration in concrete and reinforcement
- high cement–sand ratio
- corrosion in reinforcement
- use of recycled steel as reinforcement
- spalling of concrete by the corrosion of embedded reinforcing bars
- corrosion related to insufficient concrete cover
- poor concrete placement and porous concrete

Structural concerns

- the relatively low stiffness of the frames—excessive inter-storey drifts, damage to non-structural items
- pounding—column distress, possibly local collapse
- unsymmetrical buildings (U, T, L, V) in plan—torsional effects and concentration of damage at the junctures (*i.e.*, re-entrant corners)
- unsymmetrical buildings in elevation—abrupt change in lateral resistance
- vertical strength discontinuities—concentrate damage in the “soft” stories
- short column

Detailing concerns

- large tie spacing in columns lack of confinement of concrete core—shear failures.
- insufficient column lengths—concrete to spall.
- locations of inadequate splices—brittle shear failure.
- insufficient column strength for full moment hinge capacity—brittle shear failure.
- lack of continuous beam reinforcement—hinge formation during load reversals.
- inadequate reinforcing of beam column joints or location of beam bar splices at columns—joint failures.
- improper bent-up of longitudinal reinforcing in beams as shear reinforcement—shear failure during load reversal
- foundation dowels that are insufficient to develop the capacity of the column steel above—local column distress.

Seismic evaluation data

Seismic evaluation of data will provide a general idea about the building performance during an earthquake. The criteria of evaluation of building will depend on materials, strength and ductility of structural components and detailing of reinforcement.

Materials evaluation

- buildings height > 3 stories, minimum grade concrete M 20, desirable M 30 to M 40 particularly in columns of lower stories
- maximum grade of steel should be Fe 415 due to adequate ductility
- no significant deterioration in reinforcement
- no evidence of corrosion or spalling of concrete

Structural components

- evaluation of columns shear strength and drift—check for permissible limits
- evaluation of plan irregularities—check for torsional forces and concentration of forces
- evaluation of vertical irregularities—check for soft storey, mass or geometric discontinuities
- evaluation of discontinuous load path—check for ground floor columns, projected cantilever beam and ductile detailing at beam–column joints
- evaluation of beam–column joints—check for strong column–weak beams
- evaluation of pounding—check for drift control or building separation
- evaluation of interaction between frame and infill—check for force distribution in frames and overstressing of frames

Structural detailing

Flexural members

- limitation of sectional dimensions
- limitation on minimum and maximum flexural reinforcement—at least two continuous reinforced bars at top and bottom of the members

- restriction of lap splices
- development length requirements—for longitudinal bars
- shear reinforcement requirements—stirrup and tie hooks, tie spacing, bar splices

Columns

- limitation of sectional dimensions
- longitudinal reinforcement requirement
- transverse reinforcement requirements—stirrup and tie hooks, column tie spacing, column bar splices
- special confining requirements

Foundation

- column steel doweled into the foundation

Non-structural components

- cornices, parapet, and appendages are anchored
- exterior cladding and veneer are well anchored

Note: Structural detailing in the structural member should comply with IS 13920: 1993

28.2.2 Field Evaluation/Visual Inspection Method

Visual inspection is an integral part of evaluation, and in fact, is the most widely used form of Non-Destructive Evaluation (NDE). Visual inspection can provide a wealth of information that may lead to positive identification of the cause of observed distress. Before performing a detailed visual inspection, the investigator must be familiar with the type of damage and its cause and be able to distinguish between recent damage and pre-existing damage, ensuring that the observed damage may or may not prove to be dangerous for the structures. It is not always true that the observed damage is due to earthquake; it may be due to some other reasons as well.

Procedure for visual inspection method

The procedure for visual inspection method and its limitations are described in the following sections (FEMA 306, 1999).

Description

- perform a walk through visual inspection to become familiar with the structure
- gather background documents and information on the design, construction, maintenance, and operation of the structure
- plan the complete investigation
- perform a detailed visual inspection and observe type of damage—cracks spalls and delaminations, permanent lateral displacement, and buckling or fracture of reinforcement, estimating of drift
- observe damage documented on sketches—interpreted to assess the behaviour during earthquake

- perform any necessary sampling—basis for further testing

Equipments

- optical magnification—allows a detailed view of local areas of distress
- stereomicroscope—that allow a three dimensional view of the surface. Investigator can estimate the elevation difference in surface features by calibrating the focus adjustment screw
- fiberscopes and bore scopes—allow inspection of regions that are inaccessible to the naked eye
- tape—to measure the dimension of structure, length of cracks
- flashlight—to aid in lighting the area to be inspected, particularly in post-earthquake evaluation, power failure
- crack comparator—to measure the width of cracks at representative locations, two types—plastic cards and magnifying lens comparators
- pencil—to draw the sketch of cracks
- sketchpad—to prepare a representation of wall elevation, indicating the location of cracks, spalling, or other damage, records of significant features such as non-structural elements
- camera—for photographs or video tape of the observed cracking

Execution

- to identify the location of vertical structural elements—columns or walls
- to sketch the elevation with sufficient details—dimensions, openings, observed damage such as cracks, spalling, and exposed reinforcing bars, width of cracks
- to take photographs of cracks—use marker, paint or chalk to highlight the fine cracks or location of cracks in photographs
- observation of the non-structural elements—inter-storey displacement

Limitations

- applicable for surface damage that can be visualised
- no identification of inner damage—health monitoring of building, change of frequency and mode shapes

Identification of seismic damage in building components

Possible damages in building component, which are frequently observed after the earthquakes are as follows:

Seismic Evaluation of Reinforced Concrete Columns

Damaged mainly due to lack of confinement, large tie spacing, insufficient splices length, inadequate splicing at the same section, hook configurations, poor concrete quality, less than full height masonry infill partitions, and a combinations of many of the above compounded with vertical and geometrical irregularities. Failure of column has catastrophic consequences for a structure. The most common modes of failure of column are as follows.

Mode 1: Formation of plastic hinge at the base of ground level columns



Mechanism: The column, when subjected to seismic motion, its concrete begins to disintegrate and the load carried by the concrete shifts to longitudinal reinforcement of the column. This additional load causes buckling of longitudinal reinforcement. As a result the column shortens and loses its ability to carry even the gravity load (Kono and Watanabe, 2000).

Reasons: Insufficient confinement length and improper confinement in plastic hinge region due to smaller numbers of ties.

Design Consideration: This type of damage is sensitive to the cyclic moments generated during the earthquake and axial load intensity. Consideration is to be paid on plastic hinge length or length of confinement.

Mode 2: Diagonal shear cracking in mid span of columns



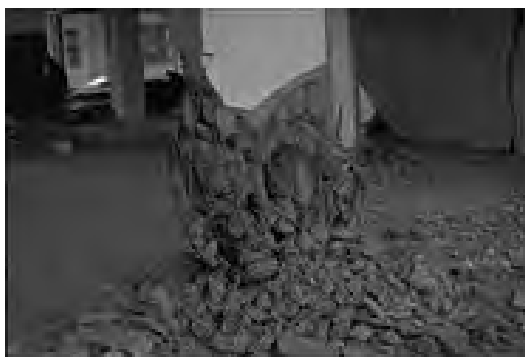
Mechanism: In older reinforced concrete building frames, column failures were more frequent since the strength of beams in such constructions was kept higher than that of the columns. This shear failure brings forth loss of axial load carrying capacity of the column. As the axial capacity diminishes, the gravity loads carried by the column are transferred to neighbouring elements

resulting in massive internal redistribution of forces, which is also amplified by dynamic effects causing spectacular collapse of building (Moehle and Sezen, 2000).

Reason: Wide spacing of transverse reinforcement.

Design Considerations: To improve understanding of column shear strength, as well as to understand how the gravity loads will be supported after a column fails in shear

Mode 3: Shear and splice failure of longitudinal reinforcement



Mechanism: Splices of column longitudinal reinforcement in older buildings were commonly designed for compression only with relatively light transverse reinforcement enclosing the lap. For example, as per IS: 456-1978, a lap splice length of 20 or 24 longitudinal bar diameters with transverse reinforcement should be equal to the least column dimension or 16 longitudinal bar diameter. Under earthquake motion, the longitudinal reinforcement may be subjected to significant tensile stresses, which require lap lengths for tension substantially exceeding those for compression. As a result slip occurs along the splice length with spalling of concrete (Wallace and Melek, 2000).

Reasons: Deficient lap splice length of column longitudinal reinforcement with lightly spaced transverse reinforcement, particularly if the splices just above the floor slab especially the splices just above the floor slab, which is very common in older construction.

Design Consideration: Lap splices should be provided only in the center half of the member length and it should be proportionate to tension splice. Spacing of transverse reinforcement as per IS 13929: 1993.

Mode 4: Shear failures in captive columns and short columns

Captive Column: Column whose deforming ability is restricted and only a fraction of its height can deform laterally. It is due to presence of adjoining non-structural elements, columns at sloping ground, partially buried basements, etc.

Short Column: Column is made shorter than neighbouring column by horizontal structural elements such as beams, girder, stair way landing slabs, use of grade beams, and ramps.

Mechanism: A reduction in the clear height of captive or short columns increases the lateral stiffness. Therefore, these columns are subjected to larger shear force during the earthquake



since the storey shear is distributed in proportion to lateral stiffness of the same floor. If these columns, reinforced with conventional longitudinal and transverse reinforcement, and subjected to relatively high axial loading, fail by splitting of concrete along their diagonals, if the axial loading level is low, the most probable mode of failure is by shear sliding along full depth cracks at the member ends. Moreover, in the case of captive column by adjoining non-structural walls, the confinement provided to the lower part of the column is so effective that usually damage is shifted to the short non-confined upper section of the column (Guevara and Garcia, 2005).

Reasons: Large shear stresses, when the structure is subjected to lateral forces are not accounted for in the standard frame design procedure.

Design Consideration: The best solution for captive column or short column is to avoid the situation otherwise use separation gap in between the non-structural elements and vertical structural element with appropriate measures against out-of-plane stability of the masonry wall.

Seismic Evaluation of Reinforced Concrete Beams

There is little evidence that the buildings have collapsed due to beam failure. Only a few examples exist in which buildings have exhibited plastic hinging in the beam. The probable regions of hinging are at and near their intersections with supporting columns. An exception may be where a heavy concentrated load is carried at some intermediate point on the span. The causes of hinging are lack of confinement of concrete core and support for the longitudinal compressive reinforcement against inelastic buckling. The shear-flexure mode of failure is most commonly observed during the earthquakes, which is described as follows.

Mode 5: Shear-flexure failure

Mechanism: Two types of plastic hinges may form in the beams of multi-storeyed framed construction depending upon the span of beams. In case of short beams or where gravity load supported by the beam is low, plastic hinges are formed at the column ends and damage occurs in the form of opening of a crack at the end of beam otherwise there is the formation of plastic hinges at and near end region of beam in the form of diagonal shear cracking.



Reasons: Lack of longitudinal compressive reinforcement, infrequent transverse reinforcement in plastic hinge zone, bad anchorage of the bottom reinforcement in to the support or slip of the longitudinal beam reinforcement, bottom steel termination at face of column.

Design Consideration: Adequate flexural and shear strength must be provided and verification by design calculation is essential. The beams should not be too stiff with respect to adjacent columns so that the plastic hinging will occur in beam rather than column. To ensure that the plastic hinges zones in beams have adequate ductility, the following considerations must be considered (Booth, 1994).

- Lower and upper limits on the amount of longitudinal flexural tension steel
- A limit on the ration of the steel on one side of the beam to that of on the other side
- Minimum requirements for the spacing and size of stirrups to restrain buckling of the longitudinal reinforcement

Seismic Evaluation of Reinforced Concrete Beam-Column Joints

Beam-column joints are critical element in frame structures and are subjected to high shear and bond-slip deformations under earthquake loading. Account for cross-sectional properties of the joint region, amount and distribution of column vertical steel, inadequate or absence of reinforcement in beam-column joints, absence of confinement of hoop reinforcement, inappropriate location of bar splices in column are the common causes of failure of beam-column joints. The most common modes of failure in beam-column joint are as follows.

Mode 6: Shear failure in beam-column joint

Mechanism: The most common failures observed in exterior joints are due to either high shear or bond (anchorage) under severe earthquakes. Plastic hinges are formed in the beams at the columns faces. As a result, cracks develop throughout the overall beam depth. Bond deterioration near the face of the column causes propagation of beam reinforcement yielding in the joint and a shortening of the bar length available for force transfer by bond causing horizontal bar slippage in the joint. In the interior joint, the beam reinforcement at both the column faces



undergoes different stress conditions (compression and tension) because of opposite signs of seismic bending moments results in failure of joint core (UNDP, 1983).

Reasons: Inadequate anchorage of flexural steel in beams, lack of transverse reinforcement.

Design considerations

Exterior Joint: The provision on anchorage stub for the beam reinforcement improves the performance of external joints by preventing spalling of concrete cover on the outside face resulting in loss of flexural strength of the column. This increases diagonal strut action as well as reduces steel congestion as the beam bars can be anchored clear of the column bars.

Interior Joint: Reliable anchorage of the beam reinforcement in the joints.

Seismic Evaluation of Reinforced Concrete Slabs

Generally slab on beams performed well during earthquakes and are not dangerous but cracks in slab creates serious aesthetic and functional problems. It reduces the available strength, stiffness and energy dissipation capacity of building for future earthquake. In flat slab construction, punching shear is the primary cause of failure. The common modes of failure are:

Mode 7: Shear cracking in slabs

Mechanism: Damage to slab often occurs due to irregularities such as large openings at concentration of earthquake forces, close to widely spaced shear walls, at the staircase flight landings.

Reasons: Existing micro cracks which widen due to shaking, differential settlement.

Design consideration

- Use secondary reinforcement in the bottom of the slab
- Avoid the use of flat slab in high seismic zones, provided this is done in conjunction with a stiff lateral load resisting system



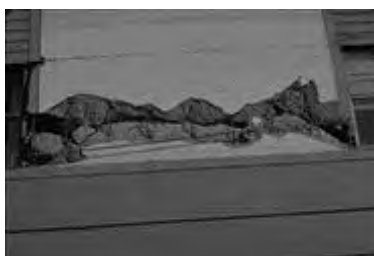
Seismic Evaluation of Reinforced Concrete Shear Walls

Shear walls generally performed well during the earthquakes. Four types of failure mode are generally observed (Penelis and Kappos, 1997).

Mode 8: Four types of failure mode are generally observed (i) Diagonal tension–compression failure in the form of cross-shaped shear cracking (ii) sliding shear failure cracking at interface of new and old concrete (iii) flexure and compression in bottom end region of wall and finally (iv) Diagonal tension in the form X shaped cracking in coupling beams.



Diagonal tension-compression failure



Sliding shear failure



Flexure and compression



Flexural/Diagonal tension



Flexural/Diagonal tension



Flexure shear cracks

Mechanism: Shear walls are subjected to shear and flexural deformation depending upon the slenderness ratio. Therefore, the damage in shear walls may generally occur due to inadequate shear and flexure capacity of wall. Slender walls are governed by their flexural strength and cracking occurs in the form of yielding of main flexure reinforcement in the plastic hinge region, normally at the base of the wall. Squat walls are governed by their shear strength and failure takes place due to diagonal tension or diagonal compression in the form of inclined cracking. Coupling beams between shear walls or piers may also damage due to inadequate shear and flexure capacity. Sometimes damage occurs at the construction joints in the form of slippage and related drift.

Reasons

- Flexural/boundary compression failure—Inadequate transverse confining reinforcement to the main flexural reinforcement near the outer edge of wall and in boundary elements
- Flexure/Diagonal tension—Inadequate horizontal shear reinforcement
- Sliding shear—Absence of diagonal reinforcement across the potential sliding planes of the plastic hinge zone
- Coupling beams—Inadequate stirrup reinforcement and no diagonal reinforcement
- Construction joint—Improper bonding between two surfaces

Design considerations

- The concrete shear walls must have boundary elements or columns thicker than walls, which will carry the vertical load after shear failure of wall.
- A proper connection between wall vs. diaphragm as well as wall vs. foundation to complete the load path.
- Proper bonding at construction joint in the form of shear friction reinforcement.
- Provision of diagonal steel in the coupling beam



Seismic Evaluation of Infill Walls

Infill panels in reinforced concrete frames are the cause of unequal distribution of lateral forces in the different frames of a building, producing vertical and horizontal irregularities etc. The common mode of failure of infill masonry are in plane or shear failure.

Mode 9: Shear failure of masonry infill

Mechanism: Frame with infill possesses much more lateral stiffness than the bare frame, and hence initially attracts most of the lateral force during an earthquake. Being brittle, the infill starts to disintegrate as soon as its strength is reached. Infills that were not adequately tied to the surrounding frames, sometimes dislodges by out-of-plane seismic excitations.

Reasons: Infill causes asymmetry of load application, resulting in increased torsional forces and changes in the distribution of shear forces between lateral load resisting system.

Design Considerations: Two strategies are possible either complete separation between infill walls and frame by providing separation joint so that the two systems do not interact or complete anchoring between frame and infill to act as an integral unit. Horizontal and vertical reinforcement may also be used to improve the strength, stiffness, and deformability of masonry infill walls.

Seismic Evaluation of Parapets

Un-reinforced concrete parapets with large height-to-thickness ratio and not improper anchoring to the roof diaphragm may also constitute a hazard. The hazard posed by a parapet increases in direct proportion to its height above building base, which has been generally observed. The common mode of failure of parapet wall is against out-of-plane forces, which is described as follows.

Mode 10: Brittle flexure out-of-plane failure



Mechanism: Parapet walls are acceleration sensitive in the out-of-plane direction; the result is that they may become disengaged and topple.

Reasons: Not properly braced.

Design Considerations: Analyzed for acceleration forces and braced and connected with roof diaphragm.

28.2.3 Concrete Distress and Deterioration Other than Earthquake

Table 28.1 summarizes the list of other causes or reasons of distress and deterioration observed in buildings other than earthquake.

TABLE 28.1 Forms of concrete distress and deterioration other than earthquake (Poston, 1997)

Description	Typical causes
Cracking	Plastic shrinkage, Drying shrinkage, Restraint, Sub-grade support deficiencies, Vapour barrier, Expansion, Corrosion of reinforcing steel, Thermal loading, Overloading, Aggregate reaction.
Scaling	Inadequate air content, Finishing problems, Freeze-thaw cycling, Chemical de-icers.
Spalling	Aggregate reaction, Corrosion, Freeze-thaw cycling, Construction problems, Poor preparation of construction joints, Early age loading.
Disintegration	Frozen concrete, Freeze-thaw cycling, Low strength, Chemical attack, Sulphate attack.
Discoloration and straining	Different cement production, Different water–cement ratios, Corrosion, Aggregates, Use of calcium chloride, Curing, Finishing, Non-uniform absorption of forms.
Honeycombing and surface voids	Poor placement, Poor consolidation, Congested reinforcement.

28.2.4 Non-destructive Testing (NDT)

Visual inspection has the obvious limitation that only visible surface can be inspected. Internal defects go unnoticed and no quantitative information is obtained about the properties of the concrete. For these reasons, a visual inspection is usually supplemented by NDT methods. Other detailed testing is then conducted to determine the extent of deterioration and to establish causes.

NDT tests for condition assessment of structures

Some methods of field and laboratory testing (FEMA, 1999; Nawy, 1997) that may assess the minimum concrete strength and condition and location of the reinforcement in order to characterize the strength, safety, and integrity are described here.

Rebound hammer/Swiss hammer

The rebound hammer is the most widely used non-destructive device for quick surveys to assess the quality of concrete. In 1948, Ernest Schmidt, a Swiss engineer, developed a device for testing concrete based upon the rebound principal strength of in-place concrete; comparison of concrete strength in different locations and provides relative difference in strength only.

Limitations

- not give a precise value of compressive strength, provide estimate strength for comparison
- sensitive to the quality of concrete; carbonation increases the rebound number
- more reproducible results from formed surface rather than finished surface; smooth hard-towelled surface giving higher values than a rough-textured surface.
- surface moisture and roughness also affect the reading; a dry surface results in a higher rebound number
- not take more than one reading at the same spot

Penetration Resistance Method—Windsor Probe Test

Penetration resistance methods are used to determine the quality and compressive strength of in-situ concrete. It is based on the determination of the depth of penetration of probes (steel rods or pins) into concrete by means of powder-actuated driver. This provides a measure of the hardness or penetration resistance of the material that can be related to its strength.

Limitations

- both probe penetration and rebound hammer test provide means of estimating the relative quality of concrete not absolute value of strength of concrete
- probe penetration results are more meaningful than the results of rebound hammer
- because of greater penetration in concrete, the probe test results are influenced to a lesser degree by surface moisture, texture, and carbonation effect
- probe test may be the cause of minor cracking in concrete

Rebar locator/convert meter

It is used to determine quantity, location, size and condition of reinforcing steel in concrete. It is also used for verifying the drawing and preparing as-built data, if no previous information is available. These devices are based on interaction between the reinforcing bars and low frequency electromagnetic fields. Commercial covermeter can be divided into two classes: those based on the principle of magnetic reluctance and those based on eddy currents.

Limitations

- difficult to interpret at heavy congestion of reinforcement or when depth of reinforcement is too great
- embedded metals sometimes affect the reading
- used to detect the reinforcing bars closest to the face

Ultrasonic pulse velocity

It is used for determining the elastic constants (modulus of elasticity and Poisson's ratio) and the density. By conducting tests at various points on a structure, lower quality concrete can be identified by its lower pulse velocity. Pulse-velocity measurements can detect the presence of voids or discontinuities within a wall; however, these measurements cannot determine the depth of the voids.

Limitations

- Moisture content—an increase in moisture content increases the pulse velocity
- Presence of reinforcement oriented parallel to the pulse propagation direction—the pulse may propagate through the bars and result in an apparent pulse velocity that is higher than that propagating through concrete
- Presence of cracks and voids—increases the length of the travel path and result in a longer travel time

Impact echo

Impact echo is a method for detecting discontinuities within the thickness of a wall. An impact-echo test system is composed of three components: an impact source, a receiving transducer, and a waveform analyzer or a portable computer with a data acquisition.

Limitations

- accuracy of results highly dependent on the skill of the engineer and interpreting the results
- The size, type, sensitivity, and natural frequency of the transducer, ability of FFT analyzer also affect the results
- Mainly used for concrete structures

Spectral Analysis of Surface Waves (SASW)

To assess the thickness and elastic stiffness of material, size and location of discontinuities within the wall such as voids, large cracks, and delimitations.

Limitations

- interpretation of results is very complex
- mainly used on slab and other horizontal surface, to determine the stiffness profiles of soil sites and of flexible and rigid pavement systems, measuring the changes in elastic properties of concrete slab

Penetrating radar

It is used to detect the location of reinforcing bars, cracks, voids or other material discontinuities, verify thickness of concrete.

Limitations

- mainly used for detecting subsurface condition of slab-on-grade
- not useful for detecting the small differences in materials

- not useful for detecting the size of bars, closely spaced bars make difficult to detect features below the layer of reinforcing steel

SUMMARY

There are many buildings that have primary structural system, which do not meet the current seismic requirements and suffer extensive damage during the earthquake. The methods for seismic evaluation of existing seismically deficient or earthquake-damaged buildings are not yet fully developed. The present chapter deals with the practical methodology for seismic evaluation of existing buildings or earthquake damaged buildings on the basis of three-tier system which are condition assessment, field inspection report and non-destructive testing. Each system is independent in itself and evaluation process can be stopped at any stage depending upon the objective of evaluation process.

REFERENCES

- [1] ATC, "Evaluating the Seismic Resistance of Existing Buildings", *ATC-14 Project*, Applied Technology Council, California, 1987.
- [2] Booth, E., *Concrete Structures in Earthquake Regions*, Longman Scientific and Technical, Longman Group UK Limited, 1994.
- [3] Carino, N.J., "Non-destructive Test Method", *Concrete Construction Engineering Handbook*, Edward G. Nawy, CRC Press, New York, 1997.
- [4] FEMA-306, "Evaluation of Earthquake Damaged Concrete and Masonry Wall Buildings", *ATC-43 Project*, Applied Technology Council, California, 1999.
- [5] Guevara, L.T. and Garcia, L.E., "The Captive and Short Column Effect", *Earthquake Spectra*, 21(1), 141-160, 2005
- [6] IS: 13935, *Ductile Detailing of Reinforced Concrete Structures Subjected to Seismic Forces*, Bureau of Indian Standards, New Delhi, 1993.
- [7] Kono, S. and Watanabe, F., "Damage Evaluation of Reinforced Concrete Columns under Multi-axial Cyclic Loadings", *The Second US-Japan Workshop on Performance Based Earthquake Engineering Methodology for Reinforced Concrete Building Structures*, PEER 2000/10, 2000.
- [8] Malhotra, V.M. and Carino, N.J., *Handbook on Non-destructive Testing of Concrete*, CRC Press, 1991.
- [9] Moehle, J.P., Wood, K.J. and Sezen, "Shear Failure and Axial Load Collapse of Existing Reinforced Concrete Columns", *The Second US-Japan Workshop on Performance Based Earthquake Engineering Methodology for Reinforced Concrete Building Structures*, PEER 2000/10, 2000.
- [10] Nawy, Edward G., *Concrete Construction Engineering Handbook*, CRC Press, New York, 1997.
- [11] Poston, W.R., "Structural Concrete Repair: General Principles and a Case Study (ch. 19)", *Concrete Construction Engineering Handbook*, Edward G. Nawy (Ed.-in-Chief), Chapter 19, CRC Press, New York, 1997.

- [12] Smith, B.S. and Carter, C., "Hypothesis for shear Failure of Brickwork", *Journal of the Structural Division, Proceedings of the American Society of Civil Engineers*, April, 1971.
- [13] UNDP/UNIDO Project RER/79/015, "Repair and Strengthening of Reinforced Concrete, Stone and Brick Masonry Buildings", *Building Construction Under Seismic Conditions in the Balkan Regions*, Vol. 5., United Nations Industrial Development Programme, Austria, 1983.
- [14] UNDP/UNIDO Project RER/79/015, "Repair and Strengthening of Reinforced Concrete, Stone and Brick Masonry Buildings", *Building Construction Under Seismic Conditions in the Balkan Regions*, Vol. 5, United Nations Industrial Development Programme, Austria, 1983.
- [15] Wallace, J.W. and Melek, M., "Column Splices: Observed Earthquake Damage, Modeling Approaches, and the PEER/UCLA Research Program", *The Second US-Japan Workshop on Performance Based Earthquake Engineering Methodology for Reinforced Concrete Building Structures*, PEER 2000/10, 2000.

Chapter 29

Seismic Retrofitting Strategies of Reinforced Concrete Buildings

29.1 INTRODUCTION

The aftermath of an earthquake manifests great devastation due to unpredicted seismic motion striking extensive damage to innumerable buildings of varying degree *i.e.* either full or partial or slight. This damage to structures in its turn causes irreparable loss of life with a large number of casualties. As a result frightened occupants may refuse to enter the building unless assured of the safety of the building from future earthquakes. It has been observed that majority of such earthquake damaged buildings may be safely reused, if they are converted into seismically resistant structures by employing a few retrofitting measures. This proves to be a better option catering to the economic considerations and immediate shelter problems rather than replacement of buildings. Moreover it has often been seen that retrofitting of buildings is generally more economical as compared to demolition and reconstruction even in the case of severe structural damage. Therefore, seismic retrofitting of building structures is one of the most important aspects for mitigating seismic hazards especially in earthquake-prone countries. Various terms are associated to retrofitting with a marginal difference like repair, strengthening, retrofitting, remoulding, rehabilitation, reconstruction etc. but there is no consensus on them. The most common definition of these terms may be summarized in Table 29.1.

The need of seismic retrofitting of buildings arises under two circumstances: (i) earthquake-damaged buildings and (ii) earthquake-vulnerable buildings that have not yet experienced severe earthquakes. The problems faced by a structural engineer in retrofitting earthquake damaged buildings are: (a) lack of standards for methods of retrofitting; (b) effectiveness of retrofitting techniques since there is a considerable dearth of experience and data on retrofitted structures; (c) absence of consensus on appropriate methods for the wide range of parameters like type of structures, condition of materials, type of damage, amount of damage, location of damage, significance of damage, condition under which a damaged element can be retrofitted etc. Therefore, a catalogue of available options regarding feasible and practical retrofitting method

TABLE 29.1 Concept of various terms associated with retrofitting

<i>Terms</i>	<i>CEB, 1995</i>	<i>Tomazevic, 1999</i>	<i>Newman, 2001</i>
Repairing To make the existing structure safer for future earthquake <i>as per IS 13935: 1993</i>	Reconstruction or renewal of any part of a damaged or deteriorated building to provide the same level of strength and ductility, which the building had, prior to the damage	“Repair” refers to the post-earthquake repair of damage, which restricts the seismic resistance of the building to its pre-earthquake state	Repairing is a process of reconstruction and renewal of the existing buildings, either wholly or in part.
Retrofitting To upgrade the earthquake resistance up to the level of the present-day codes by appropriate techniques <i>as per IS 13935: 1993</i>	Concepts including strengthening, repairing and remoulding	Increasing the seismic resistance of a damaged building is called retrofitting.	It is an upgrading of certain building system, such as mechanical, electrical, or structural, to improve performance, function, or appearance.
Strengthening To upgrade the seismic resistance of a damaged building <i>as per IS 13935: 1993</i>	Reconstruction or renewal of any part of an existing building to provide better structural capacity <i>i.e.</i> higher strength and ductility, than the original building	“Strengthening” may increase the seismic resistance of a building beyond its pre-earthquake state. Strengthening may be carried out in existing seismically deficient buildings or earthquake-damaged buildings	

Contd.

TABLE 29.1 Contd.

<i>Terms</i>	<i>CEB, 1995</i>	<i>Tomazevic, 1999</i>	<i>Newman, 2001</i>
Rehabilitation	Reconstruction or renewal of a damaged building to provide the same level of function, which the building had prior to the damage	Increasing the seismic resistance of an existing seismically deficient building is called rehabilitation.	Upgradation required to meet the present needs; it implies sensitivity to building features and a sympathetic matching of original construction.
Restoration	Rehabilitation of buildings in a certain area		More restrictive term than rehabilitation; it suggests replicating the structure as originally built. The term is most commonly applied to the buildings of historical value.
Remoulding	Reconstruction or renewal of any part of an existing building owing to change of usage or occupancy		It is a process of substantial repair or alteration that extends a building's useful life.

is needed by the structural engineer due to great variability of retrofitting requirements differing from building to building. In addition, experimental and analytical research is urgently needed to strengthen different techniques of retrofitting.

The need of retrofitting of existing earthquake vulnerable buildings may arise due to one or more than one of the following reasons *i.e.* (a) the buildings have been designed according to a seismic code, but the code has been upgraded in later years; (b) buildings designed to meet the modern seismic codes, but deficiencies exist in the design and/or construction; (c) essential buildings must be strengthened like hospitals, historical monuments and architectural buildings; (d) important buildings whose service is assumed to be essential even just after an earthquake; (e) buildings, the use of which has changed through the years; (f) buildings that are expanded, renovated or rebuilt. The problems faced by the structural engineer in case of earthquake vulnerable buildings are to obtain sufficient records of buildings such as architectural and structural drawings, structural design calculations, material properties, details of foundation and geo-technical reports, records of at least natural period of the buildings in order to evaluate the increased stiffness of buildings since strengthening techniques most often stiffen the structure reducing its natural period.

Retrofitting of existing buildings and issues of their structural safety have not received adequate attention in India. There are at present no guidelines or codes of practice available in the country for retrofitting. The methods of seismic assessment of existing buildings are not adequately developed. In some developed countries research on repair and retrofitting has been undertaken during the last two decades. Various techniques of seismic retrofitting have been developed and used in practice. The basic concepts of these techniques of retrofitting are aimed at (CEB, 1997): (a) upgradation of the lateral strength of the structure; (b) increase in the ductility of structure; (c) increase in strength and ductility. These three concepts are schematically illustrated in Figure 29.1.

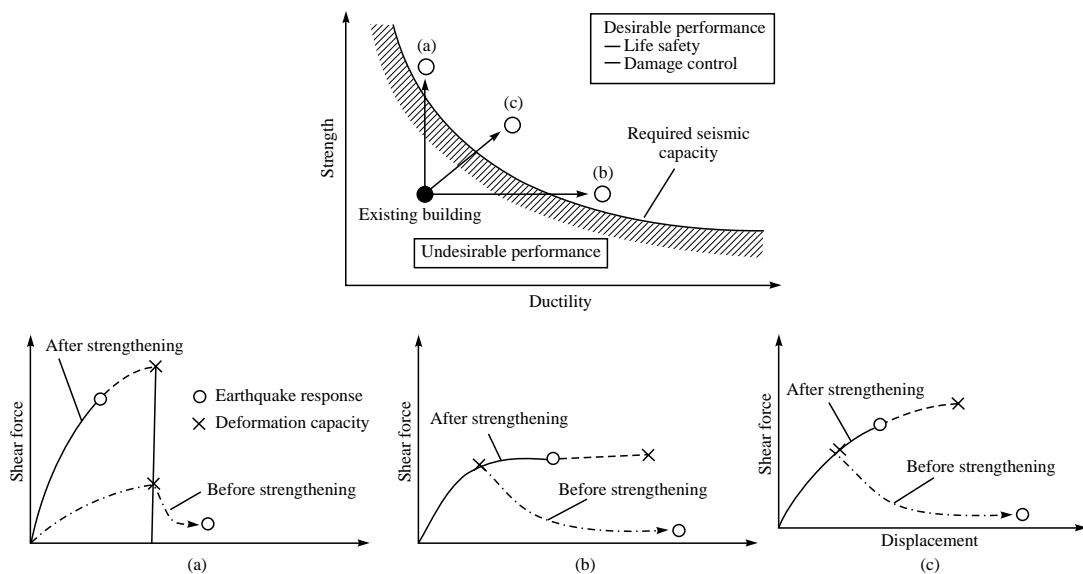


FIGURE 29.1 Aims of seismic strengthening (CEB, 1997).

The decision to repair and strengthen a structure depends not only on technical considerations as mentioned above but also on a cost/benefit analysis of the different possible alternatives. It is suggested that the cost of retrofitting of a structure should remain below 25% of the replacement as major justification of retrofitting (Nateghi and Shahbazian, 1992). The present chapter will discuss different aspects of retrofitting scheme and their limitations, side effects as well as cost considerations. The information in this chapter is gathered from the available literature and is based on the experiences of individual authors and their studies.

29.2 CONSIDERATION IN RETROFITTING OF STRUCTURES

The method of retrofitting principally depends on the horizontal and vertical load resisting system of the structure and the type of materials used for parent construction. It also relies on the technology that is feasible and economical. The understanding of mode of failure, structural behaviour and weak and strong design aspects as derived from the earthquake damage surveys exercise considerable influence on selection of retrofitting methods of buildings. Usually the retrofitting method is aimed at increasing the lateral resistance of the structure. The lateral resistance includes the lateral strength or stiffness and lateral displacement or ductility of the structures. The lateral resistance is often provided through modification or addition of retrofitting elements of an existing structure in certain areas only. The remaining elements in the structure are usually not strengthened and are assumed to carry vertical load only, but in an earthquake, all components at each floor, retrofitted or not, will undergo essentially the same lateral displacements. While modified or added elements can be designed to sustain these lateral deformations, the remaining non-strengthened elements could still suffer substantial damage unless lateral drifts are controlled. Therefore, caution must be taken to avoid an irregular stiffness distribution in the strengthened structure. Thus the ability to predict initial and final stiffness of the retrofitted structure need clarification and quantification. Consequently, it is suggested that the design of retrofitted schemes should be based on drift control rather than on strength consideration alone. The use of three-dimensional analysis is recommended to identify and locate the potential weakness of the retrofitted building.

29.3 SOURCE OF WEAKNESS IN RC FRAME BUILDING

Earthquake engineering is not a pure science; rather it has been developed through the observation of failure of structure during earthquake (Otani, 2004). Damage survey reports of past earthquakes reveal the following main sources of weakness in reinforced concrete moment resisting frame buildings.

- (i) discontinuous load path/interrupted load path/irregular load path
- (ii) lack of deformation compatibility of structural members
- (iii) quality of workmanship and poor quality of materials

29.3.1 Structural Damage due to Discontinuous Load Path

Every structure must have two load resisting systems: (a) vertical load resisting system for transferring the vertical load to the ground and (b) horizontal load resisting system for transferring the horizontal load to the vertical load system. It is imperative that the seismic forces should be properly collected by the horizontal framing system and properly transferred into vertical lateral resisting system. Any discontinuity/irregularity in this load path or load transfer may cause one of the major contributions to structural damage during strong earthquakes. In addition it must be ensured that each member both of horizontal or vertical load resisting system must be strong enough and not fail during an earthquake. Therefore, all the structural and non-structural elements must have sufficient strength and ductility and should be well connected to the structural system so that the load path must be complete and sufficiently strong.

29.3.2 Structural Damage due to Lack of Deformation

The main problems in the structural members of moment resisting frame building are the limited amount of ductility and the inability to redistribute load in order to safely withstand the deformations imposed upon in response to seismic loads. The most common regions of failure in an existing reinforced concrete frame are shown in Figure 29.2. The regions of failure may be in columns, beams, walls and beam–column joints. It is important to consider the consequences of member failure or structural performance. Inadequate strength and ductility of the structural member can and will result in local or complete failure of the system. The different modes of failure in various structural members are reviewed.

Global behaviour of frames

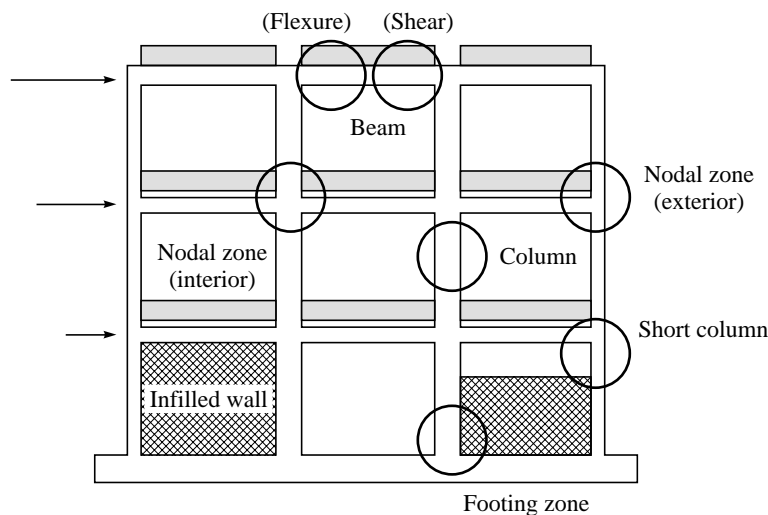


FIGURE 29.2 Possible reason of failure in moment resisting frame (Cosenza and Manfredi, 1997).

Columns

In reinforced concrete columns several interaction mechanism influences its lateral load behaviour. The main actions are associated with axial, flexure, shear, and bond as shown in Figure 29.3. The possible mode of failure and the suggested remedial measures are described in Table 29.2.

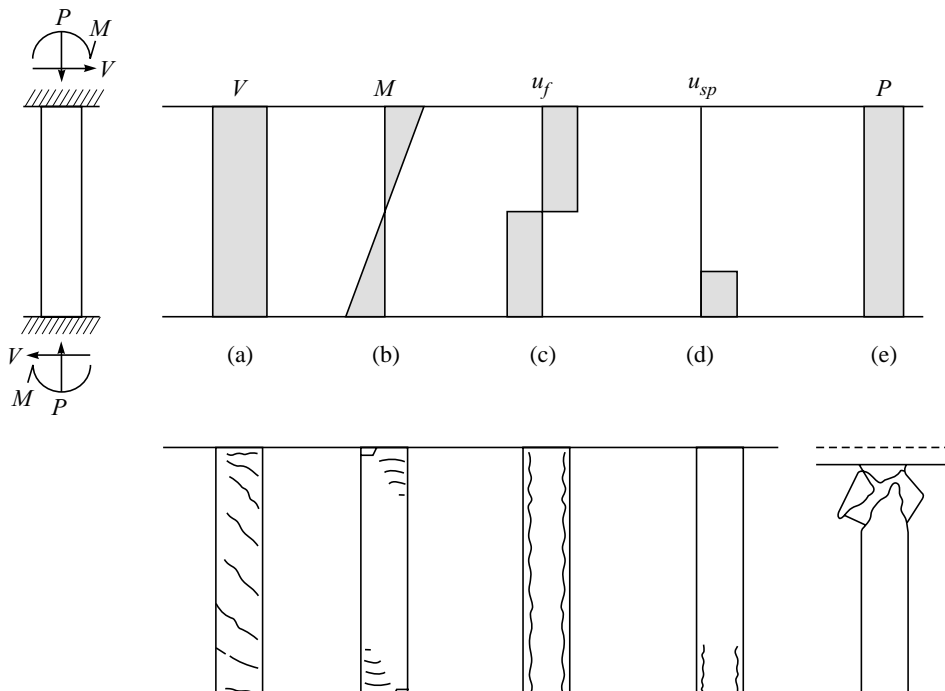


FIGURE 29.3 Action of concern force and its mode of failure in column (Lynn et al., 1996).

Beams

In reinforced concrete beams, the major problems exist at the right end, considering seismic forces left to right as shown in Figure 29.4. A *brittle shear failure* could occur due to superposing of shear forces caused by vertical loading and seismic loading.

Beam–column joints

In beam–column joint, the situation of exterior joints could be more critical if there is inadequate lateral reinforcement. In case of strong column–weak beam behaviour, the joint may be heavily stressed after beam yielding and diagonal cracking may be formed in the connection. Wide flexural cracks may develop at the beam end, partially attributable to the slip of beam reinforcement within the connection. Such shear cracking may reduce the stiffness of a building.

TABLE 29.2 Mode of failure of columns and remedial measures (Otani, 2004)

Action concern	Failure mode	Description of failure	Suggested remedial measures
Axial force and flexural	Flexural compression	<ul style="list-style-type: none"> • compression failure of concrete • buckling of longitudinal reinforcement • failure takes place near the column ends • hoop fracture 	<ul style="list-style-type: none"> • lateral confining reinforcement can delay the crushing failure of concrete • deformation capacity of column can be enhanced by providing the lateral reinforcement in the region of plastic deformation
Shear force	Diagonal tension/ Brittle shear	<ul style="list-style-type: none"> • cause diagonal tensile stress in concrete • these tensile stresses are transferred to the lateral reinforcement after cracking in concrete 	<ul style="list-style-type: none"> • provided minimum amount of lateral reinforcement (size, spacing and strength of shear reinforcement)
Shear force	Diagonal compression	<ul style="list-style-type: none"> • failure of concrete after the yielding of lateral reinforcement • not brittle as the diagonal tension failure or brittle shear failure • deformation capacity of column is limited 	<ul style="list-style-type: none"> • this failure occurs when minimum amount of lateral reinforcement is there but it is not adequate as per requirement • provides adequate lateral reinforcement as per requirement
Shear force	Diagonal compression	<ul style="list-style-type: none"> • compression failure of concrete takes place prior to the yielding of lateral reinforcement • vertical load carrying capacity of the column is lost, leading to the collapse 	<ul style="list-style-type: none"> • this failure occurs when there is excessive amount of lateral reinforcement • only up to a limit the amount of lateral reinforcement is effective for shear resistance • provides lateral reinforcement as per requirements

Contd.

TABLE 29.2 Contd.

<i>Action concern</i>	<i>Failure mode</i>	<i>Description of failure</i>	<i>Suggested remedial measures</i>
Tensile stresses	Splice failure of longitudinal reinforcement	<ul style="list-style-type: none"> • splices in older buildings were located in region of higher tensile stress because the implications for earthquake performance were inadequately understood • splices failure reduces flexural resistance of the member 	<ul style="list-style-type: none"> • splicing should be in a region of low tensile stress
Bond stresses	Bond splitting failure	<ul style="list-style-type: none"> • causes ring tension to the surrounding concrete • high flexural bond stresses may exist in members with steep moment gradient along their lengths • splitting cracks may develop along the longitudinal reinforcement, especially when the strength of concrete is low. 	<ul style="list-style-type: none"> • longitudinal reinforcement of a column should be supported by closely spaced stirrups or ties • not provide large diameters of longitudinal bars with high strength, • provide sufficient concrete cover

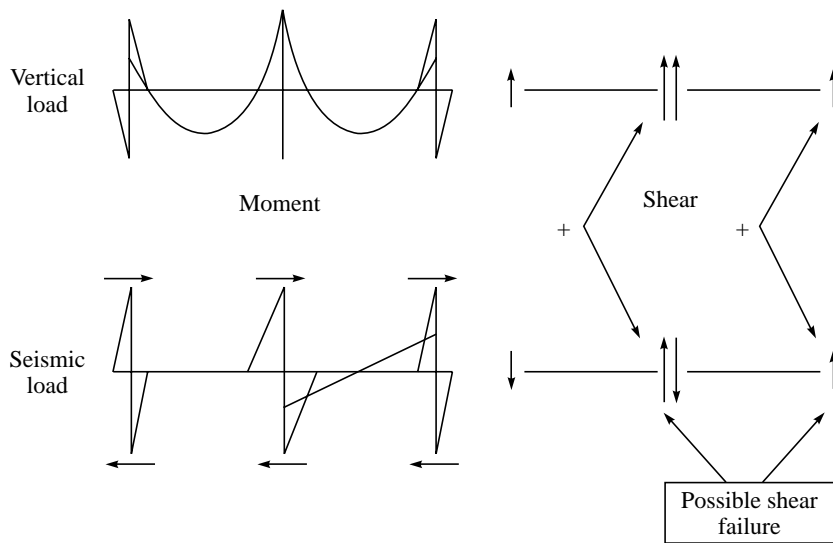


FIGURE 29.4 Behaviour of beams for vertical and seismic loading (Edoardo Cosenza and Gaetano Manfredi, 1997).

Slab

A shear failure has been observed in the case that the slab is resting directly on column capital without having any beam. The critical part of the flat plate slab system is the vertical shear transfer between the slab and column.

29.3.3 Quality of Workmanship and Materials

There are numerous instances where faulty construction practices and lack of quality control have contributed to the damage. The faulty construction practices may be like, lack of amount and detailing of reinforcement as per requirement of code particularly when the end of lateral reinforcement is not bent by 135 degrees as the code specified. Many buildings have been damaged due to poor quality control of design material strength as specified, spalling of concrete by the corrosion of embedded reinforcing bars, porous concrete, age of concrete, proper maintenance etc.

29.4 CLASSIFICATION OF RETROFITTING TECHNIQUES

There are two ways to enhance the seismic capacity of existing structures. The first is a structural-level approach of retrofitting which involves global modifications to the structural system. The second is a member level approach of retrofitting or local retrofitting which deals with an increase of the ductility of components with adequate capacities to satisfy their specific limit states. Based on the above concept the available techniques of retrofitting of reinforced concrete buildings may be classified as in Figure 29.5.

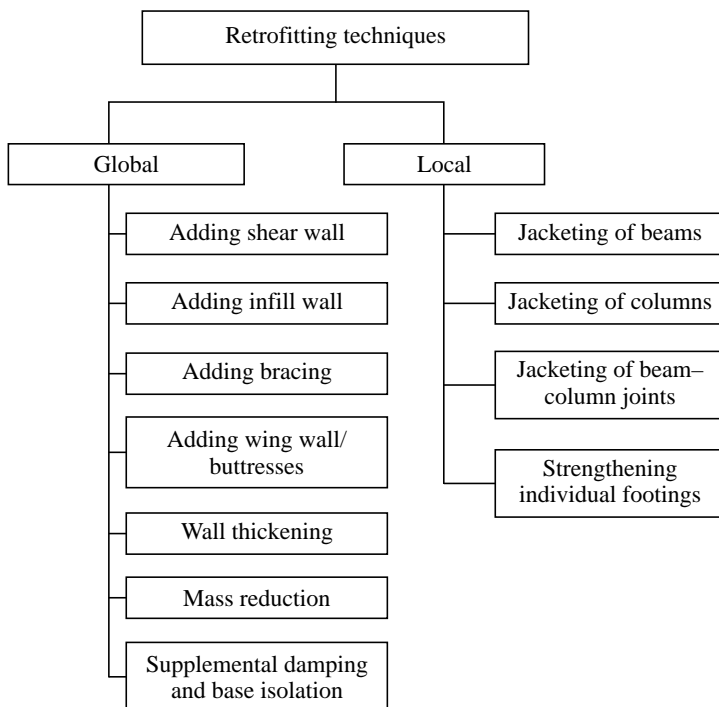


FIGURE 29.5 Global and local retrofitting methods.

Generally structural level retrofittings are applied when the entire structural lateral load resisting system is deemed to be deficient. Common approaches in this regard are employed to increase stiffness and strength with limited ductility. Achieving desired ratio between the additional stiffening and strengthening is the art of seismic retrofitting. The most common modifications include the addition of structural walls, steel braces, infill walls, base isolators or supplemental energy dissipation devices.

The addition of new reinforced concrete shear wall is the most oftenly practised device which has proved to be effective for controlling global lateral drifts and for reducing damage in frame members. Steel braces are used to make the existing buildings stiffen. Concentric or eccentric bracing schemes may be used, in the selected bays of an RC frame contributing to increase the lateral resistance of the structure. Infill wall may be employed for strengthening of reinforced concrete buildings, which has been effective in the case of one to three storey buildings that may be extended up to five stories. The lateral strength of existing columns can be increased by adding wing walls (side walls) or buttresses similar to infilling. These techniques are not so popular because it may require a vacant site around the building, and enough resistance from piles or foundation of the buttress (CEB, 1997). At some occasions it might be possible to achieve the retrofitting objectives by means of global mass reduction. Mass reduction can be accomplished by removal of upper stories, heavy cladding, partitions and stored good. Increasing the strength or stiffness of structural members such as slabs and shear wall can be achieved by thickening of members. The concept of seismic base isolation is based on decoupling of structure by introducing low horizontal stiffness bearing between the structure and the foundation. This

is found to be efficient for seismic protection of historical buildings where superstructure has a limited seismic resistance and intervention is required only at foundation level. The supplemental damping devices such as addition of viscous damper, visco-elastic damper, frictional damper in diagonals of bays of frame substantially reduces the earthquake response by dissipation of energy.

Local retrofittings are typically used either when the retrofit objectives are limited or direct treatment of the vulnerable components is needed. The most popular and frequently used method in local retrofitting is **jacketing** or **confinement** by the jackets of reinforced concrete, steel, fibre reinforced polymer (FRP), carbon fibre etc. Jacketing around the existing members increases lateral load capacity of the structure in a uniformly distributed way with a minimal increase in loading on any single foundation and with no alteration in the basic geometry of the building.

29.5 RETROFITTING STRATEGIES FOR RC BUILDINGS

The need for retrofitting or strengthening of earthquake-damaged or earthquake-vulnerable buildings in India have been tremendously increased during recent years after the devastating Bhuj earthquake with an alarming awakening for sufficient preparedness in anticipation to face future earthquakes. Many professional engineers are accustomed to the designing of new buildings but they may find themselves not fully equipped to face the challenges posed at the time of strengthening the existing buildings with a view to improve their seismic performance. This section presents the most common devices for retrofitting of reinforced concrete buildings with technical details, constructional details and limitations.

29.5.1 Structural Level (or Global) Retrofit Methods

Two approaches are used for structure-level retrofitting: (i) **conventional methods** based on increasing the seismic resistance of existing structure, and (ii) **non-conventional methods** based on reduction of seismic demands.

Conventional methods

Conventional methods of retrofitting are used to enhance the seismic resistance of existing structures by eliminating or reducing the adverse effects of design or construction. The methods include adding of shear wall, infill walls and steel braces.

Adding new shear walls

One of the most common methods to increase the lateral strength of the reinforced concrete buildings is to make a provision for additional shear walls (Figure 29.6). The technique of infilling/adding new shear walls is often taken as the best and simple solution for improving seismic performance. Therefore, it is frequently used for retrofitting of non-ductile reinforced concrete frame buildings. The added elements can be either cast-in-place or pre-cast concrete elements. New elements preferably be placed at the exterior of the building, however it may cause alteration in the appearance and window layouts. Placing of shear walls in the interior of the structure is not preferred in order to avoid interior mouldings.

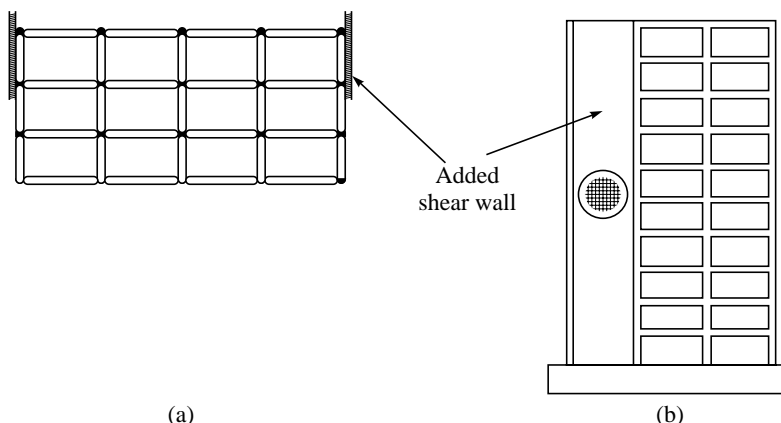


FIGURE 29.6 Increasing strength with shear walls: (a) Adding techniques (b) Infilling techniques (CEB, 1997).

Technical considerations: The addition of new shear walls to existing frame has many technical considerations which may be summarized as (a) determining the adequacy of existing floor and roof slabs to carry the seismic forces; (b) transfer of diaphragm shear into the new shear walls with dowels; (c) adding new collector and drag members to the diaphragm; (d) increase in the weight and concentration of shear by the addition of wall which may affect the foundations.

Constructional considerations: The first consideration during construction is to find locations where walls can be added and well located which may align to the full height of the building to minimize torsion (Wyllie, 1996). It is often desirable to locate walls adjacent to the beam between columns so that only minimum slab demolition is required with connections made to beam at the sides of columns. The design of the shear wall may be similar to new construction. The longitudinal reinforcement must be placed at the ends of the wall running continuously through the entire height. In order to realize this end, the reinforcement has to pass through holes in slabs and around the beams to avoid interference. To achieve both conditions, boundary elements can be used. Although it would also be convenient to have continuous shear reinforcement but in its absence, the walls must be adequately connected to the beams, slabs and columns ensuring proper shear transfer through shear connectors. Wall thickness also varies from 15 to 25 cm (6 to 10 inch) and is normally placed externally. This retrofitting system is only adequate for concrete structures, which bring forth a big increase in the lateral capacity and stiffness. A reasonable structural ductility may be achieved if the wall is properly designed with a good detailing. The connection to the existing structure has to be carefully designed to guarantee shear transfer.

Limitations: The main limitations of this method are: (i) increase in lateral resistance but it is concentrated at a few places, (ii) increased overturning moment at foundation causes very high uplifting that needs either new foundations or strengthening of the existing foundations, (iii) increased dead load of the structure, (iv) excessive destruction at each floor level results in functional disability of the buildings, (v) possibilities of adequate attachment between the new walls and the existing structure, (vi) closing of formerly open spaces can have major negative impact on the interior of the building or exterior appearance.

Adding steel bracings

Another method of strengthening is the use of steel bracing, which also has similar advantages. The structural details of connection between bracing and column are shown in Figure 29.7. The installation of steel bracing members can be an effective solution when large openings are required. This scheme of the use of steel bracing has a potential advantage over other schemes for the following reasons:

- higher strength and stiffness can be proved,
- opening for natural light can be made easily,
- amount of work is less since foundation cost may be minimized,
- the bracing system adds much less weight to the existing structure,
- most of the retrofitting work can be performed with prefabricated elements and disturbance to the occupants may be minimized.

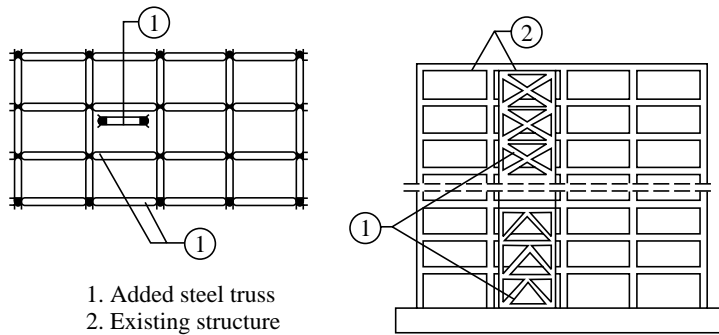


FIGURE 29.7 Reinforced concrete building retrofitted with steel bracing (UNDP, 1983).

Technical considerations: The steel bracing system can be used for steel structures as well as concrete structures; several researchers have reported successful results while using steel bracing to upgrade the strength and stiffness of reinforced concrete structures. It has performed well-exhibited linear behaviour even up to twice the design code force. The effective slenderness ratio of brace should be kept relatively low so that braces are effective in compression as well as tension, suggested l/r ratio are 80 to 60 or even lower. Collector's members are recommended for transferring forces between the frame and bracing system. Careful consideration of connections of strengthening elements to the existing structures and to the foundations have to be consciously designed to ensure proper shear transfer. Column shear failure is not specifically prevented; therefore close attention must be given to limit drifts of the strengthened frame. Local reinforcement to the columns may be needed to bear the increased load generated on them. The epoxies threaded rods have proved to be quite effective in connecting the bracing system to the concrete frame and in transferring the forces.

Constructional considerations: The available dead load of structure has to be considered to determine the amount or number of bays of bracing that can be mobilized to resist overturning uplift, as steel bracing is relatively light. Bracing bays usually require vertical columns at ends to resist overturning forces to work vertically, as chords of a cantilever truss are arranged horizontally at each floor level. It is to be connected to the horizontal diaphragms by collectors

or an opposite system of diagonals can be added to complete the truss network. Tension in braces should be avoided except in the case of light, simple buildings. Braces should have relatively low slenderness ratios so that they can function effectively during compression. Members are to be selected to provide acceptable slenderness ratio and to make simple connection, which in turn develops the strength of the member.

Limitations: Some inconveniences may be experienced with steel bracing, e.g. lack of information about the seismic behaviour of the added bracing; undesirable changes take place regarding the original architectural feature of the building. Moreover lack of cost efficiency and field experience may also cause inconvenience. In addition to this, steel bracing system may be sensitive to construction errors or omissions, which cause reduction in member capacity at a section. Section failure can impact the overall performance of the system. A moderate to high level of skilled labour is necessary for construction, due to the need for member fit-up adjustment and welding. Close quality control particularly with respect to welding is essential.

Adding infill walls

Strengthening of existing reinforced moment resisting frames often involves addition of infill walls. It is an effective and economical method for improving strength and reducing drift of existing frames (Figure 29.8a). But a relatively strong masonry infill may result in a failure of the columns of existing frame (Figure 29.8b). By proper selection of the infill masonry strength along with prevention of its premature separation from the columns, a more desirable failure mode can be achieved. Anchorage of the masonry to the frame is a critical factor in determining an overall performance. With proper anchorage, it should be possible to force failure in the masonry and prevent a premature shear/flexure column failure.

Technical consideration: A review of the literature has brought to light the high sensitivity of frame performance to relative values of infill strength, column strength and stiffness and beam strength. This exhibits three basic failure modes for masonry infilled frames as quantified by are: (E1-Dakhakhni et al., 2003).

Mode 1: Corner Crushing of the infill at least one of its loaded corners—associated with strong infill surrounded by a strong frame

Mode 2: Diagonal shear cracking in the form of a crack connecting the two loaded corners—associated with strong infill surrounded by a weak frame or a frame with weak joints and strong members

Mode 3: Frame Failure in the form of plastic hinges in the columns or the beam column connection—also associated with strong infill surrounded by a weak frame or frame with weak joints and strong members.

Constructional considerations: The infill wall capacity is usually governed by dead load column to resist overturning uplift. Number of infill wall depends on the building seismic loads alongwith shear and upliftment from single bay full height. Determination of number of bays of infill wall is needed in both directions to prevent uplift and locate walls in appropriate bays. Moreover design forces are transferred to new infill panels using shear friction. If columns have compression splices that are weak in tension, strengthening of column splices will be necessary.

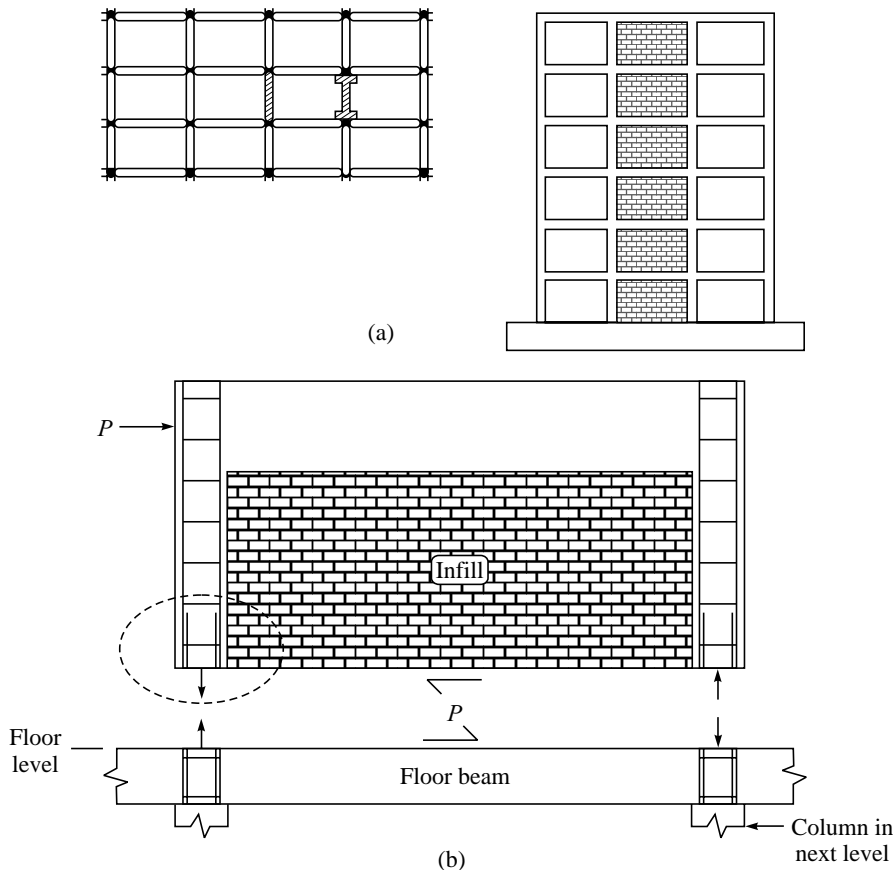


FIGURE 29.8 (a) Adding infill walls in reinforced concrete frame (UNDP, 1983, (b) Column lap splices subjected to large axial force due to frame wall action (Valluvan, Kreger and Jirsa, 1993).

There are two approaches for strengthening of column splices (Valluvan, Kreger and Jirsa, 1992). The first consists of making spliced bars continuous so that forces could lie transferred directly without relying on the bond strength between spliced bars and surrounding concrete. The other is to involve the region to improve bond along spliced bars. External reinforcement around the splice region significantly improves confinement and splice strength. The external reinforcement must be grouted in order to permit it to effectively confine the concrete. Addition of internal ties to the splice region has not been an effective method for strengthening column splices, because removal of concrete reduces the effectiveness of concrete cover and the splice strength more than additional ties improve it.

Limitations: The benefit of retrofitting by infill walls is often limited by failure of splices in existing columns, which act as boundary elements for new infill walls. As a result, some columns in the frame are subjected to large axial tensile forces, which may exceed the capacity of column splices that have originally been designed both for little or no flexure and only for either compression prior to seismic code or only for gravity loads without consideration of seismic loads.

Non-conventional methods

In recent years, several alternative approaches are being used in the retrofitting of structures. Among them, seismic base isolation and addition of supplemental device techniques are the most popular. These techniques proceed with quite a different philosophy in that sense that it is fundamentally conceived to reduce the horizontal seismic forces. The applications of these techniques in retrofitting are also in infancy state; hence, the technical literature related to their application, future performance, advantage and problems have not been thoroughly investigated. However, a brief discussion about these techniques has been made here.

Seismic base isolation

Base isolation proceeds with quite a different philosophy in the sense that this concept is fundamentally concerned to reduce the horizontal seismic forces (Delfosse and Delfosse, 1992). It is a powerful and relatively cheaper method of seismic rehabilitation of buildings. Its main advantages are: (a) better protection against earthquake due to the decreasing of shears, (b) superstructure will need no reinforcement, (c) foundation system will not need any reinforcement to resist the overturning moments, which are much smaller than those of initial design, (d) least interrupting the building activities, since the work is carried out in the basement with no loss of income during rehabilitation programme, (e) least temporary work is required.

A typical base isolation system is evolved by the use of rubber bearing located at the base of the building, most often just below the first floor, under columns or shear walls. Rubber bearing consists of laminated layers of rubber and steel plates strongly bound together during the vulcanizing process of rubber. They are designed with a vertical stiffness, which is usually 300 to 1000 times higher than the horizontal stiffness. Such a system increases the first natural period in both the horizontal directions in between the range of 1 to 2.5 seconds and the response acceleration decreases accordingly (except for building on soft soils for which natural period should be increased up to 3 sec or more). Damping usually comprised between 5% and 10% critical, but can jump to as high as 20% with the addition of damper. Base isolation techniques have created considerable interest among architects and engineers in developed nations like France, USA, Japan etc. A building filled with well designed base isolation behaves like one degree of freedom system.

Figures 29.9 and 29.10 show the step-by-step process of base isolation retrofit of building supported by columns and pile respectively.

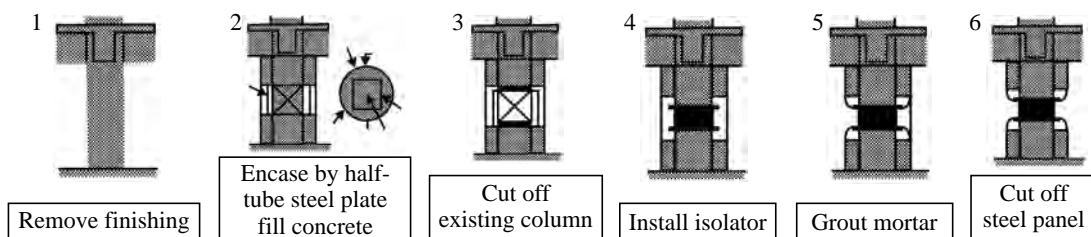


FIGURE 29.9 Process of seismic retrofitting by base isolation in mid-storey isolation (Kawamura, 2000).

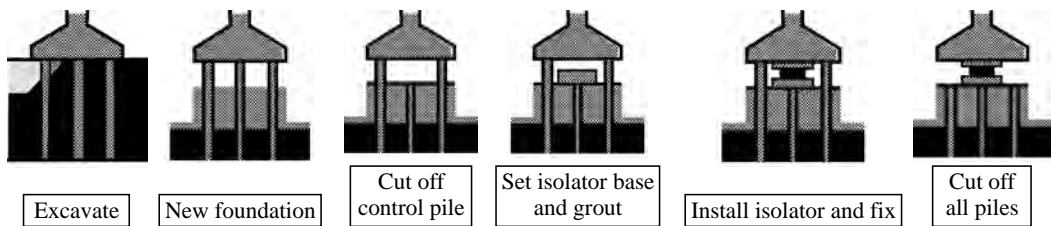


FIGURE 29.10 Process of seismic retrofitting by base isolation in building resting on pile (Kawamura, 2000).

Supplemental damping devices

Use of supplemental damping may be an effective method to resist seismic force. The most commonly used approaches to add supplemental dampers to a structure are installing of viscous damper or visco-elastic damper, frictional damper, and hysteretic dampers as components of braced frames (Figure 29.11).

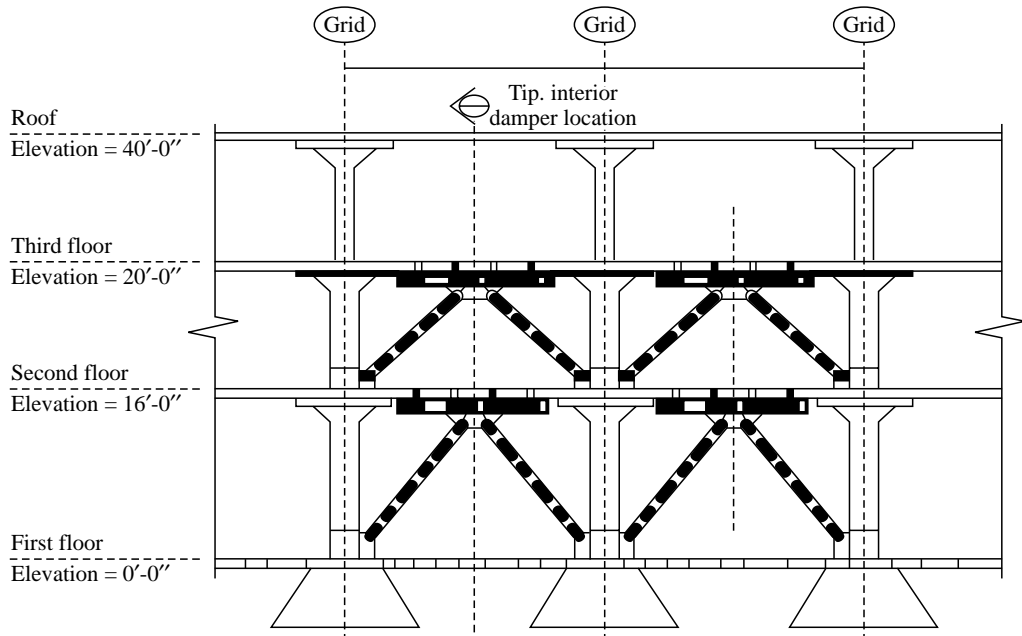


FIGURE 29.11 Building retrofitted with visco-elastic damper in first and second stories (Buckle, 2000).

29.5.2 Member Level (or Local) Retrofit Methods

The member-level retrofit or local retrofit approach is to upgrade the strength of the members, which are seismically deficient. This approach is more cost effective as compared to the structural level retrofit. The most common method of enhancing the individual member strength

is jacketing. It includes the addition of concrete, steel, or fibre reinforced polymer (FRP) jackets for use in confining reinforced concrete columns, beams, joints and foundation. A brief discussion of jacketing and its application on various members are discussed below.

Jacketing/confinement

Jacketing is the most popularly used methods for strengthening of building columns. The most common types of jackets are steel jacket, reinforced concrete jacket, fibre reinforced polymer composite jacket, jacket with high tension materials like carbon fibre, glass fibre etc. The main purposes of jacketing are: (i) to increase concrete confinement by transverse fibre/reinforcement, especially for circular cross-sectional columns, (ii) to increase shear strength by transverse fibre/reinforcement, (iii) to increase flexural strength by longitudinal fibre/reinforcement provided they are well anchored at critical sections. Transverse fibre should be wrapped all around the entire circumference of the members possessing close loops sufficiently overlapped or welded in order to increase concrete confinement and shear strength. This is how members with circular cross-section will get better confinement than member with rectangular cross-section. Where square or rectangular cross-sections are to be jacketed, circular/oval/elliptical jackets are most oftenly used and the space between the jacket and column is filled with concrete. Such types of multi-shaped jackets provide a high degree of confinement by virtue of their shape to the splice region proving to be more effective. Rectangular jackets typically lack the flexural stiffness needed to fully confine the concrete. However, circular and oval jackets may be less desirable due to (i) need of large space in the building potential difficulties of fitting in the jackets with existing partition walls, exterior cladding, and non-structural elements and (ii) where an oval or elliptical jacket has sufficient stiffness to confine the concrete along the long dimension of the cross-section is open to question (Figure 29.12). The longitudinal fibres similar to longitudinal reinforcement can be effective in increasing the flexural strength of member although they cannot effectively increase the flexural capacity of building frames because the critical moments are located at beam–column ends where most of the longitudinal fibres are difficult to pierce through to get sufficient anchorage.

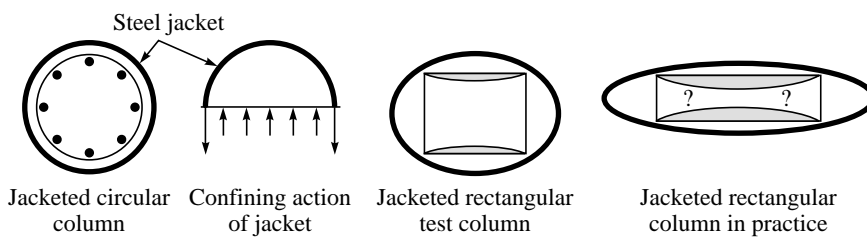


FIGURE 29.12 Various shapes of retrofitting jackets (Aschheim, 1997).

Note: Shading shows areas of reduced confinement effectiveness

Technical considerations

The main objective of jacketing is to increase the seismic capacity of the moment resisting framed structures. In almost every case, the columns as well as beams of the existing structure have been jacketed. In comparison to the jacketing of reinforced concrete columns, jacketing

of reinforced concrete beams with slabs is difficult yielding good confinement because slab causes hindrance in the jacket. In structures with waffle slab, the increase in stiffness obtained by jacketing columns and some of the ribs, have improved the efficiency of structures. In some cases, foundation grids are strengthened and stiffened by jacketing their beams. An increase in strength, stiffness and ductility or a combination of them can be obtained. There may be several options for the jacketing of members as shown in Figure 29.13. Usually the existing member is wrapped with a jacket of concrete reinforced with longitudinal steel and ties or with welded wire fibre, steel plate, similar to other strengthening schemes, the design of jackets should also include the probable redistribution of loads in the structure. A change in the dynamic properties of the structure may lead to a change in the lateral forces induced by an earthquake. Jacketing serves to improve the lateral strength and ductility by confinement of compression concrete. It should be noted that retrofitting of a few members with jacketing or some other enclosing techniques might not be effective enough to improve the overall behaviour of the structure, if the remaining members are not ductile.

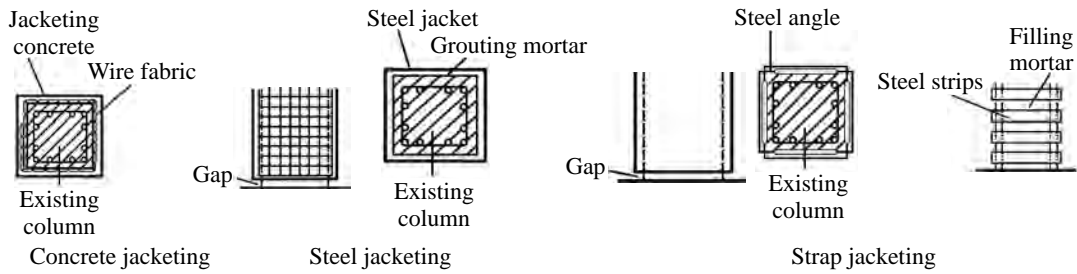


FIGURE 29.13 Types of jacketing of columns (Sugano, 1981)

Jacketing of columns

Jacketing of columns consists of added concrete with longitudinal and transverse reinforcement around the existing columns. This type of strengthening improves the axial and shear strength of columns while the flexural strength of column and strength of the beam–column joints remain the same. It is also observed that the jacketing of columns is not successful for improving the ductility. A major advantage of column jacketing is that it improves the lateral load capacity of the building in a reasonably uniform and distributed way and hence avoiding the concentration of stiffness as in the case of shear walls. This is how major strengthening of foundations may be avoided. In addition the original function of the building can be maintained, as there are no major changes in the original geometry of the building with this technique. The jacketing of columns is generally carried out by two methods: (i) reinforced concrete jacketing and (ii) steel jacketing.

Reinforced concrete jacketing

Reinforced concrete jacketing can be employed as a repair or strengthening scheme. Damaged regions of the existing members should be repaired prior to their jacketing. There are two main purposes of jacketing of columns: (i) increase in the shear capacity of columns in order to

accomplish a strong column–weak beam design and (ii) to improve the column's flexural strength by the longitudinal steel of the jacket made continuous through the slab system and anchored with the foundation. It is achieved by passing the new longitudinal reinforcement through holes drilled in the slab and by placing new concrete in the beam–column joints as is illustrated in Figure 29.14.

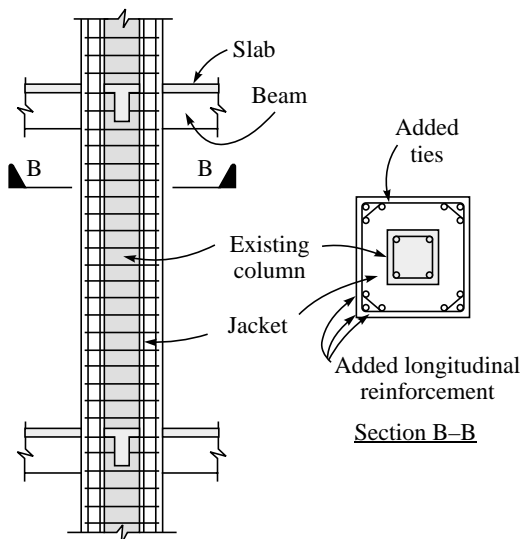


FIGURE 29.14 Construction techniques for column jacketing (Rodriguez and Park, 1991).

Rehabilitated sections are designed in this way so that the flexural strength of columns should be greater than that of the beams. Transverse steel above and below the joint has been provided with details, which consists of two L-shaped ties that overlap diagonally in opposite corners. The longitudinal reinforcement usually is concentrated in the column corners because of the existence of the beams where bar bundles have been used as shown in Figure 29.15. It is recommended that not more than 3 bars be bundled together. Windows are usually bored through the slab to allow the steel to go through as well as to enable the concrete casting process. Figure 29.16 shows the options for the detailing of the longitudinal reinforcement to avoid the excessive use of bundles. In some cases jacketing has been applied only within the storey as a

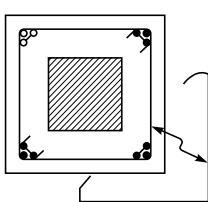


FIG. 29.15

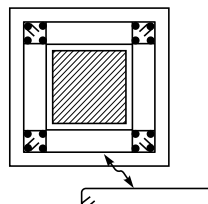


FIG. 29.16

FIGURES 29.15 and 29.16 Details for provision of longitudinal reinforcement (Teran and Ruiz, 1992).

local strengthening as shown in Figure 29.17. Table 29.3 furnished the details for reinforced concrete jacketing extracted from the UNDP/UNIDO, 1983.

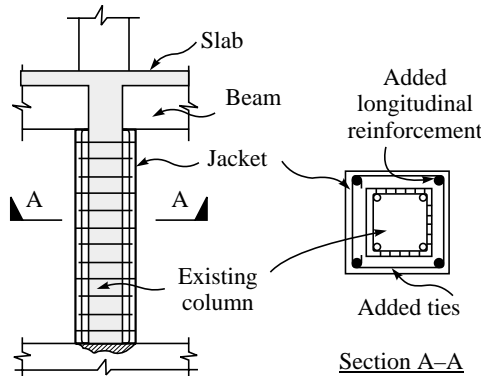


FIGURE 29.17 Local strengthening of reinforced concrete columns (Rodriguez and Park, 1991).

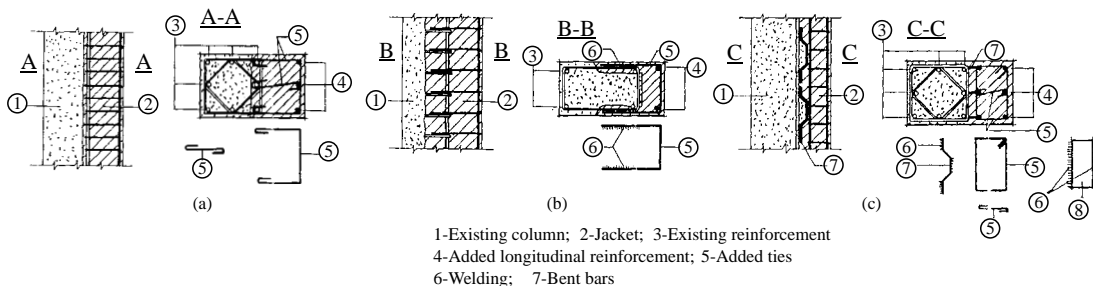
TABLE 29.3 Details for reinforced concrete jacketing (UNDP/UNIDO, 1983)

Properties of jackets	<ul style="list-style-type: none"> Match with the concrete of the existing structure Compressive strength greater than that of the existing structures by 5 N/mm^2 (50 kg/cm^2), or at least equal to that of the existing structure
Minimum width of jacket	<ul style="list-style-type: none"> 10 cm for concrete cast-in-place and 4 cm for shotcrete If possible, four-sided jacket should be used A monolithic behaviour of the composite column should be assured Narrow gap should be provided to prevent any possible increase in flexural capacity
Minimum area of longitudinal reinforcement	<ul style="list-style-type: none"> $3A/f_y$, where, A is the area of contact in cm^2 and f_y is in kg/cm^2 Spacing should not exceed six times of the width of the new elements (the jacket in the case) up to the limit of 60 cm. percentage of steel in the jacket with respect to the jacket area should be limited between 0.015 and 0.04 At least, a #5 bar should be used at every corner for a four sided jacket
Minimum area of transverse reinforcement	<ul style="list-style-type: none"> Designed and spaced as per earthquake design practice Minimum bar diameter used for ties is not less than 10 mm or $1/3$ of the diameter of the biggest longitudinal bar. The ties should have 135-degree hooks with 10 bar diameter anchorage. Due to the difficulty of manufacturing 135-degree hooks on the field, ties made up of multiple pieces, can be used.

Contd.

TABLE 29.3 Contd.

Shear stress in the interface	<ul style="list-style-type: none"> Provide adequate shear transfer mechanism to assured monolithic behaviour A relative movement between both concrete interfaces (between the jacket and the existing element) should be prevented. Chipping the concrete cover of the original member and roughening its surface may improve the bond between the old and the new concrete. For four-sided jacket, the ties should be used to confine and for shear reinforcement to the composite element For 1, 2, 3 side jackets, as shown in Figures 29.18, special reinforcement should be provided to enhance a monolithic behaviour.
Connectors	<ul style="list-style-type: none"> Connectors should be anchored in both the concrete such that it may develop at least 80% of their yielding stress. Distributed uniformly around the interface, avoiding concentration in specific locations. It is better to use reinforced bars (rebar) anchored with epoxy resins of grouts as shown in Figure 29.18(a).

**FIGURE 29.18 Different methods of column jacketing (UNDP, 1983).**

Steel jacketing

Local strengthening of columns has been frequently accomplished by jacketing with steel plates. A general feature of steel jacketing is mentioned in Table 29.4.

TABLE 29.4 Details of steel jacketing (Aboutaha, Engelhardt, Jirsa and Kreger, 1996)

Steel plate thickness	<ul style="list-style-type: none"> At least 6 mm
Height of jacket	<ul style="list-style-type: none"> 1.2 to 1.5 times splice length in case of flexural columns Full height of column in case of shear columns

Contd.

TABLE 29.4 Contd.

Shape of jackets	<ul style="list-style-type: none"> Rectangular jacketing, prefabricated two L-shaped panels <i>The use of rectangular jackets has proved to be successful in case of small size columns up to 36 inch width that have been successfully retrofitted with $\frac{1}{4}$" thick steel jackets combined with adhesive anchor bolt, but has been less successful on larger rectangular columns. On larger columns, rectangular jackets appear to be incapable to provide adequate confinement.</i>
Free ends of jackets	<ul style="list-style-type: none"> Welded throughout the height of jacket, size of weld $\frac{1}{4}$"
Bottom clearance	<ul style="list-style-type: none"> 38 mm (1.5 inch), steel jacket may be terminated above the top of footing to avoid any possible bearing of the steel jacket against the footing, to avoid local damage to the jacket and/or an undesirable or unintended increase in flexural capacity
Gap between steel jacket and concrete column	<ul style="list-style-type: none"> 25 mm (1 inch) fill with cementations grout
Size of anchor bolt	<ul style="list-style-type: none"> 25 mm (1 inch) in diameter and 300 mm (12") long embedded in 200 mm (8") into concrete column Bolts were installed through pre-drilled holes on the steel jacket using an epoxy adhesive
Number of anchor bolts	<ul style="list-style-type: none"> Two anchor bolts are intended to stiffen the steel jacket and improve confinement of the splice

FRP jacketing

Several researchers have investigated the possibility and feasibility of fibre reinforced polymer composite jackets for seismic strengthening of columns winding them with high strength carbon fibres around column surface to add spiral hoops (Figure 29.19). The merits of this method are: (i) carbon fibre is flexible and can be made to contact the surface tightly for a high degree of confinement; (ii) confinement is of high degree because carbon fibres is of high strength and high modules of elasticity are used; (iii) the carbon fibre has light weight and rusting does not occur (Katsumata et al., 1988).

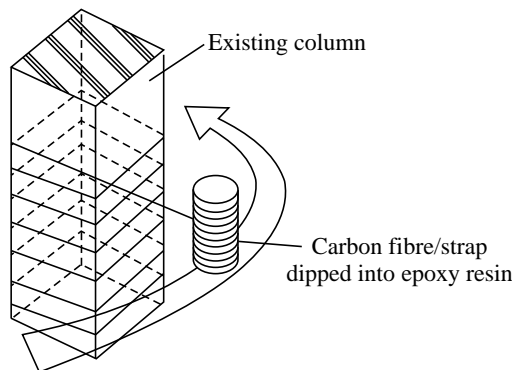


FIGURE 29.19 Carbon fibre winding (Katsumata and Kobatake, 1996).

Limitations: There are some disadvantages associated with the column jacketing technique as well, (i) in some cases the presence of beams may require majority of new longitudinal bars to be bundled into the corners of the jacket; (ii) with the presence of the existing column it is difficult to provide cross ties for new longitudinal bars which are not at the corners of the jackets; (iii) jacketing is based mostly on engineering judgment as there is a dearth of guidelines.

Beam jacketing

Jacketing of beams is recommended for several purposes as it gives continuity to the columns and increases the strength and stiffness of the structure. While jacketing a beam, its flexural resistance must be carefully computed to avoid the creation of a strong beam–weak column system. In the retrofitted structure, there is a strong possibility of change of mode of failure and redistribution of forces as a result of jacketing of column, which may consequently causes beam hinging. The location of the beam critical section and the participation of the existing reinforcement should be taken into consideration. Jacketing of beam may be carried out under different ways (Teran and Ruiz, 1992), the most common are one-sided jackets or 3- and 4-sided jackets (Figure 29.20).

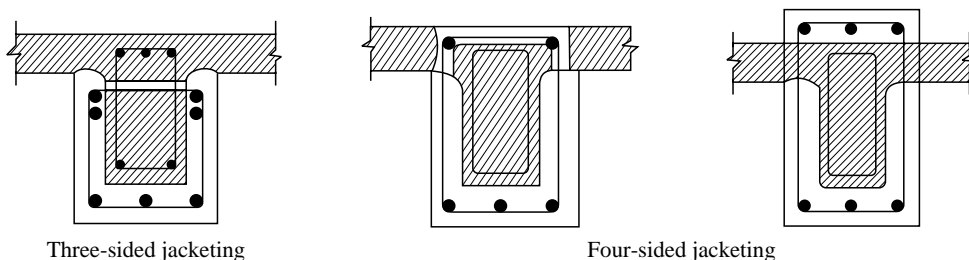


FIGURE 29.20 Different ways of beam jacketing (Teran and Ruiz, 1992).

At several occasions, the slab has been perforated to allow the ties to go through and to enable the casting of concrete. The beam should be jacketed through its whole length. The reinforcement has also been added to increase beam flexural capacity moderately and to produce high joint shear stresses. Top bars crossing the orthogonal beams are put through holes and the bottom bars have been placed under the soffit of the existing beams, at each side of the existing column. Beam transverse steel consists of sets of U-shaped ties fixed to the top jacket bars and of inverted U-shaped ties placed through perforations in the slab, closely spaced ties have been placed near the joint region where beam hinging is expected to occur (Figure 29.21). The main features of reinforcement details of beam jacketing are given in Table 29.5.

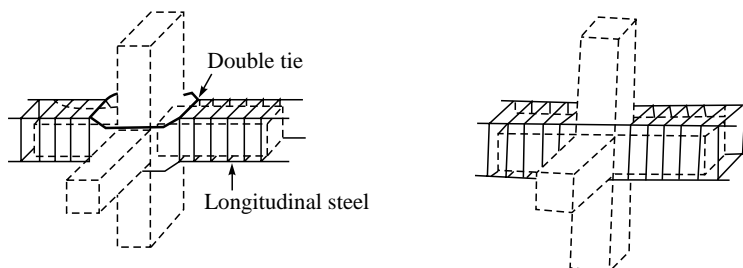


FIGURE 29.21 Continuity of longitudinal steel in jacketed beams (Teran and Ruiz, 1992).

TABLE 29.5 Reinforcement details of beam jackets (UNDP/UNIDO, 1983)

Minimum width for jacket	<ul style="list-style-type: none"> • 8 cm if concrete cast in place or 4 cm for shotcrete
Longitudinal reinforcement	<ul style="list-style-type: none"> • Percentage of steel on the jacket should be limited to 50 of the total area of the composite section
Shear reinforcement	<ul style="list-style-type: none"> • Ignore the effect of existing shear reinforcement • New reinforcement should have 135 hooks and at each corner of the tie there must be at least one longitudinal bar. • The bar used for the tie should have at least 8 mm diameter • Multiple piece ties can be used, as discussed before for columns
Depth of jacketed beam	<ul style="list-style-type: none"> • Span/depth ratio • Storey height • Ductile behaviour

Although these guidelines can give a rational basis for practical design, research still needs to address critical aspects in the behaviour of jacketed elements. The change in behaviour in jacketed elements, whose shear span/depth ratios are significantly reduced, due to their jacketing, needs to be clarified.

Beam-column joint jacketing

A joint may be defined as the part of the column that is located through the depth of the beams, and which intersect that column. This critical region should have enough confinement and shear capacity. However, due to lack of space in the joint region it is difficult enough to provide an adequate confinement. Alcocer (1992) has assessed experimentally the behaviour of several beam columns sub-assemblages, where the joint is confined with a steel cage as is shown in Figure 29.22. Test results have indicated that jacketing has been effective in rehabilitating the joint, with improving the strength, stiffness and energy dissipation characteristics of the existing joint. In these specimens, the dissipation of energy has been mainly concentrated at the beam's ends. It is also very important to point out the need to have a very strong column as compared to the beam to avoid driving of the column or joint into significant inelastic behaviour.

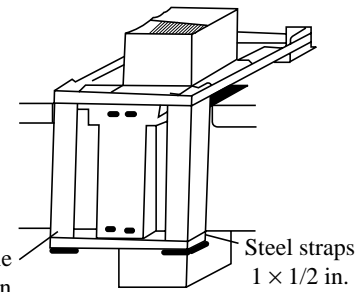


FIGURE 29.22 Steel cage assembled in the joint (Alcocer, 1992).

Slab column connection

The most critical type of structural damage is the slab column connection which results in the punching shear failure due to the transfer of unbalanced moments. The retrofitting of slab column connection is beneficial for the prevention of punching shear failures. A considerable amount of research carried out in this regard (Tuo and Durani, 1994; Farbey et al., 1993;

Martinez et al., 1994) has reported that adding concrete capitals or steel plates on both sides of slab can prevent punching shear failures (Bai, 2003).

Foundations

The repair and retrofitting of foundations is principally required due to two types of problems: (i) the change of loads on the foundation by strengthening the structure and (ii) the failure of foundation itself. In the first case, the most common practice has been the reinforced concrete jacketing of basement beams and the addition of new piles. Generally segmented concrete piles have been used for retrofitting (Iglesias, 1986).

29.6 COMPARATIVE ANALYSIS OF METHODS OF RETROFITTING

A large number of existing reinforced concrete buildings retrofitted by various seismic retrofitting schemes in Japan are shown in Figure 29.23. This data are collected by **Japan Concrete Institute** on practices of seismic retrofitting of 157 existing buildings constructed between 1933 and 1975 in Japan (Endo et al., 1984). More than one methods were adopted simultaneously in many cases. The most frequently used methods of retrofitting have been addition of shear walls in 82% cases, column jacketing used in 33% cases, while adding of steel bracing has been adopted only in 2% cases, mainly because of the difficulty of connecting the braces to the existing concrete frame. Repairing work with epoxy resin has been carried out in 20% cases.

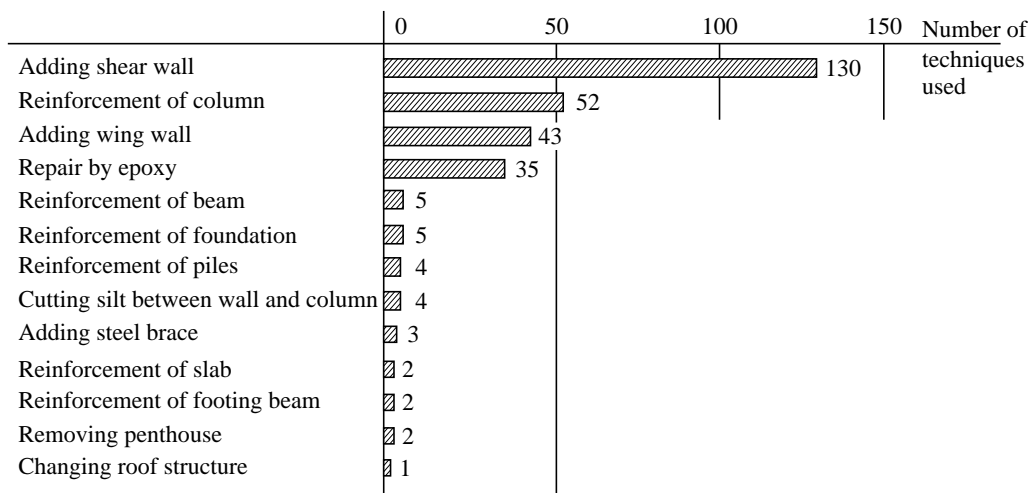


FIGURE 29.23 Repair and strengthening techniques used for 157 buildings in Japan (Endo et al., 1984).

Typical lateral load–displacement relationships of different strengthening techniques are presented in Figure 29.24. It may be observed that the strengthening techniques significantly increase the lateral strength and stiffness in comparison to unstrengthened frame, however it is

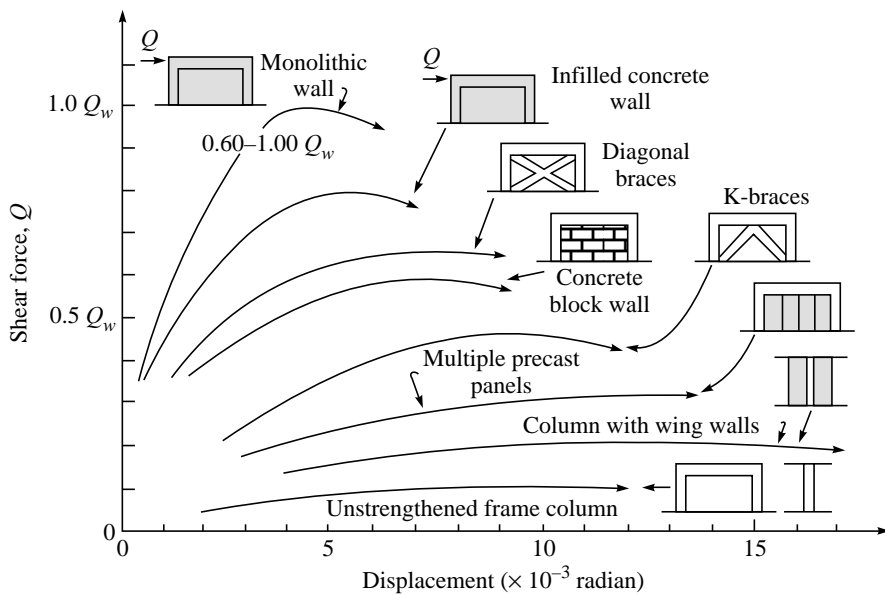


FIGURE 29.24 Typical load–displacement relationship for different strengthening techniques (Sugano, 1981).

only a qualitative indication. Table 29.6 presents a comparison of different aspects involved in retrofitting. It is based on the author's experimental study of one-bay, one-storey simple frame, which was strengthened by different techniques.

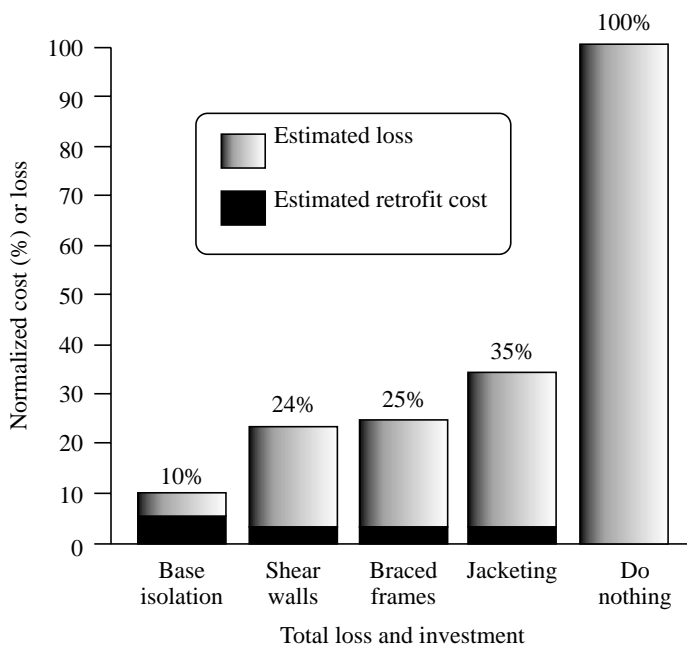
TABLE 29.6 Feasibility study of strengthened one-storey frame (Gates et al., 1992)

Strengthened schemes	Construction		Cost	Structural capacity		
	Workability	Weight		Stiffness	Strength	Ductility
Infilled concrete wall	Much work	Heavy (1.00)	Cheap (1.00)	High (1.00)	High (1.00)	Low (1.00)
Infilled concrete block wall	Easy work (1.00)	Heavy (1.00)	Slightly expensive (1.61)	Low (0.30)	Low (0.30)	Low (1.13)
Compression brace	Simple connection, easy work (0.39)	Light	Slightly expensive (1.47)	Low (0.27)	Low (0.63)	High (1.70)
Tension brace	Easy work but accuracy needed (0.44)	Light (2.93)	Expensive	Low (0.24)	Low (0.67)	High (1.70)

Table 29.7 illustrates the qualitative comparison of the four alternative retrofitting schemes: (a) base isolation plus exterior diagonal bracing; (b) conventional diagonal braced frames on the exterior; (c) exterior shear walls in the perimeter frame; and (d) jacketing of the non-ductile concrete beams and columns (Gates, Nester and Whitby, 1992). Figure 29.25 illustrates the quantifiable losses associated with earthquake under each of the retrofit solutions

TABLE 29.7 Comparison of alternative retrofit schemes (Gates et.al., 1992)

<i>Partial list of retrofit schemes</i>	<i>Base isolation</i>	<i>Braced frames</i>	<i>External shear walls</i>	<i>Jacketing</i>	<i>Do nothing</i>
<i>Seismic Risks @ MCE</i>					
Life safety-injury	Minor	Moderate	Moderate	Moderate	Extensive
Life loss	Not expected	Not expected	Not expected	Not expected	Some
Equipment damage	Minor	Moderate	Moderate	Moderate	Extensive
Business interruption	hours-days	weeks	weeks	weeks-months	months or relocation
<i>Construction</i>					
Business impact	Low	Medium	Medium	High	—
Architectural impact	Low-Moderate	Low-Moderate	High	Low	—
Schedule (Years)	3	1.75	2	1.5	—
Project cost (Ratios)	2.2	1.0	1.2	1.0	—
<i>Impact of Engineering Uncertainties</i>					
Ground motion	High	Medium	Medium	Low	—
Design and analysis	Low	Low	Low	Low	—
Constructibility	Medium	Low	Low	Medium	—
<i>History of Performance in Earthquakes</i>					
	Some	Moderate	Extensive	Some	Extensive

**FIGURE 29.25 Risk assessment summary in terms of quantifiable costs (Gates et al., 1992).**

as well as the do-nothing alternative. Superimposed on this figure is the estimated retrofitting cost for each scheme.

SUMMARY

Retrofitting of seismically-deficient buildings or earthquake-damaged building is one of the most challenging tasks, which structural engineers face in the aftermath of an earthquake. There are at present no guidelines or code of practice available in the country for seismic retrofitting. The chapter presents a state-of-the-art documentation on the methods available for seismic retrofitting and their pros and cons. The methods of retrofitting are divided into two categories, namely, structural retrofitting and member retrofitting. The methods for structural retrofitting are adding shear walls, adding steel bracing, adding infill walls, seismic base isolation and supplemental damping devices. The most common method of enhancing the individual member strength is jacketing. It includes the addition of concrete, steel, or fibre reinforced polymer (FRP) jackets for use in confining reinforced concrete columns, beams, joints and foundation. A comparative analysis has also been made for different methods of retrofitting depending on effectiveness and cost.

REFERENCES

- [1] Aboutaha, R.S., Engelhardt, M.D., Jirsa, J.O. and Kreger, M.E, "Retrofit of Concrete Column with Inadequate Lap Splices by the Use of Rectangular Steel Jackets", *Earthquake Spectra*, Volume 12, No. 4, November, 1996.
- [2] Alcocer, S.M., "Rehabilitation of RC Frame Connections Using Jacketing", *Tenth World Conference on Earthquake Engineering*, Madrid, Spain, 19–24 July, 1992.
- [3] Aschheim, M. "Seismic Vulnerability, Evaluation, Retrofit, and New Design of California Bridges—An Overview", D.P. Abrams and G.M. Calvi (Eds.), *US–Italian Workshop on Seismic Evaluation and Retrofit*, NCEER–97–0003, 1997.
- [4] Bai, J.W., "Seismic Retrofit for Reinforced Concrete Building Structures", *Consequences-Based Engineering (CBE) Institute Final Report*, Texas A&M University, Mid-America Earthquake Center (from Internet), 2003.
- [5] Buckle, I.G., "Passive Control of Structures for Seismic Loads", *Twelfth World Conference on Earthquake Engineering*, Paper No. 2825, 2000.
- [6] CEB, *Fastenings for Seismic Retrofitting—State-of-the Art-Report*, Thomas Telford, 1997.
- [7] Delfosse, G.C. and Delfosse, P.G., "Seismic Rehabilitation of a Shear Wall Building by means of Base Isolation", *Tenth World Conference on Earthquake Engineering*, Madrid, Spain, 19–24 July, 1992.
- [8] Edoardo, Cosenza and Gaetano, Manfredi, "Some Remarks on the Evaluation and Strengthening of Under-designed R.C. Frame Buildings", *U.S.–Italian Workshop on Seismic Evaluation and Retrofit*, D.P. Abrams and G.M. Calvi (Eds.), NCEER–97–0003, 1997.

- [9] El-Dakhakhni, W.W. Elgaaly, M., and Hamid, A.A., "Three-Strut Model for Concrete Masonry-Infilled Steel Frames", *Journal of Structural Engineering*, Vol. 129, No. 2, 2003.
- [10] Endo, T. et. al., "Practices of Seismic Retrofit of Existing Concrete Structures in Japan", *Eighth World Conference on Earthquake Engineering*, San Francisco, 1984.
- [11] Gates, W.E., Nester, M.R., and Whitby, T.R., "Managing Seismic Risk: A Case History of Seismic Retrofit for a Non-ductile Reinforced Concrete Frame High Rise Office Building", *Tenth World Conference on Earthquake Engineering*, Madrid, Spain, 19–24 July, 1992.
- [12] Iglesias, J., "Repairing and Strengthening of Reinforced Concrete Buildings Damaged in the 1985 Mexico City Earthquake", *The Mexico Earthquakes—1985—Factors Involved and Lessons Learned*, Michael A. Cassaro and Enrique Martinez Romero (Eds.), *Proceedings of the International Conference*, Mexico City, Mexico, ASCE Publication, September 19–21, 1986.
- [13] IS 13935, *Repair and Seismic Strengthening of Buildings—Guidelines*, Bureau of Indian Standards, New Delhi, 1993.
- [14] Jara, M., Hernandez, C., Garcia, R., and Robles, F., "The Mexico Earthquake of September 19, 1985—Typical cases of Repair and Strengthening of Concrete Buildings", *Earthquake Spectra*, Vol. 5, No. 1, 1989.
- [15] "Guideline for Seismic Evaluation of Existing Reinforced Concrete Buildings", (in Japanese), Japan Building Disaster Prevention Association (JBDPA), Akasaka, Tokyo, 1990.
- [16] Katsumata, H. and Kobatake, Y., "Seismic Retrofit with Carbon Fibres for Reinforced Concrete Columns", *Eleventh World Conference on Earthquake Engineering*, Paper No. 293, 1996.
- [17] Katsumata, H., Kobatake, Y. and Tanaka, T., "A Study on Strengthening with Carbon Fibre for Earthquake Resistant Capacity of Existing Reinforced Concrete Columns", *Ninth World Conference on Earthquake Engineering*, Vol. 7, pp. 517–522, 1988.
- [18] Kawamura, S., Sugisaki, R., Ogura, K., Maezawa, S., Tanaka, S., and Yajima, A., "Seismic Isolation Retrofit in Japan", *Twelfth World Conference on Earthquake Engineering*, Paper No. 2523, 2000.
- [19] Lynn, A.C., Moehle, J.P., Mahin, S.A., and Holmes, W.T., "Seismic Evaluation of Existing Reinforced Concrete Building Columns", *Earthquake Spectra*, Vol. 12, No. 4, 1996.
- [20] Nateghi, F. and Shahbazian, B., "Seismic Evaluation, Upgrading and Retrofitting of Structures: Recent Experiences in Iran", *Tenth World Conference on Earthquake Engineering*, Madrid, Spain, 19–24 July, 1992.
- [21] Newman, Alexander, *Structural Renovation of Buildings—Methods, Details, and Design Example*, McGraw-Hill, USA, 2001.
- [22] Otani, S. "Earthquake Resistant Design of Reinforced Concrete Buildings—Past and Future", *Journal of Advanced Concrete Technology*, Vol. 2, No. 1, 3–24, Japan Concrete Institute, 2004.
- [23] Rodriguez, M. and Park R., "Repair and Strengthening of Reinforced Concrete Buildings for Seismic Resistance", *Earthquake Spectra*, Vol. 7, No. 3, 1991.

- [24] Sugano, S., "Seismic Strengthening of Existing Reinforced Concrete Buildings in Japan", *Bulletin of the New Zealand National Society for Earthquake Engineering*, Vol. 14, No. 4, December, 1981.
- [25] Teran, A. and Ruiz, J., "Reinforced Concrete Jacketing of Existing Structures", *Tenth World Conference on Earthquake Engineering*, Madrid, Spain, 1992.
- [26] UNDP/UNIDO Project RER/79/015. "Repair and Strengthening of Reinforced Concrete, Stone and Brick Masonry Buildings", *Building Construction Under Seismic Conditions in the Balkan Regions*, Vol. 5, United Nations Industrial Development Programme, Austria, 1983.
- [27] UN Economic and Social Council, Committee on Housing, Building and Planning, "Redesign, Repair and Strengthening of Buildings in Seismic Regions", ECE/HBP/43, 1982.
- [28] Valluvan, R., Kreger, M.E., and Jirsa, J.O., "Strengthening of Column Splices for Seismic Retrofit of Non-ductile Reinforced Concrete Frames", *ACI Structural Journal*, Vol. 90, No. 4, July–Aug., 1993.
- [29] Valluvan, R., Kreger, M.E., and Jirsa, J.O., "Strengthening of Column Splices in Infilled Shear Wall", *Tenth World Conference on Earthquake Engineering*, Madrid, Spain, 19–24 July, 1992.
- [30] Wyllie, L.A. "Strengthening Strategies for Improved Seismic Performance", *Eleventh World Conference on Earthquake Engineering*, Paper No. 1424, 1996.

Chapter 30

Seismic Retrofitting of Reinforced Concrete Buildings—Case Studies

30.1 INTRODUCTION

This chapter deals with a few case studies in which the applications of the most common retrofitting schemes are employed to improve the efficiency and proficiency of either the seismically deficient vulnerable buildings or earthquake damaged buildings. In view of the mixed and complex seismic responses of retrofitted structures, heterogeneous nature of different constructions alongwith the strain dependent elastic properties of various materials hamper to bring a complete justification of the application of analytical studies. A sound qualitative basis of experimental studies or the experience of retrofitted structures during future earthquake will exactly judge and reveal the success of retrofitted structures. Since we have a considerable dearth of experience and experimental data on the behaviour and response of retrofitted structures, the case studies presented here are based on the experience obtained by the others. Incidentally, two major earthquakes of March 14 and September 19, 1979 hit a large number of reinforced concrete buildings in Mexico. Some of them were retrofitted whose efficacy came to be actually judged by the reoccurrence of an earthquake in the same region in 1985. Similar experience has been initially obtained from Turkey earthquake, 1988 in which a large number of buildings were damaged and retrofitted. This proved to be a good learning opportunity about the behaviour of the retrofitted structures. A few available case studies presented in this chapter serve as good instances for a better understanding of conventional retrofitted schemes. Some of the studies referred here are based on advance technological devices like base isolation and supplemental dampers. The information regarding suitability, effectiveness, test results of the analytical or experimental recommendations are based on the studies and experience obtained by individual authors as expressed in the published work.

30.2 METHODOLOGY FOR SEISMIC RETROFITTING OF RC BUILDINGS

A brief outline procedure followed for seismic assessment and retrofit works for a reinforced concrete building has been described here. This procedure has been adopted by the inspection team for retrofitting of reinforced concrete buildings in Turkey after the Adana–Ceyhan earthquake in Southern Turkey on June 27, 1998 (Sucuoglu, Gur and Gulkan, 2000). The survey team recommended 120 moderately damaged reinforced concrete residential apartment buildings in Ceyhan. The procedure of the method employed for 3–9-storey building stock may be followed as:

- Visit to the actual site with all documentation of buildings should be made and all structural dimensions and details should be verified. If necessary, reinforcement has to be checked on selected elements by rebar locator with some non-destructive testing (NDT) and by stripping concrete cover. Foundations should be inspected by excavating trenches at one or two exterior footings.
- An intense investigation has to be made regarding the existing concrete quality by taking 1–3 core specimens from each building and taking rebound hammer readings on a large number of structural elements calibrated with the core test results.
- Inspection of each structural and architectural element for damage should be done and the observed damage grade (none, light, moderate or heavy) on the structural and architectural plans should be accordingly marked.
- Three-dimensional linear elastic model of the existing building should be prepared and subjected to code specified vertical and lateral loads. The modulus of elasticity on concrete is to be reduced in accordance with material test results.
- The method for temporary shoring of damaged elements in buildings should be recommended. The damaged structures should be shored for vertical loads and braced for 25% of the estimated lateral loads and taking into account the live loads that will exist during construction. The most commonly used elements have been timber elements, steel elements, and tubular scaffolding (Iglesias, 1989).
- The buckling of longitudinal reinforcement, rupture of ties and crushing of concrete is often observed in columns of damaged building. In that case, the original geometry of columns is recovered by the use of hydraulic jacks.
- The seismic retrofit strategy for the building after considering all aspects should be recommended.
- The upgraded building is analyzed under code specified loading and its compliance with the code is verified.
- For selected buildings, capacity spectrum method is employed to assess the seismic performance of the retrofitted building.

30.3 CASE STUDY 1: SEISMIC RETROFITTING OF RC BUILDING WITH JACKETING AND SHEAR WALLS

Source

The Mexico Earthquake of September 19, 1985—Typical Cases of Repair and Strengthening of Concrete Buildings.

M. Jara, C. Hernandez, R. Garcia, and F. Robles
Earthquake Spectra, Vol. 5, No. 1, 1989

Typical Features of the Building

- Number of Stories—eight stories with basement
- Year of construction—1966
- Lateral load resisting system—reinforced concrete frames
- Floor system—two-way slab with beam
- Foundation—grid foundation with retaining walls around the perimeter
- Typical floor plan and elevation are shown in Figure 30.1.

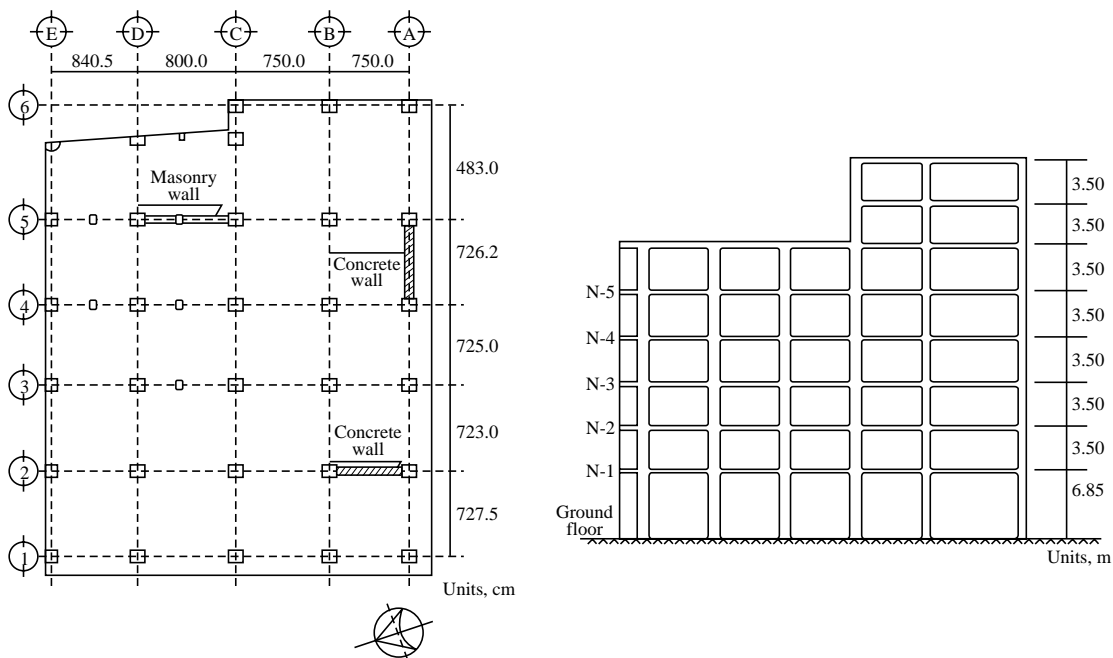


FIGURE 30.1 Plan and elevation of the building (Jara et al., 1983).

Features of Damages in Mexico Earthquake, 1979

- Minor cracks in beams and columns

Retrofitting Techniques Employed after Mexico Earthquake, 1979

- Addition of concrete shear wall in axis 2 and A
- Addition of masonry wall in axis 5

Behaviour of Retrofitted Building in Mexico Earthquake, 1985

- Severe damage such as spalling of the concrete cover and buckled bar at the interface of the walls and beam–column joints
- Main reinforcement in the columns located at the ground floor buckled and crushing of the concrete core occurred
- Most damaged columns were the columns adjacent to the added walls
- Damage attributed to the inadequate connection between the added walls and original frame connection and the poor quality of the concrete

Retrofitting Techniques Employed after Mexico Earthquake, 1985

- **Minor cracks**—Repaired by injecting epoxy resins
- **Buckled longitudinal reinforcement, broken ties, and crushed concrete**—Replacement of new reinforcement welded with the existing bars and new additionally closed ties were placed, concrete with low shrinkage properties were placed
- **Severely damaged columns adjacent to added walls**—Retrofitted with encasing in concrete with appropriate longitudinal and transverse reinforcement, existing surface should be chipped and cleaned of all loose materials. The surface was moistened before the new concrete was placed
- **Other columns**—Retrofitted with wire mesh and a cover of 50 mm of shotcrete
- **Damaged concrete wall added after 1979 earthquake**—Demolished and replaced with new concrete walls with 200 mm in thickness
- **Wall with slight damage**—repaired by injecting epoxy resins and by increasing their thickness to 200 mm
- **Added new walls** along the axis 2, 5, 6, E and A
- **Foundation**—The foundation grid was encased to permit the anchorage to the new longitudinal reinforcement. Additionally, the grid was connected to the retaining walls located around the perimeter to ensure monolithic behaviour.

Expected Performance

- Static and dynamic analysis was performed on the original undamaged building, match to the distribution of the damage observed accordingly

- Retrofitted building has been analyzed with the assumption of monolithic behaviour between old and new material
- Results indicate no additional piles to the foundation

30.4 CASE STUDY 2: SEISMIC RETROFITTING OF RC BUILDING WITH BRACING AND SHEAR WALL

Source

Seismic Retrofit of an RC Building: A Case Study

Enrique DEL VALLE CALDERON, Douglas A. FOUTCH, Keith D. HJELMSTAD, Eduardo FIGUEROA-GUTIERREZ and Arturo TENA-COLUNGA

Proceedings of Ninth World Conference on Earthquake Engineering, Tokyo-Kyoto, Japan (Vol. VII), 1988

Typical Features of the Building

- Number of stories—twelve, acting as Hotel building
- Year of construction—1927
- Lateral load resisting systems—non-ductile reinforced concrete frames
- Floor system—cast-in-place concrete joist beam construction with 2.5-inch concrete slab
- Foundation system—mat foundation (2.4 m thick) on concrete friction piles
- Typical floor plan and elevation shown in Figure 30.2

Features of Damages in Mexico Earthquake, 1979

- Extensive damage to first four stories in transverse direction
- The spandrel beams and columns in Frame 1 and 5 experienced diagonal cracking over much of their length in the first floor. In addition, the beam–column joints of these frames suffered severe cracking and spalling
- The medium column in the fourth storey of Frame 3 suffered cracking and crushing
- The foundation performed well

Retrofitting Techniques Employed

- **Cracked beams and columns**—Repaired with epoxy injection
- **The columns of Frames 1 and 5**—Encased in steel through the fourth storey level
- **Frame 1 and 5**—Braced steel frames were attached on the outside of the building in E–W direction

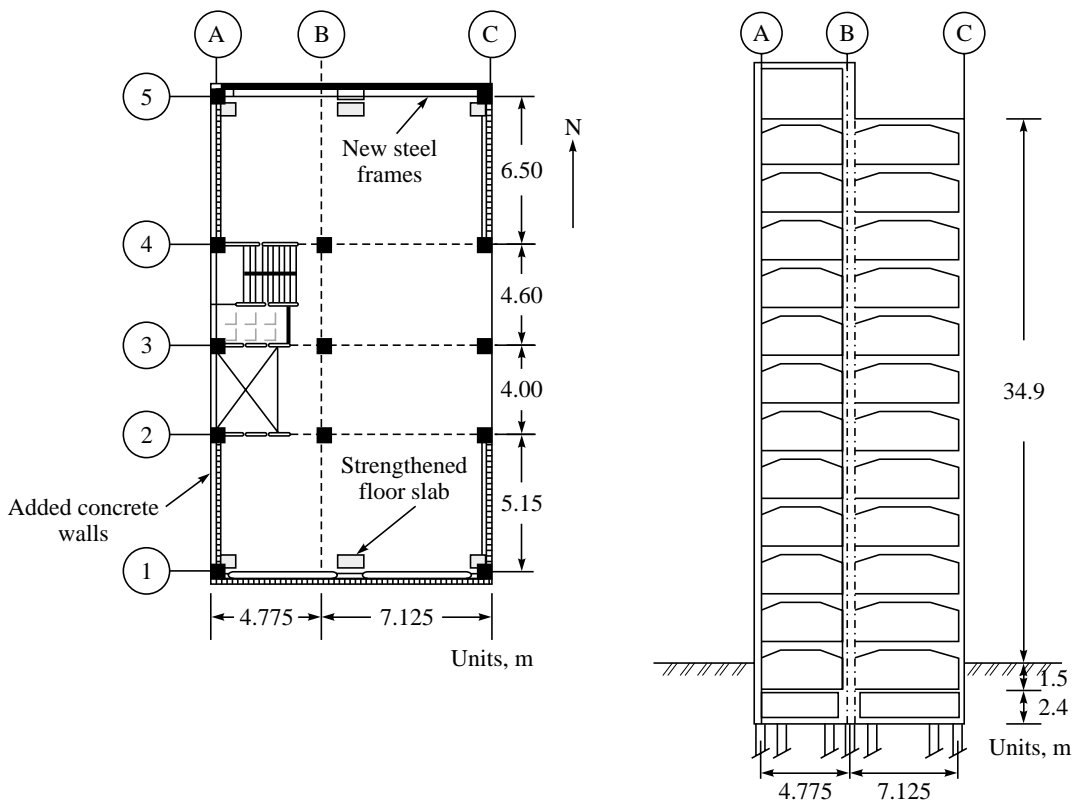


FIGURE 30.2 Plan and elevation of the building (Calderon et al., 1988).

The columns of the frames and diagonal bracing at the first level were fabricated steel boxes. The other bracing members were made from 2 channels placed toe-to-toe with gusset plate between them. New footing and piles were placed under the columns of the new frames and were attached to the original foundation to ensure monolithic action

- **Insertion of new infill reinforced concrete shear walls** in N–S direction.
The walls have been placed in the 1–2 and 4–5 bays of frames A and C for the full height of the building. Nails were inserted into the existing masonry walls

Expected Performance

- A three-dimensional response spectrum analysis has been conducted on the structure using the ground motion measured in Mexico City. Results indicate that the steel braced frames attached to the building strengthened it, and they stiffened the structure, moving its natural period away from the predominant ground period of 2.0 sec
- The retrofitted building performed well and suffered no damage during the Mexico earthquake 1985, even though it was located in the vicinity of several collapsed buildings and was located in the part of the city that experienced the strongest ground shaking

30.5 CASE STUDY 3: SEISMIC RETROFITTING OF RC BUILDING WITH STEEL BRACING

Source

Forced Vibration Studies of an RC Building Retrofit with Steel Bracing

Keith D. HJELMSTAD, Douglas A. FOUTCH, Enrique DEL VALLE, Ruth E. DOWNS

Proceedings of Ninth World Conference on Earthquake Engineering, Tokyo-Kyoto, Japan (Vol. VII), 1988

Typical Features of the Building

- Number of stories—12-storey reinforced concrete condominium apartment building
- Building details—plan size 10.8×17.45 m and height is 28.2 m above the foundation level, including penthouse
- Lateral load resisting systems—moment resisting RC frames
- Floor system—racticular waffle slab 5 cm thick with 35 cm deep ribs
- Foundation system—mat foundation (15 cm thick) underlain by deep, slender stiffening beams (140 cm \times 40 cm N-S and 140 cm \times 30 cm E-W) located along the column lines. The stiffening beams are supported on concrete friction piles
- Typical floor plan and elevation shown in Figure 30.3.

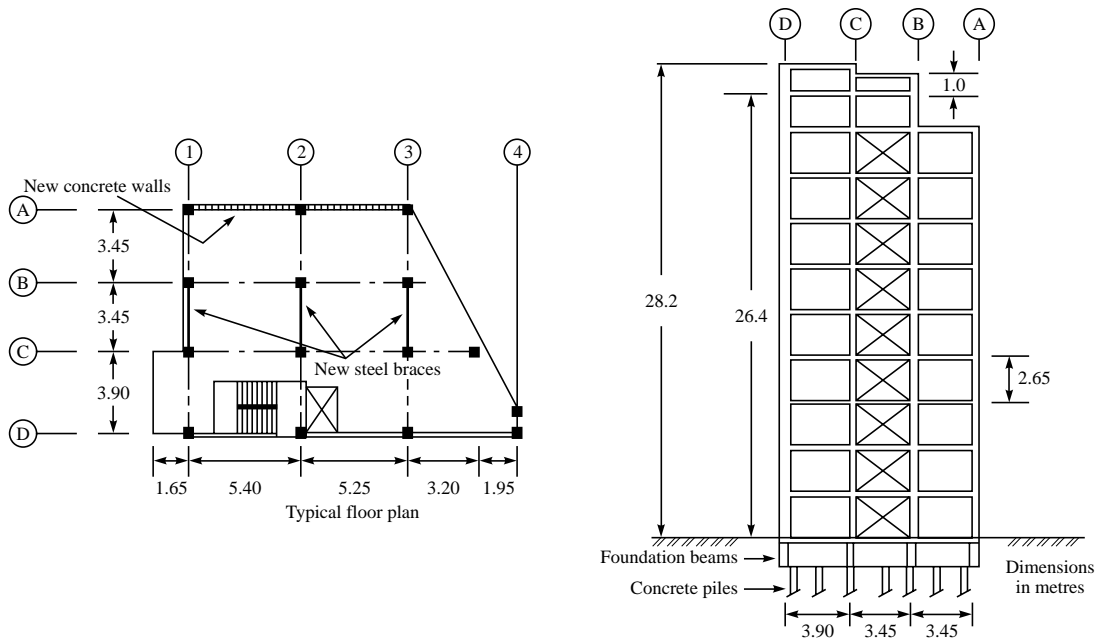


FIGURE 30.3 Plan and elevation of the building (Hjelmstad et al., 1988).

Features of Damages in Mexico Earthquake, 1979

- The building suffered extensive damage at the fourth storey columns due to pounding against an adjacent four-storey building located approximately 5 cm north of this building
- The building also experienced large inter-storey deformations of its frame; resulting in damage to the exterior walls (both longitudinal and transverse). In addition, the longitudinal and transverse partition walls were badly cracked at several levels
- No indications of the foundation failure were observed.

Retrofitting Techniques Employed

- **Diagonal steel bracing** was added to the central bay of frames 1, 2 and 3 in the transverse direction

The cross-braces were fabricated by continuously welding of two angles together toe-to-toe to form a structural box. The columns of the three braced bays were encased in a steel lattice composed of angles at the corners and diagonal flat plates. This encasement provided the additional strength necessary to carry the increased axial forces anticipated in the columns of the braced bays. These forces result from the additional overturning moment attracted to the braced bays. Special steel collars were fabricated and placed at the top and bottom of each column to facilitate the attachment of the steel cross-braces. These collars were grouted and bolted to both the original concrete columns and the adjoining slab to smooth out the transfer of forces between stories

- Insertion of new **reinforced concrete infill walls** of 4 cm thickness to all bays of the exterior longitudinal frames

The reinforcement ratio of these walls was about 0.64% in both horizontal and vertical directions. The steel braces and reinforced concrete walls increased the weight of the building approximately by 3%. No additional piles or other foundation modifications were required largely because the weight of the structure was essentially unchanged. Besides, failure of foundation was not observed following the 1979 earthquake.

Expected Performance

- The retrofitted building performed well and it suffered only minor structural damage during the 1985 Mexico earthquake, even though the intensity of shaking was much greater than in 1979
- Forced vibration studies of the building was carried out, the test result indicates that the steel-bracing scheme used to retrofit the building was an important factor in its better structural behaviour during the 1985 earthquake
- Free vibration test results show an increase in average stiffness in N-S direction by approximately 50%, which is also verified by the shape of the response spectrum. Lateral displacements were controlled and pounding against adjacent building was reduced.

30.6 CASE STUDY 4: SEISMIC RETROFITTING OF RC BUILDING BY JACKETING OF FRAMES

30.6.1 Source

The Mexico Earthquake of September 19, 1985—Typical Cases of Repairs and Strengthening of Concrete Buildings

M. Jara, C. Hernandez, R. Garcia, and F. Robles
Earthquake Spectra, Vol. 5, No. 1, 1989

Typical Features of the Building

- Number of stories—four stories with basement, ground floor and three upper floors act as a warehouse
- Typical features—corner building
- Year of construction—1959
- Lateral load resisting system—reinforced concrete frames
- Floor system—two-way slab with beam
- Foundation—mat foundation with retaining walls around the perimeter
- Typical floor plan and elevation as shown in Figure 30.4

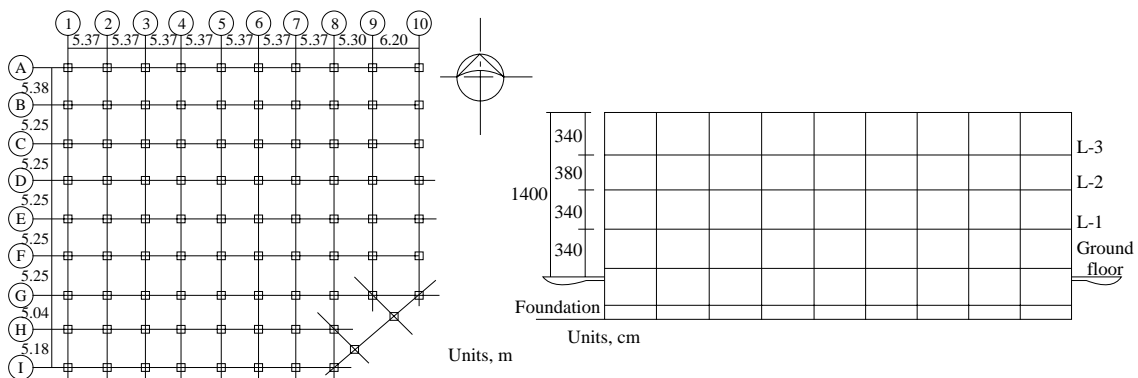


FIGURE 30.4 Plan and elevation of the building (Jara et al., 1989)

Features of Damages in Mexico Earthquake, 1985

- Severe damage at second floor level columns
- Damage consists of cracks more than 1 mm in width, loss of material and buckled bars
- The facade walls suffered extensive cracking
- Short column effect
- Excessive splicing of the longitudinal reinforcement at the same section

Retrofitting Techniques Employed

- **Concrete Jacketing**—Both beams and columns

Expected Performance

- Static analysis was performed taking into account the torsional effects
- Retrofitted building was analyzed with the assumption of monolithic behaviour between the old and the new material

30.7 CASE STUDY 5: SEISMIC RETROFITTING OF RC BUILDING WITH SHEAR WALLS AND JACKETING

Source

The Adana–Ceyhan Earthquake of June 27, 1998—Seismic Retrofit of 120 RC Buildings

Haluk SUCUOGLU, Turel GUR and Polat GULKAN

Twelfth World Conference on Earthquake Engineering, 2000

Typical Features of the Building

- Number of stories—Eight-storey reinforced concrete apartment building
- Building dimensions—floor area 245 m^2 and storey height is 3.0 m above the foundation level, including penthouse
- Design and construction—1984
- Lateral load resisting systems—moment resisting RC frames. A structural wall around the elevator
- Floor system—concrete slabs in the first six stories and joist slabs in the top two stories
- Foundation system—strip foundation in both the orthogonal directions

Features of Damages in Adana–Ceyhan (Turkey) Earthquake, 1998

- Building under moderate damage category
- Extensive damage was observed in beams especially between the first and fifth floors

Retrofitting Techniques Employed

- Infilling of appropriate frame bays by in-situ **reinforced concrete shear walls** with proper anchorage to the existing frame designed for these shear walls (Figure 30.5)
- Damaged columns or columns lacking required vertical load carrying capacity are **jacketed**. Where feasible, use of composite reinforced polymer fabric is recommended

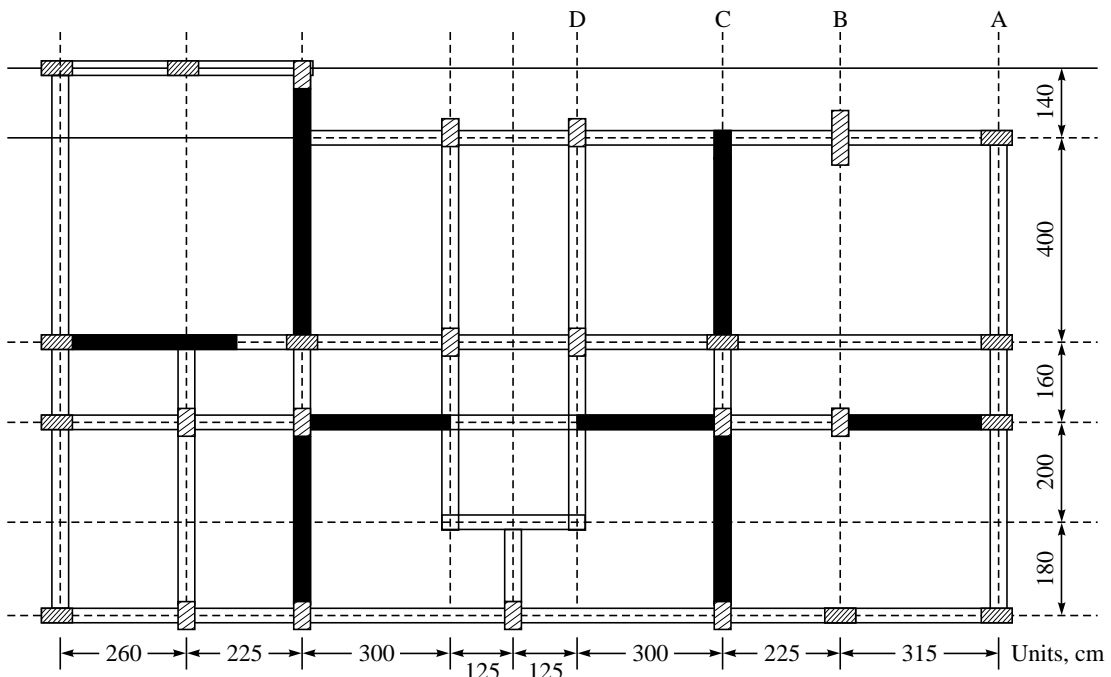


FIGURE 30.5 Strengthening schemes applied to the building (darker shading shows newly added RC walls) (Sucuoglu et al., 2000).

In the selection of seismic retrofit scheme, closing exterior window openings, intervention with the existing piping system and limiting architectural functions are avoided as much as possible

Expected Performance

- Free vibration test results indicate the lowest mode vibration periods of the original (as built) building are calculated as 0.85 s (torsion), 0.68 s (translation in the short direction) and 0.65 s (translation in long direction). In the damaged state, these periods become 1.09, 0.87 and 0.84 respectively. After adding the shear walls, periods are reduced to 0.65 s (torsion), 0.50 s (translation in the long direction) and 0.43 s (translation in short direction)
- Naturally, the reduction in natural vibration periods after seismic retrofit is due to increase in the stiffness of buildings. The study indicates that the mean increase in lateral stiffness for retrofitted building is roughly

$$\frac{k_r}{k_e} = \left[\frac{T_e}{T_r} \right]_{\text{mean}}^2 \times 1.1$$

where,

k_r = Stiffness after retrofitting

k_e = Stiffness before retrofitting

T_r = Time period after retrofitting

T_e = Time period before retrofitting

30.8 CASE STUDY 6: SEISMIC RETROFITTING OF RC BUILDING BY ADDING FRAMES

Source

The Mexico Earthquake of September 19, 1985—Typical Cases of Repair and Strengthening of Concrete Buildings

M. Jara, C. Hernandez, R. Garcia, and F. Robles
Earthquake Spectra, Vol. 5, No. 1, 1989

Typical Features of the Building

- Number of stories—eight stories consisting of ground floor with seven upper floors that act as a housing building
- Typical features—soft storey, mixed construction masonry with reinforced concrete
- Year of construction—1979
- Lateral load resisting systems—masonry bearing walls except at the ground floor. Columns are only at the ground floor
- Floor system—waffle slab at the first level and beam-block slab at the other levels
- Foundation system—grid and slab with friction piles located under each column
- Typical floor plan and elevation shown in Figure 30.6

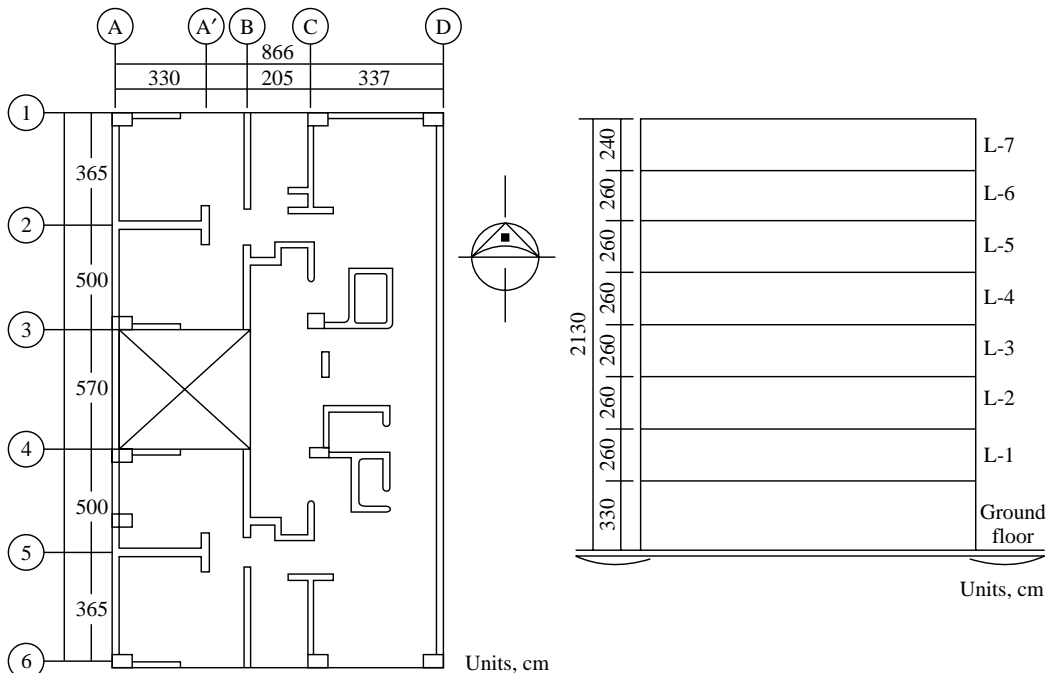


FIGURE 30.6 Plan and elevation of the building (Jara et al., 1989).

Features of Damages in Mexico Earthquake, 1985

- Severe damage occurred in masonry walls
- Foundation of the columns at the first level suffered no damage
- Principal failure direction was east–west due to irregularities in plan and insufficient area of walls in east–west direction

Retrofitting Techniques Employed

- Adding of **reinforced concrete frames** over the existing column in the ground floor along axis 1, 3, 4 and 6
- Adding **two concrete shear walls** from first level to the upper storey were placed in axis 3 and 4
- The existing masonry walls were retrofitted using **wire mesh** and 30 mm of mortar
- The cover of the existing columns was removed to permit the continuity of the new longitudinal reinforcement. The dimensions of the existing columns were increased
- The monolithic behaviour between the new frames and the floor system was provided by eliminating part of the floor system so that the new reinforcement of the frame was cast together with slab
- Foundation—The foundation grid was encased to permit the anchorage to the new longitudinal reinforcement

Expected Performance

- Four new concrete frames with concrete walls were analyzed by taking into account the torsional effects
- Retrofitted building was analyzed with the assumption of monolithic behaviour between old and new material
- The results indicate that the bearing capacity of the existing foundation was considered sufficient to resist the forces induced by the new structure

30.9 CASE STUDY 7: SEISMIC RETROFITTING OF RC BUILDING BY STEEL BRACING AND INFILL WALLS

Source

The Mexico Earthquake of September 19, 1985—Typical Cases of Repairs and Strengthening of Concrete Buildings

M. Jara, C. Hernandez, R. Garcia, and F. Robles
Earthquake Spectra, Vol. 5, No. 1, 1989

Typical Features of the Building

- Number of stories—six stories consisting of a basement, ground level with five upper floors that act as an office building
- Year of construction—1974
- Lateral load resisting systems—reinforced concrete frames
- Floor system—waffle slab
- Foundation system—mat foundation with retaining walls around the perimeter, friction piles were placed under the mat foundation
- Typical floor plan and elevation shown in Figure 30.7

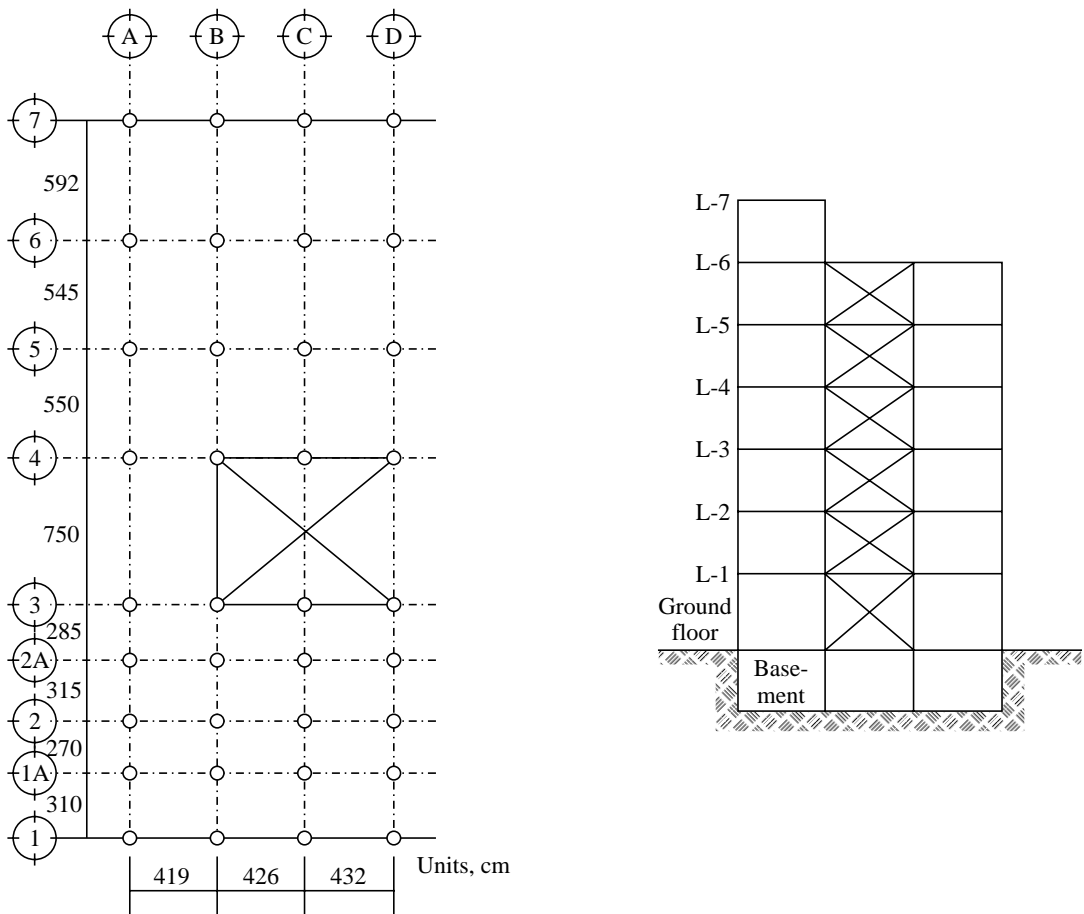


FIGURE 30.7 Plan and elevation with strengthening schemes of the building (Jara et al., 1989).

Features of Damages in Mexico Earthquake, 1985

- No significant damage during the earthquake. Only minor damage to non-structural walls
- Foundation performed well

Retrofitting Techniques Employed

- Although there is no significant damage but the owner of the building decided to retrofit it for future events and to eliminate the damage in nonstructural elements
- Steel bracing in transverse direction. Bracing consists of angle sections welded together forming a box section
- Infilled masonry walls were reinforced to stiffen the structure in the longitudinal direction. Wire mesh and shotcrete were used to strengthen the walls

Expected Performance

- Static analysis was performed to verify that the upgraded structure could resist the code loads
- The bracing frames were designed in such a way that they would carry all the lateral loads while the existing structure was considered to carry all the vertical loads

30.10 CASE STUDY 8: SEISMIC RETROFITTING OF RC BUILDING WITH SHEAR WALLS

Source

Effect of Shear Wall Location on Response of Retrofitted Multi-Storied Building

S.K. Thakkar, Pankaj Agarwal and Debasis Sinha

12th Symposium on Earthquake Engineering, IIT Roorkee, 2002

Typical Features of the Building

- Number of stories—fourteen stories (G + 13) in Zone IV
- Building details—five blocks, central block retrofitted,
- Lateral load resisting system—Ordinary Moment Reinforced Concrete Frames
- Floor system—RC beam slab construction, thickness of slab 20 cm
- Foundation system—Considered fixed at base above the raft foundation

Seismic Evaluation of Building

- Three-dimensional linear dynamic analysis of building indicates that the capacity demand (C/D) ratio of majority of the elements (beams and columns) are less than 1

Retrofitting Techniques Employed

- Addition of concrete shear wall
- Two alternative locations of shear walls considered
- Addition of shear wall in external frame and in internal frame as shown in Figure 30.8

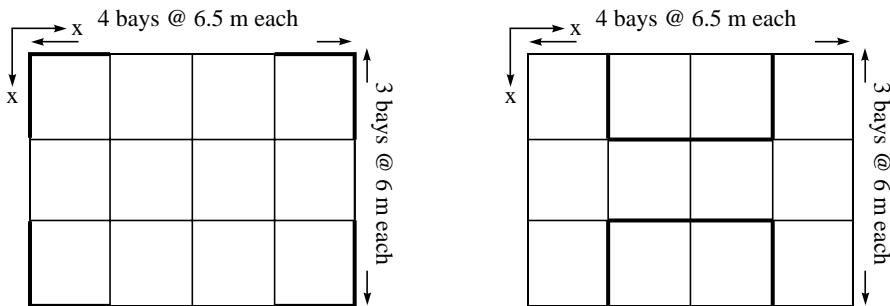


FIGURE 30.8 Two different retrofitting schemes by shear wall (Thakkar et al., 2002).

Expected Performance

- Provision of shear walls in external frames are more effective than the shear wall provided in internal frame however it is more effective for reducing base shear
- Storey drifts can be significantly decreased by addition of shear wall

30.11 CASE STUDY 9: SEISMIC RETROFITTING OF RC BUILDING BY SEISMIC BASE ISOLATION

Source

- Passive Control of Structures for Seismic Loads
Ian G. Buckle
12th World Conference on Earthquake Engineering, 2000
- Latest Advances in Seismic Isolation
William H. Robinson
Eleventh World Conference on Earthquake Engineering, 1996
- Retrofitting of Historical Building by Seismic Base Isolations
Sarvesh Kr. Jain and S.K. Thakkar
Workshop on Earthquake Disaster Preparedness, Roorkee, 1997

Typical Features of the Buildings

- Name of buildings—New Zealand Parliament House and Library, both are historical buildings
- Year of construction—1899 and 1922 respectively
- Lateral load resisting systems—seismically vulnerable un-reinforced masonry

Retrofitting Techniques Employed

- Seismic isolation chosen over conventional strengthening techniques to maintain the historic fabric of the building

- The isolation system comprises 145 lead-rubber bearings, 230 high-damping rubber bearings and 42 sliders
- Installation of the isolators required strengthening of basement walls and columns, and the provision of floor diaphragms
- The retrofit involves re-piling the building with lead rubber bearings and rubber bearing in the supports, as well as cutting a seismic gap in the 500 mm thick concrete wall
- Figure 30.9 shows the strengthening of foundation walls below NZ parliament House and location of isolators

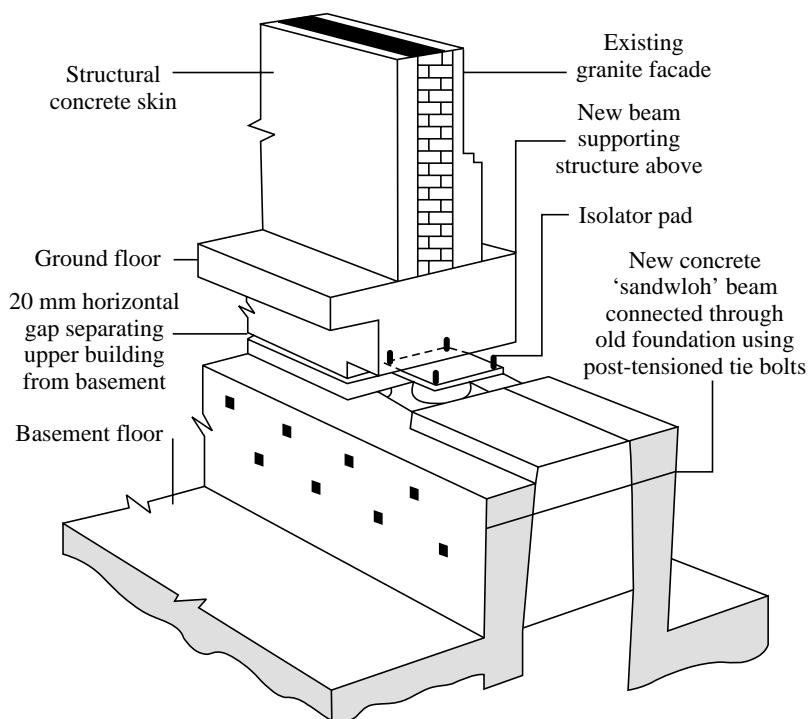


FIGURE 30.9 Strengthening of foundation walls below NZ Parliament House and location of isolators (Buckle, 2000).

Expected Performance

- The effect of the isolation is calculated as increasing the fundamental period from a value of 0.45 second to 2.5 seconds
- During an earthquake the building will be able to move in any direction on a horizontal plane up to the distance of 300 mm
- The total cost for the restoration and seismic retrofit of these two buildings was approximately US\$90 million

30.12 CASE STUDY 10: SEISMIC RETROFITTING OF RC BUILDING BY VISCOUS DAMPER

Source

Seismic Rehabilitation of a Non-Ductile Soft-Storey Concrete Structure Using Viscous Damper

H. Kit Miyamoto and Roger E. Scholl

Eleventh World Conference on Earthquake Engineering, 1996

Typical Features of the Building

- Number of stories—four-storey building consisting of ground floor with three upper floors
- Typical features—historical building, soft/weak storey structure in E–W direction, ground floor is used as commercial/retail space, and the 2nd floor and above is single occupancy apartments
- Year of construction—1927
- Lateral load resisting systems—no lateral resisting elements in North and South elevation of the building at the ground floor, except for 16" square light RC frame, Non-ductile soft/weak storey structure in the East–West direction, Non-ductile reinforced concrete frames at the first level, and conventional shear walls or braces at levels 2, 3, and 4
- Floor system—cast-in-place concrete joist beam construction with 2.5-inch concrete slab.

Features of Possible Damages

- Three-dimensional time history analysis of the original building was performed and the result indicates that the concrete columns at the ground floor level were overstressed in bending and shears due to excessive deflection and the lack of ductility detailing and strength. This type of adverse behaviour could cause total collapse of the superstructure
- At present, there is no significant damage in the structure.

Retrofitting Techniques Employed

Since the building is a National Registered building, only limited options for retrofitting were considered so that they should not affect the appearance of the landmark hotel, maximizing the retail/commercial area at the ground floor, avoiding disturbance to tenants living in apartment on the upper floors and of course should be cost effective. The finally selected retrofitting schemes are:

- **Steel moment frames with fluid viscous dampers (VDs)** at the ground floor. The steel moment frames were designed to provide stiffness, strength, and redundancy to the existing lightly reinforced concrete columns. VDs were provided to control drift at the first floor and to keep steel moment frames in the elastic range. VDs were attached to the top of the steel Chevron Braces and were strategically located to meet the above requirements

Expected Performance

- Dynamic analysis was performed on two different mathematical models of the retrofitted building. One was a simple two-dimensional stick model and the other was a complex three-dimensional finite element model. The analysis revealed that installing VDs and moment frames at the first level, reduces drift at all levels to the desired performance. In addition, using VDs is cost effective and also maintain the historical appearance and commercial utilization requirement of the building.

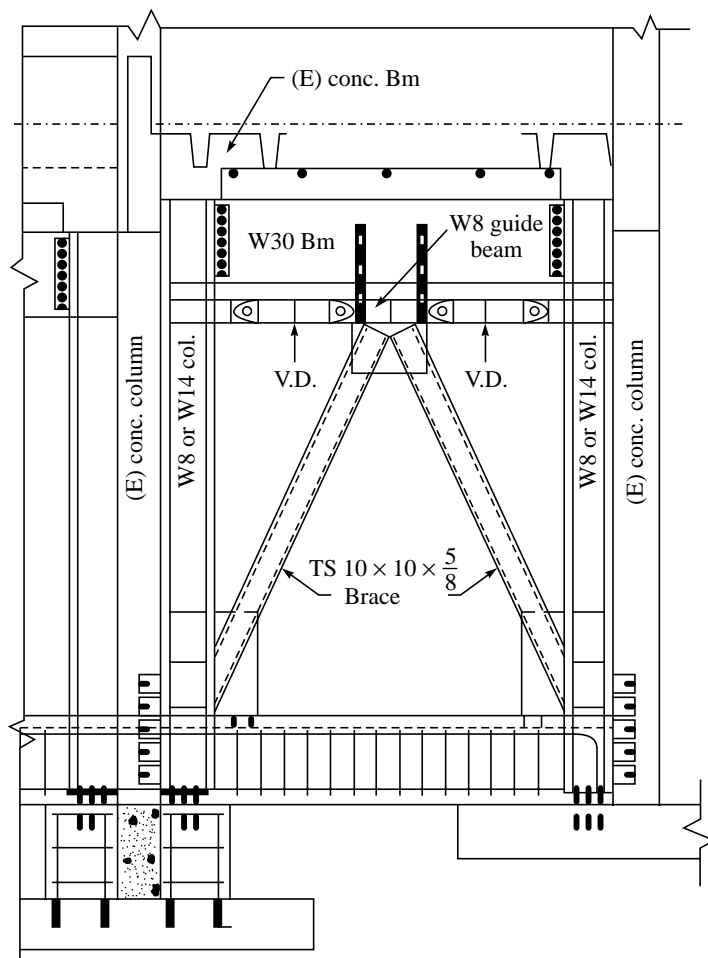


FIGURE 30.10 Typical visco damper assembly elevation (Miyamoto and Scholl, 1996).

SUMMARY

The chapter deals with the practical application of retrofitting techniques in reinforced concrete buildings in the form of case studies. Conventional and non-conventional schemes of retrofitting

are presented with their application, suitability and effectiveness. A few available case studies presented in this chapter serve as good instances for a better understanding of conventional retrofitted schemes such as addition of shear wall, bracing, infill wall, jacketing and a combination of them. Some of the studies referred here are based on advanced technological devices like base isolation and supplemental dampers. As there is a scarcity of data on the retrofitting of building in India, the case studies presented in this chapter are extracted from the available literature.

REFERENCES

- [1] Buckle, I.G., "Passive Control of Structures for Seismic Loads", *Twelfth World Conference on Earthquake Engineering*, Auckland, New Zealand, 2000.
- [2] Calderon, Valle, E.D. et al., "Seismic Retrofit of an RC Building: A Case Study", *Proceedings of Ninth World Conference on Earthquake Engineering*, Tokyo-Kyoto, Vol. VII, Japan, 1988.
- [3] Iglesias, J., "Repairing and Strengthening of Reinforced Concrete Buildings Damaged in the 1985 Mexico City Earthquake", *The Mexico Earthquakes 1985—Factors Involved and Lessons Learned*, Cassaro and Romero (Eds.). *Proceedings of the International Conference*, Mexico City, Mexico, September 19–21, ASCE Publication, 1986.
- [4] Jain, Sarvesh K. and Thakkar, S.K., "Retrofitting of Historical Building by Seismic Base Isolations", *Workshop on Earthquake Disaster Preparedness*, Roorkee, 1997.
- [5] Jara, M., et al., "The Mexico Earthquake of September 19, 1985—Typical Cases of Repair and Strengthening of Concrete Buildings", *Earthquake Spectra*, Vol. 5, No. 1, 1989.
- [6] Keith Hjelmstad D., et al., "Forced Vibration Studies of an RC Building Retrofit with Steel Bracing", *Proceedings of Ninth World Conference on Earthquake Engineering*, (Vol. VII), Tokyo-Kyoto, Japan 1988.
- [7] Miyamoto, H.K. and Scholl, R.E., "Seismic Rehabilitation of a Non-ductile Soft-storey Concrete Structure Using Viscous Damper", *Eleventh World Conference on Earthquake Engineering*, Acapulco, Mexico, 1996.
- [8] Robinson, W.H., "Latest Advances in Seismic Isolation", *Eleventh World Conference on Earthquake Engineering*, Acapulco, Mexico, 1996.
- [9] Sucuoglu, H., Gur, T. and Gulkan, P., "The ADANA-CEYHAN Earthquake of June 27, 1998: Seismic Retrofit of 120 RC Buildings", *Twelfth World Conference on Earthquake Engineering*, Auckland, New Zealand, 2000.
- [10] Thakkar, S.K., Agarwal, P., and Sinha, Debasis, "Effect of Shear Wall Location on Response of Retrofitted Multi-storied Building", *Twelfth Symposium on Earthquake Engineering*, IIT Roorkee, 2002.

Chapter 31

Seismic Provisions for Improving the Performance of Non-engineered Masonry Construction with Experimental Verifications

31.1 INTRODUCTION

Masonry is one of the most traditional, oldest materials and widely accepted medium for housing construction in India. This construction system is usually made spontaneously and informally with the help of local masons without any or only a little intervention by professional experts, therefore it is termed as **non-engineered construction**. Non-engineered construction in India is generally made with fieldstone, fired brick, concrete blocks, adobe or rammed earth, wood or a combination of locally available traditional materials. The long history of earthquakes and age-old tradition of construction should have lead to the reasoning, logic and assumption that sufficient precautionary measures are to be incorporated in these constructions to withstand the earthquake forces. But, on the contrary, this is not the case. Past experience has shown that collapse of non-engineered construction is the single largest factor contributing to the huge losses and casualties during earthquakes till now. Unfortunately, however, the subject of earthquake resistant construction of such buildings has not received the attention it deserves and the construction practices continue to ignore the warning issued by nature time and again. There may be two possibilities for this situation, either people are unaware and do not know about the earthquake resistant measure of masonry construction or they doubt the efficiency, proficiency and efficacy of these measures. The present chapter will deal with the earthquake resistant provisions in non-engineered construction in general and brick and stone masonry buildings in particular alongwith experimental verification to build confidence among the people.

31.2 CRITERIA FOR EARTHQUAKE RESISTANT PROVISIONS

The past earthquakes have revealed that masonry construction remains susceptible to earthquake forces because of (i) lack of integral action, (ii) lack of strong and ductile connections between walls, roof elements and foundation, (iii) inadequate strength for out-of-plane forces, (iv) low tensile and shear strength of mortar, (v) high in-plane stiffness of wall, (vi) low ductility and deformability capacity and (vii) heavy mass. In view of the continuous use of such buildings, it is felt necessary to increase the seismic resistance of masonry construction by providing some additional features known as **earthquake resistant (ER) measures**. The earthquake resistant measures intended to increase the seismic resistance in terms of strength and ductility. These earthquake resistant features alongwith the general guidelines are given in IS: 4326 and IS: 13928. Actually, the major features of these codes are extracted from the Monograph on "Basic Concepts of Seismic Codes" prepared by "*The International Association for Earthquake Engineering IAEE*" in 1980. IS 4326: 1993 deals with the selection of materials, special features of design and construction for earthquake resistant buildings including masonry construction using rectangular masonry units, timber construction and building with prefabricated flooring/ roofing elements. Guidelines for construction of earthquake resistant buildings using masonry of low strength particularly brick and stone masonry are covered in IS 13828: 1993 and for earthen buildings are covered in separate code in IS 13927: 1993. The basic aim for providing the earthquake resistant features as recommended in the codes is based on following concepts: (i) need of integral action, (ii) strong and ductile connections between walls, roof elements and foundation, (iii) improvement in strength for out-of-plane bending, (iv) strengthening of weaker sections by steel, timber or reinforced concrete, and (v) improving the strength of mortar, quality of construction and insertion of bonding elements. However, to develop a better understanding of the efficacy, reliability and acceptability of these measures, an experimental verification is necessary (Agarwal, 2002).

31.3 SALIENT FEATURES OF EARTHQUAKE RESISTANT PROVISIONS

The general features for improving the performance of non-engineered masonry construction recommended in IS 4326: 1993 and IS 13828: 1993 are summarized in Table 31.1.

31.4 SEISMIC STRENGTHENING FEATURES

The non-engineered building construction system should be strengthened by horizontal bands or bond beams at critical levels and vertical reinforcing bars at corners and junctions of walls. The bands form a horizontal framing system that transfer the horizontal shear induced by the earthquakes from the floors to structural walls. It also connects all the structural walls to improve the integral action. Depending upon its location in the building it may be termed as roof, lintel, sill, and plinth band. The reinforcing details of these bands are available elsewhere

TABLE 31.1 Salient features of earthquake resistant provisions recommended in IS 4326: 1993 and IS 13928: 1993

<i>Features</i>	<i>Earthquake Resistant Design and Construction of Buildings—Code of Practice (IS 4326: 1993)</i>	<i>Improving Earthquake Resistance of Low Strength Masonry Buildings—Guidelines (IS 13928: 1993)</i>
General principle	<ul style="list-style-type: none"> • Building should be light in weight, particularly roof and upper stories • Integrity and continuity in construction such that it forms a continuous load path between the foundation to all diaphragm levels, and tying all portions of building together • Projection/suspended ceiling should be avoided, otherwise reinforced and firmly attached with main structure • Building plan and elevation should be symmetrical with respect to mass and stiffness, otherwise use separation joints • Avoid close proximity (pounding), use separation • Use separated staircase, otherwise enclosed with rigid walls, if it is not possible use sliding joint • Sloping roof system should be adequately braced in both orthogonal direction (horizontal tie member and cross bracing) and should be adequately anchored into the RC band. • Foundation of building should be firm and uniform, otherwise separate the building in units. In case of loose soil, improve the soil condition 	<ul style="list-style-type: none"> • Building should be light in weight, particularly roof and upper stories • Integrity and continuity in construction such that it forms a continuous load path between the foundation to all diaphragm levels, and tying all portions of building together • Projection/suspended ceiling should be avoided, otherwise reinforced and firmly attached with main structure • Building plan and elevation should be symmetrical with respect to mass and stiffness, otherwise use separation joints • Use separated staircase, otherwise enclosed with rigid walls, if it is not possible use sliding joint • Sloping roof system should be adequately braced in both orthogonal direction (horizontal tie member and cross bracing) and should be adequately anchored into the RC band. • Gables ends of unreinforced masonry walls are anchored to all diaphragm levels • Foundation of building should be firm and uniform, otherwise separate the building in units. In case of loose soil, improve the soil condition

Contd.

TABLE 31.1 Contd.

<i>Features</i>	<i>Earthquake Resistant Design and Construction of Buildings—Code of Practice (IS 4326: 1993)</i>	<i>Improving Earthquake Resistance of Low Strength Masonry Buildings—Guidelines (IS 13928: 1993)</i>
Masonry unit	<ul style="list-style-type: none"> Well burnt bricks or solid concrete blocks having a crushing strength > 35 MPa Squared stone masonry, stone block masonry or hollow concrete block masonry, as specified in IS: 1597 (Part 2): 1992 of adequate strength Category A: M₂ (cement-sand 1:6) or M₃ (lime-cinder 1:3) or even richer M₂ (cement-lime-sand 1:2:9 or cement-sand 1:6) or richer H₂ (cement-sand 1:4) or M₁ (cement-lime-sand 1:1:6) or richer 	<p>Brick work in weak mortars</p> <ul style="list-style-type: none"> Fired bricks having a compressive strength > 3.5 MPa <p>Stone masonry</p> <ul style="list-style-type: none"> Stone masonry of random rubble or dressed stone type as IS 1597: 1967 <p>Brick work in weak mortars</p> <ul style="list-style-type: none"> Lime sand (1:3) or clay mud of good quality for brick work <p>Stone masonry</p> <ul style="list-style-type: none"> Cement sand (1:6), lime sand (1:3) or clay mud of good quality in stone masonry
Mortar	<ul style="list-style-type: none"> Category A: M₂ (cement-sand 1:6) or M₃ (lime-cinder 1:3) or even richer M₂ (cement-lime-sand 1:2:9 or cement-sand 1:6) or richer H₂ (cement-sand 1:4) or M₁ (cement-lime-sand 1:1:6) or richer 	<p>Brickwork in weak mortar</p> <ul style="list-style-type: none"> Minimum wall thickness—one brick (230 mm) in single storeyed, one brick in top storey and 1.5 bricks (350 mm) in bottom storey of up to three stories Storey height < 3.0 m, number of stories for category A, B, and C—3 stories, and category D—2 stories <p>Stone masonry</p> <ul style="list-style-type: none"> Wall thickness < 450 mm preferably 350 mm, height < 3.0 m, length < 5.0 m if exceed provide buttress, course height < 600 mm, inner and outer width should be interlocked with bond stone, maximum number of stories 2.
Wall dimension and number of stories	<ul style="list-style-type: none"> Not greater than 15 m subject to a maximum of four stories, with strengthening arrangements Straight and symmetrical in both the directions Checked in flexure as a plate or as vertical strip 	<i>Contd.</i>

TABLE 31.1 Contd.

<i>Features</i>	<i>Earthquake Resistant Design and Construction of Buildings—Code of Practice (IS 4326: 1993)</i>	<i>Improving Earthquake Resistance of Low Strength Masonry Buildings—Guidelines (IS 13928: 1993)</i>
Masonry bond	<ul style="list-style-type: none"> Usual bond but vertical joints should be broken properly from course to course Make a sloping joint by making the corner first to a height of 600 mm and then bulging the wall in between them A toothed joint perpendicular walls, alternatively in lifts of about 450 mm 	<p>Brickwork in weak mortar</p> <ul style="list-style-type: none"> Usual joints but vertical joints should be broken properly from course to course Make a sloping joint by making the corner first to a height of 600 mm and then bulging the wall in between them A toothed joint perpendicular walls, alternatively in lifts of about 450 mm <p>Stone masonry</p> <ul style="list-style-type: none"> Use bond or through stone of full-length (or a pair of about $\frac{3}{4}$ wall thickness) in every 600 mm lift but < 1.2 m horizontally. Other alternatives of bond stones are steel bars 8 to 10 mm diameter bent to S-shape or wood bars of 38 mm \times 38 mm or concrete bars of 50 mm \times 50 mm with an 8 mm diameter rod placed centrally. Door and window should be as small as possible and placed centrally as recommended Top level of openings should be the same, covered with lintel band If do not comply with code, strengthened by RC lining with 2 HYSD of 8φ Avoid arches over the opening otherwise use steel ties
Openings	<ul style="list-style-type: none"> Door and window should be as small as possible and placed centrally as recommended Top level of openings should be the same, covered with lintel band If do not comply with code, strengthened by RC lining with 2 HYSD of 8φ Avoid arches over the opening otherwise use steel ties 	<ul style="list-style-type: none"> Door and window should be as small as possible and placed centrally as recommended Top level of openings should be the same, covered with lintel band If do not comply with code, strengthened by RC lining with 2 HYSD of 8φ Avoid arches over the opening otherwise use steel ties

Contd.

TABLE 31.1 Contd.

<i>Features</i>	<i>Earthquake Resistant Design and Construction of Buildings—Code of Practice (IS 4326: 1993)</i>	<i>Improving Earthquake Resistance of Low Strength Masonry Buildings—Guidelines (IS 13928: 1993)</i>
Seismic strengthening arrangements	<ul style="list-style-type: none"> a. Masonry mortar b. Lintel band c. Roof band and gable band d. Vertical steel at corners and junctions of walls e. Vertical steel at jambs f. Bracing in plan at tie level of roof g. Plinth band h. Dowel bars <p>Category A (up to 3 stories) use only a</p> <p>Category A (up to 4 stories) use a, b, and c</p> <p>Category B (up to 3 stories) use a, b, f and g</p> <p>Category B (up to 4 stories) use a, b, c, d, f and g</p> <p>Category C (up to 2 stories) use a, b, c, f and g</p> <p>Category C (up to 4 stories) use a to g</p> <p>Category D (up to 2 stories) use a to g</p> <p>Category D (up to 4 stories) use a to h</p> <p>Category E (up to 3 stories) use a to h</p>	<p>Brickwork and stone masonry</p> <ul style="list-style-type: none"> b. Lintel band c. Roof band and gable band d. Vertical steel at corners and junctions of walls e. Bracing in plan at tie level of roof f. Plinth band <p>Category A (up to 2 stories) use c and f</p> <p>Category A (up to 3 stories) use b, c, f, g</p> <p>Category B (up to 2 stories) use b, c, f, g</p> <p>Category B (up to 3 stories) use b, c, d, f and g</p> <p>Category C (up to 1 stories) use b, c, f and g</p> <p>Category C (up to 3 stories) use b, c, d, f and g</p> <p>Category D (up to 2 stories) use b, c, d, f and g</p>

Note: The categories of construction are defined in Clause 7.1 of IS 4326: 1993 depending upon the design seismic coefficient (α_h) (Category: A ($0.04 < \alpha_h < 0.05$), B ($0.05 < \alpha_h < 0.06$), C ($0.06 < \alpha_h < 0.08$), D ($0.08 < \alpha_h < 0.12$) and E ($0.12 \leq \alpha_h$)).

(IS 4326, 13927, IAEE etc). In combination with vertical reinforcement, it improves the strength, ductility and energy dissipation capacity of masonry walls. Levels of strengthening arrangements may vary with the type of construction and seismic zones. The descriptions of each strengthening measure with its individual function are as follows:

Plinth band: This band is provided at the plinth level of walls on the top of the foundation, which is useful in sustaining differential settlements particularly when foundation soil is soft or has uneven properties.

Gable band: Gable band is provided at the top of gable masonry below the purlins. This band shall be made continuous with the roof band at the eave level. It restricts the out-of-plane failure of gable wall, which is susceptible to earthquake forces.

Roof band: Roof band is similar to lintel band but it is provided below the roof or floors. It improves the in-plane rigidity of horizontal floor diaphragms. Such band need not be provided in case of rigid diaphragm.

Lintel band: This band is provided at lintel level on all internal and external longitudinal as well as cross walls except partition walls. It provides integrity to the structure and resistance to out-of-plane wall bending. The lintel band if provided in partition walls will also enhance their stability. The purpose of lintel and roof band is to prevent the collapse of roof.

Sill band: This band is similar to lintel band but it is provided at sill level. This band reduces the effective height of masonry piers between openings. This is expected to reduce shear cracking in piers. It has not been recommended so far in codes.

Vertical steel: The vertical steel is provided at corners and junctions of walls and around jambs of doors and windows. The vertical steel in walls shall be embedded in plinth masonry of foundation, roof slab or band so as to develop its tensile strength in bond. It should pass through the lintel bands and floor slabs in all stories. It is either a steel bar of 10 mm to 12 mm diameter or a bamboo. For providing vertical steel in stone masonry a casing pipe is recommended around which masonry be built upto a height of 600 mm. The pipe is raised and the cavity is filled by 1:2:4 grade of concrete mix in case of steel bar.

31.5 EXPERIMENTAL VERIFICATION OF CODAL PROVISIONS

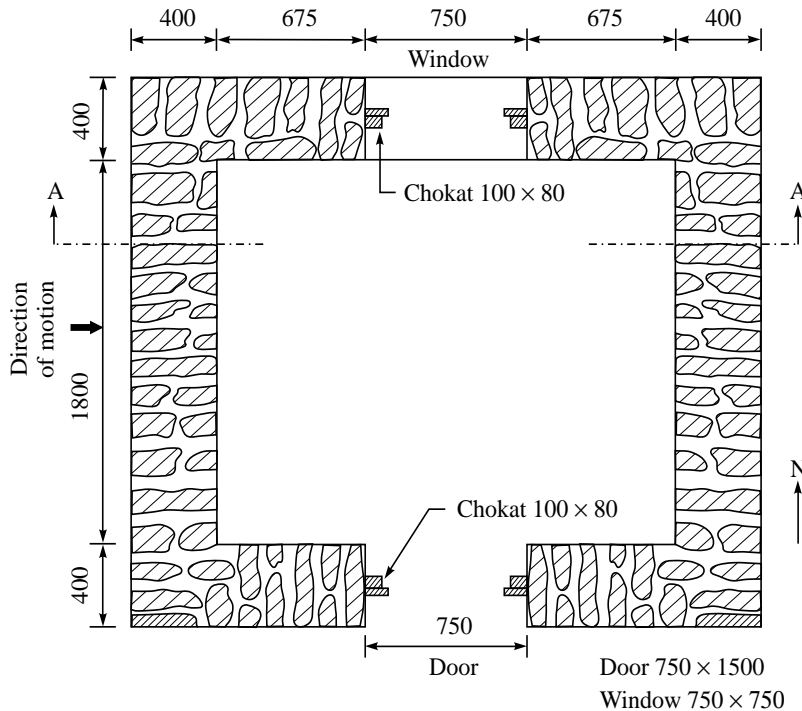
An experimental study is undertaken to carry out shock table testing of full-scale models of one storeyed stone masonry houses employing different earthquake resistant provisions under progressively increasing intensity of shock. Six stone masonry models in random rubble are tested on shock table to study the effectiveness of codal provisions for earthquake resistance measures. Out of them one model is built in a traditional way without any earthquake resistant measures while the other models with gradually increasing strengthening arrangements like roof, lintel, and sill bands alongwith corner reinforcement. The scheme of model testing is given in Table 31.2 and the details of model with strengthening features are described subsequently.

TABLE 31.2 Scheme of models testing for evaluation of earthquake resistant provisions

<i>Model no.</i>	<i>Earthquake resistant measures</i>	<i>Mortar</i>
1.	Unstrengthened (no strengthening measures)	Mud
2.	Wooden lintel and gable band	Mud
3.	Sill, lintel, gable band with corner strengthening	Mud
4.	Unstrengthened (no strengthening measures)	Cement sand (1:6)
5.	Lintel band	Cement sand (1:6)
6.	Lintel band with corner and Jamb steel	Cement sand (1:6)

31.5.1 Features of Model

The characteristics of real type of constructions as built in hilly and rural parts of India are incorporated in the construction of models. The model is single-storeyed one room of size $2.9\text{ m} \times 2.6\text{ m} \times 2.7\text{ m}$ having a thickness of walls of 40 cm constructed in random rubble stone masonry. The roof of the model is gable type. All the six models have identical layout and are connected with shear keys on shock table. The walls with windows and door openings are made in the direction of motion whereas walls without opening are orthogonal to the motion so that shock testing is performed in weaker directions. The openings in the walls are centrally located. The layout plan and elevation of the model is given in Figure 31.1(a) and 31.1(b).

**FIGURE 31.1(a) Layout plan of the model.**

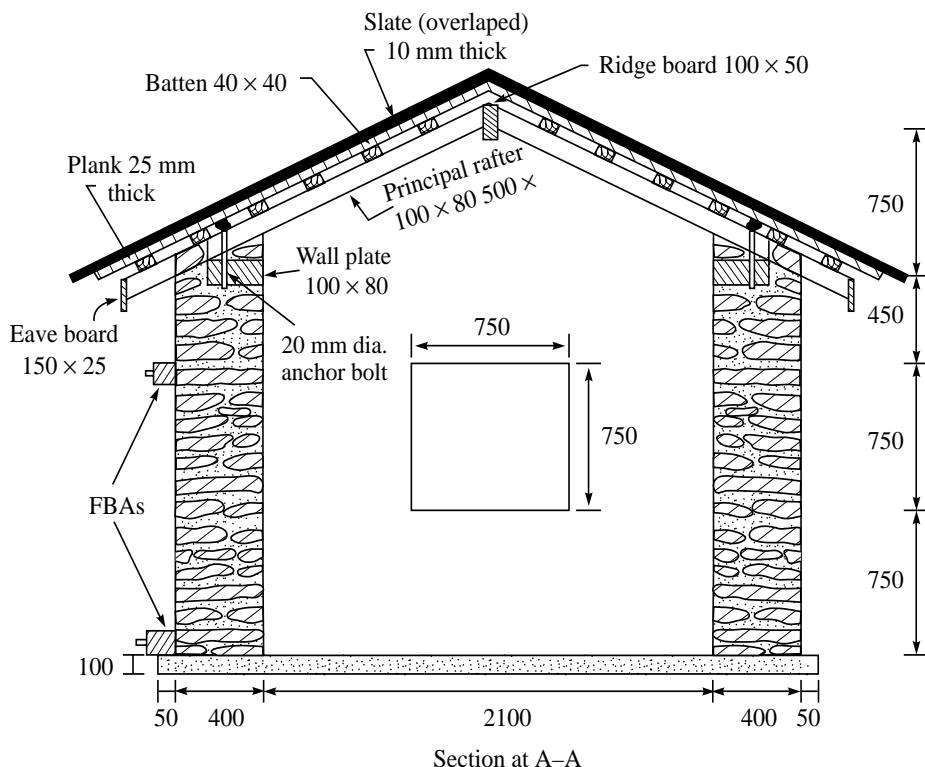


FIGURE 31.1(b) Sectional elevation of the model.

31.5.2 Seismic Strengthening Arrangements

The strengthening measures comprise horizontal bands or bond beams at critical levels and vertical reinforcing bars at corners and junctions of walls the model. Figure 31.2(a) shows the

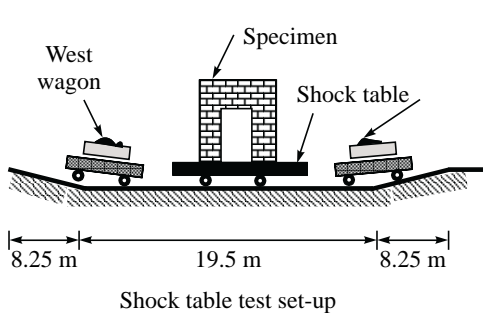


FIGURE 31.2 (a) Detail of horizontal band (main reinforcement: 2@12φ mm, transverse reinforcement: 6φ @ 150 mm) (b) Details of vertical and jamb steel (vertical reinforcement of diameter 12φ mm, casing pipe of diameter 50 mm).

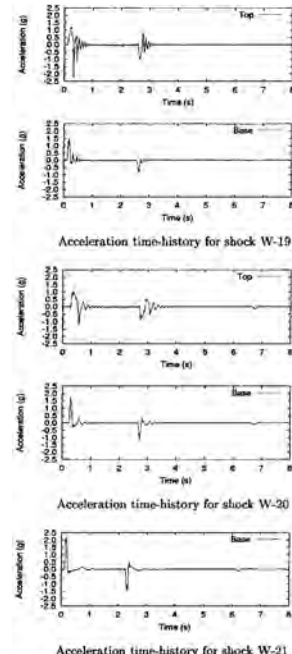
details of horizontal band at the level of roof, lintel and sill. Figure 31.2(b) demonstrates the details of providing the vertical reinforcement in stone masonry.

31.6 SHOCK TABLE TEST ON STRUCTURAL MODELS

Keightly (1977) developed **shock table** facility for conducting shock table tests on structural models at a considerably low cost. The facility consists of following components: (i) track or permanent way; (ii) shock table; (iii) dead load wagons or striking wagons; (iv) winch mechanism to pull wagons. The general arrangement of the shock table and its signature of shock are given in Figure 31.3a and 31.3b. The models constructed on the shock table are subjected to two to three shocks from one or from the opposite directions such as E-22, E-23, E-24, W-19, W-20 and W-21. The models may be tested upto the failure stage. The letters E and W designate impact from east and west direction respectively, the number designates wheel position of loading wagon. In each shock, the absolute peak accelerations at the top and bottom of the models as well as at the base of table are measured. The acceleration time histories are recorded by unidirectional **Force Balance Accelerometers (FBA-11)** mounted in the direction of loading. The peak acceleration data obtained during the shock test of models subjected to shock



(a)



(b)

**FIGURE 31.3 (a) Shock table facility (Railway wagon facility) in DEQ, IITR, Roorkee
(b) Signature of main and rebound shock in shock table test.**

table excitations for each phase of the testing is summarized in Table 31.3. The acceleration pattern along the height of the model generally shows that prior to cracking the acceleration at the top of the model is higher than that at the base but after cracking the acceleration at the top of model is smaller than that at the base of model. It is also observed that after cracking of the model the ratio of roof to base acceleration decreases in successive shocks for the same model. This indicates that the damaged lower portion of the model functions as a kind of base isolator that prevents transmission of energy into upper portion.

TABLE 31.3 Peak acceleration for different intensity of shocks

Model no.	Shock no.	Wheel position	Peak base accelerations
1	1	E-22	0.68 g
	2	E-23	1.00 g
2	1	E-22	0.70 g
	2	E-23	1.20 g
3	1	E-22	0.76 g
	2	E-23	1.30 g
	3	E-24	1.75 g
4	1	W-19	1.45 g
5	1	W-19	1.32 g
	2	W-20	1.60 g
6	1	W-19	1.47 g
	2	W-20	1.76 g
	3	W-21	2.31 g

31.6.1 Behaviour of Models in Shock Tests

The behaviour of each model with respect to pattern of cracking, identification of weak zones with the progressively increasing intensity of shocks is studied. The main observations regarding the seismic behaviour of the models are as follows:

Model 1: The model is subjected to two shocks E-22 and E-23. During the test run E-22, the diagonally oriented shear cracks develop in the shear walls in the direction of seismic motion. In the transverse walls, a continuous crack occurs around the roof level. In the second test run E-23, the model tends to fall apart. The stone begins to fall and wall is separated into several parts. The consequences of the lack of connection between the walls have become obvious. The failure mode of model 1 is that of complete collapse (Figures 31.4a and 31.4b).

Model 2: The model is subjected to two shocks E-22 and E-23. Integral behaviour of model is observed during the first test run at E-22. The extent of damage in the model is increased when the shock E-23 is applied. The mechanism of positive action of lintel band is clearly observed. The development of cracks above the lintel and the separation of walls are prevented. Also the shear and flexure cracks that develop in the model are not crossed through the lintel



(a)



(b)

FIGURE 31.4 (a) Model 1 (unstrengthened) under shock test (b) Complete collapse of model 1 at shock E-23.

band. The intensity of damage in model 2 is sharply reduced in comparison to model 1 at the same level of excitation. The failure mode of model 2 is that of partial collapse of longitudinal walls below lintel level (Figure 31.5a and 31.5b).



(a)



(b)

FIGURE 31.5 (a) Model 2 under shock test (b) Partial collapse below lintel band at shock E-23.

Model 3: The model is subjected to three shocks E-22, E-23 and E-24. In test run E-22 the model has behaved monolithically and has not exhibited any major crack. Diagonal cracks are propagated in the portion of the lintel and sill bands of shear wall during the test run E-23. The portion below the sill band manifests damage while the cross walls do not demonstrate any prominent crack. It was observed that cracking between lintel and sill level is significantly reduced with the provision of sill band. At the increased intensity of shock test run E-24, the extent of damage to the model is increased. Most of the cracks have developed below the sill level and minor damage has occurred between lintel and sill level. The vertical strengthening at corners has prevented the disintegration of the model and damage at the corners. The failure mode of model 3 is that of cracking below sill levels (Figure 31.6a and 31.6b).

Model 4: The model is subjected to one shock W-19. In spite of the use of cement sand mortar the model manifests poor performance. The separation of the orthogonal walls and the



FIGURE 31.6 (a) Model 3 under shock test (b) Cracking below sill level at E-24.

out-of-plane failure of the walls have been observed. The mere use of rich mortar without any other earthquake resistant feature is not adequate to prevent collapse of the structure. The failure mode of model 4 is also that of complete collapse (Figure 31.7a and 31.7b).



FIGURE 31.7 (a) Model 4 under shock test (b) Out-of-plane failure of Model 4.

Model 5: The model is subjected to two shocks W-19 and W-20. In test run W-19, the monolithic behaviour of the structure is observed. As a consequence of the second test run W-20 the model manifests considerable cracks. The upper north east corner of the northward shear wall is damaged severely and the joints split out. The eastward cross wall is quite damaged between the lintel and sill level while the westward cross wall shows minor cracks. The damage to the shear wall is limited upto the lintel level but the damage has occurred at the corners (Figure 31.8a and 31.8b).

Model 6: The model is tested for three shocks, W-19, W-20 and W-21. The model has shown integral behaviour during the first shock W-19. Not even a single crack is observed in the entire model. During shock 2 (W-20) the model manifests a few cracks. Under the third shock W-21



(a)



(b)

FIGURE 31.8 (a) Model 5 under shock test, strengthened with lintel band (b) Crack pattern of Model 5 at shock W-20, cracking below lintel level.

though the model has remained intact yet it is cracked considerably. The cracking is mainly concentrated between lintel and sill level (Figure 31.9a and 31.9b).



(a)



(b)

FIGURE 31.9 (a) Model 6 under shock test (b) Crack pattern of Model 6.

31.6.2 Recommendations

Some important recommendations have been arrived at from the study of shock response of stone masonry models which are highlighted below:

1. The provision of seismic band at lintel level is the minimum requirement to prevent collapse of house made in mud or cement sand mortar. The mere use of rich mortar without any other earthquake resistance measure is not adequate to prevent collapse of structures.
2. The codal provisions are effective in reducing the damage mainly above the lintel level. The brittle shear failure in wall piers still occurs. The cracking in piers can be reduced

by providing the additional horizontal band, preferably at sill level. The vertical reinforcement at the corner of model, in combination with horizontal bands increases the strength of model as well as reduces the cracking at corners.

SUMMARY

Masonry is widely used for housing construction in India and many countries of the world. The past earthquakes that have occurred in Indian subcontinent reveal that the root cause of devastation is the collapse of non-engineered masonry construction. Hence, it is necessary to increase the seismic resistance of non-engineered masonry construction by providing some additional features. The present chapter presents the summary of earthquake resistant features for improving the seismic performance of non-engineered masonry buildings. In order to develop a better understanding of the efficacy, reliability and acceptability of these measures, an experimental verification is also present. The experimental study is undertaken to carry out shock table testing of full-scale models of one storeyed stone masonry houses employing different strengthening measures under progressively increasing intensity of shock.

REFERENCES

- [1] Agarwal, P. and Thakkar, S.K., "Seismic Evaluation of Strengthening and Retrofitting Measures in Stone Masonry Houses under Shock Loading", *Workshop on Retrofitting of Structures*, IIT Roorkee, Oct. 2003.
- [2] Agarwal, P. and Thakkar, S.K., "An Experimental Study of Effectiveness of Seismic Strengthening and Retrofitting Measures in Stone Masonry Buildings", *Journal of European Earthquake Engineering*, pp. 48–64, 2002.
- [3] Agarwal, P. and Thakkar, S.K., "Study of Adequacy of Earthquake Resistance and Retrofitting Measures of Stone Masonry Buildings", *Research Highlights in Earth Systems Science*, DST Special, Vol. 2, on 'Seismicity' pp. 327–335, O.P. Verma (Ed.), Indian Geological Congress, August 2001.
- [4] Agarwal, P. and Thakkar, S.K., "Seismic Evaluation of Strengthening Measures in Stone Masonry Houses", *Eleventh Symposium on Earthquake Engineering*, University of Roorkee, Roorkee, December 17–19, 1998.
- [5] IS 13828, *Improving Earthquake Resistance of Low Strength Masonry Buildings—Guidelines*, Bureau of Indian Standards, New Delhi, 1993.
- [6] IS 4326, *Earthquake Resistant Design and Construction of Buildings—Code of Practice*, Bureau of Indian Standards, New Delhi, 1993.
- [7] IAEE, "Basic Concepts of Seismic Codes—Vol. I", *The International Association for Earthquake Engineering*, Tokyo, Japan, 1980.
- [8] Keightley, W.O., *Report on Indo-US Subcommission on Education and Culture*, Department of Earthquake Engineering, University of Roorkee, Roorkee, 1977.
- [9] Thakkar, S.K. and Agarwal, P., "Seismic Evaluation of Earthquake Resistant and Retrofitting Measures of Stone Masonry Houses", Paper No. 110, *12th WCEE*, February 2000, Auckland, New Zealand, 1999.

Chapter 32

Retrofitting of Masonry Buildings

32.1 INTRODUCTION

Masonry buildings are the most common type of construction used for housing purpose all around the world. In India masonry construction is employed in the rural, urban and hilly regions upto its optimum, since it is flexible enough to accommodate itself according to the prevailing environmental conditions. That is why more than 90% population of the country prefers to live in such houses. Although this type of construction is most oftenly preferred and most frequently employed yet it is not completely perfect with regard to seismic efficiency. It has likewise some flaws. The recent earthquakes in India reveal that its low seismic resistance has proved to be one of the principal causes of extensive damage, as compared to other modes of construction like reinforced concrete and steel. In addition improper seismic design of masonry building emerges as a sister cause of such devastation. It is evidently clear that a proper adherence to recommended earthquake resistant measures as per IS code may avoid such a heavy loss of life and property. But the already constructed, in use buildings facing the threat of further damage in future seismic activity turn out to be a challenge to earthquake engineering community which is making ceaseless perennial efforts in finding out ways to minimize the damage. In this regard retrofitting of existing buildings may emerge as a probable possibility which implies incorporation of earthquake resistant measure in either seismically deficient or earthquake damaged parent constructions. This is a difficult but essential task because firstly there is a majority of seismically deficient buildings and secondly due to economic considerations and immediate shelter requirements earthquake damaged buildings cannot be replaced or rebuilt in the event of an earthquake. Hence it is the need of the hour to retrofit well in time the seismically deficient or seismically damaged buildings as per current codes so that they may be safely reused in future.

The past experience of retrofitted buildings has not been very convincing and promising. But the recent studies show that proper retrofitting may very well upgrade the seismic resistance bringing it at par with the newly constructed earthquake resistant design construction. Innumerable conventional and non-conventional techniques have been applied and employed for retrofitting

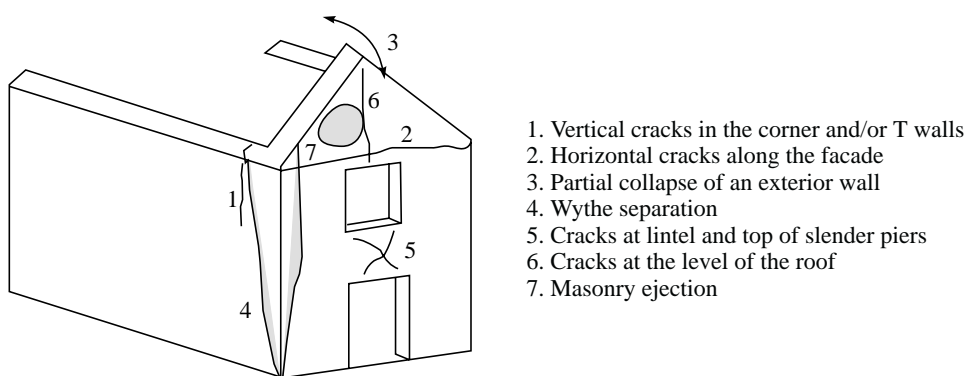
of existing masonry buildings along with their advantages and disadvantages. Such retrofitting schemes depend upon the number of factors such as material of parent construction, type of masonry, location and amount of damage etc. Some of the methods have already been recommended in the IS 13935: 1993 and IAEE guidelines. The present chapter focuses on the conventional methods of retrofitting schemes with special reference to brick and stone masonry construction along with their proper use and limitations.

32.2 FAILURE MODE OF MASONRY BUILDINGS

An appropriate selection of suitable retrofitting schemes depends entirely upon the failure mode of individual masonry construction. There are innumerable modes of failure of walls as observed by the reconnaissance team and documented in various published papers and reports. Although the type of construction, site of construction, structural typology of masonry buildings varies in different regions but the damage caused by seismic activity may be identified uniformly. The two most common modes of masonry failure may be called **out-of-plane failure** and **in-plane failure**. The structural walls perpendicular to seismic motion are subjected to out-of-plane bending results in out-of-plane failure featuring vertical cracks at the corners and in the middle of the walls. The structural walls parallel to seismic motion are subjected to in-plane forces *i.e.* bending and shear causes horizontal and diagonal cracks in the wall respectively. The other types of masonry failure are diaphragm failure, pounding, connection failure and failure of non-structural components. A brief discussion of each mode of masonry failure is described as under.

32.2.1 Out-of-plane Failure

Inadequate anchorage of the wall into the roof diaphragm and limited tensile strength of masonry and mortar unitedly causes out-of-plane failure of wall in un-reinforced masonry buildings, which are the most vulnerable. The resulting flexural stress apparently exceeds the tensile strength of masonry leading to rupture followed by collapse. Moreover long span diaphragms causes excessive horizontal flexure. Out-of-plane wall movement has been characterized as shown in Figure 32.1.



1. Vertical cracks in the corner and/or T walls
2. Horizontal cracks along the facade
3. Partial collapse of an exterior wall
4. Wythe separation
5. Cracks at lintel and top of slender piers
6. Cracks at the level of the roof
7. Masonry ejection

FIGURE 32.1 Out-of-plane failure characterization (Zuccaro and Papa, 1999).

32.2.2 In-plane Failure

In-plane failures of walls in un-reinforced masonry structures due to excessive bending or shear are most common as is evident from double diagonal (X) shear cracking. This cracking pattern frequently found in cyclic loading indicates that the planes of principal tensile stress in the walls remain incapable of withstanding repeated load reversals leading to total collapse. As the ground motion takes place for a short duration the walls are subjected to only one or two significant loading reversals and do not collapse totally. Fortunately by the time the shear cracks become unduly severe, the gravity load carrying capacity of the wall is not jeopardized. Diagonal tension i.e. "X" cracks occurs mainly in short piers, rocking (top and bottom) in slender piers. These cracks happen to be worse at lower storey. In-plane failures are characterized as in Figure 32.2.

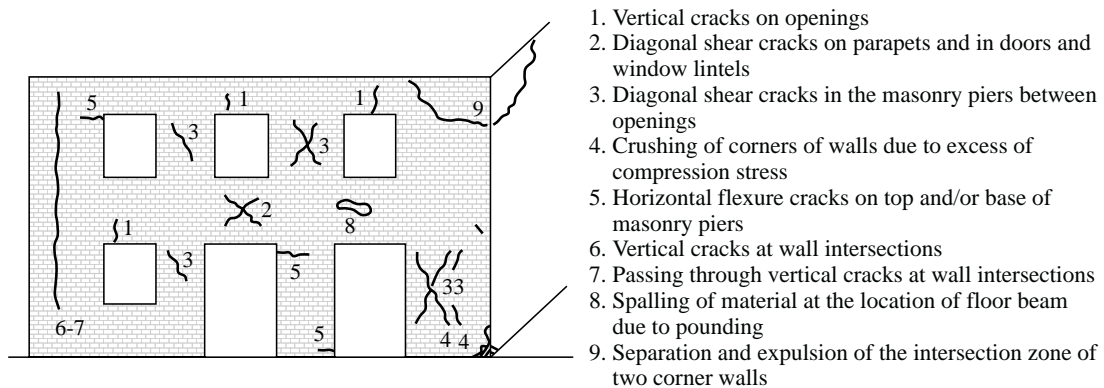


FIGURE 32.2 In-plane failure characterization (Pasquale and Orsmi, 1999).

32.2.3 Diaphragm Failure

The failure of the diaphragm is a rare phenomenon in the event of seismic motion. Damage to the diaphragm never impairs its gravity load carrying capacity. Lack of tension anchoring produces a non-bending cantilever action at the base of the wall resulting from the push of diaphragm against the wall. The in-plane rotation of the diaphragms ends and the absence of a good shear transfer between diaphragms and reaction walls account for damage at the corners of the wall. Figure 32.3 illustrates a wall failure resulting from excessive diaphragm flexibility. This problem remains non-existent in strengthened buildings and is very rare in anchored buildings. In strengthened buildings, separation remains worse at or near the centreline of the diaphragm.

32.2.4 Failure of Connection

Seismic inertial forces that originate in all elements of the building are delivered to horizontal diaphragms through structural connections. The diaphragms distribute these forces among vertical elements, which in turn transfer the forces to the foundation. Hence, an adequate connection capable to transfer the in-plane shear stress from the diaphragms to the vertical elements and to provide support to out-of-plane forces on these elements is essential between

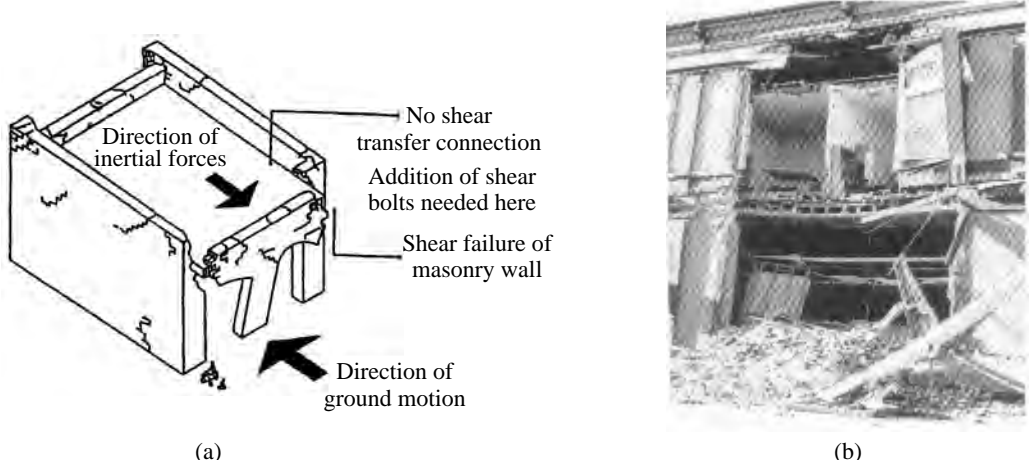


FIGURE 32.3 Failure of diaphragms (a) Shear failure, FEMA 306, 1999 (b) Failure resulting from diaphragm flexibility in Loma Prieta earthquake, 1989.

the diaphragms and the vertical elements. This type of failure is characterized by diagonal cracks disposed on both the walls' edges causing separation and collapse of corner zones (Figure 32.4). This phenomenon magnifies due to inadequately strengthened openings near the walls' edges and by floors insufficiently connected to the external walls.

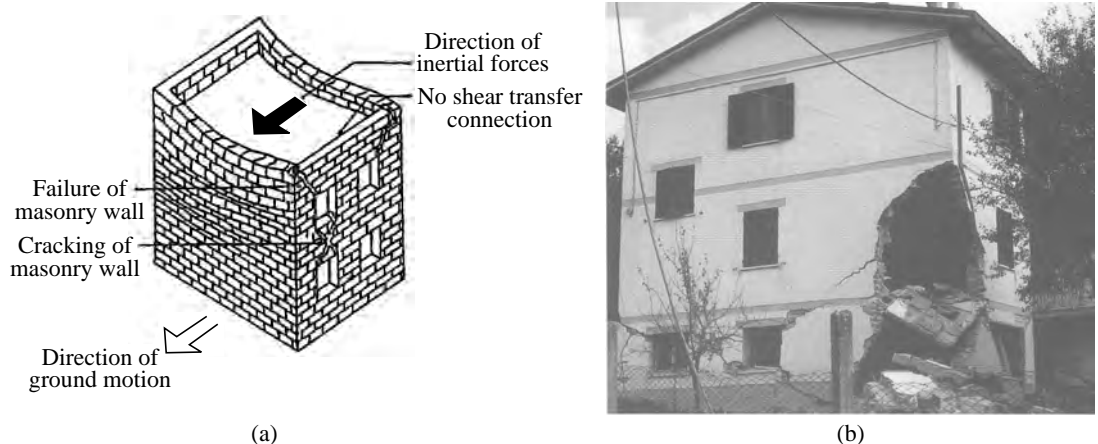
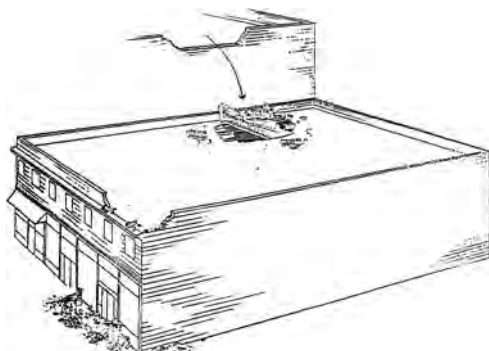


FIGURE 32.4 Failure of connection of walls (a) Characterization of failure, FEMA 306, 1999 (b) Collapse of corner zone (Dolce, Masi and Goretti, 1999).

32.2.5 Non-structural Components

The non-structural components in masonry buildings are parapet walls, partition walls, mummy, water tanks, canopies, projections, staircase etc. These non-structural elements behave like cantilevers if they remain unrestrained and are subjected to greater amplification as compared to ground motion becoming prone to failures (Figure 32.5).



(a)

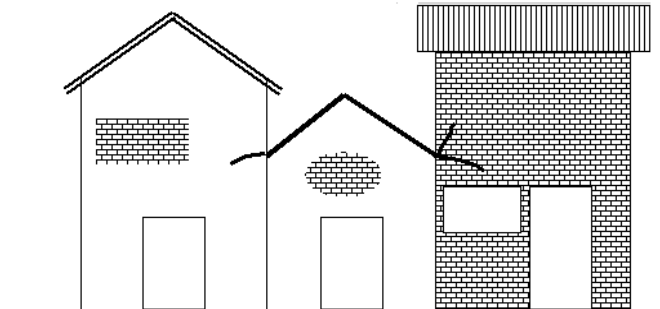


(b)

FIGURE 32.5 Failure of non-structural components (a) Parapet failure, FEMA 306, 1999 (b) Out-of-plane failure of a parapet, EERI, 1996.

32.2.6 Pounding

When adjacent roof levels of two buildings and vertical brick work faces flush with one another, the pounding action causes structural distress due to out-of-plane vibrations. Such a failure is characterized as shown in Figure 32.6.



- Vertical cracks in the adjacent walls
- Diagonal cracks due to different levels in the structures

(a)



(b)

FIGURE 32.6 Pounding failure (a) Characterization of failure (b) Minor pounding damage between buildings of different heights, EERI, 1993.

32.3 METHODS FOR RETROFITTING OF MASONRY BUILDINGS

The choice of a suitable method of retrofitting basically depends upon the structural scheme and the employed building material in the parent construction alongwith a feasible and economical

technology. Moreover an understanding of failure mode, structural behaviour with the weak and strong aspects of design as derived from the earthquake damage surveys also influence the selection of retrofitting schemes. Numerous techniques, used to retrofit seismically deficient or damaged masonry buildings, may be broadly classified into three categories on the basis of their effect on structural performance namely, (i) improving the existing masonry strength and deformability, not related to any specific objective which is similar to the repairing process of masonry structures; (ii) improving the in-plane strength of the wall or any weak zone of the section akin to local/member retrofitting and (iii) improving the structural integrity of the whole structure in terms of in-plane and out-of-plane strength or only against out-of-plane forces very much like the global/structural retrofitting. Various techniques under each scheme are described as:

32.3.1 Repair

It is a process to preserve the mechanical efficiency of a masonry structure and to increase shear resistance of walls having large internal voids. The commonly employed repairing techniques of masonry are (i) cement or epoxy injection (ii) reinforced injection (iii) grouting with cement or epoxy (iv) insertion of stones (v) re-pointing of mortar.

32.3.2 Local/Member Retrofitting

It enhances the shear resistance of un-reinforced masonry components especially against in-plane forces. Feasible retrofitting techniques are: (i) surface coatings (ii) shotcrete overlays or adhered fabric with wire mesh or FRP materials (iii) use of RC and steel frames in openings.

32.3.3 Structural/Global Retrofitting

Improving the response of existing un-reinforced masonry buildings to both gravity and seismic loads it provides them “box type” behaviour and increases the flexural strength of un-reinforced walls and piers. The most common techniques are (i) addition of reinforcement (ii) external binding or jacketing (iii) prestressing, (iv) confinements with RC element and steel sections (v) strengthening of wall intersections and (vi) strengthening of connection between walls and floor.

32.4 REPAIRING TECHNIQUES OF MASONRY

Repairing of cracks or replacement of damaged wall sections is an essential feature of repair process. It is a general assumption that repairing only helps to retain the original shape of the structure without increasing its strength. The main two problems solved during the repairing process are: (i) masonry cracking and (ii) masonry deterioration.

32.4.1 Masonry Cracking

According to Grimm, 1988, a crack may be defined as a “break, split, fracture, fissure, separation, cleavage, or elongated narrow opening visible to the normal human eye and extending from the

surface and into a masonry unit, mortar joint, interface between a masonry unit and adjacent mortar joint, or into the joint between masonry and an adjacent construction element". Besides seismic vibration, the cause of cracking is movement or strain induced by imposition of loads or by restraint of volume changes in masonry materials. Nothing can help to prevent such cracks, but at least they may be accommodated. In the case of load bearing masonry building, the seismic damage depends on the width of cracks for which repairing process needs to be defined accordingly. A well-established definition by Coburn and Spence (1992) regarding damage level is given in Table 32.1. A repairing process can be handled upto a maximum damage level of G3 grade cracking.

TABLE 32.1 Definitions of damage grades (Davenport, Burton and Nail 1999)

<i>Damage level</i>	<i>Definition for load bearing masonry</i>
G0	Undamaged
G1	Slight damage
G2	Moderate damage
G3	Heavy
G4	Partial destruction
G5	Collapse

Repairing techniques

The approach for adopting a repair process of existing or damaged masonry structures principally relies on the basis of level of cracking. The IAEE 1980 and UNDP 1983 serve as the basic source of information regarding details of techniques.

Repair of G0 and G1 grade cracks

In order to repair cracks upto a width of 5 mm, pressure injection of cement grout containing admixtures against shrinkage or epoxy is recommended. For fine cracks of upto 1 mm width epoxy injection is preferred. The procedure is shown in Figure 32.7 (*IS 13935: 1993*) and the general steps are as follows:

- Clean the external surface of the wall from the nonstructural materials
- Place the plastic injection along the surface of cracks on both sides of the member and are secure in place with the fast binding mortar. The centre-to-centre spacing of these port may be approximately equal to the thickness of the element
- After the sealant has cured, inject a low viscosity epoxy resin/or cement grout into one port at a time beginning at the lowest part of the crack, in case it is vertical, or at one end of the crack, in case it is horizontal.
- The processes of injection are to be continued until the epoxy resin/or cement grout penetrates into cracks. The injection port should be closed at this stage and injection equipment next port and so on.

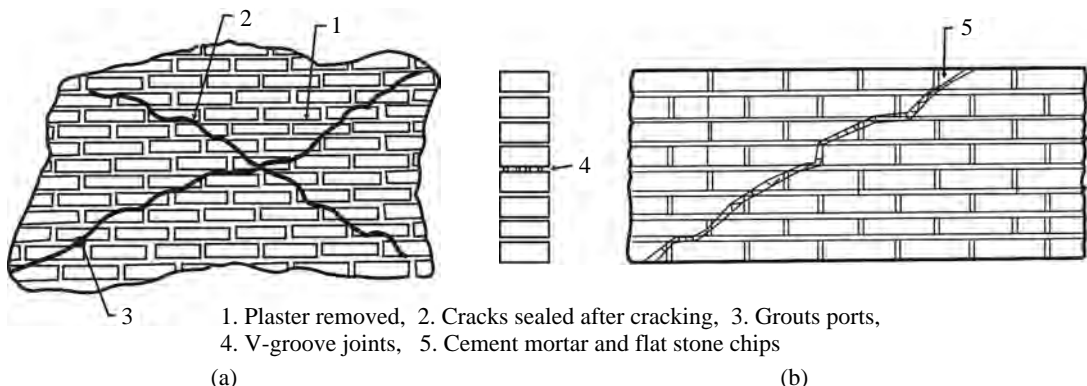
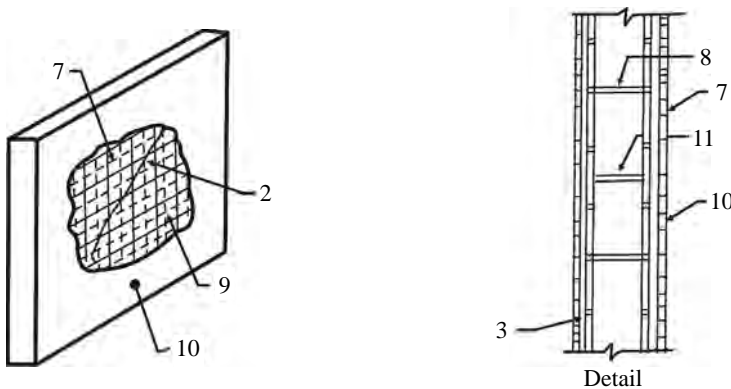


Figure 32.7: Repair of G0/G1 grade cracking (a) Grout or epoxy injection in cracks
 (b) Cement mortar and flat chips (IS 13935: 1993).

Repair of G2 grade cracks

In G2 grade cracks the repairing process remains much similar to the previous technique with an exception to insert reinforcement in every injected hole. The step to be followed for repairing of cracks is as follows: Figure 32.8 (IS 13935: 1993).



7. Wire mesh on front face, 8. Clamps, 9. Wire mesh on back face,
 10. Cement plaster, 11. Cracks in wall

FIGURE 32.8 Repair of G2 grade cracking: cement mortar and wire mesh in cracks (IS 13935: 1993).

- Remove the loose material and replace with either epoxy sand mortar or quick setting cement mortar
- Provide additional reinforcement, if necessary, and cover with mortar
- In case of damage to walls and floor diaphragms, steel mesh could be provided on the outer surface and nailed or bolted to the wall. Then it may be covered with plaster or micro concrete

- In case of much larger cracks units become loose, and the repairing process has to be more extensive than injection. In that case defined process is, UNDP, 1983, (a) remove cracked units (b) insert new units in rich mortar or the use of steel bars/stitching dogs (c) fill the void
- Same procedure can be repeated on the opposite side of the wall if necessary

Repairing of G3 grade cracks

Cracks due to loss of connection among the multi-wythe masonry walls may be categorized as G3 grade cracking. Multi-wythe wall construction practice is frequent in the rural and hilly regions of India with stone masonry houses built in poor mortars. Such wall constructions happen to be more susceptible to out-of-plane forces resulting in collapse of the outer leaf of multiple leaves stone masonry walls. There may be two possibilities of damage (i) permanent distortion of wall on both the sides as shown in Figure 32.9(a) and (ii) distortion or humping only on one side as shown in Figure 32.9(b). In the first case only the distressed portion of the wall may be removed and reconstructed since repairing is not feasible. In the second case total reconstruction may be avoided by removing only the humped side, rebuilding the wall and filling of voids with concrete or cement grout. Insertion of through stones and bond stones at regular intervals, Figure 32.9(c), may provide a good connection between the reconstructed wall and the existing wall. The details of repairing process are as follows.

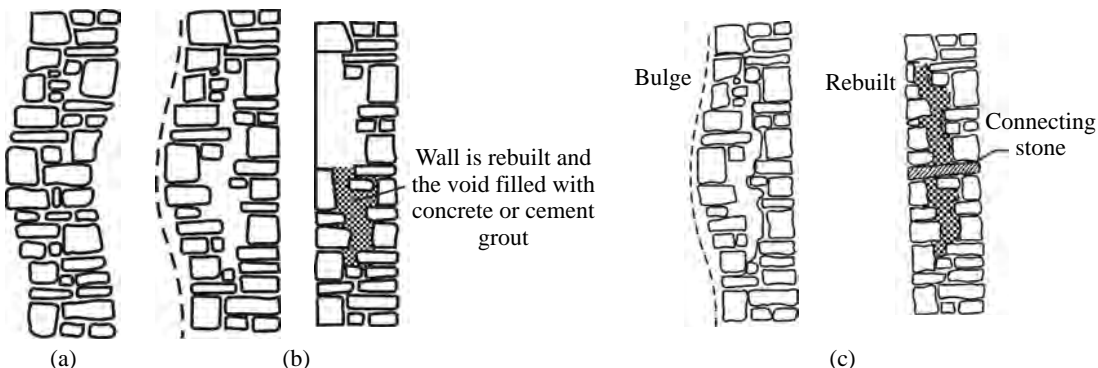
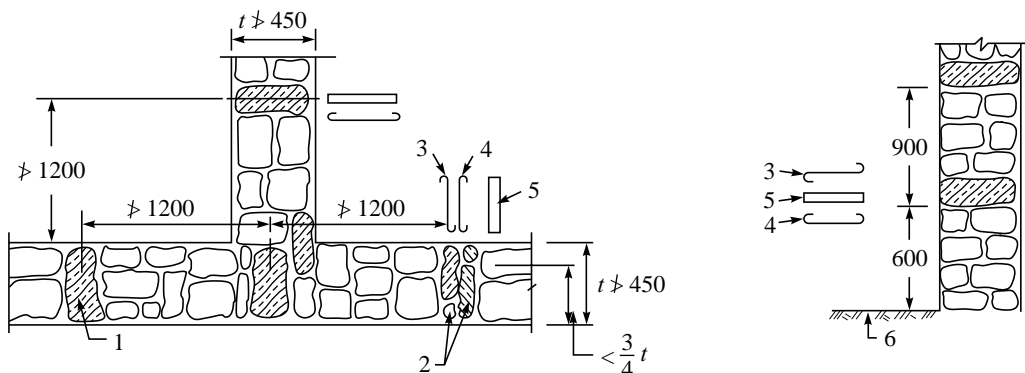


FIGURE 32.9 Repair of G3 grade cracking (a) Humping both sides of the wall (UNDP, 1983) (b) Humping one side of walls, reconstruction possible (UNDP, 1983) (c) Reconstruction of a bulged stone-masonry wall (Tomazevic, 1999).

Through stones/bond stones

In the event of an earthquake delamination and bulging of walls, vertical separation of internal and external wythe through middle of the wall thickness generally occur in stone masonry constructions. Reconstruction may be preferred if one of the layers is stable enough to be used as framework. “Through” stones of full-length equal to wall thickness may be inserted at an interval of 0.6 m in vertical direction at 1.2 m in horizontal direction. In the non-availability of full-length stones, stones in pairs each of about $\frac{3}{4}$ of the wall thickness may be used providing an overlap between them (Figure 32.10). The technique includes preparation of space in the



1. Through stone, 2. Pair of overlapping stone, 3. S-shape tie,
4. Hooked tie, 5. Wood plank, 6. Floor level

FIGURE 32.10 Insertion of “Through” stones or “Bond” elements (IS 13828: 1993).

wall, insertion of stones of equal size to the thickness of the wall and fixing of stones with cement sand mortar. Other alternatives of through stones are use of “S” shape elements of steel bars 8 to 10 ϕ or a hooked link with a cover of 25 mm from each face of the wall or wooden bars of size 38 mm \times 38 mm cross section or equivalent.

Cement grouting

Grouts are most frequently used to repair and strengthen of masonry walls having large voids or to fill the space between adjacent portions of masonry. There may be different types of grout but the most commonly used are the epoxy and cement grouts. Grout injection binds the inner and outer wythes together establishing a composite action between them for an improved out-of-plane moment capacity. The selection of grout depends on the desired strength, bonding properties and on the size of the crack network or void system. Fine grout can fill cracks as small as 0.0005 inch, while coarse grouts are useful for filling wide collar joints between the wythes. According to Newman 2001, cement grout consisting of 1 part of portland cement, $\frac{1}{2}$ part type S hydrated lime, $\frac{1}{2}$ part type fly ash may be used for repairing earthquake damaged un-reinforced masonry building.

Grout injection is a powerful rehabilitation technique, if it is handled carefully. The most evident problem arises from the lateral pressure exerted by the grout, if the wall wythes are poorly interconnected, the wall being grouted can split apart and collapse. Low lifting grouting is preferred as it reduces the hydrostatic pressure, which prevents the outward thrust of the fluid grout from displacing one of the wythes. Grouting begins from the bottom of the wall and proceeds up to the top. It is believed that the strength of grout does not influence the lateral resistance of the grouted walls. This can be explained as per Tomazevic (1999): “the potential vertical and lateral resistance of the wall is determined by the strength of the original mortar, which transfer the external loads acting on the wall from unit to unit. As confirmed by visual inspection of the crushed walls after the tests, the grout does not penetrate into original mortar. Consequently, the strength of the original mortar is not improved and hence the potential resistance of the wall does not change, although the voids have been filled with stronger materials”.

32.4.2 Masonry Deterioration

The phenomenon of masonry deterioration is somewhat unrelated to earthquakes but its repair is required to be done alongwith the repair of cracking of walls. The most common types of masonry deterioration are in **Units** due to water penetration and freeze thaw cycles and in **Mortar** due to poor quality.

Repairing techniques

Units

All damaged units are replaced by new units of same appearance and material property.

Mortar

There is evidence that a weak or deteriorated mortar is the cause of failure (in-plane as well as out-of-plane) of masonry buildings, Figure 32.11. It is suggested that before taking up the retrofitting of building, improvement in strength of mortar is necessary.

Re-pointing: Re-pointing is often carried out when the quality of the mortar happens to be poor but the units remain in good condition. This involves removal of the existing mortar up to $1/3$ of the walls thickness or at least $\frac{3}{4}$ inches from the joints on one or both sides of the wall, followed by proper cleaning of the surfaces by compressed air brush or steam of water and insertion of new mortar. If the mortar condition is extremely poor the removal is needed up to a larger depth. Steel reinforcement is sometimes placed in bed joints to improve the ductility and energy dissipation capacity of the structure. The joints are then re-pointed with cement mortar. After sufficient strength of the mortar is attained, the procedure of re-pointing is repeated on the other side of the wall. Figure 32.12 shows various steps involved in re-pointing.



FIGURE 32.11 Weak mortar led to extensive shear cracking in the building (EERI, 1996).

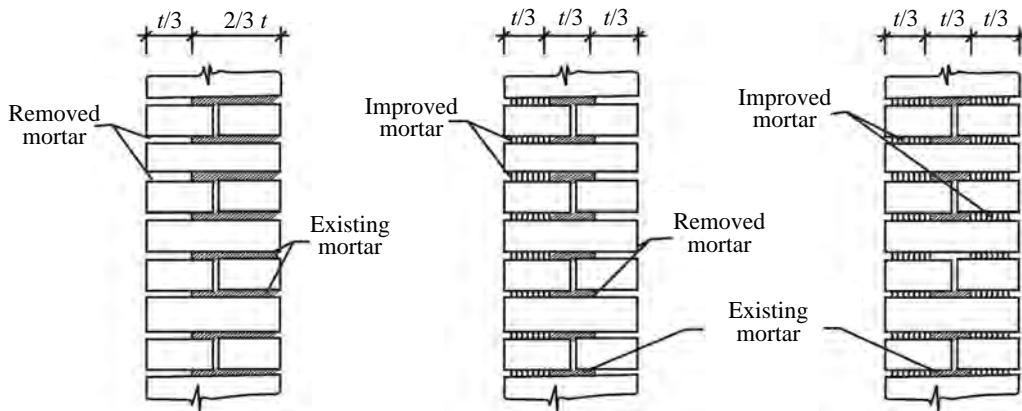


FIGURE 32.12 Re-pointing of a brick masonry wall (Tomazevic, 1999).

32.5 MEMBER RETROFITTING

32.5.1 Retrofitting Techniques

Shotcrete

In the case of weak masonry and absence of enough solid piers to resist seismic loads, shotcrete is ideally suitable for un-reinforced masonry buildings (Wyllie, 1996). A considerable number of load bearing and architectural un-reinforced masonry walls have been strengthened against seismic motion by applying a layer of shotcrete either to the outside or inside surface of the wall. **Shotcrete** is a concrete mix pneumatically applied to a solid surface (Figure 32.13a). There are two types of shotcrete usually employed namely **wet mix** for large volumes and massive section and **dry mix or gunite** for lesser volumes, thin sections and confined spaces. Better control can be achieved in handling dry mix shotcrete as compared to the wet mix due to good control of material flow (Sanders, 1984). Moreover design of concrete mix, selection of correct process and skilled workmanship are essential for effective use of shotcrete.

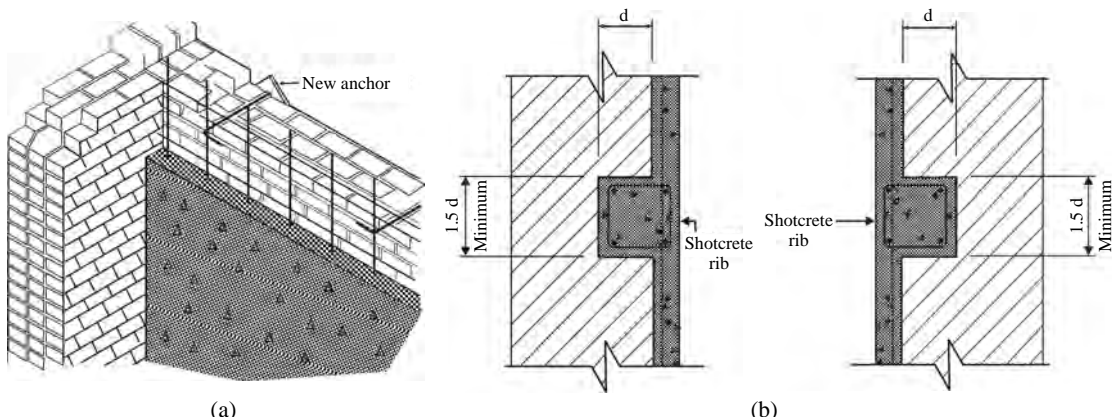


FIGURE 32.13 Strengthening existing masonry walls with shotcrete (a) New reinforced concrete (shotcrete) added to existing unreinforced masonry (Turner, 2004) (b) Plan of the shotcrete rib (Newman, 2001).

Design mix

- Shotcrete mix may be a combination of one part portland cement and three parts sand by volume (Kahn, 1984)
- Shotcrete must have compatible stiffness values to the masonry walls. A 4 to 5 inch shotcrete is often sufficient.

Applications

- Prepare surface by cleaning and removing all loose aggregate and roughening of the surface. Condition of surface whether dry, wet or epoxy coated does not affect significantly although a saturated brick, wetted surface is recommended.

- Due to high shrinkage characteristics of shotcrete, it is always necessary to provide adequate reinforcement to prevent cracks and proper curing (Turner, 2004).
- Reinforcement should be placed at mid-depth with a mat of small size 8 to 10φ bar and is cut into the wall at regular intervals, usually 2 to 3 m.
- A proper bonding with the existing walls can be achieved by providing vertical shotcrete ribs in between the floors, reinforced as columns with vertical bars and closely spaced ties. For placement practically, the width of ribs should be at least 1.5 times their depth, as shown in Figure 32.13b (Newman, 2001).
- Vertical reinforcement of vertical ribs must be anchored to floors or slab and bottom of the existing foundations with dowels
- Shotcrete may be applied either internally or externally. Caution may be taken to preserve the appearance of the building.
- Shotcrete can be used in accessible footing, footing walls, slabs, walls, columns, beams, stairs, filling of large voids etc.

Equipment

- A pressure gun, an air compressor, material hose, air and water hoses, nozzles, and sometimes a water pump (UNDP/UNIDO, 1983).

Results

Experimental tests have revealed the effectiveness of reinforced shotcrete. Some of the important findings are:

- Reinforced shotcrete in unreinforced masonry wall has proved to be an effective method as it greatly increases the in-plane diagonal strength and inelastic deflection capacity (Kahn, 1984).
- Full composite behaviour may be observed between the new shotcrete and the old masonry and the new reinforcement when properly applied on prepared surface (UNDP/UNIDO, 1983).
- Strength characteristics of shotcrete are higher due to the high compaction energy and a low water cement ratio.

Structural overlay/adhered fabric

Fibre Reinforced Plastic (FRP) has drawn considerable attention for repair and retrofitting of civil engineering structures due to their unique properties like high strength to weight ratio, stiffness to weight ratio, corrosion and fatigue resistance as against conventional materials of heavy mass with limited efficiency. FRP consisting of stiff and strong reinforcing fibre (primarily carbon and glass), held together. Table 32.2 lists of major material properties of CFRP, GPRF as compared to conventional materials of retrofitting.

There are various examples where the FRP has been successfully used for retrofitting of RC structures. Use of adhered fabric materials like Carbon Fibre Reinforced Plastic (CFRP) sheets and Glass Fibre Reinforced Polymer (GFRP) sheets are the latest developments as medium of retrofitting of RC structures. There are several examples in which FRP has been suc-

TABLE 32.2 Major material properties of FRP materials as compared to conventional materials

Type of strengthening materials	Ultimate tensile strength, σ_u in N/mm ²	Young's modulus, E in N/mm ²	Ultimate tensile strain, ϵ_u in %
Carbon-Fibre T700S	2300	152,000	1.50
GFRP Sheets, CW130-1000 (low strength, bi-directional)	98.4	12,200	0.94
GFRP Sheets, EGFW430 (high strength, uni-directional)	2040	93,100	2.4
GFRP Sheets, Sika Wrap-300G0/90	2400	70,000	3.0
Steel	235	210,000	> 5%
Shotcrete (compressive strength 34.5 MPa)	3.45	26,000	—
Epoxy resin for injection (compressive strength 65 MPa)	34	2300	—
Epoxy mortar for filling (compressive strength 79 MPa)	29	7300	0.39

cessfully used in masonry structures, which in turn has also been experimentally tested (Weng et al., 2004; Elgawady, 2004; Schveyler and Kelterborn, 1996). It is also be noted that the use of higher strength or higher modulus fibres (particularly carbon fibres) results in substantially higher level of performance, but these fibres are at present very costly to use in routine civil infrastructure applications (Karbhari, 2002).

The method of strengthening an un-reinforced masonry wall with FRP is quite simple and rapid. The surface should be roughened by grinding, and then cleaned with high air pressure and the holes are filled with epoxy mortar. Small holes are filled with epoxy resin. The FRP sheets are fixed to the surface of masonry substrate by epoxy resin, cross-wise on one or both sides of the wall. Steel plates are used to ensure non-occurrence of anchorage failure by anchoring the FRP to the slab and foundation pad (Figure 32.14).

Anchoring in slabs avoids stress concentration in masonry walls. The anchoring of sheets in the RC slab consists of steel plate pressed onto the ends of the sheets by means of bolts. The application of FRP sheets to the existing load bearing masonry shear walls significantly increases its lateral resistance and ductility. It happens to be cheaper than the reinforced shotcrete or the

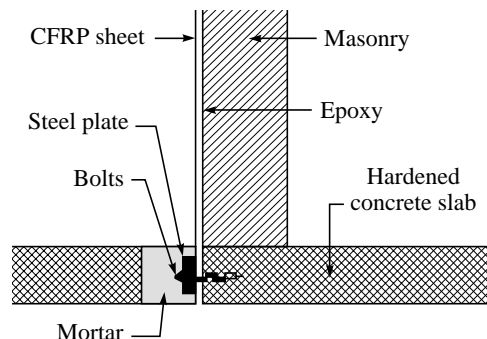


FIGURE 32.14 Strengthening existing masonry walls with FRP (Schwegler and Kelterborn, 1996).

replacement of the walls. Its construction is simple, hence can be used to retrofit seismically damaged structures or historical buildings.

RC and steel frame

The in-plane strength of masonry walls reduced due to openings. It may be increased by employing the technique which consists of making an RC or steel frame inside the opening. The weakness of the wall caused by the opening can be effectively counteracted by the frame. For better results better interaction conditions are ensured between the wall and the frame as shown in Figure 32.15a. Another alternative is to place vertical jamb steel at the edges of opening, while the horizontal edges of the opening are reinforced with reinforcement bar spanning between the jamb reinforcement as shown in Figure 32.15b. Jamb reinforcement can be inserted from a side and be anchored to foundation pad and slab or lintel band/lintel if available. The horizontal bars may be hooked at the ends or may extend past the openings edges up to an adequate distance. The last option for increasing the in-plane shear capacity is to fill with the material having similar properties (FEMA 172, 1992).

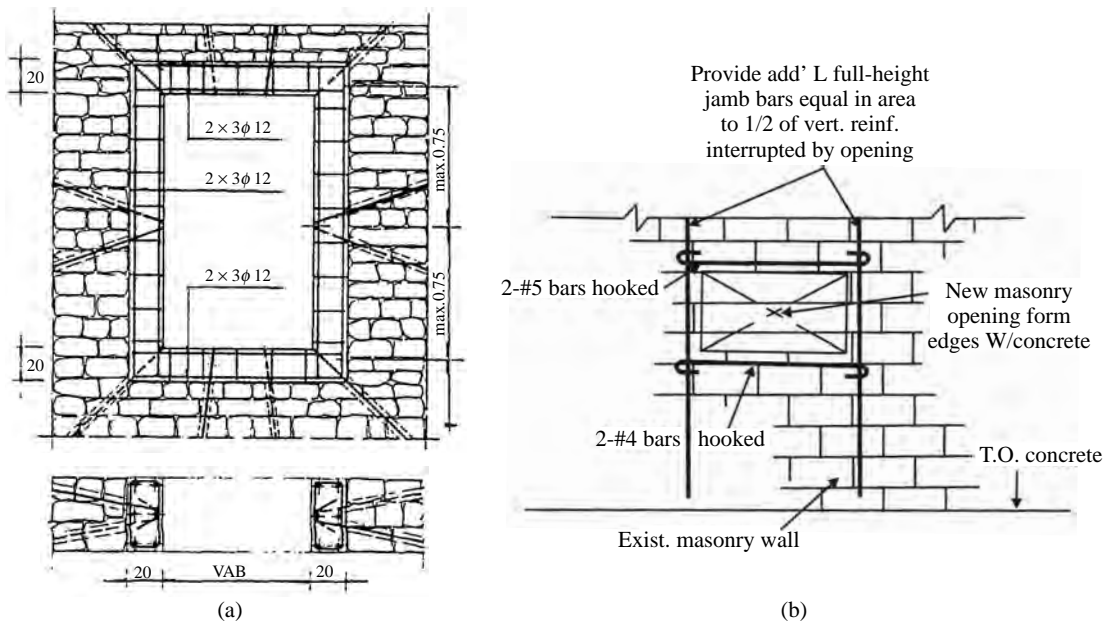


FIGURE 32.15 Strengthening techniques of an opening in unreinforced masonry wall (a) Use of a reinforced concrete frame (Modena, 1994) (b) Added reinforcing bars at the edges of an opening (Newman, 2001).

32.6 STRUCTURAL LEVEL RETROFITTING METHODS

The object of structural level retrofitting is to improve the structural integrity of the whole structure. Retrofitting techniques in this category are as follows.

32.6.1 Retrofitting Techniques

Confinements with RC elements

The techniques tend to make the existing masonry act as a “confined masonry”, in the sense that reinforced concrete elements have been inserted surrounding the wall panel or middle of the long wall, allowing the entire wall, or its portion, to act as a truss element, where the struts are inclined strip of unreinforced masonry (Figure 32.16). In this way brittle and non-ductile wall becomes more ductile and its load carrying capacity is increased several times with added confinement of the reinforced concrete elements. It is more suitable for smaller building *i.e.* upto one- to three-storey height with monolithic reinforced concrete slab and horizontal band over the load bearing walls at the lintel level.

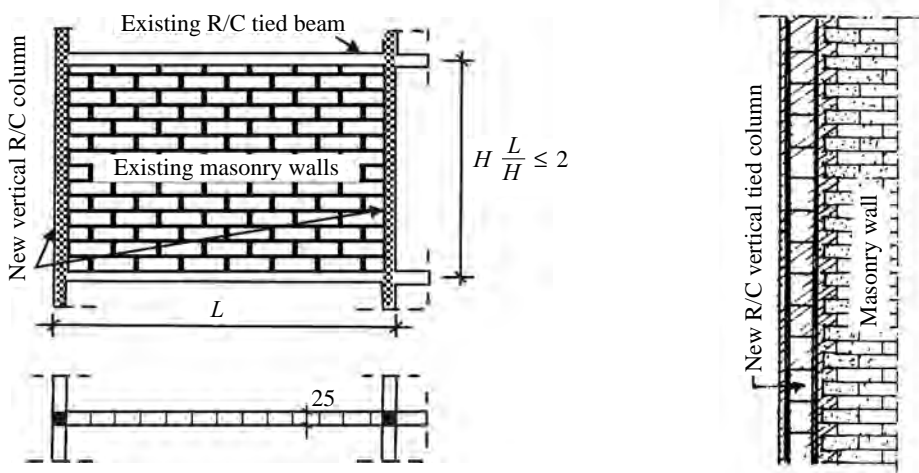


FIGURE 32.16 Strengthening of existing unreinforced masonry by confinement with RC elements (UNDP, 1983).

Following points should be considered in the design procedure (UNDP, 1983):

- Column should be thicker than wall and should not take part in the transmission of the vertical loads, and should be designed with reinforcement to resist the tensile forces due to moment and shear of the wall panel.
- Larger percentage of reinforcement should be avoided and more columns however with minimum reinforcement must be there.
- Position of the added column in the wall such that its length to height ratio of the framed wall panel should not be larger than 2:1.
- If the horizontal band is there, it should be repaired particularly at doors and window levels. Otherwise horizontal band over the load bearing walls should be provided.

Following are the points, which should be considered during construction

- Construction of the column should begin from the lowest storey and proceed upto upward unit until the work is completed

- In locations where vertical columns are to be constructed, the wall bricks are removed one by one so that contact zone between the wall and the new concrete is coggued.
- The concrete of the horizontal band should be removed and only the reinforcement should be left.
- A part of the wall on the upper floor also needs to be opened so that the reinforcement of the column can continue and be anchored in the wall above. Special attention should be given to ensure that the vertical columns are adequately anchored through the basement and to the foundation structure including local strengthening of foundation if necessary.

Confinements with steel elements

Confinements with steel sections may prove to be best solution when immediate and urgent retrofitting is required since the steel sections can be quickly installed and are easily available as compared to other equipment like shotcrete. This scheme happens to be more useful for increasing out-of-plane strength of wall.

Strengthening schemes consist of two steel sections (channel section or angle section) having full wall height placed on both the sides of the existing wall and attached to the roof or floor diaphragms. Steel sections are interconnected with each other in between by drilled anchors through masonry at regular intervals such as 50 cm as shown in Figure 32.17.

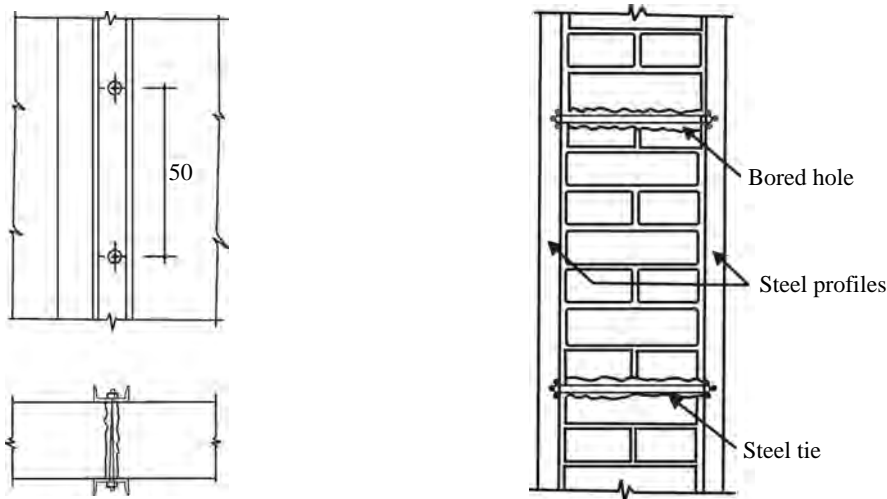


FIGURE 32.17 Strengthening of existing unreinforced masonry by confinement with steel sections (UNDP, 1983).

The same attachment may be repeated along the length of the wall such that the horizontal span is shorter than the vertical *i.e.* floor to floor. Cracks and such other distress in masonry wall may be repaired by other techniques as described earlier. The steel sections may be painted or covered with cement plaster in order to provide corrosion protection. If the exposed steel frames are visually undesirable, they may be placed within the wall.

Adding reinforcement to masonry walls

Insertion of reinforcement into the masonry wall may increase its flexural and shear capacities for which several methods exist. Reinforcement may be inserted from the side or centrally or placed externally.

Reinforcement from side may be provided by cutting vertical slots at the desired intervals (4 ft c/c, for example) in the walls either from inner or outer face depending upon easiability, feasibility, workability, operatability and aesthetic considerations. After insertion of reinforcement slots are filled with grout (Newman, 2001).

Insertion of reinforcement from the centre of the wall may take place by providing vertical cores, which may be termed as centre coring. The coring of a vertical hole should be from the top continuously through the wall into the existing footing or basement wall. The spacing of the cores is determined analytically, and is typically 4 to 5 ft in the centre. The core should be grouted with regular non-shrink grout as shown in Figure 32.18a. The advantage of centre core system is to minimise site/interior disturbance and non-disfiguring of the internal or external face of the walls. Sometimes the cutting of slot or cores weaken the masonry, because the added grout in the cores does not participate in resisting the loads that are already present. Therefore, the wall should be relieved of the existing loading to the great extent possible before this strengthening takes place.

In some cases, adding reinforcement from the insideside of the wall is insufficient, to improve its out-of-plane flexural and shear capacities or sometimes it may not be possible to provide the slots or cores in the wall. At this situation, the reinforcement is provided from the inside or outside face of the wall with a pneumatically applied (*i.e.* shotcrete) reinforced concrete (Figure 32.18b). The main challenge in this operation is to assure that the shotcrete bonds to the existing wall. To that effect, the shotcrete can be keyed into the wall at regular intervals, typically from 6 to 8 ft as discussed in previous section.

Connection between intersecting walls

Stitching of Wall Corners: Corners and wall intersection zones are always susceptible to heavy damage during earthquakes. The damaged corner and wall intersection zones may not only be repaired by sealing the cracks with grouting, but should also be strengthened by stitching. This technique is more frequently used in repair of the damaged wall corners. In such cases, holes are drilled in orthogonal wall of the structure at a regular interval of 0.5 m. After cleaning of holes with water, steel rods of about 12 mm diameter are inserted into both intersecting walls so that both walls are connected and the holes are filled with cement grout (Figure 32.19a). Other alternative of steel rod is to place long stone across the crack. Adjacent bricks or stones are removed, installing a new brick or stone, common to both walls as shown in (Figure 32.19b). This new stitching stone should be embedded in rich cement grout, at about 70 cm spacing. The gap formed between the two walls is to be filled with a rich cement grout. A wire framework is fastened to both the internal and external surfaces, and they are plastered with cement.

In case of separated wall sections as shown in Figure 32.20a, they are tied up with steel plate (*i.e.* 40 × 4 in cross section), embedded in rich cement grout in between two brick or stone layers after some bricks or stones have been removed. Such plates can be very effective in

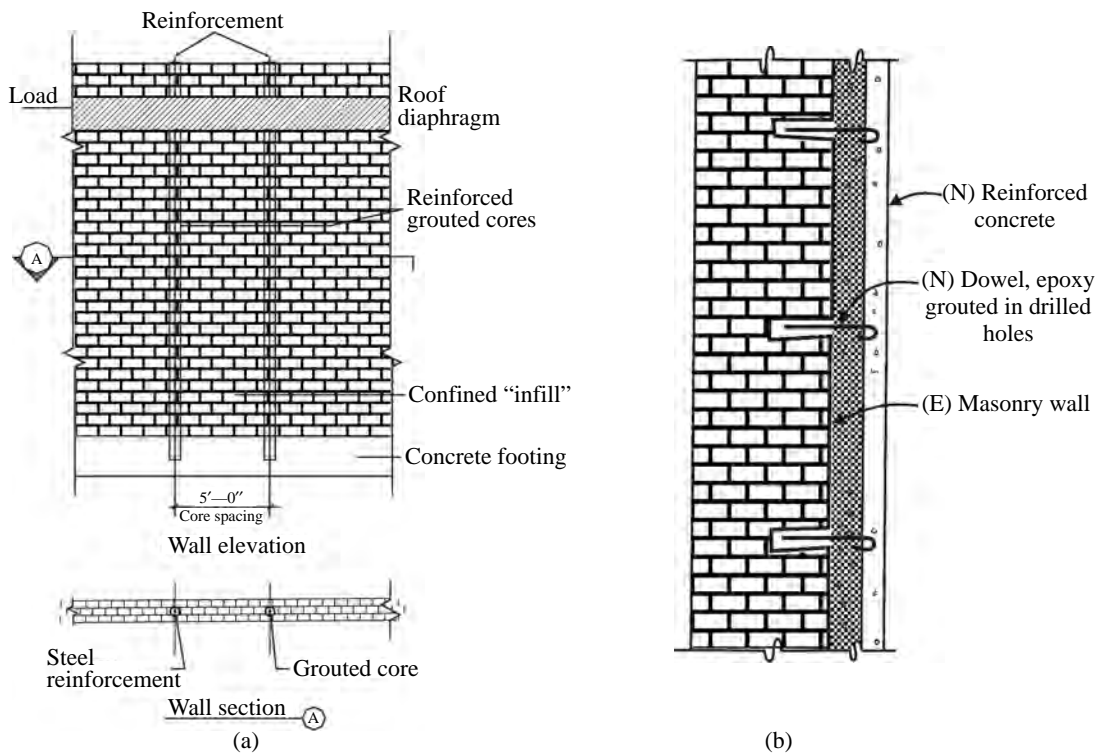


FIGURE 32.18 Strengthening of wall with added reinforcement (a) Centre core techniques (Breiholz, 2000) (b) Reinforced concrete overlay (shotcrete) (FEMA 172, 1992).

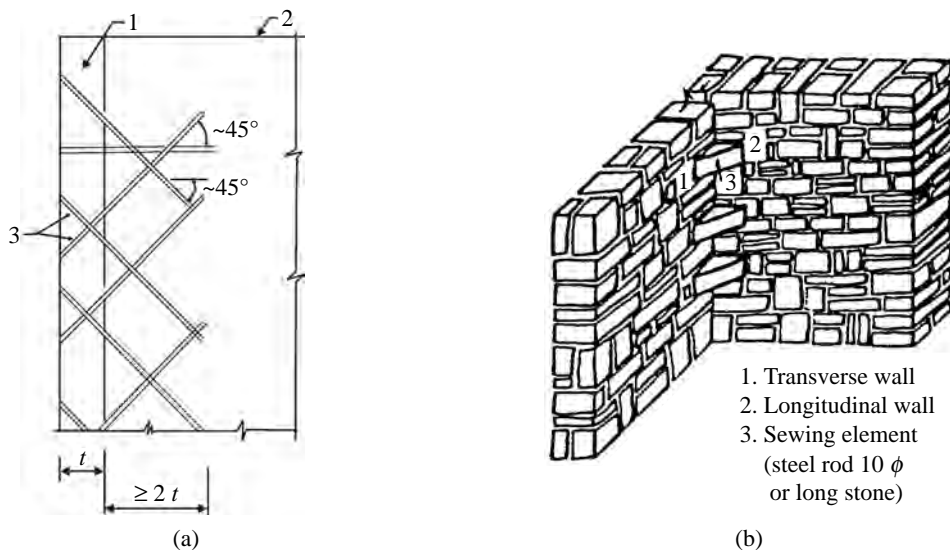


FIGURE 32.19 Strengthening of wall intersection (a) Sewing transverse walls with inclined bars (IS 13935: 1993) (b) Use of stitching stones (UNDP, 1983).

reinforcing the corner but they cannot bring the walls back to vertical position. The gap is then sealed and the surface be covered with wire trellies and plaster as mentioned above.

Another alternative of steel plate is to drill horizontal holes in the masonry through vertical crack and grouting or epoxying steel rods in the holes. In both these procedures, the remaining cracks should be filled with cement mortar. To reduce the separation prior to repair, tie rods, installed on both sides of the walls, can be used, Figure 32.20b.

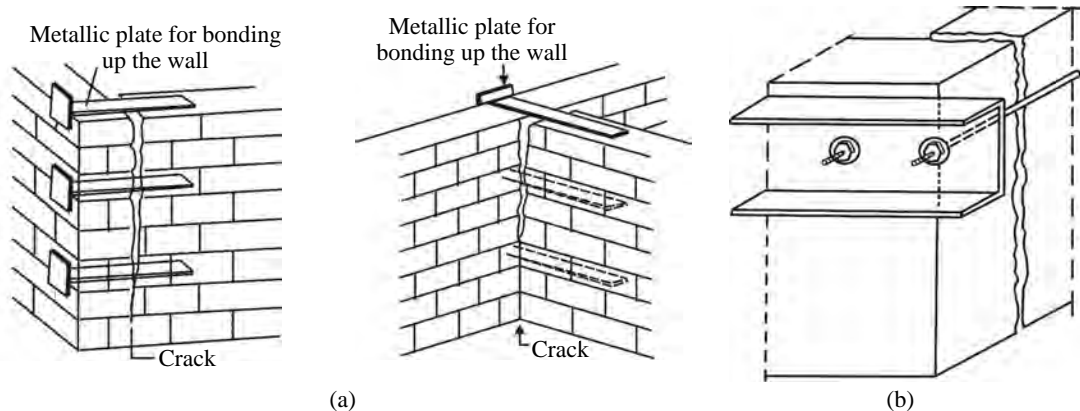


FIGURE 32.20 Strengthening of separated wall intersection (a) Use of steel plates (b) Use of tie rod (UNDP, 1983).

In case of total collapse of corner region, which is generally uncommon, strengthening is required by rebuilding of the corners with proper bond of the rebuilt part and the wall onto the contact surface (Figure 32.21a). A horizontal belt like a seismic band of thickness 15 to 20 cm, reinforcement $4 @ 16 \phi$ and stirrups 6 mm at 20 cm, should be added. A reinforced concrete corner column properly tied into the intersecting walls could be added to strengthen the wall intersection. Such column should have minimum reinforcement of $4 @ 16 \text{ mm}$ and stirrups $6\Phi \text{ mm}$ at 20 cm, (Figure 32.21b).

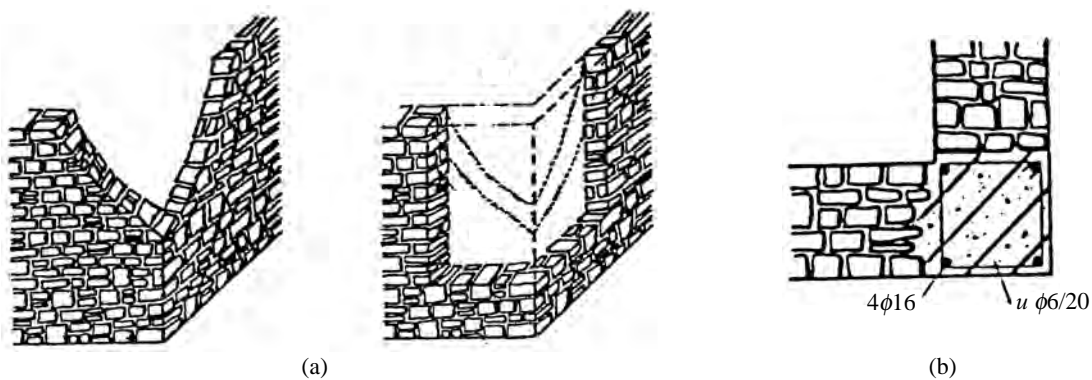
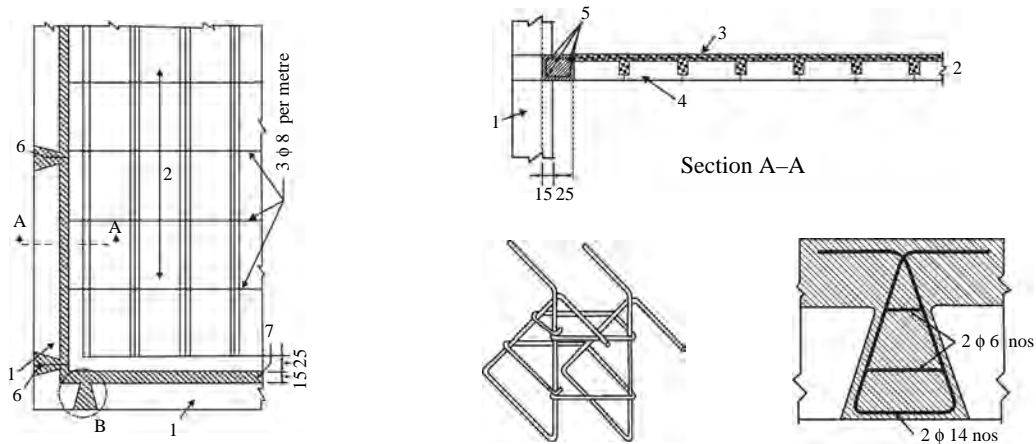


FIGURE 32.21 Strengthening of collapse wall intersection (a) Rebuilding (b) Use of RC column (UNDP, 1983).

Connection between walls and floors

The connection between the masonry walls and floor or roof is a vital link on which the distribution of earthquake forces depends. Moreover, an adequate interconnection between the walls and floor or roof also ensures a monolithic and integrated behaviour of structure to resist the earthquake forces in a unified way. A poor connection between the floors and walls is responsible for the independent behaviour of wall and transverse walls may collapse due to out-of-plane forces.

In most existing buildings, the floor and roofing joints have only gravity connection with the walls—typically, direct bearing with sparse anchorage. These gravity connections are nearly useless in resisting out-of-plane seismic force. Therefore, the roof has to be properly connected to the walls through appropriate keys, Figure 32.22.



1. Existing wall, 2. New floor, 3. Slab topping with reinforcement, 4. Prefab slab units, 5. RC band, 6. Key connecting new floor to existing wall @ 3 m, 7. Grooves cut in wall

FIGURE 32.22 Substitution of slab (IAEE, 1986).

There are two methods for stiffening an existing wooden floor connecting it to the surrounding walls. The first one is based on the use of traditional materials *i.e.* wood and steel. The floor is infact stiffened by nailing one or more layers of wood planks to the existing girders. Steel ties are then nailed directly to the girders or to the wood slab and anchored to the external face of the wall with steel fasteners. The second solution implies the creation of a composite structure formed by the wood structure and by a reinforced concrete thin slab. However it requires more complicated operations and the use of special materials, usually resins or special screws, to ensure the cooperation between the reinforced concrete slab and the wood girders. These schemes are schematically indicated in Figure 32.23a and b.

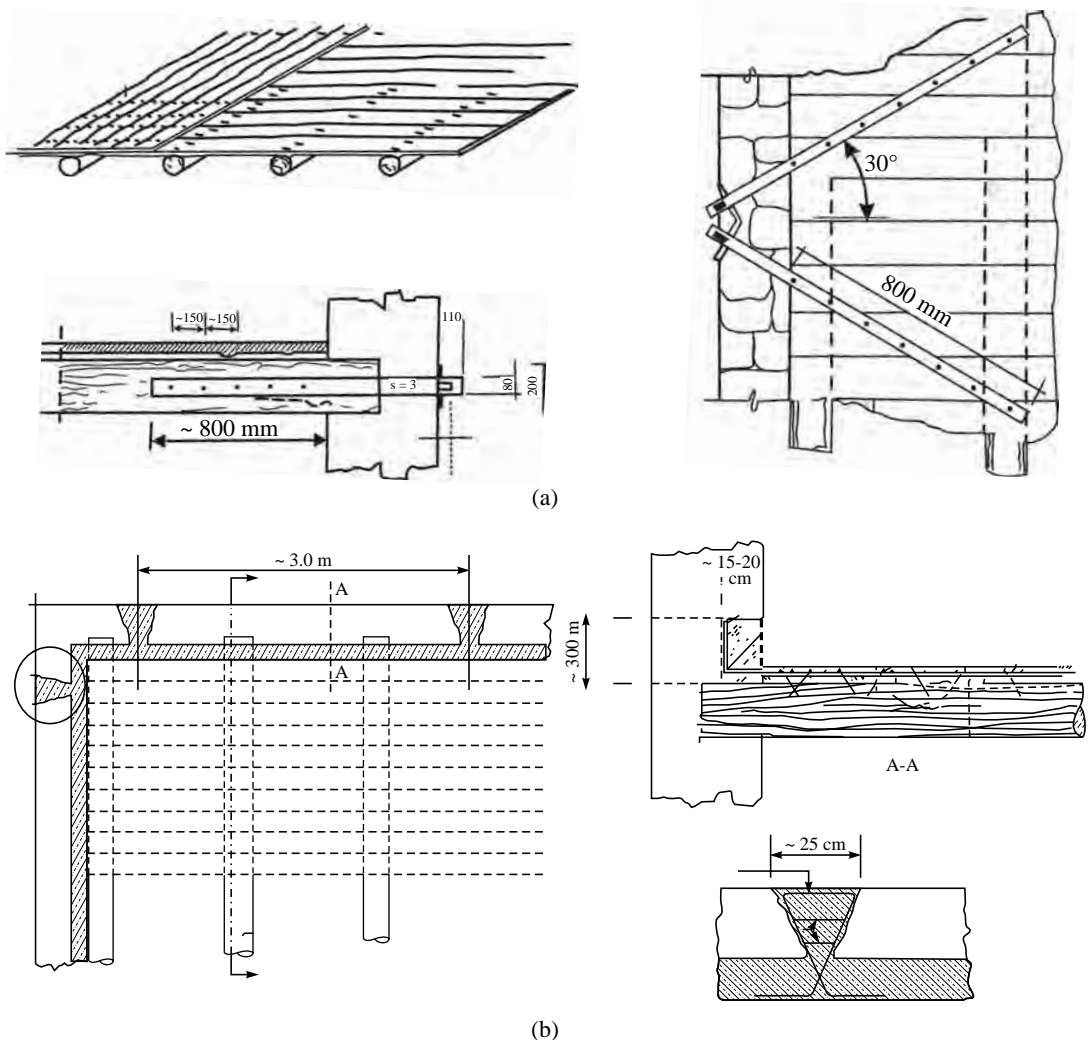


FIGURE 32.23 Strengthening of slab (a) Use of steel connections between stiffened timber floors and masonry walls (b) Use of reinforced concrete for stiffening timber floors and connecting them to masonry walls (Modena, 1994).

Pre-stressing

To increase the lateral strength, stability and integrated behaviour of load bearing walls, prestressing is a very effective and viable method of retrofitting. In prestressing of wall, two steel rods are placed on the two sides of the wall and tightened by turnbuckles as shown in Figure 32.24.

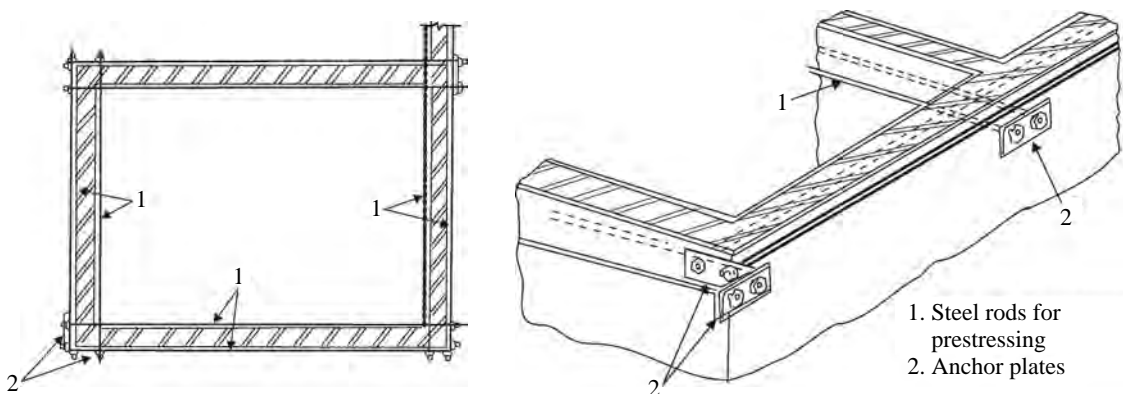


FIGURE 32.24 Strengthening of walls by prestressing (IS 13935: 1993).

External binding or jacketing

In the case of seriously damaged masonry walls, or where there is a need to strengthen the existing structure, the application of reinforced cement coating forming a jacket on one or both sides of the wall is used to improve the lateral resistance. This method of retrofitting is easy to apply and very efficient, hence it is widely used. The other alternative of reinforcing steel is **ferro-cement** or **wire fabric** like FRP materials that are more efficiently used. In retrofitting by jacketing, plaster is first removed from the damaged portion of the wall and joints between the bricks are cleaned from the mortar. The cracks and joints of the wall are first filled with cement sand (1:1) mortar. A welded wire meshes or wire fabric is placed around the entire damaged region. Steel ties are inserted at regular intervals of 0.5 m to 0.6 m in order to tie the mesh with the wall. The entire operation is followed by concreting or shotcrete of about 3 to 4 cm for simple brick work upto 8 cm or greater thickness for heavy masonry on the welded mesh. In smaller structures where continuous jackets are not desired, it is possible to add local reinforced concrete jackets only at wall corners, edges of openings and occasionally at midpoints of walls. Figure 32.25a shows the details of reinforced concrete jackets as per UNDP, 1983.

Alternate system of reinforcing the jackets can also be used. Figure 32.25b illustrates a system whereby bricks or stones are removed at regular intervals and a reinforcement cage is placed in the chase or void created and concrete or shotcrete is then placed within the chase (UNDP, 1983). This system is best utilized where only one side jacketing is provided and exposed anchor are objectionable or where heavy stone masonry makes drilling impractical. One caution with this approach is that the addition thickness of concrete may add sufficient weight and overturning forces such that the foundation will require strengthening for increased bearing area. If only isolated walls are jacketed, extremely high stress concentration and overturning forces may result, requiring special design attention. Designers are also cautioned that jacketing greatly increases the stiffness of the masonry walls and care must be taken not to introduce torsional moments into the structure.

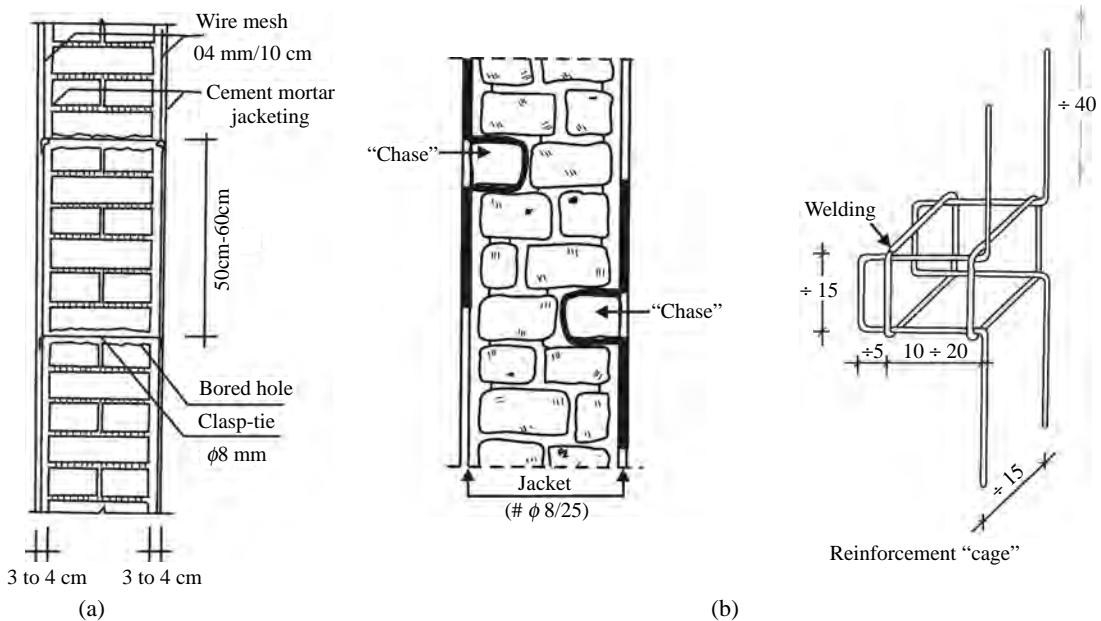


FIGURE 32.25 Methods for jacketing (a) Use of wire mesh (b) Use of reinforcement cage (UNDP, 1983).

Splint and bandage technique

The jacketing with steel mesh with micro-concrete may be used only on the outside surface walls and may be uneconomical also because of covering the entire perimeter of the building. The **splint and bandage** is another approach to strengthen the walls as well as bind them together economically. Figure 32.26 shows a scheme of strengthening by splint and bandage technique. The horizontal bands are called **bandage** while vertical steel are called **splints**. The welded mesh type of steel is to be provided on both outer and inner surfaces at critical sections. The welded mesh should be nailed to the masonry and then be covered with micro-concrete. As a minimum provision these must be provided on all-external walls along with cross-tie bars across the building in both directions and embedded in external bands. The cross-tie bars are necessary to ensure integral action of bearing walls like a crate (Thakkar, 2002).

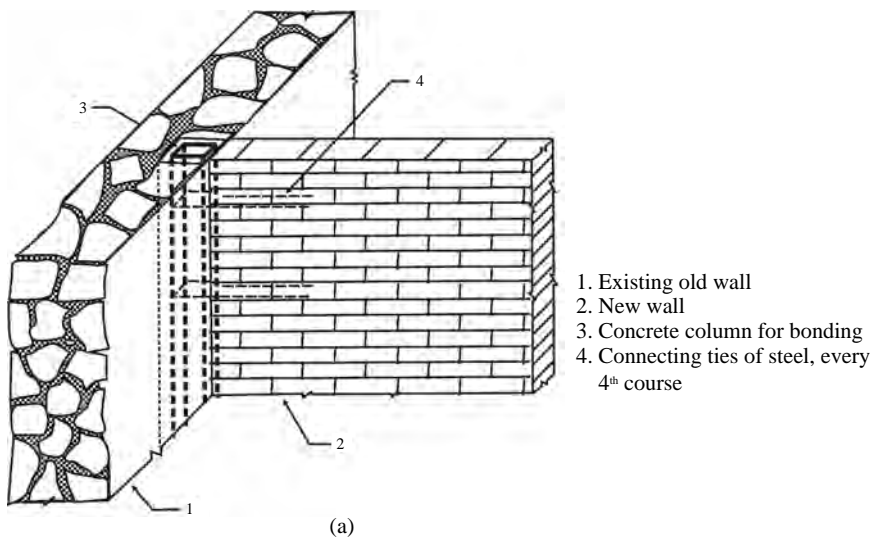
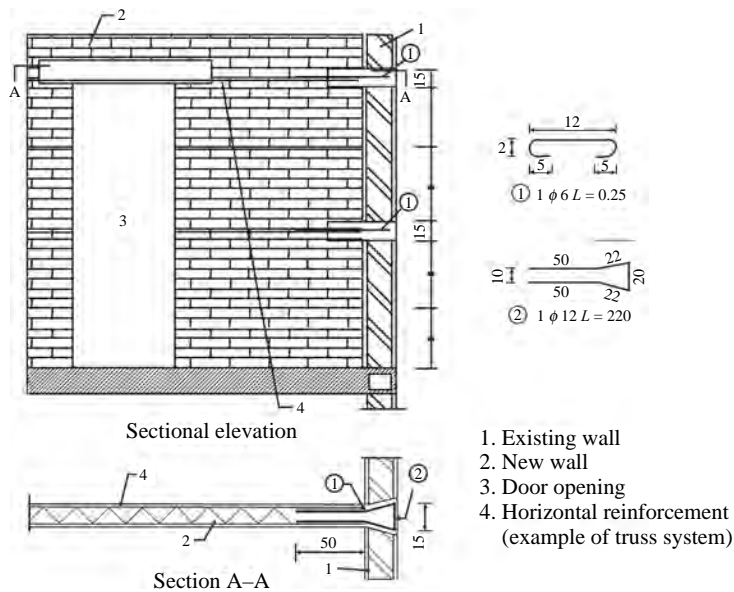


FIGURE 32.26 Strengthening by splint and bandage technique (IS 13935: 1993).

1. Wire mesh with width > 400 mm

Inserting new walls

New walls could be inserted in the existing buildings for increasing strength and for correcting deficiency caused due to asymmetry. The main problem in such modification is the connection of new wall with old wall. The link to the old walls is maintained by means of a number of keys made in old walls (IS 13935: 1993). Figure 32.27a and b shows two examples of connection of new walls to existing ones. The first case refers to a **T-junction**, the second case to a **corner junction** (IAEE, 1986).



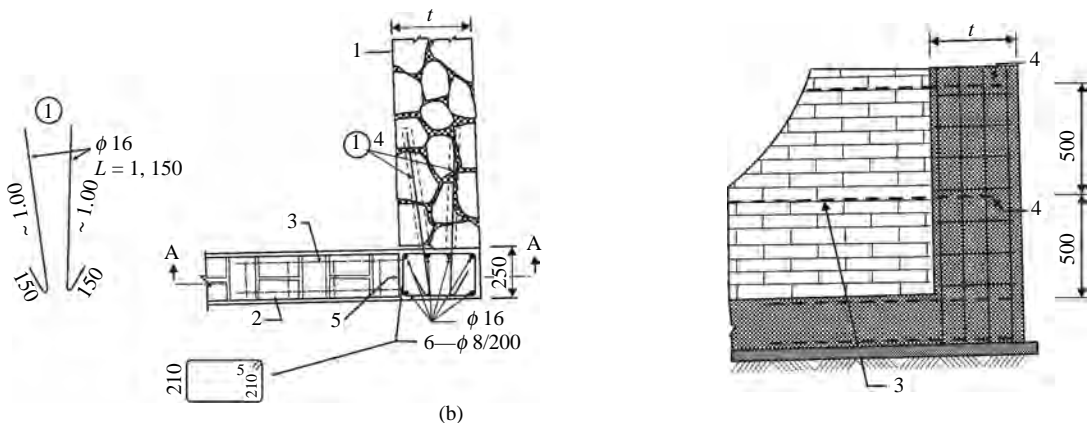


FIGURE 32.27 Inserting new walls (a) Connection of new and old brick wall and connection of new brick wall with existing stone wall at T-junction (b) Connection of new and old walls at corner junctions (IAEE, 1986).

Exterior supplemental elements

Provision of additional shear walls at the perimeter of the building or external buttresses are the examples of exterior supplemental devices to increase in-plane strength of the existing masonry walls. Figure 32.28 shows the application of external buttresses to an existing masonry building.

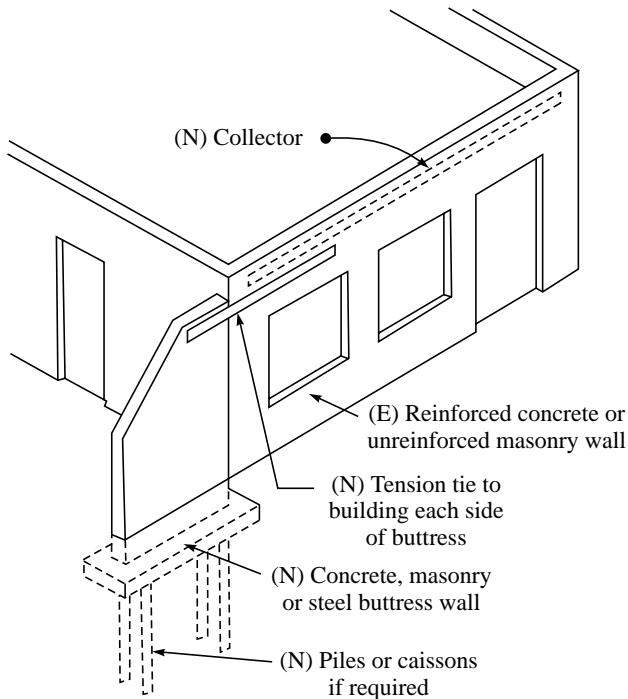


FIGURE 32.28 Strengthening of walls with external buttresses (FEMA 172, 1992).

These buttresses must have sufficient capacity against overturning forces and uplift forces therefore it requires an additional foundation. It should have proper connection with the existing walls through dowel so that the forces are transferred from the existing building to the new external vertical resisting elements. This technique has limitations in case of buildings constructed at the property lines or not having much space.

External buttresses may also be used in case of long longitudinal walls as in the case of long barrack type buildings (Figure 32.29).

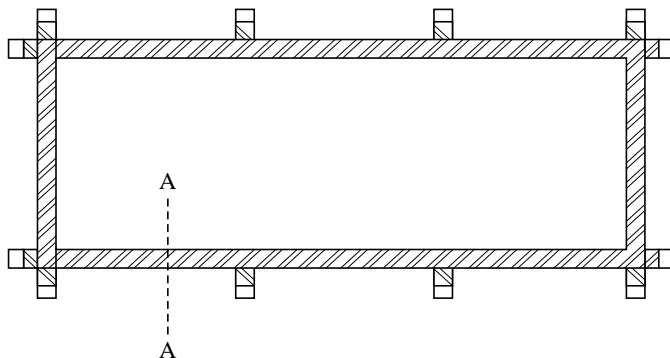


FIGURE 32.29 Strengthening of long walls by buttress (IAEE, 1986).

Strengthening of parapets

Retrofitting of unreinforced masonry parapets above public access area is a considerably effective method of minimizing hazard. The basic element of seismic retrofitting of these vulnerable parapets involves bracing parapets roofs and connecting floor diaphragms to walls through anchor as shown in Figure 32.30. Some engineers consider parapets with height to thickness ratios of less than 2.5 to be stable and in no need of strengthening.

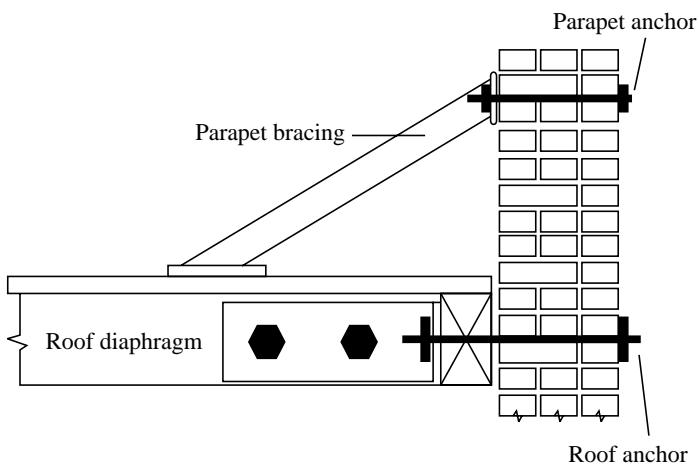


FIGURE 32.30 Details of parapet bracing (Telford, 1995).

32.7 SEISMIC EVALUATION OF RETROFITTING MEASURES IN STONE MASONRY MODELS

In the previous chapter, models 5 and 6 have been tested for earthquake resistant measures on shock table. After damage under shock loading, models were retrofitted by two different schemes and tested for evaluating the effectiveness of retrofitting techniques. Model 5 has been retrofitted with cement grouting, strengthening with wire mesh, and stitching of walls while model 6 has been retrofitted with through stones, external binding and prestressing at sill level, designated as **Model R1** and **Model R2** respectively. The Indian Standard Code IS 13935: 1993, “Repair and Seismic Strengthening of Buildings—Guidelines” furnishes the detailed specifications of techniques used for retrofitting. However, brief details of retrofitting techniques used in models have been described as (Agarwal and Thakkar, 2002):

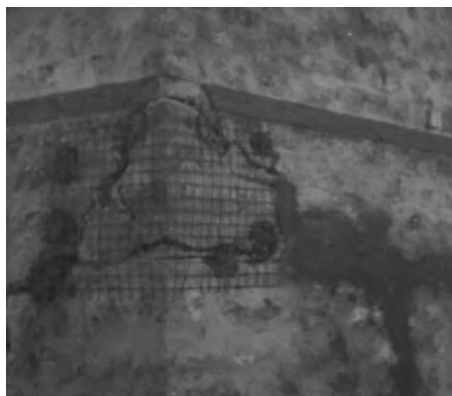
Grouting: A grout mix consisting of Portland cement and water in the ratio of 1:1 is injected into the walls through nozzles, if the cracks are fine; or with cement sand mortar (1:1), if the cracks are wide. A number of holes, preferably 2 to 4 holes in each square metre area of wall, are drilled between the stones to a depth of atleast half the thickness of walls, and injection nozzles are put into the holes.

Stitching of wall corners: In this technique, holes are drilled in orthogonal wall of the structure at a regular interval of 0.5 m. After the cleaning of holes with water, steel rods of about 12 mm diameter are inserted into both intersecting walls so that both walls are connected and the holes are filled with cement grout (Figure 32.31).



FIGURE 32.31 Stitching of damaged corner.

Strengthening of wall with wire mesh: This consists of reinforced welded wire mesh of size 50 mm × 50 mm of 3 mm diameter forming a vertical plate bounded to the wall. The mesh is anchored with the wall by steel ties at spacing of about 30 cm to 40 cm and plastered by cement sand mortar of 20 mm to 40 mm thickness on the outer surface (Figure 32.32).



(a)



(b)

FIGURE 32.32 Retrofitting techniques employed in model R1 (a) Repair with wire mesh (b) Wire mesh with cement plaster.

Through stones: Through stones are inserted at an interval of 0.5 m in horizontal direction and 1 m in vertical direction. The technique includes preparation of space in the wall, insertion of stones of size equal to the thickness of the wall and fixing the stones with the cement-sand mortar.

Tying of walls with steel ties: Holes are drilled in the wall in order to insert steel bars at both the inner and the outer sides of the model. Usually, the bars are placed symmetrically on both sides of the wall. These bars are bolted with steel plates of 3 mm thickness at the ends. The inner and outer bars are bolted simultaneously which enable the model to remain intact. As a consequence of bolting, tension in the bars applies prestress to the walls. This enhances capacity of the wall to withstand horizontal loads (Figure 32.33).



(a)



(b)

FIGURE 32.33 Retrofitting techniques employed in model R1 (a) Placing of steel ties (12φ mm) at sill level (b) Tensioning of steel ties by bolting with anchor plate.

External jacketing: In retrofitting by jacketing, plaster is first removed from the damaged portion of the wall and joints between the stones are cleaned from the mortar. The cracks and

joints of the wall are first filled by cement–sand (1:1) mortar. A welded wire mesh of size 50 mm × 50 mm with 3 mm diameter is placed around the model externally including the entire damaged region. Steel ties are inserted at regular intervals in order to tie the mesh with the wall. An overlap of the mesh of 0.25 m is maintained at the corners so that the continuity of the wire mesh is obtained. The entire operation is followed by a thick plaster 2 cm thick on the welded mesh (Figure 32.34).

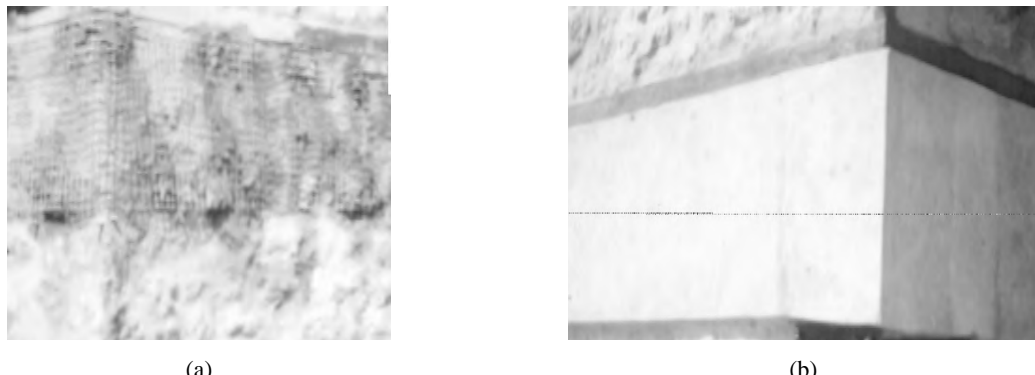


FIGURE 32.34 Retrofitting techniques employed in model R2 (a) Placing of wire mesh around model covering the damaged region (b) Cement–sand plastered on wire mesh.

32.7.1 Behaviour of Retrofitted Models

Model R1: The retrofitted model is tested with a schedule of three test runs of increasing intensity of shock W-19, W-20 and W-21. In the first shock W-19, almost no crack is noticed in the entire model. During the second shock W-20, the retrofitted model shows marked improvement in performance with a total absence of cracks and while in some regions of wall only minor cracks have occurred. On the other hand, stitching of walls has proved to be extremely useful since the stitched portion has not at all damaged. This fact underlines the efficiency of repairing techniques (Figure 32.35). As a result of the third shock W-21, the model has considerably cracked.



FIGURE 32.35 Behaviour of retrofitted model R1 (a) Model under shock test (b) Cracks pattern of Model R1.

Model R2: The retrofitted model is tested with a schedule of three test runs of increasing intensity of shock W-19, W-20 and W-21. In the first shock W-19 the model has behaved integrally and only a few cracks have developed at those portion, which have not undergone retrofitting. During shock W-20 cracking in the model has occurred mainly below sill level. But the retrofitted region of the model does not show any cracking. In shock W-21, the retrofitted portion of the model has remained entirely undamaged, yet a few minor cracks occur at the joints of wire meshes. This pattern of cracks suggests the need of a little more overlapping of the wire mesh. It is observed that the shear resistance of the retrofitted structure has significantly improved, and suffers lesser damage as compared to parent structure even subjected to a bigger shock (Figure 32.36).



FIGURE 32.36 Behaviour of retrofitted model R2 (a) Model under shock test (b) Cracks pattern of mode under shock W-21.

32.7.2 *Findings*

1. The injection of cementitious grout on localized damaged areas can restore the original strength and stiffness, which is relied from free vibration test. The scheme of repair for stitching of corners of walls avoids delamination of walls during shock test
2. The external binding (jacketing) scheme of retrofitting is effective for increasing the strength even more than the original system, as the cracks in the retrofitted models occur in a new position instead of the regions of the previous cracks. The introduction of external horizontal tie bar is helpful for reducing further cracking because of the ties of the walls behave similarly as a band and capable for resisting bending moment due to out-of-plane vibration of the wall. Moreover, external binding with welded wire mesh in damaged region not only increases the lateral resistance of the wall but also prevents shear and flexure failure of the models.

SUMMARY

The recent earthquakes in India have caused extensive damage to hundreds of masonry buildings. Such devastation after earthquake has underlined the need of retrofitting. The aim of this chapter is to summarize the retrofitting techniques of masonry buildings that are feasible and economical. Numerous techniques that are used to retrofit seismically deficient or damaged

masonry buildings are classified on the basis of their effect on structural performance. Some of the common techniques described in this chapter are cement or epoxy injection, reinforced injection, grouting with cement or epoxy, insertion of through stones and re-pointing of mortar, surface coatings, shotcrete overlays or adhered fabric with wire mesh or FRP materials, use of RC and steel frames in openings, external binding or jacketing, prestressing, confinements with RC element and steel sections, strengthening of wall intersections and strengthening of connection between walls and floor. Some of the experimental verification of these retrofitting techniques mentioned in IS 13935: 1993 is also presented.

REFERENCES

- [1] Agarwal, P., "Experimental Study of Seismic Strengthening and Retrofitting Measures in Masonry Buildings", *Ph.D. Thesis*, Department of Earthquake Engineering, IIT Roorkee, 1999.
- [2] Agarwal, P. and Thakkar, S.K., "Study of Adequacy of Earthquake Resistance and Retrofitting Measures of Stone Masonry Buildings", *Research Highlights in Earth Systems Science*, DST Special Vol. 2 on 'Seismicity' pp. 327–335, O.P. Verma (Ed.), Indian Geological Congress, August, 2001.
- [3] Agarwal, P. and Thakkar, S.K., "An Experimental Study of Effectiveness of Seismic Strengthening and Retrofitting Measures in Stone Masonry Buildings", *Journal of European Earthquake Engineering*, pp. 48–64, 2002.
- [4] Agarwal, P. and Thakkar, S.K., "Seismic Evaluation of Strengthening and Retrofitting Measures in Stone Masonry Houses under Shock Loading", *Workshop on Retrofitting of Structures*, IIT Roorkee, 2003.
- [5] Alcocer, S.M., et al., "Retrofitting of Confined Masonry Walls with Welded Wire Mesh", *Eleventh World Conference on Earthquake Engineering*, Acopulco, Mexico, 1996.
- [6] Breiholz, D.C., "Centre Core Strengthening System for Seismic Hazard Reduction of Unreinforced Masonry Bearing Wall Buildings", *Twelfth World Conference on Earthquake Engineering*, New Zealand, 2000.
- [7] Davenport, C., Burton, P., and Neill, S.O., "A GIS-based Earthquake Damage Scenario and the 28 December 1989 Earthquake of Newcastle, Australia", *International Workshop on Measures of Seismic Damage to Masonry Buildings*, Alberto Bernardini (Ed.), Monselice/Padova/Italy 25-26 June 1998, A.A. Balkema/Rotterdam/Brookfield, 1999.
- [8] Dolce, M., Masi, A., and Goretti, A., "Damage to Buildings due to 1997 Umbria-Marche Earthquake", *International Workshop on Measures of Seismic Damage to Masonry Buildings*, Alberto Bernardini (Ed.), Monselice/Padova/Italy 25-26 June 1998, A.A. Balkema/Rotterdam/Brookfield, 1999.
- [9] EERI, "Northridge Earthquake Reconnaissance Report, Vol. 2", *Earthquake Spectra*, Supplement C to Vol. 11, 1996.
- [10] EERI, "Erzincan, Turkey Earthquake Reconnaissance Report", *Earthquake Spectra*, Supplement to Vol. 9, 1993.

- [11] Elgawady, M., Lestuzzi, P., and Badoux, M., "Dynamic versus Static Cyclic Tests of Masonry Walls before and after Retrofitting with GFRP", *Thirteenth World Conference on Earthquake Engineering*, Vancouver, B.C., Canada, 2004.
- [12] FEMA 172, *NEHRP Handbook for Seismic Rehabilitation of Existing Buildings*, Building Seismic Safety Council, Washington, 1992.
- [13] Grimn, C.T., "Masonry Cracks: A Review of the Literature", *Masonry: Materials, Design, Construction, and Maintenance*, pp. 257–280, H.A. Harris, (Ed.), ASTM STP 992, American Society for Testing and Materials, Philadelphia, 1988.
- [14] IAEE, "Basic Concepts of Seismic Codes—Vol. I", *The International Association for Earthquake Engineering*, Tokyo, Japan, 1980.
- [15] IAEE, *Guidelines for Earthquake Resistant Non-engineered Construction*, ACC Limited, Thane, 2001.
- [16] IS 13935, *Repair and Seismic Strengthening of Buildings—Guidelines*, Bureau of Indian Standards, New Delhi, 1993.
- [17] Kahn, L.W., "Shotcrete Retrofit for Unreinforced Brick Masonry", *Eighth World Conference on Earthquake Engineering*, Vol. 1, San Francisco, 1984.
- [18] Karbhari, V.M., "Use of FRP Composite Materials in the Renewal of Civil Infrastructure in Seismic Region", *Second MCEER Workshop on Mitigation of Earthquake Disaster by Advanced Technologies (MEDAT-2)*, Technical Report MCEER-01-0002, 2001.
- [19] Kehoe, B.E., "Performance of Retrofitted Unreinforced Masonry Buildings", *Eleventh World Conference on Earthquake Engineering*, Acopulco, Mexico, 1996.
- [20] Modena, C., "Repair and Upgrading Techniques of Unreinforced Masonry Structures Utilized after Fruli and Compania/Basilicata Earthquakes", *Earthquake Spectra*, Vol. 10, No. 1, 1994.
- [21] Munoz, A., Quiun, D., and Tinman, M. "Repair and Seismic Retrofitting of Hospital and School Buildings in Peru", *Thirteenth World Conference on Earthquake Engineering*, Vancouver, B.C., Canada, 2004.
- [22] Nasini, U. et al., "Evaluation and Design Criteria for Restoring and Retrofitting Damaged Masonry Buildings", *Twelfth World Conference on Earthquake Engineering*, New Zealand, 2000.
- [23] Newman, Alexander, *Structural Renovation of Buildings—Methods, Details, and Design Example*, McGraw-Hill, USA, 2001.
- [24] Sanders, H.P., "A Case History—Retrofit Seismic Strengthening of John Marshall High School with Historic Restoration Objectives", *Eighth World Conference on Earthquake Engineering*, Vol. 1, San Francisco, 1984.
- [25] Schwegler, G. and Kelterborn, P., "Earthquake Resistance of Masonry Structures Strengthen with Fibre Composites", *Eleventh World Conference on Earthquake Engineering*, Acopulco, Mexico, 1996.
- [26] Spencer, R.J.S., et al., "The Performance of Strengthened Masonry Buildings in Recent European Earthquakes", *Twelfth World Conference on Earthquake Engineering*, New Zealand, 2000.
- [27] Thakkar, S.K. and Agarwal, P., "Seismic Evaluation of Earthquake Resistant and Retrofitting Measures of Stone Masonry Houses", Paper No. 110, *Twelfth World Conference on Earthquake Engineering*, New Zealand, 2000.

- [28] *Fastening for Seismic Retrofitting—State of the Art Report*, Comite Euro-International Du Beton, Thomas Telford, UK, 1995.
- [29] Tomazevic, M., *Earthquake Resistant Design of Masonry Buildings*, Imperial College Press, London, 1999.
- [30] Turner, F., “Retrofit Provisions in the International Existing Building Code”, *13th World Conference on Earthquake Engineering*, Vancouver, B.C., Canada, 2004.
- [31] UNDP, “Repair and Strengthening of Reinforced Concrete, Stone and Brick-Masonry Buildings—Volume 5”, *UNDP/UNIDO Project RER/79/015*, Vienna, 1983.
- [32] Weng, D., et al., “Experimental Study on Seismic Retrofitting of Masonry Walls Using GFRP”, *Thirteenth World Conference on Earthquake Engineering*, Vancouver, B.C., Canada, 2004.
- [32] Wyllie, L.A., “Strengthening Strategies for Improved Seismic Performance”, *Eleventh World Conference on Earthquake Engineering*, Acopulco, Mexico, 1996.

Index

- 135° hook, 356
2d plane frame model, 327
3d space frame model, 327, 331
- Absolute
 acceleration spectra, 77, 150
 response spectra, 151
 spectral response, 78
 sum method, 172
- Absorber mass, 161
- Absorbing/transmitting boundaries, 182
- Acceleration, 245
 Displacement Response Spectrum (ADRS), 79, 154
- Accelerogram, 70, 71
- Accelerometer, 134
- Acceptable risk, 57
- Accidental eccentricity, 475
- Accuracy, 141
- Active, 199
 faulting, 97
- Ad/v^2 , 92
- Adding reinforcement, 608
- Addition of structural walls, 534
- Adhered fabric, 603
- Algorithmic damping, 142, 143
- Alternate load path, 245
- Amplification factor, 64, 101, 417
- Amplitude
 parameters, 73
 spectrum, 74, 145
- Approach
 direct, 182
 substructure, 182
- Arching action, 283
- Architectural planning, 239
- Artificial
 damping, 143
 earthquake motions, 66
- Aspect ratio, 472
- Asthenosphere, 6, 30
- ATC-14 methodology, 505
- Attenuation
 law, 93, 98
 relationships, 93, 94
- Auxiliary/secondary mass, 160
- Average response acceleration coefficient, 255
- Axial, 530
- Bandage, 614
- Bands, 577
- Base, 200
 isolators, 534
 shear, 197
- Basics vectors, 164
- Basin
 edges, 63
 effects, 63
- Battering, 234
- Bayesian analysis, 98
- Beam
 column joint, 530
 elements, 334
 mechanism, 414
- Bearing wall system, 240
- Bed rock motion, 63
- Behaviour factor, 255
 of masonry assemblage, 452
- Bhuj earthquake, 207
- Bihar-Nepal earthquake, 51

- Bilateral tension, 452
- Blind fault, 97
- Body Wave Magnitude (MB), 21, 89
 - reflections, 63
 - waves, 10
- Bond, 530
 - beam, 501
 - strength, 450
 - strength of mortar, 450
- Boundary element, 366, 397, 401
- Braced steel frames, 560
- Brittle, 192
 - shear failure, 530
- Building
 - foundation, 243
 - frame system, 240
 - separation, 234
- Buttresses, 534

- Cantilevered wall, 471
- Capacity
 - based design, 421
 - demand (C/D), 505
 - design, 199, 404
 - diagram, 79, 154
- Captive column, 219
- Carbon fibre, 542, 547, 604
- Cement concrete block construction, 440
 - grouting, 600
- Centre coring, 608
 - of mass, 475, 492
 - of rigidity, 475, 476, 492
- Chamoli earthquake, 1999, 431
- Characteristic of strong motion, 91
- Characteristic value, 163
- Characteristic-swaying mode, 232
- Characteristics of earthquake ground motions, 60
- Characterization
 - of accelerogram, 71
 - of design ground motion, 61
- Chord modulus, 454
- Classical damping, 170
- Close-coupled system, 328
- Coherency function, 81
- Column
 - splices, 539
 - sway mechanism, 404, 414
- Community buildings, 254
- Complete quadratic combination (CQC), 273
- Compressional waves, 10
- Compressive strength, 449, 450, 452
 - of mortar, 451

- Concrete
 - capitals, 550
 - jacketing, 565
 - shear wall, 559
- Condition assessment, 506
- Confinement, 535
 - steel sections, 607
 - with RC elements, 606
- Connection failure, 592
- Conrad discontinuity, 31
- Construction joint, 247
- Continental drift theory, 6
- Conventional methods, 535
- Convergent boundaries, 7
- Convolution integral, 125
- Correlation between MMI and PGV, 92
- Coupled shear walls, 330, 367
- Coupling beam, 367
- Crack, 596
- Critical damping, 117, 194
- Critically damped, 117
- Cumulative effective modal mass, 175
- Cumulative tilting, 234
- Curtains, 398
- Curvature ductility, 344
- Curvature ratio, 343
- Cut-outs, 227

- D'alembert's principle, 116, 260
- Damage potential, 84
 - of a ground motion, 73
 - of earthquakes, 81
- Damageability, 198
- Damped circular natural frequency, 118
- Damping, 192, 194, 243
 - coefficient, 194
 - force, 116, 192, 194
 - matrix, 158
- Deep focus earthquakes, 88
- Deflection due to flexural bending, 471
- Deflection to shear, 471
- Degrees-of-freedom, 194
- Design
 - base shear, 253
 - basis earthquake, 252
 - criteria, 96
 - earthquake (DBE), 96
 - ground motions, 65
 - lateral force, 253, 270
 - response spectrum, 101
 - spectrum, 101, 154
- Deterministic zoning method, 56

- Diagonal steel bracing, 563
 Diagonal strut, 336
 Diagonalized modal mass matrix, 312
 Diaphragms, 227, 469
 discontinuity, 237
 failure, 592
 Digital accelerographs, 135
 Direct shear forces, 475
 Direction
 of fault rupture, 61
 one of the principal axis, 83
 to the fault-slip zone, 83
 Discontinued shear walls, 368
 Discontinuities/irregularities in the load path, 227
 Discontinuous load, 528
 Discontinuous shear wall, 227, 368
 Displacement
 ductility, 345
 method, 192
 pickup, 132
 ratio, 347
 Dissipation of seismic energy due to material damp, 63
 Distributed parameter model, 114
 Divergent boundaries, 7
 Doppler's effect, 60
 Drift control, 234
 Drift related damage, 246
 Dry mix, 602
 Dual system, 240, 397
 Ductile, 192
 coupling beams, 367
 Ductility, 193, 198, 243, 244, 342, 344
 based design, 199
 factor, 342, 347
 ratio, 342, 343
 Duhamel integral, 125
 Duration magnitude (M_D), 89
 of shaking, 60
 scale, 21
 Dynamic, 191
 analysis procedure, 253
 component, 180
 degrees of freedom, 113
 equilibrium, 192
 range, 132
 Earthen building, 440
 Earthquake
 average power, 84
 destructiveness potential, 85
 ground motion, 59, 60
 intensity, 84
 potential in a region, 90
 protection system, 199
 resistant (ER) measures, 577
 Effect of inertia, 111
 Effect of the duration of application of excitation, 123
 Effective peak acceleration (EPA), 85, 92
 Eigenvalue, 264
 problem, 163
 Eigenvector/modal, 262
 Elastic half space, 336
 Elasticity time history method, 196
 Elevators, 222
 Embedment ratio, 185
 Energy
 approach, 199
 dissipating capacity, 347
 released, 60
 Epicentres, 4
 EPV, 92
 Equation of motion, 112, 115
 Equivalent
 diagonal strut, 285
 harmonic wave, 73
 lateral force procedure, 253
 modal damping, 334
 number of yield cycles, 85
 shear wall-frame model, 330
 static analysis, 196
 static procedure, 253
 viscous damping, 199
 Evaluate the dynamic response, 137
 Evaluation, 505
 Excitation
 by multiple components, 175
 function, 314
 Expected ground motion, 60
 Experimental determination of dynamic characteristics, 119
 Exterior supplemental devices, 616
 Exterior walls, 219
 External binding, 621
 buttresses, 616
 jacketing, 619
 Factor, 344
 Failure of non-structural components, 592
 Far-coupled system, 328
 Fault
 parallel direction, 60
 rupture area, 60
 rupture parameters, 90

- Faulty construction, 211
 Ferro-cement, 613
 Fibre polymer composite jacket, 542
 Fibre reinforced plastic (FRP), 603
 Field evaluation, 506
 method, 505
 Finite element, 334
 Flexible
 base parameters, 186
 capacities of the beams, 410
 diaphragm, 469
 floor diaphragms, 332
 strength of mortar, 450
 tensile, 450
 wall, 483
 Flexural walls, 464
 Flexure, 530
 beam model, 328
 tensile strength, 455
 tension normal to bed joints, 455
 tension parallel to bed joint, 455
 Fling step, 61
 Floating
 box, 227
 box type, 209
 columns, 212
 column concept, 227
 earthquakes, 98
 Floor space index, 212
 Force balance accelerometer (FBA), 135
 flow, 227
 Forced vibration, 123
 of an MDOF system, 169
 of MDOF system, 171
 Foundation beams or ties, 246
 Foundation input motion, 183
 Fourier
 series, 120
 spectra, 144
 spectrum, 74
 Fragmentation, 398
 Free vibration, 117, 162
 Frequency content, 74
 of a time history, 75
 of ground motion, 144
 Frictional damper, 535
 FRP jacketing, 547
 Fundamental, 193
 mode, 165
 natural period, 255, 486
 Gable band, 582
 Generalised
 coordinates, 158
 eigenvalue problem, 165
 mass, 178
 Geometric attenuation, 62, 63
 Glass fibre, 542
 Global mass reduction, 534
 Global/structural retrofitting, 596
 Grillage
 elements, 334
 model, 336
 Ground motion parameter, 64, 65
 Grout, 449, 451, 600
 injection, 600
 Grouting, 618
 Gunite, 602
 Gutenberg seismic discontinuity, 32
 H/V ratio, 64
 Hammering, 215
 Hanging wall effect, 62
 Harmonic excitation, 120
 Hazard maps, 56
 Holonomic constraints, 157
 Horizontal
 bands or bond beams, 577
 construction joint, 369
 framing system, 577
 irregularities, 226
 resisting elements, 227
 seismic coefficient, 465
 Hybrid, 199
 systems, 201
 Hyperstatic, 246
 Hyperstaticity, 246
 Hysteresis behaviour, 342
 Hysteretic damping, 199
 IDNDR, 59
 Impact echo, 521
 Impedance functions, 183
 Importance factor, 254, 466
 Important service, 254
 In-plane (shear)
 failure, 593
 forces, 464
 moment, 479
 shear, 479
 Inclined beam member, 336
 Inclined truss member, 336
 Incoherence effect, 80

- Increase in axial load, 496
 Indian Institute of Technology, Roorkee, 65
 Industrial building, 159
 Inelastic deformation, 404
 Inelastic time history analysis, 197
 Inertia force, 116, 192
 Inertia matrix, 158
 Inertial interaction, 181, 334
 Infill walls, 534
 Infilled masonry walls, 570
 Influence coefficient matrix, 180
 Inplane failure, 445
 Intensity, 89
 - attenuation, 49
 - scale, 13
 Intermediate focus earthquakes, 88
 Interplate, 5
 - earthquakes, 88
 Intervention, 505
 Intraplate, 5
 - earthquakes, 88
 Inundation, 37
 Irregular, 226
 - buildings, 259
 - shaped plans, 241
 Isolated footing, 334
 Isolation, 200
 Isoseismal, 18
- Jacket with high tension materials, 542
 Jacketed, 565
 Jacketing, 535, 542
 Jamb reinforcement, 605
 Jamb steel, 498
- Kangra earthquake, 51, 55
 Killari (latur) earthquake, 56
 Kinematic interaction effects, 181
 Kinematics, 335
 Koyna earthquake, 52, 56
 Kutch earthquake, 51, 207
- Lack of deformation compatibility, 528
 Land-use planning, 66
 Lap splices, 351
 Large openings, 227
 Lateral
 - force procedure, 253
 - resistance, 528
 - strength design, 199
- Lehmann discontinuity, 31
 Linear
 - dynamic analysis, 196
 - interaction diagram, 483
 - static analysis, 196
 Lintel, 501
 - band, 582
 Liquefaction, 247
 Lithosphere, 6, 30
 Load
 - combinations, 409
 - ground response, 63
 - /member retrofitting, 596
 - path, 212, 468
 - resisting system, 239
 - retrofitting, 533
 - (richter) magnitude (ml), 89
 - site effects, 60
 Logarithmic decrement, 119
 Long duration pulse, 61
 Long natural period, 244
 Loss of resistance, 246
 Losses, 45
 Love waves, 11
 Low lifting grouting, 600
 Lumped
 - mass model, 195
 - parameter model, 114
 - system, 329
- Magnification factor, 414
 Magnitude, 89
 Masonry
 - assemblage, 452
 - buildings, 463
 - cracking, 596
 - deterioration, 596, 601
 - infill walls, 219
 - infills, 282
 - parapets, 617
 - unit, 449
 - wall, 559
- Mass
 - and stiffness matrices, 261
 - irregularities, 211, 232
 - orthonormal mode shape, 163
 - reduction, 534
 - renormalization, 163
- Master, 333
 Mathematical model, 194
 Mathematical modelling, 112

Maximum

- absolute response, 272
- considered earthquake, 252
- considered magnitude, 56
- credible earthquake (MCE), 96
- interaction effect, 410
- interaction ratio, 387
- strain energy input, 78
- MDOF system, 157
- Mean square acceleration, 84
- Measure of severity, 71, 83
- Measure of the severity of ground shaking, 81
- Mechanical dissipaters, 200
- Medvedev-Spoonheuer-karnik (MSK), 13
- Member level approach, 533
- Member/local, 203
- Mercalli intensity scale, 13
- Mesosphere, 30
- Micro-earthquake, 89
- Microtremor data, 64
- Mindlin plate element, 335
- Minimax property of Rayleigh quotient, 165
- Missing mass correction, 177, 270

Modal

- analysis procedure, 253
- combination rules, 171
- damping matrix, 312
- expansion theorem, 164
- mass, 170, 269
- participation factors, 171, 270, 315
- stiffness, 170
- stiffness matrix, 312
- shapes, 163, 243, 262
- superposition method, 196
- truncation, 175

Modified mercalli (MMI) scale, 89

Modulus

- of elasticity, 453, 470
- of rigidity, 470
- of rupture, 455

MOHO, 31

Mohorovicic discontinuity, 31

Moment, 22

- magnification factor, 414, 424
- magnitude, 22, 90

Mortar, 446, 449, 601

Movable joint, 219

(MSK) intensity scale, 89

Multi-degree-of-freedom, 197

Multiple-support excitation by differential ground, 179

Mutually orthogonal, 163

Muzaffarabad earthquake, 446

Natural

- mode shapes, 163, 255
- period, 193, 243
- time period, 262
- Near-field, 60
 - strong motion data, 60
- Newton's second law of motion, 115
- Non-destructive evaluation, 506, 509
- Non-engineered construction, 576
- Non-linear dynamic analysis, 197
- Non-linear inelastic analysis, 505
- Non-linear static analysis, 196
- Non-reference site approach, 64
- Non-stationary characteristics, 74
- Non-structural damage, 245
- Non-structural elements, 243
- Nonholonomic, 157
- Number of significant half-cycles of motion, 62

Numerical

- algorithm, 142
- integration, 141

Occurrence of an earthquake, 99

Oceanic ridges, 6

Orthogonal strength ratio, 455

Orthogonality of mode-shapes, 164

Out-of-plane, 220

- bending, 464
- buckling, 397
- failure, 445, 592
- forces, 483

Over strength, 347, 417

- factor, 415

Overdamped, 117

Overturning moment, 480, 495

P-Δ effects, 211, 231

Parapets, 220

Partial resonance, 193

Partial safety factor, 417

Passive, 199

- and active control systems, 201
- control system, 200

Path effect, 60

- /interrupted load, 528
- /irregular load path, 528

Peak ground

- acceleration (PGA), 91
- horizontal acceleration, 73
- horizontal velocity, 62
- shear force, 271
- velocity (PGV), 92

- Penetration resistance methods, 520
 Perfectly-plastic, 347
 Performance-based engineering, 79
 Period elongation, 143
 of the dominant pulse, 62
 Permanent ground displacement, 61
 Phase spectrum, 74, 145
 Physical coordinates, 316
 Piecewise-linear interpolation, 315
 Piers, 470
 Pile, 335
 Pitched roofs, 432
 Plane frame idealization, 328
 Plane frame models, 328
 Plastic hinges, 395, 404
 Plinth band, 501, 582
 Poisson process, 99
 Poisson's ratio, 449
 Poor quality of material, 211, 528
 Pounding, 233, 507, 592
 failure, 215
 Power spectrum, 75
 Predominant period, 63
 Premature deterioration, 398
 Prestressing, 612
 Primary loss, 45
 Principal axis, 83
 Prism, 451
 Probabilistic estimations of ground motion, 98
 Propagation delay, 81
 Proportional damping, 170
 Pseudo relative velocity response spectrum, 76, 148
 Pseudodynamic test, 204, 205
 Punching shear failure, 549
 Push over analysis, 197, 345, 505
 Push over curve, 79, 154
- Qualitative methods, 505
 Quality factor, 25
 of workmanship, 528
 Quasi
 -resonance, 193
 -static component, 180
 -static test, 204, 205
- Raft foundation, 335
 Random rubble stone masonry, 440
 Rapid visual screening method, 505
 Rayleigh (L_R), 11
 dissipation function, 158.
 quotient, 165
- RC or steel frame, 605
 Re-entrant, 236
 corner, 227, 233
 Re-pointing, 601
 Rebar locator/convert meter, 520
 Rebound hammer, 520
 Reciprocating machine, 159
 Reconstruction, 524
 Recurrence
 relation for constant average accelerator, 140
 relation for duhamel integral, 138
 Reduced 3d model, 328, 331
 eigenvalue problem, 178
 Redundancy, 245
 Reference site, 63
 Regression analysis, 64
 Regular, 226
 building, 259
 configurations, 226
 shapes, 241
 Rehabilitation, 524
 Reinforced concrete
 beams, 530
 construction, 208
 frames, 568
 infill walls, 563
 jacket, 542
 jacketing, 543
 masonry, 451
 shear walls, 565
 Reinforcement, 449
 Reinforcing steel, 451
 Relation between MMI and PGA, 91
 Relative
 displacement response spectra, 76
 displacement response spectrum, 148
 rigidity, 253
 velocity spectrum, 77
 Remoulding, 524
 Repairing, 524, 596
 Representative ground frequency, 153
 RESA, 65
 Resonance, 25
 Restoring force, 192
 Retrofitting, 202, 524
 Return period, 56, 99
 Richter magnitude scale, 19
 Rigid
 and flexible diaphragm, 467
 bars, 393
 diaphragm, 332, 469
 link, 329, 393
 Rigidity, 198

- Rima (Assam) earthquake, 51
- Ring of fire, 6
- Ritz base vectors, 177
- Roof, 501
 - band, 582
 - diaphragms, 469
- Rotation angle ductility ratio, 343
- Rotational ductility factor, 343
- Run-up, 37
- Rupture directivity effect, 60, 61
- Safety level, 57
- Screening method, 503
- SDOF system, 115
- Seismic, 200
- Seismic
 - base isolation, 540
 - base shear force, 465
 - demand diagram, 79
 - design code of practice, 60
 - evaluation, 202, 508
 - hazard map, 45
 - hazard zone map, 46
 - isolation, 571
 - moment, 90
 - pickups, 129
 - regionlisation map, 50
 - retrofitting, 524
 - separation, 233
 - wave propagation, 60
 - waves, 10
 - weight, 255
 - zone map of india, 253
 - zoning, 45
 - zoning map, 45, 48, 49, 50
- Seismically deficient structures, 505
- Seismicity data, 60
- Seismo-tectonic setup of india, 53
- Seismo-tectonic units, 53
- Seismogenic rupture zone, 94
- Seismology, 3
- Seismometers, 132
- Seismoresistant capacity, 239
- Semi-active, 199
- Serviceability, 198
- Servo-accelerometer, 135
- Severity of ground motion, 96
- Shaking table, 204
- Shallow focus earthquakes, 88
- Shear, 530
 - beam model, 329
 - building model, 113
- friction, 369
- wall, 464, 470, 534
- waves, 10
- Shillong earthquake, 51
- Shock table, 585
 - testing, 582
- Short
 - column, 219, 505
 - duration pulse, 61
 - natural period, 244
- Shotcrete, 602
- Sill band, 582
- Single degree-of-freedom, 194
- Slaves, 333
- Sliding joints, 222
- Soft, 211
 - or weak stories, 209
 - storey, 231, 404, 414
 - storey problem, 421
 - stories, 211, 507
- Soil
 - damping, 334
 - springs, 183
 - structure interaction, 181, 182, 195, 334
- Source effect, 60
- Spatial variation of
 - earthquake ground motion, 179
 - ground motion, 80
 - strong ground motion, 62
- Special confining reinforcement, 389
- Specification of MCE, 97
- Spectral
 - amplification, 63
 - analysis of surface waves (SASW), 521
 - intensity, 85
 - radius, 142
 - shapes, 131
- Splicing, 369
- Splints, 614
 - and bandage, 614
- Splitting tension, 450
- Spring force, 116
- Square-root-of-the-squares, 272
- SRR, 65
- SRSS rule, 172
- SSI analysis, 181
- Stability, 141
- Stack pattern, 452
- Standard eigenvalue problem, 165
- Starting transient, 122
- Static, 191
 - equilibrium, 192
- Statically indeterminate, 245

- Steady-state magnification factor, 121
 Steady-state response, 121
Steel
 braces, 534
 bracing, 570
 jacket, 542
 moment frames with fluid viscous dampers, 573
Stiffness, 192
 matrices, 178
 resistance, 192
Stitching of wall corners, 608, 618
Stodola method, 165
Stones
 bond, 599
 through, 599, 619
Strain hardening effects, 417, 423
Strength, 198
Strengthening, 524
 of wall with wire mesh, 618
Stress concentrations, 227
Stress-strain curve, 449, 453
Strong column
 motion data, 64
 motion duration, 493
 motion studies, 60
 -weak beam, 530
 -weak beam structure by, 404
Structural
 damping, 244
 dynamics, 112
 /global, 203
 integrity, 444
 level approach, 533
 level retrofittings, 534
 masonry, 449
 models, 194
 overlay, 603
Structure ductility, 345
Strut action, 219
Supplemental
 damping, 541
 damping devices, 535
 device, 540
 energy dissipation devices, 534
Support motions, 171
Surface
 apparent velocity of propagation, 81
 ground motion, 63
 topography, 63
 wave (s-wave) magnitude, 21, 89
 wave generation, 63
 waves, 10
Survivability, 198
Sweeping matrix, 167, 168
Synchronous motion, 162
Tectonic earthquakes, 88
Tectonic map, 51
Theory of elasticity, 285
Three-dimensional model, 194
Time
 history method, 311
 marching schemes, 141
 period of the building, 466
TOPI, 209, 217
Torsion, 235
 irregularity, 234
Torsional
 eccentricity, 493
 effects, 224
 moment, 493
 shear forces, 475
Transducers, 129
Transfer function of the soil column at the site, 63
Transform boundaries, 7
Transform fault boundary, 9
Triaxial compression, 452
Truncation of the modal summation, 176
Tsunami earthquake, 36
Tuned mass dampers, 200
Tuning ratio, 121, 130
Two-dimensional plane frame model, 195, 393
Tying of walls with steel ties, 619
Ultimate displacement, 343
Ultimate limit state, 198
Uncorrelated components of the ground motion, 82
Undamped
 circular natural frequency, 117
 free vibration, 262
 system, 260
Under-damped, 117
UNESCO, 59
Uniaxial compression, 452
Unit, 446, 601
 impulse response function, 124
Unity equation, 481, 482
University of Roorkee, 65
Uttarkashi, 438
V/A ratio, 73, 92

- Vector purification/deflation, 167
Velocity pickup, 132
Vertical
 acceleration, 252
 discontinuity, 212
 irregularities, 223, 226
 reinforcing, 577
 setback, 233
 steel, 582
 strength discontinuities, 507
Vibration, 111
 isolation, 127
 isolators, 128
 spectra, 131
Virtual eccentricity, 483
Visco-elastic damper, 535
Viscous
 damper, 535, 573
 damping, 192
 forces, 192
Visual inspection, 506, 509
- Water tank, 220
Wave propagation effect, 80
 in elastic medium, 181
Weak, 211
 motions, 64
 storey, 230
Web reinforcement, 369
Wide column, 393
Wing walls (side walls), 534
Winkler model, 336
Wire fabric, 613
Wire mesh, 568
- Yield
 condition, 194
 displacement, 343
 load, 343
 penetration, 359
- Wall as strip footing, 334
/pier fixed, 471
- Zero period acceleration (ZPA), 101
Zone factor, 253, 466

Earthquake Resistant Design of Structures

Pankaj Agarwal
Manish Shrikhande

This comprehensive and well-organized book presents the concepts and principles of earthquake resistant design of structures in an easy-to-read style. The use of these principles helps in the implementation of seismic design practice. The book adopts a step-by-step approach, starting from the fundamentals of structural dynamics to application of seismic codes in analysis and design of structures. The text also focusses on seismic evaluation and retrofitting of reinforced concrete and masonry buildings. The text has been enriched with a large number of diagrams and solved problems to reinforce the understanding of the concepts.

Intended mainly as a text for undergraduate and postgraduate students of civil engineering, this text would also be of considerable benefit to practising engineers, architects, field engineers and teachers in the field of earthquake resistant design of structures.

ABOUT THE AUTHORS

Pankaj Agarwal, Ph.D., is Assistant Professor at the Department of Earthquake Engineering, Indian Institute of Technology Roorkee. He has been engaged in teaching and research in earthquake resistant design of masonry and RC structures, post-damage detection and survey of earthquake affected areas and buildings, and health monitoring. Dr. Agarwal is a member of Indian Society of Earthquake Technology (ISET).

Manish Shrikhande, Ph.D., is Assistant Professor at the Department of Earthquake Engineering, Indian Institute of Technology Roorkee. He is a recipient of Young Engineer Award of Indian National Academy of Engineering (INAE) and Career Award of AICTE.

